Géométrie et percolation sur des cartes à bord aléatoires

Loïc Richier

Numéro national de Thèse : **2017LYSEN020**

THÈSE de DOCTORAT DE L'UNIVERSITÉ DE LYON

opérée par

L'École Normale Supérieure de Lyon

École Doctorale en Informatique et Mathématiques de Lyon N° 512

Discipline : Mathématiques

Soutenue publiquement le 30 Juin 2017 par :

Loïc RICHIER

GÉOMÉTRIE ET PERCOLATION SUR DES CARTES À BORD ALÉATOIRES

Devant le jury composé de :

Mme	Marie ALBENQUE	École Polytechnique	Examinatrice
M.	Jérémie BOUTTIER	CEA Saclay	Invité
M.	Nicolas CURIEN	Université Paris-Sud	Rapporteur
M.	Igor KORTCHEMSKI	École Polytechnique	Examinateur
M.	Jean-François LE GALL	Université Paris-Sud	Examinateur
M.	Grégory MIERMONT	ENS de Lyon	Directeur
M.	Jean-Christophe MOURRAT	ENS de Lyon	Examinateur

Après l'avis de :

M.	Omer ANGEL	The University of British Columbia
M.	Nicolas CURIEN	Université Paris-Sud

GÉOMÉTRIE ET PERCOLATION SUR DES CARTES À BORD ALÉATOIRES

Cette thèse porte sur des limites de grandes cartes à bord aléatoires.

Dans un premier temps, nous nous intéressons aux propriétés géométriques de telles cartes. Nous montrons d'abord des résultats concernant les limites d'échelle et les limites locales du bord de cartes de Boltzmann dont le périmètre tend vers l'infini, que nous appliquons à l'étude du modèle $O(n)$ rigide sur les quadrangulations. Ensuite, nous introduisons une famille de quadrangulations du demi-plan aléatoires avec un paramètre de torsion, dont on étudie les limites d'échelle et la structure de branchement. Enfin, nous établissons une propriété de confluence des géodésiques dans les cartes uniformes infinies du demi-plan, qui sont des limites locales de triangulations et quadrangulations à bord uniformes.

Dans un second temps, nous considérons des modèles de percolation de Bernoulli sur les cartes uniformes infinies du demi-plan. Nous calculons le seuil de percolation par site critique pour les quadrangulations, et établissons une propriété d'universalité de ces modèles de percolation au point critique à partir des probabilités de croisement. Pour finir, nous étudions la limite locale de grands amas de percolation critiques en construisant l'amas critique émergent, une triangulation uniforme infinie du demi-plan munie d'un amas de percolation critique infini.

Mots-clés. Cartes aléatoires, percolation, modèle $O(n)$, limites locales, limites d'échelle.

GEOMETRY AND PERCOLATION ON RANDOM MAPS WITH A BOUNDARY

This thesis deals with limits of large random planar maps with a boundary.

First, we are interested in geometric properties of such maps. We prove scaling and local limit results for the boundary of Boltzmann maps whose perimeter goes to infinity, which we apply to the study of the rigid $O(n)$ loop model on quadrangulations. Next, we introduce a family of random half-planar quadrangulations with a skewness parameter, and study their scaling limits and branching structure. Finally, we establish a confluence property of geodesics in uniform infinite half-planar maps, which are local limits of uniform triangulations and quadrangulations with a boundary.

Second, we consider Bernoulli percolation models on uniform infinite half-planar maps. We compute the critical site percolation threshold for quadrangulations, and prove a universality property of these percolation models at criticality involving crossing probabilities. To conclude, we study the local limit of large critical percolation clusters by defining the incipient infinite cluster, a uniform infinite half-planar triangulation equipped with an infinite critical percolation cluster.

Keywords. Random maps, percolation, $O(n)$ model, local limits, scaling limits.

Remerciements

Mes premiers remerciements sont naturellement adressés à mon directeur de thèse, Grégory Miermont. Lorsque je suis arrivé à Lyon pour un stage de M1, j'étais loin d'imaginer que j'aurais un jour à écrire ces lignes. Merci de m'avoir proposé un sujet de thèse passionnant, de m'avoir guidé avec tant de patience et de gentillesse. Merci de m'avoir soutenu et conseillé, d'avoir été toujours disponible. Merci d'avoir partagé avec un enthousiasme communicatif de nombreuses discussions mathématiques. Je suis parfois entré dans le bureau Sud 435 avec des doutes et des inquiétudes. J'en suis toujours sorti motivé et passionné.

Je remercie chaleureusement Omer Angel et Nicolas Curien d'avoir accepté de rapporter ce manuscrit. J'ai la plus grande admiration pour leurs travaux, qui ont considérablement influencé cette thèse. Je les remercie pour leur relecture très attentive et pour l'intérêt qu'ils portent à ce travail. Je suis également très reconnaissant envers Nicolas pour toutes les idées qu'il a partagées avec moi ces dernières années.

Je suis extrêmement honoré que Jean-François Le Gall fasse partie du jury de soutenance. Je garde un souvenir mémorable de ses cours, modèles de clarté et de rigueur, mais aussi de ses précieux conseils. C'est avec un très grand plaisir que je compte Marie Albenque, Jérémie Bouttier, Igor Kortchemski et Jean-Christophe Mourrat parmi les membres du jury. Je les remercie d'avoir répondu avec gentillesse à toutes les questions que j'ai pu leur poser, y compris les plus idiotes. Je suis très heureux de rejoindre Igor l'an prochain, et j'espère avoir la chance de continuer à échanger avec Jérémie et Marie. Enfin, merci à Jean-Christophe de m'avoir mis le pied à l'étrier pour l'enseignement.

Au moment d'écrire ces lignes, j'ai une pensée toute particulière pour tous mes Professeurs, qui m'ont soutenu et transmis leur passion pour les mathématiques, de l'Université Henri Poincaré à l'École Polytechnique. Je remercie Didier Schmitt de m'avoir tant encouragé, mais aussi de m'avoir appris que 100% des gagnants du Loto ont tenté leur chance. Je remercie du fond du coeur Sylvie Méléard pour ses cours passionnants, son aide inestimable, et pour l'oeil attentif qu'elle garde sur mon parcours.

Ce manuscrit ne serait rien sans mes co-auteurs. En plus de Grégory, je remercie chaleureusement Erich Baur pour tout ce que nous avons partagé ces dernières années, mathématiquement et au-delà. J'espère que cela durera encore longtemps. J'ai beaucoup de chance d'avoir pu compter sur ton amitié.

Je tiens également à remercier l'ensemble des chercheurs et chercheuses que j'ai eu la chance de rencontrer avant et pendant ma thèse. En particulier, j'ai tiré les plus grands bénéfices de mes discussions avec Timothy Budd, Philippe Chassaing, Christophe Garban et Wendelin Werner. Merci aussi à celles et ceux qui ont animé les groupes de travail (parfois aléatoires) auxquels j'ai participé, et à mes grands frères et soeurs de thèse Jérémie, Robin et Daphné pour tous les moments passés ensemble.

J'ai bénéficié d'excellentes conditions pour réaliser cette thèse grâce à l'aide de nombreuses personnes de la DGA que je souhaite sincèrement remercier.

Cette thèse a été préparée à l'Unité de Mathématiques Pures et Appliquées de l'ENS Lyon. Je remercie l'ensemble des membres du laboratoire qui rendent ce lieu agréable et propice à l'épanouissement scientifique, ainsi que les membres voisins de l'Institut Camille Jordan. Je remercie particulièrement Magalie, Virginia et Sandy dont l'efficacité n'a d'égal que la gentillesse.

Je profite de ces lignes pour remercier Denis, Emmanuel, Jean-Baptiste, Régis et Vincent avec qui j'ai eu *le plaisir, et l'honneur*, d'organiser les Soirées Mathématiques de Lyon, ainsi que celles et ceux qui ont animé les séances de football du mercredi, en particulier Bastien, Nacho et Nathalie.

L'heure est venue de remercier mes camarades de thèse de Lyon. J'ai eu la chance de partager pendant trois ans le bureau de Samuel "Footix" Le Fourn : journaliste sportif en (mauvaise) herbe, toujours de bonne humeur et d'un soutien moral permanent. J'ai passé trois excellentes années en face de toi, et tu vas me manquer. Pénalty pour Lyon ! Il n'est resté qu'un an en notre compagnie mais je ne peux pas oublier Sylvain "Le Patron" Courte : excellent quand il s'agit de la mettre au fond et modèle de gentillesse, comme toute sa famille. Merci Patron ! Alexandre "Couscous" Vérine n'a pas volé sa place dans ces lignes : homme de tous les défis et de toutes les confidences, sa présence assure une journée agréable et pimentée. La poésie, c'est pas plutôt Brassens ? Je n'oublierai pas les discussions avec Sébastien "Tournesol" Martineau, ni l'aide qu'il m'a apportée pour l'introduction de cette thèse. Merci, vieux ! Il est un peu aigri, mais Thomas "Papy" Letendre a corrigé de manière implacable mon introduction et je l'en remercie. Café ? J'ai également passé les meilleurs moments de ma thèse avec Giulia "Abuelita" Binotto. Gracias ! Bien sûr, je ne saurai oublier mes autres camarades de jeu : Alessandro, Álvaro, Bruno (voisin d'outre-Rhin), Coline (co-organisatrice en chef), Danny the dog, Juhan (la vie est belle, mais les mathématiques sont difficiles...), Mike (Olivier, la batterie !), Mohamed, Mohesh (veste à l'envers), Raymond (le joueur de tête), Romain et toutes celles et ceux que je ne peux pas citer tant la liste serait longue. Je n'oublie pas non plus mes camarades de la promotion X2010, ni ceux de Nancy et d'Orsay.

Je tiens enfin à remercier ma famille et mes amis, qui m'ont tant aidé ces dernières années. Mes retours en Lorraine durant ces trois ans m'auront fait le plus grand bien. Surtout, cette thèse doit énormément à mes parents et à ma soeur. Vous m'avez toujours encouragé, quels que soient mes choix. Vous m'avez soutenu dans les moments de doute. Je ne serais pas là sans vous. Pour toutes ces choses, merci. Mes derniers mots sont destinés à Camille, à qui je dois tant qu'il est impossible de l'écrire. Merci pour tout. Je ne sais pas ce que je ferais sans toi...

À mes parents,

Table des matières

I

Introduction

1

Présentation générale

Ce premier chapitre est consacré à une présentation succincte de la théorie des cartes aléatoires, sur laquelle reposent les travaux de cette thèse. Nous commençons par la définition d'une carte et quelques mots sur leur énumération. Ensuite, nous nous intéressons à la construction de limites de grandes cartes aléatoires, dont la taille tend vers l'infini. Nous évoquerons d'abord des *limites d'échelle* de telles cartes, qui sont des espaces métriques aléatoires compacts, puis des *limites locales*, qui sont des réseaux aléatoires infinis. Ces limites constituent les principaux objets d'étude de ce manuscrit.

Sommaire

1.1 Cartes planaires

1.1.1 Préliminaires et définitions

Cartes planaires. Les cartes sont des objets combinatoires qui apparaissent dans de nombreuses branches des mathématiques. Il en existe plusieurs définitions, mais nous présentons d'abord la plus géométrique d'entre elles. Une présentation détaillée est disponible dans les ouvrages [LZ04, MT01].

Un *graphe* G est constitué d'un ensemble de *sommets* V, d'un ensemble d'*arêtes* E et d'une relation d'incidence I qui associe à chaque arête $e \in E$ un ou deux éléments de V appelés *extrémités*. Une arête $e \in E$ avec une seule extrémité est appelée une *boucle*. Cette notion de graphe apparaît dans la littérature sous l'appellation *multigraphe non orienté*. Un *plongement* du graphe $G = (V, E, I)$ dans la sphère $\mathbb{S}^2$ est la donnée d'une application $\varphi : V \to \mathbb{S}^2$ injective, et d'une collection d'applications $(\phi_e : e \in E)$ continues de $[0, 1]$ dans $\mathbb{S}^2$, dont la restriction à $[0, 1)$ est injective et telles que $\varphi(I(e)) = \{\phi_e(0), \phi_e(1)\}$. L'ensemble $\phi_e([0, 1])$ représente l'arête e sur la sphère, et est souvent identifié avec cette dernière. Un tel plongement est dit *propre* si de plus les arêtes ne s'intersectent pas, sauf éventuellement en les sommets du graphe. Dans ce cas, les *faces* du plongement de G sont les composantes connexes de la sphère $\mathbb{S}^2$ privée de l'union des arêtes $e \in E$. Notons que chaque arête a deux orientations possibles, et on appelle *arête orientée* une arête munie de l'une de ces orientations. Une arête orientée est dite *incidente* à la face se trouvant à sa gauche. Le *degré* $\deg(f)$ d'une face f est alors le nombre d'arêtes orientées qui lui sont incidentes.

Intuitivement, le plongement d'un graphe dans la sphère est simplement un dessin du graphe sur celle-ci. La notion de carte planaire porte sur la structure combinatoire d'un tel plongement, et non sur la forme particulière des arêtes. Autrement dit, deux plongements sont dits *isomorphes* s'il existe un homéomorphisme de $\mathbb{S}^2$ préservant l'orientation induisant un isomorphisme des graphes sous-jacents.

Définition 1.1.1. Une *carte planaire* est le plongement propre d'un graphe fini connexe dans la sphère $\mathbb{S}^2$, considéré à homéomorphisme préservant l'orientation près.

Dans cette définition, l'adjectif "planaire" est associé au choix de la sphère comme surface. La notion de carte peut néanmoins être étendue à d'autres surfaces. Dans la suite, toutes les cartes que nous considérons sont implicitement planaires. Une carte est un objet plus rigide qu'un graphe. En particulier, on peut construire des cartes différentes à partir d'un même graphe (et certains graphes finis ne peuvent pas être réalisés comme une carte planaire). C'est cette rigidité qui rend plus aisée leur énumération. Pour la renforcer et supprimer les éventuelles symétries, on suppose implicitement les cartes *enracinées*, c'est-à-dire munies d'une arête orientée distinguée $e_* = (e_-, e_+)$ appelée la *racine* (marquée par une flèche dans les illustrations, voir la Figure 1.1). Le point source e_- de la racine est appelé l'*origine* de la carte. Il est parfois utile de distinguer un sommet v_* de la carte en plus de l'arête racine. On dit alors que la carte est (enracinée) *pointée*.

FIGURE 1.1 : Une carte planaire (enracinée).

Cette définition d'une carte, bien qu'intuitive, présente deux inconvénients. D'abord, le caractère combinatoire de cette notion n'est pas transparent : il n'est pas immédiat, par exemple, que le nombre de cartes ayant un nombre prescrit d'arêtes est fini. De plus, la notion de degré d'une face peut paraître à première vue arbitraire. La définition équivalente suivante clarifie ces deux aspects (voir [MT01, Section 3.2]).

Définition 1.1.2. Une carte planaire est le recollement par paires des arêtes d'un nombre fini de polygones formant une sphère topologique.

Avec ce point de vue, les faces de la carte ainsi que leur degré correspondent aux polygones initiaux (voir la Figure 1.2). On peut également obtenir une description algébrique de la carte par des permutations.

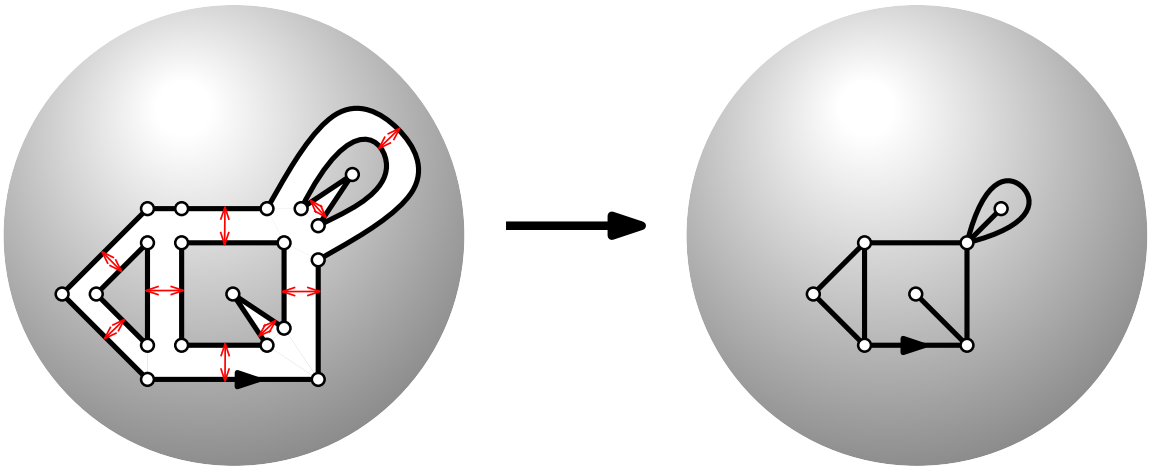

FIGURE 1.2 : Une carte planaire obtenue comme recollement de polygones.

L'ensemble des cartes est noté $\mathcal{M}_f$, et un élément de $\mathcal{M}_f$ est généralement noté $\mathbf{m}$. Les notations $\mathrm{V}(\mathbf{m})$, $\mathrm{E}(\mathbf{m})$ et $\mathrm{F}(\mathbf{m})$ désignent respectivement l'ensemble des sommets, arêtes et faces de $\mathbf{m}$. Une part importante des travaux de cette thèse concerne

les cartes *à bord*. Une carte à bord est simplement une carte $\mathbf{m}$ dans laquelle la *face racine*, c'est-à-dire la face f_* incidente à droite de l'arête racine, est interprétée comme une face *externe* (par opposition, les autres faces sont dites *internes*). Les sommets et arêtes incidents à f_* forment alors le *bord* $\partial\mathbf{m}$ de la carte, et le degré de f_* est appelé le *périmètre* $\#\partial\mathbf{m}$ de $\mathbf{m}$. Le bord d'une carte est dit *simple* s'il forme un cycle sans auto-intersection. L'ensemble des cartes à bord simple est noté $\widehat{\mathcal{M}}$.

Certaines classes de cartes planaires jouent un rôle particulier, en premier lieu les *p-angulations* qui sont les cartes dont toutes les faces ont le même degré p. On s'intéressera notamment aux *triangulations* $(p = 3)$ et aux *quadrangulations* $(p = 4)$ dont les ensembles sont notés $\mathcal{M}_f^{\triangle}$ et $\mathcal{M}_f^{\square}$ (ou parfois $\mathcal{Q}_f$). C'est également le cas des cartes *biparties*, dont les sommets peuvent être coloriés avec deux couleurs de sorte que deux sommets voisins soient toujours de couleurs différentes. De manière équivalente, une carte bipartie est une carte dont toutes les faces ont degré pair. On note leur ensemble $\mathcal{B}_f$. Plus généralement, une p-angulation (ou une carte bipartie) à bord est une carte à bord dont toutes les faces internes ont degré p (ou pair), le périmètre étant libre.

L'un des premiers résultats concernant les cartes est la fameuse formule d'Euler, qui montre que pour toute carte planaire $\mathbf{m}$,

$$\mathrm{V}(\mathbf{m}) - \mathrm{E}(\mathbf{m}) + \mathrm{F}(\mathbf{m}) = 2.$$

Toutefois, l'étude des cartes commence réellement dans les années soixante, avec les travaux de William Thomas Tutte (voir par exemple [Tut62a, Tut62b, Tut62c, Tut63, Tut68]) dont le but était de montrer le théorème des quatre couleurs : les faces de toute carte planaire peuvent être coloriées avec quatre couleurs de sorte que deux faces adjacentes soient toujours de couleurs différentes. Bien qu'il ait fallu attendre 1976 et le travail de Kenneth Appel et Wolfgang Haken pour que ce théorème soit prouvé, William Thomas Tutte parvient à énumérer de nombreuses classes de cartes, notamment via sa *méthode quadratique*. Il détermine en particulier le cardinal de l'ensemble $\mathcal{M}_n^{\square}$ des quadrangulations à n faces (qui est également le nombre de cartes à n arêtes), montrant que

$$\#\mathcal{M}_n^{\square} = \frac{2 \cdot 3^n}{(n+1)(n+2)} \binom{2n}{n}. \tag{1.1}$$

La remarquable simplicité de cette formule et sa proximité avec le n-ième nombre de Catalan, qui est le nombre d'arbres ordonnés enracinés à n arêtes, conduit à penser qu'il existe une bijection entre $\mathcal{M}_n^{\square}$ et une certaine classe d'arbres. Une telle bijection est établie en 1981 par Robert Cori et Bernard Vauquelin [CV81], puis développée par Gilles Schaeffer [Sch98]. Nous la présentons dans la Section 1.1.2, ainsi qu'une généralisation due à Jérémie Bouttier, Philippe Di Francesco et Emmanuel Guitter dans la Section 1.3.2.

Parallèlement au développement des techniques bijectives, les problèmes d'énumération de cartes apparaissent en physique théorique en raison de leur lien avec les intégrales de matrices, mis en évidence par Gerardus 't Hooft [tH74], puis par Édouard Brézin, Claude Itzykson, Giorgio Parisi et Jean-Bernard Zuber [BIPZ78].

Arbres plans. Les techniques d'énumération bijectives des cartes mentionnées au paragraphe précédent motivent l'introduction des arbres plans (ou arbres ordonnés enracinés). La définition suivante emprunte le formalisme introduit par Jacques Neveu [Nev86]. On utilise les notations anglo-saxonnes $\mathbb{N} := \{1, 2, \ldots\}$ et $\mathbb{Z}_+ := \mathbb{N} \cup \{0\}$. L'ensemble $\mathcal{U}$ des mots finis sur les entiers s'écrit alors

$$\mathcal{U} := \bigcup_{k=0}^{\infty} \mathbb{N}^k.$$

Définition 1.1.3. Un arbre plan $\mathbf{t}$ est un sous-ensemble fini de $\mathcal{U}$ (dont les éléments sont appelés les *sommets* de $\mathbf{t}$) satisfaisant les propriétés suivantes :

- Le mot vide $\emptyset$ est un élément de $\mathbf{t}$, appelé le *sommet racine* de $\mathbf{t}$.
- Pour tout $k \in \mathbb{N}$, si $u = (u_1, \ldots, u_k) \in \mathbf{t}$ alors $\widehat{u} := (u_1, \ldots u_{k-1}) \in \mathbf{t}$. Le sommet $\widehat{u}$ est appelé le *parent* de u dans $\mathbf{t}$.
- Pour tout sommet $u = (u_1, \ldots, u_k) \in \mathbf{t}$, il existe $k_u(\mathbf{t}) \in \mathbb{Z}_+$ tel que l'on ait $uj := (u_1, \ldots, u_k, j) \in \mathbf{t}$ si et seulement si $1 \leq j \leq k_u(\mathbf{t})$. L'entier $k_u(\mathbf{t})$ est le *nombre d'enfants* de u dans $\mathbf{t}$.

L'ensemble des arbres plans est noté $\mathcal{T}_f$. Notons qu'un arbre plan est précisément une carte planaire enracinée avec une unique face. Aussi, on note parfois $\mathrm{V}(\mathbf{t})$ l'ensemble des sommets de l'arbre plan $\mathbf{t} \in \mathcal{T}_f$.

Soit $\mathbf{t} \in \mathcal{T}_f$ un arbre plan. La *génération* ou *hauteur* d'un sommet $u = (u_1, \ldots, u_k)$ de $\mathbf{t}$ est $|u| = k$. Les sommets de l'arbre à hauteur paire sont appelés *sommets blancs*, et ceux à hauteur impaire *sommets noirs*. On note $\mathbf{t}_\circ$ et $\mathbf{t}_\bullet$ les ensembles correspondants. La *taille* de $\mathbf{t}$ est son nombre total de sommets $|\mathbf{t}|$.

Une manière d'énumérer les sommets d'un arbre plan $\mathbf{t}$ avec $|\mathbf{t}| = n + 1$ sommets est donnée par sa *suite de contour* $(v_0, \ldots, v_{2n})$. On l'obtient par récurrence comme suit : $v_0 = \emptyset$, et pour tout $i \in \{0, \ldots, 2n-1\}$, v_{i+1} est le premier enfant de v_i n'apparaissant pas dans $\{v_0, \ldots, v_i\}$, ou bien le parent de v_i si un tel sommet n'existe pas. On a $v_{2n} = \emptyset$, et on étend la liste sur $\mathbb{Z}_+$ par périodicité. La *fonction de contour* $C = C_{\mathbf{t}}$ de $\mathbf{t}$ est alors définie pour tout $i \in \{0, \ldots, 2n\}$ par $C(i) = |v_i|$.

1.1.2 La bijection Cori–Vauquelin–Schaeffer

Nous présentons maintenant la bijection Cori–Vauquelin–Schaeffer (CVS). Pour cela, on introduit une classe d'arbres munis d'étiquettes sur leurs sommets, appelés *arbres bien étiquetés*.

Définition 1.1.4. Un arbre bien étiqueté est une paire $(\mathbf{t}, \ell)$ formée d'un arbre plan $\mathbf{t}$ et d'une *fonction d'étiquettes* $\ell : \mathrm{V}(\mathbf{t}) \to \mathbb{Z}$ satisfaisant les propriétés suivantes :

- La racine a une étiquette nulle : $\ell(\emptyset) = 0$.
- Pour tous sommets $u, v \in \mathbf{t}$ reliés par une arête de $\mathbf{t}$, $|\ell(u) - \ell(v)| \leq 1$.

On note $\mathfrak{T}_n$ l'ensemble des arbres bien étiquetés à n arêtes. Soit $(\mathbf{t}, \ell) \in \mathfrak{T}_n$ et $(v_i : i \geq 0)$ la suite de contour de $\mathbf{t}$. Pour tout $i \geq 0$, le *successeur* de i est donné par

$$\mathrm{succ}(i) := \inf\{j > i : \ell(v_j) = \ell(v_i) - 1\}.$$

Soit $\varepsilon \in \{-1, 1\}$. La quadrangulation pointée $(\mathbf{q}, v_*) = \Phi_{\mathrm{CVS}}((\mathbf{t}, \ell), \varepsilon)$ est obtenue de la façon suivante. On commence par ajouter un sommet v_* dans l'unique face de $\mathbf{t}$, et on décide que $v_\infty = v_*$ (autrement dit, v_* reçoit l'étiquette $\min_{\mathrm{V}(t)} \ell - 1$). L'ensemble des sommets de $\mathbf{q}$ est $\mathrm{V}(\mathbf{t}) \cup \{v_*\}$, et les arêtes de $\mathbf{q}$ sont les $(v_i, v_{\mathrm{succ}(i)})$, pour $i \in \{0, \ldots, 2n-1\}$. Enfin, la racine de $\mathbf{q}$ est l'arête orientée $(v_0, v_{\mathrm{succ}(0)})$ si $\varepsilon = 1$, ou $(v_{\mathrm{succ}(0)}, v_0)$ si $\varepsilon = -1$. Un exemple se trouve dans la Figure 1.3.

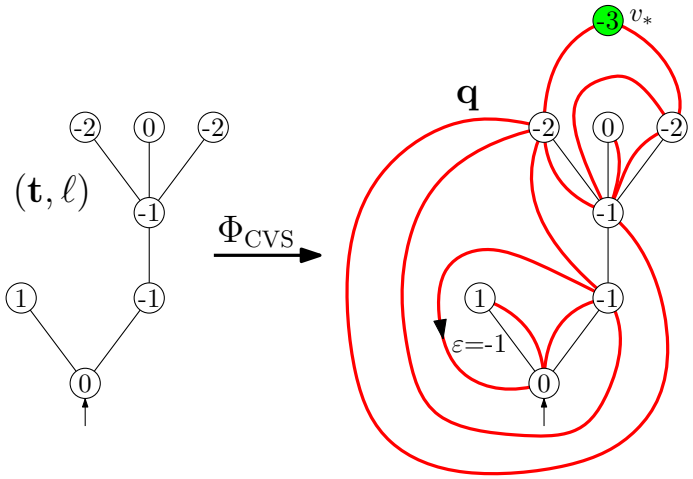

FIGURE 1.3 : La bijection Cori–Vauquelin–Schaeffer.

Il n'est pas clair *a priori* que l'objet obtenu soit une quadrangulation, ni même que l'on puisse plonger proprement $\mathbf{q}$ dans la sphère. Ces résultats font partie intégrante du théorème suivant.

Théorème 1.1.5. ([CS04, Théorème 4]) *Pour tout $n \geq 1$, l'application Φ_{CVS} est une bijection de $\mathfrak{T}_n \times \{-1, 1\}$ dans l'ensemble $\mathcal{M}_n^{\square,\bullet}$ des quadrangulations pointées à n faces.*

On déduit en particulier du Théorème 1.1.5 une preuve alternative de (1.1). La bijection Φ_{CVS} possède une propriété fondamentale, qui relie les étiquettes de l'arbre bien étiqueté $(\mathbf{t}, \ell)$ aux distances au sommet v_* dans la quadrangulation $\mathbf{q}$: si $d_{\mathrm{gr}}^{\mathbf{q}}$ désigne la distance de graphe dans $\mathbf{q}$, on a

$$d_{\mathrm{gr}}^{\mathbf{q}}(v, v_*) = \ell(v) - \min_{u \in \mathrm{V}(\mathbf{t})} \ell(u) + 1, \quad v \in \mathrm{V}(\mathbf{q}). \tag{1.2}$$

La bijection réciproque Φ_{CVS}^{-1} a également une forme explicite, voir [CV81, Sch98].

1.2 Limite d'échelle des quadrangulations uniformes

Les développements mathématiques récents autour des cartes sont motivés par des questions provenant de la physique théorique, plus précisément de la théorie de la

gravité quantique en dimension deux. Les cartes y sont utilisées comme modèle de surface discrète aléatoire, voir par exemple [AJD97]. La motivation générale est de comprendre les propriétés d'une surface, par exemple la sphère, dont la métrique aurait été choisie uniformément au hasard. Malheureusement, il est très difficile de définir une bonne notion de mesure "uniforme" sur l'ensemble des métriques Riemanniennes sur la sphère, qui est de dimension infinie. Un problème similaire apparaît si l'on cherche à définir un chemin aléatoire uniforme dans $\mathbb{R}^d$. Dans ce cas, le *mouvement brownien* est un candidat naturel, notamment parce qu'on peut l'obtenir à partir de chemins aléatoires uniformes sur $\mathbb{Z}^d$ convenablement renormalisés. C'est ce que l'on appelle une *limite d'échelle*. Cette observation suggère de construire une sphère aléatoire "uniforme" comme limite d'échelle de discrétisations de la sphère, les cartes planaires, choisies uniformément au hasard. Précisément, existe-t-il une limite d'échelle des triangulations uniformes de la sphère à n sommets lorsque n tend vers l'infini ? La question a été posée sous cette forme pour la première fois par Oded Schramm [Sch06].

1.2.1 La topologie de Gromov-Hausdorff

La premier obstacle soulevé par la stratégie précédente est celui du sens à donner à la convergence. L'idée est d'interpréter une carte comme un espace métrique en munissant l'ensemble de ses sommets de la distance de graphe. La topologie naturelle est alors celle de *Gromov-Hausdorff*. La distance de Gromov-Hausdorff entre deux espaces métriques compacts (E_1, d_1) et (E_2, d_2) est définie par

$$d_{\mathrm{GH}}(E_1, E_2) := \inf\{d_{\mathrm{H}}(\varphi_1(E_1), \varphi_2(E_2))\},$$

où l'infimum a lieu sur tous les espaces métriques (E, d) et tous les plongements isométriques $\varphi_1 : E_1 \to E$ et $\varphi_2 : E_2 \to E$ de E_1 et E_2 dans E. Ici, d_{H} désigne la distance de Hausdorff entre les ensembles compacts de E. Elle est définie pour tous sous-ensembles compacts K_1, K_2 de E par

$$d_{\mathrm{H}}(K_1, K_2) := \inf\{\varepsilon > 0 : K_1 \subseteq K_2^\varepsilon \text{ et } K_2 \subseteq K_1^\varepsilon\},$$

où K^ε est le ε-voisinage du compact K dans E : $K^\varepsilon := \{x \in E : d(x, K) \leq \varepsilon\}$.

L'application d_{GH} est une distance sur l'ensemble $\mathbb{K}$ des espaces métriques compacts, vus à isométrie près. Muni de cette distance, $\mathbb{K}$ est en fait un espace polonais (c'est-à-dire métrisable, séparable et complet). On renvoie le lecteur à [BBI01] pour davantage de détails sur cette topologie.

1.2.2 L'arbre continu brownien

La bijection CVS suggère d'utiliser dans un premier temps des quadrangulations comme discrétisations de la sphère. Soit donc Q_n une quadrangulation de la sphère à n faces uniforme, et v_* un sommet de Q_n choisi uniformément au hasard. Alors, (Q_n, v_*) est une quadrangulation pointée à n faces uniforme, c'est-à-dire tirée selon la mesure uniforme sur $\mathcal{M}_n^{\square,\bullet}$. En posant $(T_n, L_n) := \Phi_{\mathrm{CVS}}^{-1}((Q_n, v_*))$, on a donc que T_n est un arbre plan à n arêtes uniforme.

La première étape est d'étudier la limite d'échelle de l'arbre T_n lorsque n tend vers l'infini. En raison de sa distribution uniforme, la fonction de contour $C_n := C_{T_n}$ de l'arbre T_n est une marche aléatoire simple conditionnée à rester positive, et à revenir en zéro au temps $2n$. On étend C_n à $\mathbb{R}_+$ par interpolation affine (et la valeur zéro au-delà de $2n$). Par une version conditionnée du théorème de Donsker, on obtient la convergence en loi pour la topologie de la convergence uniforme

$$\left(\frac{C_n(2nt)}{\sqrt{2n}} : 0 \leq t \leq 1\right) \xrightarrow[n\to\infty]{(d)} (\mathbb{e}_t : 0 \leq t \leq 1)\,, \tag{1.3}$$

où $(\mathbb{e}_t : 0 \leq t \leq 1)$ est l'*excursion brownienne normalisée*. Pour obtenir une convergence de l'arbre T_n en tant qu'espace métrique, il est nécessaire d'introduire la notion de $\mathbb{R}$-arbre (voir [DLG05, LG05]). Soit g une fonction continue positive sur $[0,1]$, telle que $g(0) = g(1) = 0$ (une telle fonction est appelée *excursion normalisée*). On pose

$$d_g(s,t) := g(s) + g(t) - 2 \inf_{s\wedge t \leq r \leq s\vee t} g(r), \quad s,t \in [0,1],$$

et on introduit la relation d'équivalence $s \sim t$ si et seulement si $d_g(s,t) = 0$. Le $\mathbb{R}$-arbre codé par g est l'espace quotient $\mathscr{T}_g := [0,1]/\sim$ muni de la distance d_g. Intuitivement, il est obtenu en identifiant les points qui "se font face" sous le graphe de la fonction g. Le $\mathbb{R}$-arbre $(\mathscr{T}_{\mathbb{e}}, d_{\mathbb{e}})$ obtenu à partir de l'excursion brownienne normalisée est appelé *arbre continu brownien* (CRT en abrégé, pour *Continuum Random Tree*) et a été introduit par David Aldous [Ald91, Ald93]. À partir de la convergence (1.3), on obtient la convergence en loi au sens de Gromov-Hausdorff

$$\left(\mathrm{V}(T_n), \frac{1}{\sqrt{2n}} \cdot d_{\mathrm{gr}}^{T_n}\right) \xrightarrow[n\to\infty]{(d)} (\mathscr{T}_{\mathbb{e}}, d_{\mathbb{e}}). \tag{1.4}$$

1.2.3 La carte brownienne

L'objectif suivant est de comprendre la limite d'échelle de la fonction d'étiquettes L_n sur l'arbre uniforme T_n. Dans la suite, on note $L_n(i)$ l'étiquette du i-ème sommet de T_n dans l'ordre de contour (avec interpolation affine). Le résultat suivant a été obtenu dans un travail fondateur de Philippe Chassaing et Gilles Schaeffer [CS04].

Théorème 1.2.1. ([CS04, Théorème 5]) *On a la convergence en loi, pour la topologie de la convergence uniforme,*

$$\left(\frac{C_n(2nt)}{\sqrt{2n}}, \frac{L_n(2nt)}{\left(\frac{8n}{9}\right)^{1/4}} : 0 \leq t \leq 1\right) \xrightarrow[n\to\infty]{(d)} (\mathbb{e}_t, Z_t : 0 \leq t \leq 1)\,.$$

Le processus $(Z_t : 0 \leq t \leq 1)$ est appelé la *tête du serpent brownien*, et a été introduit par Jean-François Le Gall [LG99]. On peut l'interpréter comme un mouvement brownien le long des branches du $\mathbb{R}$-arbre $\mathscr{T}_{\mathbb{e}}$. Une conséquence importante de ce théorème est que le diamètre de la quadrangulation à n faces uniforme Q_n est d'ordre $n^{1/4}$. La conjecture de Schramm a finalement été démontrée indépendamment par Jean-François Le Gall [LG13] et Grégory Miermont [Mie13].

Théorème 1.2.2. ([LG13, Théorème 1.1], [Mie13, Théorème 1]) *Pour tout $n \geq 1$, soit Q_n une quadrangulation à n faces uniforme. Alors, on a la convergence en loi, au sens de Gromov-Hausdorff,*

$$\left(\mathrm{V}(Q_n), \left(\frac{9}{8n}\right)^{1/4} \cdot d_{\mathrm{gr}}^{Q_n}\right) \xrightarrow[n\to\infty]{(d)} (\mathbb{M}, D)\,.$$

L'espace métrique aléatoire compact $(\mathbb{M}, D)$ est appelé la *carte brownienne* (BM). L'existence d'une limite le long de sous-suites a d'abord été établie par Jean-François Le Gall [LG07] avant que l'unicité de la limite ne soit démontrée. Toutefois, certaines propriétés presque sûres étaient déjà établies pour toute sous-limite : la carte brownienne a dimension de Hausdorff 4 [LG07], et est homéomorphe à la sphère $\mathbb{S}^2$ [LGP08, Mie08]. Les plus courts chemins dans la carte brownienne, ou *géodésiques*, ont également été étudiés [LG10, AKM15]. La construction de la carte brownienne a été généralisée à des surfaces de genre arbitraire par Jérémie Bettinelli [Bet10, Bet12], et à des surfaces à bord par Jérémie Bettinelli et Grégory Miermont [Bet15, Bet16, BM15] qui ont en particulier étudié le *disque brownien* (BD_σ, où $\sigma > 0$ est le périmètre).

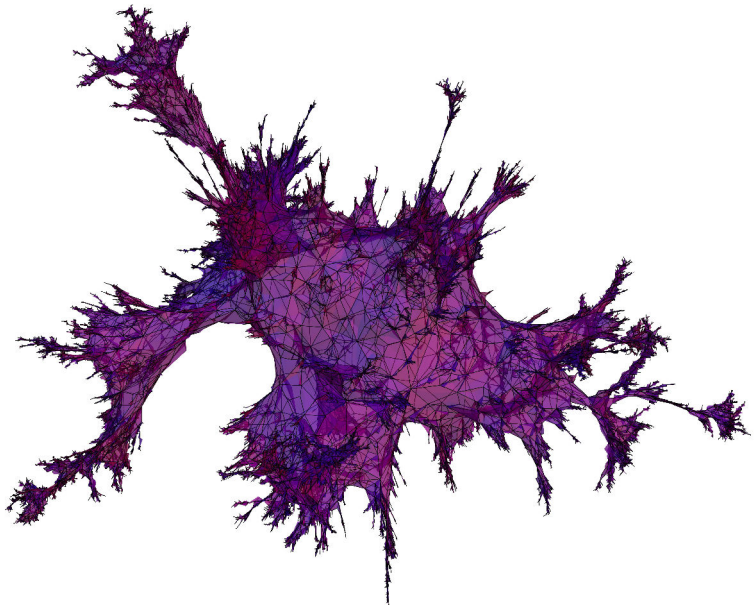

FIGURE 1.4 : Une quadrangulation à 50000 faces uniforme, par Jérémie Bettinelli.

Parallèlement au développement de la théorie des cartes aléatoires, une approche très différente de géométrie aléatoire sur la sphère a été introduite par Bertrand Duplantier et Scott Sheffield [DS11], sous le nom de *gravité quantique de Liouville*. Cette théorie s'appuie sur une approche développée en physique théorique par Aleksandr Polyakov [Pol81, KPZ88]. Les liens entre la carte brownienne et la gravité quantique de Liouville ont récemment été étudiés par Jason Miller et Scott Sheffield [MS15, MS16a, MS16b].

1.3 Limites d'échelle des cartes de Boltzmann

L'intuition derrière la construction de la carte brownienne est celle d'un objet analogue au mouvement brownien pour la sphère $\mathbb{S}^2$. Cette analogie amène deux questions naturelles. La carte brownienne possède-t-elle, comme le mouvement brownien, des propriétés d'*universalité* ? Peut-on obtenir d'autres limites d'échelle, jouant un rôle similaire à celui des *processus de Lévy* pour les marches aléatoires ? Une première forme d'universalité résulte du fait que la carte brownienne est la limite d'échelle des p-angulations uniformes, pour $p = 3$ ou $p \geq 4$ pair (voir [LG13]). La classe d'universalité de la carte brownienne est en fait bien plus large. Pour le comprendre, il est nécessaire d'introduire un modèle plus général que celui des cartes uniformes : les *cartes de Boltzmann*.

1.3.1 Limites d'échelle des arbres de Galton-Watson

Nous abordons d'abord la question de l'universalité des limites d'échelle d'arbres plans. Nous avons vu dans la Section 1.2.2 que la limite d'échelle des arbres plans uniformes est l'arbre continu brownien. Voyons comment ce résultat peut être généralisé. Un *arbre de Galton-Watson* est un arbre plan aléatoire dans lequel tous les sommets ont un nombre d'enfants indépendant et de même loi, appelée la *loi de reproduction*. Une loi de reproduction ρ est une mesure de probabilité sur $\mathbb{Z}_+$ telle que $\rho(1) < 1$, qui est dite *critique* si sa moyenne m_ρ est égale à 1, et *sous-critique* si $m_\rho < 1$.

Définition 1.3.1. Soit ρ une loi de reproduction critique ou sous-critique. La loi GW_ρ d'un arbre de Galton-Watson de loi de reproduction ρ est la mesure de probabilité sur $\mathcal{T}_f$ définie par

$$\mathsf{GW}_\rho(\mathbf{t}) = \prod_{u \in \mathbf{t}} \rho(k_u(\mathbf{t})), \quad \mathbf{t} \in \mathcal{T}_f.$$

Cette identité définit bien une mesure de probabilité sur $\mathcal{T}_f$, voir [LG05] pour plus de détails. Les arbres et processus de Galton-Watson ont d'abord été introduits par Irénée-Jules Bienaymé [Bie45], puis par Francis Galton et Henry William Watson [GW75] pour modéliser l'extinction des noms de famille nobles. Les arbres de Galton-Watson présentent le double intérêt d'avoir une *propriété de branchement* et de couvrir certaines mesures uniformes lorsqu'on les conditionne à avoir n sommets (par exemple la mesure uniforme sur les arbres plans à n sommets si ρ est la loi géométrique de paramètre $1/2$). Le résultat suivant est dû à David Aldous.

Théorème 1.3.2. ([Ald93]) *Soit ρ une loi de reproduction critique de variance $\sigma^2 \in (0, \infty)$. Pour tout $n \geq 1$, on suppose que $\mathsf{GW}_\rho(\{|\mathbf{t}| = n\}) > 0$ et on se donne T_n un arbre de loi GW_ρ conditionné à avoir n sommets. Alors, on a la convergence en loi, au sens de Gromov-Hausdorff,*

$$\left(\mathrm{V}(T_n), \frac{\sigma}{2\sqrt{n}} \cdot d_{\mathrm{gr}}^{T_n} \right) \xrightarrow[n\to\infty]{(d)} (\mathscr{T}_{\mathbb{e}}, d_{\mathbb{e}}) \,.$$

La classe d'universalité de l'arbre continu brownien s'étend donc à tous les arbres de Galton-Watson critiques conditionnés dont la loi de reproduction a une variance

finie. Néanmoins, il est possible d'obtenir d'autres limites en relâchant l'hypothèse de finitude de la variance. Une manière naturelle de procéder est de supposer la loi ρ dans le domaine d'attraction d'une loi stable de paramètre $\alpha \in (1,2)$:

$$\rho([k,\infty)) = \frac{\ell(k)}{k^\alpha}, \quad k \geq 1,$$

où ℓ est une fonction à variation lente à l'infini (i.e., $\ell(\lambda x)/\ell(x) \to 1$ quand $x \to \infty$ pour tout $\lambda > 0$) telle que $\ell(x) > 0$ pour x assez grand. Dans ce cadre, l'analogue du Théorème 1.3.2 a été obtenu par Thomas Duquesne.

Théorème 1.3.3. ([Duq03, Théorème 3.1], [Kor13, Théorème 3]) *Soit ρ une loi de reproduction critique dans le bassin d'attraction d'une loi stable de paramètre $\alpha \in (1,2)$. Pour tout $n \geq 1$, on suppose que $\mathsf{GW}_\rho(\{|\mathbf{t}| = n\}) > 0$ et on se donne T_n un arbre de loi GW_ρ conditionné à avoir n sommets. Alors, il existe une fonction à variation lente à l'infini L telle que l'on ait la convergence en loi, au sens de Gromov-Hausdorff,*

$$\left(\mathrm{V}(T_n), \frac{L(n)}{n^{1-1/\alpha}} \cdot d_{\mathrm{gr}}^{T_n}\right) \xrightarrow[n\to\infty]{(d)} (\mathscr{T}_\alpha, d_\alpha)\,.$$

L'espace métrique $(\mathscr{T}_\alpha, d_\alpha)$ est un $\mathbb{R}$-arbre, appelé l'*arbre stable* de paramètre α. Il est associé à l'excursion normalisée du *processus des hauteurs*. Ce processus a été introduit (dans une généralité bien plus grande) par Thomas Duquesne et Jean-François Le Gall [DLG02], en se basant sur des travaux de Jean-François Le Gall et Yves Le Jan [LGLJ98]. Nous ne donnons pas sa définition ici, qui est obtenue à partir d'un *processus de Lévy stable spectralement positif* de même paramètre α. L'arbre stable a été introduit plus tard par Thomas Duquesne et Jean-François Le Gall [DLG05]. Il possède des propriétés très différentes de l'arbre continu brownien. En particulier, la queue lourde de la loi de reproduction ρ provoque l'apparition de points de branchement de degré infini dans le $\mathbb{R}$-arbre limite, alors que presque sûrement, le CRT est un arbre binaire. Notons que cette construction peut être étendue à une large classe de processus de Lévy, voir [DLG02, DLG05].

1.3.2 La bijection Bouttier–Di Francesco–Guitter

L'étude de cartes plus générales que les quadrangulations nécessite d'introduire la bijection Bouttier–Di Francesco–Guitter (BDG). Elle partage certaines similarités avec la bijection CVS, mais elle est remarquablement plus générale : elle s'applique à toute carte, sans restriction sur le degré des faces. Sa présentation est plus délicate car elle fait intervenir des arbres dont les sommets sont de quatre types différents. Néanmoins, dans le cas particulier des cartes biparties, le nombre de types de sommets est réduit à deux ce qui rend la bijection plus simple à manipuler. C'est l'une des raisons pour lesquelles les modèles de cartes biparties sont privilégiés, et nous présentons maintenant la bijection dans ce cadre.

Commençons par quelques généralités sur les cartes biparties. Rappelons que $\mathcal{B}_f$ désigne l'ensemble des cartes biparties, et notons $\mathcal{B}_f^\bullet$ l'ensemble des cartes biparties pointées. Du fait de son caractère biparti, toute carte $\mathbf{m} \in \mathcal{B}_f^\bullet$ avec racine $e_* = (e_-, e_+)$

et sommet distingué v_* satisfait l'identité $|d_{\mathrm{gr}}^{\mathbf{m}}(e_+, v_*) - d_{\mathrm{gr}}^{\mathbf{m}}(e_-, v_*)| = 1$, où $d_{\mathrm{gr}}^{\mathbf{m}}$ est la distance de graphe dans $\mathbf{m}$. On dit que $(\mathbf{m}, v_*)$ est *positive* si $d_{\mathrm{gr}}^{\mathbf{m}}(e_+, v_*) = d_{\mathrm{gr}}^{\mathbf{m}}(e_-, v_*) + 1$, et *négative* sinon. Les ensembles correspondants sont notés $\mathcal{B}_+^\bullet$ et $\mathcal{B}_-^\bullet$. Par convention, la carte avec un seul sommet, notée †, appartient à $\mathcal{B}_+^\bullet$. Il existe une bijection simple entre $\mathcal{B}_+^\bullet \backslash \{\dagger\}$ et $\mathcal{B}_-^\bullet$, consistant à renverser l'orientation de la racine.

Définition et propriétés. La bijection BDG repose sur une classe d'arbres étiquetés à deux types, appelés *mobiles*.

Définition 1.3.4. Un mobile est une paire $\theta = (\mathbf{t}, \ell)$ formée d'un arbre plan $\mathbf{t}$ et d'une fonction d'étiquettes sur les sommets à hauteur paire $\ell : \mathrm{V}(\mathbf{t}_\circ) \to \mathbb{Z}$ satisfaisant les propriétés suivantes :

- La racine a une étiquette nulle : $\ell(\emptyset) = 0$.
- Pour chaque sommet $u \in \mathbf{t}_\bullet$, si $u0 = u(k_u(\mathbf{t}) + 1)$ désigne le parent $\widehat{u}$ de u, alors pour tout $1 \le i \le k_u(\mathbf{t}) + 1$, on a $\ell(ui) \ge \ell(u(i-1)) - 1$. Autrement dit, dans le sens horaire autour de u, les étiquettes décroissent au plus de un.

L'ensemble des mobiles est noté Θ. Soit $\theta = (\mathbf{t}, \ell)$ un mobile avec $|\mathbf{t}| = n + 1$ sommets. On note $(v_0^\circ, \dots, v_n^\circ)$ la suite de contour des sommets à hauteur paire dans $\mathbf{t}$. Autrement dit, pour tout $i \in \{0, \dots, n\}$, $v_i^\circ = v_{2i}$ où $(v_0, \dots, v_{2n})$ est la suite de contour de $\mathbf{t}$. Comme précédemment, cette suite est étendue à $\mathbb{Z}_+$ par périodicité, et pour tout $i \ge 0$, on définit le successeur de i par $\mathrm{succ}^\circ(i) := \inf\{j > i : \ell(v_j^\circ) = \ell(v_i^\circ) - 1\}$.

La carte bipartie positive pointée $(\mathbf{m}, v_*) = \Phi_{\mathrm{BDG}}(\theta)$ est obtenue comme suit. D'abord, si $\mathbf{t} = \{\emptyset\}$, on pose $\mathbf{m} = \dagger$. Sinon, on ajoute un sommet v_* dans l'unique face de $\mathbf{t}$, et on pose $v_\infty^\circ = v_*$. Alors, $\mathbf{m}$ est la carte dont l'ensemble des sommets est $\mathrm{V}(\mathbf{t}_\circ) \cup \{v_*\}$, et dont les arêtes sont les $(v_i^\circ, v_{\mathrm{succ}^\circ(i)}^\circ)$ pour $i \in \{0, 1, \dots, n-1\}$. L'arête racine de $\mathbf{m}$ est l'arête orientée $(v_{\mathrm{succ}^\circ(0)}^\circ, v_0^\circ)$. Voir la Figure 1.5 pour un exemple.

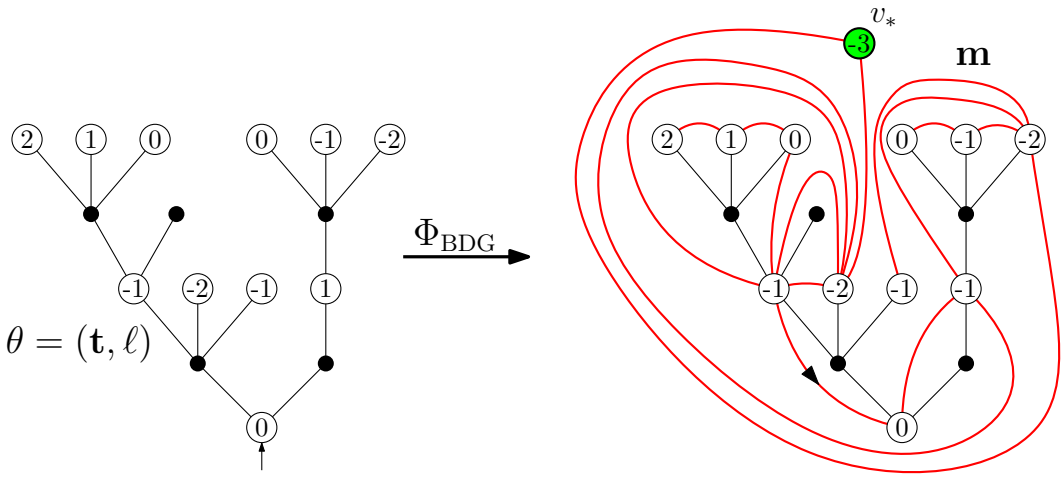

FIGURE 1.5 : La bijection Bouttier–Di Francesco–Guitter.

Théorème 1.3.5. ([BDFG04]) *L'application Φ_{BDG} est une bijection de l'ensemble des mobiles Θ (à n arêtes) dans l'ensemble $\mathcal{B}_+^\bullet$ des cartes biparties positives pointées (à n arêtes).*

La bijection Φ_{BDG} possède également des propriétés remarquables. D'abord, elle satisfait une formule analogue à (1.2) concernant les distances dans la carte. De plus, chaque face f de la carte $\mathbf{m}$ contient exactement un sommet à hauteur impaire $u \in \mathbf{t}_\bullet$, et on a alors $\deg(f) = 2(k_u(\mathbf{t}) + 1)$.

À partir de cette bijection, on peut établir des variantes pour les cartes à bord en prescrivant le degré d'une face. Le cas des quadrangulations à bord sera évoqué dans la Section 4.4.2. Notons pour conclure que cette bijection a été généralisée aux cartes de genre supérieur [CMS07, Mie09] et même à des cartes sur des surfaces non orientables [CD17].

La bijection Janson–Stefánsson. La bijection BDG fait intervenir des arbres plans aléatoires dont les sommets à hauteur paire et impaire jouent un rôle différent. On appelle un tel arbre *arbre à deux types alternés*. L'analyse de ces arbres est considérablement simplifiée si on leur applique une bijection entre arbres plans, due à Svante Janson et Sigurður Örn Stefánsson [JS15, Section 3].

Décrivons brièvement cette bijection, notée Φ_{JS}. D'abord, l'image de l'arbre à un seul sommet $\{\emptyset\}$ est $\{\emptyset\}$ lui-même. Soit donc $\mathbf{t} \in \mathcal{T}_f \backslash \{\emptyset\}$. L'arbre $\Phi_{\text{JS}}(\mathbf{t})$ a les mêmes sommets que $\mathbf{t}$, mais ses arêtes sont différentes et obtenues comme suit. Pour tout sommet blanc $u \in \mathbf{t}_\circ$, on note $u0 = \widehat{u}$ le parent de u (si $u \neq \emptyset$) et $u(k_u(\mathbf{t})+1)$ le sommet u lui-même. Pour tout $j \in \{0, 1, \dots, k_u(\mathbf{t})\}$, on ajoute alors l'arête $(uj, u(j+1))$ à $\Phi_{\text{JS}}(\mathbf{t})$. Si u est une feuille, ceci revient simplement à ajouter une arête entre u et son parent. Le sommet 1 de $\mathbf{t}$ est le sommet racine de $\Phi_{\text{JS}}(\mathbf{t})$, et son premier enfant dans $\Phi_{\text{JS}}(\mathbf{t})$ est choisi selon l'ordre lexicographique de $\mathbf{t}$. Un exemple est proposé dans la Figure 1.6.

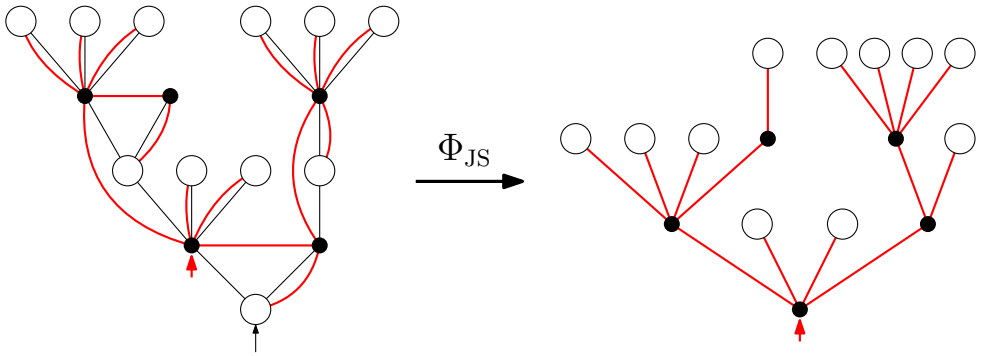

FIGURE 1.6 : La bijection Janson–Stefánsson.

Théorème 1.3.6. ([JS15, Section 3]) *Pour tout $n \geq 1$, l'application Φ_{JS} est une bijection de l'ensemble des arbres plans (à n sommets) dans lui-même.*

La propriété fondamentale de cette bijection est la suivante : chaque sommet de $\mathbf{t}_\circ$ est envoyé sur une feuille de $\Phi_{\text{JS}}(\mathbf{t})$, et chaque sommet de $\mathbf{t}_\bullet$ ayant $k \geq 0$ enfants est envoyé sur un sommet (interne) de $\Phi_{\text{JS}}(\mathbf{t})$ ayant $k+1$ enfants. Autrement dit, la bijection sépare les sommets blancs et noirs en feuilles et sommets internes.

Dans la suite, nous allons nous intéresser à une généralisation des arbres de Galton-Watson aux arbres à deux types alternés. Soit $(\rho_\circ, \rho_\bullet)$ un couple de lois de

reproduction, de moyennes respectives $m_{\rho_\circ}$ et $m_{\rho_\bullet}$. On dit que le couple $(\rho_\circ, \rho_\bullet)$ est *critique* si $m_{\rho_\circ} m_{\rho_\bullet} = 1$, et *sous-critique* si $m_{\rho_\circ} m_{\rho_\bullet} < 1$. Un *arbre de Galton-Watson à deux types alternés* de lois de reproduction $(\rho_\circ, \rho_\bullet)$ est un arbre aléatoire dans lequel chaque sommet a un nombre d'enfants distribué selon $\rho_\circ$ si sa hauteur est paire et selon $\rho_\bullet$ si sa hauteur est impaire, indépendamment de tous les autres sommets.

Définition 1.3.7. Soit $(\rho_\circ, \rho_\bullet)$ un couple de mesures de probabilités sur $\mathbb{Z}_+$, critique ou sous-critique. La loi $\mathsf{GW}_{\rho_\circ,\rho_\bullet}$ d'un arbre de Galton-Watson à deux types alternés de lois de reproduction $(\rho_\circ, \rho_\bullet)$ est la mesure de probabilité sur $\mathcal{T}_f$ définie par

$$\mathsf{GW}_{\rho_\circ,\rho_\bullet}(\mathbf{t}) = \prod_{u \in \mathbf{t}_\circ} \rho_\circ(k_u) \prod_{u \in \mathbf{t}_\bullet} \rho_\bullet(k_u), \quad \mathbf{t} \in \mathcal{T}_f.$$

La bijection Φ_{JS} simplifie beaucoup l'étude des arbres de Galton-Watson à deux types alternés grâce au résultat suivant (voir aussi [CK14a, Proposition 3.6]).

Proposition 1.3.8. [JS15, Appendice A] *Soit $(\rho_\circ, \rho_\bullet)$ un couple de lois de reproduction critique ou sous-critique, tel que $\rho_\circ$ soit la loi géométrique de paramètre $1-p \in (0,1)$: $\rho_\circ(k) = (1-p)p^k$ pour tout $k \geq 0$. Alors, la mesure image de $\mathsf{GW}_{\rho_\circ,\rho_\bullet}$ par Φ_{JS} est GW_ρ, où ρ est définie par*

$$\rho(0) = 1 - p \quad \textit{et} \quad \rho(k) = p \cdot \rho_\bullet(k-1), \quad k \in \mathbb{N}.$$

1.3.3 Mesures de Boltzmann

Dans la Section 1.3.1, nous avons défini les mesures de Galton-Watson en attribuant un poids à chaque sommet d'un arbre selon son degré. Les mesures de Boltzmann sont obtenues de manière similaire, en assignant un poids local à chaque face d'une carte selon son degré. Étant donnée une *suite de poids* $\mathsf{q} = (q_k : k \in \mathbb{N})$ de nombres réels positifs, le *poids de Boltzmann* d'une carte bipartie $\mathbf{m} \in \mathcal{B}_f$ est défini par

$$w_{\mathsf{q}}(\mathbf{m}) := \prod_{f \in \mathrm{F}(\mathbf{m})} q_{\deg(f)/2}. \tag{1.5}$$

On adopte la convention $w_{\mathsf{q}}(\dagger) = 1$. Ce poids définit une mesure σ-finie sur l'ensemble $\mathcal{B}_+^\bullet$ des cartes biparties positives pointées, dont la masse totale (ou *fonction de partition*) s'écrit

$$Z_{\mathsf{q}} := w_{\mathsf{q}}\left(\mathcal{B}_+^\bullet\right) \in [1, \infty]. \tag{1.6}$$

Naturellement, une suite de poids q est dite *admissible* si $Z_{\mathsf{q}} < \infty$. Dans ce cas, la distribution de Boltzmann $\mathbb{P}_{\mathsf{q}}^\bullet$ sur $\mathcal{B}_+^\bullet$ associée à q est définie par

$$\mathbb{P}_{\mathsf{q}}^\bullet(\mathbf{m}) := \frac{w_{\mathsf{q}}(\mathbf{m})}{Z_{\mathsf{q}}}, \quad \mathbf{m} \in \mathcal{B}_+^\bullet.$$

Puisque les ensembles $\mathcal{B}_+^\bullet \setminus \{\dagger\}$ et $\mathcal{B}_-^\bullet$ sont en bijection, q est admissible si et seulement si $w_{\mathsf{q}}(\mathcal{B}_f^\bullet) < \infty$. On peut alors définir une mesure $\mathbb{P}_{\mathsf{q}}$ sur l'ensemble $\mathcal{B}_f$ des cartes biparties par

$$\mathbb{P}_{\mathsf{q}}(\mathbf{m}) := \frac{w_{\mathsf{q}}(\mathbf{m})}{w_{\mathsf{q}}(\mathcal{B}_f)}, \quad \mathbf{m} \in \mathcal{B}_f.$$

La fonction suivante, introduite par Jean-François Marckert et Grégory Miermont dans [MM07], joue un rôle particulier dans l'analyse de la mesure $\mathbb{P}_{\mathsf{q}}^{\bullet}$:

$$f_{\mathsf{q}}(x) := \sum_{k=1}^{\infty} \binom{2k-1}{k-1} q_k x^{k-1}, \quad x \geq 0. \tag{1.7}$$

On note R_{q} le rayon de convergence de f_{q}. Remarquons que les quantités $f_{\mathsf{q}}(R_{\mathsf{q}})$, $f'_{\mathsf{q}}(R_{\mathsf{q}})$ et $f''_{\mathsf{q}}(R_{\mathsf{q}})$ sont bien définies dans $[0,\infty]$. La fonction f_{q} décrit l'admissibilité de la suite de poids q via le résultat suivant.

Proposition 1.3.9. [MM07, Proposition 1] *La suite de poids* q *est admissible si et seulement si l'équation*

$$f_{\mathsf{q}}(x) = 1 - \frac{1}{x}, \quad x > 0, \tag{1.8}$$

admet une solution. Dans ce cas, la plus petite solution est Z_{q} *et* $Z_{\mathsf{q}}^2 f'_{\mathsf{q}}(Z_{\mathsf{q}}) \leq 1$.

La fonction f_{q} étant infinie sur $(R_{\mathsf{q}},\infty]$ et $x \mapsto 1 - 1/x$ négative sur $(0,1]$, Z_{q} (de même que toute solution de (1.8)) appartient à $(1, R_{\mathsf{q}}]$. Les définitions suivantes ont d'abord été introduites dans [MM07], puis généralisées dans [BBG12c].

Définition 1.3.10. Une suite de poids admissible q est dite *critique* si $Z_{\mathsf{q}}^2 f'_{\mathsf{q}}(Z_{\mathsf{q}}) = 1$, et *sous-critique* sinon. Une suite de poids critique est dite *régulière critique* si $Z_{\mathsf{q}} < R_{\mathsf{q}}$, *générique critique* si $f''_{\mathsf{q}}(Z_{\mathsf{q}}) < \infty$, et *non générique critique* si $f''_{\mathsf{q}}(Z_{\mathsf{q}}) = \infty$.

Puisque la fonction f_{q} est de classe C^∞ sur $(0, R_{\mathsf{q}})$, toute suite de poids régulière critique est également générique critique.

Criticité, généricité et régularité. Pour toute carte $\mathbf{m} \in \mathcal{B}_+^{\bullet}$, on note $\Pi(\mathbf{m})$ l'arbre plan donné par la première coordonnée de $\Phi_{\mathrm{BDG}}^{-1}(\mathbf{m})$. On s'intéresse maintenant à la loi de cet arbre sous $\mathbb{P}_{\mathsf{q}}^{\bullet}$. Dans la suite, M désigne l'application identité sur $\mathcal{B}_+^{\bullet}$.

Proposition 1.3.11. ([MM07, Proposition 7]) *Soit* q *une suite de poids admissible. Sous* $\mathbb{P}_{\mathsf{q}}^{\bullet}$*, l'arbre plan* $\Pi(M)$ *est un arbre de Galton-Watson à deux types alternés de lois de reproduction* $(\mu_\circ, \mu_\bullet)$ *définies par*

$$\mu_\circ(k) = \frac{f_{\mathsf{q}}(Z_{\mathsf{q}})^k}{Z_{\mathsf{q}}} \quad \textit{et} \quad \mu_\bullet(k) = \frac{Z_{\mathsf{q}}^k \binom{2k+1}{k} q_{k+1}}{f_{\mathsf{q}}(Z_{\mathsf{q}})}, \qquad k \in \mathbb{Z}_+.$$

De plus, le couple $(\mu_\circ, \mu_\bullet)$ *est critique ou sous-critique, au sens où* $m_{\mu_\circ} m_{\mu_\bullet} \leq 1$.

On applique maintenant la bijection Φ_{JS} à $\Pi(\mathbf{m})$. L'arbre plan ainsi obtenu est noté $\Phi(\mathbf{m}) := \Phi_{\mathrm{JS}}(\Pi(\mathbf{m}))$. Par la Proposition 1.3.8, on obtient le résultat suivant.

Lemma 1.3.12. *Soit* q *une suite de poids admissible. Sous* $\mathbb{P}_{\mathsf{q}}^{\bullet}$*, l'arbre plan* $\Phi(M)$ *est un arbre de Galton-Watson de loi de reproduction* μ *définie par*

$$\mu(0) = 1 - f_{\mathsf{q}}(Z_{\mathsf{q}}) \quad \textit{et} \quad \mu(k) = Z_{\mathsf{q}}^{k-1} \binom{2k-1}{k-1} q_k, \quad k \in \mathbb{N}.$$

Les notions de criticité, généricité et régularité peuvent maintenant être interprétées en termes de la mesure de probabilité μ. D'abord, la moyenne m_μ de μ vérifie

$$m_\mu = 1 - \frac{1 - Z_{\mathsf{q}}^2 f'_{\mathsf{q}}(Z_{\mathsf{q}})}{Z_{\mathsf{q}}}, \tag{1.9}$$

et lorsque $m_\mu = 1$, sa variance σ_μ^2 vaut

$$\sigma_\mu^2 = Z_{\mathsf{q}}^2 f''_{\mathsf{q}}(Z_{\mathsf{q}}) + \frac{2}{Z_{\mathsf{q}}}. \tag{1.10}$$

La Définition 1.3.10 peut ainsi être reformulée de la façon suivante.

Proposition 1.3.13. *Une suite de poids* q *est critique si et seulement si* μ *est critique. Une suite de poids critique* q *est régulière critique si et seulement si* μ *a des moments exponentiels, et générique critique (respectivement non générique critique) si et seulement si* μ *a variance finie (respectivement infinie).*

Remarque 1.3.14. Nous pouvons finalement décrire les notions de la Définition 1.3.10 en termes de la mesure $\mathbb{P}_{\mathsf{q}}^\bullet$. Par la formule d'Euler et les propriétés de la bijection BDG, on a que $\#\mathrm{E}(\mathbf{m}) = |\mathbf{t}| - 1$ dès que $\Phi(\mathbf{m}) = \mathbf{t}$. Soient ξ la loi de $|\Phi(M)|$ sous $\mathbb{P}_{\mathsf{q}}^\bullet$, et G_μ (respectivement G_ξ) la fonction génératrice de μ (respectivement ξ). Alors,

$$G_\xi(s) = sG_\mu(G_\xi(s)), \quad s \in [0,1], \quad \text{et} \quad \mathbb{E}_{\mathsf{q}}^\bullet(|\Phi(M)|) = \frac{1}{1 - m_\mu}.$$

Ainsi, le nombre moyen d'arêtes $\mathbb{E}_{\mathsf{q}}^\bullet(\#\mathrm{E}(M))$ est infini si et seulement si q est critique.

À nouveau par les propriétés de la bijection BDG, la loi de reproduction $\mu_\bullet$ des sommets à hauteur impaire de $\Pi(M)$ est la loi du demi-degré d'une face typique de M sous $\mathbb{P}_{\mathsf{q}}^\bullet$. Donc, une suite critique q est régulière critique (respectivement générique critique) si et seulement si le degré d'une face typique de M a des moments exponentiels (respectivement variance finie).

1.3.4 Limites d'échelle des cartes de Boltzmann

Le but de cette section est de décrire les limites d'échelle de certaines cartes de Boltzmann. Pour cela, on s'intéresse à des cartes de Boltzmann de loi $\mathbb{P}_{\mathsf{q}}$ conditionnées à avoir n faces. Autrement dit, pour toute suite admissible q, on définit la mesure de Boltzmann $\mathbb{P}_{\mathsf{q},n}$ sur l'ensemble $\mathcal{B}_n$ des cartes biparties à n faces par

$$\mathbb{P}_{\mathsf{q},n}(\mathbf{m}) := \frac{\mathbf{1}_{\{\mathbf{m} \in \mathcal{B}_n\}} w_{\mathsf{q}}(\mathbf{m})}{w_{\mathsf{q}}(\mathcal{B}_n)}, \quad \mathbf{m} \in \mathcal{B}_f,\ n \in \mathbb{N}. \tag{1.11}$$

L'universalité de la carte brownienne est démontrée par le théorème suivant, dû à Jean-François Le Gall.

Théorème 1.3.15. ([LG13, Théorème 9.1]) *Soit* q *une suite de poids régulière critique, et pour tout* $n \geq 1$, M_n *une carte bipartie de loi* $\mathbb{P}_{\mathsf{q},n}$. *Il existe une constante* $c_{\mathsf{q}} > 0$ *telle qu'on ait la convergence en loi, au sens de Gromov-Hausdorff,*

$$\left(\mathrm{V}(M_n), \frac{c_{\mathsf{q}}}{n^{1/4}} \cdot d_{\mathrm{gr}}^{M_n}\right) \xrightarrow[n\to\infty]{(d)} (\mathbb{M}, D)\,.$$

Ce résultat est un analogue du Théorème 1.3.2, dans lequel les cartes de Boltzmann jouent le rôle des arbres de Galton-Watson. Il généralise notamment le Théorème 1.2.2 : si q est une suite admissible de la forme $q_k = g\delta_p(k)$, la carte M_n est uniforme parmi les $2p$-angulations à n faces. Le Théorème 1.3.15 a été généralisé par Cyril Marzouk [Mar16] aux suites de poids génériques critiques. La classe d'universalité de la carte brownienne est donc déterminée par une hypothèse de second moment, comme celle de l'arbre continu brownien. D'autres résultats de convergence vers la carte brownienne, y compris pour des modèles de cartes non biparties, ont été établis dans [Mie06, MW08, BLG13, ABA13, BJM14, Abr16].

L'analogie entre cartes de Boltzmann et arbres de Galton-Watson suggère l'étude de suites de poids non génériques critiques pour lesquelles la mesure de probabilité μ est dans le bassin d'attraction d'une loi stable. On peut alors espérer obtenir un objet très différent de la carte brownienne à la limite, comme c'est le cas pour les arbres.

Definition 1.3.16. Une suite de poids q est dite *non générique critique* de paramètre $\alpha \in (1,2)$ si q est critique et si la loi de reproduction μ est dans le domaine d'attraction d'une loi stable de paramètre α : il existe une fonction à variation lente à l'infini ℓ telle que

$$\mu([k,\infty)) = \frac{\ell(k)}{k^\alpha}.$$

Cette définition est plus générale que celle introduite dans [LGM11a], qui implique que la fonction ℓ est asymptotiquement constante (voir [LGM11a, Equation (13)]). Les cartes de Boltzmann avec suite de poids q non générique critique de paramètre α sont dites *à grandes faces* parce que la loi du degré d'une face typique est à queue lourde. Le résultat majeur concernant leur limite d'échelle est dû à Jean-François Le Gall et Grégory Miermont [LGM11a].

Théorème 1.3.17. ([LGM11a, Théorème 5]) *Soit* q *une suite de poids non générique critique de paramètre* $\alpha \in (1,2)$*, et pour tout* $n \geq 1$*,* M_n *une carte bipartie de loi* $\mathbb{P}_{\mathsf{q},n}$*. De toute suite strictement croissante d'entiers, on peut extraire une sous-suite le long de laquelle on ait la convergence en loi, au sens de Gromov-Hausdorff,*

$$\left(\mathrm{V}(M_n), \frac{1}{n^{1/2\alpha}} \cdot d_{\mathrm{gr}}^{M_n}\right) \xrightarrow[n\to\infty]{(d)} (\mathbb{M}_\alpha, D_\alpha)\,.$$

Dans ce résultat, la limite $(\mathbb{M}_\alpha, D_\alpha)$ dépend a priori de la sous-suite considérée. Comme pour la carte brownienne, il est conjecturé que cette limite est unique. Le candidat naturel est un espace métrique aléatoire compact qui est appelée la *carte stable* de paramètre α, également introduit dans [LGM11a]. La dimension de Hausdorff de cet espace, et de toute sous-limite, est presque sûrement égale à 2α [LGM11a, Théorème 5]. Peu de résultats sont connus à propos de la carte stable, bien que son dual ait été étudié dans [BC16, BBCK16]. Sa géométrie est supposée être très différente de celle de la carte brownienne, et fait l'objet du Chapitre 5. Comme nous le verrons, l'étude des cartes de Boltzmann et de la carte stable est également motivée par leur lien avec les modèles de physique statistique sur les cartes, notamment les modèles de boucles $O(n)$, mis en évidence par des travaux de Gaëtan Borot, Jérémie Bouttier et Emmanuel Guitter [BBG12c, BBG12b, BBG12a].

1.4 Limites locales de cartes aléatoires

Jusqu'à présent, nous nous sommes intéressés à des limites d'échelle de grandes cartes aléatoires. Autrement dit, nous avons renormalisé les distances dans ces cartes par leur taille typique de sorte à obtenir à la limite des espaces métriques aléatoires compacts. Une autre approche consiste à étudier des limites de grandes cartes aléatoires sans changement d'échelle. On obtient alors des cartes aléatoires infinies qui constituent l'un des objets d'étude principaux de cette thèse.

1.4.1 La topologie locale

La construction de cartes aléatoires infinies requiert l'introduction d'une topologie sur l'ensemble des cartes, appelée *topologie locale*. Elle a d'abord été introduite par Itai Benjamini et Oded Schramm dans [BS01]. Nous allons utiliser une définition légèrement différente due à Omer Angel et Oded Schramm [AS03].

Commençons par introduire quelques notations. Pour tout $R \geq 0$ et toute carte $\mathbf{m} \in \mathcal{M}_f$, on note $\mathbf{B}_R(\mathbf{m})$ la boule de rayon R dans $\mathbf{m}$ autour de l'origine, pour la distance de graphe. Autrement dit, $\mathbf{B}_0(\mathbf{m})$ est le sommet origine de $\mathbf{m}$, et pour tout $R \geq 1$, $\mathbf{B}_R(\mathbf{m})$ est la carte formée par tous les sommets de $\mathbf{m}$ à distance de graphe inférieure ou égale à R de l'origine, ainsi que toutes les arêtes reliant ces sommets.

La topologie locale est métrisée par la *distance locale* d_{loc}, définie par

$$d_{\text{loc}}(\mathbf{m}, \mathbf{m}') := (1 + \sup\{R \geq 0 : \mathbf{B}_R(\mathbf{m}) = \mathbf{B}_R(\mathbf{m}')\})^{-1}, \quad \mathbf{m}, \mathbf{m}' \in \mathcal{M}_f. \tag{1.12}$$

On peut effectivement montrer que d_{loc} est une distance sur $\mathcal{M}_f$, et que le complété $\mathcal{M}$ de l'espace métrique $(\mathcal{M}_f, d_{\text{loc}})$ est polonais (voir par exemple [Cur16a]). Intuitivement, deux cartes sont proches au sens de la distance locale si elles ont la même boule de rayon R autour de leur racine, pour R très grand.

Les éléments de $\mathcal{M}_\infty := \mathcal{M} \backslash \mathcal{M}_f$ sont appelés des *cartes planaires infinies*, et sont représentés par une suite $(\mathbf{m}_R : R \geq 0)$ d'éléments de $\mathcal{M}_f$ *cohérente*, au sens où $\mathbf{B}_R(\mathbf{m}_{R+1}) = \mathbf{m}_R$ pour tout $R \geq 0$. Néanmoins, une carte planaire infinie avec un seul bout (en tant que graphe) peut être vue comme une classe d'équivalence (à homéomorphisme préservant l'orientation près) de plongements propres de graphes infinis dans le plan $\mathbb{R}^2$, de sorte que tout compact de $\mathbb{R}^2$ n'intersecte qu'un nombre fini d'arêtes (voir [CMM13, Appendice] et [Cur16a, Proposition 2] pour plus de détails). Dans la suite, toutes les cartes infinies que nous considérons ont un seul bout (ou un plongement canonique dans le plan), de sorte que tout élément de $\mathcal{M}_\infty$ peut être vu comme une telle classe d'équivalence. Le bord $\partial\mathbf{m}$ d'une carte infinie $\mathbf{m} \in \mathcal{M}_\infty$ est alors formé par l'ensemble des arêtes et sommets incidents à la face externe (à droite de la racine). Le bord est infini lorsque la face externe a degré infini, et dans ce cas, il est dit *simple* s'il est isomorphe à $\mathbb{Z}$ en tant que graphe.

Une carte infinie avec un seul bout a au plus une face de degré infini. Lorsque toutes ses faces sont finies, elle décompose le plan $\mathbb{R}^2$ en une collection de domaines simplement connexes bornés et on parle d'une carte infinie *du plan*. Si au contraire elle possède un bord simple infini, elle décompose le demi-plan supérieur $\mathbb{H}$ en une

telle collection et on parle d'une carte infinie *du demi-plan* (à bord simple). Par abus de langage, une carte infinie ayant un seul bout et un bord infini est parfois également appelée carte infinie du demi-plan (à bord quelconque ou *général*). Les définitions de p-angulation et de carte bipartie (à bord) s'étendent également aux cartes infinies.

Dans la suite, on s'intéressera notamment à l'ensemble $\mathcal{T}_{\text{loc}}$ des arbres plans *localement finis*, qui sont les limites locales d'arbres plans. Ils sont également obtenus en étendant la Définition 1.1.3 aux arbres avec une infinité de sommets (de degré fini).

1.4.2 Cartes uniformes infinies du plan

Le premier résultat de convergence locale de cartes aléatoires est dû à Omer Angel et Oded Schramm [AS03].

Théorème 1.4.1. ([AS03, Théorème 1.8]) *Pour tout $n \geq 1$, soit $\mathbb{P}_n^{\triangle}$ la mesure uniforme sur l'ensemble $\mathcal{M}_n^{\triangle}$ des triangulations sans boucle à n sommets. Alors, au sens faible, pour la topologie locale,*

$$\mathbb{P}_n^{\triangle} \underset{n\to\infty}{\Longrightarrow} \mathbb{P}_\infty^{\triangle}.$$

Une variable aléatoire de loi $\mathbb{P}_\infty^{\triangle}$ est appelée *Triangulation Uniforme Infinie du Plan* (UIPT). Presque sûrement, l'UIPT a un seul bout [AS03, Théorème 1.10] et est une triangulation du plan (voir la Figure 1.7). La géométrie de cet objet et les modèles de physique statistique sur celui-ci ont été très largement étudiés. Nous y reviendrons au chapitre suivant.

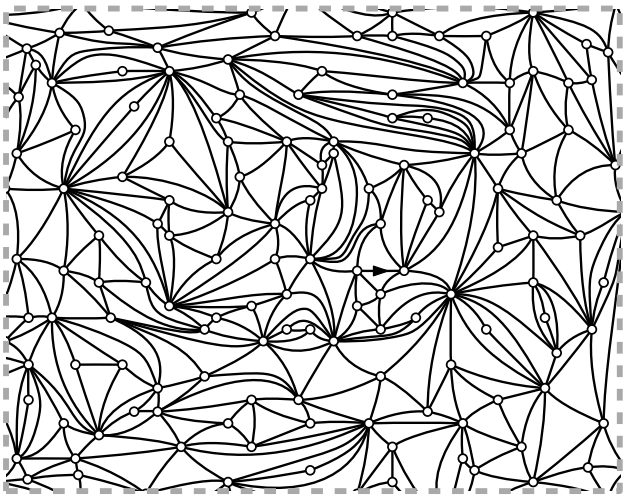

FIGURE 1.7 : La Triangulation Uniforme Infinie du Plan.

Le Théorème 1.4.1 a été étendu au cas quadrangulaire par Maxim Krikun [Kri05].

Théorème 1.4.2. ([Kri05, Théorème 1]) *Pour tout $n \geq 1$, soit $\mathbb{P}_n^{\square}$ la mesure uniforme sur l'ensemble $\mathcal{M}_n^{\square}$ des quadrangulations à n faces. Alors, au sens faible, pour la topologie locale,*

$$\mathbb{P}_n^{\square} \underset{n\to\infty}{\Longrightarrow} \mathbb{P}_\infty^{\square}.$$

De même, une variable aléatoire de loi $\mathbb{P}_\infty^{\square}$ est appelée *Quadrangulation Uniforme Infinie du Plan* (UIPQ), et l'UIPQ est presque sûrement une quadrangulation du plan.

1.4.3 Cartes uniformes infinies du demi-plan

À la suite de son travail avec Oded Schramm, Omer Angel propose dans [Ang04] d'étendre la construction de l'UIPT aux cartes à bord simple, et obtient le résultat que nous présentons maintenant. Pour tous $n \geq 0$ et $k \geq 2$, on note $\widehat{\mathcal{M}}_{n,k}^{\triangle}$ l'ensemble des triangulations sans boucle à bord simple ayant périmètre k et n sommets internes (i.e., n'appartenant pas à la face externe). Un élément de $\widehat{\mathcal{M}}_{n,k}^{\triangle}$ est parfois appelé *triangulation du k-gone* (avec n sommets internes), parce que sa face externe (simple) est un polygone de degré k.

Théorème 1.4.3. ([AS03, Théorème 5.1] et [Ang04, Théorème 2.1]) *Pour tous $n \geq 0$ et $k \geq 2$, soit $\widehat{\mathbb{P}}_{n,k}^{\triangle}$ la mesure uniforme sur $\widehat{\mathcal{M}}_{n,k}^{\triangle}$. Alors, au sens faible, pour la topologie locale,*

$$\widehat{\mathbb{P}}_{n,k}^{\triangle} \underset{n\to\infty}{\Longrightarrow} \widehat{\mathbb{P}}_{\infty,k}^{\triangle} \quad \textit{et} \quad \widehat{\mathbb{P}}_{\infty,k}^{\triangle} \underset{k\to\infty}{\Longrightarrow} \widehat{\mathbb{P}}_{\infty,\infty}^{\triangle}.$$

Une variable aléatoire de loi $\widehat{\mathbb{P}}_{\infty,k}^{\triangle}$ est appelée *Triangulation Uniforme Infinie du k-gone* (UIPT du k-gone), et a été introduite dans [AS03]. Presque sûrement, il s'agit d'une triangulation du k-gone, c'est-à-dire une triangulation infinie ayant un seul bout et un bord simple de périmètre k. En faisant tendre ce périmètre vers l'infini, on obtient la mesure de probabilité $\widehat{\mathbb{P}}_{\infty,\infty}^{\triangle}$. Une variable aléatoire ayant cette loi est appelée *Triangulation Uniforme Infinie du Demi-Plan* (UIHPT) à bord simple. Comme la terminologie l'indique, l'UIHPT est presque sûrement une triangulation du demi-plan à bord simple, ayant un seul bout et un bord simple infini (voir la Figure 1.8).

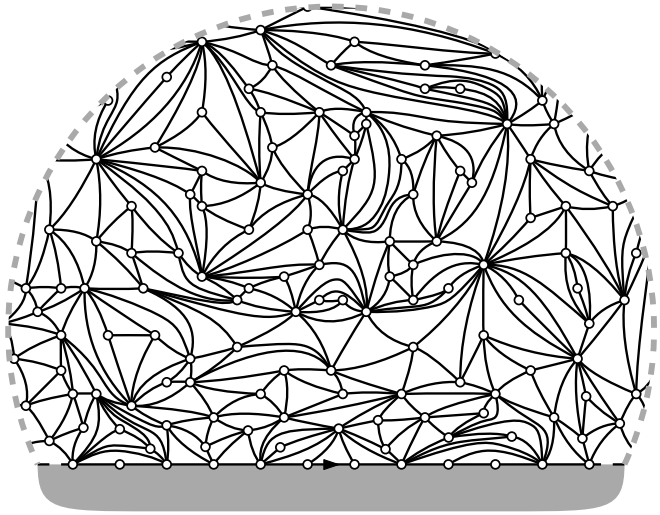

FIGURE 1.8 : La Triangulation Uniforme Infinie du Demi-Plan.

L'UIHPT apparaît également comme limite locale de cartes de type Boltzmann. Pour tout $k \geq 2$, on définit une mesure de Boltzmann sur l'ensemble des triangulations du k-gone en assignant un poids $q > 0$ à chaque sommet interne d'une triangulation. Cette construction, semblable à celle de la Section 1.3.3, est possible si et seulement si la masse totale des triangulations du k-gone (aussi appelée la fonction

de partition) est finie, c'est-à-dire

$$W_k^{\triangle}(q) := \sum_{n\geq 0} \#\widehat{\mathcal{M}}_{n,k}^{\triangle} q^n < \infty. \tag{1.13}$$

Par des résultats d'énumération (voir par exemple [Kri07]), ceci est vrai dès que $q \leq 2/27$. On note $W_k^{\triangle} := W_k^{\triangle}(2/27)$ la valeur de la fonction de partition au paramètre critique. La mesure de Boltzmann critique sur les triangulations (sans boucle) du k-gone, notée $\mathbb{W}_k^{\triangle}$, est alors définie par

$$\mathbb{W}_k^{\triangle}(\mathbf{m}) = \frac{1}{W_k^{\triangle}} \left(\frac{2}{27}\right)^n, \quad \mathbf{m} \in \widehat{\mathcal{M}}_{n,k}^{\triangle}, \quad n \in \mathbb{Z}_+. \tag{1.14}$$

Le résultat suivant est également dû à Omer Angel.

Théorème 1.4.4. ([Ang04, Théorème 2.1]) *Pour tout $k \geq 2$, soit $\mathbb{W}_k^{\triangle}$ la mesure de Boltzmann critique sur les triangulations du k-gone. Alors, au sens faible, pour la topologie locale,*

$$\mathbb{W}_k^{\triangle} \underset{k\to\infty}{\Longrightarrow} \widehat{\mathbb{P}}_{\infty,\infty}^{\triangle}.$$

Les Théorèmes 1.4.3 et 1.4.4 peuvent également être généralisés au cas des quadrangulations, voir [AC15, CM15]. Il faut néanmoins prendre garde au fait qu'une quadrangulation a nécessairement périmètre pair, et considérer l'ensemble $\widehat{\mathcal{M}}_{n,k}^{\square}$ des quadrangulations à bord simple de périmètre $2k$ ayant n sommets internes. La mesure limite $\widehat{\mathbb{P}}_{\infty,\infty}^{\square}$ est naturellement appelée la (loi de la) *Quadrangulation Uniforme Infinie du Demi-Plan* (UIHPQ) à bord simple.

La question de la limite locale des cartes uniformes à bord *général* (i.e., non nécéssairement simple) a été étudiée par Nicolas Curien et Grégory Miermont dans [CM15]. Dans la suite, pour tous $n \geq 0$ et $k \geq 1$, on note $\mathcal{M}_{n,k}^{\square}$ l'ensemble des quadrangulations à bord (général) de périmètre $2k$ ayant n faces internes.

Théorème 1.4.5. ([CM15, Théorème 2]) *Pour tous $n \geq 0$ et $k \geq 1$, soit $\mathbb{P}_{n,k}^{\square}$ la mesure uniforme sur $\mathcal{M}_{n,k}^{\square}$. Alors, au sens faible, pour la topologie locale,*

$$\mathbb{P}_{n,k}^{\square} \underset{n\to\infty}{\Longrightarrow} \mathbb{P}_{\infty,k}^{\square} \quad \textit{et} \quad \mathbb{P}_{\infty,k}^{\square} \underset{k\to\infty}{\Longrightarrow} \mathbb{P}_{\infty,\infty}^{\square}.$$

Une variable aléatoire de loi $\mathbb{P}_{\infty,\infty}^{\square}$ est appelée *Quadrangulation Uniforme Infinie du Demi-Plan* (UIHPQ) à bord général. Presque sûrement, il s'agit d'une quadrangulation du demi-plan à bord général, ayant un seul bout et un bord infini non simple.

Se pose alors la question du lien entre l'UIHPQ à bord simple $\widehat{\mathbb{P}}_{\infty,\infty}^{\square}$ et l'UIHPQ à bord général $\mathbb{P}_{\infty,\infty}^{\square}$. La réponse se trouve également dans [CM15]. Pour la comprendre, il faut introduire une décomposition des cartes à bord en leurs *composantes irréductibles*, proposée dans [BG09] (voir aussi [CM15, Section 2.2]). Les composantes irréductibles d'une carte à bord $\mathbf{m} \in \mathcal{M}$ sont les cartes à bord simple que l'on obtient à partir de $\mathbf{m}$ en coupant en deux tous les points de pincement (ou points de coupure) de son bord (voir la Figure 2.4 pour un exemple). Lorsqu'une carte $\mathbf{m}$ a une unique composante irréductible infinie (i.e., avec une infinité de sommets), on l'appelle le *noyau* de la carte et on la note $\mathrm{Core}(\mathbf{m})$.

Proposition 1.4.6. ([CM15, Proposition 6]) *Soit* $\mathbf{Q}_\infty^\infty$ *une variable aléatoire de loi* $\mathbb{P}^\square_{\infty,\infty}$. *Alors, presque sûrement,* $\mathbf{Q}_\infty^\infty$ *a une unique composante irréductible infinie notée* $\widehat{\mathbf{Q}}_\infty^\infty := \mathrm{Core}(\mathbf{Q}_\infty^\infty)$, *et* $\widehat{\mathbf{Q}}_\infty^\infty$ *a la loi* $\widehat{\mathbb{P}}^\square_{\infty,\infty}$.

Autrement dit, l'UIHPQ à bord général peut être obtenue à partir de l'UIHPQ à bord simple en attachant des quadrangulations finies aux sommets de son bord.

La construction du Théorème 1.4.5 s'étend au cas des triangulations et permet de définir la Triangulation Uniforme Infinie du Demi-Plan (UIHPT) à bord général, dont la loi est notée $\mathbb{P}^\triangle_{\infty,\infty}$. On renvoie à la Section 3.5 pour plus de détails à ce sujet.

Les Théorèmes 1.4.3 et 1.4.5 reposent sur deux techniques distinctes que nous décrivons brièvement. Ces techniques fournissent également une construction alternative de l'UIPT et de l'UIPQ. Plus généralement, elles permettent de comprendre des propriétés différentes des limites locales de cartes aléatoires.

La propriété de Markov spatiale. La *propriété de Markov spatiale* est une propriété de certains objets aléatoires d'avoir une forme d'invariance sous l'effet d'un conditionnement. Elle apparaît par exemple sur les processus *Schramm-Loewner Evolution* (SLE) ou sur le *Champ Libre Gaussien* (GFF). Certaines limites locales de cartes aléatoires possèdent également cette propriété. Intuitivement, elle affirme que lorsqu'on retire une face de la carte, les composantes connexes obtenues sont des variantes indépendantes de cette carte. En ce sens, on peut aussi l'interpréter comme une propriété de branchement. Toute la force de la propriété de Markov spatiale réside dans ses applications aux *processus d'épluchage*, dont le principe est de révéler une carte face par face. Cette idée a d'abord été introduite en physique théorique par Yoshiyuki Watabiki [Wat95], et développée dans le contexte des cartes aléatoires par Omer Angel. Il obtient d'abord une construction alternative de l'UIPT [Ang03], puis utilise ce procédé pour construire et étudier l'UIHPT [Ang04]. Les processus d'épluchage peuvent être adaptés à l'étude de différentes propriétés des cartes, comme la vitesse de croissance des boules [Ang03] ou la percolation [Ang03, Ang04, MN14, AC15]. Nous y reviendrons aux Chapitres 6 et 7. Omer Angel et Gourab Ray ont également obtenu une classification des triangulations du demi-plan satisfaisant la propriété de Markov spatiale (et une invariance par changement de racine) en une famille à un paramètre [AR15]. Les processus d'épluchage ont récemment été généralisés à une classe beaucoup plus large de cartes par Timothy Budd [Bud15].

Techniques bijectives. Les techniques dites bijectives reposent sur l'extension des bijections entre cartes finies et arbres bien étiquetés à des cartes infinies. Cette idée est due à Philippe Chassaing et Bergfinnur Durhuus [CD06], qui ont proposé une construction alternative de l'UIPQ à partir de la limite locale d'arbres bien étiquetés. L'équivalence entre cette construction et celle du Théorème 1.4.2 a été démontrée par Laurent Ménard [Mé10]. Ces techniques ont permis d'établir certaines propriétés géométriques de l'UIPQ, voir [LGM10, CMM13, CLG13]. La construction de l'UIHPQ à bord général du Théorème 1.4.5 s'appuie également sur des techniques bijectives, comme nous le verrons dans la Section 3.2.2. De même, elle a été utilisée pour étudier la géométrie de l'UIHPQ (notamment les géodésiques et les limites d'échelle de celle-ci) dans [CM15, CC15, BMR16]. Nous y reviendrons aux Chapitres 3 et 4.

1.4.4 Limites locales des cartes de Boltzmann

Pour conclure, nous présentons des résultats de limites locales des cartes de Boltzmann biparties définies dans la Section 1.3.3. Commençons par le cas des cartes de Boltzmann biparties conditionnées à avoir n faces, dont la loi $\mathbb{P}_{\mathsf{q},n}$ a été définie par (1.11). L'étude de la limite locale de ces cartes lorsque le nombre de faces tend vers l'infini a été initiée par Jakob Björnberg et Sigurður Örn Stefánsson [BS14].

Théorème 1.4.7. ([BS14, Théorème 1.1]) *Soit* q *une suite de poids admissible. Alors, au sens faible, pour la topologie locale,*

$$\mathbb{P}_{\mathsf{q},n} \underset{n\to\infty}{\Longrightarrow} \mathbb{P}_{\mathsf{q},\infty}.$$

Une variable aléatoire de loi $\mathbb{P}_{\mathsf{q},\infty}$ est appelée *Carte de Boltzmann Infinie du Plan* de paramètre q (q-IBPM). Presque sûrement, la q-IBPM a un seul bout et est une carte bipartie du plan ([BS14, Théorème 1.1]). Si l'on choisit la suite de poids $q_k = 12^{-1}\delta_2(k)$ correspondant aux quadrangulations de Boltzmann critiques (voir [BG09, Section 4.1]), $\mathbb{P}_{\mathsf{q},\infty}$ est aussi la loi $\mathbb{P}_\infty^\square$ de l'UIPQ. Ce résultat est basé sur des techniques bijectives, et a été étendu à des cartes de Boltzmann non biparties par Robin Stephenson [Ste16, Théorème 6.1]. Enfin, Nicolas Curien a obtenu une preuve alternative du Théorème 1.4.7 en utilisant des techniques d'épluchage [Cur16a, Théorème 8].

Le cas des cartes de Boltzmann à bord (général) à également été traité par Nicolas Curien [Cur16a]. Lorsqu'on considère des cartes à bord, la face racine est interprétée comme ne faisant pas partie de la carte, ce qui conduit à la définition légèrement différente du poids de Boltzmann

$$w_{\mathsf{q}}^*(\mathbf{m}) := \prod_{f\in \mathrm{F}(\mathbf{m})\setminus\{f_*\}} q_{\deg(f)/2}, \quad \mathbf{m}\in\mathcal{B}_f.$$

Pour tout $k \geq 1$, la mesure de Boltzmann sur l'ensemble $\mathcal{B}_f^{(k)}$ des cartes biparties avec un bord de taille $2k$ est alors définie par

$$\mathbb{P}_{\mathsf{q}}^{(k)}(\mathbf{m}) := \frac{\mathbf{1}_{\left\{\mathbf{m}\in\mathcal{B}_f^{(k)}\right\}} w_{\mathsf{q}}^*(\mathbf{m})}{w_{\mathsf{q}}^*\left(\mathcal{B}_f^{(k)}\right)}, \quad \mathbf{m}\in\mathcal{B}_f. \tag{1.15}$$

Ceci revient à considérer une carte de loi $\mathbb{P}_{\mathsf{q}}$ conditionnée à avoir périmètre $2k$. Le résultat s'énonce comme suit.

Théorème 1.4.8. ([Cur16a, Théorème 7]) *Soit* q *une suite de poids admissible. Alors, au sens faible, pour la topologie locale,*

$$\mathbb{P}_{\mathsf{q}}^{(k)} \underset{k\to\infty}{\Longrightarrow} \mathbb{P}_{\mathsf{q}}^{(\infty)}.$$

Une variable aléatoire de loi $\mathbb{P}_{\mathsf{q}}^{(\infty)}$ est appelée *Carte de Boltzmann Infinie du Demi-Plan* de paramètre q (q-IBHPM). Presque sûrement, la q-IBHPM est une carte bipartie du demi-plan à bord général, ayant un seul bout et un bord infini non simple [Cur16a, Théorème 7]. Pour le choix de suite de poids $q_k = 12^{-1}\delta_2(k)$ correspondant aux quadrangulations de Boltzmann critiques, $\mathbb{P}_{\mathsf{q}}^{(\infty)}$ est la loi $\mathbb{P}_{\infty,\infty}^\square$ de l'UIHPQ à bord général. Nous étudierons plus en détail le bord de ces cartes au Chapitre 5.

2

Géométrie et percolation sur des cartes à bord aléatoires

Dans ce chapitre, nous présentons nos contributions à l'étude des cartes aléatoires. Dans un premier temps, nous nous intéressons à la géométrie de cartes à bord aléatoires, ce qui correspond à la Partie II de ce manuscrit. Les résultats s'appuient sur les travaux [1] (Chapitre 3 en collaboration avec Erich Baur et Grégory Miermont), [2] (Chapitre 4 en collaboration avec Erich Baur) et [5] (Chapitre 5). Dans un second temps, nous étudierons des modèles de percolation sur des cartes aléatoires, correspondant à la Partie III de ce manuscrit. Les résultats sont issus des travaux [3] (Chapitre 6) et [4] (Chapitre 7). Les contributions originales de cette thèse sont signalées par un encadré.

Sommaire

2.1 Limites du bord des cartes de Boltzmann

Au chapitre précédent, nous avons introduit une famille de cartes aléatoires biparties, les cartes de Boltzmann, paramétrée par une suite de poids q. Nous avons vu que sous des hypothèses assez larges, la limite d'échelle des cartes de Boltzmann est un objet universel, la carte brownienne, alors que sous d'autres hypothèses impliquant que le degré d'une face typique soit à queue lourde, on obtient une famille d'espaces métriques aléatoires appelés cartes stables de paramètre $\alpha \in (1,2)$. La géométrie des cartes stables est supposée être très différente de celle de la carte brownienne en raison des grandes faces qui restent présentes à la limite. Il est conjecturé que cette géométrie admet une *transition de phase* en le paramètre α. Lorsque $\alpha \in (1,3/2)$, les grandes faces sont censées être auto-intersectantes (on parle de la *phase dense*) alors que pour $\alpha \in (3/2,2)$, on pense qu'elles sont auto-évitantes (on parle de la *phase diluée*). Voir la Figure 2.1 pour une illustration. Le but du Chapitre 5, que nous présentons maintenant, est d'aborder cette conjecture en étudiant les limites du bord des cartes de Boltzmann. Notre but est double : on commence par identifier la structure de branchement des grandes faces dans la phase dense en étudiant leur limite d'échelle, puis on établit la transition de phase à travers leur limite locale.

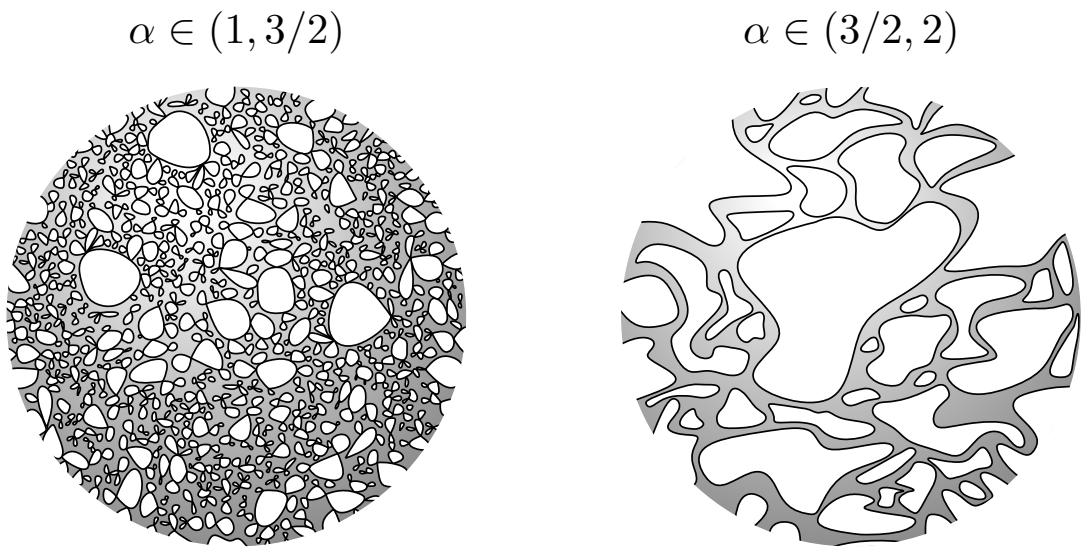

FIGURE 2.1 : Représentation schématique de la carte stable dans les phases dense $\alpha \in (1,3/2)$ et diluée $\alpha \in (3/2,2)$.

Précisément, on considère la mesure de Boltzmann $\mathbb{P}_{\mathsf{q}}^{(k)}$ avec poids q sur l'ensemble $\mathcal{B}_f^{(k)}$ des cartes biparties de périmètre $2k$ introduite dans (1.15), définie par

$$\mathbb{P}_{\mathsf{q}}^{(k)}(\mathbf{m}) := \frac{\mathbf{1}_{\left\{\mathbf{m}\in\mathcal{B}_f^{(k)}\right\}} w_{\mathsf{q}}^*(\mathbf{m})}{w_{\mathsf{q}}^*\left(\mathcal{B}_f^{(k)}\right)}, \quad \mathbf{m} \in \mathcal{B}_f.$$

Cette mesure s'obtient également en conditionnant une carte de loi $\mathbb{P}_{\mathsf{q}}$ à avoir périmètre $2k$. L'intérêt d'une telle carte réside dans son interprétation, à grande échelle,

comme une carte stable enracinée sur l'une de ses grandes faces (lorsque q est non générique critique de paramètre α). Les limites d'échelle du bord de cartes de loi $\mathbb{P}_q^{(k)}$ sont étudiées dans la Section 2.1.2, et leurs limites locales dans la Section 2.1.3. Ces résultats reposent en partie sur la notion d'*arbre à boucles*, qui fait l'objet de la Section 2.1.1 et que l'on utilisera à nouveau dans la Section 2.4.4. Nous discuterons enfin des applications de ces résultats au modèle de boucles $O(n)$ rigide sur les quadrangulations dans la Section 2.1.4.

2.1.1 Arbres à boucles

Les arbres à boucles ont d'abord été introduits par Nicolas Curien et Igor Kortchemski [CK14b] dans le but d'étudier le modèle de percolation de Bernoulli sur l'UIPT [CK14a]. Nous donnons ici une brève introduction inspirée de [CK14a], et renvoyons aux Sections 5.3.2 et 7.2.2 pour davantage de précisions.

Définition et notations. Commençons par une définition formelle d'arbre à boucles.

Définition 2.1.1. Un arbre à boucles est une carte (finie) dont toutes les arêtes sont incidentes à exactement deux faces, l'une d'entre elles étant la face racine.

On note $\mathcal{L}_f$ l'ensemble des arbres à boucles. De manière informelle, un arbre à boucles est une collection de cycles organisés selon une structure d'arbre. Il existe donc une manière d'obtenir des arbres à boucles à partir d'arbres, et inversement, que nous décrivons brièvement. Pour tout $\mathbf{t} \in \mathcal{T}_f$, l'arbre à boucles $\mathbf{l} := \mathrm{Loop}(\mathbf{t})$ est obtenu en reliant tous les voisins de chaque sommet de $\mathbf{t}_\bullet$ dans l'ordre cyclique (les arêtes et sommets noirs de $\mathbf{t}$ étant effacés). Réciproquement, pour tout $\mathbf{l} \in \mathcal{L}_f$, l'arbre plan $\mathbf{t} := \mathrm{Tree}(\mathbf{l})$, appelé l'*arbre des composantes*, est obtenu en ajoutant un sommet à l'intérieur de chaque face interne (ou *boucle*) de $\mathbf{l}$, que l'on relie par une arête à tous les sommets de cette face (les arêtes de $\mathbf{l}$ étant effacées). Les conventions d'enracinement de ces objets sont détaillées dans la Section 5.3.2, et un exemple est proposé dans la Figure 2.2.

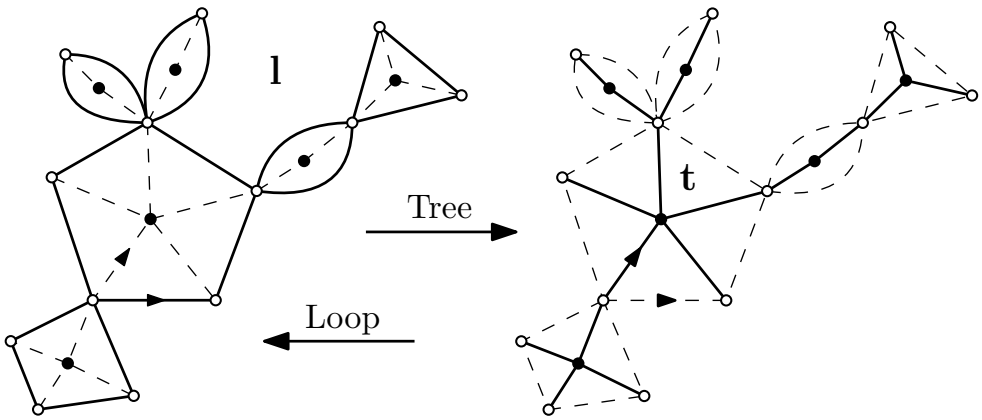

FIGURE 2.2 : Les applications Tree et Loop.

Limites locales d'arbres à boucles aléatoires. Une manière naturelle de construire des arbres à boucles aléatoires est d'utiliser les arbres de Galton-Watson à deux types de la Définition 1.3.7. Ceci motive l'étude des limites locales d'arbres de Galton-Watson dont le nombre de sommets tend vers l'infini (de tels arbres sont dits *conditionnés à survivre*). Le premier résultat de ce type est dû à Harry Kesten [Kes86b].

Théorème 2.1.2. ([Kes86b]) *Soit ρ une loi de reproduction critique. Pour tout $k \geq 1$, on suppose que $\mathsf{GW}_\rho(\{|\mathbf{t}| = k\}) > 0$ et on se donne T_k un arbre de loi GW_ρ conditionné à avoir k sommets. Alors, on a la convergence en loi pour la topologie locale*

$$T_k \xrightarrow[k\to\infty]{(d)} \mathbf{T}_\infty(\rho).$$

L'objet limite $\mathbf{T}_\infty(\rho)$ est un arbre aléatoire infini appelé *arbre de Kesten* associé à la loi de reproduction ρ. Il est composé d'un unique chemin infini partant de la racine, l'épine dorsale, sur laquelle sont attachés de part et d'autre des arbres finis.

Lorsque la loi de reproduction ρ est sous-critique (et n'a pas de moments exponentiels), un phénomène très différent se produit, connu sous le nom de *condensation*. Il a été observé d'abord dans des travaux de physique, puis considéré sous la forme que nous présentons par Þórður Jónsson et Sigurður Örn Stefánsson [JS10] (voir également [Kor15]), et généralisé par Svante Janson [Jan12]. Dans ce cas, on a convergence en loi vers un arbre limite $\mathbf{T}_\infty(\rho)$ qui possède un unique sommet de degré infini sur lequel sont attachés des arbres finis [Jan12, Théorème 7.1]. La présence d'un sommet de degré infini nécessite toutefois de considérer une topologie plus faible que la topologie locale (voir la Section 5.5.1 pour plus de détails).

Le Théorème 2.1.2 a été généralisé par Robin Stephenson au cas des arbres multitypes. Nous allons utiliser le cas particulier suivant (voir aussi [BS14]).

Théorème 2.1.3. ([Ste16, Théorème 3.1]) *Soit $(\rho_\circ, \rho_\bullet)$ un couple de lois de reproduction critique. Pour tout $k \geq 1$, on suppose que $\mathsf{GW}_{\rho_\circ,\rho_\bullet}(\{|\mathbf{t}| = k\}) > 0$ et on se donne $T_k^{\circ,\bullet}$ un arbre de loi $\mathsf{GW}_{\rho_\circ,\rho_\bullet}$ conditionné à avoir k sommets. Alors, on a la convergence en loi pour la topologie locale*

$$T_k^{\circ,\bullet} \xrightarrow[k\to\infty]{(d)} \mathbf{T}_\infty^{\circ,\bullet}(\rho_\circ, \rho_\bullet).$$

Comme précédemment, l'arbre localement fini $\mathbf{T}_\infty^{\circ,\bullet}(\rho_\circ, \rho_\bullet)$ est obtenu à partir d'une unique épine dorsale sur laquelle sont attachés des arbres finis. Dans la Proposition 5.5.3, nous montrerons un résultat analogue (pour une topologie plus faible) lorsque le couple de lois de reproduction $(\rho_\circ, \rho_\bullet)$ est sous-critique (tel que $\rho_\circ$ soit une loi géométrique et $\rho_\bullet$ n'ait pas de moment exponentiel). On observe alors un phénomène de condensation : l'arbre limite $\mathbf{T}_\infty^{\circ,\bullet}(\rho_\circ, \rho_\bullet)$ possède un unique sommet de degré infini (à hauteur impaire) sur lequel sont attachés des arbres finis. On note $\mathsf{GW}^{(\infty)}_{\rho_\circ,\rho_\bullet}$ la distribution de l'arbre $\mathbf{T}_\infty^{\circ,\bullet}(\rho_\circ, \rho_\bullet)$, qui est illustré dans la Figure 2.3. Une construction alternative est également détaillée dans la Section 5.5.1.

Nous construisons maintenant des cartes planaires infinies à partir des arbres aléatoires infinis $\mathbf{T}_\infty^{\circ,\bullet} = \mathbf{T}_\infty^{\circ,\bullet}(\rho_\circ, \rho_\bullet)$ de la manière suivante.

Dans le cas critique, $\mathbf{T}_\infty^{\circ;\bullet}$ est presque sûrement localement fini. L'application Loop peut être étendue à tout arbre plan localement fini $\mathbf{t} \in \mathcal{T}_{\text{loc}}$, en définissant $\text{Loop}(\mathbf{t})$ par la suite cohérente de cartes $(\text{Loop}(\mathbf{B}_{2R}(\mathbf{t})) : R \geq 0)$. Lorsque $\mathbf{t}$ est infini et possède un seul bout, $\text{Loop}(\mathbf{t})$ est un *arbre à boucles infini*, c'est-à-dire une carte infinie dont toutes les arêtes sont incidentes à exactement deux faces, l'une d'entre elles étant la face racine, et dont la face racine est l'unique face infinie. L'arbre à boucles aléatoire infini $\mathbf{L}_\infty = \mathbf{L}_\infty(\rho_\circ, \rho_\bullet)$ est alors défini par $\mathbf{L}_\infty := \text{Loop}(\mathbf{T}_\infty^{\circ;\bullet})$.

Dans le cas sous-critique, $\mathbf{T}_\infty^{\circ;\bullet}$ a presque sûrement un unique sommet de degré infini à hauteur impaire, et l'application Loop ne peut pas être étendue à $\mathbf{T}_\infty^{\circ;\bullet}$. Néanmoins, on peut définir une carte infinie $\mathbf{L}_\infty = \mathbf{L}_\infty(\rho_\circ, \rho_\bullet)$ à partir de $\mathbf{T}_\infty^{\circ;\bullet}$ en reliant les sommets blancs dans l'ordre cyclique autour de chaque sommet noir de $\mathbf{T}_\infty^{\circ;\bullet}$ (les arêtes de $\mathbf{T}_\infty^{\circ;\bullet}$ étant effacées). En revanche, $\mathbf{L}_\infty$ n'est pas un arbre à boucles infini au sens précédent. En fait, $\mathbf{L}_\infty$ peut être obtenue à partir du graphe de $\mathbb{Z}$ en collant sur chaque sommet un arbre à boucles fini dont la loi est explicite (voir la Section 5.5.2).

Nous verrons dans le Lemme 5.5.5 que les cartes infinies $\mathbf{L}_\infty(\rho_\circ, \rho_\bullet)$ sont également obtenues comme limite locale des arbres à boucles $L_k := \text{Loop}(T_k^{\circ,\bullet})$ lorsque k tend vers l'infini, où $T_k^{\circ,\bullet}$ un arbre de Galton-Watson de loi $\text{GW}_{\rho_\circ,\rho_\bullet}$ conditionné à avoir k sommets. Nous renvoyons à la Figure 2.3 pour une illustration, et à la Section 5.5.2 pour plus de détails.

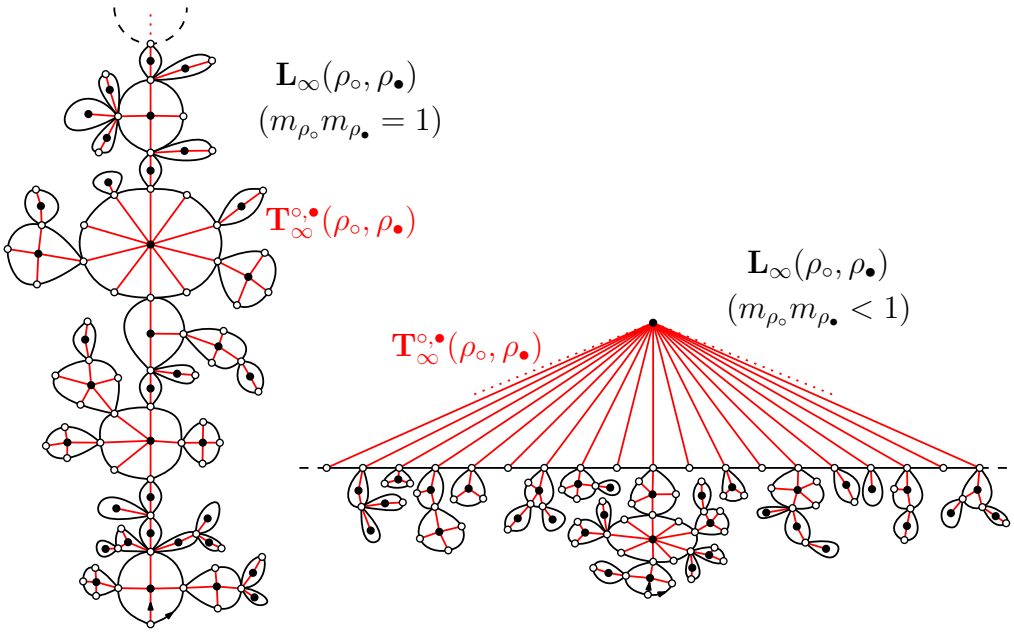

FIGURE 2.3 : La carte infinie $\mathbf{L}_\infty$ et l'arbre $\mathbf{T}_\infty^{\circ;\bullet}$ associé.

Décomposition de cartes à bord. Nous utilisons à présent la notion d'arbre à boucles pour décrire la structure de branchement de cartes à bord. Cette idée a été introduite dans [CK14a]. On commence par une définition.

Définition 2.1.4. Soit $\mathbf{m} \in \mathcal{M}$ une carte à bord. La *carte évidée* de $\mathbf{m}$ est obtenue à partir de son bord $\partial\mathbf{m}$ en dupliquant les arêtes dont les deux côtés sont incidents à la face externe. Elle est notée $\text{Scoop}(\mathbf{m})$.

Un exemple de carte évidée se trouve dans la Figure 2.4. Pour toute carte $\mathbf{m} \in \mathcal{M}_f$, Scoop($\mathbf{m}$) est un arbre à boucles et l'arbre plan **Tree**($\mathbf{m}$) := Tree(Scoop($\mathbf{m}$)) est aussi appelé l'*arbre des composantes* de $\mathbf{m}$. La carte $\mathbf{m}$ peut être reconstruite en collant à l'intérieur de chaque face interne de Scoop($\mathbf{m}$) une carte à bord simple. Ces cartes à bord simple sont exactement les composantes irréductibles de $\mathbf{m}$, obtenues en coupant les points de pincement de son bord, que nous avons introduites dans la Section 1.4.3. Ainsi, à chaque sommet u de **Tree**($\mathbf{m}$) à hauteur impaire correspond une face interne de Scoop($\mathbf{m}$), et donc une carte à bord simple de périmètre $\deg(u)$. On obtient une bijection

$$\Phi_{\mathrm{TC}} : \mathbf{m} \mapsto (\mathbf{Tree}(\mathbf{m}), (\widehat{\mathbf{m}}_u : u \in \mathbf{Tree}(\mathbf{m})_\bullet))$$

qui associe à toute carte $\mathbf{m} \in \mathcal{M}_f$ l'arbre plan $\mathbf{t} = \mathbf{Tree}(\mathbf{m})$, et une collection $(\widehat{\mathbf{m}}_u : u \in \mathbf{t}_\bullet)$ de cartes à bord simple de périmètre respectif $\deg(u)$ qui sont les composantes irréductibles de $\mathbf{m}$. Voir la Figure 2.4 pour une illustration.

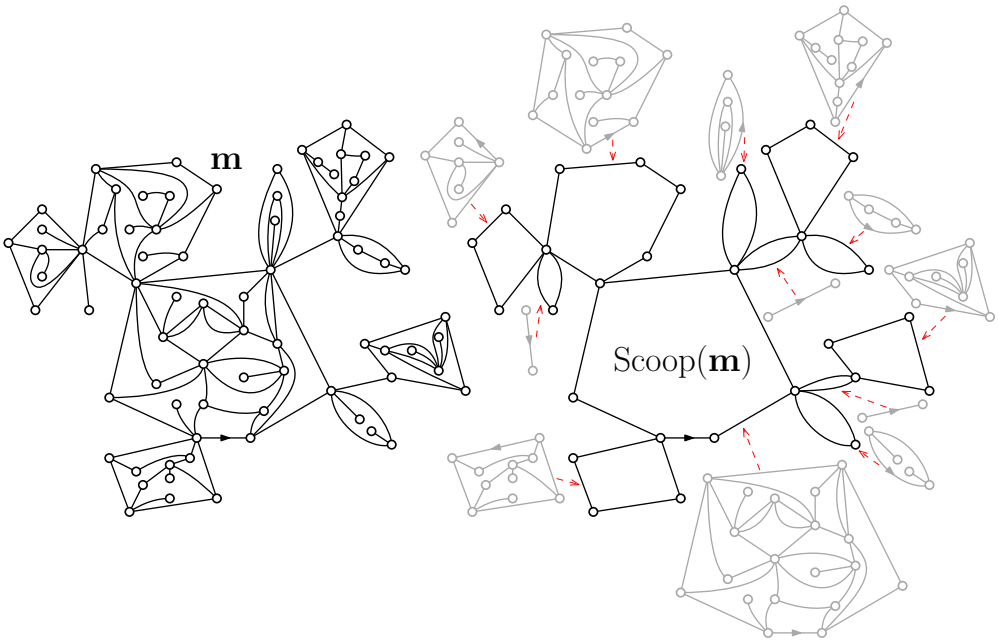

FIGURE 2.4 : La décomposition d'une carte $\mathbf{m} \in \mathcal{M}_f$ en sa carte évidée Scoop($\mathbf{m}$) et ses composantes irréductibles.

Cette décomposition peut être étendue à des cartes infinies. Dans ce cas, l'arbre des composantes $\mathbf{t} := \mathbf{Tree}(\mathbf{m})$ de $\mathbf{m} \in \mathcal{M}$ est obtenu en ajoutant un sommet à l'intérieur de chaque face interne de Scoop($\mathbf{m}$), que l'on relie par une arête à tous les sommets de cette face (les arêtes de Scoop($\mathbf{m}$) étant effacées). La carte $\mathbf{m}$ peut encore être reconstruite en collant ses composantes irréductibles $(\widehat{\mathbf{m}}_u : u \in \mathbf{t}_\bullet)$ à l'intérieur des faces de Scoop($\mathbf{m}$), comme dans le cas fini. Néanmoins, l'arbre **Tree**($\mathbf{m}$) n'est en général pas localement fini et peut avoir un sommet de degré infini.

Dans la suite, nous considérerons finalement des cartes à bord $\mathbf{m} \in \mathcal{M}$ dont toutes les composantes irréductibles sont finies. Dans ce cas, Scoop($\mathbf{m}$) est un arbre à boucles et $\mathbf{t} := \mathbf{Tree}(\mathbf{m})$ un arbre plan localement fini ayant au plus un bout. De

plus, l'application réciproque Φ_{TC}^{-1}, qui consiste à recoller les cartes à bord simple $(\widehat{\mathbf{m}}_u : u \in \mathbf{t}_\bullet)$ de périmètre respectif $\deg(u)$ dans les faces internes de $\mathrm{Loop}(\mathbf{t})$, est continue pour la topologie naturelle. Voir la Section 7.2.3 pour davantage de détails.

2.1.2 Limites d'échelle du bord des cartes de Boltzmann

Notre résultat principal concerne la limite d'échelle du bord des cartes de Boltzmann dans la phase dense $\alpha \in (1, 3/2)$.

Théorème 1

Soit q une suite de poids non générique critique de paramètre $\alpha \in (1, 3/2)$. Pour tout $k \geq 1$, soit M_k une carte de loi $\mathbb{P}_{\mathsf{q}}^{(k)}$. Alors, il existe une fonction à variation lente Λ telle qu'on ait la convergence en loi au sens de Gromov-Hausdorff

$$\left(\mathrm{V}\left(\partial M_k\right), \frac{\Lambda(k)}{(2k)^{\alpha-1/2}} \cdot d_{\mathrm{gr}}^{\partial M_k} \right) \xrightarrow[k\to\infty]{(d)} \mathscr{L}_\beta,$$

où $\mathscr{L}_\beta$ est l'arbre à boucles stable de paramètre

$$\beta := \frac{1}{\alpha - \frac{1}{2}} \in (1, 2).$$

L'*arbre à boucles stable* $\mathscr{L}_\beta$ de paramètre $\beta \in (1, 2)$ est un espace métrique aléatoire compact qui a été introduit dans [CK14b]. Intuitivement, il s'agit de l'arbre stable $\mathscr{T}_\beta$ de la Section 1.3.1 dans lequel les points de branchement de degré infini sont éclatés en des cycles. En particulier, cet objet peut être entièrement codé à partir d'une excursion de processus de Lévy stable spectralement positif de paramètre β. Sa dimension de Hausdorff est presque sûrement égale à β [CK14b, Théorème 1.1]. Une simulation se trouve dans la Figure 2.5.

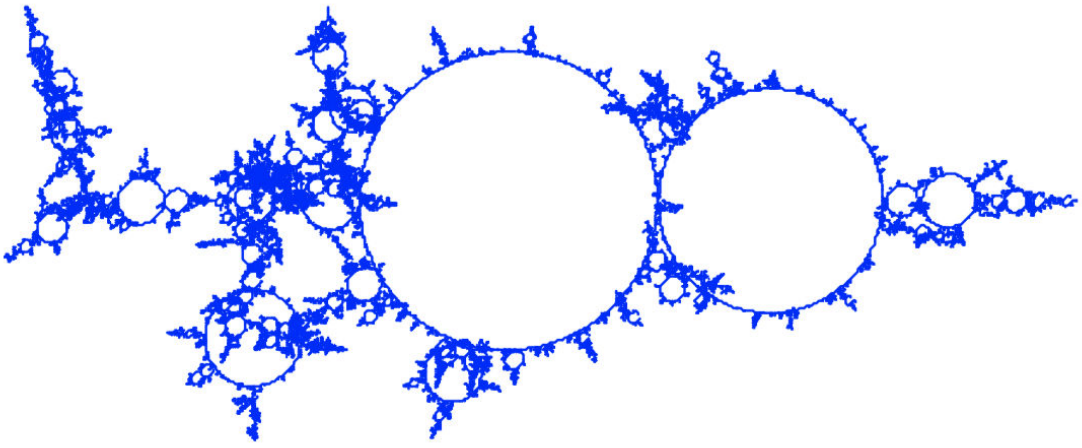

FIGURE 2.5 : Un arbre à boucles stable de paramètre $\beta = 1.07$ (par Igor Kortchemski).

Ce résultat caractérise la structure de branchement du bord d'une carte de Boltzmann dans la phase dense. Comme attendu, cette structure est non triviale : les grandes faces d'une carte de Boltzmann sont auto-intersectantes à la limite. Les cas sous-critique, dilué et générique critique restent ouverts. Nous pensons que dans les régimes dilué et générique critique, la limite d'échelle du bord est un cercle, conformément à la conjecture d'auto-évitement des grandes faces. Dans la phase sous-critique, au contraire, l'arbre continu brownien est attendu comme limite d'échelle. Nous espérons aborder ces questions dans un travail futur, et nous les discuterons plus en détail dans la Section 5.4.3.

2.1.3 Limites locales du bord des cartes de Boltzmann

Nous cherchons maintenant à établir la transition de phase de ce modèle à travers le bord des limites locales de cartes de Boltzmann. Nous avons vu dans le Théorème 1.4.8 que la mesure de probabilité $\mathbb{P}_{\mathsf{q}}^{(k)}$ admet une limite au sens faible pour la topologie locale, notée $\mathbb{P}_{\mathsf{q}}^{(\infty)}$ et appelée la loi de la Carte de Boltzmann Infinie du Demi-Plan de paramètre q (q-IBHPM).

Soit $\mathbf{M}_\infty = \mathbf{M}_\infty(\mathsf{q})$ une carte de loi $\mathbb{P}_{\mathsf{q}}^{(\infty)}$. On s'intéresse aux propriétés du bord (non simple) de $\mathbf{M}_\infty$ selon la suite de poids q. À nouveau, on décompose $\mathbf{M}_\infty$ en ses composantes irréductibles en séparant les points de pincement de son bord. On rappelle que lorsque $\mathbf{M}_\infty$ a une unique composante irréductible infinie, celle-ci est appelée le noyau de $\mathbf{M}_\infty$ et notée $\mathrm{Core}(\mathbf{M}_\infty)$. Notre résultat est le suivant.

Théorème 2

Soit q une suite de poids admissible et $\mathbf{M}_\infty = \mathbf{M}_\infty(\mathsf{q})$ la q-IBHPM. On suppose que q est sous-critique, générique critique ou non générique critique de paramètre $\alpha \in (1,2)$. Alors, il existe des mesures de probabilité $\nu_\circ$ (géométrique) et $\nu_\bullet$ telles que

$$\mathrm{Scoop}(\mathbf{M}_\infty) \overset{(d)}{=} \mathbf{L}_\infty(\nu_\circ, \nu_\bullet).$$

On observe une transition de phase :

- Si q est sous-critique ou non générique critique de paramètre $\alpha \in (1, 3/2]$, $(\nu_\circ, \nu_\bullet)$ est critique et les composantes irréductibles de $\mathbf{M}_\infty$ sont finies.
- Si q est non générique critique de paramètre $\alpha \in (3/2, 2)$ ou générique critique, $(\nu_\circ, \nu_\bullet)$ est sous-critique et $\mathbf{M}_\infty$ a un noyau à bord simple infini.

De plus, $\nu_\bullet$ a variance finie si et seulement si q est sous-critique. Sinon, $\nu_\bullet$ est dans le domaine d'attraction d'une loi stable de paramètre $(\alpha - 1/2)^{-1}$ (si $\alpha \in (1, 3/2)$), $\alpha - 1/2$ (si $\alpha \in (3/2, 2)$) ou $3/2$ (si q est générique critique).

En d'autres termes, dans la phase dense, $\mathbf{M}_\infty$ a une structure arborescente alors que dans la phase diluée, elle possède une unique composante irréductible infinie homéomorphe au demi-plan sur laquelle des cartes finies sont attachées. Une illustration se trouve dans la Figure 2.6.

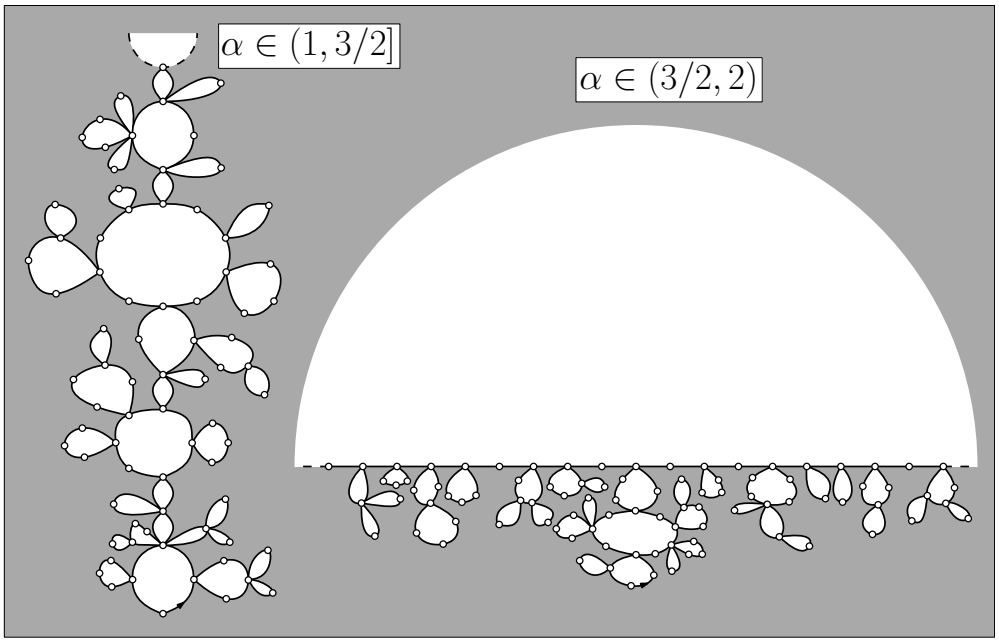

FIGURE 2.6 : Représentation schématique du bord de la q-IBHPM avec q non générique critique de paramètre $\alpha \in (1, 2)$.

Dans les phases sous-critique et dense, la q-IBHPM peut même être reconstruite à partir de l'arbre à boucles $\mathbf{L}_\infty(\nu_\circ, \nu_\bullet)$ du Théorème 2 et d'une collection de cartes de Boltzmann à bord simple indépendantes. Dans la suite, $\widehat{\mathbb{P}}_{\mathsf{q}}^{(k)}$ désigne la mesure de Boltzmann sur l'ensemble $\widehat{\mathcal{B}}_f^{(k)}$ des cartes biparties à bord simple de périmètre $2k$, définie par

$$\widehat{\mathbb{P}}_{\mathsf{q}}^{(k)}(\mathbf{m}) := \frac{\mathbf{1}_{\left\{\mathbf{m} \in \widehat{\mathcal{B}}_f^{(k)}\right\}} w_{\mathsf{q}}^*(\mathbf{m})}{w_{\mathsf{q}}^*\left(\widehat{\mathcal{B}}_f^{(k)}\right)}, \quad \mathbf{m} \in \mathcal{B}_f. \tag{2.1}$$

Proposition 3

Soit q une suite de poids sous-critique ou non générique critique de paramètre $\alpha \in (1, 3/2]$ et $\mathbf{T}_\infty^{\circ,\bullet} = \mathbf{T}_\infty^{\circ,\bullet}(\nu_\circ, \nu_\bullet)$. Conditionnellement à $\mathbf{T}_\infty^{\circ,\bullet}$, soit $(\widehat{M}_u : u \in (\mathbf{T}_\infty^{\circ,\bullet})_\bullet)$ une collection de cartes de Boltzmann biparties à bord simple indépendantes, de loi $\widehat{\mathbb{P}}_{\mathsf{q}}^{(\deg(u)/2)}$. Alors, la carte bipartie infinie

$$M_\infty = \Phi_{\mathrm{TC}}^{-1}\left(\mathbf{T}_\infty^{\circ,\bullet}, \left(\widehat{M}_u : u \in (\mathbf{T}_\infty^{\circ,\bullet})_\bullet\right)\right)$$

a la loi $\mathbb{P}_{\mathsf{q}}^{(\infty)}$ de la q-IBHPM.

Dans les régimes dilué et générique critique, nous nous attendons à ce que la carte du demi-plan à bord simple $\mathrm{Core}(\mathbf{M}_\infty)$ soit la limite locale de cartes de Boltzmann biparties à bord simple (de loi $\widehat{\mathbb{P}}_{\mathsf{q}}^{(k)}$) dont le périmètre tend vers l'infini. Dans le cas particulier de l'UIHPQ, nous avons déjà vu un tel résultat au Théorème 1.4.6. Enfin, le rôle du paramètre critique $\alpha = 3/2$ sera discuté dans la Section 5.7.

2.1.4 Application au modèle $O(n)$ rigide sur les quadrangulations

L'étude des mesures de Boltzmann est également motivée par leur lien avec les modèles de physique statistique sur les cartes, en particulier les *modèles de boucles* $O(n)$. Il s'agit de modèles d'abord introduits en physique théorique [DK88, Kos89, KS92, EZJ92, EK95, EK96, BE11], et dont l'intérêt tient notamment au fait qu'ils généralisent de nombreux modèles de physique statistique (incluant percolation de Bernoulli, modèle d'Ising, modèle de Potts et percolation FK). De manière générale, l'étude des modèles de physique statistique sur les cartes constitue un enjeu majeur de la théorie, en particulier du point de vue physique (on parle alors de modèle de gravité quantique couplé à la matière).

Dans la plupart des modèles de boucles $O(n)$ sur les cartes, le "gasket" obtenu en supprimant l'intérieur des boucles les plus à l'extérieur est une carte de Boltzmann. Ce résultat est le point de départ de l'étude menée par Gaëtan Borot, Jérémie Bouttier, et Emmanuel Guitter [BBG12c, BBG12b, BBG12a]. Ici, on s'intéresse au cas particulier du modèle de boucles $O(n)$ *rigide* sur les quadrangulations, qui a été étudié dans [BBG12c].

Définition du modèle. Commençons par une brève description du modèle. Une quadrangulation à bord *décorée par des boucles* $(\mathbf{q}, \boldsymbol{\ell})$ est une quadrangulation à bord $\mathbf{q}$ munie d'une collection de chemins simples fermés disjoints $\boldsymbol{\ell} = (\ell_1, \ell_2, \ldots)$ sur le dual de $\mathbf{q}$, appelés *boucles*. La configuration de boucles est dite *rigide* si de plus les boucles traversent les quadrangles par leurs côtés opposés. L'ensemble de tous les couples $(\mathbf{q}, \boldsymbol{\ell})$ de ce type est noté $\mathcal{O}$ (ou $\mathcal{O}_k$ si de plus $\mathbf{q}$ a périmètre $2k$).

Étant donnés $n \in (0, 2)$ et $g, h \geq 0$, on définit une mesure σ-finie sur les quadrangulations décorées en posant

$$W_{(n;g,h)}((\mathbf{q}, \boldsymbol{\ell})) := g^{\#\mathrm{F}(\mathbf{q})-|\boldsymbol{\ell}|} h^{|\boldsymbol{\ell}|} n^{\#\boldsymbol{\ell}},$$

où $|\boldsymbol{\ell}|$ est la longueur totale des boucles et $\#\boldsymbol{\ell}$ le nombre de boucles. Autrement dit, on assigne un poids g par quadrangle vide de $\mathbf{q}$, un poids h par quadrangle traversé par une boucle et enfin un poids n par boucle. On définit aussi la fonction de partition

$$F_k^\circ := \sum_{(\mathbf{q},\boldsymbol{\ell})\in\mathcal{O}_k} W_{(n;g,h)}((\mathbf{q}, \boldsymbol{\ell})), \quad k \in \mathbb{N}.$$

Lorsqu'elle est finie (ce qui ne dépend pas de k) on dit que le triplet $(n; g, h)$ est admissible et la *mesure* $O(n)$ sur $\mathcal{O}_k$ de paramètres $(n; g, h)$ est définie par

$$\mathbf{P}^{(k)}_{(n;g,h)}((\mathbf{q}, \boldsymbol{\ell})) := \frac{W_{(n;g,h)}((\mathbf{q}, \boldsymbol{\ell}))}{F_k^\circ}, \quad (\mathbf{q}, \boldsymbol{\ell}) \in \mathcal{O}_k, \quad k \in \mathbb{N}.$$

Le cas particulier $k = 1$ correspond au modèle $O(n)$ rigide sur les quadrangulations de la sphère, quitte à recoller les deux arêtes du bord entre elles. Une illustration est proposée dans la Figure 2.7. On renvoie à la Section 5.6 pour plus de détails.

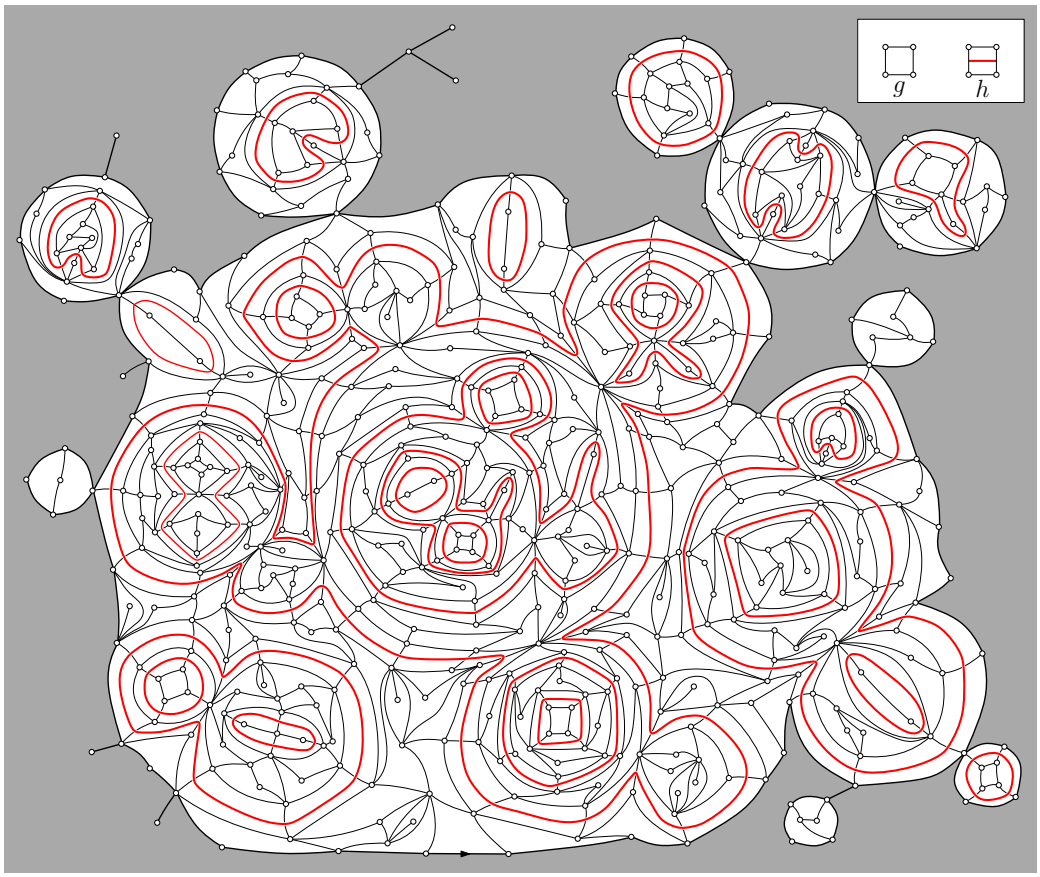

FIGURE 2.7 : Une configuration de boucles rigide sur une quadrangulation à bord.

La décomposition en gasket. La *décomposition en gasket* d'une quadrangulation décorée par des boucles $(\mathbf{q}, \boldsymbol{\ell})$ a été proposée dans [BBG12c]. Elle est obtenue en supprimant l'intérieur des boucles de $(\mathbf{q}, \boldsymbol{\ell})$ les plus à l'extérieur (par rapport à la racine de $\mathbf{q}$). Il est prouvé dans [BBG12c] (voir la Section 5.6) que dans le modèle $O(n)$ rigide sur les quadrangulations de périmètre $2k$, le gasket est une carte de Boltzmann bipartie de loi $\mathbb{P}_{\mathsf{q}}^{(k)}$, où $\mathsf{q} = \mathsf{q}(n; g, h)$ est la solution d'une certaine équation. Ceci conduit à une classification des paramètres $(n; g, h)$ en régimes (sous-)critiques et (non) génériques, selon le type de la suite de poids q. Il a également été montré dans [BBG12c] (et complètement justifié dans [Bud17, Appendice]) que ce modèle admet un diagramme de phase complet reproduit dans la Figure 2.8. En particulier, pour les choix de paramètres non génériques critiques, le gasket est une carte de Boltzmann bipartie non générique critique de paramètre α satisfaisant

$$\alpha = \frac{3}{2} \pm \frac{1}{\pi} \arccos\left(\frac{n}{2}\right).$$

Plus précisément, pour tout $n \in (0, 2)$, il existe une ligne critique $h = h_c(n; g)$ qui sépare les paramètres sous-critiques de ceux pour lesquels le modèle n'est pas défini. Le régime change le long de la ligne critique. Il y a un point spécial $(g^*(n), h^*(n))$ tel que les paramètres critiques sont non génériques critiques de paramètre $\alpha < 3/2$ (dense) lorsque $g < g^*$, et génériques critiques lorsque $g > g^*$. Le point spécial (g^*, h^*) lui-même est non générique critique de paramètre $\alpha > 3/2$ (dilué).

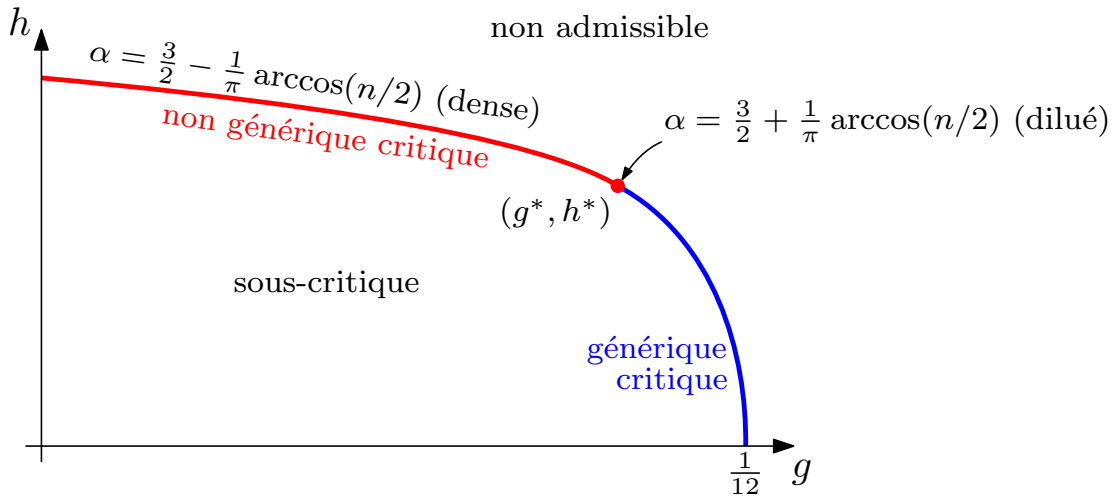

FIGURE 2.8 : Le diagramme de phase du modèle $O(n)$ rigide sur les quadrangulations.

Limites de grandes boucles. L'une des motivations de l'étude du bord des cartes de Boltzmann est la compréhension de la géométrie de grandes boucles du modèle $O(n)$ rigide sur les quadrangulations. Un tel résultat à été établi pour le modèle de percolation par site sur l'UIPT par Nicolas Curien et Igor Kortchemski [CK14a, Théorème 1.2]. Ils ont montré que la limite d'échelle du bord d'un amas de percolation critique conditionné à avoir grand périmètre est l'arbre à boucles stable de paramètre $3/2$ (voir le Théorème 2.4.4). Ils ont également conjecturé que la famille $(\mathscr{L}_\beta : \beta \in (1,2))$ apparaît comme la limite d'échelle de grandes boucles du modèle $O(n)$ sur les triangulations. L'application suivante du Théorème 1 prouve cette conjecture dans le cadre du modèle $O(n)$ rigide sur les quadrangulations.

Théorème 4

Soit $n \in (0,2)$, $g \in [0, g^*(n))$ et $h := h_c(n;g)$. Pour tout $k \geq 1$, soit (Q_k, L_k) une quadrangulation décorée de loi $\mathbf{P}^{(k)}_{(n;g,h)}$. Alors, il existe une constante $C = C(n,g,h)$ telle qu'on ait la convergence en loi au sens de Gromov-Hausdorff

$$\left(\mathrm{V}\left(\partial Q_k\right), \frac{C}{(2k)^{1/\beta}} \cdot d_{\mathrm{gr}}^{\partial Q_k}\right) \xrightarrow[k\to\infty]{(d)} \mathscr{L}_\beta,$$

où $\mathscr{L}_\beta$ est l'arbre à boucles stable de paramètre

$$\beta := \left(1 - \frac{1}{\pi}\arccos\left(\frac{n}{2}\right)\right)^{-1} \in (1,2).$$

La valeur de β dans le théorème précédent correspond effectivement à la prédiction proposée dans [CK14a].

On obtient également des résultats concernant la limite locale des boucles du modèle $O(n)$ comme conséquence du Théorème 2.

Théorème 5

Soit $n \in (0,2)$ et $g, h \geq 0$ tels que $(n; g, h)$ soit admissible. Pour tout $k \geq 1$, soit (Q_k, L_k) une quadrangulation décorée de loi $\mathbf{P}^{(k)}_{(n;g,h)}$. Alors, il existe des mesures de probabilité $\nu_\circ$ (géométrique) et $\nu_\bullet$ telles qu'on ait la convergence en loi pour la topologie locale

$$\mathrm{Scoop}(Q_k) \xrightarrow[k\to\infty]{(d)} \mathbf{L}_\infty(\nu_\circ, \nu_\bullet).$$

De plus,

- Si $(n; g, h)$ est sous-critique, $(\nu_\circ, \nu_\bullet)$ est critique et $\nu_\bullet$ a variance finie.
- Si $h = h_c(n; g)$ et $g < g^*(n)$ (phase dense), $(\nu_\circ, \nu_\bullet)$ est critique et $\nu_\bullet$ est dans le domaine d'attraction d'une loi stable de paramètre $\left(1 - \frac{1}{\pi}\arccos\left(\frac{n}{2}\right)\right)^{-1}$.
- Si $(h, g) = (h^*(n), g^*(n))$ (phase diluée), $(\nu_\circ, \nu_\bullet)$ est sous-critique et $\nu_\bullet$ est dans le domaine d'attraction d'une loi stable de paramètre $1 + \frac{1}{\pi}\arccos\left(\frac{n}{2}\right)$.
- Si $h = h_c(n; g)$ et $g > g^*(n)$ (phase générique critique), $(\nu_\circ, \nu_\bullet)$ est sous-critique et $\nu_\bullet$ est dans le domaine d'attraction d'une loi stable de paramètre $3/2$.

À première vue, les Théorèmes 4 et 5 portent sur le bord de quadrangulations décorées. Néanmoins, par la décomposition en gasket, ils s'appliquent à toute boucle conditionnée à avoir grand périmètre. Plus concrètement, on peut se donner une procédure déterministe pour choisir une boucle dans le modèle $O(n)$ rigide sur les quadrangulations de la sphère (par exemple, en choisissant la boucle la plus proche de la racine), puis conditionner cette boucle à avoir périmètre $2k$. Alors, le contour intérieur de cette boucle est le bord d'une quadrangulation décorée de loi $\mathbf{P}^{(k)}_{(n;g,h)}$. Nous renvoyons à la Section 5.6 pour davantage de précisions.

Notre approche repose sur la technique de décomposition présentée dans la Section 2.1.1. Nous pensons qu'elle peut être adaptée à d'autres modèles $O(n)$, comme ceux de [BBG12b] et [BBG12a]. Ceci inclut en particulier le modèle de Potts et de percolation FK sur des cartes générales qui ont été étudiés dans [BLR15, She11, GMS15, GS15a, GS15b, Che15]. Notons également que l'emboîtement des boucles du modèle $O(n)$ a récemment été étudié dans [BBD16] et [CCM17].

Le cas particulier de la percolation par site critique sur les triangulations, traité dans [BBG12b, Section 4.2, p.23], correspond à un modèle $O(n)$ sur des triangulations avec $n = 1$ et un bon choix de paramètres. L'exposant est le même que dans le cas quadrangulaire, à savoir $\beta = (1 - \arccos(1/2)/\pi)^{-1} = 3/2$, ce qui est cohérent avec le résultat de [CK14a, Théorème 1.2].

2.2 Quadrangulations uniformes infinies du demi-plan avec torsion

Dans cette section, nous allons introduire et étudier une famille de quadrangulations aléatoires avec un bord infini, appelées *Quadrangulations Uniformes Infinies du Demi-Plan avec torsion*. L'intérêt de cette famille réside dans son lien avec certaines *limites d'échelle locales* de quadrangulations définies dans [BMR16], que nous évoquons dans la Section 2.2.1. Les Sections 2.2.2 et 2.2.3 sont dédiées à des résultats de limites locales et de limites d'échelle locales.

2.2.1 Limites d'échelle locales de quadrangulations

L'idée générale des résultats de limites d'échelle locales de cartes aléatoires est soit de faire un "zoom arrière" sur les cartes aléatoires infinies de la Section 1.4, soit à l'inverse de faire un "zoom avant" près d'un sommet typique dans l'un des espaces métriques aléatoires compacts de la Section 1.2. On obtient ainsi des espaces métriques aléatoires non compacts. Pour ce faire, on utilise une notion de convergence mélangeant les idées de la convergence au sens de Gromov-Hausdorff et de la convergence locale : la *convergence locale au sens de Gromov-Hausdorff*, dont la définition se trouve dans la Section 4.1.2.

Le premier résultat de ce type a été montré par Nicolas Curien et Jean-François Le Gall [CLG13], qui ont obtenu le *plan brownien* (BP) comme limite de l'UIPQ lorsque les distances sont multipliées par un facteur tendant vers zéro, et de la carte brownienne BM lorsque les distances sont multipliées par un facteur tendant vers l'infini. Le plan brownien est également la limite de quadrangulations à n faces uniformes lorsque les distances sont renormalisées par un facteur négligeable devant $n^{1/4}$. Ce résultat a été étendu aux quadrangulations à bord par Erich Baur, Grégory Miermont et Gourab Ray [BMR16], qui ont introduit le *demi-plan brownien* (BHP), voir aussi [GM16]. Cet objet est obtenu comme limite de l'UIHPQ lorsque les distances sont multipliées par un facteur tendant vers zéro, ou bien comme limite du disque brownien BD_σ de périmètre σ (quelconque) près d'un point typique de son bord lorsque les distances sont multipliées par un facteur tendant vers l'infini. À l'instar du plan brownien, le demi-plan brownien est également la limite de quadrangulations à bord avec n faces internes et demi-périmètre $k_n \sim \sigma\sqrt{2n}$ uniformes lorsque les distances sont renormalisées par un facteur négligeable devant $n^{1/4}$.

Les résultats de [BMR16] sont en fait bien plus précis, et fournissent une classification complète de toutes les limites d'échelle locales non compactes de quadrangulations à bord uniformes dont le volume et le périmètre tendent vers l'infini (le cas des limites compactes ayant été traité dans [Bet15, BM15]), voir le diagramme de la Figure 2.9. Cette classification fait intervenir de nombreux espaces métriques aléatoires. On y trouve en particulier des versions infinies du disque brownien (IBD) et de l'arbre continu brownien (ICRT), ainsi qu'une version du demi-plan brownien *avec torsion* $\theta \geq 0$ (BHP_θ). On renvoie à la Section 4.3.1 pour des définitions précises.

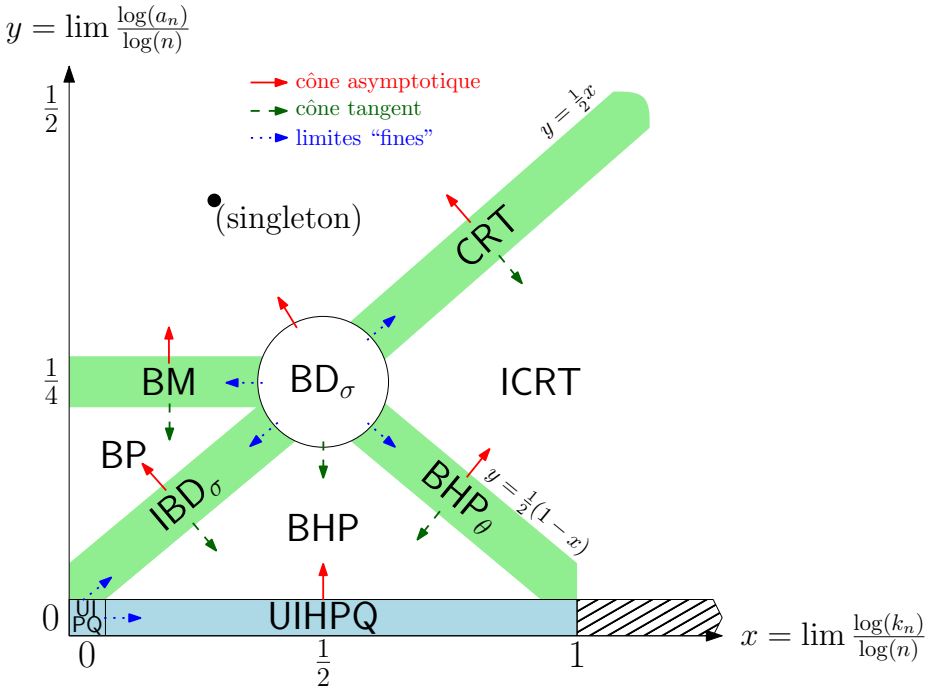

FIGURE 2.9 : La classification des limites de $(\mathrm{V}(Q_n^{k_n}), a_n^{-1} \cdot d_{\mathrm{gr}}^{Q_n^{k_n}}, \rho_n)$, avec $Q_n^{k_n}$ une quadrangulation à n faces internes de périmètre $2k_n$ uniforme (d'origine ρ_n), et a_n un facteur de renormalisation. (En fonction de $x = \log(k_n)/\log(n)$ et $y = \log(a_n)/\log(n)$.)

La classification de [BMR16] est le point de départ de notre étude. D'une part, on s'intéresse au régime $x \geq 1$ et $y = 0$ du diagramme de la Figure 2.9 (voir la partie rayée), qui n'a pas été étudié dans [BMR16]. D'autre part, on cherche à construire une quadrangulation aléatoire à bord infini qui joue vis-à-vis du demi-plan brownien avec torsion un rôle analogue à l'UIHPQ pour le demi-plan brownien.

2.2.2 Limites locales

Notre premier résultat définit les Quadrangulations Uniformes Infinies du Demi-Plan avec torsion comme limites locales de quadrangulations à bord uniformes dont le périmètre et le volume tendent vers l'infini de manière adéquate. On rappelle que pour tout $n \geq 0$ et $k \geq 1$, $\mathbb{P}_{n,k}^{\square}$ désigne la mesure uniforme sur l'ensemble $\mathcal{M}_{n,k}^{\square}$ des quadrangulations à bord (général) avec n faces internes et périmètre $2k$.

Théorème 6 (avec Erich Baur)

Soit $0 \leq p \leq 1/2$, et $(k_n : n \in \mathbb{N})$ une suite d'entiers strictement positifs tels que

$$k_n = \frac{1-2p}{p} n + o(n) \quad \text{si} \quad 0 < p \leq 1/2, \quad \text{et} \quad k_n \gg n \quad \text{si} \quad p = 0.$$

Alors, au sens faible, pour la topologie locale

$$\mathbb{P}_{n,k_n}^{\square} \underset{n\to\infty}{\Longrightarrow} \mathbb{P}_{\infty,\infty}^{\square}(p).$$

Une variable aléatoire de loi $\mathbb{P}^{\square}_{\infty,\infty}(p)$ est appelée Quadrangulation Uniforme Infinie du Demi-Plan avec torsion p (UIHPQ$_p$). Le Théorème 6 montre que la famille (UIHPQ$_p$: $0 \leq p \leq 1/2$) correspond effectivement au régime $x \geq 1$ et $y = 0$ de la Figure 2.9. L'UIHPQ$_p$ peut également être construite à partir des techniques bijectives mentionnées dans la Section 1.4.3, comme nous le verrons dans la Section 4.4.3. À partir de cette construction, on montre que la famille (UIHPQ$_p$: $0 \leq p \leq 1/2$) interpole entre l'arbre de Kesten associé à la loi géométrique critique (UIHPQ$_0$), et l'UIHPQ à bord général (UIHPQ$_{1/2}$), voir notamment la Proposition 4.2.2.

L'UIHPQ$_p$ apparaît également comme limite locale de quadrangulations de Boltzmann dont le périmètre tend vers l'infini, comme nous l'avons déjà vu au Théorème 1.4.8 pour l'UIHPQ. Précisément, on considère la mesure de Boltzmann $\mathbb{P}^{(k)}_{\mathsf{q}}$ sur les cartes biparties de périmètre $2k$, définie dans (1.15), et on se ramène aux quadrangulations en faisant le choix de suite de poids $q_k = g\delta_2(k)$. Cette suite est admissible dès que $g \leq 1/12$, critique pour $g = 1/12$ et sous-critique pour $g < 1/12$ (voir [BG09, Section 4.1]). On note $\mathbb{P}^{(k)}_{g}$ la mesure de probabilité associée.

Proposition 7 (avec Erich Baur)

Soit $0 \leq p \leq 1/2$, et $g_p := p(1-p)/3$. Alors, on a la convergence en loi pour la topologie locale

$$\mathbb{P}^{(k)}_{g_p} \underset{k\to\infty}{\Longrightarrow} \mathbb{P}^{\square}_{\infty,\infty}(p).$$

Par le Théorème 1.4.8, l'UIHPQ$_p$ est donc une Carte de Boltzmann Infinie du Demi-Plan (q-IBHPM) pour le choix précédent de suite de poids q. En particulier, l'UIHPQ$_p$ est presque sûrement une carte infinie du demi-plan à bord général. La Proposition 3 fournit ainsi une décomposition de l'UIHPQ$_p$ en une structure arborescente de quadrangulations de Boltzmann à bord simple pour $p \in [0, 1/2)$ (voir la Section 4.6). En utilisant également la Proposition 4.2.2 et le Théorème 1.4.6, ceci détermine la géométrie du bord de l'UIHPQ$_p$, qui est illustrée dans la Figure 2.10.

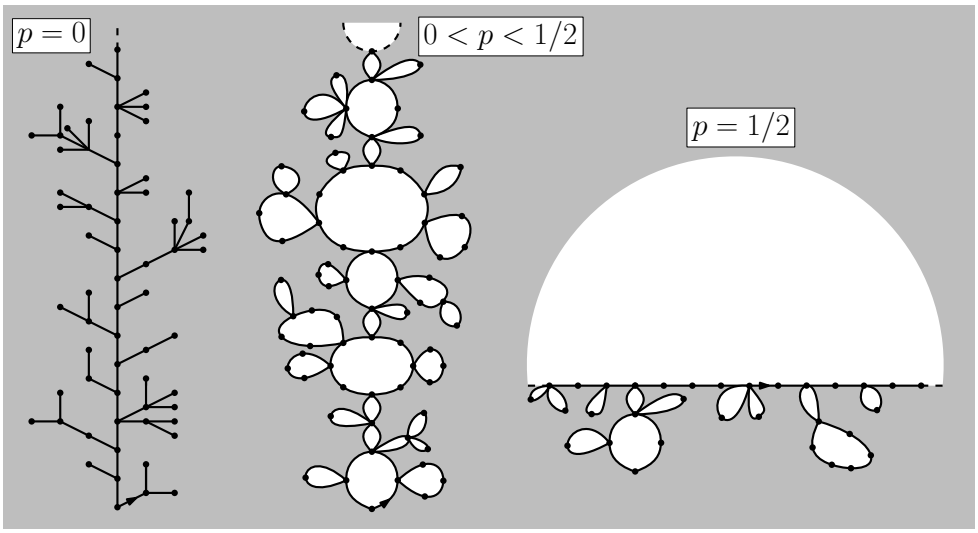

FIGURE 2.10 : Représentation schématique du bord de l'UIHPQ$_p$, pour $p \in [0, 1/2]$.

2.2.3 Limites d'échelle locales

Nous nous intéressons maintenant aux limites d'échelle locales des Quadrangulations Uniformes Infinies du Demi-Plan avec torsion. Pour $p \in [0, 1/2]$, soit $\mathbf{Q}_\infty^\infty(p)$ une variable aléatoire de loi $\mathbb{P}^{\square}_{\infty,\infty}(p)$ munie de la distance de graphe $d_{\mathrm{gr}}^{(p)}$ et de son sommet origine ρ_p. Notre résultat principal est que l'UIHPQ$_p$ approche le demi-plan brownien avec torsion BHP$_\theta$ localement au sens de Gromov-Hausdorff lorsque le paramètre de torsion et le facteur de renormalisation sont convenablement choisis.

Théorème 8 (avec Erich Baur)

Soit $\theta \geq 0$, et $(a_n : n \in \mathbb{N})$ une suite de réels strictement positifs tels que $a_n \to \infty$ quand $n \to \infty$. Soit $(p_n : n \in \mathbb{N}) \subset [0, 1/2]$ une suite de réels telle que

$$p_n = p_n(\theta, a_n) = \frac{1}{2}\left(1 - \frac{2\theta}{3a_n^2}\right) + o\left(a_n^{-2}\right).$$

Alors, on a la convergence en loi, localement au sens de Gromov-Hausdorff

$$\left(\mathrm{V}\left(\mathbf{Q}_\infty^\infty(p_n)\right), \frac{1}{a_n} \cdot d_{\mathrm{gr}}^{(p_n)}, \rho_{p_n}\right) \xrightarrow[n\to\infty]{(d)} \mathrm{BHP}_\theta.$$

En combinant [BM15, Théorème 1], [BMR16, Corollaire 3.17] et [BMR16, Théorème 3.4] avec les Théorèmes 6 et 8, on obtient le diagramme de convergence de la Figure 2.11, qui est l'analogue de ceux obtenus dans [CLG13, BMR16] pour le plan et le demi-plan browniens. Toutefois, le résultat du Théorème 8 nécessite de choisir convenablement le paramètre de torsion en fonction du facteur de renormalisation, ce qui n'est pas le cas pour la convergence de l'UIHPQ vers le BHP.

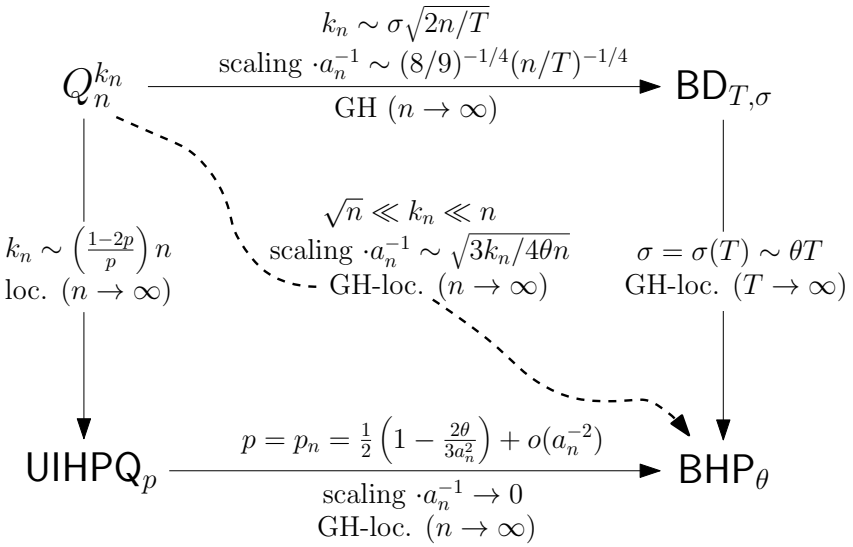

FIGURE 2.11 : Le diagramme de convergence vers le demi-plan brownien avec torsion. Dans ce diagramme, $\mathrm{BD}_{T,\sigma}$ désigne le disque brownien de volume T et de périmètre σ introduit dans [BM15], et $Q_n^{k_n}$ une quadrangulation à bord avec n faces internes et périmètre $2k_n$ uniforme.

Il est également montré dans [BMR16, Remarque 3.19] que l'on a la convergence en loi du BHP_θ vers l'ICRT, localement au sens de Gromov-Hausdorff, lorsque le paramètre de torsion θ tend vers l'infini. Il est donc naturel que l'ICRT apparaisse comme limite d'échelle locale de l'UIHPQ_{p_n}, lorsque θ est remplacé par une suite θ_n tendant vers l'infini dans la définition de p_n donnée au Théorème 8.

Théorème 9 (avec Erich Baur)

Soit $(a_n : n \in \mathbb{N})$ une suite de réels strictement positifs tels que $a_n \to \infty$ quand $n \to \infty$. Soit $(p_n, n \in \mathbb{N}) \subset [0, 1/2]$ une suite de réels telle que

$$a_n^2(1 - 2p_n) \underset{n\to\infty}{\longrightarrow} \infty.$$

Alors, on a la convergence en loi, localement au sens de Gromov-Hausdorff

$$\left(\mathrm{V}\left(\mathbf{Q}_\infty^\infty(p_n)\right), \frac{1}{a_n} \cdot d_{\mathrm{gr}}^{(p_n)}, \rho_{p_n}\right) \underset{n\to\infty}{\overset{(d)}{\longrightarrow}} \mathsf{ICRT}.$$

Ce résultat permet de compléter la classification de la Figure 2.9, en déterminant l'ensemble des convergences locales au sens de Gromov-Hausdorff de la famille $(\mathsf{UIHPQ}_p : 0 \leq p \leq 1/2)$ vers les espaces métriques aléatoires de cette classification.

2.3 Géodésiques de la quadrangulation uniforme infinie du demi-plan

Une manière de comprendre la géométrie d'un espace métrique est d'étudier ses géodésiques, ou plus courts chemins. C'est notamment une étude très fine des géodésiques qui a permis de montrer l'unicité de la carte brownienne [LG10, LG13, Mie13]. Nous nous intéressons ici aux géodésiques de limites locales de cartes aléatoires. Commençons par une définition.

Définition 2.3.1. Une géodésique γ dans un graphe G est un chemin (éventuellement infini) dans G, visitant une suite de sommets $(\gamma(0), \gamma(1), \ldots)$ de G, tel que

$$d_{\mathrm{gr}}^G(\gamma(i), \gamma(j)) = |i - j|, \quad \text{pour tous } \; i, j \in \mathbb{Z}_+.$$

Une géodésique infinie γ avec $\gamma(0) = v \in V$ est appelée *rayon géodésique* issu de v.

Dans la suite, on s'intéresse en particulier aux propriétés de *confluence* des géodésiques vers l'infini. Le cas de l'UIPQ a été traité par Nicolas Curien, Laurent Ménard et Grégory Miermont [CMM13].

Théorème 2.3.2. ([CMM13, Théorème 2]) *Soit $\mathbf{Q}_\infty$ une variable aléatoire ayant la loi de l'*UIPQ*. Presque sûrement, il existe une suite infinie $(v_1, v_2, \ldots)$ de sommets distincts de $\mathbf{Q}_\infty$ telle que tout rayon géodésique issu de l'origine dans $\mathbf{Q}_\infty$ passe par $(v_1, v_2, \ldots)$.*

Les rayons géodésiques issus de l'origine dans l'UIPQ sont confluents à l'infini. On dit que l'UIPQ a un seul *bout géodésique*. L'UIPQ satisfait également une propriété de confluence des géodésiques vers la racine, voir [CMM13, Section 3.1]. La preuve du Théorème 2.3.2 repose sur une représentation de l'UIPQ par un arbre bien étiqueté infini. Ce résultat a été étendu à l'UIHPQ (à bord général) par Alessandra Caraceni et Nicolas Curien [CC15].

Théorème 2.3.3. ([CC15, Corollaire 4.6]) *Soit $\mathbf{Q}_\infty^\infty$ une variable aléatoire ayant la loi de l'*UIHPQ *à bord général. Presque sûrement, il existe une suite infinie $(v_1, v_2, \ldots)$ de sommets distincts de $\mathbf{Q}_\infty^\infty$ telle que tout rayon géodésique issu de l'origine dans $\mathbf{Q}_\infty^\infty$ passe par $(v_1, v_2, \ldots)$.*

Notons que d'autres propriétés des géodésiques de l'UIHPQ ont été établies dans [CC15]. Les géodésiques de l'UIHPQ possèdent donc la même propriété de confluence à l'infini que celles de l'UIPQ. L'UIHPQ étant une quadrangulation à bord infini, on peut également se demander si les géodésiques visitent le bord une infinité de fois ou non. Cette question, posée par Nicolas Curien, est à l'origine du résultat suivant.

Théorème 10 (avec Erich Baur et Grégory Miermont)

Soit $\mathbf{Q}_\infty^\infty$ une variable aléatoire ayant la loi de l'UIHPQ à bord général. Presque sûrement, il existe une suite infinie $(v_1, v_2, \ldots)$ de sommets distincts **du bord** $\partial\mathbf{Q}_\infty^\infty$ de $\mathbf{Q}_\infty^\infty$ telle que tout rayon géodésique dans $\mathbf{Q}_\infty^\infty$ passe par tous les sommets $(v_1, v_2, \ldots)$, sauf éventuellement un nombre fini.

Comme dans [CMM13, CC15], notre approche repose sur une construction de l'UIHPQ par des techniques bijectives. Un rôle particulier est joué par les géodésiques dites *maximale* (la plus à gauche) et *minimale* (la plus à droite) issues de la racine, qui enserrent tous les rayons géodésiques issus de la racine (voir la Figure 2.12).

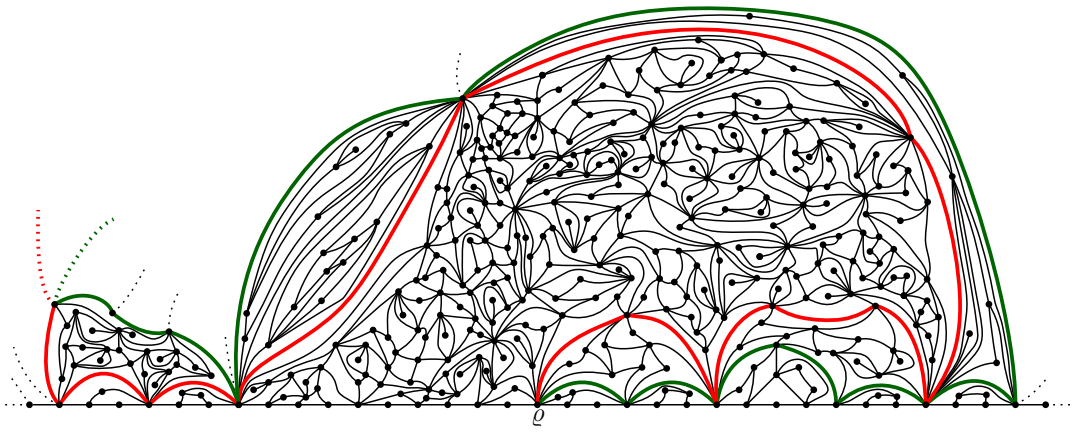

FIGURE 2.12 : L'UIHPQ et ses géodésiques maximale (rouge) et minimale (vert).

Nous montrons également que les retours au bord des rayons géodésiques issus de l'origine sont très rares, au sens suivant. On rappelle qu'un *ensemble régénératif* est un sous-ensemble $\mathcal{R}$ de $\mathbb{Z}_+$ de la forme $\mathcal{R} = \{G_0 + \ldots + G_n : n \in \mathbb{Z}_+\}$, où $(G_i : i \in \mathbb{Z}_+)$ est une famille de variables aléatoires indépendantes et de même loi.

Proposition 11 (avec Erich Baur et Grégory Miermont)

Soit $\mathbf{Q}_\infty^\infty$ une variable aléatoire ayant la loi de l'UIHPQ à bord général. Alors, il existe des ensembles régénératifs $\mathcal{R}_+$ et $\mathcal{R}_-^{\min}$ (de même loi) et $\mathcal{R}_+^{\min}$ et $\mathcal{R}_-$ (de même loi) tels que presque sûrement, pour tout rayon géodésique $\gamma = (\gamma(i) : i \in \mathbb{Z}_+)$ issu de l'origine, on ait

$$\mathcal{R}_+ \cup \mathcal{R}_-^{\min} \subseteq \{i \in \mathbb{Z}_+ : \gamma(i) \in \partial \mathbf{Q}_\infty^\infty\} \subseteq \mathcal{R}_+^{\min} \cup \mathcal{R}_-.$$

De plus, la distance δ entre deux éléments consécutifs de $\mathcal{R}_+$ (ou $\mathcal{R}_-^{\min}$) satisfait $\mathbb{P}(\delta > m) \sim 1/\ln(m)$ quand $m \to \infty$, alors que la distance δ' entre deux éléments consécutifs de $\mathcal{R}_+^{\min}$ (ou $\mathcal{R}_-$) vérifie $\mathbb{P}(\delta' > m) \sim 1/(3\ln(m))$.

Les ensembles régénératifs $\mathcal{R}_-$, $\mathcal{R}_+$, $\mathcal{R}_-^{\min}$ et $\mathcal{R}_+^{\min}$ sont en fait donnés par les retours sur le bord gauche et droit des géodésiques maximale et minimale. Enfin, nous verrons au Théorème 3.5.3 que ces résultats peuvent être étendus à l'UIHPT.

2.4 Percolation sur les cartes aléatoires

Le modèle de *percolation de Bernoulli*, introduit par Simon Broadbent et John Hammersley [BH57] figure parmi les modèles de physique statistique les plus célèbres et les plus simples. Son but est la modélisation des phénomènes de propagation dans les milieux poreux. Il possède des propriétés étonnantes et recèle des problèmes ouverts notoirement difficiles, voir [Gri99]. On peut s'attendre à ce que l'étude des modèles de physique statistique dans des réseaux eux-mêmes aléatoires soit plus complexe que dans des réseaux euclidiens (réguliers). Par exemple, la récurrence de la marche aléatoire simple symétrique sur l'UIPT (conjecturée dès 2003 dans [AS03]) a été démontrée en 2012 par Ori Gurel-Gurevich et Asaf Nachmias [GGN12], alors que ce résultat est classique sur $\mathbb{Z}^2$. Néanmoins, certaines propriétés des cartes aléatoires, notamment la propriété de Markov spatiale, permettent de simplifier l'étude d'autres modèles de physique statistique sur les cartes aléatoires comme la percolation.

Dans la suite, nous allons nous intéresser à des problèmes naturels du point de vue du modèle de percolation, comme le calcul des seuils critiques dans la Section 2.4.2, les propriétés d'universalité au point critique dans la Section 2.4.3 ou encore la forme de grandes interfaces et amas dans la Section 2.4.4.

2.4.1 Définition du modèle

Le modèle de percolation de Bernoulli sur un graphe est défini en déclarant chaque sommet (arête, face) *ouvert* (ou noir) avec probabilité $p \in [0,1]$ et *fermé* (ou blanc) sinon, indépendamment des autres sommets (arêtes, faces). On distingue donc trois modèles : la percolation par site (ou par sommet), par arête, et par face.

Soit $\mathbb{P}$ une mesure de probabilité sur l'ensemble $\mathcal{M}$ des cartes (éventuellement infinies). Pour toute carte $\mathbf{m} \in \mathcal{M}$, on définit la mesure sur l'ensemble $\{0,1\}^{e(\mathbf{m})}$ des

coloriages de $\mathbf{m}$ (où $e(\mathbf{m})$ est l'ensemble des sommets, arêtes ou faces de $\mathbf{m}$) :

$$\mathcal{P}_p^{e(\mathbf{m})} := (p\delta_1 + (1-p)\delta_0)^{\otimes e(\mathbf{m})}.$$

La mesure de probabilité $\mathbf{P}_p$ induite par le modèle de percolation sur une carte de loi $\mathbb{P}$ est définie sur l'ensemble des cartes coloriées $\{(\mathbf{m}, c) : \mathbf{m} \in \mathcal{M}, c \in \{0,1\}^{e(\mathbf{m})}\}$ par

$$\mathbf{P}_p(\mathrm{d}\mathbf{m}\mathrm{d}c) := \mathbb{P}(\mathrm{d}\mathbf{m})\mathcal{P}_p^{e(\mathbf{m})}(\mathrm{d}c).$$

En d'autres termes, $\mathbf{P}_p$ est la mesure sur l'ensemble des cartes coloriées telle que la carte a la loi $\mathbb{P}$, et conditionnellement à celle-ci, le coloriage est donné par une percolation de Bernoulli de paramètre p. Lorsque $\mathbb{P}$ ne charge que des cartes à bord infini (par exemple l'UIHPT et l'UIHPQ), on travaille souvent conditionnellement au coloriage du bord de la carte, que l'on appelle la *condition au bord*.

2.4.2 Seuils de percolation

Une propriété importante du modèle de percolation est l'existence d'une *transition de phase*. Pour la comprendre, il faut s'intéresser aux *amas* ou *clusters* de percolation. Pour simplifier, on se contente des définitions pour le cas de la percolation par site. L'amas de percolation ouvert issu du sommet v d'une carte coloriée est l'ensemble des sommets reliés à v par un chemin formé entièrement de sommets ouverts, ainsi que toutes les arêtes reliant ces sommets (de même pour l'amas fermé). On considérera également l'*enveloppe* $\mathcal{H}$ d'un amas $\mathcal{C}$, qui est la carte coloriée obtenue en ajoutant à $\mathcal{C}$ toutes les composantes connexes finies de son complémentaire dans la carte. Voir la Figure 2.13 pour un exemple, et la Section 7.2.1 pour plus de détails.

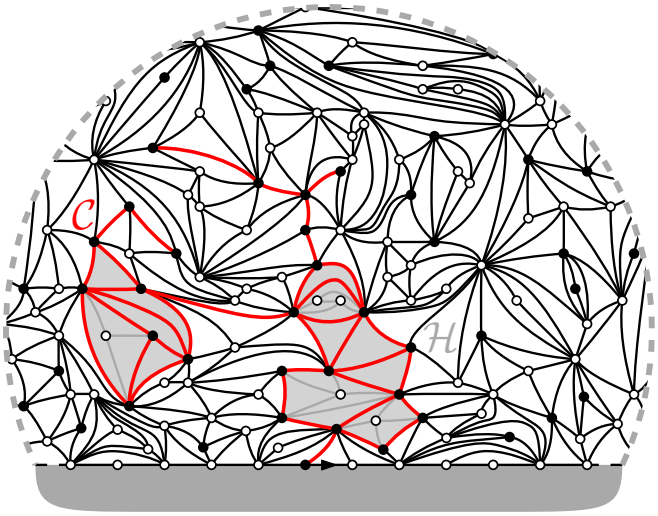

FIGURE 2.13 : Un amas de percolation $\mathcal{C}$ dans l'UIHPT et son enveloppe $\mathcal{H}$.

Définissons maintenant le *seuil de percolation* (ou *point critique*). L'*évènement de percolation* est réalisé lorsque le nombre total de sommets $|\mathcal{C}|$ de l'amas ouvert issu de l'origine $\mathcal{C}$ est infini. La probabilité de percolation est alors définie par

$$\Theta(p) := \mathbf{P}_p(|\mathcal{C}| = \infty), \quad p \in [0,1].$$

Par un argument de couplage, on peut montrer que Θ est une fonction croissante. Il existe donc un point critique p_c, appelé seuil de percolation, tel que

$$\begin{cases} \Theta(p) = 0 & \text{si} \quad p < p_c \\ \Theta(p) > 0 & \text{si} \quad p > p_c \end{cases}.$$

Le calcul des seuils de percolation est un objectif très naturel. Dans les réseaux réguliers, on dispose d'une formule exacte pour les seuils de percolation par site sur le réseau triangulaire, et par arête sur les réseaux triangulaire et carré. En ce qui concerne les cartes aléatoires, le premier seuil a avoir été calculé est le seuil de percolation par site sur l'UIPT, par Omer Angel [Ang03].

Théorème 2.4.1. ([Ang03, Théorème 1.5]) *Le seuil de percolation par site sur l'*UIPT *est*

$$p_c = \frac{1}{2}.$$

De plus, il n'y a pas de percolation au point critique presque sûrement : $\Theta(p_c) = 0$.

Plus tard, Laurent Ménard et Pierre Nolin [MN14, Théorème 1] sont parvenus à calculer, entre autres, le seuil de percolation par arête sur l'UIPQ, égal à $1/3$. Enfin, Nicolas Curien [Cur16a, Théorème 13] a obtenu une formule fermée pour les seuils de percolation par arête et par face sur toutes les Cartes de Boltzmann Infinies du Plan (q-IBPM). Tous ces résultats reposent sur des techniques d'épluchage.

L'étude des seuils de percolation sur les cartes uniformes infinies du demi-plan est plus aisée, en raison de la forme plus simple prise par la propriété de Markov spatiale. On s'intéresse maintenant à l'UIHPT et l'UIHPQ (à bord simple). Les résultats suivants ont été obtenus par Omer Angel et Nicolas Curien [Ang04, AC15].

Théorème 2.4.2. ([Ang04, AC15]) *Les seuils de percolation dans l'*UIHPT *sont donnés par*

$$p_{c,\text{site}}^{\triangle} = \frac{1}{2}, \quad p_{c,\text{arête}}^{\triangle} = \frac{1}{4} \quad \textit{et} \quad p_{c,\text{face}}^{\triangle} = \frac{4}{5}.$$

*Les seuils de percolation dans l'*UIHPQ *sont donnés par*

$$p_{c,\text{arête}}^{\square} = \frac{1}{3} \quad \textit{et} \quad p_{c,\text{face}}^{\square} = \frac{3}{4}.$$

De plus, il n'y a pas de percolation au point critique presque sûrement.

Ces résultats ont également été étendus, pour la percolation par arête et par faces, à toutes les Cartes de Boltzmann Infinies du Demi-Plan (q-IBHPM) par Nicolas Curien [Cur16a, Théorèmes 10 et 12]. Le résultat suivant complète le Théorème 2.4.2. Ici, la condition au bord *libre* signifie que les sommets du bord de la carte sont ouverts avec probabilité p et fermés sinon, indépendamment de tous les autres sommets.

Théorème 12

Le seuil de percolation par site sur l'UIHPQ avec condition au bord libre est donné par

$$p_{c,\text{site}}^{\square} = \frac{5}{9}.$$

De plus, il n'y a pas de percolation au point critique presque sûrement.

À première vue, le cas de la percolation par site sur l'UIHPQ peut sembler plus délicat parce que le processus d'épluchage standard est mal défini. On peut toutefois contourner cette difficulté en utilisant un processus d'épluchage adapté (voir l'Algorithme 6.3.1). Dans l'esprit des résultats de [AC15] et [Cur16a], on obtient également une expression des seuils de percolation par site dans l'UIHPT et l'UIHPQ en termes de quantités associées au processus d'épluchage (voir le Théorème 6.3.9). Ce résultat est toujours ouvert dans le cas des Cartes de Boltzmann Infinies du Demi-Plan. Un encadrement de $p_{c,\text{site}}^{\square}$ a également été obtenu par Jakob Björnberg et Sigurður Örn Stefánsson [BS15, Proposition 1.4].

2.4.3 Universalité de la percolation au point critique

Une part importante de la théorie de la percolation dans les réseaux réguliers consiste à étudier les propriétés des modèles au point critique. L'un des résultats les plus spectaculaires dans cette direction a été obtenu par Stanislav Smirnov [Smi01], qui a montré l'invariance conforme asymptotique des *probabilités de croisement* pour la percolation par site dans le réseau triangulaire, ainsi que la *formule de Cardy* (qui en donne une formule explicite). En s'inspirant du résultat de Stanislav Smirnov, Omer Angel a introduit dans [Ang04] une notion de probabilité de croisement asymptotique dans l'UIHPT. Pour cela, on considère un modèle de percolation par site critique sur l'UIHPT ($p = 1/2$), avec la condition au bord de la Figure 2.14, où $a, b \geq 0$ sont fixés et $\lambda > 0$ est un facteur d'échelle.

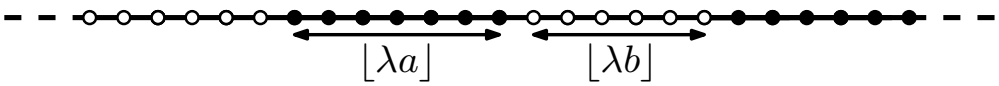

FIGURE 2.14 : La condition au bord pour l'étude des probabilités de croisement.

L'*évènement de croisement* $\mathsf{C}(\lambda a, \lambda b)$ est réalisé si les deux segments ouverts du bord sont reliés par un chemin ouvert, c'est-à-dire s'ils font partie du même amas de percolation. On s'intéresse à la limite d'échelle de la probabilité de cet évènement lorsque le paramètre λ tend vers l'infini. Le résultat suivant est dû à Omer Angel.

Théorème 2.4.3. ([Ang04, Théorème 3.3]) *Soient $a, b \geq 0$. Pour la percolation par site critique sur l'*UIHPT*, on a*

$$\lim_{\lambda\to\infty} \mathbf{P}_{p_c}\left(\mathsf{C}_{site}^{\triangle}(\lambda a, \lambda b)\right) = \frac{1}{\pi}\arccos\left(\frac{b-a}{a+b}\right).$$

Ce résultat peut être considéré comme un analogue de la formule de Cardy dans l'UIHPT, où l'on utilise le demi-plan comme domaine de référence au lieu d'un triangle équilatéral. Dans les réseaux réguliers, une conjecture importante appelée *conjecture d'universalité de Cardy* stipule que la limite d'échelle des probabilités de croisement (au point critique) ne doit pas dépendre de la maille du réseau (triangulaire, carré, hexagonal...) ni du type de modèle de percolation (par site, par arête, par face). Le but du résultat suivant est de vérifier partiellement cette conjecture dans les cartes uniformes infinies du demi-plan.

Théorème 13

Soient $a, b \geq 0$. Pour les modèles de percolation par site, par arête et par face critiques sur l'UIHPT et l'UIHPQ,

$$\lim_{\lambda \to \infty} \mathbf{P}_{p_c} \left(\mathsf{C}(\lambda a, \lambda b) \right) = \frac{1}{\pi} \arccos \left(\frac{b-a}{a+b} \right).$$

En d'autres termes, la limite d'échelle des probabilités de croisement est la même pour la percolation par site, par arête et par face sur l'UIHPT et l'UIHPQ au point critique.

Ce résultat illustre l'universalité de la percolation au point critique dans les cartes uniformes infinies du demi-plan. Il repose également des techniques d'épluchage.

2.4.4 Limites de grands amas de percolation critiques

Un objectif naturel de la théorie de la percolation, et plus généralement de la physique statistique, est de comprendre la géométrie de grandes interfaces et de grands amas au point critique. En ce qui concerne la percolation sur les cartes aléatoires, le résultat le plus important a été obtenu par Nicolas Curien et Igor Kortchemski [CK14a], dans le cadre de la percolation par site critique sur l'UIPT. Pour tout $k \geq 1$, on note $\partial \mathcal{H}_k$ le bord de l'enveloppe de l'amas ouvert issu de l'origine, conditionné à avoir périmètre k.

Théorème 2.4.4. ([CK14a, Théorème 1.2]) *Dans le modèle de percolation par site critique sur l'*UIPT *($p = 1/2$), on a la convergence en loi au sens de Gromov-Hausdorff*

$$\left(\mathrm{V}\left(\partial \mathcal{H}_k\right), \frac{3^{-1/3}}{k^{2/3}} \cdot d_{\mathrm{gr}}^{\partial \mathcal{H}_k} \right) \xrightarrow[k \to \infty]{(d)} \mathscr{L}_{3/2},$$

où $\mathscr{L}_{3/2}$ est l'arbre à boucles stable de paramètre $3/2$.

Ce résultat nous a notamment servi de référence pour les Théorèmes 4 et 5, qui traitent des limites de grandes boucles dans le modèle $O(n)$ rigide sur les quadrangulations. Le but de cette section est de décrire d'une part la limite locale de grands amas de percolation critiques dans l'UIHPT, mais aussi la limite locale de l'UIHPT toute entière conditionnée à avoir un amas de percolation critique *infini*. Cette idée est due à Harry Kesten [Kes86a], qui a construit un tel objet pour la percolation par arête critique sur le réseau carré $\mathbb{Z}^2$ sous le nom d'*amas critique émergent*. Dans le résultat suivant $[-n, n]^2$ désigne l'ensemble $\{(i, j) : -n \leq i, j \leq n\}$ et $\{0 \leftrightarrow \mathbb{Z}^2 \backslash [-n, n]^2\}$ l'évènement "l'origine est reliée à $\mathbb{Z}^2 \backslash [-n, n]^2$ par un chemin ouvert".

Théorème 2.4.5. ([Kes86a]) *Pour la percolation par arête sur $\mathbb{Z}^2$, les limites*

$$\lim_{n \to \infty} \mathbf{P}_{p_c} \left(\cdot \mid 0 \leftrightarrow \mathbb{Z}^2 \backslash [-n, n]^2 \right) \quad \textit{et} \quad \lim_{p \downarrow p_c} \mathbf{P}_p \left(\cdot \mid |\mathcal{C}| = \infty \right)$$

existent et sont égales. La mesure de probabilité limite, notée $\mathbf{P}_{\mathsf{IIC}}$, est appelée (loi de l') amas critique émergent de la percolation par arête sur $\mathbb{Z}^2$.

La mesure de probabilité $\mathbf{P}_{\text{IIC}}$ présente un caractère universel, en ce sens qu'elle apparaît à la fois en conditionnant un amas critique à être grand, mais aussi en conditionnant un amas sur-critique à être infini et en faisant décroître le paramètre p vers la valeur critique p_c. Le Théorème 2.4.5 est en fait valable dans une plus grande généralité, voir [Kes86a].

On se place maintenant dans le modèle de percolation par site sur l'UIHPT. Avant d'énoncer les résultats, on commence par quelques définitions.

Collier uniforme infini. Les *colliers* sont des cartes qui ont d'abord été introduites dans [BBG12c] pour étudier le modèle $O(n)$, voir également [CK14a]. Dans le cadre qui nous intéresse, un *collier infini* est une triangulation du demi-plan à bord simple sans sommet interne. Considérons le graphe de $\mathbb{Z}$ plongé dans le plan, enraciné en l'arête $(0,1)$. Soit $(z_i : i \in \mathbb{N})$ une suite de variables de loi de Bernoulli de paramètre $1/2$ indépendantes. On définit la marche aléatoire simple

$$S_k := \sum_{i=1}^{k} z_i, \quad k \in \mathbb{N}.$$

Le *collier uniforme infini* est la carte infinie obtenue à partir de $\mathbb{Z}$ en ajoutant les arêtes $\{(-S_k, k+1-S_k) : k \in \mathbb{N}\}$ de manière propre (voir la Figure 2.15).

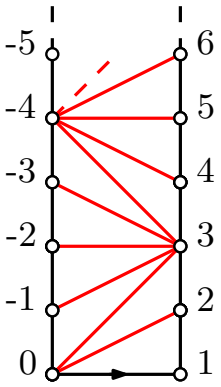

FIGURE 2.15 : Le collier uniforme infini.

Dans la suite, nous allons nous intéresser au recollement de cartes à bord le long de colliers. Soient $\mathbf{m}, \mathbf{m}' \in \mathcal{M}_\infty$ des cartes à bord infini, et $\mathbf{n}$ un collier infini. Le recollement $\Psi_{\mathbf{n}}(\mathbf{m}, \mathbf{m}')$ de $\mathbf{m}$ et $\mathbf{m}'$ le long de $\mathbf{n}$ est obtenu en identifiant le bord droit de $\mathbf{m}$ avec le bord gauche de $\mathbf{n}$, et le bord gauche de $\mathbf{m}'$ avec le bord droit de $\mathbf{n}$. On définit de manière similaire le recollement $\Psi_{(\mathbf{n},\mathbf{n}')}(\mathbf{m}, \mathbf{m}', \mathbf{m}'')$ de trois cartes à bord infini $\mathbf{m}$, $\mathbf{m}'$ et $\mathbf{m}''$ le long d'une paire de collier infinis $(\mathbf{n}, \mathbf{n}')$. On renvoie à la Section 7.2.3 pour une description détaillée.

Décomposition de l'UIHPT. Notre premier résultat consiste en une décomposition de l'UIHPT le long d'une interface de percolation critique. Cette idée apparaît pour la première fois dans des travaux de Bertrand Duplantier, Jason Miller et Scott Sheffield [DMS14]. Pour cela, on considère un modèle de percolation par site critique sur

l'UIHPT ($p = 1/2$) avec la condition au bord "ouvert-fermé" de la Figure 2.16. On note $\mathcal{H}_b$ et $\mathcal{H}_w$ les enveloppes des amas de percolation issus de l'origine et de la cible de l'arête racine. Soient **Tree**$(\mathcal{H}_b)$ et **Tree**$(\mathcal{H}_w)$ leurs arbres des composantes, et

$$\left\{M_u^b : u \in \textbf{Tree}(\mathcal{H}_b)_\bullet\right\} \quad \text{et} \quad \left\{M_u^w : u \in \textbf{Tree}(\mathcal{H}_w)_\bullet\right\}$$

leurs composantes irréductibles (i.e., la seconde composante de $\Phi_{\text{TC}}(\mathcal{H}_b)$ et $\Phi_{\text{TC}}(\mathcal{H}_w)$). Notons que les conditions au bord des composantes irréductibles sont déterminées par leur enveloppe.

FIGURE 2.16 : La condition au bord "ouvert-fermé".

Dans la suite, on note $\mathbf{W}_k^{\triangle}$ la mesure induite par le modèle de percolation de paramètre $1/2$ sur une triangulation de Boltzmann de loi $\mathbb{W}_k^{\triangle}$ (définie dans (1.14)), avec une condition au bord à préciser. On introduit également les mesures de probabilité

$$\mu_\circ(k) := \frac{2}{3}\left(\frac{1}{3}\right)^k \quad \text{et} \quad \mu_\bullet(k) := 6W_{k+1}^{\triangle}9^{-k}, \quad k \in \mathbb{Z}_+.$$

La fonction de partition $W_k^{\triangle}$ a été définie dans (1.13). En utilisant ses propriétés (voir la Section 7.2.1), on peut montrer que le couple $(\mu_\circ, \mu_\bullet)$ est critique. Enfin, on rappelle que $\text{GW}_{\mu_\circ,\mu_\bullet}^{(\infty)}$ désigne la loi de l'arbre de Galton-Watson à deux types conditionné à survivre $\mathbf{T}_\infty^{\circ,\bullet}(\mu_\circ, \mu_\bullet)$ introduit dans le Théorème 2.1.3. Cet arbre a presque sûrement une unique épine dorsale. Lorsqu'on supprime tous les sommets à gauche (respectivement à droite) de cette épine à l'exception des enfants des sommets de hauteur impaire, on obtient une variante de l'arbre $\mathbf{T}_\infty^{\circ,\bullet}(\mu_\circ, \mu_\bullet)$ dont la loi est notée $\text{GW}_{\mu_\circ,\mu_\bullet}^{(\infty,l)}$ (respectivement $\text{GW}_{\mu_\circ,\mu_\bullet}^{(\infty,r)}$). On renvoie le lecteur à la Section 7.2.2 pour une description détaillée de ces arbres aléatoires infinis et de leur convention d'enracinement. Notre résultat est le suivant.

Théorème 14

Dans le modèle de percolation de Bernoulli par site critique sur l'UIHPT avec condition au bord "ouvert-fermé" :

- Les arbres des composantes **Tree**$(\mathcal{H}_b)$ et **Tree**$(\mathcal{H}_w)$ sont indépendants de loi respective $\text{GW}_{\mu_\circ,\mu_\bullet}^{(\infty,l)}$ et $\text{GW}_{\mu_\circ,\mu_\bullet}^{(\infty,r)}$.
- Conditionnellement à **Tree**$(\mathcal{H}_b)$ et **Tree**$(\mathcal{H}_w)$, les composantes irréductibles $\{M_u^b : u \in \textbf{Tree}(\mathcal{H}_b)_\bullet\}$ et $\{M_u^w : u \in \textbf{Tree}(\mathcal{H}_w)_\bullet\}$ sont des triangulations de Boltzmann à bord simple indépendantes munies d'un modèle de percolation critique, de loi $\mathbf{W}_{\deg(u)}^{\triangle}$.

Enfin l'UIHPT est obtenue comme le recollement $\Psi_{\mathbf{N}}(\mathcal{H}_b, \mathcal{H}_w)$ de $\mathcal{H}_b$ et $\mathcal{H}_w$ le long d'un collier uniforme infini $\mathbf{N}$ indépendant de $(\mathcal{H}_b, \mathcal{H}_w)$.

Le Théorème 14 peut être vu comme une version discrète de [DMS14, Théorème 1.16-1.17] (voir la Section 7.6 pour davantage de précisions à ce sujet), et est illustré dans la Figure 2.17. Il peut en fait être énoncé sans faire référence au modèle de percolation et est en ce sens un résultat de décomposition de l'UIHPT.

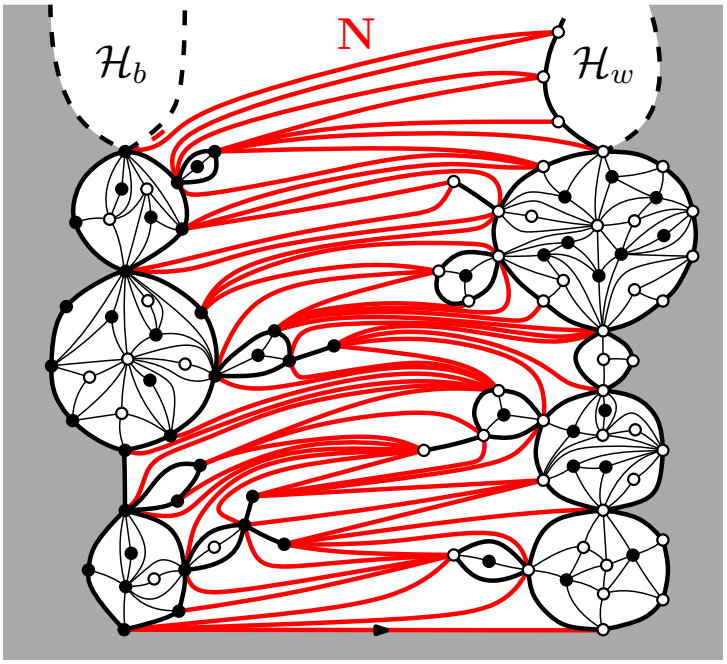

FIGURE 2.17 : La décomposition de l'UIHPT en ses amas de percolation et un collier uniforme infini.

Amas critique émergent de l'UIHPT. On considère à présent un modèle de percolation par site de paramètre p sur l'UIHPT avec la condition au bord "fermé-ouvert-fermé" de la Figure 2.18. Dans une carte avec une telle condition au bord, on note $\mathcal{H}$, $\mathcal{H}_l$ et $\mathcal{H}_r$ les enveloppes des amas issus de l'origine et de ses voisins sur le bord. Soient **Tree**$(\mathcal{H})$, **Tree**$(\mathcal{H}_l)$ et **Tree**$(\mathcal{H}_r)$ leurs arbres des composantes, et

$$\{M_u : u \in \textbf{Tree}(\mathcal{H})_\bullet\}, \quad \{M_u^l : u \in \textbf{Tree}(\mathcal{H}_l)_\bullet\} \quad \text{et} \quad \{M_u^r : u \in \textbf{Tree}(\mathcal{H}_r)_\bullet\}$$

leurs composantes irréductibles (i.e., les secondes composantes de $\Phi_{\text{TC}}(\mathcal{H})$, $\Phi_{\text{TC}}(\mathcal{H}_l)$ et $\Phi_{\text{TC}}(\mathcal{H}_r)$). À nouveau, les conditions au bord des composantes irréductibles sont déterminées par leurs enveloppes.

FIGURE 2.18 : La condition au bord "fermé-ouvert-fermé".

L'exploration de l'interface de percolation entre l'origine et le sommet à sa gauche sur le bord révèle un chemin ouvert dans l'UIHPT. La taille maximale atteinte par ce chemin lors de l'exploration (en effaçant les boucles) est appelée la *hauteur* $h(\mathcal{C})$ de l'amas ouvert issu de l'origine $\mathcal{C}$, et sera précisément définie dans la Section 7.5.1.

Théorème 15

Soit $\mathbf{P}_p$ la loi du modèle de percolation par site de paramètre p sur l'UIHPT avec condition au bord "fermé-ouvert-fermé". Alors, au sens faible pour la topologie locale, les limites

$$\lim_{p\downarrow p_c} \mathbf{P}_p(\cdot \mid |\mathcal{C}| = \infty) \quad \text{et} \quad \lim_{n\to\infty} \mathbf{P}_{p_c}(\cdot \mid h(\mathcal{C}) \geq n)$$

existent et sont égales. La mesure de probabilité limite, notée $\mathbf{P}_{\mathsf{IIC}}$, est appelée (loi de l') *amas critique émergent* de l'UIHPT ou IIC. Presque sûrement, l'IIC est une triangulation coloriée du demi-plan à bord simple avec condition au bord "fermé-ouvert-fermé". De plus, dans l'IIC :

- Les arbres des composantes $\mathbf{Tree}(\mathcal{H})$, $\mathbf{Tree}(\mathcal{H}_l)$ et $\mathbf{Tree}(\mathcal{H}_r)$ sont indépendants de lois respectives $\mathsf{GW}^{(\infty)}_{\mu_\circ,\mu_\bullet}$, $\mathsf{GW}^{(\infty,l)}_{\mu_\circ,\mu_\bullet}$ et $\mathsf{GW}^{(\infty,r)}_{\mu_\circ,\mu_\bullet}$.
- Conditionnellement à $\mathbf{Tree}(\mathcal{H})$, $\mathbf{Tree}(\mathcal{H}_l)$ et $\mathbf{Tree}(\mathcal{H}_r)$, les composantes irréductibles $\{M_u : u \in \mathbf{Tree}(\mathcal{H})_\bullet\}$, $\{M^l_u : u \in \mathbf{Tree}(\mathcal{H}_l)_\bullet\}$ et $\{M^r_u : u \in \mathbf{Tree}(\mathcal{H}_r)_\bullet\}$ sont des triangulations de Boltzmann à bord simple indépendantes munies d'un modèle de percolation critique, de loi $\mathbf{W}^{\triangle}_{\deg(u)}$.

Enfin, l'IIC est obtenu comme le recollement $\Psi_{(\mathbf{N}_l,\mathbf{N}_r)}(\mathcal{H}_l,\mathcal{H},\mathcal{H}_r)$ de $\mathcal{H}_l$, $\mathcal{H}$ et $\mathcal{H}_r$ le long d'une paire de colliers uniformes infinis indépendants $(\mathbf{N}_l,\mathbf{N}_r)$, également indépendants de $(\mathcal{H}_l,\mathcal{H},\mathcal{H}_r)$.

Comme dans le Théorème 2.4.5, on retrouve une forme d'universalité par rapport au conditionnement de l'amas de l'origine à être grand. Toutefois, on utilise ici un conditionnement différent dans le cas critique, qui est plus adapté à l'utilisation des techniques d'épluchage. La loi du bord de l'amas critique infini peut être comparée au résultat obtenu dans le Théorème 5 pour le modèle $O(n)$ sur les quadrangulations, ainsi qu'au Théorème 2.4.4. En particulier, grâce à l'asymptotique de la fonction de partition $W^{\triangle}_k$ (voir [AC15, Section 2.2]), la mesure de probabilité $\mu_\bullet$ est dans le bassin d'attraction d'une loi stable de paramètre $3/2$, qui est l'exposant associé aux modèles de percolation critiques sur les triangulations.

Les Théorèmes 14 et 15 sont étroitement liés. La décomposition de l'IIC montre que lorsqu'on conditionne l'amas issu de l'origine a être infini dans l'UIHPT, on lui ajoute *ex-nihilo* un arbre à boucles infini dont les boucles sont des triangulations indépendantes (voir la Figure 2.19). Ceci décrit comment l'évènement de probabilité nulle par rapport auquel on conditionne déforme la géométrie de la triangulation aléatoire du demi-plan sous-jacente.

Pour conclure, mentionnons quelques perspectives liées aux Théorèmes 14 et 15. Nous avons vu dans la Section 2.2.1 que l'UIHPQ admet une limite localement au sens de Gromov-Hausdorff : le demi-plan brownien (BHP). Il est alors naturel de conjecturer, en passant à la limite dans la décomposition du Théorème 14, que le BHP s'obtient comme le recollement d'arbres à boucles stables infinis dont les boucles sont remplies par des disques browniens. Toutefois, la définition d'un tel recollement

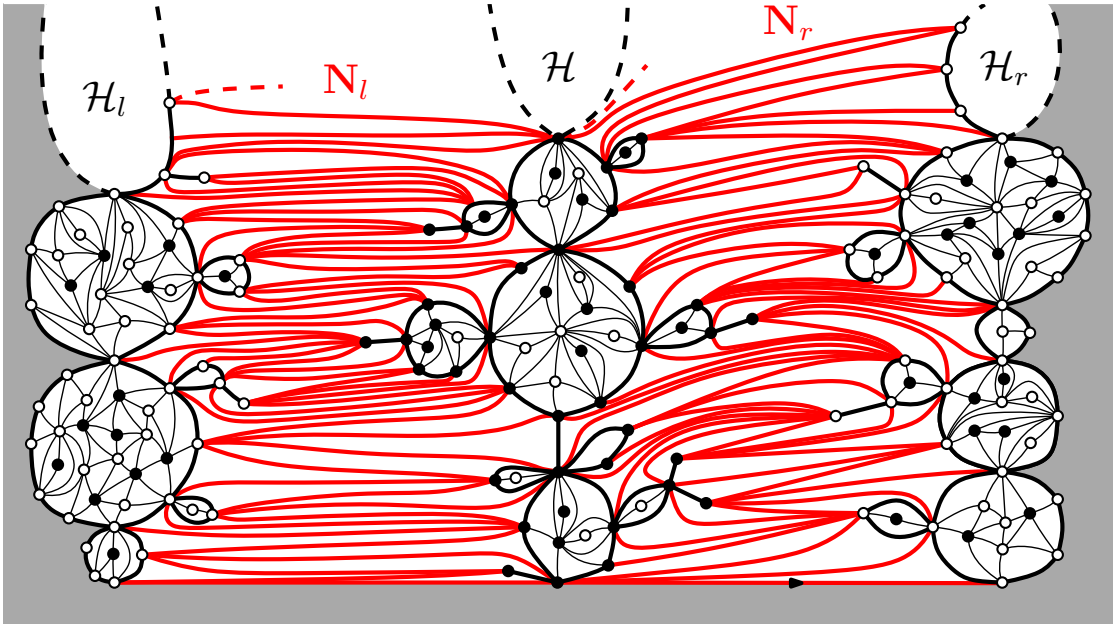

FIGURE 2.19 : La décomposition de l'IIC en ses enveloppes de percolation et deux colliers uniformes infinis.

est très délicate. De la même façon, on peut espérer définir l'amas critique émergent du BHP via le Théorème 15. Ces questions sont reliées à [DMS14, She10], où des recollements de surfaces quantiques sont étudiés, ainsi qu'à [GM17], où il est montré que l'interface de percolation (pour la percolation par face sur l'UIHPQ) converge vers un processus SLE de paramètre 6 sur le BHP.

II

Géométrie de grandes cartes à bord aléatoires

3

Geodesics of the uniform infinite half-planar quadrangulation

We show that all geodesic rays in the uniform infinite half-planar quadrangulation (UIHPQ) intersect the boundary infinitely many times, answering thereby a recent question of Curien. However, the possible intersection points are sparsely distributed along the boundary. As an intermediate step, we show that geodesic rays in the UIHPQ are proper, a fact that was recently established by Caraceni and Curien in [CC15] by a reasoning different from ours. Finally, we argue that geodesic rays in the uniform infinite half-planar triangulation behave in a very similar manner, even in a strong quantitative sense.

This Chapter is adapted from joint work with Erich Baur and Grégory Miermont [1] (published in ALEA : Latin American Journal of Probability and Mathematical Statistics, XIII(2):1123-1149, 2016). It contains the proof of Theorem 10 and Proposition 11.

Contents

3.1 Introduction

The uniform infinite half-planar quadrangulation UIHPQ provides a natural model of (discrete) random half-planar geometry. It arises as a local limit of finite-size quadrangulations with a boundary, when the number of quadrangles and the size of the boundary tend to infinity in a suitable way. We give more precise statements with references in the next section.

The full-plane equivalent of the UIHPQ is the so-called uniform infinite planar quadrangulation (UIPQ), which was introduced by Krikun [Kri05], after Angel and Schramm's pioneering work on triangulations [AS03]. It is proved in [CMM13] that geodesic rays (i.e., infinite one-ended geodesics) starting from the root in the UIPQ satisfy a confluence property towards infinity (and, as it is also shown, towards the root): Almost surely, there exists an infinite set of vertices such that every geodesic ray emanating from the origin passes through all the vertices of this set. In other words, geodesic rays in the UIPQ are essentially unique, in the sense that the Gromov boundary of the UIPQ contains only a single point.

In a recent work [CC15], Caraceni and Curien showed that the analog coalescence property of geodesics holds in the half-planar model UIHPQ: There is with probability one an infinite sequence of distinct vertices, which are all hit by every geodesic ray emanating from the root. Our main result of this paper shows that this property holds in the UIHPQ in a very strong sense.

Theorem 3.1.1. *Almost surely, every geodesic ray in the* UIHPQ *hits the boundary infinitely many times. More specifically, almost surely there is an infinite sequence of distinct vertices all lying on the boundary of the* UIHPQ*, such that every geodesic ray passes through every point of this sequence except maybe for a finite number.*

After having introduced some notation, we will outline our strategy for proving Theorem 3.1.1 at the beginning of Section 3.3. In Section 3.4, we obtain more precise information on the set of times (and points) of intersection with the boundary, see Proposition 3.4.3. More specifically, by analyzing two distinguished geodesics starting from the root vertex, we will construct an infinite set of boundary vertices, which contains all possible points of intersection with any geodesic ray. See Figure 3.1. Our construction will imply that geodesic rays hit both "sides" of the boundary (see Section 3.2.2 for the exact terminology) infinitely many times; however, the time between two hits has a logarithmic tail. Section 3.5 contains an extension of our results to the uniform infinite half-planar triangulation UIHPT, see Theorem 3.5.3.

The UIHPQ considered here has a non-simple boundary, meaning that the boundary vertices cannot be connected by a simple curve. In other words, there are pinch-points along the boundary. The analog of the UIHPQ with a simple boundary, which we denote by $\text{UIHPQ}^{(s)}$ (see [AC15, CM15], and [Ang04] for the triangular analog), can be constructed by a pruning procedure applied to the UIHPQ, cf. [CM15], and this construction will allow us to argue in Corollary 3.3.7 that our results on geodesics transfer to the $\text{UIHPQ}^{(s)}$.

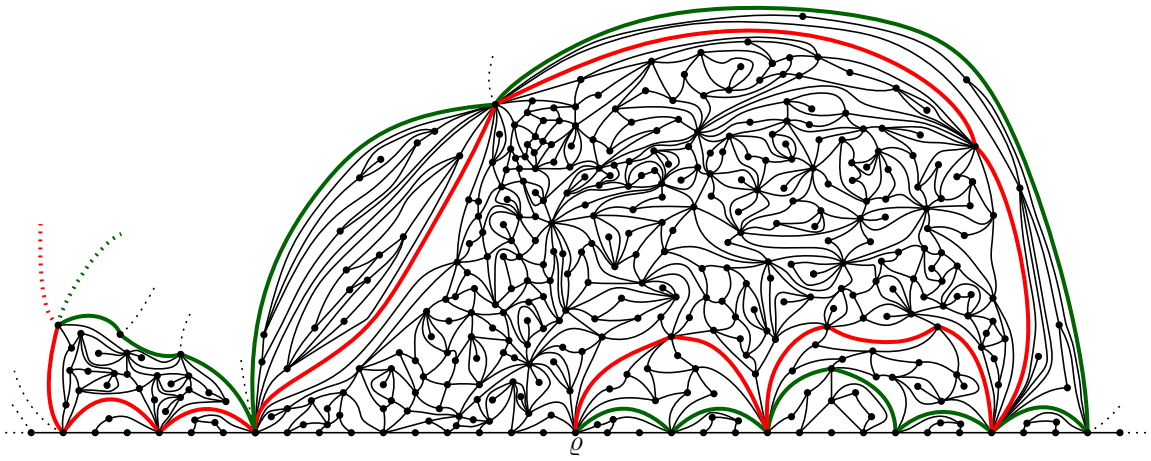

Figure 3.1: Artistic drawing of the UIHPQ (here, for simplicity, with a simple boundary) with two distinguished geodesics emanating from the root vertex ρ called the *maximal* or *leftmost geodesic* (in red) and the *minimal* or *rightmost geodesic* (in green). All geodesic rays starting from ρ lie in between the maximal and minimal geodesic. Their joint intersection points with the boundary are thus intersection points for *any* geodesic ray emanating from ρ.

The uniform infinite planar quadrangulation UIPQ contains a distinguished infinite sequence of vertices, the so-called *spine*. This sequence can be interpreted as a self-avoiding infinite path in the UIPQ, which is, as it is shown in [CMM13], almost surely hit only a *finite* number of times by the collection of geodesic rays starting from the root. This result should be seen in comparison with our Theorem 3.1.1, see Remark 3.3.5 for more on this. In particular, in the UIPQ, there are self-avoiding paths of infinite length which are finally avoided by any geodesic ray. As our arguments leading to Theorem 3.1.1 show, such paths do not exist in the UIHPQ: Any infinite self-avoiding path in the UIHPQ must cross any geodesic ray infinitely often.

The fact that the spine is eventually left by the collection of geodesic rays emanating from the root is a key step in [CMM13] to prove the confluence property towards infinity, and our approach borrows to some extent from the ideas presented there.

We will rely on a Schaeffer-type encoding of the UIHPQ going back to [Sch98, BDFG04, CM15] in terms of uniformly labeled critical Galton-Watson trees, which are attached to the down-steps of a two-sided simple random walk. The key observation for Theorem 3.1.1 is expressed in Proposition 3.3.1. There, we find the exact distribution of the minimal label, which is attained in the trees attached to an excursion above -1 of the simple random walk. A related quantity is studied in Lemma 14 in [CMM13], see also Remark 3.3.5 below. In the last section, we argue that a variant of the Schaeffer-type encoding can be used to construct the uniform infinite half-planar triangulation UIHPT, and then a similar strategy works for the UIHPT as well, resulting in Theorem 3.5.3. In particular, somewhat surprisingly, we will see that geodesic rays in the UIHPT behave in a quantitatively very similar manner.

3.2 The uniform infinite half-planar quadrangulation

The UIHPQ is an infinite random quadrangulation with an infinite boundary, which comes equipped with an oriented root edge lying on the boundary. Let us first briefly recall the notion of planar quadrangulations with a boundary.

3.2.1 Planar maps and quadrangulations with a boundary

A finite planar map is a finite connected graph properly embedded in the two-dimensional sphere, that is, in such a way that edges intersect only at their endpoints. As usual, we regard two such maps as being equivalent, if they differ only by a homeomorphism that preserves the orientation of the sphere.

The faces of a planar map are the connected components of the complement of the union of its edges. The degree of a face is the number of its incident edges, where, as usual, an edge that lies entirely in a face is counted twice.

A planar map is a *quadrangulation with a boundary*, if all faces have degree four, except possibly one face called the root face, which can have an arbitrary (even) degree. The edges surrounding the root face form the boundary of the quadrangulation. We do not require the boundary to be a simple curve.

The size of a quadrangulation with a boundary is the number (possibly infinite) of its non-root or inner faces. The size of the boundary, which is also called the perimeter of the map, is given by the degree of the root face. Note that since quadrangulations are bipartite, the perimeter is an even number.

Provided the perimeter is non-zero, in which case the map is seen as a single vertex map, we root such a quadrangulation by specifying one distinguished oriented edge on the boundary, in such a way that the root face lies to the right of that edge. The origin of the root edge is called the root vertex. We write $\mathcal{Q}_f$ for the set of all finite (rooted) quadrangulations with a boundary. Of course, if the perimeter of an element $\mathbf{q} \in \mathcal{Q}_f$ is equal to four, we may view $\mathbf{q}$ more naturally as a quadrangulation without boundary.

Equipped with the usual graph distance d_{gr}, the vertex set $V(\mathbf{m})$ of a rooted planar map $\mathbf{m}$ is a pointed metric space. Let us next recall the so-called *local topology* on the set $\mathcal{Q}_f$ (or more generally, on the set of finite rooted maps).

Given a rooted planar map $\mathbf{m}$ with root vertex ϱ, we denote by $\mathbf{B}_r(\mathbf{m})$ for $r \geq 0$ the combinatorial ball of radius r, that is, the submap of $\mathbf{m}$ containing all vertices v of $\mathbf{m}$ with $d_{\mathrm{gr}}(\varrho, v) \leq r$, together with the edges of $\mathbf{m}$ connecting such vertices. Now if $\mathbf{m}$ and $\mathbf{m}'$ are two rooted planar maps, the local distance between $\mathbf{m}$ and $\mathbf{m}'$ is defined as

$$d_{\mathrm{loc}}(\mathbf{m}, \mathbf{m}') = (1 + \sup\{r \geq 0 : \mathbf{B}_r(\mathbf{m}) = \mathbf{B}_r(\mathbf{m}')\})^{-1}.$$

The local topology is the topology induced by d_{loc}, and we write $\mathcal{Q}$ for the completion of $\mathcal{Q}_f$ with respect to d_{loc}. Elements in $\mathcal{Q} \backslash \mathcal{Q}_f$ are called *infinite quadrangulations with a boundary*.

The UIHPQ $\mathbf{Q}_\infty^\infty$ is a random (rooted) infinite quadrangulation with an infinite boundary, which can be obtained as a local limit of random elements in $\mathcal{Q}_f$, in the following ways.

Firstly, let Q_n^σ be uniformly chosen among all rooted quadrangulations of size n with a boundary of size 2σ, $\sigma \in \mathbb{N} = \{1, 2, \ldots\}$. Curien and Miermont proved in [CM15] that with respect to d_{loc},

$$Q_n^\sigma \xrightarrow[n\to\infty]{(d)} \mathbf{Q}_\infty^\sigma, \quad \mathbf{Q}_\infty^\sigma \xrightarrow[\sigma\to\infty]{(d)} \mathbf{Q}_\infty^\infty.$$

Here, $\mathbf{Q}_\infty^\sigma$ is the so-called uniform infinite planar quadrangulation with a boundary of length 2σ, see [CM15] for a precise description. Similar convergences hold if Q_n^σ is chosen uniformly among all rooted quadrangulations of size n with a simple boundary of size 2σ, that is, if Q_n^σ is a uniform rooted quadrangulation of the 2σ-gon with n inner faces. In this case, the limiting map when first $n \to \infty$ and then $\sigma \to \infty$ is the uniform infinite planar quadrangulation with a simple boundary UIHPQ$^{(s)}$, as alluded to above (see [AC15] for details).

Secondly, the UIHPQ $\mathbf{Q}_\infty^\infty$ arises also as the local limit of random elements in $\mathcal{Q}_f$ when the boundary grows simultaneously with the size of the map. More specifically, assume that σ_n grows much slower than n. Then it is shown in [BMR16] that

$$Q_n^{\sigma_n} \xrightarrow[n\to\infty]{(d)} \mathbf{Q}_\infty^\infty.$$

In [CM15], the UIHPQ $\mathbf{Q}_\infty^\infty$ is constructed from an extended Schaeffer-type mapping applied to a so-called *uniform infinite treed bridge* of infinite length, and we will recall and work with this construction in the following section.

A new construction of the UIHPQ which is better suited to study the metric balls around the root has recently been given in [CC15]. Although we will work with the first construction, we adopt some notation from there.

In the following section, we introduce certain deterministic objects which encode (non-random) infinite quadrangulations via a Schaeffer-type mapping. Randomized versions of these objects will then encode the UIHPQ.

3.2.2 A Schaeffer-type construction

Well-labeled trees and infinite treed bridges. Recall the definition of a (rooted) finite planar tree τ, see, e.g., [LGM11b]. We denote by $|\tau|$ the number of its edges and write $V(\tau)$ for the vertex set of τ.

A *well-labeled tree* (τ, ℓ) is a pair of a rooted planar tree τ and integer labels $\ell = (\ell(u))_{u\in V(\tau)}$, which are attached to the vertices of τ, according to the following rule: Whenever $u, v \in V(\tau)$ are connected by an edge, then $|\ell(u) - \ell(v)| \le 1$.

For $k \in \mathbb{Z}$, we let LT_k be the set of all finite well-labeled plane trees, whose root is labeled k. The set of all well-labeled plane trees is denoted $\mathsf{LT} = \cup_{k\in\mathbb{Z}}\mathsf{LT}_k$.

As in [CM15] or [CC15], we will work with so-called *treed bridges*. We will only need their infinite versions, which we define next. First, an *infinite bridge* is a two-sided sequence $\mathsf{b} = (\mathsf{b}(i) : i \in \mathbb{Z})$ with $\mathsf{b}(0) = 0$ and $|\mathsf{b}(i+1) - \mathsf{b}(i)| = 1$. An index i

for which $\mathsf{b}(i+1) = \mathsf{b}(i) - 1$ is called a *down-step* of b. The set of all down-steps of b is denoted $\mathsf{DS}(\mathsf{b})$.

Definition 3.2.1. We call *infinite treed bridge* a pair (b, T), where b is an infinite bridge and T is a mapping from $\mathsf{DS}(\mathsf{b})$ to LT with the property that $T(i) \in \mathsf{LT}_{\mathsf{b}(i)}$, i.e., $T(i)$ is a well-labeled tree whose root has label $\mathsf{b}(i)$.

We write $\mathsf{TB}^{-\infty}$ for the set of all infinite treed bridges which have the property that $\inf_{i\in\mathbb{Z}_+} \mathsf{b}(i) = -\infty$ and $\inf_{i\in\mathbb{Z}_-} \mathsf{b}(i) = -\infty$, where $\mathbb{Z}_+ = \{0, 1, 2, \ldots\}$, $\mathbb{Z}_- = \{\ldots, -2, -1, 0\}$.

The Bouttier–Di Francesco–Guitter mapping. We now construct a mapping Φ, which we call the Bouttier–Di Francesco–Guitter mapping, that sends elements in $\mathsf{TB}^{-\infty}$ to infinite quadrangulations with an infinite boundary. The uniform infinite half-planar quadrangulation UIHPQ is then obtained from applying Φ to a random element $(\mathsf{b}_\infty, T_\infty)$ in $\mathsf{TB}^{-\infty}$, whose law we specify in the next section.

We stress that usually (e.g., in [CM15], or in [CC15]), the Bouttier–Di Francesco–Guitter mapping is first introduced as a bijection between finite versions of treed bridges and (rooted and pointed) finite-size quadrangulations with a boundary. Then it is argued that the mapping can be extended to elements in $\mathsf{TB}^{-\infty}$, yielding infinite quadrangulations. However, since we will here only work with infinite quadrangulations, we directly describe the mapping as a function

$$\Phi : \mathsf{TB}^{-\infty} \longrightarrow \mathcal{Q}.$$

Let $(\mathsf{b}, T) \in \mathsf{TB}^{-\infty}$. It is convenient to work with the following representation of (b, T) in the plane: We identify $\mathsf{b} = (\mathsf{b}(i) : i \in \mathbb{Z})$ with the labeled bi-infinite line, which is obtained from connecting the neighboring vertices of $\mathbb{Z}$ by edges and assigning to $i \in \mathbb{Z}$ the label $\mathsf{b}(i)$. Then we graft a proper embedding of the tree $T(i)$ for $i \in \mathsf{DS}(\mathsf{b})$ to the vertex i in the upper half-plane, by identifying the root of $T(i)$ with the vertex i. See Figure 3.2. Note our small abuse of notation: We denote here by $i \in \mathsf{DS}(\mathsf{b})$ an index of b as well as a vertex of the representation of b.

The vertex set of such a representation of (b, T) is therefore given by $\mathbb{Z}$ and the union of the tree vertices of $T(i)$, $i \in \mathsf{DS}(\mathsf{b})$, where we interpret the root of $T(i)$ and the vertex $i \in \mathbb{Z}$ as one and the same vertex. Following the wording of [CC15], we call the vertices which belong to the trees $T(i)$, $i \in \mathsf{DS}(\mathsf{b})$, *real vertices*, and the vertices $j \in \mathbb{Z}$ above which no trees are grafted, i.e., the vertices j that do not correspond to down-steps of b, *phantom vertices*. A *corner* of (the representation of) (b, T) is an angular sector between two consecutive edges, in the clockwise contour or left-to-right order. Henceforth we shall consider only *real corners*, i.e., corners that are incident to real vertices and lie in the upper half-plane. By a small abuse of notation, given a vertex $v \in T(i)$, $i \in \mathsf{DS}(\mathsf{b})$, we shall simply write $\ell(v)$ for its label, and we let $\ell(c) = \ell(v)$ if c is a corner incident to v.

We now consider the bi-infinite sequence of corners $(c_i)_{i\in\mathbb{Z}}$ obtained from ordering the real corners of (b, T) according to the left-to-right order, where we agree that c_0 is the left-most real corner with label 0, which appears in $T(i)$, $i \in \mathsf{DS}(\mathsf{b}) \cap \mathbb{Z}_+$. See

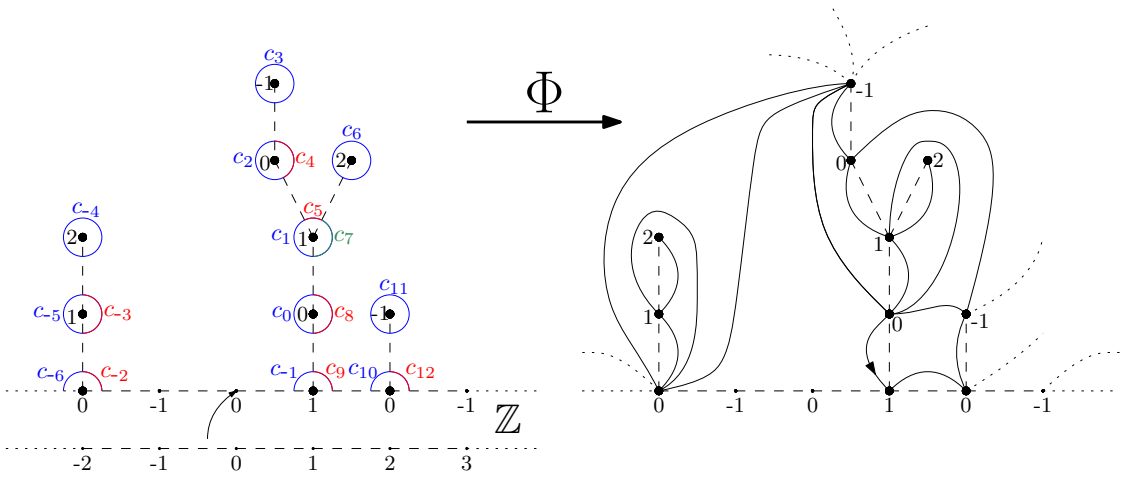

Figure 3.2: The Bouttier–Di Francesco–Guitter mapping. Vertex 0 of $\mathbb{Z}$ is indicated by an arrow. The visible trees are attached to the vertices -2, 1 and 2 of $\mathbb{Z}$, which are labeled 0, 1 and 0, respectively. These vertices correspond to down-steps of the bridge.

again Figure 3.2. For $i \in \mathbb{Z}$, we denote by $\mathrm{succ}(c_i)$ the first corner among $c_{i+1}, c_{i+2}, \ldots$, which has label $\ell(c_i) - 1$. Note that such a corner always exists, since $\inf_{i \in \mathbb{Z}_+} \mathsf{b}(i) = -\infty$. We call $\mathrm{succ}(c_i)$ the *successor* of i. As indicated on the right side of Figure 3.2, we draw for every $i \in \mathbb{Z}$ an arc between the corner c_i and $\mathrm{succ}(c_i)$ in the upper half-plane, in such a way that arcs do only possibly intersect at their endpoints. We finally erase the phantom vertices and the edges that stem from the representation of (b, T). We obtain a locally finite quadrangulation M with an infinite boundary ∂M, which we root in the (oriented) edge that corresponds to the first step of the bridge to the right of 0. A detailed explanation of this correspondence is given in the next section. In other words, the root face that lies to the right of the root edge has infinite degree, and the edges surrounding it form the (infinite) boundary ∂M of the map.

We let $\Phi((\mathsf{b}, T)) = M$ be the rooted infinite quadrangulation with an infinite boundary obtained in this way.

Identification of the boundary. If we identify $\mathbb{Z}$ with the bi-infinite line by connecting neighboring vertices with an edge, then the Bouttier–Di Francesco–Guitter mapping establishes a one-to-one correspondence between the edges of $\mathbb{Z}$ and those of the boundary ∂M of $M = \Phi((\mathsf{b}, T))$, as it is visible in Figures 3.2 and 3.3. More precisely, for a given (b, T), we define a function

$$\varphi : \mathbb{Z} \to V(\partial M)$$

as follows: Vertex $i \in \mathbb{Z}$ of the representation of b (which is labeled $\mathsf{b}(i)$) is mapped to itself, if i is a real vertex. By definition, this is the case if and only if $i \in \mathsf{DS}(\mathsf{b})$. Otherwise, we search for the next real corner to the right of i which has label $\mathsf{b}(i)$, and define $\varphi(i)$ to be the vertex incident to it. Then the edge $\{i, i+1\}$ of $\mathbb{Z}$ corresponds to a unique edge from $\varphi(i)$ to $\varphi(i+1)$ of ∂M, and the assignment is one-to-one. Instead of being more formal, we refer to Figure 3.3.

We will call $\varphi(\mathbb{Z}_-)$ and $\varphi(\mathbb{Z}_+)$ the *left* and *right part* of the boundary of M, respectively. Of course, $\partial M = \varphi(\mathbb{Z}_-) \cup \varphi(\mathbb{Z}_+)$. Moreover, M is rooted in the (oriented) edge between $\varphi(0)$ and $\varphi(1)$.

Construction of the UIHPQ. Recall the definition of LT_k for $k \in \mathbb{Z}$. Let ρ_k be the Boltzmann measure on LT_k given by $\rho_k((\tau, \ell)) = 12^{-|\tau|}/2$. The measure ρ_k is the law of a so-called *uniformly labeled critical geometric Galton-Watson tree*. This means that if (τ, ℓ) is distributed according to ρ_k, then τ has the law of a Galton-Watson tree with a geometric offspring distribution of parameter $1/2$. Moreover, conditionally on τ, $\ell : V(\tau) \to \mathbb{Z}$ is the random labeling of τ such that the root receives label k, and independently for each edge $e = \{u, v\}$ of τ, $\ell(u) - \ell(v)$ is uniformly distributed over $\{-1, 0, 1\}$. We refer, e.g., to [LGM11b, Section 2.2] for more details.

Let $\mathsf{b}_\infty = (\mathsf{b}_\infty(i) : i \in \mathbb{Z})$ be a two-sided simple symmetric random walk with $\mathsf{b}_\infty(0) = 0$, that is, $(\mathsf{b}_\infty(i) : i \in \mathbb{Z}_+)$ and $(\mathsf{b}_\infty(i) : i \in \mathbb{Z}_-)$ are two independent simple symmetric random walks starting from 0.

Conditionally on b_∞, define a (random) function $T_\infty : \mathsf{DS}(\mathsf{b}_\infty) \to \mathsf{LT}$ by letting $T_\infty(i)$ for $i \in \mathsf{DS}(\mathsf{b}_\infty)$ be a well-labeled tree with law $\rho_{\mathsf{b}_\infty(i)}$, independently in $i \in \mathsf{DS}(\mathsf{b}_\infty)$.

We call the random element $(\mathsf{b}_\infty, T_\infty)$ of $\mathsf{TB}^{-\infty}$ a *uniform infinite treed bridge*.

Definition 3.2.2. The UIHPQ $\mathbf{Q}_\infty^\infty = (V(\mathbf{Q}_\infty^\infty), d_{\mathrm{gr}}, \varrho)$ is the random infinite quadrangulation with an infinite boundary obtained from applying the Bouttier–Di Francesco–Guitter mapping to a uniform infinite treed bridge $(\mathsf{b}_\infty, T_\infty)$, i.e.,

$$\mathbf{Q}_\infty^\infty = \Phi\left((\mathsf{b}_\infty, T_\infty)\right).$$

We will write $\ell_\infty(v)$ for the label of a vertex $v \in V(T_\infty(i))$, $i \in \mathsf{DS}(\mathsf{b}_\infty)$, which we also identify with a vertex of $\mathbf{Q}_\infty^\infty$ via the Bouttier–Di Francesco–Guitter mapping.

3.2.3 Geodesics in the UIHPQ

Let $G = (V(G), E(G))$ be a graph. A *geodesic* in G is a path of possibly infinite length, which visits a sequence (or chain) of vertices $\gamma = (\gamma(0), \gamma(1), \ldots)$ of G such that for $i, j \in \mathbb{Z}_0$ for which γ is defined, $d_{\mathrm{gr}}(\gamma(i), \gamma(j)) = |i - j|$. An infinite geodesic γ with $\gamma(0) = v \in V(G)$ is called a *geodesic ray* started at v.

Note that we view a geodesic as a sequence of concatenated edges. In particular, if G is a non-simple graph as in the case of the UIHPQ, a geodesic is usually not specified by its vertices alone.

Let $(\mathsf{b}, T) \in \mathsf{TB}^{-\infty}$ be an infinite treed bridge. We will now define particular geodesic rays in the infinite quadrangulation $\Phi((\mathsf{b}, T))$. Recall the definition of the sequence of corners $(c_i)_{i \in \mathbb{Z}}$ obtained from ordering the real corners of (b, T) according to the contour order, as well as the definition of the successor-mapping; see Section 3.2.2. We write $\mathrm{succ}^{(i)}$ for the i-fold composition of the successor-mapping and denote by $\mathcal{V}(c)$ the vertex incident to the corner c.

Definition 3.2.3 (Maximal geodesic)**.** Let $(\mathsf{b}, T) \in \mathsf{TB}^{-\infty}$, and let $v \in V(\Phi((\mathsf{b}, T)))$ be a vertex of the quadrangulation associated to (b, T). Let c be the leftmost (real)

corner of (b, T) incident to v. Then the *maximal geodesic* started at v is given by the chain of vertices incident to the iterated successors of c, that is, $\gamma^v_{\max}(0) = v$, and then for $i \in \mathbb{N}$,

$$\gamma^v_{\max}(i) = \mathcal{V}(\mathrm{succ}^{(i)}(c)),$$

and with edges connecting $\mathrm{succ}^{(i)}(c)$ to $\mathrm{succ}^{(i+1)}(c)$ for $i \in \mathbb{Z}_+$.

We will simply write $\gamma_{\max}$ for the maximal geodesic started from the root ϱ. See Figure 3.3 for an illustration of the maximal geodesic in the UIHPQ. It is a direct consequence of the definition that maximal geodesics finally coalesce. Indeed, consider the first vertex incident to a corner c_i for $i \in \mathbb{Z}_+$, which is visited by $\gamma^v_{\max}$. Let v' be the first vertex incident to a corner c_j, $j \geq i$, which is visited by $\gamma_{\max}$. Then v' is also visited by $\gamma^v_{\max}$, and from that moment on, $\gamma^v_{\max}$ and $\gamma_{\max}$ coincide.

Of special interest is the class of *proper geodesics*, which generalizes the construction of maximal geodesics, in the sense that the connecting edges do not necessarily emanate from leftmost corners.

Definition 3.2.4 (Proper geodesic)**.** A geodesic ray γ is *proper*, if for every $i \in \mathbb{Z}_+$,

$$\ell(\gamma(i+1)) = \ell(\gamma(i)) - 1.$$

It turns out that in the UIHPQ, almost surely every geodesic ray is proper. This fact has already been proved in [CC15], but we will give an alternative proof in Corollary 3.3.6. In particular, it makes sense to call maximal geodesics *leftmost geodesics*. In Section 3.4, we shall also consider *minimal* or *rightmost geodesics*.

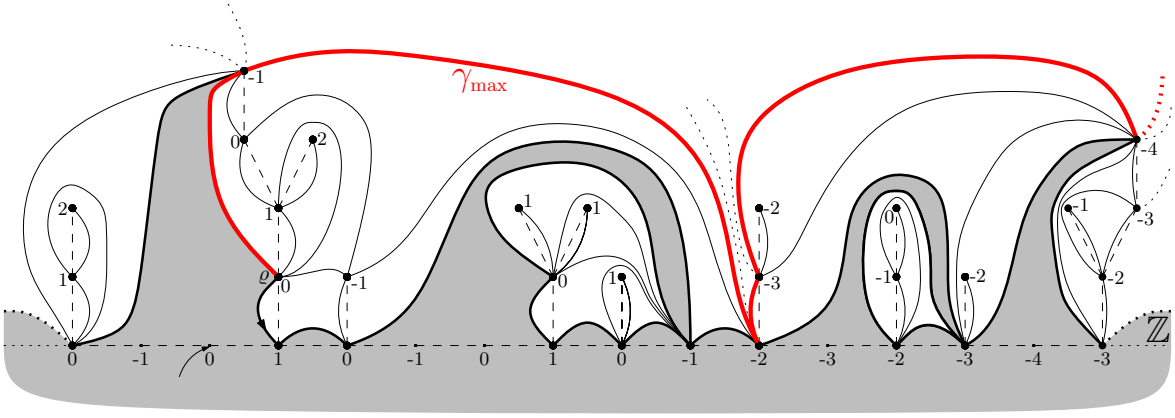

Figure 3.3: The UIHPQ and its maximal geodesic $\gamma_{\max}$.

3.3 Proof of the main results

To begin with, let us describe our **general strategy** for proving Theorem 3.1.1.

We will first show that the maximal geodesic $\gamma_{\max}$ hits both parts of the boundary of the UIHPQ infinitely many times, see Proposition 3.3.4 below. For that purpose, we will study the sets $\mathcal{R}_+$ and $\mathcal{R}_-$ of intersection times of $\gamma_{\max}$ with the right and left part

of the boundary. It turns out that both $\mathcal{R}_+$ and $\mathcal{R}_-$ are regenerative sets. Moreover, we find a representation of these sets in terms of the infinite treed bridge encoding the UIHPQ, which involves the minimal label attained in the trees between two subsequent minima of the bridge. The crucial step is formulated as Proposition 3.3.1 below, where we compute the exact distribution of such a minimal label. Once we know that $\gamma_{\max}$ touches both parts of the boundary infinitely often, we also know that every geodesic ray must cross $\gamma_{\max}$ infinitely many times. From this, we readily deduce that any geodesic ray is proper, as it was already shown in [CC15, Proposition 4.8] for geodesic rays started from the root vertex, by means different from ours. Since any proper geodesic ray lies finally in between $\gamma_{\max}$ and the boundary, an appeal to Proposition 3.3.4 allows us to conclude the proof of Theorem 3.1.1.

We first introduce some more notation. Let $(\mathsf{b}, T) \in \mathsf{TB}^{-\infty}$ be an infinite treed bridge. For $j \in \mathbb{Z}_+$, we write

$$H_j(\mathsf{b}) = \inf\{m \in \mathbb{Z}_+ : \mathsf{b}(m) = -j\}, \quad H'_j = \sup\{m \in \mathbb{Z}_- : \mathsf{b}(m) = -j\}$$

for the first time b hits $-j$ to the right of zero or to the left of zero, respectively. Note that both $H_j(\mathsf{b})$ and $H'_j(\mathsf{b})$ are finite for each $j \in \mathbb{Z}_+$, almost surely.

Moreover, for $i \in \mathsf{DS}(\mathsf{b})$, we write $\ell_i = (\ell_i(u))_{u \in V(T(i))}$ for the labels of the vertices of the tree $T(i) \in \mathsf{LT}_{\mathsf{b}(i)}$. Recall that if r is the root vertex of $T(i)$, then $\ell_i(r) = \mathsf{b}(i)$.

For $j \in \mathbb{Z}_+$, we let

$$\Delta_j((\mathsf{b}, T)) = \max_{i \in \mathsf{DS}(\mathsf{b}) \cap [H_j, H_{j+1})} - \left(\min_{u \in V(T(i))} \ell_i(u) + j \right), \quad \text{and}$$
$$\Delta'_j((\mathsf{b}, T)) = \max_{i \in \mathsf{DS}(\mathsf{b}) \cap [H'_{j+1}, H'_j)} - \left(\min_{u \in V(T(i))} \ell_i(u) + j \right),$$

where $H_j = H_j(\mathsf{b}_\infty)$, and $H'_j = H'_j(\mathsf{b}_\infty)$. In words, $\Delta_j((\mathsf{b}, T)) \in \mathbb{Z}_+$ is the absolute value of the minimal label shifted by $|\mathsf{b}(H_j)| = j$ in the trees $T(i)$ that are attached to the infinite bridge b on $[H_j, H_{j+1})$. A similar interpretation holds for $\Delta'_j((\mathsf{b}, T))$. We simply write Δ_j and Δ'_j for the random numbers $\Delta_j((\mathsf{b}_\infty, T_\infty))$ and $\Delta'_j((\mathsf{b}_\infty, T_\infty))$, where $(\mathsf{b}_\infty, T_\infty)$ is a uniform infinite treed bridge as specified in Section 3.2.2. The strong Markov property shows that Δ_j has the same law as Δ_0, and Δ'_j has the same law as Δ'_0, for each $j \in \mathbb{Z}_+$. As we show next, their distributions can be computed explicitly.

Proposition 3.3.1. *We have for $m \in \mathbb{N}$,*

$$\mathbb{P}(\Delta_0 \geq m) = \frac{1}{m+1}, \quad \textit{and} \quad \mathbb{P}(\Delta'_0 \geq m) = \frac{1}{m+3}.$$

Proof. We first consider Δ_0. The statement for Δ'_0 will then follow from a symmetry argument. Let $m \in \mathbb{N}$. We set $g(m) = \mathbb{P}(\Delta_0 < m)$. Moreover, let $h(m) = \mathbb{P}(\min_{u \in V(\tau)} \ell(u) > -m)$, where (τ, ℓ) is distributed according to ρ_0; see Section 3.2.2. We decompose the path of b on $[0, H_1)$ into its excursions above 1, as shown in Figure 3.4. For Δ_0 to be smaller than m, the labels in every excursion above 1 have to be larger than $-(m+1)$, while the minimal label of the tree grafted to the last step of the excursion has to be larger than $-m$.

A standard application of the strong Markov property shows that these excursions, shifted by -1, have the same law as b on $[0, H_1)$, so that the quantity $g(m)$ satisfies the recursive equation

$$g(m) = \frac{1}{2}h(m)\sum_{k=0}^{\infty}\left(\frac{1}{2}g(m+1)\right)^k = \frac{h(m)}{2-g(m+1)}. \tag{3.1}$$

We stress that (3.1) is in spirit of the arch decomposition as described in Section V.4.1 of [FS09]; see also (2.1) and (2.2) of [BG12] for related decompositions.

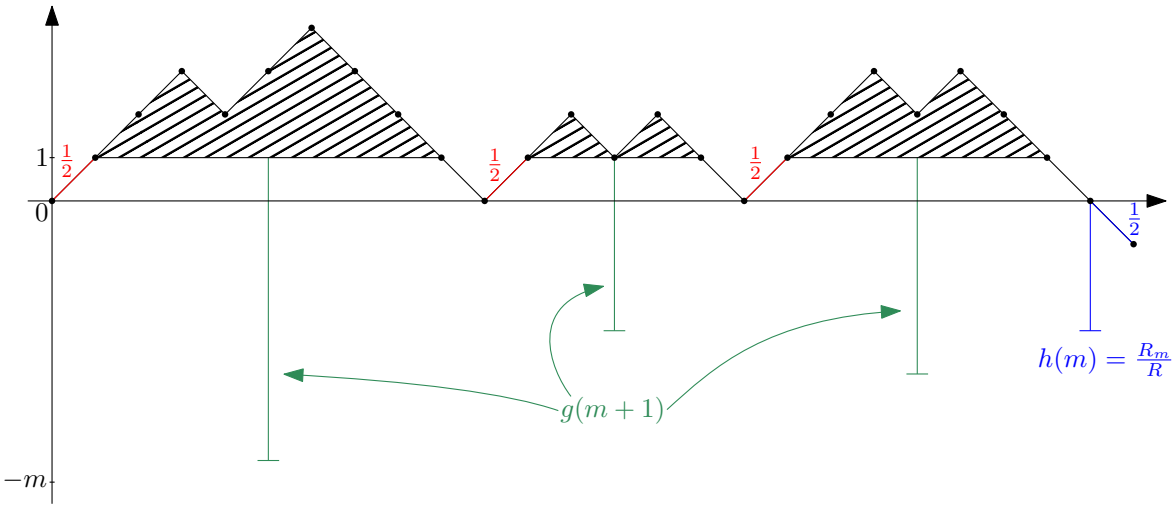

Figure 3.4: The decomposition of the probability $g(m)$.

From the Bouttier–Di Francesco–Guitter bijection for quadrangulations of a finite size, see, e.g., [BDFG04], well-labeled trees are in bijection with rooted and pointed quadrangulations, the pointed vertex being at distance $\min_{u\in V(\tau)}\ell(u) - 1$ from the root. In [BG12], the generating function for quadrangulations with weight g_4 per face and distance less than or equal to m between the root and the pointed vertex, called the *distance-dependent two-point function* and denoted R_m, is proved to satisfy (see [BG12, (6.18)])

$$R_m = R\frac{(1-y^m)(1-y^{m+3})}{(1-y^{m+1})(1-y^{m+2})},$$

where $R = R(g_4) = \lim_{m\to\infty} R_m$ is the generating function of rooted and pointed quadrangulations with weight g_4 per face, and $y = y(g_4)$ is the solution of the so-called characteristic equation (see [BG12, (6.17)]). In our special case corresponding to a critical weight per face given by $g_{4,\mathrm{cr}} = 1/12$, the solution of the characteristic equation simplifies to $y = 1$. Taking the limit $y \uparrow 1$ in the last display, this implies

$$R_m = R\frac{m(m+3)}{(m+1)(m+2)}.$$

Since the partition function is given by R, we therefore get

$$h(m) = \mathbb{P}\left(-\min_{u\in V(\tau)}\ell(u) \le m-1\right) = \frac{R_m}{R} = 1 - \frac{2}{(m+1)(m+2)}. \tag{3.2}$$

By the way, we note that $h(m)$ as already been calculated before in [CD06, Proposition 2.4]; see Remark 3.3.3 below. Letting $f(m) = \mathbb{P}(\Delta_0 \geq m) = 1 - g(m)$, we obtain from (3.1) and the last display

$$f(m) - f(m+1) + f(m)f(m+1) = \frac{2}{(m+1)(m+2)} \quad \text{for all } m \in \mathbb{N}.$$

Our claim about Δ_0 now follows from the following

Lemma 3.3.2. *Consider the non-linear system*

$$\begin{cases} f(m) - f(m+1) + f(m)f(m+1) &= \frac{2}{(m+1)(m+2)} \quad \text{for all } m \in \mathbb{N}, \\ f(0) &= 1, \\ \lim_{m\to\infty} f(m) &= 0. \end{cases} \tag{3.3}$$

Then the only solution f of (3.3) with $f(m) \in (0,1)$ for all $m \in \mathbb{N}$ is given by $f(m) = 1/(m+1)$, $m \in \mathbb{Z}_+$.

Proof. It is elementary to check that $f(m) = 1/(m+1)$, $m \in \mathbb{Z}_+$, is a solution of (3.3) with $f(\mathbb{N}) \subset (0,1)$, so it remains to show uniqueness. We first prove the following statement:

If $f_1, f_2 : \mathbb{Z}_+ \to (0,1)$ are two solutions of (3.3) such that $f_1(m) < f_2(m)$ for some $m \in \mathbb{N}$, then $f_1(m+k) < f_2(m+k)$ for all $k \in \mathbb{Z}_+$. (3.4)

Indeed, assume $f_1(m) < f_2(m)$ for some $m \in \mathbb{N}$. We show that then also $f_1(m+1) < f_2(m+1)$. Since f_1 is a solution of (3.3), we can use (3.3) to express $f_1(m+1)$ in terms of $f_1(m)$ and obtain

$$f_1(m+1) = \frac{(m+1)(m+2)f_1(m) - 2}{(m+1)(m+2)(1-f_1(m))} < \frac{(m+1)(m+2)f_2(m) - 2}{(m+1)(m+2)(1-f_2(m))} = f_2(m+1).$$

An iteration of the argument shows $f_1(m+k) < f_2(m+k)$ for all $k \in \mathbb{Z}_+$ and hence (3.4).

Now assume there are two solutions $f_1, f_2 : \mathbb{Z}_+ \to (0,1)$ of (3.3) with $f_1 \neq f_2$. Then there exists $\varepsilon > 0$ and $m \in \mathbb{N}$ such that $f_2(m) - f_1(m) > \varepsilon$ or $f_1(m) - f_2(m) > \varepsilon$. By symmetry, we may assume the former. Since both f_1 and f_2 solve (3.3), we obtain for their difference

$$f_2(m) - f_1(m) - (f_2(m+1) - f_1(m+1)) + f_2(m)f_2(m+1) - f_1(m)f_1(m+1) = 0. \tag{3.5}$$

By assumption, $f_2(m) - f_1(m) > \varepsilon$, which implies by (3.4) that

$$f_2(m)f_2(m+1) - f_1(m)f_1(m+1) > 0.$$

Therefore, we obtain from (3.5) that also $f_2(m+1) - f_1(m+1) > \varepsilon$. Iterating the argument, we see $\lim_{m\to\infty} f_2(m) \geq \varepsilon$, a contradiction to $\lim_{m\to\infty} f_2(m) = 0$. □

We continue the proof of Proposition 3.3.1 and turn to the distribution of Δ_0'. By time-reversal, $(\mathsf{b}_\infty(i) : H_1' < i \leq 0)$ has the same law as $(\mathsf{b}_\infty(i) : 0 \leq i < H_1)$. Moreover, down-steps i of $(\mathsf{b}_\infty(i) : H_1' < i \leq 0)$ belong to $\mathsf{DS}(\mathsf{b}_\infty)$, and as shown in

Figure 3.5, independent trees with law $\rho_{\mathsf{b}_\infty(i)}$ are assigned to them. However, $H'_1 - 1$ is an up-step of the bridge, where no tree is attached to, while $H_1 - 1$ is a down-step. As a consequence, if we modify T_∞ by attaching an independent tree with law ρ_0 to $H'_1 - 1$, the whole process $(\mathsf{b}_\infty, T_\infty)$ has the same law on $[0, H_1]$ as on $[H'_1, 0]$. Thus, for every $m \in \mathbb{Z}_+$,

$$\mathbb{P}(\Delta_0 < m) = \mathbb{P}(\Delta'_0 < m)h(m),$$

which gives from the first part of the proposition that for every $m \in \mathbb{N}$,

$$\mathbb{P}(\Delta'_0 \geq m) = \frac{1}{m+3}.$$

This concludes the proof of Proposition 3.3.1. □

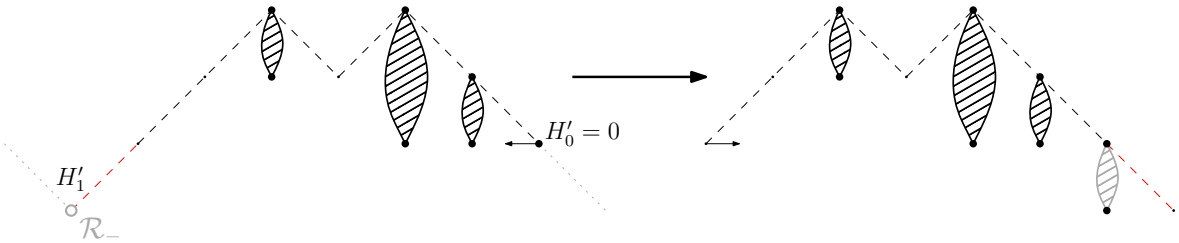

Figure 3.5: The symmetry argument between excursions of b_∞.

Remark 3.3.3. Note that as an intermediate step in the proof of Proposition 3.3.1, we explicitly compute the distribution of a minimal label in a well-labeled tree (τ, ℓ) with law ρ_0, cf. Display (3.2). As it was pointed out to us by the referee, the calculation of $h(m)$ was already performed in [CD06, Proposition 2.4]. In [CMM13, Lemma 12], it is (only) shown that the tail distribution behaves asymptotically like $2/m^2$ as m tends to infinity. The methods of [CMM13] rely on the fact that the label function ℓ has its continuous analog in the so-called Brownian snake. We stress that for our purpose, the asymptotic tail behavior of the minimal label of (τ, ℓ) would not provide enough information, see Remark 3.3.5 below.

We let $\mathbf{Q}_\infty^\infty = \Phi((\mathsf{b}_\infty, T_\infty))$ be the UIHPQ defined in terms of a uniform infinite treed bridge $(\mathsf{b}_\infty, T_\infty)$. Recall the identification of $\mathbb{Z}$ with $\partial\mathbf{Q}_\infty^\infty$ via the function φ. Our presentation is now similar to that of [CMM13, Section 3.2.2]. From now on, $\gamma_{\max}$ will denote the maximal geodesic in the UIHPQ emanating from the root ϱ. By construction of the Bouttier–Di Francesco–Guitter mapping and by definition of $\gamma_{\max}$, a vertex $\varphi(j) \in \partial\mathbf{Q}_\infty^\infty$ for $j \in \mathbb{Z}_+$ is hit by $\gamma_{\max}$ if and only if it is incident to the first (real) corner in contour order starting from c_0 with label $\ell_\infty(\varphi(j))$, i.e., if and only if

$$\min\{\ell_{\infty,i}(v) : v \in V(T_\infty(i)),\, i \in \mathsf{DS}(\mathsf{b}_\infty),\, 0 \leq i \leq j-1\} > \mathsf{b}_\infty(j),$$

where $\ell_{\infty,i}$ denotes the labeling of $T_\infty(i)$. In particular, if we introduce the set of intersection times of the maximal geodesic with the right boundary of the UIHPQ,

$$\mathcal{R}_+ = \{j \in \mathbb{Z}_+ : \gamma_{\max}(j) \in \varphi(\mathbb{Z}_+)\},$$

we have

$$\mathcal{R}_+ = \mathbb{Z}_+ \setminus \bigcup_{j\geq 0} (j, j+\Delta_j].$$

See Figure 3.6 for an illustration. It follows from the last display that $\mathcal{R}_+$ can be represented as the set $\{G_0 + G_1 + \cdots + G_n : n \in \mathbb{Z}_+\}$, where $G_0 = 0$, and $(G_i : i \in \mathbb{N})$ is a sequence of i.i.d. variables with

$$G_1 = \inf\left\{i > 0 : \max\{j + \Delta_j : 0 \leq j \leq i-1\} < i\right\}. \tag{3.6}$$

In particular, $\mathcal{R}_+$ is a discrete regenerative set, and the renewal theorem shows that the asymptotic frequency of $\mathcal{R}_+$ is given by

$$|\mathcal{R}_+| = \lim_{n\to\infty} \frac{\#\mathcal{R}_+ \cap \{1,\ldots,n\}}{n} = \frac{1}{\mathbb{E}[G_1]}. \tag{3.7}$$

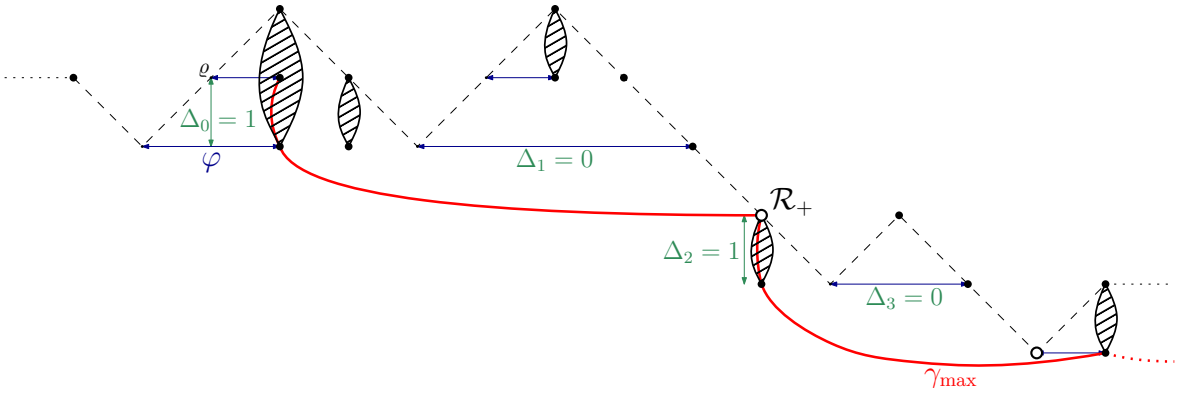

Figure 3.6: Alternative representation of the UIHPQ and its maximal geodesic $\gamma_{\max}$ as depicted in Figure 3.3. (Trees are represented by the striped almonds, whose lower endpoints indicate the minimal label in the corresponding tree.)

We will also study the set of intersection times of the maximal geodesic with the left part of the boundary,

$$\mathcal{R}_- = \{j \in \mathbb{Z}_+ : \gamma_{\max}(j) \in \varphi(\mathbb{Z}_-)\}.$$

Using again the construction of the UIHPQ via the Bouttier–Di Francesco–Guitter mapping, we can express this set as

$$\mathcal{R}_- = \mathbb{Z}_+ \setminus \bigcup_{j\geq 0} (j, j+\Delta'_j].$$

Similarly to $\mathcal{R}_+$, we have $\mathcal{R}_- = \{G'_0 + G'_1 + \cdots + G'_n : n \in \mathbb{Z}_+\}$, where again $G'_0 = 0$, and $(G'_i : i \in \mathbb{N})$ is an i.i.d. family of random variables specified by

$$G'_1 = \inf\left\{i > 0 : \max\{j + \Delta'_j : 0 \leq j \leq i-1\} < i\right\}. \tag{3.8}$$

Note that $(G'_i : i \in \mathbb{N})$ is also independent of $(G_i : i \in \mathbb{N})$. Indices $j \in \mathcal{R}_-$ correspond to (certain) up-steps of the bridge and thus to phantom vertices. Then, the associated vertex $\varphi(j)$ is incident to the first (real) corner in contour order starting from c_0 with label $\ell_\infty(\varphi(j))$ and is therefore visited by the maximal geodesic.

We now formulate the key proposition of this paper.

Proposition 3.3.4. *We have for $i \in \mathbb{N}$,*

$$\mathbb{P}(i \in \mathcal{R}_+) = \frac{1}{i+1}, \quad \text{and} \quad \mathbb{P}(i \in \mathcal{R}_-) = \frac{3}{i+3}.$$

Also, almost surely, both $\mathcal{R}_+$ and $\mathcal{R}_-$ are infinite sets, and the maximal geodesic $\gamma_{\max}$ hits the left as well as the right part of the boundary of the UIHPQ *infinitely many times. However, this happens with asymptotic frequency zero: $|\mathcal{R}_+| = 0$ and $|\mathcal{R}_-| = 0$ almost surely.*

Proof. The arguments for $\mathcal{R}_+$ and $\mathcal{R}_-$ are entirely similar. Let us first consider $\mathcal{R}_+$. By Proposition 3.3.1 in the last equation, we have for $i \in \mathbb{N}$

$$\begin{aligned}\mathbb{P}(i \in \mathcal{R}_+) &= \mathbb{P}\left(\max\{j + \Delta_j : 0 \le j \le i-1\} < i\right) \\ &= \prod_{j=0}^{i-1} \left(1 - \mathbb{P}\left(\Delta_0 \ge i - j\right)\right) = \prod_{j=1}^{i} \left(1 - \mathbb{P}\left(\Delta_0 \ge j\right)\right) \\ &= \exp\left(\sum_{j=1}^{i} \ln\left(1 - \frac{1}{j+1}\right)\right) = \frac{1}{i+1}.\end{aligned}$$

We deduce from the last display that

$$\mathbb{E}\left[\#\mathcal{R}_+\right] = \sum_{i=0}^{\infty} \mathbb{P}(i \in \mathcal{R}_+) = \infty.$$

From this, we readily infer that $\#\mathcal{R}_+ = \infty$ almost surely: Indeed, if the contrary were true, then necessarily $G_1 = \infty$ with some probability $\alpha > 0$. However, then the number of points in $\mathcal{R}_+$ different from 0 is geometrically distributed with parameter α, a contradiction to $\mathbb{E}[\#\mathcal{R}_+] = \infty$. The fact that $|\mathcal{R}_+| = 0$ follows from (3.7) and Proposition 3.3.1. Concerning $\mathcal{R}_-$, we simply have to replace Δ_0 by Δ_0' in the above argumentation. An application of Proposition 3.3.1 shows $\mathbb{P}(i \in \mathcal{R}_-) = 3/(i+3)$, and the remaining statements for $\mathcal{R}_-$ follow from the same reasoning as above. □

Albeit being infinite, the sets $\mathcal{R}_+$ and $\mathcal{R}_-$ are rather sparse. We will make this more precise in Section 3.4.

Remark 3.3.5. The last proposition should be compared with [CMM13, Proposition 15]. Proposition 3.3.1 has its counterpart in Lemma 14 of [CMM13], where it is shown that the quantity corresponding to $\mathbb{P}\left(\Delta_0 \ge m\right)$ behaves asymptotically like $2/m$ for m tending to infinity. The multiplicative factor being larger than 1, this implies in the context considered there that the number of intersections between the maximal geodesic and the spine of the UIPQ is *finite* almost surely. Here, in the setting of the UIHPQ, we find an exact formula for $\mathbb{P}\left(\Delta_0 \ge m\right)$, which came somewhat as a surprise and is the key observation that leads to Proposition 3.3.4. We emphasize that an equivalent of the form $\mathbb{P}\left(\Delta_0 \ge m\right) \sim 1/m$ would not be sufficient to deduce that $\mathcal{R}_+$ is an infinite set, and the same for $\mathcal{R}_-$.

For the intersection of the independent regenerative sets $\mathcal{R}_+$ and $\mathcal{R}_-$, we have for $i \in \mathbb{Z}_+$

$$\mathbb{P}\left(i \in \mathcal{R}_+ \cap \mathcal{R}_-\right) = \frac{3}{(i+1)(i+3)},$$

and with arguments similar to those in the proof of Proposition 3.3.4, we get that the left and right boundary of the UIHPQ intersect *finitely* many times. Actually, we have here obtained a new proof of the fact shown in [CM15] that the UIHPQ contains a well-defined *core*, that is an infinite submap homeomorphic to the half-plane. In [CM15], the well-definedness of the core was obtained by a limiting argument, starting from an infinite quadrangulation with a simple boundary of a finite (randomized) size, while we prove this result directly in terms of the UIHPQ.

Since any maximal geodesic finally coincides with $\gamma_{\max}$, Proposition 3.3.4 implies that any maximal geodesic has infinitely many intersection points with the left and right part of the boundary of the UIHPQ. We now prove that all geodesic rays in the UIHPQ are proper. Theorem 3.1.1 will then readily follow. The following result was already established in Proposition 4.8 of [CC15] for geodesic rays started from the root vertex, by similar but different arguments.

Corollary 3.3.6 (see Proposition 4.8 of [CC15]). *Almost surely, all geodesics rays in the* UIHPQ $\mathbf{Q}_\infty^\infty = \Phi((\mathsf{b}_\infty, T_\infty))$ *are proper.*

Proof. Here, we propose a simple proof that uses the result of Proposition 3.3.4. Let η be an infinite self-avoiding path in $\mathbf{Q}_\infty^\infty$. Since by the above proposition, the maximal geodesic $\gamma_{\max}$ intersects the left and right boundary infinitely often, the path η also intersects $\gamma_{\max}$ infinitely often, as indicated by Figure 3.7.

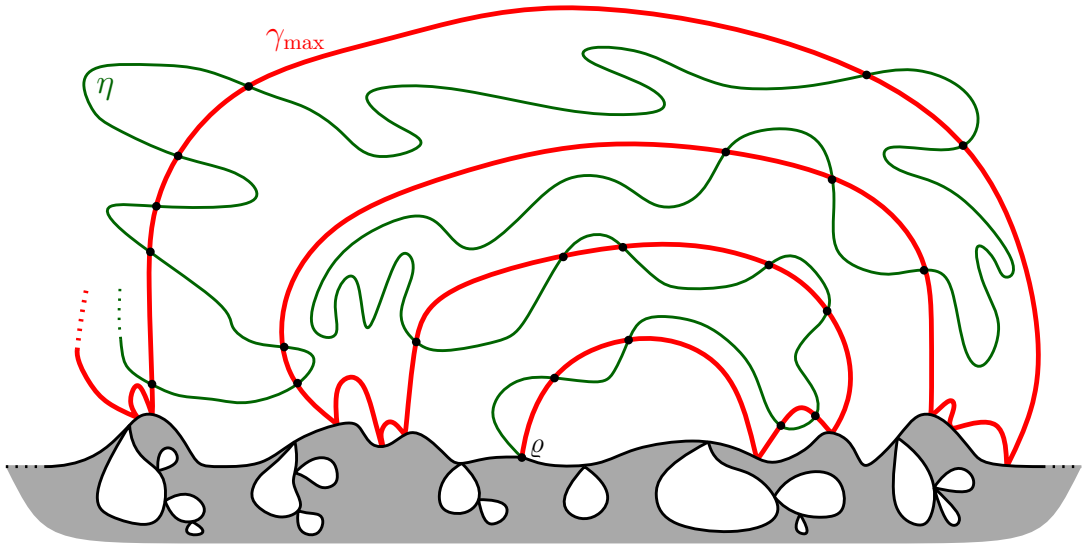

Figure 3.7: The infinite path η intersects $\gamma_{\max}$ infinitely many times.

Let γ be a geodesic ray in $\mathbf{Q}_\infty^\infty$. To simplify notation, we assume that γ starts at the root ϱ (if not, one should consider the maximal geodesic started from $\gamma(0)$). The above remark applied to $\eta = \gamma$ shows that γ and $\gamma_{\max}$ intersect infinitely many times. Let $(u_i : i \in \mathbb{Z}_+)$ be the sequence of vertices at which γ and $\gamma_{\max}$ intersect, with $u_0 = \varrho$ and such that u_i is visited before u_j if $i < j$. Then, for every $i \in \mathbb{Z}_+$, by definition of the maximal geodesic,

$$d_{\mathrm{gr}}(u_{i+1}, u_i) = \ell_\infty(u_i) - \ell_\infty(u_{i+1}).$$

Because labels differ at most by one between neighboring vertices of the map, the length of the segment of γ between u_i and u_{i+1} is at least $\ell_\infty(u_i) - \ell_\infty(u_{i+1}) = d_{\mathrm{gr}}(u_{i+1}, u_i)$. Therefore, equality must hold since γ is a geodesic, and this implies that labels always decrease by one as γ goes from u_i to u_{i+1}, meaning that γ is proper on this segment. This finishes the proof. □

The proof of Theorem 3.1.1 is now an immediate consequence of our foregoing considerations.

Proof of Theorem 3.1.1. For the purpose of the proof, we will assume that the UIHPQ is given in terms of a uniform infinite treed bridge, $\mathbf{Q}_\infty^\infty = \Phi((\mathsf{b}_\infty, T_\infty))$. Let γ be a geodesic ray. By Corollary 3.3.6, we can assume that γ is proper. Hence each edge of γ connects a real corner of $(\mathsf{b}_\infty, T_\infty)$ to its successor. Now let $n_0 \in \mathbb{Z}_+$ be the first instant when the maximal geodesic emanating from $v = \gamma(0)$ hits the left part of the boundary. We have seen above that n_0 is finite almost surely. By definition, $\gamma^v_{\max}$ always connects leftmost corners to their successors. In particular, the embedding of γ in the upper half-plane (in terms of the Bouttier–Di Francesco–Guitter mapping) lies in between $(\gamma^v_{\max}(n) : n \geq n_0)$ and the boundary of the map, see Figure 3.8. Otherwise said, vertices of the right part of the boundary which are visited by $(\gamma^v_{\max}(n) : n \geq n_0)$ are also visited by any other proper geodesic started at v. Since $\gamma^v_{\max}$ coincides after a finite number of steps with $\gamma_{\max}$, the maximal geodesic started from the root ϱ, Proposition 3.3.4 concludes the proof. □

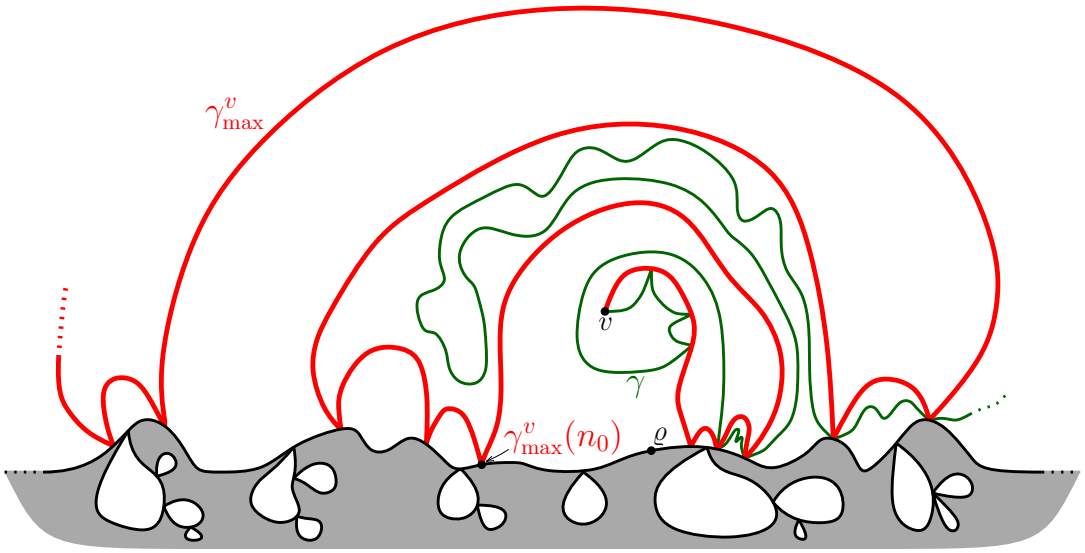

Figure 3.8: The geodesic γ lies in between $(\gamma^v_{\max}(n) : n \geq n_0)$ and the boundary of the map.

Corollary 3.3.7. *Theorem 3.1.1 remains true if the* UIHPQ *is replaced by its analog with a simple boundary, the* UIHPQ$^{(s)}$.

Proof. We give only a sketch proof, since the statement is essentially a consequence of the pruning construction of the UIHPQ$^{(s)}$ out of the UIHPQ, as explained in [CM15]

(see, in particular, Proposition 6 in this work). Roughly speaking, after removing the finite quadrangulations which hang off from the pinch-points of the boundary of the UIHPQ, a core consisting of a unique infinite quadrangulation with an infinite simple boundary remains, which has, after a rooting operation, the law of the UIHPQ$^{(s)}$. Since geodesics started from the core of the UIHPQ do not visit the finite quadrangulations that are attached to the pinch-points of the boundary (the pinch-points would be visited twice), Theorem 3.1.1 applies to the UIHPQ$^{(s)}$ as well. □

3.4 Sparseness of the intersections with the boundary

From Theorem 3.1.1, we know that every geodesic ray in the UIHPQ hits the boundary infinitely many times. The goal of this section is to show that these hitting times and hitting points are, however, sparsely distributed, in a way that we will make precise in Proposition 3.4.3 below.

For that purpose, recall that the sets $\mathcal{R}_+$ and $\mathcal{R}_-$ of intersection times of the maximal geodesic with the right and left part of the boundary, respectively, admit the representation

$$\mathcal{R}_+ = \{G_0 + G_1 + \cdots + G_n : n \in \mathbb{Z}_+\}, \quad \mathcal{R}_- = \{G'_0 + G'_1 + \cdots + G'_n : n \in \mathbb{Z}_+\},$$

where $G_0 = G'_0 = 0$, and the families $(G_i : i \in \mathbb{N})$ and $(G'_i : i \in \mathbb{N})$ consist of i.i.d. random variables specified by (3.6) and (3.8), respectively. We find the following asymptotic behavior.

Lemma 3.4.1. *For m tending to infinity, we have*

$$\mathbb{P}(G_1 = m) \sim \frac{1}{m \ln^2 m}, \quad \mathbb{P}(G'_1 = m) \sim \frac{1}{3m \ln^2 m}.$$

Proof. We first look at G_1. For $n \in \mathbb{Z}_+$, let $u_n = \mathbb{P}(n \in \mathcal{R}_+)$, $f_n = \mathbb{P}(G_1 = n)$. Note that $f_0 = 0$ and $u_0 = 1$. A classical decomposition (see, e.g., Section XIII.3 in [Fel68]) of u_n according to the smallest non-zero element in $\mathcal{R}_+$, i.e., according to the value of G_1, gives the recursive relation

$$u_n = f_1 u_{n-1} + f_2 u_{n-2} + \cdots + f_n u_0, \quad n \in \mathbb{N}.$$

For the generating functions $U(s) = \sum_{n\geq 0} u_n s^n$ and $F(s) = \sum_{n\geq 0} f_n s^n$, the last relation implies

$$U(s) = \frac{1}{1 - F(s)}, \quad |s| < 1.$$

Using that $\mathbb{P}(n \in \mathcal{R}_+) = 1/(n+1)$, see Proposition 3.3.4, we obtain for $0 < |s| < 1$ the expression $U(s) = -(1/s)\ln(1-s)$. Therefore,

$$F(s) = 1 - s \ln^{-1}\left(\frac{1}{1-s}\right), \quad |s| < 1.$$

Standard singularity analysis, see, e.g., (24) on page 387 of [FS09], yields the first claim. For G'_1, we use that $\mathbb{P}(n \in \mathcal{R}_-) = 3/(n+3)$, see again Proposition 3.3.4. For

the generating function $H(s) = \sum_{n\geq 0} \mathbb{P}(G_1' = n)s^n$, this gives similarly to above the relation

$$H(s) = 1 - (s^3/3)\left(\ln\left(\frac{1}{1-s}\right) - s^2/2 - s\right)^{-1}, \quad |s| < 1.$$

Since $1 - H(s) \sim (1/3)(1 - F(s))$ as $s \to 1$, an application of [FS09, Theorem IV.4] finishes the proof of the second claim. □

Remark 3.4.2. The above lemma should be compared with the asymptotics of the returns to zero of a recurrent two-dimensional random walk $S = (S_n : n \in \mathbb{Z}_+)$. For concreteness, let us assume that S is the simple symmetric random walk on $\mathbb{Z}^2$ started from zero. Let $\mathcal{R}$ be the regenerative set of return times to zero of S. One has the representation $\mathcal{R} = \{G_0 + G_1 + \cdots + G_n : n \in \mathbb{Z}_+\}$, where $G_0 = 0$, and $(G_i : i \in \mathbb{N})$ are the waiting times between two consecutive returns. Then, as $m \to \infty$, we get the asymptotics ([Spi01, Chapter III, Section 16, Example 1])

$$\mathbb{P}(m \in \mathcal{R}) \sim \frac{1}{\pi m} \quad \text{and} \quad \mathbb{P}(G_1 = m) \sim \frac{\pi}{m \ln^2 m}.$$

Coming back to geodesics in the UIHPQ, we note that Lemma 3.4.1 gives precise quantitative information on the number of steps between two consecutive visits of the boundary by the maximal geodesic $\gamma_{\max}$. The distance measured along the boundary between two consecutive times of intersection is bounded from below by the number of steps of $\gamma_{\max}$ in between these times.

In the proof of Theorem 3.1.1, we have seen that any geodesic ray γ is finally enclosed between $\gamma_{\max}$ and the boundary of the UIHPQ. *A priori,* this does not exclude the existence of a geodesic ray that visits the boundary with a much higher frequency than $\gamma_{\max}$. We will now argue that this is not the case.

In this regard, it is convenient to introduce the *minimal geodesic* in the UIHPQ emanating from the root ϱ. Given $(\mathsf{b}_\infty, T_\infty)$ and v a real vertex of $(\mathsf{b}_\infty, T_\infty)$, we write $c^{(r)}(v)$ for the rightmost corner incident to v. Note that in the list of corners $(c_i)_{i\in\mathbb{Z}}$ as specified in Section 3.2.2, $c^{(r)}(v)$ appears as the last corner incident to v (in the lexicographical order).

The minimal geodesic $\gamma_{\min}$ starting from ϱ is then given by the chain of vertices $\gamma_{\min}(0) = \varrho$, and for $i \in \mathbb{N}$,

$$\gamma_{\min}(i) = \mathcal{V}\left(\mathrm{succ}\left(c^{(r)}(\gamma_{\min}(i-1))\right)\right).$$

The edge set of $\gamma_{\min}$ is given by the edges connecting $c^{(r)}(\gamma_{\min}(i))$ to $c^{(r)}(\gamma_{\min}(i+1))$ for $i \in \mathbb{Z}_+$.

Similarly to above, one defines for $\gamma_{\min}$ the (random) sets of intersection times with the right and left part of the boundary, respectively,

$$\mathcal{R}_+^{\min} = \{j \in \mathbb{Z}_+ : \gamma_{\min}(j) \in \varphi(\mathbb{Z}_+)\}, \quad \mathcal{R}_-^{\min} = \{j \in \mathbb{Z}_+ : \gamma_{\min}(j) \in \varphi(\mathbb{Z}_-)\}.$$

The following symmetry argument shows that the random set $\mathcal{R}_+^{\min}$ (defined in terms of $\gamma_{\min}$) has the same law as $\mathcal{R}_-$ (defined in terms of $\gamma_{\max}$). Consider the mapping that associates to a (possibly infinite) rooted planar map $\mathbf{m}$ its "mirror" $\overleftarrow{\mathbf{m}}$, which

is obtained from applying a symmetry with respect to any line of the plane, and reversing the orientation of the root edge. This transformation is better understood by seeing a planar map as a gluing of polygons: Then, the map $\overleftarrow{\mathbf{m}}$ is obtained by reversing the orientation of the polygons forming $\mathbf{m}$, and that of the root edge. Now, it is seen that this transformation preserves the uniform measure on quadrangulations with a fixed size and perimeter, and thus the law of the UIHPQ. Finally, recall that the maximal and minimal geodesics started at the root vertex are also the leftmost and rightmost geodesics, respectively, and are thus exchanged by the "mirror" mapping. It follows that $\mathcal{R}_+^{\min}$ and $\mathcal{R}_-$ have the same law, and, by the same symmetry argument, $\mathcal{R}_-^{\min}$ has the same law as $\mathcal{R}_+$.

As a direct consequence of the way edges are drawn in the Bouttier–Di Francesco–Guitter construction of the UIHPQ, and of the fact that every geodesic ray is proper, see Corollary 3.3.6, we notice that any geodesic ray γ lies finally in between $\gamma_{\max}$ and $\gamma_{\min}$. Indeed, this is the case from the first vertex on hit by γ that is incident to a corner c_i with $i \in \mathbb{Z}_+$. See Figure 3.9 for an illustration. From the constructions of $\gamma_{\max}$ and $\gamma_{\min}$, we see that $\mathcal{R}_+$ is a subset of $\mathcal{R}_+^{\min}$, and similarly $\mathcal{R}_-^{\min}$ is a subset of $\mathcal{R}_-$.

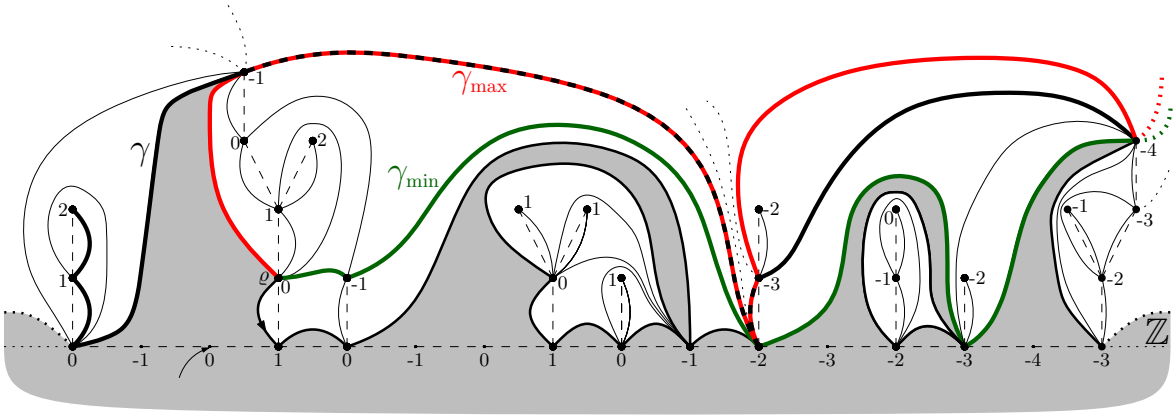

Figure 3.9: The geodesic γ (black bold) started at the leftmost vertex labeled 2 is enclosed by $\gamma_{\min}$ (green bold) and $\gamma_{\max}$ (red bold) after it first hits the latter (at the topmost vertex labeled -1).

We collect our observations in the following proposition, which should be read as an extension to Theorem 3.1.1. For simplicity, we restrict ourselves to geodesic rays emanating from the root vertex; see, however, the remark below the proposition.

Proposition 3.4.3. *Almost surely, for any geodesic ray $\gamma = (\gamma(i) : i \in \mathbb{Z}_+)$ in the* UIHPQ $\mathbf{Q}_\infty^\infty = \Phi((\mathsf{b}_\infty, T_\infty))$ *started from the root vertex, we have the inclusions*

$$\mathcal{R}_+ \cup \mathcal{R}_-^{\min} \subseteq \{i \in \mathbb{Z}_+ : \gamma(i) \in \partial \mathbf{Q}_\infty^\infty\} \subseteq \mathcal{R}_+^{\min} \cup \mathcal{R}_-.$$

The random sets $\mathcal{R}_+$ and $\mathcal{R}_-^{\min}$ (as well as $\mathcal{R}_+^{\min}$ and $\mathcal{R}_-$) have the same law. The distance δ between two consecutive times in $\mathcal{R}_+$ (or $\mathcal{R}_-^{\min}$) exhibits the tail behavior $\mathbb{P}(\delta > m) \sim 1/\ln m$ as $m \to \infty$, whereas the distance δ' between two consecutive times in $\mathcal{R}_+^{\min}$ (or $\mathcal{R}_-$) satisfies $\mathbb{P}(\delta' > m) \sim 1/(3 \ln m)$.

Remark 3.4.4. Let $\gamma = (\gamma(i) : i \in \mathbb{Z}_+)$ be any geodesic ray in the UIHPQ (not necessarily started from the root vertex), and let v be the first vertex to the right of the root ϱ which is hit by both γ and $\gamma_{\max}$. Let n, $n' \in \mathbb{Z}_+$ such that $\gamma(n) = \gamma_{\max}(n') = v$, and set $j = n - n'$. Now consider the shifted geodesic $\gamma_j(i) = \gamma(i + j)$, $i \geq \max\{0, -j\}$. On the event of full probability where γ, $\gamma_{\max}$ and $\gamma_{\min}$ are proper, we have the inclusions

$$\left(\mathcal{R}_+ \cup \mathcal{R}_-^{\min}\right) \setminus \{0, \dots, n'\} \subseteq \{i \geq \max\{0, -j\} : \gamma_j(i) \in \partial \mathbf{Q}_\infty^\infty\} \subseteq \mathcal{R}_+^{\min} \cup \mathcal{R}_-.$$

3.5 Extension to the uniform infinite half-planar triangulation

The uniform infinite half-planar triangulation UIHPT is an infinite triangulation of the half-plane. A variation with a simple boundary (i.e., the triangular analog to the UIHPQ$^{(s)}$) was introduced by Angel in [Ang04].

In this part, we will argue that the intersection times with the boundary of geodesics in the UIHPT behave in way comparable to that in the UIHPQ. More precisely, it turns out that the right part of the boundary is hit by the maximal geodesic started from the root with exactly the same frequency as in the UIHPQ, whereas the distribution of the hitting times of the left part of the boundary undergoes a slight change.

In order to avoid too much repetition, we will not treat the case of the UIHPT in full detail. We will rather argue that the strategy developed for the UIHPQ applies to the UIHPT as well, and then sketch how the computations have to be modified. Our discussion will therefore lack a certain rigor, but should enable the reader to fill in the remaining details. In order to make a clear distinction to the UIHPQ, some of our quantities considered in this section will be decorated with the tilde sign.

Triangulations, or more generally (rooted and pointed) planar maps with prescribed face valences, can be encoded in terms of labeled trees called *mobiles*, as shown in [BDFG04]. Let us briefly recall the encoding: First, label each vertex of the map by its distance from the pointed vertex minus the distance from the pointed vertex to the origin of the root edge. Put a new vertex without label in the center of each face. Now walk around each face F in the clockwise order, and look at each of its incident edges. If for an edge e, the label decreases by 1 when walking clockwise around F, then connect the endpoint of e with the larger label to the (unlabeled) vertex in the middle of F. If the labels of the endpoints of e are both equal to n, say, add a *flagged vertex* with flag n in the middle of e and connect the flagged vertex with two new edges to the two central vertices of the faces incident to e. In the third case, that is, for edges where the labels increase when walking around the face F, do nothing. See Figure 3.10. By removing all the original edges of the map together with the pointed vertex, one obtains a *mobile*, i.e., a plane tree with three types of vertices: labeled and unlabeled vertices, and flagged vertices.

Note that by construction, flagged vertices have degree 2, and unlabeled vertices are in one-to-one correspondence with the faces of the map. Moreover, the degree of the corresponding face equals twice the number of labeled vertices plus the number

of flagged vertices that are connected to the unlabeled vertex in the mobile. In particular, an unlabeled vertex associated to a triangular face has either three flagged vertices or a flagged vertex and a labeled vertex incident to it.

Figure 3.10: The construction of a mobile. The black dots represent unlabeled vertices of the mobile. They are put in the centers of the faces of the map. On the left, the bold line represents a mobile edge associated to an edge of the map, which connects a vertex labeled n to a vertex labeled $n-1$. On the right, the bold line represents a mobile edge associated to an edge connecting two vertices with label n. The flagged vertex is represented by a lozenge and receives label n, too.

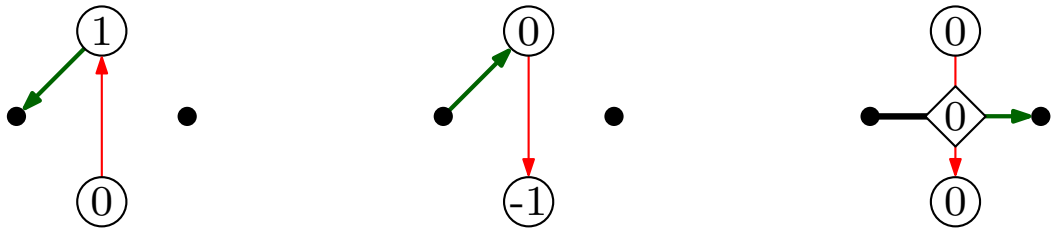

Figure 3.11: The rooting convention. The red arrow represents the root edge of the map, and the green bold arrow is the associated root edge of the mobile.

The root edge of a planar map allows to distinguish a root edge in the mobile, as depicted in Figure 3.11. If the root edge of the map connects two vertices with label 0, see the right most case in Figure 3.11, it is convenient to regard the encoding mobile as a pair of *half-mobiles* with root flag 0 each, i.e., mobiles which have one distinguished flagged vertex of degree 1 called the root flag, which receives label 0. There is a bijection between rooted pointed planar maps on the one hand and rooted mobiles and pairs of half-mobiles on the other hand. We refer to [BDFG04] and [BG12] for more details.

In terms of generating functions, prescribing the number of faces of a certain degree k amounts to attach a weight to each face of degree k. For our purpose, we now specialize in triangulations corresponding to the critical weight sequence $g_k = g_{3,\mathrm{cr}}\delta_3(k)$, where $g_{3,\mathrm{cr}} = 2^{-1}3^{-3/4}$, see, e.g., [Mie06]. In this regard, let R_m (or S_m) denote the corresponding generating function of rooted mobiles (or half-mobiles) with root label (or root flag) 0, which have their labels all strictly larger than $-m$ and their flags all larger or equal to $-m$, cf. [BG12]. Letting $R = \lim_{m\to\infty} R_m$ and $S = \lim_{m\to\infty} S_m$, an analysis of (6.2) in [BG12] shows that $R = \sqrt{3}$ and $S = 3^{1/4}\left(\sqrt{3}-1\right)$, but this will be of no importance here. Note that R and S are the

partition functions for rooted mobiles with root label 0 and half-mobiles with root flag 0, respectively, subject to $g_k = g_{3,\mathrm{cr}}\delta_3(k)$.

In order to motivate our construction of the UIHPT, let us first consider rooted pointed triangulations with a boundary of perimeter $n \in \mathbb{Z}_+$. This means that all faces except the root face are triangles, the root face being incident to n edges (loops and multiple edges are allowed). We choose such a triangulation $\mathbf{m}$ according to the Boltzmann law $\rho(\mathbf{m}) = g_{3,\mathrm{cr}}^{\#F(\mathbf{m})}/Z$, where $F(\mathbf{m})$ denotes the set of faces of $\mathbf{m}$ without the root face (which receives no weight), and Z is the normalizing partition function. Denote by d the distance between the pointed vertex of $\mathbf{m}$ and the origin of the root edge. Following Section 2.4 of [BDFG04], we associate to the map a (random) path $(X^{[n]}(i) : 0 \le i \le n)$ that encodes the clockwise sequence of distances minus d between the pointed vertex of the map and the vertices incident to the root face, with $X^{[n]}(0)$ given by the origin of the root edge (so that $X^{[n]}(0) = 0$).

We decompose the associated mobile around the unlabeled vertex v lying in the center of the root face of the map. Then each down- or level-step of $X^{[n]}$ corresponds to a labeled or a flagged vertex, respectively, which is connected to v by an edge, see Figure 3.10. By removing v and its incident edges, one obtains a sequence of rooted mobiles and half-mobiles. More precisely, a down-step i of $X^{[n]}$ corresponds to a rooted mobile with root label $X^{[n]}(i)$, while a level-step i of $X^{[n]}$, that is, an i with $X^{[n]}(i+1) = X^{[n]}(i)$, corresponds to a half-mobile with root flag $X^{[n]}(i)$. This decomposition is bijective. Letting n grow, this incites us to define the following two-sided random walk. Let $C = 2\sqrt{R} + S$, and consider $\tilde{\mathsf{b}}_\infty = (\tilde{\mathsf{b}}_\infty(i) : i \in \mathbb{Z})$ with $\tilde{\mathsf{b}}_\infty(0) = 0$, such that the increments $(\tilde{\mathsf{b}}_\infty(i+1) - \tilde{\mathsf{b}}_\infty(i) : i \in \mathbb{Z}_+)$ are i.i.d. with law

$$\mathbb{P}\left(\tilde{\mathsf{b}}_\infty(i+1) - \tilde{\mathsf{b}}_\infty(i) = \pm 1\right) = \frac{\sqrt{R}}{C}, \quad \mathbb{P}\left(\tilde{\mathsf{b}}_\infty(i+1) - \tilde{\mathsf{b}}_\infty(i) = 0\right) = \frac{S}{C},$$

and $(\tilde{\mathsf{b}}_\infty(i) : i \in \mathbb{Z}_-)$ is an i.i.d. copy of $(\tilde{\mathsf{b}}_\infty(i) : i \in \mathbb{Z}_+)$. One can show that for fixed $\ell \in \mathbb{N}$, there is the convergence

$$\left(X^{[n]}([i]) : -\ell \le i \le \ell\right) \xrightarrow[n\to\infty]{(d)} \left(\tilde{\mathsf{b}}_\infty(i) : -\ell \le i \le \ell\right),$$

with $[i]$ denoting the representative of i modulo n in $\{0, \dots, n-1\}$.

We proceed now similarly to the construction of the UIHPQ: Conditionally on $\tilde{\mathsf{b}}_\infty$, we identify $\tilde{\mathsf{b}}_\infty$ with $\mathbb{Z}$ equipped with the labels $(\tilde{\mathsf{b}}_\infty(i) : i \in \mathbb{Z})$, and graft independently to each down-step $i \in \mathsf{DS}(\tilde{\mathsf{b}}_\infty)$ a mobile θ in the upper half-plane with root label $\tilde{\mathsf{b}}_\infty(i)$, distributed according to the Boltzmann measure $\rho^{(R)}(\theta) = g_{3,\mathrm{cr}}^{\#\bullet(\theta)}/R$ (where $\bullet(\theta)$ denotes the set of unlabeled vertices of θ). Moreover, writing $\mathsf{LS}(\tilde{\mathsf{b}}_\infty)$ for the set of level-steps of $\tilde{\mathsf{b}}_\infty$, we graft to each $i \in \mathsf{LS}(\tilde{\mathsf{b}}_\infty)$ independently a half-mobile θ' with root flag $\tilde{\mathsf{b}}_\infty(i)$, distributed according to $\rho^{(S)}(\theta') = g_{3,\mathrm{cr}}^{\#\bullet(\theta')}/S$. We obtain what we call a *uniform infinite mobile bridge* $(\tilde{\mathsf{b}}_\infty, \tilde{T}_\infty)$, where $\tilde{T}_\infty$ is now a collection of independent mobiles and half-mobiles associated to the down- and level-steps of $\tilde{\mathsf{b}}_\infty$, respectively.

Each realization of $(\tilde{\mathsf{b}}_\infty, \tilde{T}_\infty)$ is naturally embedded in the upper-half plane, similarly to the description in Section 3.2.2. Recall that mobiles and half-mobiles come with three types of vertices. We call here a labeled vertex of a mobile or a half-mobile

a *real vertex* , and a real corner (of the embedding) is a corner in the upper half-plane incident to a real vertex. Note that flagged vertices are not real vertices.

We write $(c_i)_{i\in\mathbb{Z}}$ for the sequence of real corners in the left-to-right order, again with c_0 being the leftmost corner incident to the root vertex. As in the construction of the UIHPQ, we now connect each real corner c_i to its successor, that is the first corner among $c_{i+1}, c_{i+2}, \dots$ with label $\ell(c_i) - 1$. Additionally, we connect both corners of the flagged vertices to the corresponding next real corner in the contour order with the *same* label. See Figure 3.12 for an illustration.

We finally erase the unlabeled vertices and the flagged vertices, interpreting the two outgoing arcs from a flagged vertex which we added as a single edge. We also erase all the edges and non-real vertices that stem from the representation of $(\tilde{\mathfrak{b}}_\infty, \tilde{T}_\infty)$ in the plane. We obtain what we call the *uniform infinite half-planar triangulation* UIHPT. The bi-infinite line $\mathbb{Z}$ can again be identified with the boundary of the UIHPT. In particular, it makes sense to speak of the left or right part of the boundary. We root the UIHPT according to the convention described in Section 3.2.2.

Remark 3.5.1. We stress that the above construction does not make use of the particular form of the weight sequence and can therefore be carried through for maps corresponding to other critical or sub-critical Boltzmann weights. For the choice $g_k = (1/12)\delta_4(k)$, we rediscover the construction of the UIHPQ as described in Section 3.2.2. Note that for bipartite maps, we have $S = 0$, i.e., there are no half-mobiles.

We may now define maximal (and minimal) geodesics in the UIHPT. Note that vertices of the UIHPT correspond to real vertices of the encoding. Analogously to the UIHPQ, the maximal geodesic started at vertex v is given by the infinite chain of vertices which are incident to the iterated successors of the leftmost real corner c belonging to v.

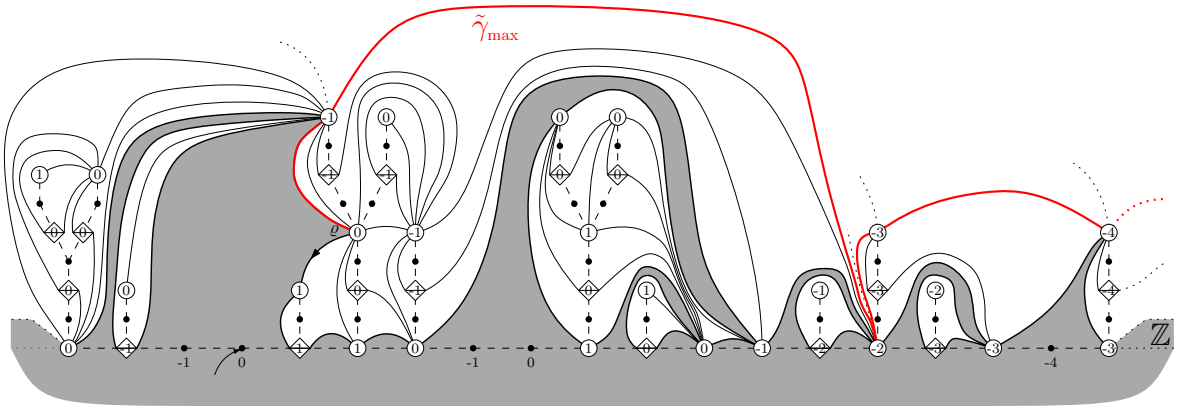

Figure 3.12: The construction of the UIHPT from an infinite mobile bridge, with its maximal geodesic $\tilde{\gamma}_{\max}$.

Similarly, by starting from the rightmost corner, we define the minimal geodesic emanating from v, and we write $\tilde{\gamma}_{\max}$ (or $\tilde{\gamma}_{\min}$) for the maximal (or minimal) geodesic starting from the root vertex. Moreover, we let $\tilde{\mathcal{R}}_+$ and $\tilde{\mathcal{R}}_-$ (or $\tilde{\mathcal{R}}_+^{\min}$ and $\tilde{\mathcal{R}}_-^{\min}$)

denote the set of intersection times of $\tilde{\gamma}_{\max}$ (or $\tilde{\gamma}_{\min}$) with the right and left part of the boundary, respectively.

For characterizing $\tilde{\mathcal{R}}_+$ and $\tilde{\mathcal{R}}_-$ as regenerative sets, we may argue as in the case of the UIHPQ. For $j \in \mathbb{Z}_+$, let

$$\tilde{\Delta}_j = \max_{i \in \mathsf{DS}(\tilde{\mathsf{b}}_\infty) \cup \mathsf{LS}(\tilde{\mathsf{b}}_\infty) \cap [H_j, H_{j+1})} - \left(\min_{u \in V(\tilde{T}_\infty(i))} \ell_i(u) + j \right).$$

Here, $H_j = H_j(\tilde{\mathsf{b}}_\infty)$, and in hopefully obvious notation, $\tilde{T}_\infty(i)$ is the mobile (in the case $i \in \mathsf{DS}(\tilde{\mathsf{b}}_\infty)$) or half-mobile (in the case $i \in \mathsf{LS}(\tilde{\mathsf{b}}_\infty)$) grafted to the vertex i, and $\ell_i(u)$ for $u \in V(\tilde{T}_\infty(i))$ represents its label. By replacing H_j with H'_j, we define $\tilde{\Delta}'_j$ in a similar fashion.

Proposition 3.5.2. *We have for* $m \in \mathbb{N}$,

$$\mathbb{P}\left(\tilde{\Delta}_0 \geq m\right) = \frac{1}{m+1}, \quad \textit{and} \quad \mathbb{P}\left(\tilde{\Delta}'_0 \geq m\right) = \frac{1}{m+2}.$$

Proof. We first look at $\tilde{\Delta}_0$. Let $m \in \mathbb{N}$. Put $\tilde{g}(m) = 1 - \mathbb{P}\left(\tilde{\Delta}_0 \geq m\right)$. The arch decomposition corresponding to (3.1) reads

$$\begin{aligned}\tilde{g}(m) &= \sum_{k=0}^{\infty} \left(\sum_{k'=0}^{\infty} \left(\frac{S_m}{C}\right)^{k'} \frac{\sqrt{R}}{C} \tilde{g}(m+1) \right)^k \sum_{\ell=0}^{\infty} \left(\frac{S_m}{C}\right)^{\ell} \frac{\sqrt{R}}{C} \frac{R_m}{R} \\ &= \frac{1}{1 - \left(\frac{1}{1-\frac{S_m}{C}} \frac{\sqrt{R}}{C}\right) \tilde{g}(m+1)} \frac{1}{1 - \frac{S_m}{c}} \frac{\sqrt{R}}{C} \frac{R_m}{R};\end{aligned}$$

see Figure 3.13. The formula for $\tilde{g}$ is equivalent to

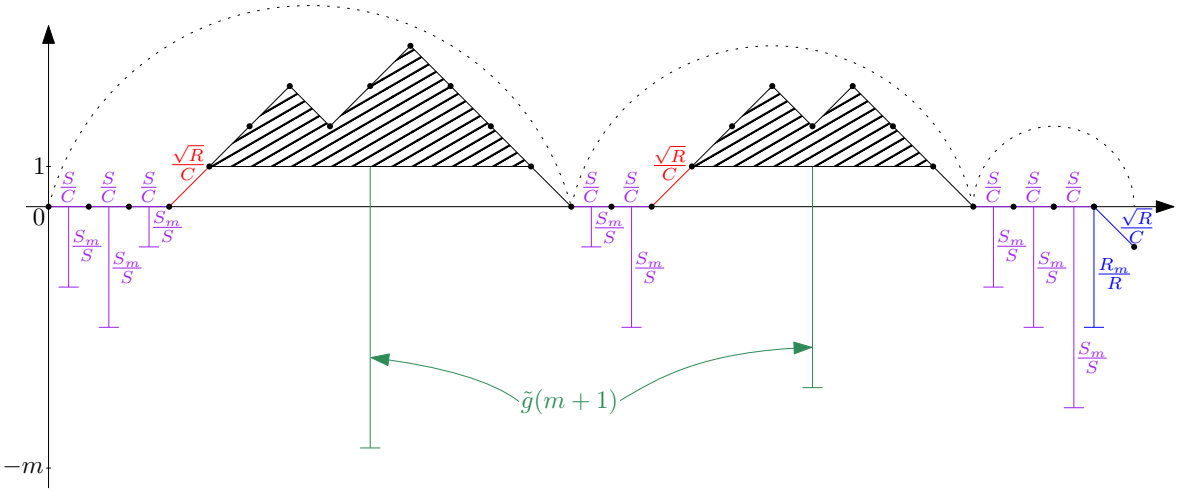

Figure 3.13: The decomposition of the probability $\tilde{g}(m)$.

$$\tilde{g}(m) \left(\frac{C}{\sqrt{R}} - \frac{S_m}{S} \frac{S}{\sqrt{R}} - \tilde{g}(m+1) \right) = \frac{R_m}{R}. \tag{3.9}$$

We note along the way that the last expression is universal, in the sense that it does not depend on the particular choice of the Boltzmann weights $(g_k)_{k \in \mathbb{N}}$.

Back to the triangular case, by letting $y \uparrow 1$ in (6.8) of [BG12], which corresponds to the choice of $g_3 = g_{3,\mathrm{cr}}$, we obtain the relations

$$\frac{R_m}{R} = \frac{m(m+2)}{(m+1)^2}, \quad \frac{S_m}{S} = 1 - \frac{g_3 R^2}{S}\frac{2}{(m+1)(m+2)}, \quad m \in \mathbb{N}.$$

Since $C = 2\sqrt{R} + S$ and $2g_{3,\mathrm{cr}}R^{3/2} = 1$, see (6.7) of [BG12], Equation (3.9) turns into

$$\tilde{g}(m)\left(2 + \frac{1}{(m+1)(m+2)} - \tilde{g}(m+1)\right) = \frac{m(m+2)}{(m+1)^2},$$

or, with $\tilde{f}(m) = 1 - \tilde{g}(m)$,

$$\tilde{f}(m) - \tilde{f}(m+1) + \tilde{f}(m)\tilde{f}(m+1) + \frac{\tilde{f}(m) - 1}{(m+1)(m+2)} = \frac{1}{(m+1)^2}. \tag{3.10}$$

Of course, the last display resembles very much Equation (3.3) for f, and in fact, $\tilde{f}(m) = 1/(m+1)$ is also a solution of (3.10). Rewriting (3.10) as

$$\tilde{f}(m+1) = \frac{(m+1)^2\tilde{f}(m) - 1}{(m+1)^2(1 - \tilde{f}(m))} - \frac{1}{(m+1)(m+2)},$$

we check with the same arguments as in the proof of Lemma 3.3.2 that $\tilde{f}(m) = 1/(m+1)$ is the only solution of (3.10) with $\tilde{f}(m) \in (0,1)$ for $m \in \mathbb{N}$, $\tilde{f}(0) = 1$ and $\lim_{m\to\infty} \tilde{f}(m) = 0$. This shows $\mathbb{P}(\tilde{\Delta}_0 \geq m) = 1/(m+1)$, as claimed. The law of $\tilde{\Delta}_0'$ is now computed as in the proof of Proposition 3.3.1, using

$$\mathbb{P}\left(\tilde{\Delta}_0 < m\right) = \mathbb{P}\left(\tilde{\Delta}_0' < m\right)\frac{R_m}{R} = \mathbb{P}\left(\tilde{\Delta}_0' < m\right)\frac{m(m+2)}{(m+1)^2}.$$

□

With the last proposition at hand, we obtain with the arguments given in the proof of Proposition 3.3.4 that

$$\mathbb{P}\left(i \in \tilde{\mathcal{R}}_+\right) = \frac{1}{i+1}, \quad \mathbb{P}\left(i \in \tilde{\mathcal{R}}_-\right) = \frac{2}{i+2}, \quad i \in \mathbb{Z}_+.$$

In particular, we again deduce that $\tilde{\gamma}_{\mathrm{max}}$ hits both parts of the boundary in the UIHPT infinitely many times. More precisely, comparing the last display with the analogous results obtained for $\mathcal{R}_+$ and $\mathcal{R}_-$, we conclude that the intersection times of $\tilde{\gamma}_{\mathrm{max}}$ with the right part of the boundary have exactly the same distribution as the corresponding times of γ_{max} in the UIHPQ. On the contrary, the maximal geodesic visits the left part of the boundary slightly more often in the UIHPQ than in the UIHPT.

A symmetry argument similar to above shows that $\tilde{\mathcal{R}}_+^{\min}$ has the same law as $\tilde{\mathcal{R}}_-$, and we have the inclusions $\tilde{\mathcal{R}}_+ \subset \tilde{\mathcal{R}}_+^{\min}$ and $\tilde{\mathcal{R}}_-^{\min} \subset \tilde{\mathcal{R}}_-$. Using that $\tilde{\gamma}_{\mathrm{max}}$ is proper and hits both parts of the boundary infinitely many times, we deduce from arguments very close to those in the proof of Corollary 3.3.6 that almost surely, all geodesic rays in the UIHPT are proper. Finally, adapting the arguments leading to Theorem 3.1.1 and Proposition 3.4.3, we arrive at the following theorem, whose details of proof we leave to the reader. We write $\tilde{\mathbf{M}}_\infty^\infty$ for the UIHPT constructed in terms of an uniform infinite mobile bridge $(\tilde{\mathsf{b}}_\infty, \tilde{T}_\infty)$.

Theorem 3.5.3. *On a set of full probability, the following holds in the* UIHPT $\tilde{\mathbf{M}}_\infty^\infty$*: Every geodesic ray hits the boundary of the* UIHPT *infinitely many times. Moreover, if* $\gamma = (\gamma(i) : i \in \mathbb{Z}_+)$ *is a geodesic ray emanating from the root vertex, we have the inclusions*

$$\tilde{\mathcal{R}}_+ \cup \tilde{\mathcal{R}}_-^{\min} \subseteq \{i \in \mathbb{Z}_+ : \gamma(i) \in \partial\tilde{\mathbf{M}}_\infty^\infty\} \subseteq \tilde{\mathcal{R}}_+^{\min} \cup \tilde{\mathcal{R}}_-.$$

The random sets $\tilde{\mathcal{R}}_+$ *and* $\tilde{\mathcal{R}}_-^{\min}$ *(as well as* $\tilde{\mathcal{R}}_+^{\min}$ *and* $\tilde{\mathcal{R}}_-$*) have the same law. The distance* δ *between two consecutive times in* $\tilde{\mathcal{R}}_+$ *(or* $\tilde{\mathcal{R}}_-^{\min}$*) exhibits the tail behavior* $\mathbb{P}(\delta > m) \sim 1/\ln m$ *as* $m \to \infty$*, whereas the distance* δ' *between two consecutive times in* $\tilde{\mathcal{R}}_+^{\min}$ *(or* $\tilde{\mathcal{R}}_-$*) satisfies* $\mathbb{P}(\delta' > m) \sim 1/(2\ln m)$.

Concluding remarks. Angel constructed in [Ang04] the uniform infinite triangulation with an infinite *simple* boundary, and we expect that Theorem 3.5.3 can be transferred to the model of Angel by a pruning procedure, as in the case of the UIHPQ$^{(s)}$. Moreover, since the above construction of the UIHPT (or the UIHPQ) can be extended to general limits of critical or sub-critical Boltzmann maps, the same methods can in principle be applied to study the intersection of geodesic rays with the boundary for the full class of models obtained in this way.

However, as it should be clear from Remark 3.3.5, intersection properties of geodesics as studied in this paper are delicate, and our approach requires exact calculations (or at least non-asymptotic bounds). In the pure quadrangular and triangular cases at criticality, the expressions for R_m and S_m are particularly simple, so that we can compute the laws of Δ_0 and $\tilde{\Delta}_0$ explicitly. See (5.11) of [BG12] for the general form of R_m, which involves so-called Hankel determinants. For a more general treatment, Equation (3.9) is model-independent and may serve as a starting point for further investigations.

Acknowledgments. We would like to thank Nicolas Curien for asking us whether geodesic rays in the UIHPQ intersect the boundary infinitely often. Moreover, we thank Jérémie Bouttier for a helpful discussion, and the referee for pointing us to [CD06, Proposition 2.4].

4

Uniform infinite half-planar quadrangulations with skewness

We introduce a one-parameter family of random infinite quadrangulations of the half-plane, which we call the *uniform infinite half-planar quadrangulations with skewness* (UIHPQ_p for short, with $p \in [0, 1/2]$ measuring the skewness). They interpolate between Kesten's tree corresponding to $p = 0$ and the usual UIHPQ with a general boundary corresponding to $p = 1/2$. As we make precise, these models arise as local limits of uniform quadrangulations with a boundary when their volume and perimeter grow in a properly fine-tuned way, and they represent all local limits of (sub)critical Boltzmann quadrangulations whose perimeter tend to infinity. Our main result shows that the family $(\mathsf{UIHPQ}_p)_p$ approximates the Brownian half-planes BHP_θ, $\theta \geq 0$, recently introduced in [BMR16]. For $p < 1/2$, we give a description of the UIHPQ_p in terms of a looptree associated to a critical two-type Galton-Watson tree conditioned to survive.

This Chapter is adapted from joint work with Erich Baur [2] (preprint). It contains the proof of Theorems 6, 8 and 9 as well as Proposition 7.

Contents

4.1 Introduction

4.1.1 Overview

The purpose of this paper is to introduce and study a one-parameter family of random infinite quadrangulations of the half-plane, which we denote by $(\mathsf{UIHPQ}_p)_{0\leq p\leq 1/2}$ and call the *uniform infinite half-planar quadrangulations with skewness*. Two members play a particular role: The choice $p = 0$ corresponds to Kesten's tree, cf. Proposition 4.2.2 below, whereas the choice $p = 1/2$ corresponds to the standard uniform infinite half-planar quadrangulation UIHPQ with a general boundary.

Kesten's tree [Kes86b] is a random infinite planar tree, which we may view as a degenerate quadrangulation with an infinite boundary, but no inner faces. It arises as the local limit of critical Galton-Watson trees conditioned to survive. The standard $\mathsf{UIHPQ}(= \mathsf{UIHPQ}_{1/2})$ forms the half-planar analog of the uniform infinite planar quadrangulation introduced by Krikun [Kri05], after the seminal work of Angel and Schramm [AS03] on triangulations of the plane. Curien and Miermont [CM15] showed that the UIHPQ arises as a local limit of uniformly chosen quadrangulations of the two-sphere with n inner faces and a boundary of size 2σ, upon letting first $n \to \infty$ and then $\sigma \to \infty$ (see Angel [Ang04] for the case of triangulations with a simple boundary).

We will define each UIHPQ_p in Section 4.4 by means of an extension of the Bouttier–Di Francesco–Guitter mapping to infinite quadrangulations with a boundary. In the first part of this paper, we will discuss various local limits and scaling limits which involve the family $(\mathsf{UIHPQ}_p)_p$. More precisely, in Theorem 4.2.1, we will see that each UIHPQ_p appears as a local limit as n tends to infinity of uniform quadrangulations $Q_n^{\sigma_n}$ with n inner faces and a boundary of size $2\sigma_n$, for an appropriate choice of $\sigma_n = \sigma_n(p) \to \infty$. In Proposition 4.2.3, we argue that the family $(\mathsf{UIHPQ}_p)_p$ consists precisely of the infinite quadrangulations with a boundary which are obtained as local limits $\sigma \to \infty$ of subcritical Boltzmann quadrangulations with a boundary of size 2σ. This result will prove helpful in our description of the UIHPQ_p given in Theorem 4.2.10.

We will then turn to distributional scaling limits of the family $(\mathsf{UIHPQ}_p)_p$ in the so-called *local Gromov-Hausdorff topology*. In Theorems 4.2.6 and 4.2.7, we will clarify the connection between the (discrete) quadrangulations UIHPQ_p and the family $(\mathsf{BHP}_\theta)_{\theta\geq 0}$ of Brownian half-spaces with skewness θ introduced in [BMR16]. More specifically, upon rescaling the graph distance by a factor $a_n^{-1} \to 0$, we prove that each BHP_θ is the distributional limit of the rescaled spaces $a_n^{-1} \cdot \mathsf{UIHPQ}_{p_n}$, if $p_n = p_n(\theta, a_n)$ is adjusted in the right manner (Theorem 4.2.6). In our setting, convergence in the local Gromov-Hausdorff sense amounts to show convergence of rescaled metric balls around the roots of a fixed but arbitrarily large radius in the usual Gromov-Hausdorff topology; see Section 4.1.2.

In [BMR16], a classification of all possible non-compact scaling limits of pointed uniform random quadrangulations with a boundary $(V(Q_n^{\sigma_n}), a_n^{-1} d_{\mathrm{gr}}, \rho_n)$ has been given, depending on the asymptotic behavior of the boundary size $2\sigma_n$ and on the

choice of the scaling factor $a_n \to \infty$ (in the local Gromov-Hausdorff topology, with the distinguished point ρ_n lying on the boundary). In this paper, we address the boundary regime corresponding to the portion $x \geq 1$ of the $y = 0$ axis in Figure 4.1 (in hashed marks), which was left untouched in [BMR16]. As we show, it corresponds to a regime of unrescaled local limits, namely the family $(\mathsf{UIHPQ}_p)_p$.

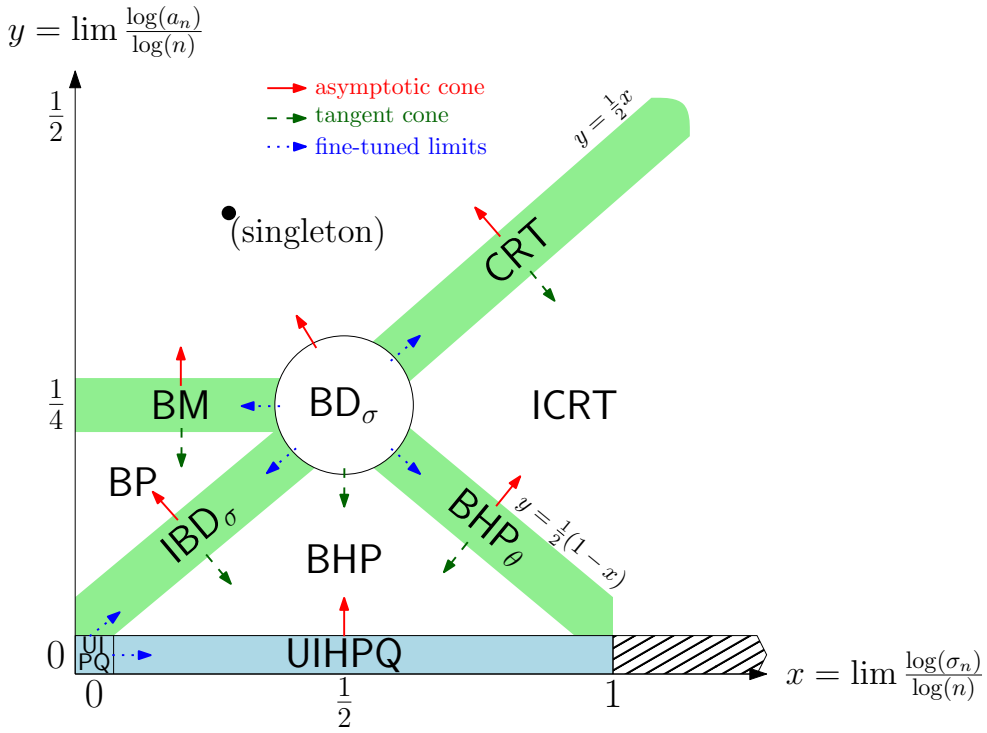

Figure 4.1: In [BMR16], all possible limits for the rescaled spaces $(V(Q_n^{\sigma_n}), a_n^{-1} d_{\mathrm{gr}}, \rho_n)$ are discussed. The x-axis represents the limit values for the logarithm of the boundary length $\log(\sigma_n)/\log(n)$ in units of $\log(n)$, and the y-axis corresponds to the limit of the logarithm of the scaling factor $\log(a_n)/\log(n)$ in units of $\log(n)$. The focus of this paper lies on the hashed region.

We finally give a branching characterization of the UIHPQ_p when $p < 1/2$. For that purpose, we will adapt the concept of discrete random looptrees introduced by Curien and Kortchemski [CK14b]. We will see that the UIHPQ_p admits a representation in terms of a looptree associated to a two-type version of Kesten's infinite tree. Informally, we will replace each vertex u at odd height in Kesten's tree by a cycle of length $\deg(u)$, which connects the vertices incident to u. Here, $\deg(u)$ stands for the degree (i.e., the number of neighbors) of u in the tree. We then fill in the cycles of the looptree with a collection of independent quadrangulations with a simple boundary, which are drawn according to a subcritical Boltzmann law. As we show in Theorem 4.2.10, the space constructed in this way has the law of the UIHPQ_p. Discrete looptrees and their scaling limits have found various applications in the study of large-scale properties of random planar maps, for instance in the description of the boundary of percolation clusters on the uniform infinite planar triangulation; see the work [CK14a], which served as the main inspiration for our characterization of

the UIHPQ$_p$. From our description, we immediately infer that simple random walk is recurrent on the UIHPQ$_p$ for $p < 1/2$.

It is well-known that the standard UIHPQ with a simple boundary satisfies the so-called *spatial Markov property*, which allows, in particular, the use of peeling techniques. In [AR15], Angel and Ray classified all triangulations (without self-loops) of the half-plane satisfying the spatial Markov property and translation invariance. They form a one-parameter family $(\mathbb{H}_\alpha)_\alpha$ parametrized by $\alpha \in [0, 1)$. The parameter $\alpha = 2/3$ corresponds to the standard UIHPT with a simple boundary, the triangular equivalent of the UIHPQ with a simple boundary. When $\alpha > 2/3$ (the supercritical case), $\mathbb{H}_\alpha$ is of hyperbolic nature and exhibits an exponential volume growth. On the contrary, when $\alpha < 2/3$ (the subcritical case), it has a tree-like structure. We believe that the family $(\text{UIHPQ}_p)_p$ is a quadrangular equivalent to the triangulations in the subcritical phase of [AR15]. Note that contrary to the UIHPQ$_p$, the spaces $\mathbb{H}_\alpha$ for $\alpha < 2/3$ have a half-plane topology, due to the conditioning to have a simple boundary. However, there exists almost surely infinitely many cut-edges connecting the left and right boundaries; see [Ray14, Proposition 4.11]. This should be seen as an equivalent to the branching structure formulated in Theorem 4.2.10 below. Our methods in this paper are different from [AR15, Ray14] as we do not use peeling techniques.

In [Cur16b], Curien studied full-plane analogs of the family $(\mathbb{H}_\alpha)_\alpha$. With similar (peeling) techniques, he constructed a (unique) one-parameter family of random infinite planar triangulations indexed by $\kappa \in (0, 2/27]$, which satisfy a slightly adapted spatial Markov property. The critical case $\kappa = 2/27$ corresponds to the standard UIPT with a simple boundary of Angel and Schramm [AS03]. The regime $\kappa \in (0, 2/27)$ parallels the supercritical (or hyperbolic) phase $\alpha > 2/3$ of [AR15], whereas it is shown that there is no subcritical phase. Recently, a near-critical scaling limit of hyperbolic nature called the hyperbolic Brownian half-plane has been studied by Budzinski [Bud16]. It is obtained from rescaling the triangulations of Curien [Cur16b] and letting $\kappa \to 2/27$ at the right speed. Theorem 1 of [Bud16] bears some structural similarities with our Theorem 4.2.6 below, although it concerns a different regime.

Structure of the paper. The rest of this paper is structured as follows. In the following section, we introduce some (standard) concepts and notation around quadrangulations, which will be used throughout this text. Moreover, we recapitulate the local topology and the local Gromov-Hausdorff topology. In Section 4.2, we state our main results, which concern local limits, scaling limits, and structural properties of the family $(\text{UIHPQ}_p)_p$. Section 4.3 reviews the definition of the family of Brownian half-planes $(\text{BHP}_\theta)_\theta$, and of various random trees, which are used both to describe the distributional limits of the family $(\text{UIHPQ}_p)_p$ as well as their branching structure.

In Section 4.4, we construct the UIHPQ$_p$. We first explain the Bouttier–Di Francesco–Guitter encoding of quadrangulations with a boundary and then define the UIHPQ$_p$ in terms of the encoding objects. We are then in position to prove our limit statements; see Section 4.5. In the final Section 4.6, we prove our main result characterizing the tree-like structure of the UIHPQ$_p$ when $p < 1/2$, as well as recurrence of simple random walk.

4.1.2 Some standard notation and definitions

Notation. We write

$$\mathbb{N} = \{1, 2, \ldots\}, \quad \mathbb{Z}_+ = \mathbb{Z}_{\geq 0} = \mathbb{N} \cup \{0\}, \quad \mathbb{Z}_{<0} = \{-1, -2, \ldots\}.$$

For two sequences $(a_n)_n$, $(b_n)_n \subset \mathbb{N}$, we write $a_n \ll b_n$ or $b_n \gg a_n$ if $a_n/b_n \to 0$ as $n \to \infty$. Given two measurable subsets $U, V \subset \mathbb{R}$, we denote by $\mathcal{C}(U, V)$ the space of continuous functions from U to V, equipped with the usual compact-open topology, i.e., uniform convergence on compact subsets. We write $\|\nu\|_{\text{TV}}$ for the total variation norm of a probability measure ν.

As a general notational rule for this paper, if we drop p from the notation, we work with the case $p = 1/2$. For example, we write UIHPQ (and not $\text{UIHPQ}_{1/2}$) for the standard uniform infinite half-planar quadrangulation.

Planar maps. By a *planar map* we mean, as usual, an equivalence class of a proper embedding of a finite connected graph in the two-sphere, where two embeddings are declared to be equivalent if they differ only by an orientation-preserving homeomorphism of the sphere. Loops and multiple edges are allowed. Our planar maps will be rooted, meaning that we distinguish an oriented edge called the *root edge*. Its origin is the root vertex of the map. The faces of a planar map are formed by the components of the complement of the union of its edges.

Quadrangulations with a boundary. A *quadrangulation with a boundary* is a finite planar map $\mathbf{q}$, whose faces are quadrangles except possibly one face called the *outer face*, which may an have arbitrary even degree. The edges incident to the outer face form the *boundary* $\partial\mathbf{q}$ of $\mathbf{q}$, and their number $\#\partial\mathbf{q}$ (counted with multiplicity) is the size or *perimeter* of the boundary. In general, we do not assume that the boundary edges form a simple curve. We will root the map by selecting an oriented edge of the boundary, such that the outer face lies to its right. The *size* of $\mathbf{q}$ is given by the number of its *inner faces*, i.e., all the faces different from the outer face.

We write $\mathcal{Q}_n^{(\sigma)}$ for the (finite) set of all rooted quadrangulations with n inner faces and a boundary of size 2σ, $\sigma \in \mathbb{Z}_+$. By convention, $\mathcal{Q}_0^{(0)} = \{\dagger\}$ consists of the unique vertex map.

More generally, $\mathcal{Q}_f$ will denote the set of all finite rooted quadrangulations with a boundary, and $\mathcal{Q}_f^{(\sigma)} \subset \mathcal{Q}_f$ the set of all finite rooted quadrangulations with 2σ boundary edges, for $\sigma \in \mathbb{Z}_+$.

Similarly, we let $\widehat{\mathcal{Q}}_f$ be the set of all finite rooted quadrangulations with a simple boundary, meaning that the edges of their outer face form a cycle without self-intersection. We denote by $\widehat{\mathcal{Q}}_f^{(\sigma)} \subset \widehat{\mathcal{Q}}_f$ the subset of finite rooted quadrangulations with a simple boundary of size 2σ. Note that $\mathcal{Q}_0^{(1)}$ consists of the map having one oriented edge and thus a simple boundary.

Uniform quadrangulations with a boundary. Throughout this text, we write Q_n^σ for a quadrangulation chosen uniformly at random in $\mathcal{Q}_n^{(\sigma)}$. We denote by ρ_n the root

vertex of Q_n^σ, i.e., the origin of the root edge. By equipping the set of vertices $V(Q_n^\sigma)$ with the graph distance d_{gr}, we view the triplet $(V(Q_n^\sigma), d_{\mathrm{gr}}, \rho_n)$ as a random rooted metric space.

Boltzmann quadrangulations with a boundary. We will also work with various Boltzmann measures. For a finite rooted quadrangulation $\mathbf{q} \in \mathcal{Q}_f$, we write $\mathrm{F}(\mathbf{q})$ for the set of inner faces of $\mathbf{q}$. Given non-negative weights g per inner face and $\sqrt{z}$ per boundary edge, we let

$$F(g,z) = \sum_{\mathbf{q}\in\mathcal{Q}_f} g^{\#\mathrm{F}(\mathbf{q})} z^{\#\partial\mathbf{q}/2}.$$

When this partition function is finite, we may define the associated Boltzmann distribution

$$\mathbb{P}_{g,z}(\mathbf{q}) = \frac{g^{\#\mathrm{F}(\mathbf{q})} z^{\#\partial\mathbf{q}/2}}{F(g,z)}, \quad \mathbf{q} \in \mathcal{Q}_f.$$

The statement of Proposition 4.2.3 below deals with Boltzmann-distributed quadrangulations of a fixed boundary size 2σ, for $\sigma \in \mathbb{Z}_+$. In this case, the associated partition function and Boltzmann distribution read

$$F_\sigma(g) = \sum_{\mathbf{q}\in\mathcal{Q}_f^{(\sigma)}} g^{\#\mathrm{F}(\mathbf{q})}, \quad \mathbb{P}_g^{(\sigma)}(\mathbf{q}) = \frac{g^{\#\mathrm{F}(\mathbf{q})}}{F_\sigma(g)}, \quad \mathbf{q} \in \mathcal{Q}_f^{(\sigma)},$$

whenever $g \geq 0$ is such that $F_\sigma(g)$ is finite. The Boltzmann distribution $\mathbb{P}_g^{(\sigma)}$ is related to $\mathbb{P}_{g,z}$ by conditioning the latter with respect to the boundary length, i.e., $\mathbb{P}_g^{(\sigma)}(\mathbf{q}) = \mathbb{P}_{g,z}(\mathbf{q} \mid \mathcal{Q}_f^{(\sigma)})$.

When studying quadrangulations with a simple boundary, the partition functions are

$$\widehat{F}(g,z) = \sum_{\mathbf{q}\in\widehat{\mathcal{Q}}_f} g^{\#\mathrm{F}(\mathbf{q})} z^{\#\partial\mathbf{q}/2}, \quad \widehat{F}_\sigma(g) = \sum_{\mathbf{q}\in\widehat{\mathcal{Q}}_f^{(\sigma)}} g^{\#\mathrm{F}(\mathbf{q})},$$

and the Boltzmann distributions take the form

$$\widehat{\mathbb{P}}_{g,z}(\mathbf{q}) = \frac{g^{\#\mathrm{F}(\mathbf{q})}}{\widehat{F}_\sigma(g,z)}, \quad \mathbf{q} \in \widehat{\mathcal{Q}}_f, \quad \widehat{\mathbb{P}}_g^{(\sigma)}(\mathbf{q}) = \frac{g^{\#\mathrm{F}(\mathbf{q})}}{\widehat{F}_\sigma(g)}, \quad \mathbf{q} \in \widehat{\mathcal{Q}}_f^{(\sigma)}.$$

Remark 4.1.1. In the notation of [BG09], the generating function F is denoted W_0, while $\widehat{F}$ is denoted $\tilde{W}_0$. The index zero stands for the distance between the origin of the root edge and the marked vertex, so that these generating functions count unpointed quadrangulations.

Local topology. Our unrescaled limit results hold with respect to the *local topology* first studied by Benjamini and Schramm [BS01]: For two rooted planar maps $\mathbf{m}$ and $\mathbf{m}'$, the local distance between $\mathbf{m}$ and $\mathbf{m}'$ is

$$d_{\mathrm{loc}}(\mathbf{m},\mathbf{m}') = \left(1 + \sup\{r \geq 0 : \mathbf{B}_r(\mathbf{m}) = \mathbf{B}_r(\mathbf{m}')\}\right)^{-1},$$

where $\mathbf{B}_r(\mathbf{m})$ denotes the combinatorial ball of radius r around the root ρ of $\mathbf{m}$, i.e., the submap of $\mathbf{m}$ consisting of all the vertices v of $\mathbf{m}$ with $d_{\mathrm{gr}}(\rho, v) \leq r$ and all the

edges of $\mathfrak{m}$ between such vertices. The set $\mathcal{Q}_f$ of all finite rooted quadrangulations with a boundary is not complete for the distance d_{loc}; we have to add infinite quadrangulations. We shall write $\mathcal{Q}$ for the completion of $\mathcal{Q}_f$ with respect to d_{loc}. The UIHPQ$_p$ will be defined as a random element in $\mathcal{Q}$.

Around the Gromov-Hausdorff metric. The pointed Gromov-Hausdorff distance measures the distance between (pointed) compact metric spaces, where the latter are viewed up to isometries. More specifically, given two elements $\mathbf{E} = (E, d, \rho)$ and $\mathbf{E}' = (E', d', \rho')$ in the space $\mathbb{K}$ of isometry classes of pointed compact metric spaces, their Gromov-Hausdorff distance is defined as

$$d_{\text{GH}}(\mathbf{E}, \mathbf{E}') = \inf \left\{ d_{\text{H}}(\varphi(E), \varphi'(E)) \vee \delta(\varphi(\rho), \varphi'(\rho')) \right\},$$

where the infimum is taken over all isometric embeddings $\varphi : E \to F$ and $\varphi' : E' \to F$ of E and E' into the same metric space (F, δ), and d_{H} is the usual Hausdorff distance between compacts of F. The space $(\mathbb{K}, d_{\text{GH}})$ is complete and separable.

Our results on scaling limits involve non-compact pointed metric spaces and hold in the so-called *local Gromov-Hausdorff sense*, which we briefly recall next. Given a pointed complete and locally compact length space $\mathbf{E}$ and a sequence $(\mathbf{E}_n)_n$ of such spaces, $(\mathbf{E}_n)_n$ converges in the local Gromov-Hausdorff sense to $\mathbf{E}$ if for every $r \geq 0$,

$$d_{\text{GH}}(B_r(\mathbf{E}_n), B_r(\mathbf{E})) \to 0 \quad \text{as } n \to \infty.$$

Here and in what follows, given a pointed metric space $\mathbf{F} = (F, d, \rho)$, $B_r(\mathbf{F}) = \{x \in F : d(x, \rho) \leq r\}$ denotes the closed ball of radius r around ρ, viewed as a subspace of $\mathbf{F}$ equipped with the metric structure inherited from $\mathbf{F}$. For $\lambda > 0$, $\lambda \cdot \mathbf{F}$ stands for the rescaled pointed metric space $(F, \lambda d, \rho)$, so that in particular $\lambda \cdot B_r(\mathbf{F}) = B_{\lambda r}(\lambda \cdot \mathbf{F})$.

As a discrete map, the UIHPQ$_p$ is not a length space in the sense of [BBI01]. However, by identifying each edge with a copy of the unit interval $[0, 1]$ (and by extending the metric isometrically), one obtains a complete locally compact length space (pointed at the root vertex). By construction, balls of the same radius and around the same points in the UIHPQ$_p$ and in the approximating length space are at Gromov-Hausdorff distance at most 1 from each other. Therefore, local Gromov-Hausdorff convergence for the (rescaled) UIHPQ$_p$, see Theorems 4.2.6 and 4.2.7 below, follows indeed from the convergence of balls as stated above.

4.2 Statements of the main results

4.2.1 Local limits

Our first result states that each member of the family $(\text{UIHPQ}_p)_{0 \leq p \leq 1/2}$ can be seen as a local limit $n \to \infty$ of uniform quadrangulations with n inner faces and a boundary of size $2\sigma_n$, provided $\sigma_n = \sigma_n(p)$ is chosen in the right manner.

Theorem 4.2.1. *Fix $0 \leq p \leq 1/2$, and let $(\sigma_n, n \in \mathbb{N})$ be a sequence of positive integers satisfying*

$$\sigma_n = \frac{1-2p}{p} n + o(n) \quad \text{if } 0 < p \leq 1/2, \quad \text{and} \quad \sigma_n \gg n \quad \text{if } p = 0.$$

For every $n \in \mathbb{N}$, let $Q_n^{\sigma_n}$ be uniformly distributed in $\mathcal{Q}_n^{(\sigma_n)}$. Then we have the local convergence for the metric d_{loc} as $n \to \infty$,

$$Q_n^{\sigma_n} \xrightarrow{(d)} \mathsf{UIHPQ}_p.$$

In fact, we will prove a stronger result than mere local convergence: We will establish an isometry of balls of growing radii around the roots, where the maximal growth rate of the radii is given by $\xi_n = \min\{n^{1/4}, \sqrt{n/\gamma_n}\}$, for $\gamma_n = \max\{\sigma_n - \frac{1-2p}{p} n,\, 1\}$. We defer to Proposition 4.5.4 for the exact statement. The case $p = 1/2$ corresponding to the regime $\sigma_n = o(n)$ is already covered by [BMR16, Proposition 3.11] and is only included for completeness.

The convergence in the case $p = 0$ with $\sigma_n \gg n$ is somewhat simpler. However, it is *a priori* not obvious that the UIHPQ_0 as defined in Section 4.4 is actually Kesten's tree (see Section 4.3.2 for a definition of the latter).

Proposition 4.2.2. *The space UIHPQ_0 has the law of Kesten's tree $\mathbf{T}_\infty$ associated to the critical geometric probability distribution $(\mu_{1/2}(k), k \in \mathbb{Z}_+)$ given by $\mu_{1/2}(k) = 2^{-(k+1)}$.*

Interestingly, the fact that the UIHPQ_0 is Kesten's tree can also be derived as a special case from Theorem 4.2.10 below; see Remark 4.2.11. We prefer, however, to give a direct proof of the proposition based on our construction of the UIHPQ_0.

The UIHPQ_p for $0 \le p \le 1/2$ is also obtained as a local limit of Boltzmann quadrangulations with growing boundary size. This result will be important to describe the tree-like structure of the UIHPQ_p when $p < 1/2$. More specifically, the family $(\mathsf{UIHPQ}_p)_p$ is precisely given by the collection of all local limits $\sigma \to \infty$ of Boltzmann quadrangulations with a boundary of size 2σ and weight $g \le g_c = 1/12$ per inner face. The value $g_c = 1/12$ is critical (see [BG09, Section 4.1]) and corresponds to the choice $p = 1/2$.

Proposition 4.2.3. *Fix $0 \le p \le 1/2$, and set $g_p = p(1-p)/3$. For every $\sigma \in \mathbb{Z}_+$, let $Q_\sigma(p)$ be a random rooted quadrangulation distributed according to the Boltzmann measure $\mathbb{P}_{g_p}^{(\sigma)}$. Then we have the local convergence for the metric d_{loc} as $\sigma \to \infty$,*

$$Q_\sigma(p) \xrightarrow{(d)} \mathsf{UIHPQ}_p.$$

Remark 4.2.4. For $p = 1/2$, the above proposition states convergence of critical Boltzmann quadrangulations with a boundary towards the UIHPQ, as it was already proved in [Cur16a, Theorem 7] by means of peeling techniques. In view of the above proposition, it is moreover implicit from the same theorem that an infinite random map with the law of the UIHPQ_p does exist. For the case of half-planar triangulations (with a simple boundary), see [Ang04]. When $p = 0$, there is no inner quadrangle almost surely and $Q_\sigma(0)$ is a uniform tree with σ edges (i.e., a Galton-Watson tree with geometric offspring law conditioned to have σ edges), which converges locally towards Kesten's tree; see, for example, [Jan12, Theorem 7.1].

Remark 4.2.5. Let us write $\mathcal{M}(\mathcal{Q})$ for the set of probability measures on the completion $\mathcal{Q}$, and equip it with the usual weak topology. Then it is easily seen by our methods that the mapping $[0, 1/2] \ni p \mapsto \mathrm{Law}(\mathsf{UIHPQ}_p) \in \mathcal{M}(\mathcal{Q})$ is continuous.

4.2.2 Scaling limits

Our next results address scaling limits of the family $(\mathsf{UIHPQ}_p)_p$. In [BMR16], a one-parameter family of (non-compact) random rooted metric spaces called the *Brownian half-planes* BHP_θ with skewness $\theta \geq 0$ was introduced. See Section 4.3.1 for a quick reminder. The Brownian half-plane BHP_0 corresponding to the choice $\theta = 0$ forms the half-planar analog of the Brownian plane introduced in [CLG13] and arises from zooming-out the UIHPQ around the root vertex; see [BMR16, Theorem 3.6], and [GM16, Theorem 1.10]). Here, we will see more generally that the family $(\mathsf{UIHPQ}_p)_p$ approximates the space BHP_θ for each $\theta \geq 0$ in the local Gromov-Hausdorff sense, provided p is appropriately fine-tuned (depending on θ).

Theorem 4.2.6. *Let $\theta \geq 0$. Let $(a_n, n \in \mathbb{N})$ be a sequence of positive reals with $a_n \to \infty$ as $n \to \infty$. Let $(p_n, n \in \mathbb{N}) \subset [0, 1/2]$ be a sequence satisfying*

$$p_n = p_n(\theta, a_n) = \frac{1}{2}\left(1 - \frac{2\theta}{3a_n^2}\right) + o\left(a_n^{-2}\right).$$

Then, in the sense of the local Gromov-Hausdorff topology as $n \to \infty$,

$$a_n^{-1} \cdot \mathsf{UIHPQ}_{p_n} \xrightarrow{(d)} \mathsf{BHP}_\theta.$$

The space BHP_θ satisfies the scaling property $\lambda \cdot \mathsf{BHP}_\theta \overset{(d)}{=} \mathsf{BHP}_{\theta/\lambda^2}$. It was shown in Remark 3.19 of [BMR16] that Aldous' infinite continuum random tree ICRT, whose definition is reviewed in Section 4.3.2, is the asymptotic cone of the BHP_θ around its root, implying $\mathsf{BHP}_\theta \to \mathsf{ICRT}$ in law as $\theta \to \infty$. In particular, formally, we may think of the BHP_∞ as the ICRT. In view of Theorem 4.2.6, it is therefore natural to expect that the ICRT appears also as the scaling limit of the UIHPQ_{p_n}, provided θ in the definition of p_n is replaced by a sequence $\theta_n \to \infty$, that is, if $a_n^2(1 - 2p_n) \to \infty$ as $n \to \infty$. This is indeed the case.

Theorem 4.2.7. *Let $(a_n, n \in \mathbb{N})$ be a sequence of positive reals with $a_n \to \infty$. Let $(p_n, n \in \mathbb{N}) \subset [0, 1/2]$ be a sequence satisfying*

$$a_n^2(1 - 2p_n) \to \infty \quad \text{as } n \to \infty.$$

Then, in the sense of the local Gromov-Hausdorff topology as $n \to \infty$,

$$a_n^{-1} \cdot \mathsf{UIHPQ}_{p_n} \xrightarrow{(d)} \mathsf{ICRT}.$$

As special cases of the previous two theorems, we mention

Corollary 4.2.8. *Let $p \in [0, 1/2]$, and let $(a_n, n \in \mathbb{N})$ be a sequence of positive reals with $a_n \to \infty$. Then, in the sense of the local Gromov-Hausdorff topology as $n \to \infty$,*

$$a_n^{-1} \cdot \mathsf{UIHPQ}_p \xrightarrow{(d)} \begin{cases} \mathsf{ICRT} & \text{if} \quad 0 \leq p < 1/2 \\ \mathsf{BHP} & \text{if} \quad p = 1/2 \end{cases}.$$

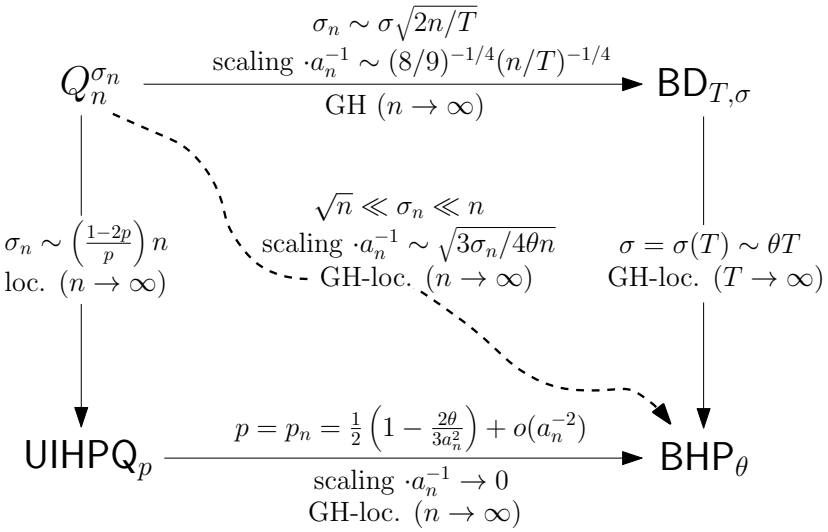

Figure 4.2: Illustration of various convergences explaining the connections between the spaces UIHPQ_p, BHP_θ and $\mathsf{BD}_{T,\sigma}$. For simplicity, the cases $\theta = 0$ and $\theta = \infty$ are left out. The top-most horizontal convergence represents [BM15, Theorem 1] and holds for $T, \sigma > 0$ fixed. If the volume T of $\mathsf{BD}_{T,\sigma}$ is blown up and the perimeter σ grows linearly in T such that $\sigma(T) \sim \theta T$, the space BHP_θ appears as the distributional local Gromov-Hausdorff limit of the disks $\mathsf{BD}_{T,\sigma(T)}$ around their roots ([BMR16, Corollary 3.17]). On the other hand, BHP_θ is approximated by uniform quadrangulations $Q_n^{\sigma_n}$ ([BMR16, Theorem 3.4]), or by the UIHPQ_p when $p = p(a_n, \theta)$ depends in the right way on θ and a_n (Theorem 4.2.6). The UIHPQ_p for fixed $p \in [0, 1/2]$ in turn arises as the local limit of $Q_n^{\sigma_n}$, provided the boundary lengths are properly chosen (Theorem 4.2.1).

Note that for the family $(\mathbb{H}_\alpha)_\alpha$ of half-planar triangulations studied in [AR15, Ray14], convergence towards the ICRT in the subcritical regime $\alpha < 2/3$ is conjectured in [Ray14, Section 2.1.2].

Remark 4.2.9. We stress that the spaces BHP_θ can also be understood as Gromov-Hausdorff scaling limits of uniform quadrangulations $Q_n^{\sigma_n} \in \mathcal{Q}_n^{(\sigma_n)}$; see [BMR16, Theorems 3.3, 3.4, 3.5]. More specifically, the BHP_θ for $\theta \in (0, \infty)$ arises when $\sqrt{n} \ll \sigma_n \ll n$ and the graph metric is rescaled by a factor a_n^{-1} satisfying $3\sigma_n a_n^2/(4n) \to \theta$ as n tends to infinity. The Brownian half-plane BHP_0 corresponding to the choice $\theta = 0$ appears more generally when $1 \ll \sigma_n \ll n$ and $1 \ll a_n \ll \min\{\sqrt{\sigma_n}, \sqrt{n/\sigma_n}\}$. Finally, the ICRT corresponding to $\theta = \infty$ appears when $\sigma_n \gg \sqrt{n}$ and $\max\{1, \sqrt{n/\sigma_n}\} \ll a_n \ll \sqrt{\sigma_n}$.

We may as well view the spaces BHP_θ as local scaling limits around the roots of the so-called Brownian disks $\mathsf{BD}_{T,\sigma}$ of volume $T > 0$ and perimeter $\sigma > 0$ introduced in [BM15]. More concretely, it was proved in [BMR16, Corollaries 3.17, 3.18] that when both T and $\sigma = \sigma(T)$ tend to infinity such that $\sigma(T)/T \to \theta \in [0, \infty]$, then the BHP_θ is the local Gromov-Hausdorff limit in law of the disk $\mathsf{BD}_{T,\sigma(T)}$ around a boundary point chosen according to the boundary measure of the latter. Figure 4.2 depicts some convergences involving the families UIHPQ_p and BHP_θ.

4.2.3 Tree structure

We will prove that for $p < 1/2$, the UIHPQ$_p$ can be represented as a collection of independent finite quadrangulations with a simple boundary glued along a tree structure. The tree structure is encoded by the looptree associated to a two-type version of Kesten's tree, and the finite quadrangulations are distributed according to the Boltzmann distribution $\widehat{\mathbb{P}}_g^{(\sigma)}$ on quadrangulations with a simple boundary of size 2σ. Precise definitions of the encoding objects are postponed to Section 4.3.

For $0 \leq p \leq 1/2$, let $g_p = p(1-p)/3$ and $z_p = (1-p)/4$. Let $F(g,z)$ be the partition function of the Boltzmann measure on finite rooted quadrangulations with a boundary, with weight g per inner face and $\sqrt{z}$ per boundary edge. Let moreover $\widehat{F}_k(g)$ be the partition function of the Boltzmann measure on finite rooted quadrangulations with a simple boundary of perimeter $2k$, with weight g per inner face.

We introduce two probability measures $\mu_\circ$ and $\mu_\bullet$ on $\mathbb{Z}_+$ by setting

$$\mu_\circ(k) = \frac{1}{F(g_p,z_p)}\left(1 - \frac{1}{F(g_p,z_p)}\right)^k, \quad k \in \mathbb{Z}_+,$$
$$\mu_\bullet(2k+1) = \frac{1}{F(g_p,z_p)-1}\left[z_p F^2(g_p,z_p)\right]^{k+1} \widehat{F}_{k+1}(g_p), \quad k \in \mathbb{Z}_+,$$

with $\mu_\bullet(k) = 0$ if k even. Exact expressions for $F(g_p,z_p)$ and $\widehat{F}_{k+1}(g_p)$ are given in (4.18) and (4.19) below. The fact that $\mu_\bullet$ is a probability distribution is a consequence of Identity (2.8) in [BG09]. We will prove in Lemma 4.6.3 that the pair $(\mu_\circ, \mu_\bullet)$ is critical for $0 \leq p < 1/2$, in the sense that the product of their respective means equals one, and subcritical if $p = 1/2$, meaning that the product of their means is strictly less than one. Moreover, both measures have small exponential moments. Our main result characterizing the structure of the UIHPQ$_p$ for $0 \leq p < 1/2$ is the following.

Theorem 4.2.10. *Let $0 \leq p < 1/2$, and let* Loop$(\mathbf{T}_\infty^{\circ,\bullet})$ *be the infinite looptree associated to Kesten's two-type tree $\mathbf{T}_\infty^{\circ,\bullet} = \mathbf{T}_\infty^{\circ,\bullet}(\mu_\circ,\mu_\bullet)$. Glue into each inner face of* Loop$(\mathbf{T}_\infty^{\circ,\bullet})$ *of degree 2σ an independent Boltzmann quadrangulations with a simple boundary distributed according to $\widehat{\mathbb{P}}_{g_p}^{(\sigma)}$. Then, the resulting infinite quadrangulation is distributed as the* UIHPQ$_p$.

The gluing operation fills in each (rooted) loop a finite-size quadrangulation with a simple boundary, which has the same perimeter as the loop. The two boundaries are glued together, such that the root edges of the loop and the quadrangulation get identified; see Remark 4.3.6. Figure 4.3 depicts the above representation of the UIHPQ$_p$ in the case $0 < p < 1/2$, as well as the borderline cases $p = 0$ and $p = 1/2$. The branching structure of the standard UIHPQ $=$ UIHPQ$_{1/2}$ has been investigated by Curien and Miermont [CM15]. They show that the UIHPQ can be seen as the uniform infinite half-planar quadrangulation with a simple boundary (represented by the big white semicircle in Figure 4.3), together with a collection of finite-size quadrangulations with a general boundary, which are attached to the infinite simple boundary.

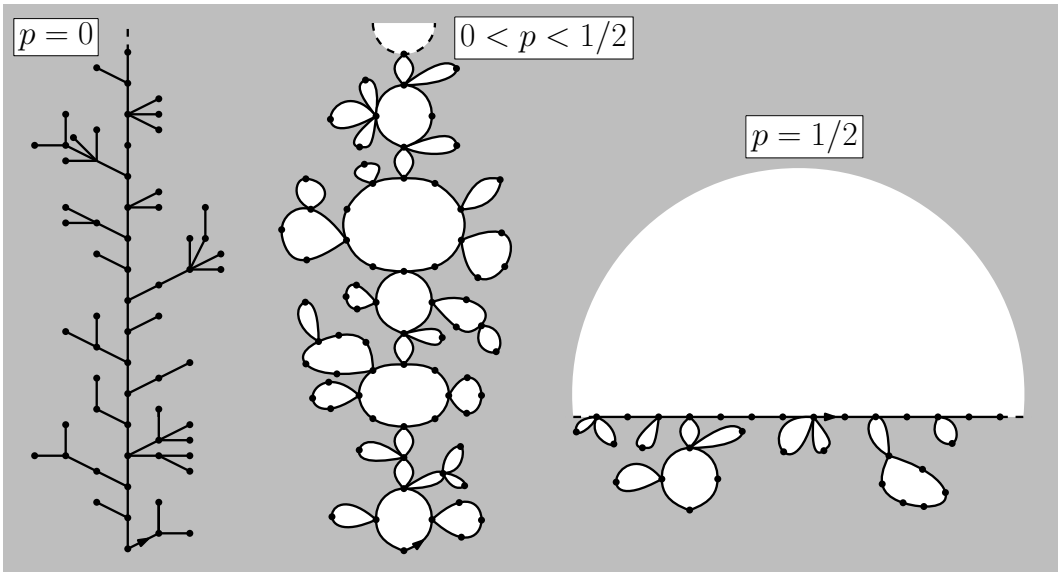

Figure 4.3: Schematic representation of the UIHPQ$_p$ for $p \in [0, 1/2]$. On the left: The UIHPQ$_0$, that is, Kesten's tree associated to the critical geometric offspring distribution $\mu_{1/2}$. On the right: The standard uniform infinite half-planar quadrangulation UIHPQ with a general boundary. The white parts are understood to be filled in with quadrangulations, the big white semicircle representing the half-plane. In the middle: The UIHPQ$_p$ with skewness parameter p. The white parts represent the (finite-size) quadrangulations with a simple boundary which are glued into the loops of the infinite looptree Loop$(\mathbf{T}_\infty^{\circ,\bullet})$ associated to a two-type version $\mathbf{T}_\infty^{\circ,\bullet}(\mu_\circ, \mu_\bullet)$ of Kesten's tree.

Remark 4.2.11. In the case $p = 0$, the above theorem can be seen as a restatement of Proposition 4.2.2. Indeed, in this case, one finds that $\mu_\circ = \mu_{1/2}$ is the critical geometric probability law, and $\mu_\bullet$ is the Dirac-distribution δ_1. By construction, all the inner faces of Loop$(\mathbf{T}_\infty^{\circ,\bullet})$ have then degree 2, and the gluing of a Boltzmann quadrangulation distributed according to $\widehat{\mathbb{P}}^{(1)}_{g_0=0}$ simply amounts to close the face, by identifying its edges. One finally recovers Kesten's (one-type) tree associated to the offspring law $\mu_{1/2}$, as already found in Proposition 4.2.2.

Remark 4.2.12. In Chapter 3, we proved that geodesics in the standard UIHPQ intersect both the left and right part of the boundary infinitely many times (see Section 3.2.3 for the exact terminology). However, up to removing finite quadrangulations that hang off from the boundary, the UIHPQ has the topology of a half-plane. Consequently, left and right parts of the boundary intersect only finitely many times. The branching structure described in Theorem 4.2.10 implies that the left and right parts of the boundary of the UIHPQ$_p$ for $p < 1/2$ have *infinitely* many intersection points. As a consequence, any infinite self-avoiding path intersects both boundaries infinitely many times.

Our tree-like description of the UIHPQ$_p$ for $0 \leq p < 1/2$ readily implies that simple random walk on the UIHPQ$_p$ is recurrent. For $p = 0$, this result is due to Kesten [Kes86b].

Corollary 4.2.13. *Let $0 \leq p < 1/2$. Almost surely, simple random walk on the* UIHPQ$_p$ *is recurrent.*

Somewhat informally, the tree structure describing the UIHPQ$_p$ in the case $p < 1/2$ shows that there is an essentially unique way for the random walk to move to infinity. Said otherwise, the walk reduces essentially to a random walk on the half-line reflected at the origin, which is, of course, recurrent. We give a precise proof in terms of electric networks in Section 4.6.

Remark 4.2.14. As far as the standard uniform infinite half-planar quadrangulation UIHPQ corresponding to $p = 1/2$ is concerned, Angel and Ray [AR16] prove recurrence of the triangular analog with a simple boundary, the half-plane UIPT. They construct a full-plane extension of the half-plane UIPT using a decomposition into layers and then adapt the methods of Gurel-Gurevich and Nachmias [GGN12], and Benjamini and Schramm [BS01]. It is believed that the arguments of [AR16] can be extended to the UIHPQ, too. Ray proves in [Ray14] of recurrence of the half-plane models $\mathbb{H}_\alpha$ when $\alpha < 2/3$. In [BS14], Björnberg and Stefánsson prove that the (local) limit of bipartite Boltzmann planar maps is recurrent, for every choice of the weight sequence.

We believe that the mean displacement of a random walker after n steps on the UIHPQ$_p$ for $p < 1/2$ is of order $n^{1/3}$, as for Kesten's tree (case $p = 0$). We will not pursue this further in this paper.

Let us finally mention another consequence of Theorem 4.2.10 concerning percolation thresholds. See, e.g., [AC15] for the terminology of Bernoulli percolation on random lattices.

Corollary 4.2.15. *Let $0 \leq p < 1/2$. The critical thresholds for Bernoulli site, bond and face percolation on the* UIHPQ$_p$ *are almost surely equal to one.*

Therefore, percolation on the UIHPQ$_p$ changes drastically depending on whether the skewness parameter p (not to be confused the the percolation parameter) is less or equal to $1/2$: In the standard UIHPQ $=$ UIHPQ$_{1/2}$, the critical thresholds are known to be $5/9$ for site percolation, see Chapter 6, and $1/3$ for edge percolation and $3/4$ for face percolation, see [AC15]. The proof of the corollary follows immediately from Theorem 4.2.10.

4.3 Random half-planes and trees

In this section, we begin with a review of the one-parameter family of Brownian half-planes BHP$_\theta$, $\theta \geq 0$, introduced in [BMR16] (see also [GM16] for the case $\theta = 0$).

We then gather certain concepts around trees, which play an important role throughout this paper. We properly define the ICRT, two-type Galton-Watson trees and Kesten's infinite versions thereof, looptrees and the so-called tree of components.

4.3.1 The Brownian half-planes BHP_θ

We need some preliminary notation. Given a function $f = (f_t, t \in \mathbb{R})$, we set $\underline{f}_t = \inf_{[0,t]} f$ for $t \geq 0$ and $\underline{f}_t = \inf_{(-\infty,t]} f$ for $t < 0$. Moreover, if $f = (f_t, t \geq 0)$ is a real-valued function indexed by the positive reals, its Pitman transform $\pi(f)$ is defined by

$$\pi(f)_t = f_t - 2\underline{f}_t.$$

In case $B = (B_t, t \geq 0)$ is a standard one-dimensional Brownian motion, its Pitman transform $\pi(B) = (\pi(B)_t, t \geq 0)$ is equal in law to a three-dimensional Bessel process, which has in turn the law of the modulus of a three-dimensional Brownian motion.

Now fix $\theta \in [0, \infty)$. The Brownian half-plane BHP_θ with skewness θ is defined in terms of its contour and label processes $X^\theta = (X^\theta_t, t \in \mathbb{R})$ and $W^\theta = (W^\theta_t, t \in \mathbb{R})$. They are characterized as follows.

- $(X^\theta_t, t \geq 0)$ has the law of a one-dimensional Brownian motion $B = (B_t, t \geq 0)$ with drift $-\theta$ and $B_0 = 0$, and $(X^\theta_{-t}, t \geq 0)$ has the law of the Pitman transform of an independent copy of B.
- Given X^θ, the (label) function W^θ has same distribution as $(\gamma_{-\underline{X}^\theta_t} + Z^\theta_t, t \in \mathbb{R})$, where
  - given X^θ, $Z^\theta = (Z^\theta_t, t \in \mathbb{R}) = Z^{X^\theta - \underline{X}^\theta}$ is a continuous modification of the centered Gaussian process with covariances given by
  $$\mathbb{E}\left[Z^\theta_s Z^\theta_t\right] = \min_{[s\wedge t, s\vee t]} X^\theta - \underline{X}^\theta,$$
  - $(\gamma_x, x \in \mathbb{R})$ is a two-sided Brownian motion with $\gamma_0 = 0$ and scaled by the factor $\sqrt{3}$, independent of Z^θ.

The process Z^θ is usually called the (head of the) random snake driven by $X^\theta - \underline{X}^\theta$, see [LG99] for more on this. Next, we define two pseudo-metrics d_{X^θ} and d_{W^θ} on $\mathbb{R}$,

$$d_{X^\theta}(s,t) = X^\theta_s + X^\theta_t - 2\min_{[s\wedge t, s\vee t]} X^\theta, \quad \text{and} \quad d_{W^\theta}(s,t) = W^\theta_s + W^\theta_t - 2\min_{[s\wedge t, s\vee t]} W^\theta.$$

The pseudo-metric D_θ associated to BHP_θ is defined as the maximal pseudo-metric d on $\mathbb{R}$ satisfying $d \leq d_{W^\theta}$ and $\{d_{X^\theta} = 0\} \subseteq \{D_\theta = 0\}$. According to Chapter 3 of [BBI01], it admits the expression $(s, t \in \mathbb{R})$

$$D_\theta(s,t) = \inf\left\{ \sum_{i=1}^k d_{W^\theta}(s_i, t_i) : \begin{array}{l} k \in \mathbb{N},\ s_1, \ldots, s_k, t_1, \ldots, t_k \in \mathbb{R}, s_1 = s, t_k = t, \\ d_{X^\theta}(t_i, s_{i+1}) = 0 \text{ for every } i \in \{1, \ldots, k-1\} \end{array} \right\}.$$

Definition 4.3.1. The Brownian half-plane BHP_θ has the law of the pointed metric space $(\mathbb{R}/\{D_\theta = 0\}, D_\theta, \rho_\theta)$, with the distinguished point ρ_θ is given by the equivalence class of 0.

Note that D_θ stands here also for the induced metric on the quotient space. It follows from standard scaling properties of X^θ and W^θ that for $\lambda > 0$, $\lambda \cdot \mathsf{BHP}_\theta = \mathsf{BHP}_{\theta/\lambda^2}$ in distribution. In particular, BHP_0 is scale-invariant. It was shown in [BMR16] that for every $\theta \geq 0$, BHP_θ has a.s. the topology of the closed half-plane $\overline{\mathbb{H}} = \mathbb{R} \times \mathbb{R}_+$.

4.3.2 Random trees and some of their properties

The infinite continuum random tree ICRT**.** Introduced by Aldous in [Ald91], the ICRT is a random rooted real tree that forms the non-compact analog of the usual continuum random tree CRT. Consider the stochastic process $(X_t, t \in \mathbb{R})$ such that $(X_t, t \geq 0)$ and $(X_{-t}, t \geq 0)$ are two independent one-dimensional standard Brownian motions started at zero. Define on $\mathbb{R}$ the pseudo-metric

$$d_X(s,t) = X_s + X_t - 2 \min_{[s\wedge t, s\vee t]} X.$$

Definition 4.3.2. The ICRT is the continuum random real tree $\mathscr{T}_X$ coded by X, i.e., the ICRT has the law of the pointed metric space $(\mathscr{T}_X, d_X, [0])$, where $\mathscr{T}_X = \mathbb{R}/\{d_X = 0\}$, and the distinguished point is given by the equivalence class of 0.

The ICRT is scale-invariant, meaning that $\lambda\cdot$ICRT $=$ ICRT in distribution for $\lambda > 0$, and invariant under re-rooting. We remark that the ICRT is often defined in terms of two independent three-dimensional Bessel processes $(X_t, t \geq 0)$ and $(X_{-t}, t \geq 0)$. Since the Pitman transform π turns a Brownian motion into a three-dimension Bessel processes, it is readily seen that both definitions give rise to the same random tree.

(Sub)critical (two-type) Galton-Watson trees. We recall the formalism of (finite or infinite) plane trees, i.e., rooted ordered trees. The size $|\mathbf{t}| \in \mathbb{Z}_+ \cup \{\infty\}$ of $\mathbf{t}$ is given by its number of edges, and we shall write $\mathcal{T}_f$ for the set of all finite plane trees.

We will often use the fact that if GW_ν denotes the law of a Galton-Watson tree with critical or subcritical offspring distribution ν, then

$$\mathsf{GW}_\nu(\mathbf{t}) = \prod_{u \in V(\mathbf{t})} \nu(k_u(\mathbf{t})), \quad t \in \mathcal{T}_f, \tag{4.1}$$

where for $u \in V(\mathbf{t})$, $k_u(\mathbf{t})$ is the number of offspring of the vertex u in $\mathbf{t}$. See, for example, [LG05, Proposition 1.4]). In the case where $\nu = \mu_p$ is the geometric offspring distribution of parameter $p \in [0, 1/2]$, (4.1) becomes

$$\mathsf{GW}_{\mu_p}(\mathbf{t}) = p^{|\mathbf{t}|}(1-p)^{|\mathbf{t}|+1}. \tag{4.2}$$

From the last display, the connection to random walks becomes apparent. Namely, let $(S^{(p)}(m), m \in \mathbb{Z}_+)$ be a random walk on the integers starting from $S^{(p)}(0) = 0$ with increments distributed according to $p\delta_1 + (1-p)\delta_{-1}$. Define the first hitting time of -1 by

$$T_{-1}^{(p)} = \inf\{m \in \mathbb{N} : S^{(p)}(m) = -1\}.$$

Then it is readily deduced from (4.2) that the size $|\mathbf{t}|$ of $\mathbf{t}$ under GW_{μ_p} and $(T_{-1}^{(p)} - 1)/2$ are equal in distribution; see, e.g., [Pit06, Section 6.3].

Given a finite or infinite plane tree, it will be convenient to say that vertices at even height of $\mathbf{t}$ are white, and those at odd height are black. We use the notation $\mathbf{t}_\circ$ and $\mathbf{t}_\bullet$ for the associated subsets of vertices. We next define two-type Galton-Watson trees associated to a pair $(\nu_\circ, \nu_\bullet)$ of probability measures on $\mathbb{Z}_+$.

Definition 4.3.3. The *two-type Galton-Watson tree* with a pair of offspring distributions $(\nu_\circ, \nu_\bullet)$ is the random plane tree such that vertices at even height have offspring distribution $\nu_\circ$, vertices at odd height have offspring distribution $\nu_\bullet$, and the numbers of children of the different vertices are independent.

In this context, the pair $(\nu_\circ, \nu_\bullet)$ is said to be *critical* if and only if the mean vector $(m_\circ, m_\bullet)$ satisfies $m_\circ m_\bullet = 1$. Then, the law $\mathsf{GW}_{\nu_\circ,\nu_\bullet}$ of such a tree is characterized by

$$\mathsf{GW}_{\nu_\circ,\nu_\bullet}(\mathbf{t}) = \prod_{u\in\mathbf{t}_\circ} \nu_\circ(k_u(\mathbf{t})) \prod_{u\in\mathbf{t}_\bullet} \nu_\bullet(k_u(\mathbf{t})), \quad t \in \mathcal{T}_f.$$

Kesten's tree and its two-type version. We next briefly review critical Galton-Watson trees conditioned to survive; see [Kes86b] or [LP16], and [Ste16] for the multi-type case.

Proposition 4.3.4 (Theorem 3.1 in [Ste16])**.** *Let* GW *be the law of a critical (either one or two-type) Galton-Watson tree. For every $n \in \mathbb{N}$, assume that* $\mathsf{GW}(\{\#V(\mathbf{t}) = n\}) > 0$*, and let T_n be a tree with law* GW *conditioned to have n vertices. Then, we have the local convergence for the metric d_{loc} as $n \to \infty$ to a random infinite tree $\mathbf{T}_\infty$,*

$$T_n \xrightarrow{(d)} \mathbf{T}_\infty.$$

In the case $\mathsf{GW} = \mathsf{GW}_\nu$ for ν a critical one-type offspring distribution, $\mathbf{T}_\infty = \mathbf{T}_\infty(\nu)$ is often called *Kesten's tree* associated to ν, and simply Kesten's tree if $\nu = \mu_{1/2}$. We will use the same terminology if $(\nu_\circ, \nu_\bullet)$ is a critical pair of offspring distributions and $\mathsf{GW} = \mathsf{GW}_{\nu_\circ,\nu_\bullet}$. In this case, we rather write $\mathbf{T}_\infty^{\circ,\bullet} = \mathbf{T}_\infty^{\circ,\bullet}(\nu_\circ, \nu_\bullet)$ for Kesten's tree associated to $(\nu_\circ, \nu_\bullet)$ (the exponent indicates the two-type nature of the tree). Note that the condition $\mathsf{GW}(\{\#V(\mathbf{t}) = n\}) > 0$ can be relaxed, provided we can find a subsequence along which this condition is satisfied.

Galton-Watson trees conditioned to survive enjoy an explicit construction, which we briefly recall for the two-type case. Details can be found in [Ste16]. Let $(\nu_\circ, \nu_\bullet)$ be a critical pair of offspring distributions with mean $(m_\circ, m_\bullet)$, and recall that the size-biased distributions $\bar{\nu}_\circ$ and $\bar{\nu}_\bullet$ are defined by

$$\bar{\nu}_\circ(k) = \frac{k\nu_\circ(k)}{m_\circ} \quad \text{and} \quad \bar{\nu}_\bullet(k) = \frac{k\nu_\bullet(k)}{m_\bullet}, \quad k \in \mathbb{Z}_+.$$

Kesten's tree $\mathbf{T}_\infty^{\circ,\bullet}$ associated to $(\nu_\circ, \nu_\bullet)$ is an infinite locally finite (two-type) tree that has a.s. a unique infinite self-avoiding path called the *spine*. It is constructed as follows. The root vertex (white) is the first vertex on the spine. It has size-biased offspring distribution $\bar{\nu}_\circ$. Among its offspring, a child (black) is chosen uniformly at random to be the second vertex on the spine. It has size-biased offspring distribution $\bar{\nu}_\bullet$, and a child (white) chosen uniformly at random among its offspring becomes the third vertex on the spine. The spine is constructed by iterating this procedure.

The construction of the tree is completed by specifying that vertices at even (resp. odd) height lying not on the spine have offspring distribution $\nu_\circ$ (resp. $\nu_\bullet$), and that the numbers of offspring of the different vertices are independent.

The construction is similar in the mono-type case. In the particular case when $\nu = \mu_{1/2}$ is the geometric distribution with parameter $1/2$, Kesten's tree can be represented by an infinite half-line (isomorphic to $\mathbb{N}$) and a collection of independent Galton-Watson trees with law $\mathsf{GW}_{\mu_{1/2}}$ grafted to the left and to the right of every vertex on the spine; see, for instance, [Jan12, Example 10.1]. We will exploit this representation in our proof of Proposition 4.2.2.

Random looptrees. Our description of the UIHPQ_p in Theorem 4.2.10 makes use of so-called *looptrees*, which were introduced in [CK14b]. A looptree can informally be seen as a collection of loops glued along a tree structure. The following presentation is inspired by [CK14a, Section 2.3]. We use, however, slightly different definitions which are better suited to our purpose. In particular, given a plane tree $\mathbf{t}$, we will only replace vertices $v \in \mathbf{t}_\bullet$ at *odd* height by loops of length $\deg(u)$. Consequently, several loops may be attached to one and the same vertex (at even height).

Let us now make things more precise. Let $\mathbf{t}$ be a finite plane tree, and recall that vertices at even height are white, and those at odd height are black (with respective subsets of vertices $\mathbf{t}_\circ$ and $\mathbf{t}_\bullet$). We associate to $\mathbf{t}$ a rooted looptree $\mathrm{Loop}(\mathbf{t})$ as follows. Around every (black) vertex in $\mathbf{t}_\bullet$, we connect its incident white vertices in cyclic order, so that they form a loop. Then $\mathrm{Loop}(\mathbf{t})$ is the planar map obtained from erasing the black vertices and the edges of $\mathbf{t}$. We root $\mathrm{Loop}(\mathbf{t})$ at the edge connecting the origin of $\mathbf{t}$ to the last child of its first sibling in $\mathbf{t}$; see Figure 4.4.

The reverse application associates to a looptree $\mathbf{l}$ a plane tree, which we call the *tree of components* $\mathrm{Tree}(\mathbf{l})$. In order to obtain $\mathrm{Tree}(\mathbf{l})$ from $\mathbf{l}$, we add a new vertex in every internal face of $\mathbf{l}$ and connect this vertex to all the vertices of the face. The root edge of $\mathrm{Tree}(\mathbf{l})$ connects the origin of $\mathbf{l}$ to the new vertex added in the face incident to the left side of the root edge of $\mathbf{l}$.

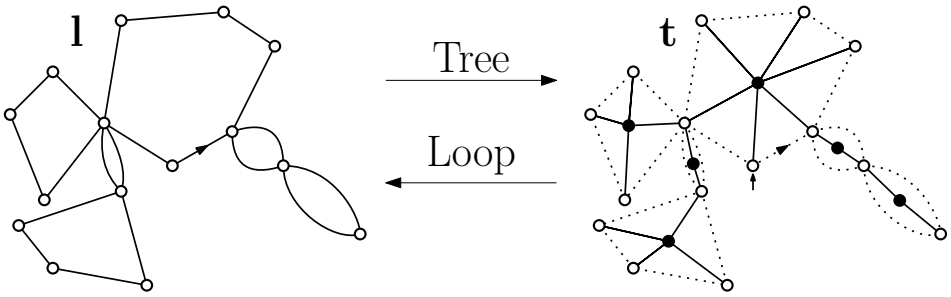

Figure 4.4: A looptree and the associated tree of components.

The procedures Tree and Loop extend to infinite but locally finite trees, by considering the consistent sequence of maps $\{\mathrm{Loop}(\mathbf{B}_{2k}(\mathbf{t})) : k \in \mathbb{Z}_+\}$. We will be interested in the random infinite looptree associated to Kesten's two-type tree.

Definition 4.3.5. If $(\nu_\circ, \nu_\bullet)$ is a critical pair of offspring laws and $\mathbf{T}_\infty^{\circ,\bullet}$ the corresponding Kesten's tree, we call the random infinite looptree $\mathrm{Loop}(\mathbf{T}_\infty^{\circ,\bullet})$ *Kesten's looptree* associated to $\mathbf{T}_\infty^{\circ,\bullet}$.

Note that a formal way to construct Loop($\mathbf{T}_\infty^{\circ,\bullet}$) is to define it as the local limit of Loop($T_n^{\circ,\bullet}$), where $T_n^{\circ,\bullet}$ is a two-type Galton-Watson tree with offspring distribution $(\nu_\circ, \nu_\bullet)$ conditioned to have n vertices.

Remark 4.3.6. In a looptree $\mathfrak{l}$, every loop is naturally rooted at the edge whose origin is the closest vertex to the origin of $\mathfrak{l}$, such that the outer face of $\mathfrak{l}$ lies on the right of that edge. The gluing of a (rooted) quadrangulation with a simple boundary of perimeter 2σ into a loop of the same length is then determined by the convention that the root edge of the quadrangulation is glued on the root edge of the loop.

4.4 Construction of the UIHPQ$_p$

A Schaeffer-type bijection due to Bouttier, Di Francesco and Guitter [BDFG04] encodes quadrangulations with a boundary in terms of labeled trees that are attached to a bridge. We shall first describe a bijective encoding of finite-size planar quadrangulations, and then extend it to infinite quadrangulations with an infinite boundary. This will allow us to construct and define the UIHPQ$_p$ for $p \in [0, 1/2]$ in terms of the encoding objects, which we define first.

4.4.1 The encoding objects

We briefly review well-labeled trees, forests, bridges and contour and label functions. Our notation bears similarities to [CM15, CC15, BMR16], differs, however, at some places. Each of these references already contains the construction of the standard UIHPQ.

Forest and bridges. A *well-labeled tree* $(\mathbf{t}, \ell)$ is a pair consisting of a finite rooted plane tree $\mathbf{t}$ and a labeling $(\ell(u))_{u\in V(\mathbf{t})}$ of its vertices $V(\mathbf{t})$ by integers, with the constraints that the root vertex receives label zero, and $|\ell(u) - \ell(v)| \leq 1$ if u and v are connected by an edge.

A *well-labeled forest* with $\sigma \in \mathbb{N}$ trees is a pair $(\mathfrak{f}, \mathfrak{l})$, where $\mathfrak{f} = (\mathbf{t}_0, \dots, \mathbf{t}_{\sigma-1})$ is a sequence of σ rooted plane trees, and $\mathfrak{l} : V(\mathfrak{f}) \to \mathbb{Z}$ is a labeling of the vertices $V(\mathfrak{f}) = \cup_{i=0}^{\sigma-1} V(\mathbf{t}_i)$ such that for every $0 \leq i \leq \sigma - 1$, the pair $(\mathbf{t}_i, \mathfrak{l} \restriction V(\mathbf{t}_i))$ is a well-labeled tree. Similarly, a *well-labeled infinite forest* is a pair $(\mathfrak{f}, \mathfrak{l})$, where $\mathfrak{f} = (\mathbf{t}_i, i \in \mathbb{Z})$ is an infinite collection of rooted plane trees, together with a labeling $\mathfrak{l} : \cup_{i\in\mathbb{Z}} V(\mathbf{t}_i) \to \mathbb{Z}$ such that for each $i \in \mathbb{Z}$, the restriction of $\mathfrak{l}$ to $V(\mathbf{t}_i)$ turns $\mathbf{t}_i$ into a well-labeled tree.

A *bridge of length* 2σ for $\sigma \in \mathbb{N}$ is a sequence $\mathsf{b} = (\mathsf{b}(0), \mathsf{b}(1), \dots, \mathsf{b}(2\sigma - 1))$ of 2σ integers with $\mathsf{b}(0) = 0$ and $|\mathsf{b}(i + 1) - \mathsf{b}(i)| = 1$ for $0 \leq i \leq 2\sigma - 1$, where we agree that $\mathsf{b}(2\sigma) = 0$. In a similar manner, an *infinite bridge* is a two-sided sequence $\mathsf{b} = (\mathsf{b}(i) : i \in \mathbb{Z})$ with $\mathsf{b}(0) = 0$ and $|\mathsf{b}(i + 1) - \mathsf{b}(i)| = 1$ for all $i \in \mathbb{Z}$.

Given a bridge b, an index i for which $\mathsf{b}(i + 1) = \mathsf{b}(i) - 1$ is called a *down-step* of b. The set of all down-steps of b is denoted $\mathsf{DS}(\mathsf{b})$. If b is a bridge of length 2σ, $\mathsf{DS}(\mathsf{b})$ has σ elements, and we write $\mathsf{d}_\mathsf{b}^\downarrow(i)$ for the ith largest element in $\mathsf{DS}(\mathsf{b})$, for $i = 1, \dots, \sigma$. If b is an infinite bridge and $i \in \mathbb{N}$, $\mathsf{d}_\mathsf{b}^\downarrow(i)$ denotes the ith largest element

in $\mathsf{DS}(\mathsf{b}) \cap \mathbb{Z}_+$, and $\mathsf{d}_\mathsf{b}^\downarrow(-i)$ denotes the ith largest element in $\mathsf{DS}(\mathsf{b}) \cap \mathbb{Z}_{<0}$. If there is no danger of confusion, we write simply $\mathsf{d}^\downarrow$ instead of $\mathsf{d}_\mathsf{b}^\downarrow$.

The size of a forest $\mathfrak{f}$ is the number $|\mathfrak{f}| \in \mathbb{Z}_+ \cup \{\infty\}$ of tree edges. If $\mathfrak{f} = (\mathbf{t}_0, \dots, \mathbf{t}_{\sigma-1})$ and $u \in V(\mathbf{t}_i)$, we write $\mathsf{H}_\mathfrak{f}(u)$ for the height of u in the tree $\mathbf{t}_i$, i.e., the graph distance to the root of $\mathbf{t}_i$. Moreover, $\mathcal{I}_\mathfrak{f}(u) = i$ denotes the index of the tree the vertex u belongs to. Both $\mathsf{H}_\mathfrak{f}$ and $\mathcal{I}_\mathfrak{f}$ extend in the obvious way to infinite forests. If it is clear which forest we are referring to, we drop the subscript $\mathfrak{f}$ in H and $\mathcal{I}$.

We let $\mathfrak{F}_\sigma^n = \{(\mathfrak{f}, \mathfrak{l}) : \mathfrak{f} \text{ has } \sigma \text{ trees and size } |\mathfrak{f}| = n\}$ be the set of all well-labeled forests of size n with σ trees and write $\mathfrak{F}_\infty$ for the set of all well-labeled infinite forests. The set of all bridges of length 2σ is denoted $\mathfrak{B}_\sigma$. As far as infinite bridges are concerned, it will be sufficient to consider only those bridges b which satisfy $\inf_{i\in\mathbb{N}} \mathsf{b}(i) = -\infty$ and $\inf_{i\in\mathbb{N}} \mathsf{b}(-i) = -\infty$, and we denote the set of them by $\mathfrak{B}_\infty$.

Contour and label function. We first consider the case $((\mathfrak{f}, \mathfrak{l}), \mathsf{b}) \in \mathfrak{F}_\sigma^n \times \mathfrak{B}_\sigma$ for some $n, \sigma \in \mathbb{N}$. By a slight abuse of notation, we write $\mathfrak{f}(0), \dots, \mathfrak{f}(2n+\sigma-1)$ for the contour exploration of $\mathfrak{f}$, that is, the sequence of vertices (with multiplicity) which we obtain from walking around the trees $\mathbf{t}_0, \dots, \mathbf{t}_{\sigma-1}$ of $\mathfrak{f}$, one after the other in the contour order. See the left side of Figure 4.5. We define the *contour function* of $(\mathfrak{f}, \mathfrak{l})$ by

$$C_\mathfrak{f}(j) = \mathsf{H}(\mathfrak{f}(j)) - \mathcal{I}(\mathfrak{f}(j)), \quad 0 \le j \le 2n + \sigma - 1.$$

Note that $C_\mathfrak{f}(2n+\sigma-1) = \sigma-1$, since the last visited vertex by the contour exploration is the root of $\mathbf{t}_{\sigma-1}$. We extend $C_\mathfrak{f}$ to $[0, 2n+\sigma]$ by first letting $C_\mathfrak{f}(2n+\sigma) = -\sigma$, and then by linear interpolation between integers, so that $C_\mathfrak{f}$ becomes a continuous real-valued function on $[0, 2n + \sigma]$ starting at zero and ending at $-\sigma$.

The *label function* associated to $((\mathfrak{f}, \mathfrak{l}), \mathsf{b})$ is obtained from shifting the vertex label $\mathfrak{l}(\mathfrak{f}(j))$ by the value of the bridge b evaluated at its $(\mathcal{I}(\mathfrak{f}(j))+1)$th down-step. Formally,

$$\mathfrak{L}_\mathfrak{f}(j) = \mathfrak{l}(\mathfrak{f}(j)) + \mathsf{b}\left(\mathsf{d}^\downarrow\left(\mathcal{I}(\mathfrak{f}(j)) + 1\right)\right), \quad 0 \le j \le 2n + \sigma - 1.$$

We let $\mathfrak{L}_\mathfrak{f}(2n + \sigma) = 0$ and again linearly interpolate between integer values, so that $\mathfrak{L}_\mathfrak{f}$ becomes an element of $\mathcal{C}([0, 2n + \sigma], \mathbb{R})$. Contour and label functions are depicted on the right side of Figure 4.5.

In the case $((\mathfrak{f}, \mathfrak{l}), \mathsf{b}) \in \mathfrak{F}_\infty \times \mathfrak{B}_\infty$, we explore the trees of $\mathfrak{f}$ in the following way: First, $(\mathfrak{f}(0), \mathfrak{f}(1), \dots)$ is the sequence of vertices of the contour paths of the trees $\mathbf{t}_i, i \in \mathbb{Z}_+$, in the left-to-right order, starting from the root of $\mathbf{t}_0$. Then, we let $(\mathfrak{f}(-1), \mathfrak{f}(-2), \dots)$ be the sequence of vertices of the contour paths $\mathbf{t}_{-1}, \mathbf{t}_{-2}, \dots$, in the counterclockwise or right-to-left order, starting from the root of $\mathbf{t}_{-1}$; see the left side of Figure 4.6. Contour and label functions $C_\mathfrak{f}$ and $\mathfrak{L}_\mathfrak{f}$ are defined similarly to the finite case, namely

$$\begin{aligned}
C_\mathfrak{f}(j) &= \mathsf{H}(\mathfrak{f}(j)) - \mathcal{I}(\mathfrak{f}(j)), \quad j \in \mathbb{Z}, \\
\mathfrak{L}_\mathfrak{f}(j) &= \mathfrak{l}(\mathfrak{f}(j)) + \mathsf{b}\left(\mathsf{d}^\downarrow\left(\mathcal{I}(\mathfrak{f}(j)) + 1\right)\right), \quad j \in \mathbb{Z}_{\ge 0}, \\
\mathfrak{L}_\mathfrak{f}(j) &= \mathfrak{l}(\mathfrak{f}(j)) + \mathsf{b}\left(\mathsf{d}^\downarrow\left(\mathcal{I}(\mathfrak{f}(j))\right)\right), \quad j \in \mathbb{Z}_{<0}.
\end{aligned}$$

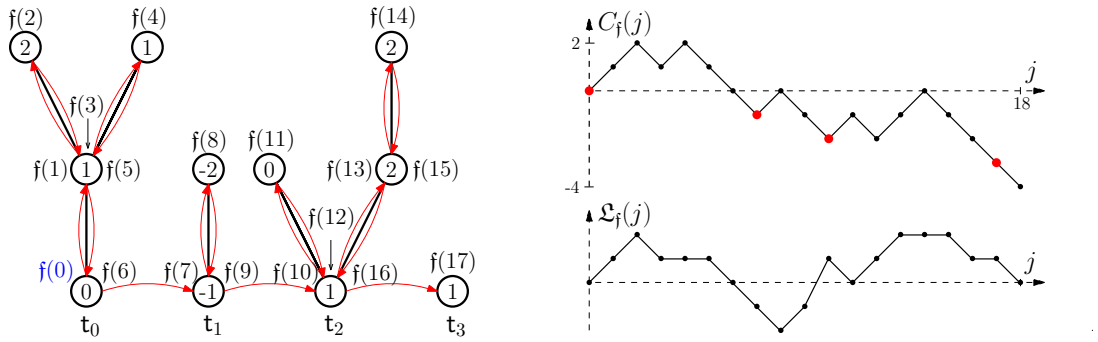

Figure 4.5: Contour and label functions $C_\mathfrak{f}$ and $\mathfrak{L}_\mathfrak{f}$ of an element $((\mathfrak{f},\mathfrak{l}),\mathfrak{b}) \in \mathfrak{F}_4^7 \times \mathfrak{B}_4$. The left side depicts the contour exploration of $\mathfrak{f}$. The labels on the vertices are given by $\mathfrak{L}_\mathfrak{f}(j)$, $j = 0,\dots,18$. Note that the values of $\mathfrak{b}$ at its four down-steps are equal to the values of $\mathfrak{L}_\mathfrak{f}$ at the tree roots: In this example, we have $\mathfrak{b}(\mathrm{d}^\downarrow(1)) = 0$, $\mathfrak{b}(\mathrm{d}^\downarrow(2)) = -1$, and $\mathfrak{b}(\mathrm{d}^\downarrow(3)) = \mathfrak{b}(\mathrm{d}^\downarrow(4)) = 1$. The red dots on the right indicate the encoding of a new tree.

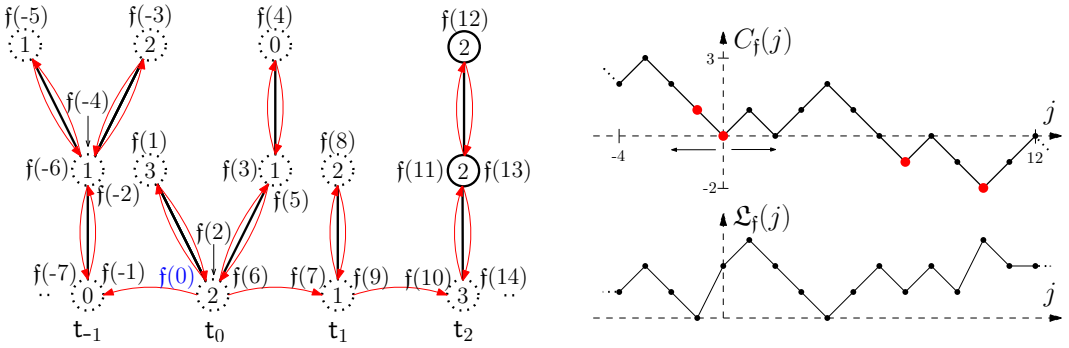

Figure 4.6: Contour and label functions $C_\mathfrak{f}$ and $\mathfrak{L}_\mathfrak{f}$ of an element $((\mathfrak{f},\mathfrak{l}),\mathfrak{b}) \in \mathfrak{F}_\infty \times \mathfrak{B}_\infty$. The left side depicts the two-sided contour exploration of $\mathfrak{f}$. The labels are given by $\mathfrak{L}_\mathfrak{f}(j)$, where now $j \in \mathbb{Z}$. The values of the infinite bridge $\mathfrak{b}$ at its first three down-steps to the right of 0 read here $\mathfrak{b}(\mathrm{d}^\downarrow(1)) = 2$, $\mathfrak{b}(\mathrm{d}^\downarrow(2)) = 1$ and $\mathfrak{b}(\mathrm{d}^\downarrow(3)) = 3$, while the first down-step to the left of zero has value $\mathfrak{b}(\mathrm{d}^\downarrow(-1)) = 0$. The arrows below the contour function indicate the direction of the encoding, and the red dots mark again the encoding of a new tree.

Note that the asymmetry in the definition of $\mathfrak{L}_\mathfrak{f}$ stems from the numbering of the trees. By linear interpolation between integer values, we interpret $C_\mathfrak{f}$, $\mathfrak{L}_\mathfrak{f}$, and sometimes also $\mathfrak{l}$, as continuous functions (from $\mathbb{R}$ to $\mathbb{R}$).

4.4.2 The Bouttier–Di Francesco–Guitter mapping

We denote the set of all rooted pointed quadrangulations with n inner faces and 2σ boundary edges by

$$\mathcal{Q}_n^{(\bullet,\sigma)} = \left\{(\mathfrak{q}, v^\bullet) : \mathfrak{q} \in \mathcal{Q}_n^{(\sigma)}, v^\bullet \in V(\mathfrak{q})\right\},$$

where $v^\bullet$ stands for the distinguished pointed vertex. In the following part, we briefly recall the definition of the bijection $\Phi_n : \mathfrak{F}_\sigma^n \times \mathfrak{B}_\sigma \to \mathcal{Q}_n^{(\bullet,\sigma)}$ introduced in [BDFG04].

The encoding of finite quadrangulations. We represent an element $((\mathfrak{f}, \mathfrak{l}), \mathfrak{b}) \in \mathfrak{F}_\sigma^n \times \mathfrak{B}_\sigma$ in the plane as follows. Firstly, we view $\mathfrak{b}$ as a cycle of length 2σ: We start from a distinguished vertex labeled $\mathfrak{b}(0) = 0$ and label the remaining $2\sigma - 1$ vertices in the counterclockwise order by the values $\mathfrak{b}(1), \mathfrak{b}(2), \ldots, \mathfrak{b}(2\sigma - 1)$. Then we graft the trees $(\mathbf{t}_0, \ldots, \mathbf{t}_{\sigma-1})$ of $\mathfrak{f}$ to the σ down-steps $0 \leq i_0 < i_1 < \cdots < i_{\sigma-1} \leq 2\sigma - 1$ of $\mathfrak{b}$, such that $\mathbf{t}_j$ is grafted on the vertex corresponding to the value $\mathfrak{b}(i_j)$, in the interior of the cycle. We do it in such a way that different trees do not intersect. The vertices of $\mathbf{t}_j$ are equipped with their labels shifted by $\mathfrak{b}(i_j)$. Figure 4.7 illustrates this procedure.

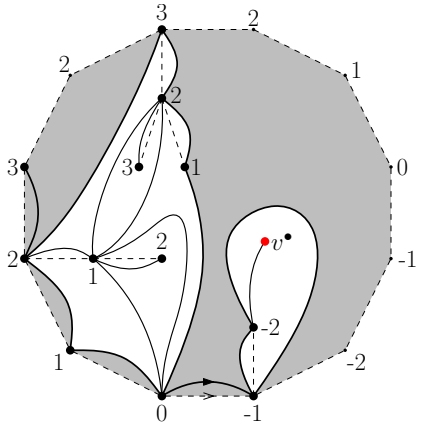

Figure 4.7: A representation of an element $((\mathfrak{f}, \mathfrak{l}), \mathfrak{b}) \in \mathfrak{F}_6^6 \times \mathfrak{B}_6$ in the plane and the associated rooted pointed quadrangulation $(\mathbf{q}, v^\bullet) = \Phi_n((\mathfrak{f}, \mathfrak{l}), \mathfrak{b})$. The distinguished vertex of the cycle is the down-most vertex labeled 0. The trees are grafted to the 6 down-steps of $\mathfrak{b}$ (here, $\mathrm{d}^\downarrow(1) = 0$, $\mathrm{d}^\downarrow(2) = 1$, $\mathrm{d}^\downarrow(3) = 8$, $\mathrm{d}^\downarrow(4) = 10$, $\mathrm{d}^\downarrow(5) = 11$, and $\mathrm{d}^\downarrow(6) = 12$). The tree edges are indicated by the dashed lines in the interior of the cycle. Note that three trees (those above the first, fourth and sixth down-step) consist of a single vertex. The labels in a tree are shifted by the bridge value of the down-step above which the tree is attached. Note that the 12 boundary edges of the cycle are in a order-preserving correspondence with the 12 boundary edges of $\mathbf{q}$. (The two edges of $\mathbf{q}$ which lie entirely in the outer face are counted twice.)

We now build a rooted and pointed quadrangulation $(\mathbf{q}, v^\bullet)$ out of $((\mathfrak{f}, \mathfrak{l}), \mathfrak{b})$. First, we put an extra vertex $v^\bullet$ in the interior of the cycle representing $\mathfrak{b}$. The set of vertices of $\mathbf{q}$ is given by the tree vertices $V(\mathfrak{f}) \cup \{v^\bullet\}$. As for the edges of $\mathbf{q}$, we define for $0 \leq i \leq 2n + \sigma - 1$ the successor $\mathrm{succ}(i) \in [0, 2n + \sigma - 1] \cup \{\infty\}$ of i to be the first element k in the list $(i + 1, \ldots, 2n + \sigma - 1, 0, \ldots, i - 1)$ (from left to right) which has label $\mathfrak{L}_\mathfrak{f}(k) = \mathfrak{L}_\mathfrak{f}(i) - 1$. If there is no such element, we put $\mathrm{succ}(i) = \infty$. We extend the contour exploration $\mathfrak{f}(0), \ldots, \mathfrak{f}(2n+\sigma-1)$ of $\mathfrak{f}$ by setting $\mathfrak{f}(\infty) = v^\bullet$. We follow the exploration starting from the vertex $\mathfrak{f}(0)$ (which is the root of $\mathbf{t}_0$) and draw for each $0 \leq i \leq 2n + \sigma - 1$ an arc between $\mathfrak{f}(i)$ and $\mathfrak{f}(\mathrm{succ}(i))$, such that arcs do not cross. Except for the leaves, a vertex of $\mathfrak{f}$ is visited at least twice in the contour exploration,

so that there are in general several arcs connecting the vertices $\mathfrak{f}(i)$ and $\mathfrak{f}(\mathrm{succ}(i))$. The edges of $\mathbf{q}$ are given by all these arcs between the vertices $V(\mathfrak{f}) \cup \{v^\bullet\}$.

It only remains to root the quadrangulation. To that aim, we observe from Figure 4.7 that the 2σ boundary edges of $\mathbf{q}$ are in a order-preserving correspondence with the 2σ cycle edges. We root $\mathbf{q}$ at the edge corresponding to the first edge of the cycle (starting from the distinguished edge, in the clockwise order), oriented in such a way that the face of degree 2σ becomes the outer face (i.e., lies to the right of the root edge). Upon erasing the tree and cycle edges of the representation of $((\mathfrak{f},\mathfrak{l}),\mathfrak{b})$, and the vertices of $\mathfrak{b}$ corresponding to up-steps, we obtain a rooted pointed quadrangulation $(\mathbf{q}, v^\bullet)$. A description of the reverse mapping $\Phi_n^{-1} : \mathcal{Q}_n^{(\bullet,\sigma)} \to \mathfrak{F}_\sigma^n \times \mathfrak{B}_\sigma$ can be found in [BDFG04] or [Bet15].

The encoding of infinite quadrangulations. Recall that $\mathcal{Q}$ is the completion of the set of finite rooted quadrangulations with a boundary with respect to d_{loc}. The aim of this section is to extend Φ_n to a mapping

$$\Phi : (\cup_{n,\sigma\in\mathbb{N}} \mathfrak{F}_\sigma^n \times \mathfrak{B}_\sigma) \cup (\mathfrak{F}_\infty \times \mathfrak{B}_\infty) \longrightarrow \mathcal{Q}.$$

We proceed as follows. If $((\mathfrak{f},\mathfrak{l}),\mathfrak{b}) \in \mathfrak{F}_\sigma^n \times \mathfrak{B}_\sigma$, we put $\Phi((\mathfrak{f},\mathfrak{l}),\mathfrak{b}) = \Phi_n((\mathfrak{f},\mathfrak{l}),\mathfrak{b})$. (We forget the distinguished vertex of $\Phi_n((\mathfrak{f},\mathfrak{l}),\mathfrak{b})$ and view the quadrangulation as an element in $\mathcal{Q}_n^{(\sigma)} \subset \mathcal{Q}$.)

Now assume $((\mathfrak{f},\mathfrak{l}),\mathfrak{b}) \in \mathfrak{F}_\infty \times \mathfrak{B}_\infty$. We consider the following representation of $((\mathfrak{f},\mathfrak{l}),\mathfrak{b})$ in the upper half-plane: First, we identify $\mathfrak{b}$ with the bi-infinite line obtained from connecting $i \in \mathbb{Z}$ to $i+1$ by an edge. Vertex i is labeled $\mathfrak{b}(i)$. We attach the trees $\mathfrak{t}(0), \mathfrak{t}(1), \ldots$ of $\mathfrak{f}$ to the down-steps of $\mathfrak{b}$ to the right of 0, and the trees $\mathfrak{t}(-1), \mathfrak{t}(-2), \ldots$ to the down-steps of $\mathfrak{b}$ to the left of -1, everything in the upper half-plane. Again, the labels in a tree are shifted by the underlying bridge label.

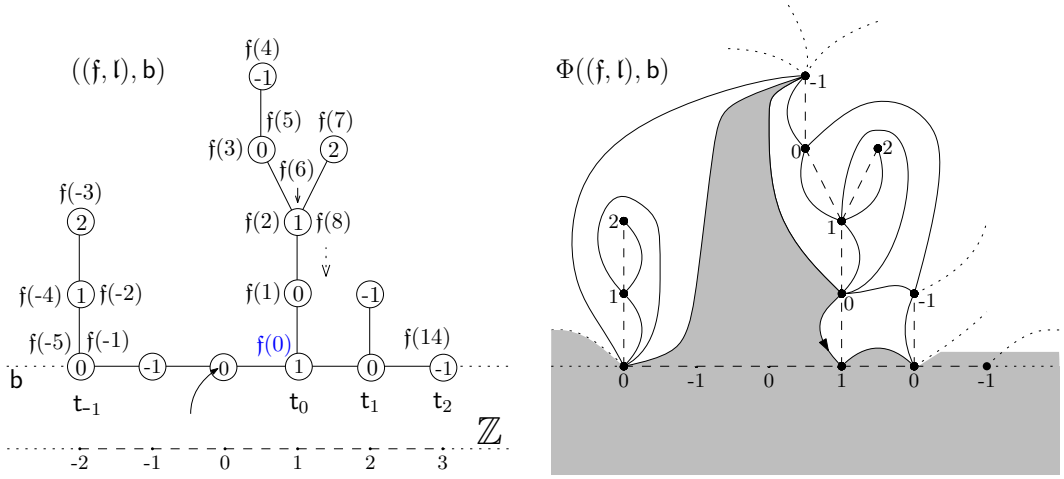

Figure 4.8: The Bouttier–Di Francesco–Guitter mapping applied to an element $((\mathfrak{f},\mathfrak{l}),\mathfrak{b}) \in \mathfrak{F}_\infty \times \mathfrak{B}_\infty$. On the right hand side, the arcs connect the vertices $\mathfrak{f}(i)$ with $\mathfrak{f}(\mathrm{succ}_\infty(i))$, for $i \in \mathbb{Z}$. The other vertices and edges of the representation of $((\mathfrak{f},\mathfrak{l}),\mathfrak{b})$ on the left hand side do not appear in the quadrangulation. The oriented arc on the right indicated by an arrow represents the root edge of the map.

Similarly to the finite case, the vertex set of $\mathbf{q} = \Phi((\mathfrak{f}, \mathfrak{l}), \mathsf{b})$ is given by $V(\mathfrak{f})$; here, we add no additional vertex. For specifying the edges, we let the successor $\mathrm{succ}_\infty(i)$ of $i \in \mathbb{Z}$ be the smallest number $k > i$ such that $\mathfrak{L}_\mathfrak{f}(k) = \mathfrak{L}_\mathfrak{f}(i) - 1$. Since by assumption $\inf_{i\in\mathbb{N}} \mathsf{b}(i) = -\infty$, $\mathrm{succ}_\infty(i)$ is a finite number. We next connect the vertices $\mathfrak{f}(i)$ and $\mathfrak{f}(\mathrm{succ}_\infty(i))$ by an arc for any $i \in \mathbb{Z}$, such that the resulting map is planar. The arcs form the edges of the infinite rooted quadrangulation $\mathbf{q}$ we are about to construct. In order to root the map, we observe that the bi-infinite line $\mathbb{Z}$ is in correspondence with the boundary edges of $\mathbf{q}$, and we choose the edge corresponding to $\{0, 1\}$ as the root edge of $\mathbf{q}$ (oriented such that the outer face lies to its right). A representation of $((\mathfrak{f}, \mathfrak{l}), \mathsf{b})$ and of the resulting quadrangulation $\Phi((\mathfrak{f}, \mathfrak{l}), \mathsf{b})$ is depicted in Figure 4.8.

4.4.3 Definition of the UIHPQ$_p$

We are now in position to construct the UIHPQ$_p$ by means of the above mapping Φ applied to a (random) element in $\mathfrak{F}_\infty \times \mathfrak{B}_\infty$, which we introduce first.

Let $\mathbf{t}$ be a finite random plane tree. Conditionally on $\mathbf{t}$, we assign to $\mathbf{t}$ a random uniform labeling ℓ of its vertices, so that the pair $(\mathbf{t}, \ell)$ becomes a well-labeled tree. Namely, given $\mathbf{t}$, we first equip each edge of $\mathbf{t}$ with an independent random variable uniformly distributed in $\{-1, 0, 1\}$. Then we define the label $\ell(u)$ of a vertex $u \in V(\mathbf{t})$ to be the sum over all labels along the unique (non-backtracking) path from the tree root to u.

We consider Galton-Watson trees with a (sub-)critical geometric offspring law μ_p of parameter p, $p \in [0, 1/2]$, that is, $\mu_p(k) = p^k(1-p)$, $k \in \mathbb{Z}_+$. If $\mathbf{t}$ is such a tree, we call it a *p-Galton-Watson tree*. Equipped with a random uniform labeling ℓ as described before, we say that the pair $(\mathbf{t}, (\ell(u))_{u\in V(\mathbf{t})})$ is a *uniformly labeled p-Galton-Watson tree*.

A *uniformly labeled infinite p-forest* is a random element $(\mathfrak{f}_\infty^{(p)}, \mathfrak{l}_\infty^{(p)})$ taking values in $\mathfrak{F}_\infty$, such that $(\mathbf{t}_i, \mathfrak{l}_\infty^{(p)} \restriction V(\mathbf{t}_i))$, $i \in \mathbb{Z}$, are independent uniformly labeled p-Galton-Watson trees.

A *uniform infinite bridge* is a random element $\mathsf{b}_\infty = (\mathsf{b}_\infty(i), i \in \mathbb{Z})$ in $\mathfrak{B}_\infty$ such that b_∞ has the law of a two-sided simple symmetric random walk starting from $\mathsf{b}_\infty(0) = 0$. We stress that our wording differs from [BMR16], where a uniform infinite bridge refers to a two-sided random walk with a geometric offspring law of parameter $1/2$. See also Lemma 4.5.3 below.

Definition 4.4.1. Fix $p \in [0, 1/2]$. Let $(\mathfrak{f}_\infty^{(p)}, \mathfrak{l}_\infty^{(p)})$ be a uniformly labeled infinite p-forest, and independently of $(\mathfrak{f}_\infty^{(p)}, \mathfrak{l}_\infty^{(p)})$, let b_∞ be a uniform infinite bridge. Then the UIHPQ$_p$ with skewness parameter p is given by the (rooted) random infinite quadrangulation $\mathbf{Q}_\infty^\infty(p) = (V(\mathbf{Q}_\infty^\infty(p)), d_{\mathrm{gr}}, \rho)$ with an infinite boundary, which is obtained from applying the Bouttier–Di Francesco–Guitter mapping Φ to $((\mathfrak{f}_\infty^{(p)}, \mathfrak{l}_\infty^{(p)}), \mathsf{b}_\infty)$. In case $p = 1/2$, we simply write $\mathbf{Q}_\infty^\infty$, which denotes then the (standard) uniform infinite half-planar quadrangulation with a general boundary.

Remark 4.4.2. Let $\mathfrak{f}_\infty^{(p)}$ be the encoding forest of the UIHPQ$_p$. Instead of working with metric balls around the root vertex in the UIHPQ$_p$, it will – due to the specific

construction of the latter – often be more practical to consider metric balls around the vertex corresponding to the tree root $\mathfrak{f}_\infty^{(p)}(0)$ in the UIHPQ$_p$. Similarly, if $Q_n^\sigma \in \mathcal{Q}_n^{(\sigma)}$ is a uniform quadrangulation and $\mathfrak{f}_n$ its encoding forest, it will be more natural to consider balls around $\mathfrak{f}_n(0)$ in Q_n^σ. Since the distance between $\mathfrak{f}_\infty^{(p)}(0)$ or $\mathfrak{f}_n(0)$ and the root of the map is stochastically bounded (it may also be zero), this makes no difference in terms of scaling limits whatsoever; see [BMR16, Lemma 5.6]. We shall use the notation $B_r^{(0)}(\mathbf{Q}_\infty^\infty(p))$ for the metric ball of radius r around $\mathfrak{f}_\infty^{(p)}(0)$ in the UIHPQ$_p$. Analogously, we define $B_r^{(0)}(Q_n^\sigma)$.

4.5 Proofs of the limit results

4.5.1 The UIHPQ$_p$ as a local limit of uniform quadrangulations

In this part, we prove Theorem 4.2.1 and Proposition 4.2.2. We begin with the former. The case $p = 1/2$ has already been treated in [BMR16], and the case $p = 0$ will be considered afterwards, so we first fix $0 < p < 1/2$ and let $(\sigma_n, n \in \mathbb{N})$ be a sequence of positive integers satisfying $\sigma_n = \frac{1-2p}{p} n + o(n)$. Recall that rooted pointed quadrangulations in $\mathcal{Q}_n^{(\bullet,\sigma_n)}$ are in one-to-one correspondence with elements in $\mathfrak{F}_{\sigma_n}^n \times \mathfrak{B}_{\sigma_n}$. For proving Theorem 4.2.1, the key step is to control the law of the first k trees in a forest $\mathfrak{f}_n$ chosen uniformly at random in $\mathfrak{F}_{\sigma_n}^n$, for k arbitrarily large but fixed. We will see in Lemma 4.5.1 below that their law is close to the law of k independent p-Galton-Watson trees when n is sufficiently large. Together with a convergence result of bridges (Lemma 4.5.3), this allows us to couple contour and label functions of $Q_n^{\sigma_n}$ and the UIHPQ$_p$, such that with high probability, we have equality of balls of a constant radius around the roots in $Q_n^{\sigma_n}$ and the UIHPQ$_p$, respectively. This readily implies the theorem.

We begin with the necessary control over the trees. Since the result on the tree convergence is of some interest on its own, we formulate an optimal version, which is stronger than we what need for mere local convergence as stated in Theorem 4.2.1. The exact formulation depends on the error term in the expression for σ_n. Let us put

$$\gamma_n = \max\left\{\sigma_n - \frac{1-2p}{p} n,\ 1\right\}. \tag{4.3}$$

Lemma 4.5.1. *Fix $0 < p < 1/2$, and let $(\sigma_n, n \in \mathbb{N})$ be a sequence of positive integers satisfying $\sigma_n = \frac{1-2p}{p} n + o(n)$. Define γ_n in terms of σ_n and p. Let $(\mathbf{t}_i)_{1\le i\le \sigma_n}$ be a family of σ_n independent $1/2$-Galton-Watson trees, and let $(\mathbf{t}_i^{(p)})_{1\le i\le \sigma_n}$ be a family of σ_n independent p-Galton-Watson trees. Then, if $(k_n, n \in \mathbb{N})$ is a sequence of positive integers satisfying $k_n \le \sigma_n$ and $k_n = o\left(\min\{n^{1/2}, n/\gamma_n\}\right)$ as $n \to \infty$, we have*

$$\lim_{n\to\infty} \left\| \mathrm{Law}\Big((\mathbf{t}_i)_{1\le i\le k_n} \,\Big|\, \sum_{i=1}^{\sigma_n} |\mathbf{t}_i| = n\Big) - \mathrm{Law}\left((\mathbf{t}_i^{(p)})_{1\le i\le k_n}\right) \right\|_{\mathrm{TV}} = 0.$$

Remark 4.5.2. We stress that if we only know $\gamma_n = o(n)$ as assumed in the statement of Theorem 4.2.1, we can at least choose k_n equals an (arbitrary) large constant

$k \in \mathbb{N}$. This suffices in any case to show local convergence towards the UIHPQ$_p$; see Proposition 4.5.4 below. Lemma 4.5.1 may be seen as a complement to the results on coupling of trees in [BMR16]; it treats a regime not considered in that work.

Proof. We write $\mathbb{P}_n$ for the conditional law of $(\mathbf{t}_i)_{1\le i\le k_n}$ given $\sum_{i=1}^{\sigma_n}|\mathbf{t}_i| = n$, and $\mathbb{Q}_n$ for the (unconditioned) law of $(\mathbf{t}_i^{(p)})_{1\le i\le k_n}$. Given a family $\mathfrak{f}$ of k_n trees, we write $\mathbf{v}(\mathfrak{f})$ for the sum of their sizes, i.e., the total number of edges. Note that

$$\mathrm{supp}(\mathbb{P}_n) = \mathrm{supp}(\mathbb{Q}_n) \cap \{\mathfrak{f} : \mathbf{v}(\mathfrak{f}) \le n\}.$$

We now proceed in two steps. First, we show that for each $\varepsilon > 0$, there exists a constant $K > 0$ such that

$$\mathbb{Q}_n\left(\{\mathfrak{f} : \mathbf{v}(\mathfrak{f}) > Kk_n\}\right) \le \varepsilon, \quad \mathbb{P}_n\left(\{\mathfrak{f} : \mathbf{v}(\mathfrak{f}) > Kk_n\}\right) \le \varepsilon. \tag{4.4}$$

We then show that for large enough n, we have for any $\mathfrak{f} \in \mathrm{supp}(\mathbb{P}_n)$ of total size $\mathbf{v}(\mathfrak{f}) \le Kk_n$,

$$1 - \varepsilon \le \left|\frac{\mathbb{P}_n(\mathfrak{f})}{\mathbb{Q}_n(\mathfrak{f})}\right| \le 1 + \varepsilon. \tag{4.5}$$

Clearly, (4.4) and (4.5) imply the claim of the lemma. We first prove (4.4). Let $(S^{(p)}(m), m \in \mathbb{Z}_+)$ be a random walk on the integers starting from $S^{(p)}(0) = 0$ with increments distributed according to $p\delta_1 + (1-p)\delta_{-1}$. Set, for $\ell \in \mathbb{Z}$,

$$T_\ell^{(p)} = \inf\left\{m \in \mathbb{N} : S^{(p)}(m) = \ell\right\}.$$

Note that $S^{(p)}(m) + (1-2p)m$, $m \in \mathbb{Z}_+$, is a martingale. We now use that the total size of k_n trees under $\mathbb{Q}_n$ and $(T_{-k_n}^{(p)} - k_n)/2$ are equal in distribution; see the discussion in Section 4.3.2. Applying Markov's inequality in the second and the optional stopping theorem in the third step, we obtain for K large enough

$$\mathbb{Q}_n\left(\mathbf{v} > Kk_n\right) = \mathbb{P}\left(T_{-k_n}^{(p)} > (2K+1)k_n\right) \le \frac{\mathbb{E}[T_{-k_n}^{(p)}]}{(2K+1)k_n} = \frac{1}{(1-2p)(2K+1)} \le \varepsilon.$$

For bounding the second probability in (4.4), we let $(S(m), m \in \mathbb{Z}_+)$ be a simple symmetric random walk started from $S(0) = 0$ and write T_ℓ for its first hitting time of $\ell \in \mathbb{Z}$. Then

$$\mathbb{P}_n\left(\mathbf{v} > Kk_n\right) = \mathbb{P}\left(T_{-k_n} > Kk_n \,|\, T_{-\sigma_n} = 2n + \sigma_n\right).$$

Let us abbreviate $N = 2n + \sigma_n$, and $K_n = \lceil Kk_n \rceil$. We recall Kemperman's formula; see [Pit06, Section 6.1]. Applying first the Markov property at time K_n and then Kemperman's formula to both the nominator and denominator gives, for large n,

$$\begin{aligned}
&\mathbb{P}\left(T_{-k_n} > K_n \,|\, T_{-\sigma_n} = N\right) = \mathbb{E}\left[\mathbf{1}_{\{T_{-k_n} > K_n\}} \frac{\mathbb{P}\left(T_{-\sigma_n} = N \,|\, S(K_n)\right)}{\mathbb{P}\left(T_{-\sigma_n} = N\right)}\right] \\
&= \mathbb{E}\left[\mathbf{1}_{\{T_{-k_n} > K_n\}} \frac{\sigma_n(\sigma_n + S(K_n))}{N(N - K_n)} \frac{\mathbb{P}\left(S(N) = -\sigma_n \,|\, S(K_n)\right)}{\mathbb{P}\left(S(N) = -\sigma_n\right)}\right] \\
&\le 2\,\mathbb{P}\left(S(K_n) > -k_n \,|\, S(N) = -\sigma_n\right).
\end{aligned}$$

Let $(\tilde{S}(m), m \in \mathbb{Z}_+)$ be the random walk starting from $\tilde{S}(0) = 0$ with steps

$$1 + \frac{\sigma_n}{N} \quad \text{with probability } \frac{1 - \sigma_n/N}{2}, \qquad -1 + \frac{\sigma_n}{N} \quad \text{with probability } \frac{1 + \sigma_n/N}{2}.$$

Clearly, $(\tilde{S}(m), m \in \mathbb{Z}_+)$ is a martingale, and we find the relation

$$\mathbb{P}\left(S(K_n) \geq -k_n \,\middle|\, S(N) = -\sigma_n\right) = \mathbb{P}\left(\tilde{S}(K_n) \geq K_n \frac{\sigma_n}{N} - k_n \,\middle|\, \tilde{S}(N) = 0\right).$$

We now estimate

$$\begin{aligned}
&\mathbb{P}\left(\tilde{S}(K_n) \geq K_n \frac{\sigma_n}{N} - k_n \,\middle|\, \tilde{S}(N) = 0\right) \\
&\leq \mathbb{P}\left(\tilde{S}(N) \geq 0\right)^{-1} \mathbb{P}\left(\tilde{S}(K_n) \geq K_n \frac{\sigma_n}{N} - k_n\right) \leq 3 \frac{\mathbb{E}\left[\tilde{S}(K_n)^2\right]}{(K_n \frac{\sigma_n}{N} - k_n)^2} \leq \frac{12 K_n}{(K_n \frac{\sigma_n}{N} - k_n)^2}.
\end{aligned}$$

Here, in the next to last inequality, we have used Doob's inequality, as well as the bound $\mathbb{P}(\tilde{S}(N) \geq 0) \geq 1/3$ for large n, which is a direct consequence of the martingale central limit theorem. Since σ_n/N remains bounded away from zero (recall that $p < 1/2$), the last expression on the right hand side can be made arbitrarily small, upon choosing K large. This proves $\mathbb{P}_n(\mathbf{v} > K k_n) \leq \varepsilon$ for K large enough, and hence (4.4) holds.

We turn to (4.5). First, observe that for a fixed $\mathfrak{f}$ in the support of $\mathbb{P}_n$, $\mathbb{P}_n(\mathfrak{f})$ is the probability to see k_n particular trees of total size $\mathbf{v}(\mathfrak{f})$ in a forest consisting of σ_n trees with total size n. An application of Kemperman's formula gives

$$\mathbb{P}_n(\mathfrak{f}) = \frac{\frac{\sigma_n - k_n}{2(n - \mathbf{v}(\mathfrak{f})) + \sigma_n - k_n} 2^{2(n - \mathbf{v}(\mathfrak{f})) + \sigma_n - k_n} \mathbb{P}\left(S(2(n - \mathbf{v}(\mathfrak{f})) + \sigma_n - k_n) = \sigma_n - k_n\right)}{\frac{\sigma_n}{2n + \sigma_n} 2^{2n + \sigma_n} \mathbb{P}\left(S(2n + \sigma_n) = \sigma_n\right)}.$$

Since $k_n \ll n$, we have for large $n \in \mathbb{N}$ and all families $\mathfrak{f}$ of k_n trees with $\mathbf{v}(\mathfrak{f}) \leq K k_n$,

$$1 - \varepsilon \leq \left| \frac{\frac{\sigma_n - k_n}{2(n - \mathbf{v}(\mathfrak{f})) + \sigma_n - k_n} 2^{2(n - \mathbf{v}(\mathfrak{f})) + \sigma_n - k_n}}{\frac{\sigma_n}{2n + \sigma_n} 2^{2n + \sigma_n}} 2^{2\mathbf{v}(\mathfrak{f}) + k_n} \right| \leq 1 + \varepsilon.$$

On the other hand, we know from (4.2) that $\mathbb{Q}_n(\mathfrak{f}) = p^{\mathbf{v}(\mathfrak{f})}(1-p)^{\mathbf{v}(\mathfrak{f}) + k_n}$. Display (4.5) will therefore follow if we show that for large n and all $\mathfrak{f}$ with $\mathbf{v}(\mathfrak{f}) \leq K k_n$,

$$1 - \varepsilon \leq \left| \frac{\mathbb{P}\left(S(2(n - \mathbf{v}(\mathfrak{f})) + \sigma_n - k_n) = \sigma_n - k_n\right)}{\mathbb{P}\left(S(2n + \sigma_n) = \sigma_n\right)} ((2p)^{-\mathbf{v}(\mathfrak{f})} (2(1-p))^{-(\mathbf{v}(\mathfrak{f}) + k_n)} \right| \leq 1 + \varepsilon. \tag{4.6}$$

For a given $\mathfrak{f}$ with $\mathbf{v}(\mathfrak{f}) \leq K k_n$, let us abbreviate $y_n = 2(n - \mathbf{v}(\mathfrak{f})) + \sigma_n - k_n$, $x_n = \sigma_n - k_n$, and $v_n = \mathbf{v}(\mathfrak{f})$. Clearly,

$$\frac{\mathbb{P}\left(S(2(n - v_n) + \sigma_n - k_n) = \sigma_n - k_n\right)}{\mathbb{P}\left(S(2n + \sigma_n) = \sigma_n\right)} = \frac{\binom{y_n}{\frac{y_n - x_n}{2}}}{\binom{2n + \sigma_n}{n}} 2^{2v_n + k_n}.$$

Combining the last two displays, it remains to show that

$$1 - \varepsilon \leq \left| \frac{y_n! (n + \sigma_n)! n!}{\frac{y_n - x_n}{2}! \frac{y_n + x_n}{2}! (2n + \sigma_n)!} p^{-v_n} (1-p)^{-(v_n + k_n)} \right| \leq 1 + \varepsilon.$$

The constants in the following error terms are uniform in the choice of $\mathfrak{f}$ satisfying $v_n = \mathbf{v}(\mathfrak{f}) \le Kk_n$. By Stirling's formula and a rearrangement of the terms, we obtain

$$\frac{y_n!(n+\sigma_n)!n!}{\frac{y_n-x_n}{2}!\frac{y_n+x_n}{2}!(2n+\sigma_n)!} = (1+o(1)) \underbrace{\left(\frac{y_n}{2n+\sigma_n}\right)^{2n+\sigma_n}\left(\frac{n}{n-v_n}\right)^{n}\left(\frac{n+\sigma_n}{(y_n+x_n)/2}\right)^{n+\sigma_n}}_{=\mathrm{I}} \times \underbrace{\left(\frac{n-v_n}{y_n}\right)^{v_n}\left(\frac{(y_n+x_n)/2}{y_n}\right)^{v_n+k_n}}_{=\mathrm{II}}.$$

Recall that $k_n = o\left(\min\{n^{1/2}, n/\gamma_n\}\right)$ and $v_n \le Kk_n$. We replace x_n and y_n by their values and obtain for the product I of the first three factors

$$\mathrm{I} = \exp\left(-(2v_n+k_n)\right)\exp\left((v_n+k_n)\right)\exp\left(v_n\right)\left(1+O(k_n^2/n)\right) = 1+o(1).$$

Recalling the particular form of σ_n for the product II of the last two factors, we arrive at

$$\mathrm{II} = p^{v_n}(1-p)^{v_n+k_n}\left(1+O(\gamma_n/n)\right)^{2v_n+k_n} = p^{v_n}(1-p)^{v_n+k_n}\left(1+o(1)\right).$$

This proves (4.6) and hence the lemma. □

We continue with a convergence result for uniform bridges $\mathsf{b}_n \in \mathfrak{B}_{\sigma_n}$ towards b_∞.

Lemma 4.5.3. *Let $(\sigma_n, n \in \mathbb{N})$ be a sequence of positive integers satisfying $\sigma_n \to \infty$ as $n \to \infty$. Let b_n be uniformly distributed in $\mathfrak{B}_{\sigma_n}$, and let b_∞ be a uniform infinite bridge as specified in Section 4.4. Then, if k_n is a sequence of positive integers with $k_n \le \sigma_n$ and $k_n = o(\sigma_n)$ as $n \to \infty$,*

$$\lim_{n\to\infty} \|\mathrm{Law}((\mathsf{b}_n(2\sigma_n-k_n),\dots,\mathsf{b}_n(2\sigma_n-1),\mathsf{b}_n(0),\mathsf{b}_n(1),\dots,\mathsf{b}_n(k_n))) - \mathrm{Law}((\mathsf{b}_\infty(-k_n),\dots,\mathsf{b}_\infty(-1),\mathsf{b}_\infty(0),\mathsf{b}_\infty(1),\dots,\mathsf{b}_\infty(k_n)))\|_{\mathrm{TV}} = 0.$$

The proof follows from a small adaption of [BMR16, Proof of Lemma 5.5] and is left to the reader. We stress, however, that in [BMR16], b_n and b_∞ were defined in a slightly different manner, by grouping the $+1$-steps between two subsequent down-steps together to one "big" jump. Clearly, this does change the argument only in a minor way.

We are now in position to formulate an appropriate coupling of balls.

Proposition 4.5.4. *Fix $0 < p < 1/2$, and let $(\sigma_n, n \in \mathbb{N})$ be a sequence of positive integers satisfying $\sigma_n = \frac{1-2p}{p}n + o(n)$. Define γ_n in terms of σ_n as under (4.3), and put $\xi_n = \min\{n^{1/4}, \sqrt{n/\gamma_n}\}$. Then, given any $\varepsilon > 0$, there exist $\delta > 0$ and $n_0 \in \mathbb{N}$ such that for every $n \ge n_0$, we can construct on the same probability space copies of $Q_n^{\sigma_n}$ and the UIHPQ_p such that with probability at least $1-\varepsilon$, the metric balls $B_{\delta\xi_n}(Q_n^{\sigma_n})$ and $B_{\delta\xi_n}(\mathsf{UIHPQ}_p)$ of radius $\delta\xi_n$ around the roots in the corresponding spaces are isometric.*

The local convergence of $Q_n^{\sigma_n}$ towards UIHPQ_p is a weaker statement, hence Theorem 4.2.1 in the case $0 < p < 1/2$ will follow from the proposition.

Proof. The proof is in spirit of [BMR16, Proof of Proposition 3.11], requires, however, some modifications. We will indicate at which place we may simply adopt the reasoning. We consider a random uniform element $((\mathfrak{f}_n, \mathfrak{l}_n), \mathsf{b}_n) \in \mathfrak{F}^n_{\sigma_n}$, and a triplet $((\mathfrak{f}^{(p)}_\infty, \mathfrak{l}^{(p)}_\infty), \mathsf{b}_\infty)$ consisting of a uniformly labeled infinite p-forest together with an (independent) uniform infinite bridge b_∞. We let $(Q^{\sigma_n}_n, v^\bullet) = \Phi_n((\mathfrak{f}_n, \mathfrak{l}_n), \mathsf{b}_n)$ and $\mathbf{Q}^\infty_\infty(p) = \Phi((\mathfrak{f}^{(p)}_\infty, \mathfrak{l}^{(p)}_\infty), \mathsf{b}_\infty)$ be the quadrangulations obtained by applying the Bouttier–Di Francesco–Guitter mapping to $((\mathfrak{f}_n, \mathfrak{l}_n), \mathsf{b}_n)$ and $((\mathfrak{f}^{(p)}_\infty, \mathfrak{l}^{(p)}_\infty), \mathsf{b}_\infty)$, respectively. Recall that $\mathfrak{f}_n = (\mathbf{t}_0, \dots, \mathbf{t}_{\sigma_n - 1})$ consists of σ_n trees. For $0 \le k \le \sigma_n - 1$, we let $\mathbf{t}(\mathfrak{f}_n, k) = \mathbf{t}_k$, i.e., $\mathbf{t}(\mathfrak{f}_n, k)$ is the tree of $\mathfrak{f}_n$ with index k, and we put $\mathbf{t}(\mathfrak{f}_n, \sigma_n) = \mathbf{t}(\mathfrak{f}_n, 0)$. In a similar manner, $\mathbf{t}(\mathfrak{f}^{(p)}_\infty, k)$ denotes the tree of $\mathfrak{f}^{(p)}_\infty$ indexed by $k \in \mathbb{Z}$.

By Lemma 4.5.1, we find $\delta' > 0$ and $n'_0 \in \mathbb{N}$ such that for $n \ge n'_0$, we can construct $((\mathfrak{f}_n, \mathfrak{l}_n), \mathsf{b}_n)$ and $((\mathfrak{f}^{(p)}_\infty, \mathfrak{l}^{(p)}_\infty), \mathsf{b}_\infty)$ on the same probability space such that with $A_n = \lfloor \delta' \xi_n^2 \rfloor$, the event

$$\begin{aligned}\mathcal{E}^1(n, \delta') = \quad & \Big\{ \mathbf{t}(\mathfrak{f}_n, i) = \mathbf{t}(\mathfrak{f}^{(p)}_\infty, i),\ \mathbf{t}(\mathfrak{f}_n, \sigma_n - i) = \mathbf{t}(\mathfrak{f}^{(p)}_\infty, -i) \text{ for all } 0 \le i \le A_n \Big\} \\ & \cap \Big\{ \mathfrak{l}_n|_{\mathbf{t}(\mathfrak{f}_n, i)} = \mathfrak{l}^{(p)}_\infty|_{\mathbf{t}(\mathfrak{f}^{(p)}_\infty, i)},\ \mathfrak{l}_n|_{\mathbf{t}(\mathfrak{f}_n, \sigma_n - i)} = \mathfrak{l}^{(p)}_\infty|_{\mathbf{t}(\mathfrak{f}^{(p)}_\infty, -i)} \text{ for all } 0 \le i \le A_n \Big\}\end{aligned}$$

has probability at least $1 - \varepsilon/8$. We now fix such a δ' for the rest of the proof. Recall that by our construction of the Bouttier–Di Francesco–Guitter bijection, the trees of $\mathfrak{f}_n$ are attached to the down-steps $\mathsf{d}^\downarrow_n(i) = \mathsf{d}^\downarrow_{\mathsf{b}_n}(i)$ of b_n, $1 \le i \le \sigma_n$, and similarly, the trees of $\mathfrak{f}^{(p)}_\infty$ are attached to the down-steps $\mathsf{d}^\downarrow_\infty(i) = \mathsf{d}^\downarrow_{\mathsf{b}_\infty}(i)$ of b_∞, where now $i \in \mathbb{Z}$. In view of the above event, this incites us to consider additionally the event

$$\begin{aligned}\mathcal{E}^2(n, \delta') = \quad & \Big\{ \mathsf{b}_n(i) = \mathsf{b}_\infty(i) \text{ for all } 1 \le i \le \mathsf{d}^\downarrow_\infty(A_n + 1) \Big\} \\ & \cap \Big\{ \mathsf{b}_n(2\sigma_n - i) = \mathsf{b}_\infty(i) \text{ for all } \mathsf{d}^\downarrow_\infty(-A_n) \le i \le -1 \Big\}.\end{aligned}$$

Note that on $\mathcal{E}^2(n, \delta')$, we automatically have $\mathsf{d}^\downarrow_n(i) = \mathsf{d}^\downarrow_\infty(i)$ for $1 \le i \le A_n + 1$, and $\mathsf{d}^\downarrow_n(\sigma_n - i + 1) = \mathsf{d}^\downarrow_\infty(-i)$ for $1 \le i \le A_n$. Trivially, we have that $\mathsf{d}^\downarrow_\infty(A_n + 1) \ge A_n + 1$ and $\mathsf{d}^\downarrow_\infty(-A_n) \le -A_n$, but also, with probability tending to 1, $\mathsf{d}^\downarrow_\infty(A_n + 1) \le 3A_n$ and $\mathsf{d}^\downarrow_\infty(-A_n) \ge -3A_n$. Since, in any case, $A_n = o(\sigma_n)$, we can ensure by Lemma 4.5.3 that the event $\mathcal{E}^2(n, \delta')$ has probability at least $1 - \varepsilon/8$ for large n.

Now for $\delta > 0$, $n \in \mathbb{N}$, define the events

$$\mathcal{E}^3(n, \delta) = \left\{ \min_{[0, \mathsf{d}^\downarrow_\infty(A_n + 1)]} \mathsf{b}_\infty < -5\delta\xi_n,\ \min_{[\mathsf{d}^\downarrow_\infty(-A_n), -1]} \mathsf{b}_\infty < -5\delta\xi_n \right\},$$

$$\mathcal{E}^4(n, \delta) = \left\{ \min_{[\mathsf{d}^\downarrow_\infty(A_n + 1) + 1,\, \mathsf{d}^\downarrow_\infty(-A_n) - 1]} \mathsf{b}_n < -5\delta\xi_n \right\}.$$

By invoking Donsker's invariance principle together with Lemma 4.5.3 for the event $\mathcal{E}^3$ (and again the fact that $A_n + 1 \le \mathsf{d}^\downarrow_\infty(A_n + 1) \le 3A_n$ and $-3A_n \le \mathsf{d}^\downarrow_\infty(-A_n) \le -A_n$ with high probability), we deduce that for small $\delta > 0$, provided n is large enough,

$$\mathbb{P}\left(\mathcal{E}^3(n, \delta)\right) \ge 1 - \varepsilon/8, \quad \text{and} \quad \mathbb{P}\left(\mathcal{E}^4(n, \delta)\right) \ge 1 - \varepsilon/8.$$

We will now assume that $n_0 \ge n'_0$ and $\delta > 0$ are such that for all $n \ge n_0$, the above bounds hold true, and work on the event $\mathcal{E}^1(n, \delta') \cap \mathcal{E}^2(n, \delta') \cap \mathcal{E}^3(n, \delta) \cap \mathcal{E}^4(n, \delta)$ of

probability at least $1-\varepsilon/2$. We consider the forest obtained from restricting $\mathfrak{f}_n$ to the first A_n+1 and the last A_n trees,

$$\mathfrak{f}'_n = (\mathbf{t}(\mathfrak{f}_n,0),\dots,\mathbf{t}(\mathfrak{f}_n,A_n),\mathbf{t}(\mathfrak{f}_n,\sigma_n-A_n),\dots,\mathbf{t}(\mathfrak{f}_n,\sigma_n-1))\,.$$

Similarly, we define $\mathfrak{f}'^{(p)}_\infty$. We recall the cactus bounds in the version stated in [BMR16, (4.4) of Section 4.5]. Applied to $Q_n^{\sigma_n}$, it shows that for vertices $v\in V(\mathfrak{f}_n)\backslash V(\mathfrak{f}'_n)$, with d_n denoting the graph distance,

$$d_n(\mathfrak{f}_n(0),v)\geq -\max\left\{\min_{[0,\,\mathsf{d}^{\downarrow}_\infty(A_n+1)]}\mathsf{b}_n,\ \min_{[\mathsf{d}^{\downarrow}_\infty(-A_n),2\sigma_n]}\mathsf{b}_n\right\}\geq 5\delta\xi_n.$$

Applying now the analogous cactus bound [BMR16, (4.6) of Section 4.5] to the infinite quadrangulation $\mathbf{Q}^\infty_\infty(p)$, we obtain the same lower bound for vertices $v\in V(\mathfrak{f}^{(p)}_\infty)\backslash V(\mathfrak{f}'^{(p)}_\infty)$, with d_n replaced by the graph distance $d^{(p)}_\infty$ in $\mathbf{Q}^\infty_\infty(p)$, and $\mathfrak{f}_n(0)$ replaced by the vertex $\mathfrak{f}^{(p)}_\infty(0)$ of $\mathbf{Q}^\infty_\infty(p)$. We recall the definition of the metric balls $B^{(0)}_r(Q_n^{\sigma_n})$ and $B^{(0)}_r(\mathbf{Q}^\infty_\infty(p))$; see Remark 4.4.2. By the same arguments as in [BMR16, Proof of Proposition 3.11], we then deduce that vertices at a distance at most $5\delta\xi_n-1$ from $\mathfrak{f}_n(0)$ in $Q_n^{\sigma_n}$ agree with those at a distance at most $5\delta\xi_n-1$ from $\mathfrak{f}^{(p)}_\infty(0)$ in $\mathbf{Q}^\infty_\infty(p)$. Moreover,

$$d_n(u,v)=d^{(p)}_\infty(u,v)\quad\text{whenever } u,v\in B^{(0)}_{2\delta\xi_n}(Q_n^{\sigma_n}).$$

This proves that the balls $B^{(0)}_{2\delta\xi_n}(Q_n^{\sigma_n})$ and $B^{(0)}_{2\delta\xi_n}(\mathbf{Q}^\infty_\infty(p))$ are isometric on an event of probability at least $1-\varepsilon/2$. In order to conclude, it suffices to observe that the distances from $\mathfrak{f}_n(0)$ resp. $\mathfrak{f}^{(p)}_\infty(0)$ to the root vertex in $Q_n^{\sigma_n}$ resp. $\mathbf{Q}^\infty_\infty(p)$ are stochastically bounded; see again Remark 4.4.2. Clearly, this implies that with probability tending to 1 as n increases, we have the inclusions $B_{\delta\xi_n}(Q_n^{\sigma_n})\subset B^{(0)}_{2\delta\xi_n}(Q_n^{\sigma_n})$ and $B_{\delta\xi_n}(\mathbf{Q}^\infty_\infty(p))\subset B^{(0)}_{2\delta\xi_n}(\mathbf{Q}^\infty_\infty(p))$. □

As mentioned at the beginning, the case $p=1/2$ has been treated in [BMR16, Proof of Proposition 3.11]: It is proved there that for δ small, the balls of radius $\delta\min\{\sqrt{\sigma_n},\sqrt{n/\sigma_n}\}$ in $Q_n^{\sigma_n}$ and in the standard $\mathsf{UIHPQ}=\mathsf{UIHPQ}_{1/2}$ can be coupled with high probability, implying of course again local convergence of $Q_n^{\sigma_n}$ towards the UIHPQ.

Finally, it remains to consider the case $p=0$ corresponding to $\sigma_n\gg n$. This case is easy. We have the following coupling lemma.

Lemma 4.5.5. *Let $(\sigma_n,n\in\mathbb{N})$ be a sequence of positive integers satisfying $\sigma_n\gg n$. Put $\xi_n=\sigma_n/n$. Then, given any $\varepsilon>0$, there exist $\delta>0$ and $n_0\in\mathbb{N}$ such that for every $n\geq n_0$, we can construct on the same probability space copies of $Q_n^{\sigma_n}$ and the UIHPQ_0 such that with probability at least $1-\varepsilon$, the metric balls $B_{\delta\xi_n}(Q_n^{\sigma_n})$ and $B_{\delta\xi_n}(\mathsf{UIHPQ}_0)$ of radius $\delta\xi_n$ around the roots in the corresponding spaces are isometric.*

Proof. Let $((\mathfrak{f}_n,\mathfrak{l}_n),\mathsf{b}_n)\in\mathfrak{F}^n_{\sigma_n}\times\mathfrak{B}_{\sigma_n}$ be uniformly distributed. By exchangeability of the trees, it follows that if $k_n=o(\sigma_n/n)$, then the first and last k_n trees of $\mathfrak{f}_n$ are all singletons with a probability tending to one. Applying Lemma 4.5.3, we can ensure that the event

$$\{\mathsf{b}_n(i)=\mathsf{b}_\infty(i),\ \mathsf{b}_n(2\sigma_n-i)=\mathsf{b}_\infty(-i),\ 1\leq i\leq k_n\}$$

has a probability as large as we wish, provided n is large enough. Given $\varepsilon > 0$, the same arguments as in the proof of Proposition 4.5.4 yield an equality of balls $B_{\delta\xi_n}(Q_n^{\sigma_n})$ and $B_{\delta\xi_n}(\mathsf{UIHPQ}_0)$ for δ small and n large enough, on an event of probability at least $1-\varepsilon$. □

Let us now show that the space UIHPQ_0 defined in terms of the Bouttier–Di Francesco–Guitter mapping in Section 4.4.3 is nothing else than Kesten's tree associated to the critical geometric offspring law $\mu_{1/2}$.

Proof of Proposition 4.2.2. Let $\mathsf{b}_\infty = (\mathsf{b}_\infty(i), i \in \mathbb{Z})$ be a uniform infinite bridge, and let $(\mathfrak{f}_\infty^{(0)}, \mathfrak{l}_\infty^{(0)})$ be the infinite forest where all trees are just singletons (with label 0); see Section 4.4.3. The UIHPQ_0 is distributed as the infinite map $\mathbf{Q}_\infty^\infty(0) = \Phi((\mathfrak{f}_\infty^{(0)}, \mathfrak{l}_\infty^{(0)}), \mathsf{b}_\infty)$. Since every vertex in $\mathfrak{f}_\infty^{(0)}$ defines a single corner, properties of the Bouttier–Di Francesco–Guitter mapping (Section 4.4.2) imply that $\mathbf{Q}_\infty^\infty(0)$ is a tree almost surely. Moreover, the set of vertices of $\mathbf{Q}_\infty^\infty(0)$ is identified with the set of down-steps $\mathsf{DS}(\mathsf{b}_\infty)$ of the bridge. Following Section 3.2.3 of Chapter 3, conditionally on b_∞, we introduce a function $\varphi : \mathbb{Z} \to \mathsf{DS}(\mathsf{b}_\infty)$ that associates to $i \in \mathbb{Z}$ the next down-step $\geq i$ with label $\mathsf{b}_\infty(i)$ (and i is mapped to itself if $i \in \mathsf{DS}(\mathsf{b}_\infty)$). According to our rooting convention, the root edge of $\mathbf{Q}_\infty^\infty(0)$ connects $\varphi(0)$ to $\varphi(1)$. Note that φ is not injective almost surely.

We recall that Kesten's tree can be represented by a half-line of vertices $s_0, s_1, \ldots$, together with a collection of independent Galton-Watson trees with offspring law $\mu_{1/2}$ grafted to the left and right side of each vertex s_i, $i \in \mathbb{Z}_+$. We will now argue that the UIHPQ_0 $\mathbf{Q}_\infty^\infty(0)$ has the same structure. In this regard, let us introduce the stopping times

$$S_i = \inf\{k \in \mathbb{Z}_+ : \mathsf{b}_\infty(k) = -i\}, \quad i \in \mathbb{Z}_+,$$

and denote by s_i the vertex of $\mathbf{Q}_\infty^\infty(0)$ given by $\varphi(S_i)$. Together with their connecting edges, the collection $(s_i, i \in \mathbb{Z}_+)$ forms a spine (i.e., an infinite self-avoiding path) in $\mathbf{Q}_\infty^\infty(0)$.

The subtree rooted at s_i on the left side of the spine is encoded by the excursion $\{\mathsf{b}_\infty(k) : S_i \leq k \leq S_{i+1}\}$, in a way we describe next; see Figure 4.9 for an illustration. First note that by the Markov property, these subtrees for $i \in \mathbb{Z}$ are i.i.d.. In order to determine their law, let us consider the subtree encoded by the excursion $\{\mathsf{b}_\infty(k) : 0 \leq k \leq S_1\}$ of b_∞. This subtree is rooted at $s_0 = \emptyset$, and the number of offspring of s_0 is the number of down-steps with label 1 between 0 and S_1. Otherwise said, this is the number $\#\{0 < k < S_1 : \mathsf{b}_\infty(k) = 0\}$ of excursions of b_∞ above 0 between 0 and S_1. By the Markov property, this quantity follows the geometric distribution $\mu_{1/2}$ of parameter $1/2$. One can now repeat the argument for each child of s_0, by considering the corresponding excursion above 0 encoding its progeny tree, inside the mother excursion. We obtain that the subtree stemming from s_0 on the left of the spine has indeed the law of a Galton-Watson tree with offspring distribution $\mu_{1/2}$.

The subtrees attached to the vertices s_i, $i \in \mathbb{Z}_+$, on the right of the spine can be treated by a symmetry argument. Namely, letting

$$S_i' = \inf\{k \in \mathbb{Z}_+ : \mathsf{b}_\infty(-k) = -i\}, \quad i \in \mathbb{Z}_+,$$

we observe that the subtree rooted at s_i to the right of the spine is coded by the (reversed) excursion $\{\mathsf{b}_\infty(k) : -S'_{i+1} \leq k \leq -S'_i\}$. With the same argument as above, we see that it has the law of an (independent) $\mu_{1/2}$-Galton Watson tree. This concludes the proof. □

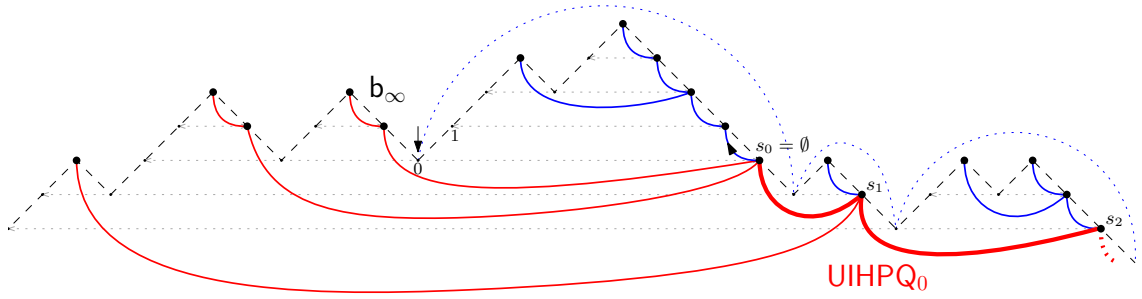

Figure 4.9: The construction of the UIHPQ$_0$ from a uniform infinite bridge b_∞. The spine is shown in bold red arcs. The trees on the left of the spine are drawn in blue and enclosed by dotted blue half-circles, which indicate the corresponding excursions of b_∞ encoding these trees. The trees on the right of the spine are drawn in red, as the spine itself.

4.5.2 The UIHPQ$_p$ as a local limit of Boltzmann quadrangulations

This section is devoted to the proof of Proposition 4.2.3. It is convenient to first prove the analogous result for pointed maps. For that purpose, we first extend the definitions of Boltzmann measures from Section 4.1.2 to pointed maps and then use a "de-pointing" argument. We use the notation $\mathcal{Q}_f^\bullet$ for the set of finite rooted pointed quadrangulations, and we write $\mathcal{Q}_f^{(\bullet,\sigma)}$ for the set of finite pointed rooted quadrangulations with 2σ boundary edges. The corresponding partition functions read

$$F^\bullet(g,z) = \sum_{\mathbf{q}\in\mathcal{Q}_f^\bullet} g^{\#\mathrm{F}(\mathbf{q})} z^{\#\partial\mathbf{q}/2}, \quad F_\sigma^\bullet(g) = \sum_{\mathbf{q}\in\mathcal{Q}_f^{(\bullet,\sigma)}} g^{\#\mathrm{F}(\mathbf{q})},$$

and the associated pointed Boltzmann distributions are defined by

$$\mathbb{P}_{g,z}^\bullet(\mathbf{q}) = \frac{g^{\#\mathrm{F}(\mathbf{q})} z^{\#\partial\mathbf{q}/2}}{F^\bullet(g,z)}, \quad \mathbf{q}\in\mathcal{Q}_f^\bullet, \quad \mathbb{P}_g^{(\bullet,\sigma)}(\mathbf{q}) = \frac{g^{\#\mathrm{F}(\mathbf{q})}}{F_\sigma^\bullet(g)}, \quad \mathbf{q}\in\mathcal{Q}_f^{(\bullet,\sigma)}.$$

We will need the following enumeration result for pointed rooted maps. By [Bud15, (23)] and [BG09, Section 3.3], we have for every $0 \leq p \leq 1/2$

$$F_\sigma^\bullet(g_p) = \binom{2\sigma}{\sigma}\left(\frac{1}{1-p}\right)^\sigma, \quad \sigma\in\mathbb{Z}_+. \tag{4.7}$$

Note that the result (3.29) in [BG09] cannot be used directly, due to a difference in the rooting convention (there, the root vertex has to be chosen among the vertices of the boundary that are closest to the marked point).

Recall that $g_p = p(1-p)/3$ for $0 \le p \le 1/2$. The first step towards the proof of Proposition 4.2.3 is the following convergence result for pointed Boltzmann quadrangulations.

Proposition 4.5.6. *Let $0 \le p \le 1/2$. For every $\sigma \in \mathbb{Z}_+$, let $Q_\sigma^\bullet(p)$ be a random rooted pointed quadrangulation distributed according to $\mathbb{P}_{g_p}^{(\bullet,\sigma)}$. Then, we have the local convergence for the metric d_{loc} as $\sigma \to \infty$*

$$Q_\sigma^\bullet(p) \xrightarrow{(d)} \mathsf{UIHPQ}_p,$$

Proof. Let $\mathfrak{q} \in \mathcal{Q}_f^{(\sigma)}$, and $((\mathfrak{f},\mathfrak{l}),\mathfrak{b}) \in \cup_{n\ge 0}\mathfrak{F}_\sigma^n \times \mathfrak{B}_\sigma$ such that $\mathfrak{q} = \Phi((\mathfrak{f},\mathfrak{l}),\mathfrak{b})$. Moreover, let $(\mathfrak{f}_\sigma^{(p)}, \mathfrak{l}_\sigma^{(p)})$ be a uniformly labeled p-forest with σ trees, i.e., a collection of σ independent uniformly labeled p-Galton-Watson trees, and let $\mathfrak{b}_\sigma$ be uniformly distributed in $\mathfrak{B}_\sigma$ and independent of $(\mathfrak{f}_\sigma^{(p)}, \mathfrak{l}_\sigma^{(p)})$. We have

$$\begin{aligned}\mathbb{P}\left(\Phi\big((\mathfrak{f}_\sigma^{(p)}, \mathfrak{l}_\sigma^{(p)}), \mathfrak{b}_\sigma\big) = \mathfrak{q}\right) &= \mathbb{P}\left(\big((\mathfrak{f}_\sigma^{(p)}, \mathfrak{l}_\sigma^{(p)}), \mathfrak{b}_\sigma\big) = ((\mathfrak{f},\mathfrak{l}),\mathfrak{b})\right)\\ &= \left(\frac{p(1-p)}{3}\right)^{|\mathfrak{f}|} \frac{(1-p)^\sigma}{\binom{2\sigma}{\sigma}} = \frac{g_p^{\#\mathrm{F}(\mathfrak{q})}}{F_\sigma^\bullet(g_p)},\end{aligned}$$

Here, for the first equality in the second line, we have used (4.2), the fact that the label differences are i.i.d. uniform in $\{-1,0,1\}$, and $|\mathfrak{B}_\sigma| = \binom{2\sigma}{\sigma}$. The last equality follows from the enumeration result (4.7) and the fact that the number of edges of $\mathfrak{f}$ equals the number of faces of $\mathfrak{q}$. Thus, $Q_\sigma^\bullet(p)$ is distributed as $\Phi((\mathfrak{f}_\sigma^{(p)}, \mathfrak{l}_\sigma^{(p)}), \mathfrak{b}_\sigma)$.

Now observe that $\mathfrak{f}_\sigma^{(p)}$ is already a collection of σ independent p-Galton-Watson trees, and Lemma 4.5.3 allows us to couple the first and last $o(\sigma)$ steps of $\mathfrak{b}_\sigma$ with those of a uniform infinite bridge $\mathfrak{b}_\infty$. With exactly the same reasoning as in Proposition 4.5.4, we therefore obtain with high probability an isometry of balls $B_{\delta\sqrt{\sigma}}(Q_\sigma^\bullet(p))$ and $B_{\delta\sqrt{\sigma}}(\mathsf{UIHPQ}_p)$ for all σ sufficiently large, provided δ is small enough. The stated local convergence follows. □

Proposition 4.2.3 is a consequence of the foregoing result and the following depointing argument inspired by [Abr16, Proposition 14]. According to Remark 4.2.4, it suffices to consider the case $p \in [0, 1/2)$.

In the following, by a small abuse of notation, we interpret $\mathbb{P}_{g_p}^{(\bullet,\sigma)}$ as a probability measure on $\mathcal{Q}_f$ by simply forgetting the marked point.

Lemma 4.5.7. *Let $0 \le p < 1/2$. Then,*

$$\lim_{\sigma\to\infty} \left\| \mathbb{P}_{g_p}^{(\sigma)} - \mathbb{P}_{g_p}^{(\bullet,\sigma)} \right\|_{\mathrm{TV}} = 0.$$

Proof. Let $\#V$ be the mapping $\mathfrak{q} \mapsto \#V(\mathfrak{q})$, which assigns to a finite quadrangulation $\mathfrak{q}$ its number of vertices. We have the absolute continuity relation [BM15, (5)]

$$\mathrm{d}\mathbb{P}_{g_p}^{(\sigma)}(\mathfrak{q}) = \frac{K_\sigma}{\#V(\mathfrak{q})} \mathrm{d}\mathbb{P}_{g_p}^{(\bullet,\sigma)}(\mathfrak{q}),$$

where $K_\sigma = (\mathbb{E}_{g_p}^{(\bullet,\sigma)}[1/\#V)])^{-1}$. Then,

$$\left\| \mathbb{P}_{g_p}^{(\sigma)} - \mathbb{P}_{g_p}^{(\bullet,\sigma)} \right\|_{\mathrm{TV}} = \frac{1}{2} \sup_{F:\mathcal{Q}_f^{(\sigma)}\to[-1,1]} \left| \mathbb{E}_{g_p}^{(\sigma)}[F] - \mathbb{E}_{g_p}^{(\bullet,\sigma)}[F] \right| \le \mathbb{E}_{g_p}^{(\bullet,\sigma)}\left[\left| 1 - \frac{K_\sigma}{\#V} \right| \right]. \tag{4.8}$$

Let $(\mathbf{t}_0^{(p)}, \dots, \mathbf{t}_{\sigma-1}^{(p)})$ be a collection of independent p-Galton-Watson trees. The proof of Proposition 4.5.6 shows that under $\mathbb{P}_{g_p}^{(\bullet,\sigma)}$, $\#V$ has the same law as

$$1 + \sum_{i=0}^{\sigma-1} \#V(\mathbf{t}_i^{(p)}).$$

Note that the summand $+1$ accounts for the pointed vertex, which is added to the tree vertices in the Bouttier–Di Francesco–Guitter mapping. Using the fact that $\#V(\mathbf{t}_0^{(p)})$ has the same law as $(T_{-1}^{(p)}+1)/2$, where $T_{-1}^{(p)}$ is the first hitting time of -1 of a random walk with step distribution $p\delta_1 + (1-p)\delta_{-1}$, an application of the optional stopping theorem gives

$$\mathbb{E}_{g_p}^{(\bullet,\sigma)}[\#V] = 1 + \sigma\mathbb{E}\left[\#V(\mathbf{t}_0^{(p)})\right] = 1 + \sigma\left(\frac{1-p}{1-2p}\right).$$

Moreover, using $p < 1/2$ and the description in terms of $T_{-1}^{(p)}$, it is readily checked that the random variable $\#V(\mathbf{t}_0^{(p)})$ has small exponential moments. Cramer's theorem thus ensures that for every $\delta > 0$, there exists a constant $C_\delta > 0$ such that

$$\mathbb{P}_{g_p}^{(\bullet,\sigma)}\left(\left|\#V - \mathbb{E}_{g_p}^{(\bullet,\sigma)}[\#V]\right| > \delta\sigma\right) \leq \exp(-C_\delta\sigma).$$

We now proceed similarly to [Abr16, Lemma 16]. Let X_σ be distributed as the variable $\#V/\mathbb{E}_{g_p}^{(\bullet,\sigma)}[\#V]$ under $\mathbb{P}_{g_p}^{(\bullet,\sigma)}$. Note that $X_\sigma^{-1} \leq \mathbb{E}_{g_p}^{(\bullet,\sigma)}[\#V]$ $\mathbb{P}_{g_p}^{(\bullet,\sigma)}$-a.s. since $\#V \geq 1$. Moreover, it is seen that $\{|X_\sigma^{-1} - 1| > \delta\} \subset \{|X_\sigma| < 1/2\} \cup \{|X_\sigma - 1| > \delta/2\}$. From these observations, we obtain

$$\begin{aligned}\mathbb{E}\left[\left|X_\sigma^{-1} - 1\right|\right] &\leq \delta + \mathbb{E}\left[\left|X_\sigma^{-1} - 1\right| \mathbf{1}_{\{|X_\sigma^{-1}-1|>\delta\}}\right] \\ &\leq \delta + \left(\mathbb{E}_{g_p}^{(\bullet,\sigma)}[\#V] + 1\right)\mathbb{P}\left(|X_\sigma - 1| > \frac{\delta}{2} \wedge \frac{1}{2}\right).\end{aligned}$$

The preceding two displays show that the expected number of vertices grows linearly in σ, and the probability on the right decays exponentially fast in σ. Since $\delta > 0$ was arbitrary, we deduce that $X_\sigma^{-1} \longrightarrow 1$ as $\sigma \to \infty$ in $\mathbb{L}^1$. Finally,

$$\mathbb{E}_{g_p}^{(\bullet,\sigma)}\left[\left|1 - \frac{K_\sigma}{\#V}\right|\right] = \mathbb{E}\left[\left|1 - \frac{X_\sigma^{-1}}{\mathbb{E}[X_\sigma^{-1}]}\right|\right] \leq \frac{1}{\mathbb{E}[X_\sigma^{-1}]}\left(\left|\mathbb{E}[X_\sigma^{-1}] - 1\right| + \mathbb{E}[|X_\sigma^{-1} - 1|]\right) \longrightarrow 0$$

as $\sigma \to \infty$, which concludes the proof by (4.8). □

4.5.3 The BHP_θ as a local scaling limit of the UIHPQ_p's

In this section, we prove Theorem 4.2.6. For the reminder, we fix a sequence $(a_n, n \in \mathbb{N})$ of positive reals tending to infinity and let $r > 0$ be given. Similarly to [BMR16, Proof of Theorem 3.4], the main step is to establish an absolute continuity relation of balls around the roots of radius ra_n between the UIHPQ_p for $p \in (0, 1/2]$ and the $\mathsf{UIHPQ} = \mathsf{UIHPQ}_{1/2}$. To this aim, we compute the Radon-Nikodym derivative of the encoding contour function of the UIHPQ_p with respect to that of the UIHPQ on an interval of the form $[-sa_n^2, sa_n^2]$ for $s > 0$. From Theorem 3.8 of [BMR16]

we know that $a_n^{-1} \cdot \mathsf{UIHPQ} \to \mathsf{BHP}_0$ in distribution in the local Gromov-Hausdorff topology, jointly with a uniform convergence on compacts of (rescaled) contour and label functions. An application of Girsanov's theorem shows that the limiting Radon-Nikodym derivative turns the contour function of BHP_0 into the contour function of BHP_θ, which allows us to conclude.

In order to make these steps rigorous, we begin with some notation specific to this section. Let $f \in \mathcal{C}(\mathbb{R}, \mathbb{R})$ and $x \in \mathbb{R}$. We define the last (first) visit to x to the left (right) of 0,

$$U_x(f) = \inf\{t \leq 0 : f(t) = x\} \in [-\infty, 0], \quad T_x(f) = \inf\{t \geq 0 : f(t) = x\} \in [0, \infty].$$

We agree that $U_x(f) = -\infty$ if the set over which the infimum is taken is empty, and, similarly, $T_x(f) = \infty$ if the second set is empty. We will also apply U_x to functions in $\mathcal{C}((-\infty, 0], \mathbb{R})$, and T_x to functions in $\mathcal{C}([0, \infty), \mathbb{R})$.

If $f \in \mathcal{C}(\mathbb{R}, \mathbb{R})$ is the contour function of an infinite p-forest for some $p \in (0, 1/2]$ (or part of it defined on some interval), and if $x \in \mathbb{N}$, we use the notation

$$\mathbf{v}(f, x) = \frac{1}{2}\left(T_{-x}(f) - U_x(f) - 2x\right)$$

for the total number of edges of the $2x$ trees that are encoded by f along the interval $[U_x(f), T_{-x}(f)]$. We set $\mathbf{v}(f, x) = \infty$ if $U_x(f)$ or $T_{-x}(f)$ is unbounded.

Given $s > 0$, we put for $n \in \mathbb{N}$

$$s_n = \lfloor (3/2) s a_n^2 \rfloor.$$

Now let $p \in (0, 1/2]$. Throughout this section, as usual, we assume that $((\mathfrak{f}_\infty^{(p)}, \mathfrak{l}_\infty^{(p)}), \mathsf{b}_\infty)$ and $((\mathfrak{f}_\infty, \mathfrak{l}_\infty), \mathsf{b}_\infty)$ encode the UIHPQ_p $\mathbf{Q}_\infty^\infty(p)$ and the standard UIHPQ $\mathbf{Q}_\infty^\infty$, respectively (see Definition 4.4.1). We stress that since the skewness parameter p does not affect the law of the infinite bridge b_∞, we can and will use the same bridge in the construction of both $\mathbf{Q}_\infty^\infty(p)$ and $\mathbf{Q}_\infty^\infty$. We denote by $(C_\infty^{(p)}, \mathfrak{L}_\infty^{(p)})$ and $(C_\infty, \mathfrak{L}_\infty)$ the associated contour and label functions, viewed as elements in $\mathcal{C}(\mathbb{R}, \mathbb{R})$.

For understanding how the balls of radius ra_n for some $r > 0$ around the roots in $\mathbf{Q}_\infty^\infty(p)$ and $\mathbf{Q}_\infty^\infty$ are related to each other, we need to control the contour functions $C_\infty^{(p)}$ and C_∞ on $[U_{s_n}, T_{-s_n}]$ for a suitable choice of $s = s(r)$. In this regard, we first formulate an absolute continuity relation between the probability laws $\mathbb{P}_{s,n}^{(p)}$ and $\mathbb{P}_{s,n}$ on $\mathcal{C}(\mathbb{R}, \mathbb{R})$ defined as follows:

$$\begin{aligned}
\mathbb{P}_{n,s}^{(p)} &= \mathrm{Law}\left(\left(C_\infty^{(p)}(t \vee U_{s_n}(C_\infty^{(p)}) \wedge T_{-s_n}(C_\infty^{(p)})), t \in \mathbb{R}\right)\right), \\
\mathbb{P}_{n,s} &= \mathrm{Law}\left((C_\infty(t \vee U_{s_n}(C_\infty) \wedge T_{-s_n}(C_\infty)), t \in \mathbb{R})\right).
\end{aligned}$$

Lemma 4.5.8. *Let $p \in (0, 1)$ and $s > 0$. The laws $\mathbb{P}_{n,s}^{(p)}$ and $\mathbb{P}_{n,s}$ are absolutely continuous with respect to each other: For any $f \in \mathrm{supp}(\mathbb{P}_{n,s}^{(p)})(= \mathrm{supp}(\mathbb{P}_{n,s}))$, with s_n as above,*

$$\mathbb{P}_{n,s}^{(p)}(f) = (4p(1-p))^{\mathbf{v}(f, s_n)} \left(2(1-p)\right)^{2s_n} \mathbb{P}_{n,s}(f).$$

Proof. By definition of $C_\infty^{(p)}$ and C_∞, each element $f \in \mathcal{C}(\mathbb{R}, \mathbb{R})$ in the support of $\mathbb{P}_{n,s}^{(p)}$ lies also in the support of $\mathbb{P}_{n,s}$ and vice versa (note that $p \notin \{0, 1\}$).

More specifically, for such an f supported by these laws, $\mathbb{P}^{(p)}_{n,s}(f)$ resp. $\mathbb{P}_{n,s}(f)$ is the probability of a particular realization of $2s_n$ independent p-Galton-Watson trees resp. $(1/2)$-Galton-Watson trees with $\mathbf{v}(f, s_n)$ tree edges in total. Therefore, by (4.2),

$$\mathbb{P}^{(p)}_{n,s}(f) = p^{\mathbf{v}(f,s_n)}(1-p)^{\mathbf{v}(f,s_n)}(1-p)^{2s_n}, \quad \text{and} \quad \mathbb{P}_{n,s}(f) = 2^{-2(\mathbf{v}(f,s_n)+s_n)}.$$

This proves the lemma. □

We turn to the proof of Theorem 4.2.6. To that aim, we will work with rescaled and stopped versions of $(C^{(p)}_\infty, \mathfrak{L}^{(p)}_\infty)$ and $(C_\infty, \mathfrak{L}_\infty)$, which encode the information of the first $s_n = \lfloor (3/2)sa_n^2 \rfloor$ trees to the right of zero, and of the first s_n trees to the left zero. Specifically, we let

$$\begin{aligned}
C^{\infty,p}_{n,s} &= \left(C^{\infty,p}_{n,s}(t), t \in \mathbb{R}\right) = \left(\frac{1}{(3/2)a_n^2} C^{(p)}_\infty\left((9/4)a_n^4 t \vee U_{s_n}(C^{(p)}_\infty) \wedge T_{-s_n}(C^{(p)}_\infty)\right), t \in \mathbb{R}\right),\\
\mathfrak{L}^{\infty,p}_{n,s} &= \left(\mathfrak{L}^{\infty,p}_{n,s}(t), t \in \mathbb{R}\right) = \left(\frac{1}{a_n} \mathfrak{L}^{(p)}_\infty\left((9/4)a_n^4 t \vee U_{s_n}(C^{(p)}_\infty) \wedge T_{-s_n}(C^{(p)}_\infty)\right), t \in \mathbb{R}\right),\\
C^{\infty}_{n,s} &= \left(C^{\infty}_{n,s}(t), t \in \mathbb{R}\right) = \left(\frac{1}{(3/2)a_n^2} C_\infty\left((9/4)a_n^4 t \vee U_{s_n}(C_\infty) \wedge T_{-s_n}(C_\infty)\right), t \in \mathbb{R}\right),\\
\mathfrak{L}^{\infty}_{n,s} &= \left(\mathfrak{L}^{\infty}_{n,s}(t), t \in \mathbb{R}\right) = \left(\frac{1}{a_n} \mathfrak{L}_\infty\left((9/4)a_n^4 t \vee U_{s_n}(C_\infty) \wedge T_{-s_n}(C_\infty)\right), t \in \mathbb{R}\right).
\end{aligned}$$

Following our notation from Section 4.3.1, we denote by $X^\theta = (X^\theta(t), t \in \mathbb{R})$ and $W^\theta = (W^\theta(t), t \in \mathbb{R})$ the contour and label functions of the limit space BHP_θ. We also put

$$\begin{aligned}
X^{\theta,s} &= \left(X^{\theta,s}(t), t \in \mathbb{R}\right) = \left(X^\theta\left(t \vee U_s(X^\theta) \wedge T_{-s}(X^\theta)\right), t \in \mathbb{R}\right),\\
W^{\theta,s} &= \left(W^{\theta,s}(t), t \in \mathbb{R}\right) = \left(W^\theta\left(t \vee U_s(X^\theta) \wedge T_{-s}(X^\theta)\right), t \in \mathbb{R}\right).
\end{aligned}$$

Accordingly, we write X^0, W^0 and $X^{0,s}, W^{0,s}$ for the corresponding functions associated to BHP_0. We will make use of the following joint convergence.

Lemma 4.5.9. *Let $r, s > 0$. Then, in the notation from above, we have the joint convergence in law in $\mathcal{C}(\mathbb{R}, \mathbb{R}) \times \mathcal{C}(\mathbb{R}, \mathbb{R}) \times \mathbb{K}$,*

$$\left(C^\infty_{n,s}, \mathfrak{L}^\infty_{n,s}, B^{(0)}_r\left(a_n^{-1} \cdot \mathbf{Q}^\infty_\infty\right)\right) \xrightarrow{(d)} \left(X^{0,s}, W^{0,s}, B_r(\mathsf{BHP}_0)\right).$$

Moreover, for $n \to \infty$

$$\frac{\mathbf{v}(C_\infty, s_n)}{(9/4)a_n^4} \xrightarrow{(d)} \frac{1}{2}\left(T_{-s} - U_s\right)(X^0).$$

Proof. Both statements are proved in [BMR16]; to give a quick reminder, first note by standard random walk estimates that for each $\delta > 0$, there exists a constant $c_\delta > 0$ such that $\mathbb{P}(v(C_\infty, s_n) > c_\delta a_n^4) \leq \delta$; see [BMR16, Proof of Lemma 6.18] for details. Together with the joint convergence in law in $\mathcal{C}(\mathbb{R}, \mathbb{R})^2 \times \mathbb{K}$ obtained in [BMR16, (6.30) of Remark 6.17], which reads

$$\left(\frac{C_\infty((9/4)a_n^4 \cdot)}{(3/2)a_n^2}, \frac{\mathfrak{L}_\infty((9/4)a_n^4 \cdot)}{a_n}, B^{(0)}_r\left(a_n^{-1} \cdot \mathbf{Q}^\infty_\infty\right)\right) \xrightarrow{(d)} \left(X^0, W^0, B_r(\mathsf{BHP}_0)\right),$$

the first claim of the statement follows, and the second is then a consequence of this. □

We turn now to the Proof of Theorem 4.2.6.

Proof of Theorem 4.2.6. We fix a sequence $(p_n, n \in \mathbb{N}) \subset (0, 1/2]$ of the form

$$p_n = \frac{1}{2}\left(1 - \frac{2\theta}{3a_n^2}\right) + o\left(a_n^{-2}\right).$$

By Remark 4.4.2 and the observations in Section 4.1.2, the claim follows if we show that for all $r > 0$, as $n \to \infty$,

$$B_r^{(0)}\left(a_n^{-1} \cdot \mathbf{Q}_\infty^\infty(p_n)\right) \xrightarrow{(d)} B_r(\mathsf{BHP}_\theta)$$

in distribution in $\mathbb{K}$. At this point, recall that $B_r^{(0)}(a_n^{-1} \cdot \mathbf{Q}_\infty^\infty(p_n)) = a_n^{-1} \cdot B_{ra_n}^{(0)}(\mathbf{Q}_\infty^\infty(p_n))$ is the (rescaled) ball of radius ra_n around the vertex $\mathfrak{f}_\infty^{(p_n)}(0)$ in $\mathbf{Q}_\infty^\infty(p_n)$. We consider the event

$$\mathcal{E}^1(n,s) = \left\{ \min_{[0,\, s_n]} \mathsf{b}_\infty < -3ra_n,\ \min_{[-s_n,\, 0]} \mathsf{b}_\infty < -3ra_n \right\}.$$

We define a similar event in terms of the two-sided Brownian motion $\gamma = (\gamma(t), t \in \mathbb{R})$ scaled by the factor $\sqrt{3}$, which forms part of the construction of the space BHP_θ given in Section 4.3.1,

$$\mathcal{E}^2(s) = \left\{ \min_{[0,s]} \gamma < -3r,\ \min_{[-s,0]} \gamma < -3r \right\}.$$

Using the cactus bound, it was argued in [BMR16, Proof of Theorem 3.4] that on the event $\mathcal{E}^1(n,s)$, for any $p \in (0,1/2]$, the ball $B_{ra_n}^{(0)}(\mathbf{Q}_\infty^\infty(p))$ viewed as a submap of $\mathbf{Q}_\infty^\infty(p)$ is a measurable function of $(C_{n,s}^{\infty,p}, \mathfrak{L}_{n,s}^{\infty,p})$. (In [BMR16], only the case $p = 1/2$ was considered, but the argument remains exactly the same for all p, since the encoding bridge b_∞ does not depend on the choice of p.) Similarly, on $\mathcal{E}^2(s)$, the ball $B_r(\mathsf{BHP}_\theta)$ for any $\theta \geq 0$ is a measurable function of $(X^{\theta,s}, W^{\theta,s})$.

Now let $\varepsilon > 0$ be given. By the (functional) central limit theorem, we find that for $s > 0$ and $n_0 \in \mathbb{N}$ sufficiently large, it holds that for all $n \geq n_0$, $\mathbb{P}(\mathcal{E}^1(n,s)) \geq 1 - \varepsilon$. By choosing s possibly larger, we can moreover ensure that $\mathbb{P}(\mathcal{E}^2(s)) \geq 1 - \varepsilon$. We fix such $s > 0$ and $n_0 \in \mathbb{N}$ such that for all $n \geq n_0$, both events $\mathcal{E}^1(n,s)$ and $\mathcal{E}^2(s)$ have probability at least $1 - \varepsilon$.

Next, consider the laws $\mathbb{P}_{n,s}^{(p_n)}$ and $\mathbb{P}_{n,s}$ defined just above Lemma 4.5.8, and put for $f \in \mathcal{C}(\mathbb{R}, \mathbb{R})$

$$\lambda_{n,s}(f) = (4p_n(1-p_n))^{\mathbf{v}(f,s_n)}\,(2(1-p_n))^{2s_n}. \tag{4.9}$$

Then, with $F : \mathcal{C}(\mathbb{R},\mathbb{R})^2 \times \mathbb{K} \to \mathbb{R}$ measurable and bounded, Lemma 4.5.8 shows

$$\begin{aligned}\mathbb{E}\left[F\left(C_{n,s}^{\infty,p_n}, \mathfrak{L}_{n,s}^{\infty,p_n}, B_r^{(0)}\left(a_n^{-1} \cdot \mathbf{Q}_\infty^\infty(p_n)\right)\right) \mathbf{1}_{\mathcal{E}^1(n,s)}\right] \\ = \mathbb{E}\left[\lambda_{n,s}(C_\infty) F\left(C_{n,s}^\infty, \mathfrak{L}_{n,s}^\infty, B_r^{(0)}\left(a_n^{-1} \cdot \mathbf{Q}_\infty^\infty\right)\right) \mathbf{1}_{\mathcal{E}^1(n,s)}\right].\end{aligned} \tag{4.10}$$

Note that on the left side, we consider the closed ball of radius ra_n around the vertex $\mathfrak{f}_\infty(0)$ in the UIHPQ_{p_n} $\mathbf{Q}_\infty^\infty(p_n)$, whereas on the right side, we look at the corresponding ball in the standard UIHPQ $\mathbf{Q}_\infty^\infty$ with contour and label functions C_∞ and $\mathfrak{L}_\infty$. Plugging in the value of p_n in (4.9), we get

$$\lambda_{n,s}(f) = \left(1 + \frac{2\theta}{3a_n^2} + o(a_n^{-2})\right)^{2s_n} \left(1 - \frac{4\theta^2}{9a_n^4} + o(a_n^{-4})\right)^{\mathbf{v}(f,s_n)}. \tag{4.11}$$

Applying both statements of Lemma 4.5.9, and using (4.11), it follows that for large $n \geq n_1(\varepsilon)$

$$\Big|\mathbb{E}\left[\lambda_{n,s}(C_\infty)F\left(C^\infty_{n,s}, \mathfrak{L}^\infty_{n,s}, B^{(0)}_r\left(a_n^{-1}\cdot \mathbf{Q}^\infty_\infty\right)\right)\right] - \mathbb{E}\left[\exp\left(2s\theta - (T_{-s}-U_s)(X^0)\theta^2/2\right)F\left(X^{0,s}, W^{0,s}, B_r\left(\mathsf{BHP}_0\right)\right)\right]\Big| \leq \varepsilon. \quad (4.12)$$

The rest of the proof is now similar to [BMR16, Proof of Theorem 3.4]. Applying Pitman's transform and Girsanov's theorem, we have for continuous and bounded $G : \mathcal{C}(\mathbb{R},\mathbb{R})^2 \to \mathbb{R}$

$$\mathbb{E}\left[\exp\left(2s\theta - (T_{-s}-U_s)(X^0)\theta^2/2\right)G\left(X^{0,s}, W^{0,s}\right)\right] = \mathbb{E}\left[G\left(X^{\theta,s}, W^{\theta,s}\right)\right].$$

On $\mathcal{E}^2(s)$, $B_r(\mathsf{BHP}_0)$ is a measurable function of $(X^{0,s}, W^{0,s})$, and $B_r(\mathsf{BHP}_\theta)$ is given by the *same* measurable function of $(X^{\theta,s}, W^{\theta,s})$. Consequently,

$$\mathbb{E}\left[\exp\left(2s\theta - (T_{-s}-U_s)(X^0)\theta^2/2\right)F\left(X^{0,s}, W^{0,s}, B_r\left(\mathsf{BHP}_0\right)\right)\mathbf{1}_{\mathcal{E}^2(s)}\right] = \mathbb{E}\left[F\left(X^{\theta,s}, W^{\theta,s}, B_r\left(\mathsf{BHP}_\theta\right)\right)\mathbf{1}_{\mathcal{E}^2(s)}\right]. \quad (4.13)$$

Recall that the events $\mathcal{E}^1(n,s)$ and $\mathcal{E}^2(s)$ have probability at least $1-\varepsilon$. Using this fact together with (4.10), (4.12), (4.13) and the triangle inequality, we find a constant $C = C(F,s,\theta)$ such that for sufficiently large n,

$$\left|\mathbb{E}\left[F\left(C^{\infty,p_n}_{n,s}, \mathfrak{L}^{\infty,p_n}_{n,s}, B^{(0)}_r\left(a_n^{-1}\cdot \mathbf{Q}^\infty_\infty(p_n)\right)\right)\right] - \mathbb{E}\left[F\left(X^{\theta,s}, W^{\theta,s}, B_r\left(\mathsf{BHP}_\theta\right)\right)\right]\right| \leq C\varepsilon.$$

This implies the theorem. □

4.5.4 The ICRT as a local scaling limit of the UIHPQ$_p$'s

Theorem 4.2.7 states that the ICRT appears as the distributional limit of $a_n^{-1}\cdot\mathsf{UIHPQ}_{p_n}$ when $a_n \to \infty$ and $p_n \in [0,1/2]$ satisfies $a_n^2(1-2p_n) \to \infty$ as $n \to \infty$. In essence, the idea behind the proof is the following. Fix $r > 0$, and sequences $(a_n)_n$ and $(p_n)_n$ with the above properties. It turns out that in the UIHPQ_{p_n}, vertices at a distance less than ra_n from the root are to be found at a distance of order $o(a_n)$ from the boundary. Therefore, upon rescaling the graph distance by a factor a_n^{-1}, the scaling limit of the UIHPQ_{p_n} in the local Gromov-Hausdorff sense will agree with the scaling limit of its boundary. Upon a rescaling by a_n^2 in time and a_n^{-1} in space, the encoding bridge b_∞ converges to a two-sided Brownian motion, which in turn encodes the ICRT.

The above observations are most naturally turned into a proof using the description of the Gromov-Hausdorff metric in terms of correspondences between metric spaces; see [BBI01, Theorem 7.3.25]. Lemma 4.5.13 below captures the kind of correspondence we need to construct. Our strategy of showing convergence of quadrangulations with a boundary towards a tree has already been successfully implemented before; see, for instance, [Bet15, Proof of Theorem 5].

For the reminder of this section, we write $((\mathfrak{f}^{(n)}_\infty, \mathfrak{l}^{(n)}_\infty), \mathsf{b}_\infty)$ for a uniformly labeled infinite p_n-forest together with an (independent) uniform infinite bridge b_∞, and we assume that the UIHPQ_{p_n} is given in terms of $((\mathfrak{f}^{(n)}_\infty, \mathfrak{l}^{(n)}_\infty), \mathsf{b}_\infty)$, via the Bouttier–Di

Francesco–Guitter mapping. We interpret the associated contour function $C_\infty^{(n)}$, the bridge b_∞ and the (unshifted) labels $\mathfrak{l}_\infty^{(n)}$ as elements in $\mathcal{C}(\mathbb{R},\mathbb{R})$ (by linear interpolation); see Section 4.4.1.

The core of the argument lies in the following lemma, which gives the necessary control over distances to the boundary, via a control of the labels $\mathfrak{l}_\infty^{(n)}$. We will use it at the very end of the proof of Theorem 4.2.7, which follows afterwards.

Lemma 4.5.10. *Let $(a_n, n\in\mathbb{N})$ be a sequence of positive reals tending to infinity, and $(p_n, n\in\mathbb{N})\subset[0,1/2)$ be a sequence satisfying $a_n^2(1-2p_n)\to\infty$ as $n\to\infty$. Then, in the notation from above, we have the distributional convergence in $\mathcal{C}(\mathbb{R},\mathbb{R}^2)$ as $n\to\infty$,*

$$\left(\left(\frac{1}{a_n^2}C_\infty^{(n)}\left(\frac{a_n^2}{1-2p_n}s\right),\frac{1}{a_n}\mathfrak{l}_\infty^{(n)}\left(\frac{a_n^2}{1-2p_n}s\right),s\in\mathbb{R}\right)\xrightarrow{(d)}((-s,0),s\in\mathbb{R})\,.\right.$$

Proof. We have to show joint convergence of $C_\infty^{(n)}$ and $\mathfrak{l}_\infty^{(n)}$ on any interval of the form $[-K,K]$, for $K>0$. Due to an obvious symmetry in the definition of the contour function, we may restrict ourselves to intervals of the form $[0,K]$. Fix $K>0$, and put $\theta_n=(1-2p_n)^{-1}a_n^2$. We first show that $a_n^{-2}C_\infty^{(n)}(\theta_n s)$, $s\in\mathbb{R}$, converges on $[0,K]$ to $g(s)=-s$ in probability. For that purpose, recall that $C_\infty^{(n)}$ on $[0,\infty)$ has the law of an linearly interpolated random walk started from 0 with step distribution $p_n\delta_1+(1-p_n)\delta_{-1}$. Set $K_n=\lceil K\theta_n\rceil$, and let $\delta>0$. By using Doob's inequality in the second line,

$$\begin{aligned}\mathbb{P}\Big(\sup_{s\in[0,K]}\left|a_n^{-2}C_\infty^{(n)}(\theta_n s)+s\right|>\delta\Big)&\le\mathbb{P}\Big(\sup_{0\le i\le K_n}\left|C_\infty^{(n)}(i)+(1-2p_n)i\right|>\delta a_n^2\Big)\\&\le\frac{1}{\delta^2a_n^4}\mathbb{E}\left[\left|C_\infty^{(n)}(K_n)+(1-2p_n)K_n\right|^2\right]\le\frac{4K_n}{\delta^2a_n^4}\le\frac{4K}{\delta^2a_n^2(1-2p_n)}.\end{aligned}\tag{4.14}$$

Thanks to our assumption on p_n, the right hand side converges to zero, and the convergence of the contour function is established. Showing joint convergence together with the (rescaled) labels $\mathfrak{l}_\infty^{(n)}$ is now rather standard: First, we may assume by Skorokhod's theorem that $a_n^{-2}C_\infty^{(n)}(\theta_n s)$ converges on $[0,K]$ almost surely. Now fix $0\le s\le K$. Conditionally given $C_\infty^{(n)}$ on $[0,K\theta_n]$, we have by construction, for $(\eta_i, i\in\mathbb{N})$ a sequence of i.i.d. uniform random variables on $\{-1,0,1\}$, and with $\underline{C}_\infty^{(n)}(\lfloor\theta_n s\rfloor)=\min_{[0,\lfloor\theta_n s\rfloor]}C_\infty^{(n)}$,

$$\mathfrak{l}_\infty^{(n)}(\lfloor\theta_n s\rfloor)\overset{(d)}{=}\sum_{i=1}^{C_\infty^{(n)}(\lfloor\theta_n s\rfloor)-\underline{C}_\infty^{(n)}(\lfloor\theta_n s\rfloor)}\eta_i.\tag{4.15}$$

Conditionally given $C_\infty^{(n)}$ on $[0,K\theta_n]$, for $\delta>0$, Chebycheff's inequality gives

$$\mathbb{P}\left(\mathfrak{l}_\infty^{(n)}(\lfloor\theta_n s\rfloor)>\delta a_n\,|\,C_\infty^{(n)}\restriction[0,\theta_n s]\right)\le\frac{1}{\delta^2a_n^2}\left(C_\infty^{(n)}(\lfloor\theta_n s\rfloor)-\underline{C}_\infty^{(n)}(\lfloor\theta_n s\rfloor)\right).$$

By our assumption, $a_n^{-2}(C_\infty^{(n)}(\lfloor\theta_n s\rfloor)-\underline{C}_\infty^{(n)}(\lfloor\theta_n s\rfloor))$ converges to zero almost surely, and we conclude

$$\left(a_n^{-2}C_\infty^{(n)}(\lfloor\theta_n s\rfloor),a_n^{-1}\mathfrak{l}_\infty^{(n)}(\lfloor\theta_n s\rfloor)\right)\xrightarrow{(d)}(-s,0)\quad\text{as } n\to\infty.$$

Since both $C_\infty^{(n)}$ and $\mathfrak{l}_\infty^{(n)}$ are Lipschitz almost surely, the claim follows with $\lfloor \theta_n s \rfloor$ replaced by $\theta_n s$. Joint finite-dimensional convergence can now be shown inductively: As for two-dimensional convergence on $[0, K]$, we simply note that when $0 \le s_1 < s_2 \le K$ are such that $C_\infty^{(n)}(\lfloor \theta_n s_1 \rfloor)$ and $C_\infty^{(n)}(\lfloor \theta_n s_2 \rfloor)$ encode vertices of different trees of $\mathfrak{f}_\infty^{(n)}$, then, conditionally on $C_\infty^{(n)} \restriction [0, \lfloor \theta_n s_2 \rfloor]$, $\mathfrak{l}_\infty^{(n)}(\lfloor \theta_n s_1 \rfloor)$ and $\mathfrak{l}_\infty^{(n)}(\lfloor \theta_n s_2 \rfloor)$ are independent sums of i.i.d. uniform variables on $\{-1, 0, 1\}$, and we have a representation similar to (4.15). If $C_\infty^{(n)}(\lfloor \theta_n s_1 \rfloor)$ and $C_\infty^{(n)}(\lfloor \theta_n s_2 \rfloor)$ encode vertices of one and the same tree of $\mathfrak{f}_\infty^{(n)}$, then, with the abbreviation

$$\check{C}_\infty^{(n)}(s_1, s_2) = \min_{[\lfloor \theta_n s_1 \rfloor, \lfloor \theta_n s_2 \rfloor]} C_\infty^{(n)} - \underline{C}_\infty^{(n)}(\lfloor \theta_n s_1 \rfloor),$$

it holds that

$$\mathfrak{l}_\infty^{(n)}(\lfloor \theta_n s_1 \rfloor) \overset{(d)}{=} \sum_{i=1}^{\check{C}_\infty^{(n)}(s_1,s_2)} \eta_i + \sum_{i=\check{C}_\infty^{(n)}(s_1,s_2)+1}^{C_\infty^{(n)}(\lfloor \theta_n s_1 \rfloor)} \eta'_i,$$

$$\mathfrak{l}_\infty^{(n)}(\lfloor \theta_n s_2 \rfloor) \overset{(d)}{=} \sum_{i=1}^{\check{C}_\infty^{(n)}(s_1,s_2)} \eta_i + \sum_{i=\check{C}_\infty^{(n)}(s_1,s_2)+1}^{C_\infty^{(n)}(\lfloor \theta_n s_2 \rfloor)} \eta'_i,$$

where $(\eta'_i, i \in \mathbb{N})$ is an i.i.d. copy of $(\eta_i, i \in \mathbb{N})$. Using almost sure convergence of $a_n^{-2} C_\infty^{(n)}(\theta_n s)$ on $[0, K]$ and an argument similar to that in the one-dimensional convergence considered above, we get convergence of $(a_n^{-2} C_\infty^{(n)}(\theta_n s), a_n^{-1} \mathfrak{l}_\infty^{(n)}(\theta_n s))$ on $[0, K]$, as wanted. Some more details can be found in [LGM11b, Proof of Theorem 4.3]. Higher-dimensional convergence is now shown inductively and is left to the reader. It remains to show tightness of the rescaled labels. We begin with the following lemma.

Lemma 4.5.11. *Let $K > 0$, $(a_n, n \in \mathbb{N})$ and $(p_n, n \in \mathbb{N})$ be as above. Then, for any $q \ge 2$, there exists a constant $C_q > 0$ such that for any $n \in \mathbb{N}$ and any $0 \le s_1, s_2 \le K$, we have (with $\theta_n = (1 - 2p_n)^{-1} a_n^2$, as before)*

$$a_n^{-2q}\, \mathbb{E}\left[\left| C_\infty^{(n)}(\theta_n s_1) - C_\infty^{(n)}(\theta_n s_2) \right|^q \right] \le C_q |s_1 - s_2|^{q/2}.$$

Proof. If $|s_1 - s_2| \le \theta_n^{-1}$, then, using linearity of $C_\infty^{(n)}$,

$$a_n^{-2q}\, \mathbb{E}\left[\left| C_\infty^{(n)}(\theta_n s_1) - C_\infty^{(n)}(\theta_n s_2) \right|^q \right] \le a_n^{-2q} \theta_n^q |s_1 - s_2|^q \le a_n^{-2q} \theta_n^{q/2} |s_1 - s_2|^{q/2}.$$

Since $a_n^{-2q} \theta_n^{q/2} \le a_n^{-q} (1 - 2p_n)^{-q/2} \to 0$ by assumption on p_n, the claim of the lemma follows in this case. Now let $|s_1 - s_2| > \theta_n^{-1}$. We may assume $s_2 \ge s_1$. Using the triangle inequality and again the assumption on p_n, we see that it suffices to establish the claim in the case where $\theta_n s_1$ and $\theta_n s_2$ are integers. In this case, by definition of $C_\infty^{(n)}$,

$$C_\infty^{(n)}(\theta_n s_2) - C_\infty^{(n)}(\theta_n s_1) \overset{(d)}{=} \Big(\sum_{i=1}^{\theta_n(s_2 - s_1)} \vartheta_i \Big) - \theta_n (s_2 - s_1)(1 - 2p_n),$$

where $(\vartheta_i, i \in \mathbb{N})$ are (centered) i.i.d. random variables with distribution $p_n\delta_{2(1-p_n)} + (1-p_n)\delta_{-2p_n}$. Using that $|a+b|^q \le 2^{q-1}(|a|^q + |b|^q)$ for reals a, b, we get

$$\mathbb{E}\left[\left|C_\infty^{(n)}(\theta_n s_2) - C_\infty^{(n)}(\theta_n s_1)\right|^q\right] \le 2^{q-1}\Big(\mathbb{E}\Big[\Big|\sum_{i=1}^{\theta_n(s_2-s_1)} \vartheta_i\Big|^q\Big] + \theta_n^q(1-2p_n)^q(s_2-s_1)^q\Big).$$

The second term within the parenthesis is equal to $a_n^{2q}|s_2-s_1|^q \le K^{q/2}a_n^{2q}|s_2-s_1|^{q/2}$. As for the sum, we apply Rosenthal's inequality and obtain for some constant $C_q' > 0$,

$$\mathbb{E}\Big[\Big|\sum_{i=1}^{\theta_n(s_2-s_1)} \vartheta_i\Big|^q\Big] \le C_q'\theta_n^{q/2}|s_2-s_1|^{q/2}.$$

Using once more that $a_n^{-2q}\theta_n^{q/2} \to 0$ by assumption on p_n, the lemma is proved. □

Let $\kappa > 0$. By the theorem of Kolmogorov-Čentsov (see [KS91, Theorem 2.8]), it follows from the above lemma that there exists $M = M(\kappa) > 0$ such that for all $n \in \mathbb{N}$, the event

$$\mathcal{E}_n = \left\{\sup_{0\le s<t\le K} \frac{|C_\infty^{(n)}(\theta_n s) - C_\infty^{(n)}(\theta_n t)|}{a_n^2|s-t|^{2/5}} \le M\right\}$$

has probability at least $1-\kappa$. We will now work conditionally given $\mathcal{E}_n$.

Lemma 4.5.12. *In the setting from above, there exists a constant $C' > 0$ such that for all $n \in \mathbb{N}$ and all $0 \le s_1, s_2 \le K$,*

$$\mathbb{E}\left[a_n^{-6}|\mathfrak{l}_\infty^{(n)}(\theta_n s_1) - \mathfrak{l}_\infty^{(n)}(\theta_n s_2)|^6 \,\middle|\, \mathcal{E}_n\right] \le C'|s_1-s_2|^{6/5}.$$

Tightness of the conditional laws of $a_n^{-1}\mathfrak{l}_\infty^{(n)}(\theta_n s)$, $0 \le s \le K$, given $\mathcal{E}_n$ is a standard consequence of this lemma; see [KS91, Problem 4.11]). Since κ in the definition of $\mathcal{E}_n$ can be chosen arbitrarily small, tightness of the unconditioned laws of the rescaled labels follows, and so does Lemma 4.5.10. □

It therefore only remains to prove Lemma 4.5.12.

Proof of Lemma 4.5.12. With arguments similar to the proof of Lemma 4.5.11, we see that it suffices to prove the claim in the case where $\theta_n s_1$ and $\theta_n s_2$ are integers (and $s_1 \le s_2$). Let

$$\Delta C_\infty^{(n)}(s_1, s_2) = C_\infty^{(n)}(\theta_n s_1) + C_\infty^{(n)}(\theta_n s_2) - 2\min_{[\theta_n s_1, \theta_n s_2]} C_\infty^{(n)}.$$

By definition of $(C_\infty^{(n)}, \mathfrak{l}_\infty^{(n)})$, conditionally given $C_\infty^{(n)}$ on $[0, K]$, the random variable $|\mathfrak{l}_\infty^{(n)}(\theta_n s_2) - \mathfrak{l}_\infty^{(n)}(\theta_n s_1)|$ is distributed as a sum of i.i.d. variables η_i with the uniform law on $\{-1, 0, 1\}$. By construction, the sum involves at most $\Delta C_\infty^{(n)}(s_1, s_2)$ summands: Indeed, it involves exactly $\Delta C_\infty^{(n)}(s_1, s_2)$ many summands if $C_\infty^{(n)}(\theta_n s_1)$ and $C_\infty^{(n)}(\theta_n s_2)$ encode vertices of the same tree, and less than $\Delta C_\infty^{(n)}(s_1, s_2)$ many summands if they

encode vertices of different trees. Again with Rosenthal's inequality, we thus obtain for some $\tilde{C} > 0$,

$$\mathbb{E}\left[a_n^{-6}|\mathfrak{l}_\infty^{(n)}(\theta_n s_2) - \mathfrak{l}_\infty^{(n)}(\theta_n s_1)|^6 \,\middle|\, \mathcal{E}_n\right] \leq a_n^{-6}\mathbb{E}\left[\left|\sum_{i=1}^{\Delta C_\infty^{(n)}(s_1,s_2)} \eta_i\right|^6 \,\middle|\, \mathcal{E}_n\right] \leq \tilde{C} a_n^{-6}\mathbb{E}\left[|\Delta C_\infty^n(s_1,s_2)|^3 \,\middle|\, \mathcal{E}_n\right].$$

On $\mathcal{E}_n$, we have the bound

$$a_n^{-2}|\Delta C_\infty^n(s_1,s_2)| \leq 2 \sup_{0\leq s<t\leq K} \frac{|C_\infty^n(\theta_n s) - C_\infty^n(\theta_n t)|}{a_n^2|s-t|^{2/5}}|s_1-s_2|^{2/5} \leq M|s_1-s_2|^{2/5},$$

and the claim of the lemma follows. □

Finally, for proving Theorem 4.2.7, we will make use of the following lemma.

Lemma 4.5.13 (Lemma 5.7 of [BMR16]). *Let $r \geq 0$. Let $\mathbf{E} = (E, d, \rho)$ and $\mathbf{E}' = (E', d', \rho')$ be two pointed complete and locally compact length spaces. Consider a subset $\mathcal{R} \subset E \times E'$ which has the following properties:*

- *$(\rho, \rho') \in \mathcal{R}$,*
- *for all $x \in B_r(\mathbf{E})$, there exists $x' \in E'$ such that $(x, x') \in \mathcal{R}$,*
- *for all $y' \in B_r(\mathbf{E}')$, there exists $y \in E$ such that $(y, y') \in \mathcal{R}$.*

Then, $d_{\mathrm{GH}}(B_r(\mathbf{E}), B_r(\mathbf{E}')) \leq (3/2)\sup\{|d(x,y) - d'(x',y')| : (x,x'),(y,y') \in \mathcal{R}\}$.

A proof is given in [BMR16]. Although $\mathcal{R}$ is not necessarily a correspondence in the sense of [BBI01], we might call the supremum on the right side of the inequality the *distortion* of $\mathcal{R}$.

Proof of Theorem 4.2.7. We let $(a_n, n \in \mathbb{N})$ and $(p_n, n \in \mathbb{N}) \subset [0, 1/2]$ be two sequences as in the statement, and, as mentioned at the beginning of this section, we assume that the UIHPQ$_{p_n}$ $\mathbf{Q}_\infty^\infty(p_n)$ with skewness parameter p_n is encoded in terms of $((\mathfrak{f}_\infty^{(n)}, \mathfrak{l}_\infty^{(n)}), \mathsf{b}_\infty)$. Local Gromov-Hausdorff convergence in law of $a_n^{-1} \cdot \mathbf{Q}_\infty^\infty(p_n)$ towards the ICRT follows if we prove that for each $r \geq 0$,

$$B_r^{(0)}\left(a_n^{-1} \cdot \mathbf{Q}_\infty^\infty(p_n)\right) \xrightarrow{(d)} B_r(\mathsf{ICRT}) \tag{4.16}$$

in distribution in $\mathbb{K}$, where we recall again that $B_r^{(0)}(a_n^{-1} \cdot \mathbf{Q}_\infty^\infty(p_n))$ denotes the ball of radius r around the vertex $\mathfrak{f}_\infty^{(n)}(0)$ in the rescaled UIHPQ$_{p_n}$.

We will show the claim for $r = 1$. The proof follows essentially the line of argumentation in [BMR16, Proof of Theorem 3.5]; since the argument is short, we repeat the main steps for completeness. We will apply Lemma 4.5.13 in the following way. The ICRT takes the role of the space $\mathbf{E}'$, with the equivalence class $[0]$ of zero being the distinguished point. Then, we consider for each $n \in \mathbb{N}$ the space $a_n^{-1} \cdot \mathbf{Q}_\infty^\infty(p_n)$ pointed at $\mathfrak{f}_\infty^{(n)}(0)$, which takes the role of $\mathbf{E}$ in the lemma. We construct a subset

$\mathcal{R}_n \subset E \times E'$ with the properties of Lemma 4.5.13, such that its distortion, that is, the quantity $\sup\{|d(x,y) - d'(x',y')| : (x,x'),(y,y') \in \mathcal{R}_n\}$, is of order $o(1)$ for n tending to infinity. By Lemma 4.5.13, this will prove (4.16). We remark that $\mathbf{Q}_\infty^\infty(p_n)$ is not a length space, hence Lemma 4.5.13 seems not applicable at first sight. However, as explained in Section 4.1.2, by identifying each edge with a copy of $[0,1]$ and upon extending the graph metric isometrically, we may identify $\mathbf{Q}_\infty^\infty(p_n)$ with the (associated) length space, which we denote by $\mathsf{Q}_\infty^\infty(p_n) = (V(\mathsf{Q}_\infty^\infty(p_n)), d_{\mathrm{gr}}, \rho)$. Here and in what follows, d_{gr} is the graph metric isometrically extended to $\mathsf{Q}_\infty^\infty(p_n)$. Note that the vertex set $V(\mathfrak{f}_\infty^{(n)})$ may be viewed as a subset of $\mathsf{Q}_\infty^\infty(p_n)$, and between points of $V(\mathfrak{f}_\infty^{(n)})$, the distances d_{gr} and d_{gr} agree. Moreover, as a matter of fact, every point in $\mathsf{Q}_\infty^\infty(p_n)$ is at distance at most $1/2$ away from a vertex of $\mathfrak{f}_\infty^{(n)}$.

Recall that $(\mathsf{b}_\infty(t), t \in \mathbb{R})$ has the law of a (linearly interpolated) two-sided symmetric simple random walk with $\mathsf{b}_\infty(0) = 0$. Let $X = (X_t, t \in \mathbb{R})$ be a two-sided Brownian motion with $X_0 = 0$. By Donsker's invariance principle, we deduce that as n tends to infinity,

$$\left(a_n^{-1}\mathsf{b}_\infty(a_n^2 t), t \in \mathbb{R}\right) \xrightarrow{(d)} (X_t, t \in \mathbb{R})\,. \tag{4.17}$$

Using Skorokhod's representation theorem, we can assume that the above convergence holds almost surely on a common probability space, uniformly over compacts. Now let $\delta > 0$, and fix $\alpha > 0$ and $n_0 \in \mathbb{N}$ such that the event

$$\mathcal{E}(n,\alpha) = \left\{\max\left\{\min_{[0,\alpha]} X, \min_{[-\alpha,0]} X\right\} < -1\right\} \bigcap \left\{\max\left\{\min_{[0,\alpha a_n^2]} \mathsf{b}_\infty, \min_{[-\alpha a_n^2,0]} \mathsf{b}_\infty\right\} < -a_n\right\}$$

has probability at least $1-\delta$ for $n \geq n_0$. From now on, we argue on the event $\mathcal{E}(n,\alpha)$. We moreover assume that the ICRT $(\mathscr{T}_X, d_X, [0])$ is defined in terms of X, and we write $p_X : \mathbb{R} \to \mathscr{T}_X$ for the canonical projection.

Recall that the vertices of $\mathfrak{f}_\infty^{(n)} = (\mathbf{t}_i, i \in \mathbb{Z})$ are identified with the vertices of $\mathbf{Q}_\infty^\infty(p_n)$. The mapping $\mathcal{I}(v) \in \mathbb{Z}$ gives back the index of the tree a vertex $v \in V(\mathfrak{f}_\infty^{(n)})$ belongs to. We extend $\mathcal{I}$ to the elements of the length space $\mathsf{Q}_\infty^\infty(p_n)$ as follows. By viewing $V(\mathfrak{f}_\infty^{(n)})$ as a subset of $\mathsf{Q}_\infty^\infty(p_n)$ as explained above, we associate to every point u of $\mathsf{Q}_\infty^\infty(p_n)$ its closest vertex $v \in V(\mathfrak{f}_\infty^{(n)})$ satisfying $\mathsf{d}_{\mathrm{gr}}(\mathfrak{f}_\infty^{(n)}(0), v) \geq d_{\mathrm{gr}}(\mathfrak{f}_\infty^{(n)}(0), u)$. Note again $\mathsf{d}_{\mathrm{gr}}(v,u) \leq 1/2$. Put

$$A_n = \{u \in \mathsf{Q}_\infty^\infty(p_n) : \mathcal{I}(u) \in [-\alpha a_n^2, \alpha a_n^2]\}.$$

A direct application of the cactus bound [BMR16, (4.6) of Section 4.5] shows that on $\mathcal{E}(n,\alpha)$,

$$\mathsf{d}_{\mathrm{gr}}(\mathfrak{f}_\infty^{(n)}(0), u) > a_n \quad \text{whenever } \mathcal{I}(u) \notin A_n,$$

implying that the set A_n contains the ball $B_1^{(0)}(\mathsf{Q}_\infty^\infty(p_n))$ of radius 1 around the vertex $\mathfrak{f}_\infty^{(n)}(0)$. Moreover, still on $\mathcal{E}(n,\alpha)$,

$$d_X([0], t) > 1 \quad \text{whenever } |t| > \alpha.$$

We now define $\mathcal{R}_n \subset \mathsf{Q}_\infty^\infty(p_n) \times \mathscr{T}_X$ by

$$\mathcal{R}_n = \left\{(u, p_X(t)) : u \in A_n, t \in [-\alpha,\alpha] \text{ with } \mathcal{I}(u) = \lfloor t a_n^2 \rfloor\right\}.$$

Letting $\mathbf{E} = (\mathsf{Q}_\infty^\infty(p_n), a_n^{-1}\mathsf{d}_{\mathrm{gr}}, \mathfrak{f}_\infty^{(n)}(0))$, $\mathbf{E}' = (\mathscr{T}_X, d_X, [0])$, $r = 1$, we find that given the event $\mathcal{E}(n,\alpha)$, the set $\mathcal{R}_n$ satisfies the requirements of Lemma 4.5.13. We are now in the setting of [BMR16, Proof of Theorem 3.5]: All what is left to show is that on $\mathcal{E}(n,\alpha)$, the distortion of $\mathcal{R}_n$ converges to 0 in probability. However, with the same arguments as in the cited proof and using the convergence (4.17), we obtain

$$\limsup_{n\to\infty} \sup\left\{|\mathsf{d}_{\mathrm{gr}}(x,y) - d_X(x',y')| : (x,x'),(y,y') \in \mathcal{R}_n\right\} \leq \limsup_{n\to\infty} \frac{5\left(\sup_{A_n} \mathfrak{l}_\infty^{(n)} - \inf_{A_n} \mathfrak{l}_\infty^{(n)}\right)}{a_n}.$$

An appeal to Lemma 4.5.10 shows that the right hand side is equal to zero, and the proof of the theorem is completed. □

4.6 Proofs of the structural properties

4.6.1 The branching structure behind the UIHPQ_p

In this section, we describe the branching structure of the UIHPQ_p and prove Theorem 4.2.10. We will first study a similar mechanism behind Boltzmann quadrangulations Q and Q_σ drawn according to $\mathbb{P}_{g_p,z_p}$ and $\mathbb{P}_{g_p}^{(\sigma)}$, respectively (Proposition 4.6.1 and Corollary 4.6.2), and then pass to the limit $\sigma \to \infty$ using Proposition 4.2.3.

To begin with, we follow an idea of [CK14a]: We associate to a (finite) rooted map a tree that describes the branching structure of the boundary of the map. Precisely, for every finite rooted quadrangulation $\mathbf{q}$ with a boundary, we define the so-called *scooped-out quadrangulation* $\mathrm{Scoop}(\mathbf{q})$ as follows. We keep only the boundary edges of $\mathbf{q}$ and duplicate those edges which lie entirely in the outer face (i.e., whose both sides belong to the outer face). The resulting object is a rooted looptree; see Figure 4.10.

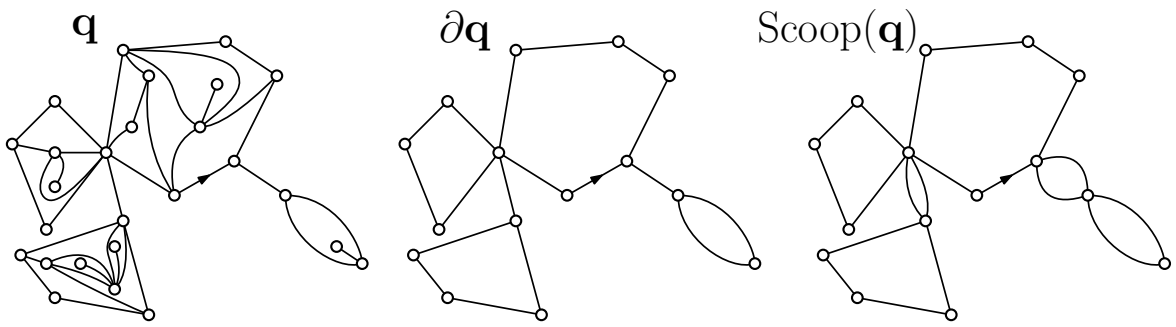

Figure 4.10: A rooted quadrangulation, its boundary and the associated scooped-out quadrangulation.

To a scooped-out quadrangulation $\mathrm{Scoop}(\mathbf{q})$ we associate its tree of components $\mathrm{Tree}(\mathrm{Scoop}(\mathbf{q}))$ as defined in Section 4.3.2. Following [CK14a], we call this tree, by a slight abuse of terminology, the tree of components of $\mathbf{q}$ and use the notation

$\mathbf{t} = \mathbf{Tree}(\mathbf{q})$. It is seen that vertices in $\mathbf{t}_\bullet$ have even degree in $\mathbf{t}$, due to the bipartite nature of $\mathbf{q}$.

By gluing the appropriate rooted quadrangulation with a simple boundary into each cycle of $\mathrm{Scoop}(\mathbf{q})$, we recover the quadrangulation $\mathbf{q}$. This provides a bijection

$$\Phi_{\mathrm{TC}} : \mathbf{q} \mapsto (\mathbf{Tree}(\mathbf{q}), (\widehat{\mathbf{q}}_u : u \in \mathbf{Tree}(\mathbf{q})_\bullet))$$

between, on the one hand, the set $\mathcal{Q}_f$ of finite rooted quadrangulations with a boundary and, on the other hand, the set of plane trees $\mathbf{t}$ with vertices at odd height having even degree, together with a collection $(\widehat{\mathbf{q}}_u : u \in \mathbf{t}_\bullet)$ of rooted quadrangulations with a simple boundary and respective perimeter $\deg(u)$, for $\deg(u)$ the degree of u in $\mathbf{t}$. We remark that the inverse mapping Φ_{TC}^{-1} can be extended to an infinite but locally finite tree together with a collection of quadrangulations with a simple boundary attached to vertices at odd height, yielding in this case an infinite rooted quadrangulation $\mathbf{q}$.

We recall from Section 4.1.2 the definitions of the Boltzmann laws $\mathbb{P}_{g,z}$ and $\mathbb{P}_g^{(\sigma)}$, and their analogs with support on quadrangulations with a simple boundary, $\widehat{\mathbb{P}}_{g,z}$ and $\widehat{\mathbb{P}}_g^{(\sigma)}$. Their corresponding partition functions are F, F_σ and $\widehat{F}$, $\widehat{F}_\sigma$. We are now interested in the law of the tree of components under $\mathbb{P}_{g,z}$. To begin with, we adapt some enumeration results from [BG09] to our setting. For every $0 \le p \le 1/2$, recall that $g_p = p(1-p)/3$ and $z_p = (1-p)/4$. Then, (3.15), (3.27) and (5.16) of [BG09] all together provide the identities

$$F(g_p, z_p) = \frac{2}{3}\frac{3-4p}{1-p}, \quad F_\sigma(g_p) = \frac{(2\sigma)!}{\sigma!(\sigma+2)!}\left(2 + \sigma\frac{1-2p}{1-p}\right)\left(\frac{1}{1-p}\right)^\sigma, \tag{4.18}$$

for $0 \le p \le 1/2$ and $\sigma \in \mathbb{Z}_+$. Moreover, for $\sigma \in \mathbb{N}$ and $0 < p \le 1/2$,

$$\widehat{F}_\sigma(g_p) = \left(\frac{p}{3(1-p)^2}\right)^\sigma \frac{(3\sigma-2)!}{\sigma!(2\sigma-1)!}\left(\frac{3\sigma(1-p)}{p} + 2 - 3\sigma\right), \tag{4.19}$$

while $\widehat{F}_0(g_p) = 1$. If $p = 0$ and hence $g_p = 0$, then $\widehat{F}_k(0) = \delta_0(k) + \delta_1(k)$ for all $k \in \mathbb{Z}_+$. (Indeed, under the maps with no inner faces, the vertex map and the map consisting of one oriented edge are the only maps with a simple boundary.)

We already introduced in Section 4.2.3 two probability measures $\mu_\circ$ and $\mu_\bullet$ on $\mathbb{Z}_+$ given by

$$\mu_\circ(k) = \frac{1}{F(g_p, z_p)}\left(1 - \frac{1}{F(g_p, z_p)}\right)^k, \quad k \in \mathbb{Z}_+, \tag{4.20}$$

$$\mu_\bullet(2k+1) = \frac{1}{F(g_p, z_p) - 1}\left[z_p F^2(g_p, z_p)\right]^{k+1} \widehat{F}_{k+1}(g_p), \quad k \in \mathbb{Z}_+, \tag{4.21}$$

with $\mu_\bullet(k) = 0$ if k even. The tree of components of the scooped-out quadrangulation $\mathrm{Scoop}(Q)$ when Q is drawn according to $\mathbb{P}_{g_p,z_p}$ may now be characterized as follows.

Proposition 4.6.1. *Let $0 \le p \le 1/2$, and let Q be distributed according to $\mathbb{P}_{g_p,z_p}$. Then the tree of components $\mathbf{Tree}(Q)$ is a two-type Galton-Watson tree with offspring distribution $(\mu_\circ, \mu_\bullet)$ as given above. Moreover, conditionally on $\mathbf{Tree}(Q)$, the quadrangulations*

with a simple boundary associated to Q via the bijection Φ_{TC} are independent with respective Boltzmann distribution $\widehat{\mathbb{P}}_{g_p}^{(\deg(u)/2)}$ for $u \in \mathbf{Tree}(Q)_\bullet$, where $\deg(u)$ denotes the degree of u in $\mathbf{Tree}(Q)$.

Proof. Note that vertices at even height of $\mathbf{Tree}(Q)$ have an odd number of offspring almost surely. Let $\mathbf{t}$ be a finite plane tree satisfying this property. Let also $(\widehat{\mathbf{q}}_u : u \in \mathbf{t}_\bullet)$ be a collection of rooted quadrangulations with a simple boundary and respective perimeters $\deg(u)$, and set $\mathbf{q} = \Phi_{\mathrm{TC}}^{-1}(\mathbf{t}, (\widehat{\mathbf{q}}_u : u \in \mathbf{t}_\bullet))$. Then, writing $(\Phi_{\mathrm{TC}})_* \mathbb{P}$ for the push-forward measure of $\mathbb{P}$ by Φ_{TC},

$$(\Phi_{\mathrm{TC}})_* \mathbb{P}_{g_p,z_p} (\mathbf{t}, (\widehat{\mathbf{q}}_u : u \in \mathbf{t}_\bullet)) = \frac{z_p^{\#\partial\mathbf{q}/2} g_p^{\#\mathrm{F}(\mathbf{q})}}{F(g_p,z_p)} = \frac{1}{F(g_p,z_p)} \prod_{u\in\mathbf{t}_\bullet} z_p^{\deg(u)/2} g_p^{\#\mathrm{F}(\widehat{\mathbf{q}}_u)}.$$

For every $c > 0$, we have

$$1 = \prod_{u\in\mathbf{t}_\circ} c^{k_u} \left(\frac{1}{c}\right)^{\#\mathbf{t}_\bullet} \quad \text{and} \quad \frac{1}{c} = \prod_{u\in\mathbf{t}_\bullet} c^{k_u} \left(\frac{1}{c}\right)^{\#\mathbf{t}_\circ}.$$

Applying the first equality with $c = 1 - 1/F(g_p,z_p)$ and the second equality with $c = F(g_p,z_p)$ gives

$$\begin{aligned}(\Phi_{\mathrm{TC}})_* \mathbb{P}_{g_p,z_p} (\mathbf{t}, (\widehat{\mathbf{q}}_u : u \in \mathbf{t}_\bullet)) &= \prod_{u\in\mathbf{t}_\circ} \frac{1}{F(g_p,z_p)} \left(1 - \frac{1}{F(g_p,z_p)}\right)^{\deg(u)-1} \\ &\times \prod_{u\in\mathbf{t}_\bullet} \frac{1}{F(g_p,z_p)-1} \left(z_p F^2(g_p,z_p)\right)^{\deg(u)/2} \widehat{F}_{\deg(u)/2}(g_p) \prod_{u\in\mathbf{t}_\bullet} \frac{g_p^{\#\mathrm{F}(\widehat{\mathbf{q}}_u)}}{\widehat{F}_{\deg(u)/2}(g_p)},\end{aligned}$$

where we agree that $0/0 = 0$. Therefore,

$$(\Phi_{\mathrm{TC}})_* \mathbb{P}_{g_p,z_p} (\mathbf{t}, (\widehat{\mathbf{q}}_u : u \in \mathbf{t}_\bullet)) = \prod_{u\in\mathbf{t}_\circ} \mu_\circ(k_u) \prod_{u\in\mathbf{t}_\bullet} \mu_\bullet(k_u) \prod_{u\in\mathbf{t}_\bullet} \widehat{\mathbb{P}}_{g_p}^{(\deg(u)/2)}(\widehat{\mathbf{q}}_u),$$

which is the expected result. □

Corollary 4.6.2. *Let $0 \le p \le 1/2$, $\sigma \in \mathbb{N}$, and let Q be distributed according to $\mathbb{P}_{g_p}^{(\sigma)}$. Then the tree of components $\mathbf{Tree}(Q)$ is a two-type Galton-Watson tree with offspring distribution $(\mu_\circ, \mu_\bullet)$ conditioned to have $2\sigma+1$ vertices. Moreover, conditionally on $\mathbf{Tree}(Q)$, the quadrangulations with a simple boundary associated to Q via the bijection Φ_{TC} are independent with respective Boltzmann distribution $\widehat{\mathbb{P}}_{g_p}^{(\deg(u)/2)}$, for $u \in \mathbf{Tree}(Q)_\bullet$.*

Proof. Observing that $\#V(\mathbf{Tree}(\mathbf{q})) = \#\partial\mathbf{q} + 1$ for every rooted quadrangulation $\mathbf{q}$, we obtain

$$\begin{aligned}\mathbb{P}_{g_p,z_p}(\mathcal{Q}_f^{(\sigma)}) &= (\Phi_{\mathrm{TC}})_* \mathbb{P}_{g_p,z_p} (\{\mathbf{t} \in \mathcal{T}_f : \#V(\mathbf{t}) = 2\sigma+1\}) \\ &= \mathsf{GW}_{\mu_\circ,\mu_\bullet}(\{\mathbf{t} \in \mathcal{T}_f : \#V(\mathbf{t}) = 2\sigma+1\}).\end{aligned}$$

Now let $\mathbf{t}$ be a finite plane tree with an odd number of offspring at even height, and let $(\widehat{\mathbf{q}}_u : u \in \mathbf{t}_\bullet)$ and $\mathbf{q}$ be as in the proof of Proposition 4.6.1. Then,

$$(\Phi_{\mathrm{TC}})_* \mathbb{P}_{g_p}^{(\sigma)} (\mathbf{t}, (\widehat{\mathbf{q}}_u : u \in \mathbf{t}_\bullet)) = \frac{\mathbf{1}_{\{\#\partial\mathbf{q}=2\sigma\}}}{\mathbb{P}_{g_p,z_p}(\mathcal{Q}_f^{(\sigma)})} \prod_{u\in\mathbf{t}_\circ} \mu_\circ(k_u) \prod_{u\in\mathbf{t}_\bullet} \mu_\bullet(k_u) \prod_{u\in\mathbf{t}_\bullet} \widehat{\mathbb{P}}_{g_p}^{(\deg(u)/2)}(\widehat{\mathbf{q}}_u),$$

which concludes the proof. □

Lemma 4.6.3. *For $0 \leq p < 1/2$, the pair $(\mu_\circ, \mu_\bullet)$ is critical and both $\mu_\circ$ and $\mu_\bullet$ have small exponential moments. For $p = 1/2$, the pair $(\mu_\circ, \mu_\bullet)$ is subcritical (and $\mu_\bullet$ has no exponential moment).*

Proof. Recall that $(\mu_\circ, \mu_\bullet)$ is critical if and only if the product of their respective means $m_\circ$ and $m_\bullet$ equals one. Since by (4.20), $\mu_\circ$ is the geometric law with parameter $1 - 1/F(g_p, z_p)$, we have

$$m_\circ = F(g_p, z_p) - 1.$$

For $m_\bullet$, we let $G_{\mu_\bullet}$ denote the generating function of $\mu_\bullet$. By (4.21), it follows that

$$G_{\mu_\bullet}(s) = \frac{1}{F(g_p, z_p) - 1} \frac{1}{s} \left(\widehat{F}\left[g_p, z_p F^2(g_p, z_p) s^2\right] - 1 \right), \quad s > 0.$$

Then, Identity (2.8) of [BG09] ensures that $\widehat{F}(g, zF^2(g, z)) = F(g, z)$ for all non-negative weights g and z. When differentiating this relation with respect to the variable z, we obtain

$$\partial_z \widehat{F}(g, zF^2(g, z)) = \frac{\partial_z F(g, z)}{F^2(g, z) + 2zF(g, z)\partial_z F(g, z)}. \tag{4.22}$$

Writing

$$\partial_z F(g_p, z_p) = \sum_{\sigma \geq 0} \sigma F_\sigma(g_p) z_p^{\sigma - 1},$$

and using the exact expression for $F_\sigma(g_p)$ from (4.18), we see by means of Stirling's formula that $\partial_z F(g_p, z_p) = \infty$ for $p \in [0, 1/2)$, and $\partial_z F(g_p, z_p) < \infty$ for $p = 1/2$. Thus, for $p \in [0, 1/2)$,

$$\partial_z \widehat{F}(g_p, z_p F^2(g_p, z_p)) = \frac{1}{2 z_p F(g_p, z_p)},$$

whereas if $p = 1/2$, the derivative on the left-hand side in (4.22) is strictly smaller than the right-hand side for $g = g_p$, $z = z_p$. Finally, applying Identity (2.8) of [BG09] once again, we get

$$\begin{aligned} m_\bullet &= G'_{\mu_\bullet}(1) \\ &= \frac{1}{F(g_p, z_p) - 1} \left(- \left(\widehat{F}\left[g_p, z_p F^2(g_p, z_p)\right] - 1 \right) + 2 z_p F^2(g_p, z_p) \partial_z \widehat{F}\left[g_p, z_p F^2(g_p, z_p)\right] \right). \end{aligned}$$

As a consequence, $m_\circ m_\bullet = 1$ if $p < 1/2$, and $m_\circ m_\bullet < 1$ if $p = 1/2$. The fact that $\mu_\circ$ has exponential moments is clear. For $\mu_\bullet$, one sees from (4.19) that the power series

$$\sum_{k \geq 0} x^k \widehat{F}_k(g_p)$$

has radius of convergence $\widehat{r}_p = 4(1-p)^2/(9p)$, while (4.18) ensures that

$$z_p F^2(g_p, z_p) = \frac{(1-4p)^2}{9(1-p)}.$$

Again, for $p \in [0, 1/2)$, $\widehat{r}_p > z_p F^2(g_p, z_p)$, and these quantities are equal for $p = 1/2$. Thus, there exists $s > 1$ such that $G_{\mu_\bullet}(s) < \infty$ if and only if $p < 1/2$, which concludes the proof. □

We are now ready to prove Theorem 4.2.10.

Proof of Theorem 4.2.10. Fix $0 \leq p < 1/2$. We denote by Q_∞ the random quadrangulation with an infinite boundary as constructed in the statement of Theorem 4.2.10, and let Q_σ be distributed according to $\mathbb{P}_{g_p}^{(\sigma)}$. In view of Proposition 4.2.3, it is sufficient to prove that in the local sense, as $\sigma \to \infty$,

$$Q_\sigma \xrightarrow{(d)} Q_\infty. \tag{4.23}$$

For every real $r \geq 1$ and every (finite or infinite) plane tree $\mathbf{t}$, we define $\mathrm{Cut}_r(\mathbf{t})$ as the finite plane tree obtained from pruning all the vertices at a height larger than $2r$ in $\mathbf{t}$. If $\mathbf{q} \in \mathcal{Q}$ is a quadrangulation with a boundary such that $\Phi_{\mathrm{TC}}(\mathbf{q}) = (\mathbf{t}, (\widehat{\mathbf{q}}_u : u \in \mathbf{t}_\bullet))$, we define $\mathrm{Cut}_r(\mathbf{q})$ to be the quadrangulation obtained from gluing the maps $(\widehat{\mathbf{q}}_u : u \in \mathrm{Cut}_r(\mathbf{t})_\bullet)$ in the associated loops of $\mathrm{Loop}(\mathrm{Cut}_r(\mathbf{t}))$. With this definition, we have $B_r(\mathbf{q}) \subset \mathrm{Cut}_r(\mathbf{q})$ for every $r \geq 1$, where we recall that $B_r(\mathbf{q})$ stands for the closed ball of radius r around the root in $\mathbf{q}$.

Let $r \geq 1$ and $\mathbf{q} \in \mathcal{Q}_f$ such that $\Phi_{\mathrm{TC}}(\mathbf{q}) = (\mathbf{t}, (\widehat{\mathbf{q}}_u : u \in \mathbf{t}_\bullet))$. Using Proposition 4.6.1 and Corollary 4.6.2, we get

$$\mathbb{P}\left(\mathrm{Cut}_r\left(Q_\sigma\right) = \mathbf{q}\right) = \mathrm{GW}_{\mu_\circ,\mu_\bullet}^{(2\sigma+1)}\left(\mathrm{Cut}_r = \mathbf{t}\right) \prod_{u \in \mathbf{t}_\bullet} \widehat{\mathbb{P}}_{g_p}^{(\deg(u)/2)}\left(\widehat{\mathbf{q}}_u\right),$$

where we use the notation $\mathrm{GW}_{\mu_\circ,\mu_\bullet}^{(2\sigma+1)}$ for the $(\mu_\circ, \mu_\bullet)$-Galton-Watson tree conditioned to have $2\sigma+1$ vertices and interpret Cut_r as the random variable $\mathbf{t} \mapsto \mathrm{Cut}_r(\mathbf{t})$. Applying Proposition 4.3.4, we get as $\sigma \to \infty$

$$\mathbb{P}\left(\mathrm{Cut}_r\left(Q_\sigma\right) = \mathbf{q}\right) \longrightarrow \mathrm{GW}_{\mu_\circ,\mu_\bullet}^{(\infty)}\left(\mathrm{Cut}_r = \mathbf{t}\right) \prod_{u \in \mathbf{t}_\bullet} \widehat{\mathbb{P}}_{g_p}^{(\deg(u)/2)}\left(\widehat{\mathbf{q}}_u\right) = \mathbb{P}\left(\mathrm{Cut}_r\left(Q_\infty\right) = \mathbf{q}\right).$$

We proved that for every $r \geq 1$, as $\sigma \to \infty$,

$$\mathrm{Cut}_r\left(Q_\sigma\right) \xrightarrow{(d)} \mathrm{Cut}_r\left(Q_\infty\right).$$

Since $B_r(\mathbf{q}) \subset \mathrm{Cut}_r(\mathbf{q})$ for every $r \geq 1$ and $\mathbf{q} \in \mathcal{Q}$, (4.23) holds and the theorem follows. □

4.6.2 Recurrence of simple random walk

In this final part, we prove Corollary 4.2.13, stating that simple random walk on the UIHPQ_p for $0 \leq p < 1/2$ is almost surely recurrent. We will use a criterion from the theory of electrical networks; see, e.g., [LP16, Chapter 2] for an introduction into these techniques.

Proof of Corollary 4.2.13. Fix $0 \leq p < 1/2$. We interpret the UIHPQ_p as an electrical network, by equipping each edge with a resistance of strength one. A cutset $\mathcal{C}$ between the root vertex and infinity is a set of edges that separates the root from infinity, in the sense that every infinite self-avoiding path starting from the root has to pass through at least one edge of $\mathcal{C}$. By the criterion of Nash-Williams, cf. [LP16,

(2.13)], it suffices to show that there is a collection $(\mathcal{C}_n, n \in \mathbb{N})$ of disjoint cutsets such that $\sum_{n=1}^{\infty}(1/\#\mathcal{C}_n) = \infty$ almost surely, i.e., for almost every realization of the UIHPQ_p.

We recall the construction of the UIHPQ_p in terms of the looptree associated to Kesten's two-type tree $\mathbf{T}_\infty^{\circ,\bullet} = \mathbf{T}_\infty^{\circ,\bullet}(\mu_\circ, \mu_\bullet)$. Note that the white vertices in $\mathbf{T}_\infty^{\circ,\bullet}$, i.e., the vertices at even height, represent vertices in the UIHPQ_p. More precisely, by construction, they form the boundary vertices of the latter. In particular, the white vertices on the spine of $\mathbf{T}_\infty^{\circ,\bullet}$ are to be found in the UIHPQ_p, and we enumerate them by $v_1, v_2, v_3, \ldots$, such that v_1 is the root vertex, and $d_{\mathrm{gr}}(v_j, v_1) \geq d_{\mathrm{gr}}(v_i, v_1)$ for $j \geq i$. Now observe that for $i \in \mathbb{N}$, v_i and v_{i+1} lie on the boundary of one common finite-size quadrangulation with a simple boundary, which we denote by $\widehat{\mathbf{q}}_{v_i}$, in accordance with notation in the proof of Theorem 4.2.10.

We define $\mathcal{C}_i$ to be the set of all the edges of $\widehat{\mathbf{q}}_{v_i}$. Clearly, for each $i \in \mathbb{N}$, $\mathcal{C}_i$ is a cutset between the root vertex and infinity, and for $i \neq j$, $\mathcal{C}_i$ and $\mathcal{C}_j$ are disjoint. The sizes $\#\mathcal{C}_i$, $i \in \mathbb{N}$, are i.i.d. random variables. More specifically, using the construction of the UIHPQ_p in terms of Kesten's looptree, the law of $\#\mathcal{C}_1$ can be described as follows: First, draw a random variable Y according to the size-biased offspring distribution $\bar{\mu}_\bullet$, and then, conditionally on Y, $\#\mathcal{C}_1$ is distributed as the number of edges of a Boltzmann quadrangulation with law $\widehat{\mathbb{P}}_{g_p}^{((Y+1)/2)}$, where $g_p = p(1-p)/3$. Obviously, $\#\mathcal{C}_1$ is finite almost surely, implying $\sum_{n=1}^{\infty}(1/\#\mathcal{C}_n) = \infty$ almost surely, and recurrence of the simple symmetric random walk on the UIHPQ_p follows. □

Remark 4.6.4. Let us end with a remark concerning the structure of the UIHPQ_p for $p < 1/2$. Note that with probability $\bar{\mu}_\bullet(1) > 0$, a cutset $\mathcal{C}_i$ as constructed in the above proof consists exactly of one edge. By independence and Borel-Cantelli, we thus find with probability one an infinite sequence of such cutsets $\mathcal{C}_{i_1}, \mathcal{C}_{i_2}, \ldots$ consisting of one edge only. In particular, this proves that the UIHPQ_p for $p < 1/2$ admits a decomposition into a sequence of almost surely finite i.i.d. quadrangulations $Q_i(p)$ with a non-simple boundary (whose laws can explicitly be derived from Theorem 4.2.10), such that $Q_i(p)$ and $Q_j(p)$ get connected by a single edge if and only if $|i-j| = 1$. This parallels the decomposition of the spaces $\mathbb{H}_\alpha$ for $\alpha < 2/3$ found in [Ray14, Display (2.3)].

Acknowledgments. We warmly thank Grégory Miermont for stimulating discussions and advice.

5

Limits of the boundary of Boltzmann maps

We discuss asymptotics for the boundary of critical Boltzmann planar maps under the assumption that the distribution of the degree of a typical face is in the domain of attraction of a stable distribution with parameter $\alpha \in (1,2)$. First, in the dense phase corresponding to $\alpha \in (1,3/2)$, we prove that the scaling limit of the boundary is the random stable looptree with parameter $(\alpha - 1/2)^{-1}$. Second, we show the existence of a phase transition through local limits of the boundary: in the dense phase, the boundary is tree-like, while in the dilute phase corresponding to $\alpha \in (3/2,2)$, it has a component homeomorphic to the half-plane. As an application, we identify the limits of loops conditioned to be large in the rigid $O(n)$ loop model on quadrangulations, proving thereby a conjecture of Curien & Kortchemski.

This Chapter is adapted from the work [5] (preprint). It contains the proof of Theorems 1, 2, 4 and 5 as well as Proposition 3.

Contents

5.1 Introduction

The purpose of this work is to investigate local limits, in the sense of Angel & Schramm, and scaling limits, in the Gromov-Hausdorff sense, of the boundary of bipartite Boltzmann planar maps conditioned to have a large perimeter.

Given a sequence $\mathsf{q} = (q_1, q_2, \ldots)$ of nonnegative real numbers and a planar map $\mathbf{m}$ which is bipartite (i.e., with faces of even degree), the associated Boltzmann weight is

$$w_{\mathsf{q}}(\mathbf{m}) := \prod_{f \in \text{Faces}(\mathbf{m})} q_{\deg(f)/2}.$$

The sequence q is admissible if these weights form a finite measure on the set of pointed bipartite maps (with a distinguished oriented edge and vertex). We also say that q is critical if moreover the expected number of edges of the map is infinite under this measure (see Remark 5.2.5 for details).

One can then generate a large planar map by choosing it with a probability proportional to its weight among the set of planar maps with n faces (or vertices). The scaling limits of such large random planar maps have attracted a lot of attention. The first model to be considered was the uniform measure on $2p$-angulations, in which all faces have the same degree $2p$. In this case, Le Gall [LG07] proved the subsequential convergence towards a random metric space called the *Brownian map*, first introduced by Marckert & Mokkadem in [MM06] and whose distribution has been characterized later by Le Gall [LG13] and Miermont [Mie13]. This result has been extended by Le Gall [LG13] to critical sequences q such that the degree of a typical face has small exponential moments (while the first results on this model were obtained by Marckert & Miermont [MM07]). The result also holds for critical sequences q such that the degree of a typical face has a finite variance, as shown in the recent work [Mar16] (such a sequence q is called *generic critical*). Convergence towards the Brownian map has also been established in the non-bipartite case in [Mie06, MW08]. All these results demonstrate the universality of the Brownian map, whose geometry is now well understood [LGP08, LG10].

For a different behaviour to arise, Le Gall & Miermont suggested in [LGM11a] to assume, besides criticality, that the degree of a typical face is in the domain of attraction of a stable law with parameter $\alpha \in (1, 2)$. The weight sequence q is then called *non-generic critical* with parameter α. Under slightly stronger assumptions, they proved the convergence (along a subsequence) towards a one-parameter family of random metric spaces called the *stable maps* with parameter α. These maps offer a geometry which is very different from that of the Brownian map, because of large faces that remain present in the scaling limit. Their duals are studied in the recent works [BC16, BBCK16], but a lot of questions remain open.

The stable maps are believed to have a phase transition at $\alpha = 3/2$. The regime $\alpha \in (1, 3/2)$ is called the *dense phase* because the large faces of the map are supposed to be self-intersecting in the limit, while in the regime $\alpha \in (3/2, 2)$, called the *dilute phase*, they are supposed to be self-avoiding. See Figure 5.1 for an illustration.

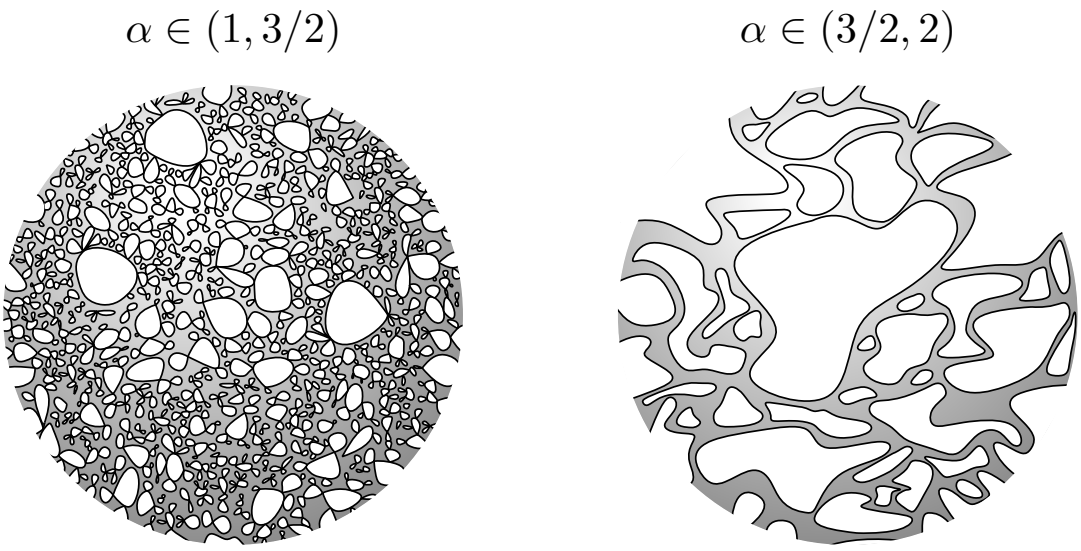

Figure 5.1: Schematic representation of the stable map in the dense phase $\alpha \in (1, 3/2)$ and the dilute phase $\alpha \in (3/2, 2)$.

The aim of this work is twofold: first, we identify the branching structure of the large faces in the dense phase via *scaling limits*. Then, we establish the phase transition through *local limits* of large faces.

Precisely, we consider Boltzmann distributions on bipartite maps with a boundary, meaning that the face on the right of the root edge (the root face) is interpreted as the boundary $\partial\mathbf{m}$ of the map $\mathbf{m}$, and receives no weight. Any admissible weight sequence q provides a probability measure $\mathbb{P}_{\mathsf{q}}^{(k)}$ on the set of bipartite maps with perimeter $\#\partial\mathbf{m} = 2k$, for every $k \geq 0$ (see Section 5.2.2). At large scale, this can be seen a as an (unpointed) stable map rooted on a large face. Our main result is the following.

Theorem 5.1.1. *Let* q *be a non-generic critical sequence with parameter* $\alpha \in (1, 3/2)$. *For every* $k \geq 0$, *let* M_k *be a random planar map with distribution* $\mathbb{P}_{\mathsf{q}}^{(k)}$. *Then, there exists a slowly varying function* Λ *such that in distribution for the Gromov-Hausdorff topology,*

$$\frac{\Lambda(k)}{(2k)^{\alpha-1/2}} \cdot \partial M_k \xrightarrow[k\to\infty]{(d)} \mathscr{L}_\beta,$$

where $\mathscr{L}_\beta$ *is the random stable looptree with parameter*

$$\beta := \frac{1}{\alpha - \frac{1}{2}} \in (1, 2).$$

The random stable looptrees $(\mathscr{L}_\beta : \beta \in (1, 2))$ are compact metric spaces introduced by Curien & Kortchemski in [CK14b], that can informally be seen as the random stable trees of Duquesne & Le Gall [DLG02, DLG05], in which branching points are turned into topological circles. Random stable looptrees also appear as the scaling limits of discrete *looptrees* [CK14b], which are loosely speaking collections of cycles glued along a tree structure. They have Hausdorff dimension β almost surely [CK14b, Theorem 1.1]. A simulation is given in Figure 5.2.

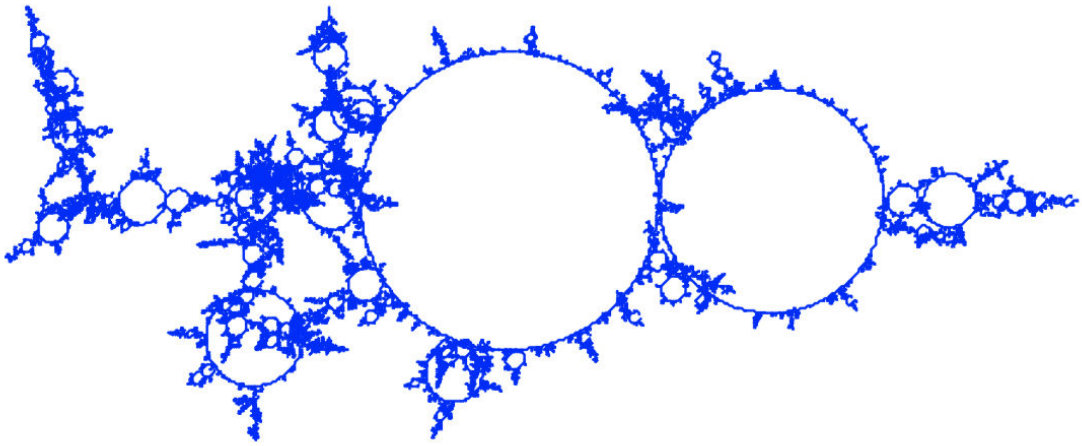

Figure 5.2: A random stable looptree with parameter $\beta = 1.07$ (by Igor Kortchemski).

The result of Theorem 5.1.1 covers the dense case, but the subcritical, dilute and generic critical regimes remain open. We believe that in the dilute and generic critical phases, the scaling limit of ∂M_k is a circle. Furthermore, in the subcritical phase, the *Continuum Random Tree* [Ald91, Ald93] is expected to arise as a scaling limit. We will discuss these questions in greater detail in Section 5.4, and hope to investigate them in a future work.

The local limits of Boltzmann bipartite planar maps with a boundary have been studied by Curien in [Cur16a]. He proved that for any admissible weight sequence q, we have the weak convergence for the local topology

$$\mathbb{P}_{\mathsf{q}}^{(k)} \underset{k\to\infty}{\Longrightarrow} \mathbb{P}_{\mathsf{q}}^{(\infty)}.$$

The probability measure $\mathbb{P}_{\mathsf{q}}^{(\infty)}$ is supported on bipartite maps with an infinite boundary, and called the (law of the) Infinite Boltzmann Half-Planar Map with weight sequence q (or q-IBHPM for short). We now let $\mathbf{M}_\infty = \mathbf{M}_\infty(\mathsf{q})$ be a planar map with distribution $\mathbb{P}_{\mathsf{q}}^{(\infty)}$.

We are interested in the behaviour of the boundary $\partial\mathbf{M}_\infty$ of $\mathbf{M}_\infty$, depending on the weight sequence q. In general, $\partial\mathbf{M}_\infty$ is not simple and has self-intersections, called cut-vertices (or pinch-points). Then, $\mathbf{M}_\infty$ can be decomposed in *irreducible components*, i.e., bipartite maps with a simple boundary attached by cut-vertices of $\partial\mathbf{M}_\infty$. When $\mathbf{M}_\infty$ has a unique infinite irreducible component, we call this component the *core* of $\mathbf{M}_\infty$. For technical reasons, it is more convenient to study the *scooped-out* map $\mathrm{Scoop}(\mathbf{M}_\infty)$ instead of $\partial\mathbf{M}_\infty$. This map is obtained by duplicating the edges of $\partial\mathbf{M}_\infty$ whose both sides belong to the root face.

It is no surprise that the boundary of $\mathbf{M}_\infty$ is a local limit version of looptrees. Let us briefly sketch their construction, details being postponed to Section 5.5.2. Given a pair of offspring distributions $(\rho_\circ, \rho_\bullet)$, a two-type alternated Galton-Watson tree is a random tree in which vertices at even (resp. odd) height have offspring distribution $\rho_\circ$ (resp. $\rho_\bullet$) all independently of each other. As in the monotype case, we can make

sense of such trees conditioned to survive, and denote the limiting infinite tree by $\mathbf{T}_\infty^{\circ,\bullet} = \mathbf{T}_\infty^{\circ,\bullet}(\rho_\circ, \rho_\bullet)$. When $(\rho_\circ, \rho_\bullet)$ is critical (meaning that the product of the means equals one), Stephenson established in [Ste16] that $\mathbf{T}_\infty^{\circ,\bullet}$ is a two-type version of *Kesten's tree* ([Kes86b], see also [LP16]). In particular, $\mathbf{T}_\infty^{\circ,\bullet}$ is locally finite and has a unique *spine*. On the contrary, we will prove in Proposition 5.5.3, under additional assumptions, that when $(\rho_\circ, \rho_\bullet)$ is subcritical, $\mathbf{T}_\infty^{\circ,\bullet}$ has a unique vertex with infinite degree (at odd height). This is an expression of the *condensation* phenomenon first observed in the monotype case by Jonsson & Stefánsson ([JS10], see also [Kor15]). We now define an infinite planar map $\mathbf{L}_\infty = \mathbf{L}_\infty(\rho_\circ, \rho_\bullet)$ out of the tree structure given by $\mathbf{T}_\infty^{\circ,\bullet}$, by taking each vertex at odd height in $\mathbf{T}_\infty^{\circ,\bullet}$ and connecting its neighbours by edges in cyclic order. Therefore, $\mathbf{L}_\infty$ has only finite faces in the critical regime, while a (unique) infinite face arises in the subcritical regime. Note that $\rho_\bullet$ dictates the size of the finite faces in $\mathbf{L}_\infty$. We can now state our local limit result.

Theorem 5.1.2. *Let* q *be an admissible weight sequence, and* $\mathbf{M}_\infty = \mathbf{M}_\infty(\mathsf{q})$ *the* q-IBHPM. *We assume that* q *is either subcritical, generic critical or non-generic critical with parameter* $\alpha \in (1, 2)$. *Then, there exists probability measures* $\nu_\circ$ *(geometric) and* $\nu_\bullet$ *such that*

$$\mathrm{Scoop}(\mathbf{M}_\infty) \overset{(d)}{=} \mathbf{L}_\infty(\nu_\circ, \nu_\bullet).$$

A phase transition is observed:

- *If* q *is subcritical or non-generic critical with parameter* $\alpha \in (1, 3/2]$, $(\nu_\circ, \nu_\bullet)$ *is critical and* $\mathbf{M}_\infty$ *has only finite irreducible components.*
- *If* q *is non-generic critical with parameter* $\alpha \in (3/2, 2)$ *or generic critical,* $(\nu_\circ, \nu_\bullet)$ *is subcritical and* $\mathbf{M}_\infty$ *has a well-defined core with an infinite simple boundary.*

Moreover, $\nu_\bullet$ *has finite variance if and only if* q *is subcritical. Otherwise,* $\nu_\bullet$ *is in the domain of attraction of a stable distribution, with parameter* $(\alpha - 1/2)^{-1}$ *(if* $\alpha \in (1, 3/2)$*),* $\alpha - 1/2$ *(if* $\alpha \in (3/2, 2)$*) or* $3/2$ *(if* q *is generic critical).*

In other words, in the dense phase, $\mathbf{M}_\infty$ is tree-like, while in the dilute phase, it has an irreducible component homeomorphic to the half-plane on which finite maps are grafted (see Figure 5.3 for an illustration). In the subcritical and dense phases, the q-IBHPM can even be recovered from the infinite looptree $\mathbf{L}_\infty$ and a collection of independent Boltzmann bipartite maps with a simple boundary, as shown in Proposition 5.5.8. Note that such collections of random combinatorial structures attached to a tree also appear in the recent work [Stu16]. In the dilute and generic critical regimes, we expect the map with an infinite simple boundary $\mathrm{Core}(\mathbf{M}_\infty)$ to be the local limit of Boltzmann bipartite maps constrained to have a simple boundary when the perimeter goes to infinity, as shown in the quadrangular case in [CM15] (see Section 5.5.3 for more on this).

The critical parameter $\alpha = 3/2$ plays a special role that we will discuss in Section 5.7. In this setting, we will deal with a specific weight sequence q introduced in [ABM16].

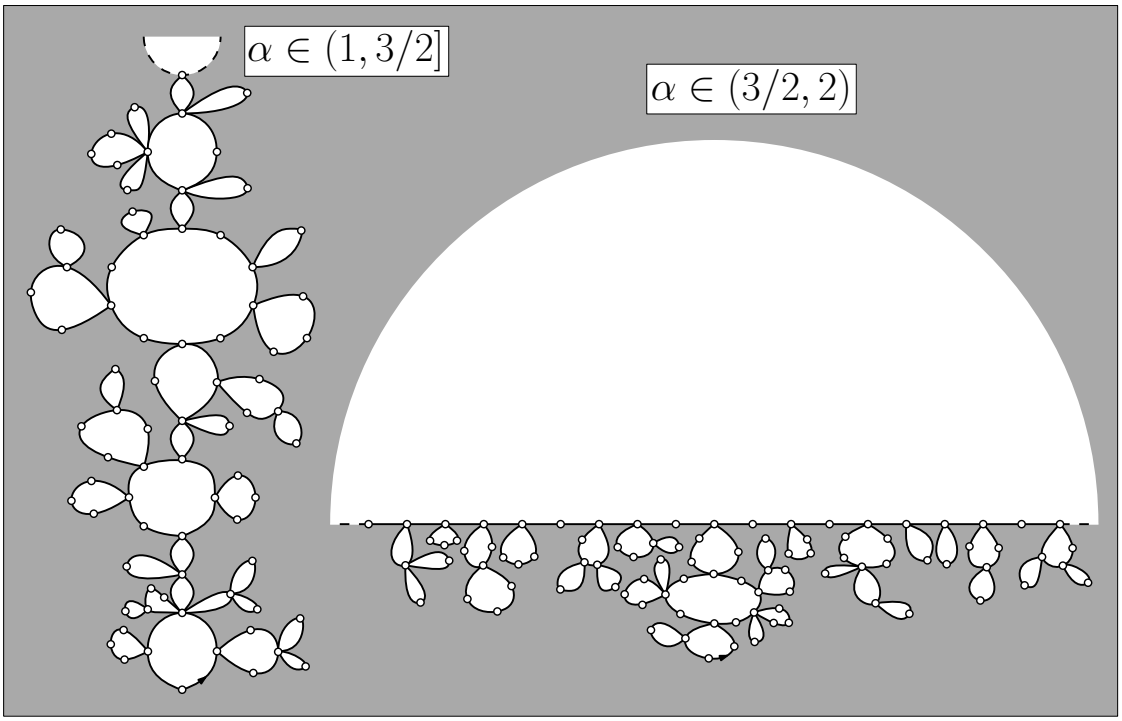

Figure 5.3: Schematic representation of the boundary of the q-IBHPM for q non-generic critical with parameter $\alpha \in (1, 2)$.

The study of Boltzmann distributions such that q is non-generic critical with parameter $\alpha \in (1, 2)$ is also motivated by the connection with statistical physics models on random maps. Here, we are interested in the *rigid* $O(n)$ *loop model* on quadrangulations, studied by Borot, Bouttier & Guitter in [BBG12c]. We now give a brief description of this model, and refer to Section 5.6 for details.

A *loop-decorated* quadrangulation with a boundary $(\mathbf{q}, \boldsymbol{\ell})$ is a planar map $\mathbf{q}$ whose faces all are quadrangles (except the root face), together with a collection of non-crossing loops $\boldsymbol{\ell} = (\ell_1, \ell_2, \ldots)$ drawn on the dual of $\mathbf{q}$. The configuration is called *rigid* if loops cross quadrangles only through their opposite sides. Given $n \in (0, 2)$ and $g, h \geq 0$, we define a measure on loop-decorated quadrangulations by

$$W_{(n;g,h)}((\mathbf{q}, \boldsymbol{\ell})) := g^{\#\mathrm{Faces}(\mathbf{q})-|\boldsymbol{\ell}|} h^{|\boldsymbol{\ell}|} n^{\#\boldsymbol{\ell}},$$

where $|\boldsymbol{\ell}|$ is the total length of the loops and $\#\boldsymbol{\ell}$ is the number of loops. Provided this measure is finite, it induces a probability measure $\mathbf{P}^{(k)}_{(n;g,h)}$ on loop-decorated quadrangulations with a boundary of perimeter $2k$, for every $k \geq 0$. We are particularly interested in the case $k = 1$, which corresponds to the rigid $O(n)$ loop model on quadrangulations of the sphere, simply by gluing the two edges of the boundary together. See Figure 5.4 for an illustration.

In [BBG12c], Borot, Bouttier & Guitter introduced the *gasket* of a loop-decorated quadrangulation, obtained by pruning the interior of the outermost loops. They proved that in the rigid $O(n)$ loop model on quadrangulations with perimeter $2k$, the gasket is a Boltzmann bipartite planar map with distribution $\mathbb{P}^{(k)}_{\mathsf{q}}$, where $\mathsf{q} = \mathsf{q}(n; g, h)$ is the solution of a certain equation. This leads to a classification of the parameters of

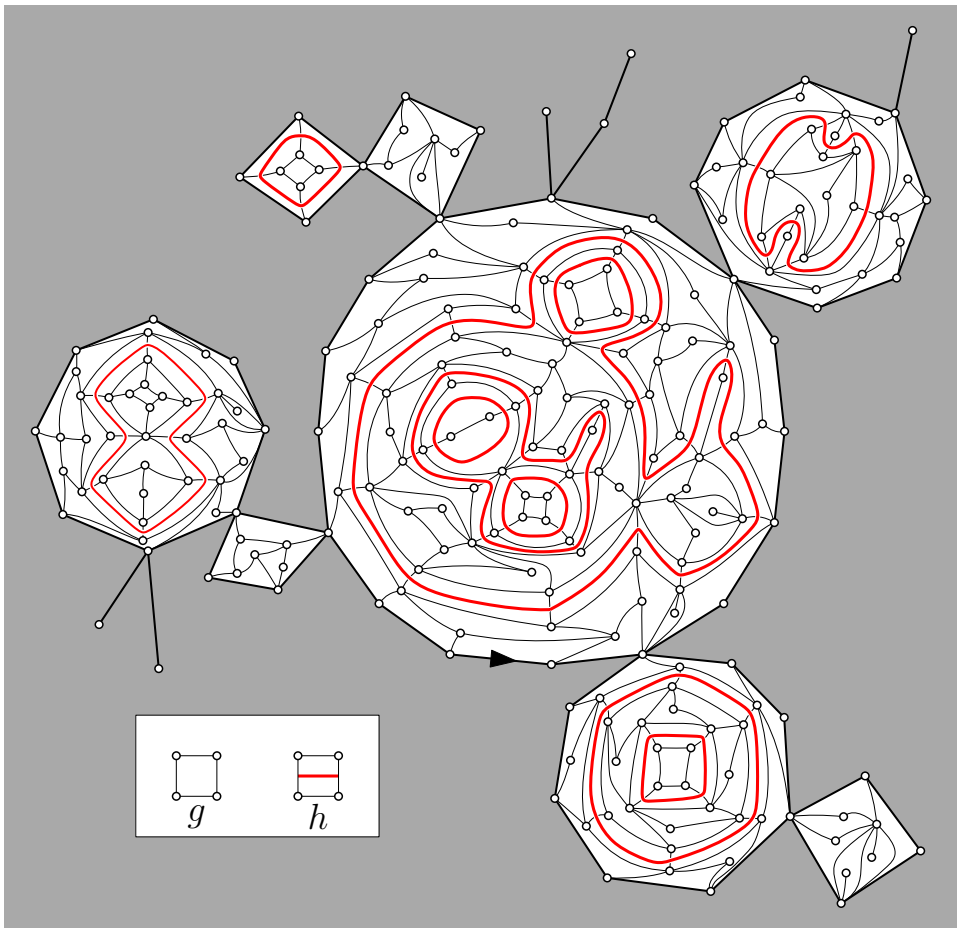

Figure 5.4: A rigid loop configuration $\boldsymbol{\ell}$ on a quadrangulation with a boundary $\mathbf{q}$.

the $O(n)$ loop model into subcritical and (non-)generic critical regimes, depending on the type of the weight sequence $\mathbf{q}$. It has been argued in [BBG12c] (and fully justified in [Bud17, Appendix]) that the model admits a complete phase diagram, shown in Figure 5.5. In particular, for non-generic critical parameters, the gasket is a non-generic Boltzmann bipartite map with parameter α satisfying

$$\alpha = \frac{3}{2} \pm \frac{1}{\pi} \arccos\left(\frac{n}{2}\right).$$

In this work, we are motivated by the study of the geometry of large loops in the rigid $O(n)$ loop model on quadrangulations. More generally, the geometry of large interfaces in statistical physics models on random maps is of great interest. In [CK14a], Curien and Kortchemski studied percolation on random triangulations of the sphere. They proved that the boundary of (the hull of) a critical percolation cluster conditioned to be large converges after proper rescaling towards the random stable looptree with parameter $3/2$. They also conjecture that the whole family $(\mathscr{L}_\beta : \beta \in (1,2))$ appears as a scaling limit of large loops in the $O(n)$ model on triangulations. The following application of Theorem 5.1.1 proves this conjecture for the rigid $O(n)$ loop model on quadrangulations.

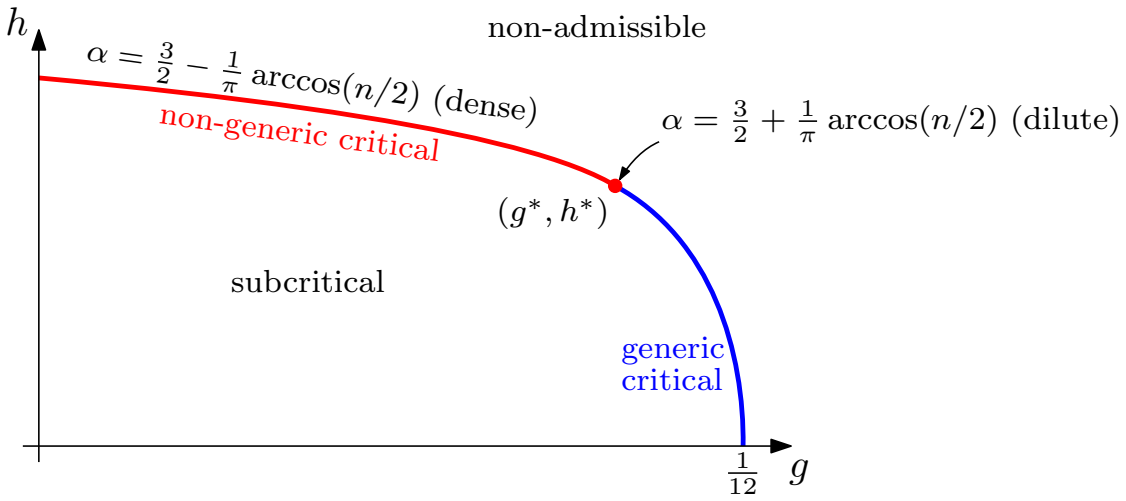

Figure 5.5: The phase diagram of the rigid $O(n)$ loop model on quadrangulations. For every $n \in (0,2)$, there exists a critical line $h = h_c(n;g)$ that separates the subcritical and ill-defined parameters. The regime changes along the critical line. There is a special point $(g^*(n), h^*(n))$ such that the parameters are non-generic critical with parameter $\alpha < 3/2$ (dense) for $g < g^*$, and generic critical for $g > g^*$. The special point (g^*, h^*) itself is non-generic critical with parameter $\alpha > 3/2$ (dilute).

Theorem 5.1.3. *Let $n \in (0,2)$, $g \in [0, g^*(n))$ and $h := h_c(n;g)$. For every $k \geq 0$, let (Q_k, L_k) be a loop-decorated quadrangulation with distribution $\mathbf{P}^{(k)}_{(n;g,h)}$. Then, there exists a constant $C = C(n,g,h)$ such that in distribution for the Gromov-Hausdorff topology,*

$$\frac{C}{(2k)^{1/\beta}} \cdot \partial Q_k \xrightarrow[k\to\infty]{(d)} \mathscr{L}_\beta,$$

where $\mathscr{L}_\beta$ is the random stable looptree with parameter

$$\beta := \left(1 - \frac{1}{\pi}\arccos\left(\frac{n}{2}\right)\right)^{-1} \in (1,2).$$

Note that the value of β in Theorem 5.1.3 fits the prediction of [CK14a].

We also obtain local limit results regarding large loops of the $O(n)$ model from Theorem 5.1.2 and its proof.

Theorem 5.1.4. *Let $n \in (0,2)$ and $g, h \geq 0$ such that $(n;g,h)$ is admissible. For every $k \geq 0$, let (Q_k, L_k) be a loop-decorated quadrangulation with distribution $\mathbf{P}^{(k)}_{(n;g,h)}$. Then, there exists probability measures $\nu_\circ$ (geometric) and $\nu_\bullet$ such that in distribution for the local topology,*

$$\mathrm{Scoop}(Q_k) \xrightarrow[k\to\infty]{(d)} \mathbf{L}_\infty(\nu_\circ, \nu_\bullet).$$

Moreover,

- *If $(n;g,h)$ is subcritical, $(\nu_\circ, \nu_\bullet)$ is critical and $\nu_\bullet$ has finite variance.*

- *If $h = h_c(n;g)$ and $g < g^*(n)$ (the dense case), $(\nu_\circ, \nu_\bullet)$ is critical and $\nu_\bullet$ is in the domain of attraction of a stable distribution with parameter $\left(1 - \frac{1}{\pi}\arccos\left(\frac{n}{2}\right)\right)^{-1}$.*
- *If $(h,g) = (h^*(n), g^*(n))$ (the dilute case), $(\nu_\circ, \nu_\bullet)$ is subcritical and $\nu_\bullet$ is in the domain of attraction of a stable distribution with parameter $1 + \frac{1}{\pi}\arccos\left(\frac{n}{2}\right)$.*
- *If $h = h_c(n;g)$ and $g > g^*(n)$ (the generic critical case), $(\nu_\circ, \nu_\bullet)$ is subcritical and $\nu_\bullet$ is in the domain of attraction of a stable distribution with parameter $3/2$.*

This result should be compared to the local limit of critical percolation clusters conditioned to be large in random half-planar triangulations, studied in Chapter 7.

At first glance, Theorems 5.1.3 and 5.1.4 hold only for the boundary of loop-decorated quadrangulations. However, by the gasket decomposition, they apply to *any* loop conditioned to be large in the rigid $O(n)$ loop model. To make it more concrete, on can choose any deterministic procedure to pick a loop in the rigid $O(n)$ loop model on quadrangulations of the sphere (e.g. the loop that is the closest to the root edge) and condition this loop to have perimeter $2k$. Then, the *inner contour* of this loop is the boundary of a loop-decorated quadrangulation with distribution $\mathbf{P}^{(k)}_{(n;g,h)}$. See Proposition 5.6.1 and Remark 5.6.2 for more details.

Our approach is based on the decomposition of bipartite planar maps with a general boundary into a tree of bipartite planar maps with a simple boundary, which is inspired by [CK14a] and described in Section 5.3. In order to deduce the results from this decomposition, we need estimates on the partition function of bipartite maps with a simple boundary. This is done in Section 5.2.3, by means of a simple relation between the generating functions of bipartite maps with a general (resp. simple) boundary (see Lemma 5.2.10).

This method is quite robust, and only needs estimates on the partition function of the model as an input. For this reason, we believe that our proofs can be adapted to more general statistical physics models on random planar maps for which Borot, Bouttier & Guitter proved results similar to those of [BBG12c]. For instance, general $O(n)$ loop models on triangulations with *bending energy* [BBG12b] or *domain symmetry breaking* [BBG12a]. This last case covers in particular the *Potts model* and *Fortuin-Kasteleyn percolation* on general planar maps, that have been studied in [BLR15, She11, GMS15, GS15a, GS15b, Che15]. An interesting example is the critical Bernoulli percolation model on random triangulations, treated in [BBG12b, Section 4.2, p.23]. This corresponds to a $O(n)$ loop model on triangulations for $n = 1$ and a suitable choice of the parameters. The asymptotics are similar to the quadrangular case, and we get the exponent $\beta = (1 - \arccos(1/2)/\pi)^{-1} = 3/2$, which is consistent with the result of [CK14a].

5.2 Boltzmann distributions

Notation. Throughout this work, we use the notation

$$\mathbb{N} := \{1, 2, \ldots\} \quad \text{and} \quad \mathbb{Z}_+ := \mathbb{N} \cup \{0\}.$$

5.2.1 Boltzmann distributions on bipartite maps

Maps. A *planar map* is a proper embedding of a finite connected graph in the two-dimensional sphere $\mathbb{S}^2$, considered up to orientation-preserving homeomorphisms. The faces of a planar map are the connected components of the complement of the embedding, and the degree $\deg(f)$ of a face f is the number of its incident oriented edges. The sets of vertices, edges and faces of a planar map $\mathbf{m}$ are denoted by $\mathrm{V}(\mathbf{m})$, $\mathrm{E}(\mathbf{m})$ and $\mathrm{F}(\mathbf{m})$. For technical reasons, the planar maps we consider are always *rooted*, which means that an oriented edge $e_* = (e_-, e_+)$, called the *root edge*, is distinguished. The face f_* incident on the right of the root edge is called the *root face*. A planar map *with a boundary* $\mathbf{m}$ is a map in which we consider the root face as an *external face*, whose incident edges and vertices form the *boundary* $\partial\mathbf{m}$ of the map. The non-root faces are then called *internal* and the degree $\#\partial\mathbf{m}$ of the external face is the *perimeter* of the map.

In this paper, we consider *bipartite* planar maps, in which all face degrees are even. We denote by $\mathcal{B}_f$ set of bipartite planar maps, and by $\mathcal{B}_f^{(k)}$ be the set of bipartite planar maps with perimeter $2k$, for $k \geq 0$. By convention, the "vertex map" $\dagger$ consisting of a single vertex is considered as the only element of $\mathcal{B}_f^{(0)}$. We will also consider *pointed* bipartite maps, which have a marked vertex v_*. A pointed bipartite map $\mathbf{m}$ such that $\mathrm{d}_{\mathbf{m}}(e_+, v_*) = \mathrm{d}_{\mathbf{m}}(e_-, v_*) + 1$ is said to be *positive*, and the corresponding set is denoted by $\mathcal{B}_+^\bullet$ (by convention, $\dagger \in \mathcal{B}_+^\bullet$). Finally, we use the notation M for the identity mapping on $\mathcal{B}_f$.

Boltzmann distributions. We now recall the construction of Boltzmann distributions, and first deal with positive bipartite maps. Given a *weight sequence* $\mathsf{q} = (q_k : k \in \mathbb{N})$ of nonnegative real numbers, the *Boltzmann weight* of a bipartite planar map $\mathbf{m}$ is defined by

$$w_{\mathsf{q}}(\mathbf{m}) := \prod_{f \in \mathrm{F}(\mathbf{m})} q_{\deg(f)/2}. \tag{5.1}$$

By convention, we set $w_{\mathsf{q}}(\dagger) = 1$. This defines a σ-finite measure on $\mathcal{B}_+^\bullet$ with total mass (or *partition function*)

$$Z_{\mathsf{q}} := w_{\mathsf{q}}\left(\mathcal{B}_+^\bullet\right) \in [1, \infty]. \tag{5.2}$$

Naturally, a weight sequence q is said to be *admissible* if $Z_{\mathsf{q}} < \infty$. This is our basic assumption in the next part. Then, the Boltzmann distribution $\mathbb{P}_{\mathsf{q}}^\bullet$ associated to q is defined by

$$\mathbb{P}_{\mathsf{q}}^\bullet(\mathbf{m}) := \frac{w_{\mathsf{q}}(\mathbf{m})}{Z_{\mathsf{q}}}, \quad \mathbf{m} \in \mathcal{B}_+^\bullet.$$

Following [MM07], we introduce the function

$$f_{\mathsf{q}}(x) := \sum_{k=1}^{\infty} \binom{2k-1}{k-1} q_k x^{k-1}, \quad x \geq 0, \tag{5.3}$$

whose radius of convergence is denoted by R_{q}. By [MM07, Proposition 1], a weight sequence q is admissible iff the equation

$$f_{\mathsf{q}}(x) = 1 - \frac{1}{x}, \quad x > 0 \tag{5.4}$$

has a solution. In that case, the smallest such solution is Z_{q} and $Z_{\mathsf{q}}^2 f'_{\mathsf{q}}(Z_{\mathsf{q}}) \leq 1$. In particular, we have $Z_{\mathsf{q}} \in (1, R_{\mathsf{q}}]$. The following definitions were introduced in [MM07, BBG12c].

Definition 5.2.1. An admissible weight sequence q is *critical* if $Z_{\mathsf{q}}^2 f'_{\mathsf{q}}(Z_{\mathsf{q}}) = 1$, and *subcritical* otherwise. A critical weight sequence is *regular critical* if $Z_{\mathsf{q}} < R_{\mathsf{q}}$, *generic critical* if $f''_{\mathsf{q}}(Z_{\mathsf{q}}) < \infty$, and *non-generic critical* otherwise.

The function f_{q} being of class C^∞ on $(0, R_{\mathsf{q}})$, a regular weight sequence is indeed generic.

The above classification of weight sequences is closely related to the Bouttier–Di Francesco–Guitter bijection [BDFG04]. The inverse Φ_{BDG}^{-1} of this bijection associates to every map $\mathbf{m} \in \mathcal{B}_+^\bullet$ a tree $\Pi(\mathbf{m})$, together with labels on vertices at even height. The study is simplified by using additionally a bijection Φ_{JS} due to Janson and Stefánsson [JS15, Section 3]. This bijection will be of independent interest in the next part, so we give a detailed presentation in Section 5.3.1. We are interested in the application that associates to $\mathbf{m} \in \mathcal{B}_+^\bullet$ the tree $\Phi(\mathbf{m}) := \Phi_{\mathrm{JS}}(\Pi(\mathbf{m}))$. By combining [MM07, Proposition 7] and [JS15, Appendix A] (see also Proposition 5.3.1), we get the following.

Lemma 5.2.2. *Let q be an admissible weight sequence. Then, under $\mathbb{P}_{\mathsf{q}}^\bullet$, the plane tree $\Phi(M)$ is a Galton-Watson tree with offspring distribution μ defined by*

$$\mu(0) = 1 - f_{\mathsf{q}}(Z_{\mathsf{q}}) \quad \textit{and} \quad \mu(k) = Z_{\mathsf{q}}^{k-1} \binom{2k-1}{k-1} q_k, \quad k \in \mathbb{N}.$$

The definition of Galton-Watson trees is postponed to Section 5.3.1. Recall that the offspring distribution μ is called critical (resp. subcritical) iff it has mean $m_\mu = 1$ (resp. $m_\mu < 1$). Lemma 5.2.2 has a simple expression in terms of the generating function G_μ of μ, which reads

$$G_\mu(s) := \sum_{k=0}^{\infty} s^k \mu(k) = 1 - f_{\mathsf{q}}(Z_{\mathsf{q}}) + s f_{\mathsf{q}}(s Z_{\mathsf{q}}), \quad s \in [0,1]. \tag{5.5}$$

The notions of criticality, regularity and genericity are now easily defined in terms of the offspring distribution μ. First, we find

$$m_\mu = 1 - \frac{1 - Z_{\mathsf{q}}^2 f'_{\mathsf{q}}(Z_{\mathsf{q}})}{Z_{\mathsf{q}}}, \tag{5.6}$$

and assuming $m_\mu = 1$, the variance σ_μ^2 of μ reads

$$\sigma_\mu^2 = Z_{\mathsf{q}}^2 f''_{\mathsf{q}}(Z_{\mathsf{q}}) + \frac{2}{Z_{\mathsf{q}}}. \tag{5.7}$$

We obtain from Definition 5.2.1 the following result.

Proposition 5.2.3. *An admissible weight sequence q is critical iff μ is critical. A critical weight sequence q is regular critical iff μ has small exponential moments, and generic critical (resp. non-generic critical) iff μ has finite (resp. infinite) variance.*

In this paper, we are particularly interested in the non-generic critical case.

Definition 5.2.4. A weight sequence q is *non-generic critical* with parameter $\alpha \in (1,2)$ if q is critical and the distribution μ is in the domain of attraction of a stable law with parameter α: there exists a slowly varying function ℓ on $\mathbb{R}_+$ (eventually positive) such that

$$\mu([k,\infty)) = \frac{\ell(k)}{k^\alpha}.$$

Recall that by definition, a measurable function ℓ is slowly varying (at infinity) if it satisfies $\ell(\lambda x)/\ell(x) \to 1$ as $x \to \infty$, for every $\lambda > 0$. We emphasize that Definition 5.2.4 is slightly more general than that introduced in [LGM11a], which implies that the slowly varying function ℓ is asymptotically constant (and is also the framework in [BBG12c, BC16, BBCK16, Cur16a]).

Remark 5.2.5. The classification of weight sequences can be translated in terms of $\mathbb{P}^\bullet_{\mathsf{q}}$ by properties of Φ_{BDG}. First, we have $\mathbb{E}^\bullet_{\mathsf{q}}(\#\mathrm{E}(M)) = \infty$ iff q is critical. Then, the probability measure $\mu_\bullet(k) := \mu(k+1)/f_{\mathsf{q}}(Z_{\mathsf{q}})$ is interpreted as the law of (half) the degree of a typical face of the map under $\mathbb{P}^\bullet_{\mathsf{q}}$. Thus, a critical sequence q is regular critical (resp. generic critical) iff the degree of a typical face has small exponential moments (resp. finite variance). Moreover, q is non-generic critical with parameter $\alpha \in (1,2)$ iff the degree of a typical face is in the domain of attraction of a stable distribution with parameter α.

We conclude by translating Proposition 5.2.3 in terms of the Laplace transform L_μ of μ. First, if q is subcritical, μ has finite mean $m_\mu < 1$ and

$$L_\mu(t) := G_\mu(e^{-t}) = 1 - m_\mu t + o(t) \quad \text{as } t \to 0^+. \tag{5.8}$$

When q is generic critical, μ has mean $m_\mu = 1$ and finite variance σ_μ^2 which yields

$$L_\mu(t) = 1 - t + \frac{\sigma_\mu^2 + 1}{2} t^2 + o(t^2) \quad \text{as } t \to 0^+. \tag{5.9}$$

The situation is different when q is non-generic critical with parameter $\alpha \in (1,2)$. By Karamata's Abelian theorem [BGT89, Theorem 8.1.6], we get

$$L_\mu(t) = 1 - t + |\Gamma(1-\alpha)| t^\alpha \ell\,(1/t) + o(t^\alpha \ell\,(1/t)) \quad \text{as } t \to 0^+. \tag{5.10}$$

5.2.2 Boltzmann distributions on maps with a boundary

We now deal with maps that have a boundary. The root face f_* is then considered as external to the map, and receives no weight. This amounts to using the Boltzmann weights

$$w^*_{\mathsf{q}}(\mathbf{m}) := \prod_{f \in \mathrm{F}(\mathbf{m}) \setminus \{f_*\}} q_{\deg(f)/2}. \tag{5.11}$$

Let us introduce the partition functions for bipartite maps with a fixed perimeter

$$F_k := \sum_{\mathbf{m} \in \mathcal{B}_f^{(k)}} w^*_{\mathsf{q}}(\mathbf{m}), \quad k \in \mathbb{Z}_+, \tag{5.12}$$

where we hide the dependence in the sequence q in the notation. These quantities are finite if q is admissible. For $\mathsf{q} = 0$, F_k is the k-th Catalan number. In particular, for any weight sequence q, $F_k > 0$ for every $k \geq 0$ (and $F_0 = 1$). The associated Boltzmann measure on bipartite maps with fixed perimeter is defined by

$$\mathbb{P}_{\mathsf{q}}^{(k)}(\mathbf{m}) := \frac{\mathbf{1}_{\left\{\mathbf{m}\in\mathcal{B}_f^{(k)}\right\}} w_{\mathsf{q}}^*(\mathbf{m})}{F_k}, \quad \mathbf{m} \in \mathcal{B}_f,\ k \in \mathbb{Z}_+. \tag{5.13}$$

This is the probability measure we focus on. The aim of this section is to give asymptotics for the partition function F_k. For this purpose, we define the generating function

$$F(x) := \sum_{k=0}^{\infty} F_k x^k, \quad x \geq 0, \tag{5.14}$$

whose radius of convergence is denoted by r_{q}. We borrow ideas of [BBG12c, Section 3.1] and [Cur16a, Section 5.1], but we need to extend these results due to our more general definition of a non-generic critical weight sequence. The idea is to let the (admissible) weight sequence q vary by adding a weight $u \in [0,1]$. We let $\mathsf{q}(u) := (u^{k-1}\mathsf{q}_k : k \in \mathbb{N})$, and set $Z_{\mathsf{q}}(u) := Z_{\mathsf{q}(u)}$. Using the universal form of the generating function for pointed Boltzmann maps [Bud15, Proposition 2, Section A.1] and Euler's formula, we obtain (see [Cur16a, Equation (5.2)])

$$F_k = \binom{2k}{k} \int_0^1 (uZ_{\mathsf{q}}(u))^k \mathrm{d}u, \quad k \in \mathbb{Z}_+. \tag{5.15}$$

In the setting of [LGM11a], the asymptotics of F_k would follow from Laplace's method, see [BBG12c, Cur16a]. Here, we use a different technique based on Karamata's Tauberian theorem. First, the function $X_{\mathsf{q}}(u) := uZ_{\mathsf{q}}(u)$ is increasing from $[0,1]$ to $[0, Z_{\mathsf{q}}]$. It is also continuous as a normally converging series of continuous functions and thus invertible on $[0,1]$, with inverse denoted by Y_{q}. Since $Z_{\mathsf{q}}(u)$ is the smallest solution of (5.4) with $\mathsf{q} = \mathsf{q}(u)$, we have by (5.5)

$$Y_{\mathsf{q}}(x) = x - xf_{\mathsf{q}}(x) = 1 + x - Z_{\mathsf{q}}G_{\mu}(x/Z_{\mathsf{q}}), \quad x \in [0, Z_{\mathsf{q}}].$$

This proves that Y_{q} is of class C^∞ on $(0, Z_{\mathsf{q}})$. Coming back to the integral in (5.15),

$$\int_0^1 (uZ_{\mathsf{q}}(u))^k \mathrm{d}u = \int_0^{Z_{\mathsf{q}}} x^k Y_{\mathsf{q}}'(x)\mathrm{d}x = Z_{\mathsf{q}}^{k+1} \int_0^{\infty} e^{-t(k+1)} Y_{\mathsf{q}}'(Z_{\mathsf{q}}e^{-t})\mathrm{d}t.$$

We now introduce the increasing function

$$U(t) := \int_0^t Z_{\mathsf{q}}e^{-u}Y_{\mathsf{q}}'(Z_{\mathsf{q}}e^{-u})\mathrm{d}u = 1 - Y_{\mathsf{q}}(Z_{\mathsf{q}}e^{-t}) = -Z_{\mathsf{q}}e^{-t} + Z_{\mathsf{q}}L_{\mu}(t), \quad t \geq 0.$$

On the one hand, the integral is expressed in terms of the Laplace transform of U:

$$\int_0^1 (uZ_{\mathsf{q}}(u))^k \mathrm{d}u = Z_{\mathsf{q}}^k \int_0^{\infty} e^{-kt} U(\mathrm{d}t),$$

and on the other hand from (5.8), (5.9) and (5.10), as $t \to 0^+$,

$$U(t) = \begin{cases} Z_{\mathsf{q}}(1-m_\mu)t + o(t) & (\mathsf{q} \text{ subcritical}) \\ Z_{\mathsf{q}}\sigma_\mu^2 t^2/2 + o(t^2) & (\mathsf{q} \text{ generic critical}) \\ Z_{\mathsf{q}}|\Gamma(1-\alpha)|t^\alpha \ell(1/t) + o(t^\alpha \ell(1/t)) & (\mathsf{q} \text{ non-generic critical } \alpha) \end{cases}.$$

We can thus apply Karamata's Tauberian theorem [BGT89, Theorem 1.7.1']. Using also Stirling's formula for the binomial coefficient in (5.15), we get

$$F_k \underset{k\to\infty}{\sim} \begin{cases} \dfrac{Z_{\mathsf{q}}(1-m_\mu)(4Z_{\mathsf{q}})^k}{\sqrt{\pi}k^{3/2}} & (\mathsf{q} \text{ subcritical}) \\ \dfrac{Z_{\mathsf{q}}\sigma_\mu^2(4Z_{\mathsf{q}})^k}{\sqrt{\pi}k^{5/2}} & (\mathsf{q} \text{ generic critical}) \\ \dfrac{Z_{\mathsf{q}}\alpha\sqrt{\pi}(4Z_{\mathsf{q}})^k \ell(k)}{\sin(\pi(\alpha-1))k^{\alpha+1/2}} & (\mathsf{q} \text{ non-generic critical } \alpha) \end{cases}, \tag{5.16}$$

where we used the identity $\Gamma(1-\alpha)\Gamma(1+\alpha) = \alpha\pi/\sin(\pi\alpha)$ for $\alpha \in (1,2)$. The quantity $a := \alpha + 1/2$ is of particular importance and governs the asymptotic behaviour of the partition function. Following [Cur16a], we introduce a notation for weight sequences.

Notation. An admissible weight sequence q is said of type $a = 3/2$ if it is subcritical, of type $a = 5/2$ if it is generic critical and of type $a \in (3/2, 5/2)$ if it is non-generic critical with parameter $\alpha = a - 1/2$.

This allows us to write (5.16) in a unified way. Let

$$c_{3/2} := \frac{Z_{\mathsf{q}}(1-m_\mu)}{\sqrt{\pi}}, \quad c_{5/2} := \frac{Z_{\mathsf{q}}\sigma_\mu^2}{\sqrt{\pi}} \quad \text{and} \quad c_a := \frac{Z_{\mathsf{q}}(a-1/2)\sqrt{\pi}}{\sin(\pi(a-3/2))}, \quad a \in (3/2, 5/2), \tag{5.17}$$

and set the convention that $\ell = 1$ if $a \in \{3/2, 5/2\}$. Then,

$$F_k \underset{k\to\infty}{\sim} \frac{c_a(4Z_{\mathsf{q}})^k \ell(k)}{k^a}, \quad a \in [3/2, 5/2]. \tag{5.18}$$

We now derive from these asymptotics a singular expansion for the generating function F, whose radius of convergence is $r_{\mathsf{q}} = (4Z_{\mathsf{q}})^{-1}$. In particular, $0 < r_{\mathsf{q}} \le 1/4$ if q is admissible. We also have $1 < F(r_{\mathsf{q}}) < \infty$, and $F'(r_{\mathsf{q}}) < \infty$ iff $a \in (2, 5/2]$. For $k \ge 0$, let

$$\zeta(k) := \frac{F_k r_{\mathsf{q}}^k}{F(r_{\mathsf{q}})} \underset{k\to\infty}{\sim} \frac{c_a \ell(k)}{k^a F(r_{\mathsf{q}})}.$$

The function $k \mapsto k^{-a}\zeta(k)$ is slowly varying, so that Karamata's theorem (direct half) [BGT89, Proposition 1.5.10] yields

$$\sum_{j \ge k} \zeta(j) \underset{k\to\infty}{\sim} (a-1)k\zeta(k) \underset{k\to\infty}{\sim} \frac{c_a \ell(k)}{k^{a-1}F(r_{\mathsf{q}})}.$$

We can now apply Karamata's Abelian theorem [BGT89, Theorem 8.1.6] to get the asymptotics of the Laplace transform L_ζ of ζ. For $a \in [3/2, 2)$, we find

$$L_\zeta(t) = 1 - \frac{\Gamma(2-a)c_a}{F(r_\mathsf{q})} t^{a-1}\ell\left(1/t\right) + o(t^{a-1}\ell\left(1/t\right)) \quad \text{as } t \to 0^+,$$

while for $a \in (2, 5/2]$,

$$L_\zeta(t) = 1 - m_\zeta t + \frac{|\Gamma(2-a)|c_a}{F(r_\mathsf{q})} t^{a-1}\ell\left(1/t\right) + o(t^{a-1}\ell\left(1/t\right)) \quad \text{as } t \to 0^+.$$

The function ℓ_1 defined for $y \geq 0$ by $\ell_1(y) = \ell(-(\log(1-1/y))^{-1})$ is slowly varying at infinity by stability properties of slowly varying functions [BGT89, Proposition 1.3.6]. We obtain from the formula $G_\zeta(s) = L_\zeta(-\log(s))$ that for $a \in [3/2, 2)$,

$$G_\zeta(s) = 1 - \frac{\Gamma(2-a)c_a}{F(r_\mathsf{q})}(1-s)^{a-1}\ell_1\left(\frac{1}{1-s}\right)(1+o(1)) \quad \text{as } s \to 1^-,$$

and for $a \in (2, 5/2]$,

$$G_\zeta(s) = 1 - m_\zeta(1-s) + \frac{|\Gamma(2-a)|c_a}{F(r_\mathsf{q})}(1-s)^{a-1}\ell_1\left(\frac{1}{1-s}\right)(1+o(1)) \quad \text{as } s \to 1^-.$$

The singular expansion of F follow from the identity $F(xr_\mathsf{q}) = F(r_\mathsf{q})G_\zeta(x)$. Note that $m_\zeta = r_\mathsf{q}F'(r_\mathsf{q})/F(r_\mathsf{q})$, and let $\kappa_a := c_a|\Gamma(2-a)|$. Recall also that $\ell_1 = 1$ for $a \in \{3/2, 5/2\}$.

Proposition 5.2.6. *Let* q *be a weight sequence of type* a*. For* $a \in [3/2, 2)$*,*

$$F(x) = F(r_\mathsf{q}) - \kappa_a\left(1 - \frac{x}{r_\mathsf{q}}\right)^{a-1}\ell_1\left(\frac{1}{1-\frac{x}{r_\mathsf{q}}}\right)(1+o(1)) \quad \textit{as } x \to r_\mathsf{q}^-,$$

and for $a \in (2, 5/2]$*,*

$$F(x) = F(r_\mathsf{q}) - r_\mathsf{q}F'(r_\mathsf{q})\left(1 - \frac{x}{r_\mathsf{q}}\right) + \kappa_a\left(1 - \frac{x}{r_\mathsf{q}}\right)^{a-1}\ell_1\left(\frac{1}{1-\frac{x}{r_\mathsf{q}}}\right)(1+o(1)) \ \textit{as } x \to r_\mathsf{q}^-.$$

Remark 5.2.7. This method fails in the special case $a = 2$, which is momentarily excluded. Indeed, Karamata's Abelian theorem [BGT89, Theorem 8.1.6] requires a different assumption for integer powers [BGT89, Equation (8.1.11c)] that we cannot prove to be satisfied in general (see [BGT89, Proposition 1.5.8] and the comments below). This issue can be bypassed by making additional assumptions on the weight sequence, which is done in Section 5.7 .

5.2.3 Boltzmann distributions on maps with a simple boundary

The aim of this section is to obtain asymptotics for bipartite maps that have a simple boundary, which will be of particular interest in the next part. A planar map with a *simple boundary* is a planar map whose boundary is a cycle with no self-intersection. Their set is denoted by $\widehat{\mathcal{B}}_f$. Consistently, for every $k \geq 0$, $\widehat{\mathcal{B}}_f^{(k)}$ is the set of bipartite

maps with a simple boundary of perimeter $2k$. A generic element of $\widehat{\mathcal{B}}_f$ is denoted by $\widehat{\mathbf{m}}$, and $\dagger \in \widehat{\mathcal{B}}_f^{(0)}$ by convention.

The partition function for bipartite maps with a simple boundary and fixed perimeter is

$$\widehat{F}_k := \sum_{\widehat{\mathbf{m}} \in \widehat{\mathcal{B}}_f^{(k)}} w_{\mathsf{q}}^*(\widehat{\mathbf{m}}), \quad k \in \mathbb{Z}_+. \tag{5.19}$$

These are finite if q is admissible. The associated Boltzmann measure is defined by

$$\widehat{\mathbb{P}}_{\mathsf{q}}^{(k)}(\mathbf{m}) := \frac{\mathbf{1}_{\left\{\mathbf{m} \in \widehat{\mathcal{B}}_f^{(k)}\right\}} w_{\mathsf{q}}^*(\mathbf{m})}{\widehat{F}_k}, \quad \mathbf{m} \in \mathcal{B}_f,\ k \in \mathbb{Z}_+, \tag{5.20}$$

and the associated generating function by

$$\widehat{F}(x) := \sum_{k=0}^{\infty} \widehat{F}_k x^k \quad x \geq 0. \tag{5.21}$$

The radius of convergence of $\widehat{F}$ is denoted by $\widehat{r}_{\mathsf{q}}$. Note that $\widehat{F}_0 = 1$ for any weight sequence, while if $\mathsf{q} = 0$, $\widehat{F}_k = \delta_0(k) + \delta_1(k)$ (the vertex map and the map with a single oriented edge are the only bipartite maps with a simple boundary and no internal face). When we consider the Boltzmann measure $\widehat{\mathbb{P}}_{\mathsf{q}}^{(k)}$, we implicitly assume that $\widehat{F}_k > 0$.

We will prove the following analogue of Proposition 5.2.6 for Boltzmann maps with a simple boundary, which is the technical core of this paper. The constants $(\widehat{c}_a : a \in \{3/2\} \cup (2, 5/2])$ and the slowly varying functions $\widehat{\ell}_1$ (also depending on a) will be defined at the end of the section, see (5.27) and (5.28).

Proposition 5.2.8. *Let q be a weight sequence of type a. For $a = 3/2$, as $y \to r_{\mathsf{q}} F^2(r_{\mathsf{q}})^+$,*

$$\widehat{F}(y) = F(r_{\mathsf{q}}) \left(1 - \frac{1}{2}\left(1 - \frac{y}{r_{\mathsf{q}} F^2(r_{\mathsf{q}})}\right) + \widehat{c}_{3/2}\left(1 - \frac{y}{r_{\mathsf{q}} F^2(r_{\mathsf{q}})}\right)^2 (1 + o(1))\right).$$

For $a \in (3/2, 2) \cup (2, 5/2]$, $\widehat{F}$ has radius of convergence $\widehat{r}_{\mathsf{q}} = P(r_{\mathsf{q}})$. Moreover, for $a \in (3/2, 2)$,

$$\widehat{F}(y) = F(r_{\mathsf{q}}) \left(1 - \frac{1}{2}\left(1 - \frac{y}{\widehat{r}_{\mathsf{q}}}\right) + \left(1 - \frac{y}{\widehat{r}_{\mathsf{q}}}\right)^{\frac{1}{a-1}} \widehat{\ell}_1\left(\frac{1}{1 - \frac{y}{\widehat{r}_{\mathsf{q}}}}\right)(1 + o(1))\right) \text{ as } y \to \widehat{r}_{\mathsf{q}}^{+},$$

and for $a \in (2, 5/2]$,

$$\widehat{F}(y) = F(r_{\mathsf{q}}) \left(1 - \frac{\widehat{c}_a}{2}\left(1 - \frac{y}{\widehat{r}_{\mathsf{q}}}\right) + \left(1 - \frac{y}{\widehat{r}_{\mathsf{q}}}\right)^{a-1} \widehat{\ell}_1\left(\frac{1}{1 - \frac{y}{\widehat{r}_{\mathsf{q}}}}\right)(1 + o(1))\right) \text{ as } y \to \widehat{r}_{\mathsf{q}}^{+}.$$

Remark 5.2.9. One may wonder if we can use the theory of singularity analysis [FS09, Chapter 6] to get an asymptotic expansion of the partition function $\widehat{F}_k$. However, it is not clear that the so-called delta-analyticity assumption is satisfied in this context. We will use instead Karamata's Tauberian theorem, which provides a weaker

result. In the subcritical case, we do not know if the radius of convergence of the generating function $\widehat{F}$ equals $r_{\mathsf{q}}F^2(r_{\mathsf{q}})$ or not.

In the special case of quadrangulations, corresponding to the weights $q_k = q\delta_2(k)$, computations can be carried out explicitly using [BG09]. First, q is admissible if $q \leq 1/12$ and critical if $q = 1/12$. The generating function F satisfies from [BG09, Equations (3.4), (3.11) and (3.15)]

$$r_{\mathsf{q}} = \frac{1}{4R(q)} \quad \text{and} \quad F(r_{\mathsf{q}}) = 2(1 - qR^2(q)),$$

where

$$R(q) := \frac{1-\sqrt{1-12q}}{6q}, \quad 0 < q \leq \frac{1}{12}.$$

Furthermore, the generating function $\widehat{F}$ has from [BG09, Equation (5.16)] radius of convergence given by

$$\widehat{r}_{\mathsf{q}} = \frac{4}{27qR^3(q)}.$$

We conclude that $\widehat{r}_{\mathsf{q}} > r_{\mathsf{q}}F^2(r_{\mathsf{q}})$ for subcritical quadrangulations. Moreover, [BG09, Equation (5.16)] also provides an equivalent of the partition function for quadrangulations:

$$\widehat{F}_k \underset{k\to\infty}{\sim} \frac{2\sqrt{3}\widehat{r}_{\mathsf{q}}^{\,-k}}{27\sqrt{\pi}k^{5/2}} \ (\mathsf{q} \text{ critical}) \quad \text{and} \quad \widehat{F}_k \underset{k\to\infty}{\sim} \frac{\sqrt{3}\widehat{r}_{\mathsf{q}}^{\,-k}}{27\sqrt{\pi}k^{3/2}}\left(\frac{1}{qR^2(q)} - 3\right) \ (\mathsf{q} \text{ subcritical}).$$

Our approach relies on a simple relation between the generating functions F and $\widehat{F}$, which was first observed in [BIPZ78] (see also [BG09] for quadrangulations). This relation itself is based on the following decomposition of bipartite maps.

Let $\mathbf{m} \in \mathcal{B}_f$ be a bipartite map with a boundary. By splitting $\mathbf{m}$ at the pinch points of $\partial\mathbf{m}$, we obtain connected components that are bipartite maps with a simple boundary, called the irreducible components of $\mathbf{m}$ in [BG09] and [CM15, Section 2.2]. These components are rooted at the oriented edge of $\partial\mathbf{m}$ which is the closest to the root edge of $\mathbf{m}$ (and such that the root face lies on its right). Let $\widehat{\mathbf{m}} \in \widehat{\mathcal{B}}_f$ be the irreducible component of $\mathbf{m}$ containing the root edge. Then, $\widehat{\mathbf{m}}\backslash \mathrm{V}(\partial\widehat{\mathbf{m}})$ disconnects $\mathbf{m}$ into $\#\partial\widehat{\mathbf{m}}$ connected components (with the same rooting convention). This provides an unambiguous decomposition of $\mathbf{m}$ into $\widehat{\mathbf{m}} \in \widehat{\mathcal{B}}_f$ and a collection $(\mathbf{m}_i : 1 \leq i \leq \#\partial\widehat{\mathbf{m}})$ of elements of $\mathcal{B}_f$ attached to the vertices of $\partial\widehat{\mathbf{m}}$. See Figure 5.6 for an illustration.

Lemma 5.2.10. *For every $x \geq 0$, we have*

$$F(x) = \widehat{F}\left(xF^2(x)\right).$$

In particular, the radius of convergence of $\widehat{F}$ satisfies $\widehat{r}_{\mathsf{q}} \geq r_{\mathsf{q}}F^2(r_{\mathsf{q}})$.

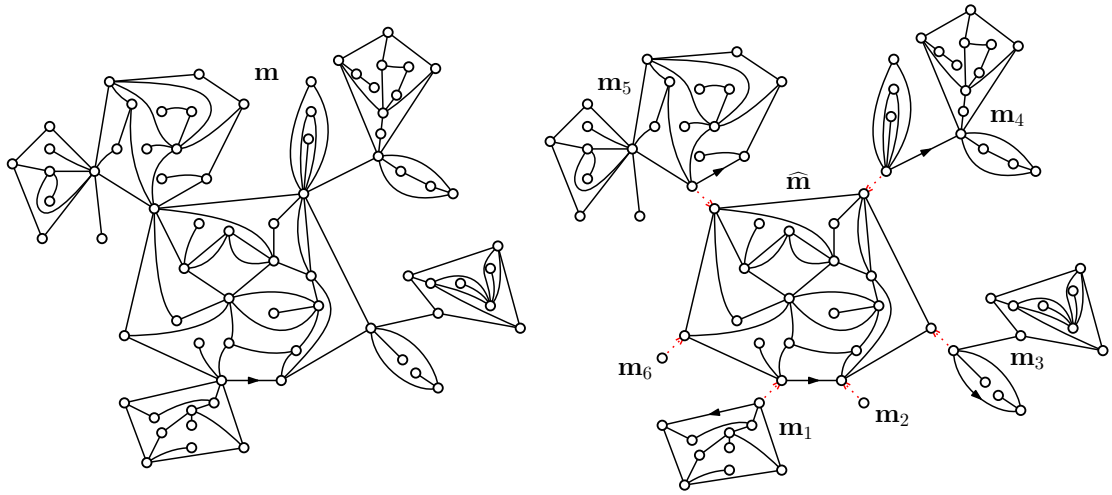

Figure 5.6: The decomposition of a bipartite map $\mathbf{m}$.

Proof. Let $x \geq 0$. By the above decomposition, we have

$$\begin{aligned} F(x) = \sum_{\mathbf{m}\in\mathcal{B}_f} x^{\#\partial\mathbf{m}/2} w_{\mathsf{q}}^*(\mathbf{m}) &= \sum_{\mathbf{m}\in\mathcal{B}_f} x^{\#\partial\widehat{\mathbf{m}}/2} w_{\mathsf{q}}^*(\widehat{\mathbf{m}}) \prod_{i=1}^{\#\partial\widehat{\mathbf{m}}} x^{\#\partial\mathbf{m}_i/2} w_{\mathsf{q}}^*(\mathbf{m}_i) \\ &= \sum_{\widehat{\mathbf{m}}\in\widehat{\mathcal{B}}_f} x^{\#\partial\widehat{\mathbf{m}}/2} w_{\mathsf{q}}^*(\widehat{\mathbf{m}}) \left(\sum_{\mathbf{m}\in\mathcal{B}_f} x^{\#\partial\mathbf{m}/2} w_{\mathsf{q}}^*(\mathbf{m}) \right)^{\#\partial\mathbf{m}} \\ &= \sum_{\widehat{\mathbf{m}}\in\widehat{\mathcal{B}}_f} \left(xF^2(x)\right)^{\#\partial\widehat{\mathbf{m}}/2} w_{\mathsf{q}}^*(\widehat{\mathbf{m}}) = \widehat{F}\left(xF^2(x)\right). \end{aligned}$$

We have that $F(x) < \infty$ if $x < r_{\mathsf{q}}$. Additionally, the function $x \mapsto xF^2(x)$ is continuous increasing on $[0, r_{\mathsf{q}})$, so that $\widehat{F}(y) < \infty$ if $y < r_{\mathsf{q}}F^2(r_{\mathsf{q}})$. We deduce that $\widehat{r}_{\mathsf{q}} \geq r_{\mathsf{q}}F^2(r_{\mathsf{q}})$. □

We now use this relation to derive a singular expansion of $\widehat{F}$ from Proposition 5.2.6. Let us introduce the function

$$P(x) := xF^2(x), \quad x \geq 0.$$

The function P is continuous and increasing from $[0, r_{\mathsf{q}}]$ onto $[0, r_{\mathsf{q}}F^2(r_{\mathsf{q}})]$, with inverse P^{-1}. The results of Proposition 5.2.6 readily transfer to P. For $a \in [3/2, 2)$,

$$P(x) = P(r_{\mathsf{q}}) - \kappa'_a \left(1 - \frac{x}{r_{\mathsf{q}}}\right)^{a-1} \ell_1\left(\frac{1}{1-\frac{x}{r_{\mathsf{q}}}}\right)(1+o(1)) \quad \text{as } x \to r_{\mathsf{q}}^-, \tag{5.22}$$

and for $a \in (2, 5/2]$,

$$P(x) = P(r_{\mathsf{q}}) - C_{\mathsf{q}}\left(1 - \frac{x}{r_{\mathsf{q}}}\right) + \kappa'_a \left(1 - \frac{x}{r_{\mathsf{q}}}\right)^{a-1} \ell_1\left(\frac{1}{1-\frac{x}{r_{\mathsf{q}}}}\right)(1+o(1)) \quad \text{as } x \to r_{\mathsf{q}}^-, \tag{5.23}$$

where $C_{\mathsf{q}} := r_{\mathsf{q}}F(r_{\mathsf{q}})(F(r_{\mathsf{q}}) + 2r_{\mathsf{q}}F'(r_{\mathsf{q}})) > 0$ and $\kappa'_a := 2r_{\mathsf{q}}F(r_{\mathsf{q}})\kappa_a$. We now invert this expansion to get that of P^{-1}, and treat the cases $a \in [3/2, 2)$ and $a \in (2, 5/2]$

separately. Recall that a measurable function f is regularly varying (at infinity) with index $\gamma \in \mathbb{R}$ if it satisfies $f(\lambda x)/f(x) \to \lambda^\gamma$ as $x \to \infty$, for every $\lambda > 0$.

Lemma 5.2.11. *Let f be a continuous decreasing regularly varying function with index $-\gamma < 0$. Then, f is invertible and the function $y \mapsto f^{-1}(1/y)$ is regularly varying with index $1/\gamma$.*

Proof. Observe that $x \mapsto 1/f(x)$ is regularly varying with index $\gamma > 0$. From [BGT89, Theorem 1.5.12], there exists g regularly varying with index $1/\gamma$ such that

$$\frac{1}{f(g(x))} \sim x \quad \text{as } x \to \infty.$$

One version of g is the inverse $y \mapsto f^{-1}(1/y)$ of $x \mapsto 1/f(x)$, defined for y large enough since f vanishes at infinity. Thus, $y \mapsto f^{-1}(1/y)$ is regularly varying with index $1/\gamma$. □

Let $a \in [3/2, 2)$. From (5.22), we know that

$$R(x) := P(r_{\mathsf{q}}) - P(r_{\mathsf{q}}(1 - 1/x)) \sim \kappa'_a x^{1-a} \ell_1(x) \quad \text{as } x \to \infty,$$

thus R is regularly varying with index $-(a-1) < 0$. Moreover, R is continuous decreasing on $[1, \infty)$ with inverse R^{-1} defined by

$$R^{-1}(y) = \left(1 - \frac{1}{r_{\mathsf{q}}} P^{-1}(P(r_{\mathsf{q}}) - y)\right)^{-1}, \quad y \in (0, P(r_{\mathsf{q}})].$$

Using Lemma 5.2.11, we get that $y \mapsto R^{-1}(1/y)$ is regularly varying with index $1/(a-1)$, so that [BGT89, Theorem 1.4.1] ensures the existence of a positive slowly varying function $\bar{\ell}_1$ such that

$$R^{-1}(1/y) = y^{\frac{1}{a-1}} \bar{\ell}_1(y), \quad y \in [1/P(r_{\mathsf{q}}), \infty).$$

As a consequence,

$$P^{-1}(y) = r_{\mathsf{q}} - r_{\mathsf{q}} \left(P(r_{\mathsf{q}}) - y\right)^{\frac{1}{a-1}} \left(\bar{\ell}_1\left(\frac{1}{P(r_{\mathsf{q}}) - y}\right)\right)^{-1}, \quad y \in [0, P(r_{\mathsf{q}})). \tag{5.24}$$

When $a = 3/2$, $\ell_1 = 1$ so that computation can be made more explicit. Indeed, we find

$$R(x) \sim \frac{\kappa'_{3/2}}{\sqrt{x}} \quad \text{as } x \to \infty.$$

Then, the function $Q(x) := R((\kappa'_{3/2}/x)^2)$ is continuous increasing from $(0, \kappa'_{3/2}]$ onto $(0, P(r_{\mathsf{q}})]$ with inverse Q^{-1}. Additionally, Q is right-differentiable at 0 with $Q'(0^+) = 1$, so that Q^{-1} is right-differentiable at 0 and $(Q^{-1})'(0^+) = 1$. Thus, $Q^{-1}(y) \sim y$ as $y \to 0^+$ and we get

$$R^{-1}(y) = \left(\frac{\kappa'_{3/2}}{Q^{-1}(y)}\right)^2 \sim \left(\frac{\kappa'_{3/2}}{y}\right)^2 \quad \text{as } y \to 0^+.$$

As a conclusion,

$$P^{-1}(y) = r_{\mathsf{q}} - \frac{r_{\mathsf{q}}}{(\kappa'_{3/2})^2}\left(P(r_{\mathsf{q}}) - y\right)^2 (1 + o(1)) \quad \text{as } y \to P(r_{\mathsf{q}})^-. \tag{5.25}$$

We are now interested in the case where $a \in (2, 5/2]$. From (5.23), we have

$$R(x) := C_{\mathsf{q}}^{-1}\left[P(r_{\mathsf{q}}) - P(r_{\mathsf{q}}(1-x))\right] = x - \frac{\kappa'_a}{C_{\mathsf{q}}} x^{a-1}\ell_1\left(1/x\right)(1 + o(1)) \quad \text{as } x \to 0^+.$$

The function R is continuous increasing on $[0, 1]$, with inverse R^{-1} defined by

$$R^{-1}(y) = 1 - \frac{1}{r_{\mathsf{q}}} P^{-1}(P(r_{\mathsf{q}}) - C_{\mathsf{q}} y), \quad y \in [0, C_{\mathsf{q}}^{-1} P(r_{\mathsf{q}})].$$

It also satisfies $R'(0^+) = 1$, $(R^{-1})'(0^+) = 1$ and thus $R^{-1}(y) \sim y$ as $y \to 0^+$. In particular, $y \mapsto R^{-1}(1/y)$ is regularly varying with index -1 and by [BGT89, Proposition 1.5.7], the function $\bar{\ell}_1(y) := \ell_1(1/R^{-1}(1/y))$ is slowly varying. We get

$$R^{-1}(y) - y \sim \frac{\kappa'_a}{C_{\mathsf{q}}}\left(R^{-1}(y)\right)^{a-1}\ell_1\left(1/R^{-1}(y)\right) \sim \frac{\kappa'_a}{C_{\mathsf{q}}} y^{a-1}\bar{\ell}_1\left(1/y\right) \quad \text{as } y \to 0^+,$$

and to conclude, as $y \to P(r_{\mathsf{q}})^-$,

$$P^{-1}(y) = r_{\mathsf{q}} - \frac{r_{\mathsf{q}}}{C_{\mathsf{q}}}\left(P(r_{\mathsf{q}}) - y\right) - \frac{\kappa'_a}{C_{\mathsf{q}}^a}\left(P(r_{\mathsf{q}}) - y\right)^{a-1}\bar{\ell}_1\left(\frac{C_{\mathsf{q}}}{P(r_{\mathsf{q}}) - y}\right)(1 + o(1)). \tag{5.26}$$

We can now introduce the constants involved in the statement of Proposition 5.2.8,

$$\widehat{c}_{3/2} := \frac{P(r_{\mathsf{q}})^2}{2(\kappa'_{3/2})^2} - \frac{1}{8} \quad \text{and} \quad \widehat{c}_a = 1 - \frac{P(r_{\mathsf{q}})}{C_{\mathsf{q}}} \in (0, 1) \quad \text{for } a \in (2, 5/2]. \tag{5.27}$$

and the functions $\widehat{\ell}_1$ defined by

$$\widehat{\ell}_1(y) := \frac{P(r_{\mathsf{q}})^{\frac{1}{a-1}}}{2\bar{\ell}_1\left(\frac{y}{P(r_{\mathsf{q}})}\right)}, \ a \in (3/2, 2) \ \text{ and } \ \widehat{\ell}_1(y) := \frac{\kappa'_a P(r_{\mathsf{q}})^{a-1}}{2C_{\mathsf{q}}^a}\bar{\ell}_1\left(\frac{C_{\mathsf{q}} y}{P(r_{\mathsf{q}})}\right), \ a \in (2, 5/2]. \tag{5.28}$$

These functions are positive slowly varying, from [BGT89, Proposition 1.3.6]. Note that for $a = 5/2$, we have $\ell_1 = 1$ so that $\widehat{\ell}_1$ is constant.

Proof of Proposition 5.2.8. By Lemma 5.2.10, we have that $\widehat{F}(r_{\mathsf{q}} F^2(r_{\mathsf{q}})) = F(r_{\mathsf{q}})$, as well as

$$\widehat{F}(y) = \sqrt{\frac{y}{P^{-1}(y)}}, \quad 0 < y \le P(r_{\mathsf{q}}).$$

We obtain asymptotic expansions for $\widehat{F}$ around $P(r_{\mathsf{q}})$ from (5.24), (5.25), and (5.26). These expansions are singular for $a \neq 3/2$, and thus $\widehat{F}$ is not of class C^∞ at $P(r_{\mathsf{q}})$. Together with Lemma 5.2.10, this proves that the radius of convergence of $\widehat{F}$ is $\widehat{r}_{\mathsf{q}} = P(r_{\mathsf{q}})$ in these cases. □

5.3 Structure of the boundary of Boltzmann maps

5.3.1 Random trees and the Janson–Stefánsson bijection

We focus on the branching structure of the boundary of Boltzmann bipartite maps. We start with generalities on plane trees.

Trees. A (finite) plane tree $\mathbf{t}$ [LG05, Nev86] is a finite subset of the set of finite sequences of positive integers

$$\mathcal{U} := \bigcup_{n\in\mathbb{Z}_+} \mathbb{N}^n$$

satisfying the following properties. First, $\emptyset \in \mathbf{t}$ and is called the *root vertex*. Then, for every $u = (u_1, \dots, u_k) \in \mathbf{t}$, $\widehat{u} := (u_1, \dots, u_{k-1}) \in \mathbf{t}$ (and is called the *parent* of u in $\mathbf{t}$). Finally, for every $u = (u_1, \dots, u_k) \in \mathbf{t}$, there exists $k_u = k_u(\mathbf{t}) \in \mathbb{Z}_+$ (the number of children of u in $\mathbf{t}$) such that $uj := (u_1, \dots, u_k, j) \in \mathbf{t}$ iff $1 \le j \le k_u$. The height $|u|$ of a vertex $u = (u_1, \dots, u_k) \in \mathbf{t}$ is $|u| = k$. The vertices at even height are called white, and those at odd height are called black. We let $\mathbf{t}_\circ$ and $\mathbf{t}_\bullet$ be the corresponding subsets of vertices of $\mathbf{t}$. The total number of vertices of a tree $\mathbf{t}$ is denoted by $|\mathbf{t}|$. The set of finite plane trees is denoted by $\mathcal{T}_f$. We use the notation T for the identity mapping on $\mathcal{T}_f$.

Given a probability measure ρ on $\mathbb{Z}_+$, a *Galton-Watson tree* with offspring distribution ρ is a random tree in which every vertex has a number of children distributed according to ρ, all independently of each other. The tree is called critical (resp. subcritical) if the mean m_ρ of ρ is equal to 1 (resp. less than 1). In these cases, its distribution GW_ρ is characterized by

$$\mathsf{GW}_\rho(\mathbf{t}) = \prod_{u\in\mathbf{t}} \rho(k_u), \quad \mathbf{t} \in \mathcal{T}_f. \tag{5.29}$$

We will also deal with (alternated) *two-type Galton-Watson trees* with offspring distribution $(\rho_\circ, \rho_\bullet)$, in which every vertex at even (resp. odd) generation has a number of children distributed according to $\rho_\circ$ (resp. $\rho_\bullet$), all independently of each other. Such a tree is critical (resp. subcritical) if $m_{\rho_\circ} m_{\rho_\bullet} = 1$ (resp. $m_{\rho_\circ} m_{\rho_\bullet} < 1$). Then, its distribution $\mathsf{GW}_{\rho_\circ,\rho_\bullet}$ is characterized by

$$\mathsf{GW}_{\rho_\circ,\rho_\bullet}(\mathbf{t}) = \prod_{u\in\mathbf{t}_\circ} \rho_\circ(k_u) \prod_{u\in\mathbf{t}_\bullet} \rho_\bullet(k_u), \quad \mathbf{t} \in \mathcal{T}_f. \tag{5.30}$$

The Janson–Stefánsson bijection. We now describe the Janson–Stefánsson bijection Φ_{JS} introduced in [JS15, Section 3]. First, $\Phi_{\mathrm{JS}}(\{\emptyset\}) = \{\emptyset\}$. For $\mathbf{t} \neq \{\emptyset\}$, $\Phi_{\mathrm{JS}}(\mathbf{t})$ has the same vertices as $\mathbf{t}$ but different edges defined as follows. For every $u \in \mathbf{t}_\circ$, set the convention that $u0 = \widehat{u}$ (if $u \neq \emptyset$) and $u(k_u + 1) = u$. Then, for every $j \in \{0, 1, \dots, k_u\}$, add the edge $(uj, u(j+1))$ to $\Phi_{\mathrm{JS}}(\mathbf{t})$. If u is a leaf, this amounts to adding an edge between u and its parent. We obtain a tree $\Phi_{\mathrm{JS}}(\mathbf{t})$ embedded in the plane. The vertex 1 of $\mathbf{t}$ is the root vertex of $\Phi_{\mathrm{JS}}(\mathbf{t})$, and its first children in $\Phi_{\mathrm{JS}}(\mathbf{t})$ is chosen according to the lexicographical order of $\mathbf{t}$. For further notice, we give a brief

description of the inverse application Φ_{JS}^{-1}. For $\mathbf{t} \neq \{\emptyset\}$, $\Phi_{\mathrm{JS}}^{-1}(\mathbf{t})$ has the same vertices as $\mathbf{t}$, and its edges can be defined as follows. For every leaf $u \in \mathbf{t}$, let $(u_1, u_2, \ldots)$ be the sequence of vertices after u in the contour order of $\mathbf{t}$, and let $\ell(u)$ be the largest index such that $u_1, \ldots, u_{\ell(u)}$ all are ancestors of u in $\mathbf{t}$. Then, add an edge between u and u_k in $\Phi_{\mathrm{JS}}^{-1}(\mathbf{t})$ for every $k \in \{1, \ldots, \ell(u)\}$. We obtain a tree $\Phi_{\mathrm{JS}}^{-1}(\mathbf{t})$ embedded in the plane, and choose the last leaf u' of $\mathbf{t}$ in contour order as the root vertex, and $u'_{\ell(u)}$ as its first child.

The application Φ_{JS} is a bijection from $\mathcal{T}_f$ onto itself. It has the property that every vertex of $\mathbf{t}_\circ$ is mapped to a leaf of $\Phi_{\mathrm{JS}}(\mathbf{t})$, and every vertex of $\mathbf{t}_\bullet$ with $k \geq 0$ children is mapped to a vertex of $\Phi_{\mathrm{JS}}(\mathbf{t})$ with $k+1$ children. See Figure 5.7 for an illustration.

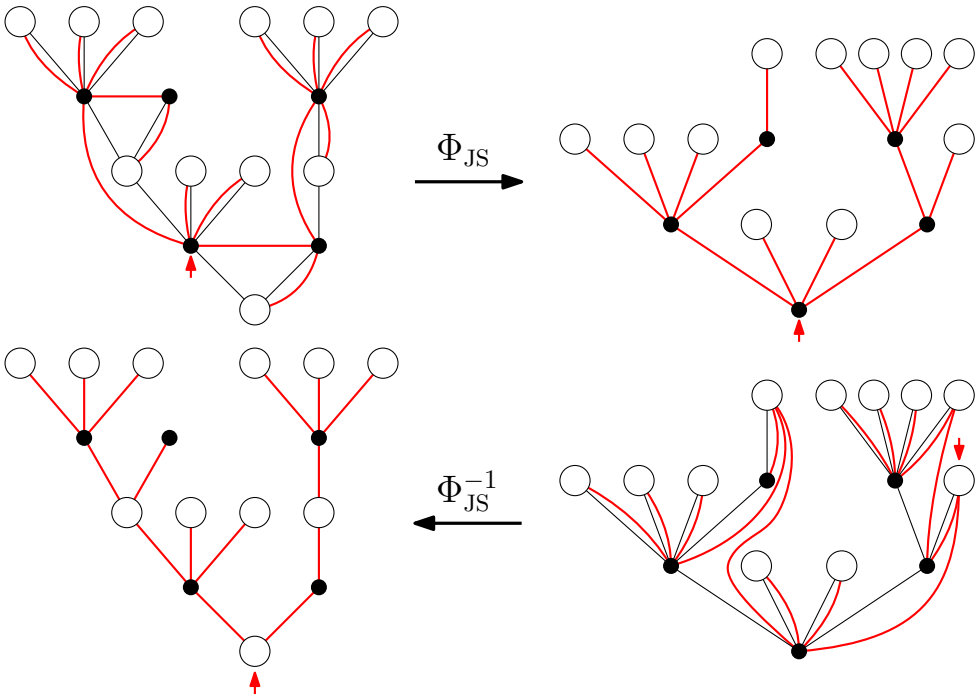

Figure 5.7: The Janson–Stefánsson bijection and its inverse application.

This bijection greatly simplifies the study of alternated two-type Galton-Watson trees, because of the following result of [JS15] (see also [CK14a, Proposition 3.6]).

Proposition 5.3.1. [JS15, Appendix A] *Let $\rho_\circ$ and $\rho_\bullet$ be probability measures on $\mathbb{Z}_+$ such that $m_{\rho_\circ} m_{\rho_\bullet} \leq 1$ and $\rho_\circ$ has geometric distribution with parameter $1-p \in (0,1)$: $\rho_\circ(k) = (1-p)p^k$ for $k \geq 0$. Then, the image of $\mathsf{GW}_{\rho_\circ,\rho_\bullet}$ under Φ_{JS} is GW_ρ, where*

$$\rho(0) = 1-p \quad \textit{and} \quad \rho(k) = p \cdot \rho_\bullet(k-1), \quad k \in \mathbb{N}.$$

Note that $m_\rho - p = (1-p) m_{\rho_\circ} m_{\rho_\bullet}$, so that $(\rho_\circ, \rho_\bullet)$ is critical iff ρ itself is critical.

5.3.2 Random looptrees and scooped-out maps

We now introduce random looptrees and their *tree of components* to represent the boundary of a planar map as a tree. This idea goes back to [CK14a], while random

looptrees were first introduced in [CK14b]. The following presentation is inspired by [CK14a, Section 2.3].

Random looptrees. A looptree is a planar map whose edges are incident to two distinct faces, one of them being the root face (such a map is also called edge-outerplanar). We denote the set of finite looptrees by $\mathcal{L}_f$. Informally, a looptree is a collection of simple cycles glued along a tree structure. Consistently, there is a way to build looptrees from trees and conversely.

We associate to every plane tree $\mathbf{t} \in \mathcal{T}_f$ a looptree $\mathrm{Loop}(\mathbf{t})$ as follows. For every (black) vertex $u \in \mathbf{t}_\bullet$, connect all the incident (white) vertices of u in cyclic order. Then, $\mathrm{Loop}(\mathbf{t})$ is the planar map obtained when discarding the black vertices and the edges of $\mathbf{t}$. The root edge of $\mathrm{Loop}(\mathbf{t})$ connects the origin of $\mathbf{t}$ to the last child of its first offspring in $\mathbf{t}$. The inverse application associates to a looptree $\mathbf{l} \in \mathcal{L}_f$ a plane tree $\mathrm{Tree}(\mathbf{l})$, called the tree of components, as follows. We add an extra vertex in every internal face of $\mathbf{l}$, which we connect by an edge to all the vertices of this face. The plane tree $\mathrm{Tree}(\mathbf{l})$ is then obtained by discarding the edges of $\mathbf{l}$. The root edge of $\mathrm{Tree}(\mathbf{l})$ connects the origin of $\mathbf{l}$ to the vertex lying inside the internal face incident to the root edge of $\mathbf{l}$. This is illustrated in Figure 5.8.

Remark 5.3.2. In a looptree $\mathbf{l}$, every internal face is rooted at the oriented edge whose origin is the closest vertex to the origin of $\mathbf{l}$, and such that the root face of $\mathbf{l}$ lies on its right. The gluing of a planar map with a simple boundary of perimeter k into an internal face of degree k is then determined by the convention that the root edges of the map and the face match.

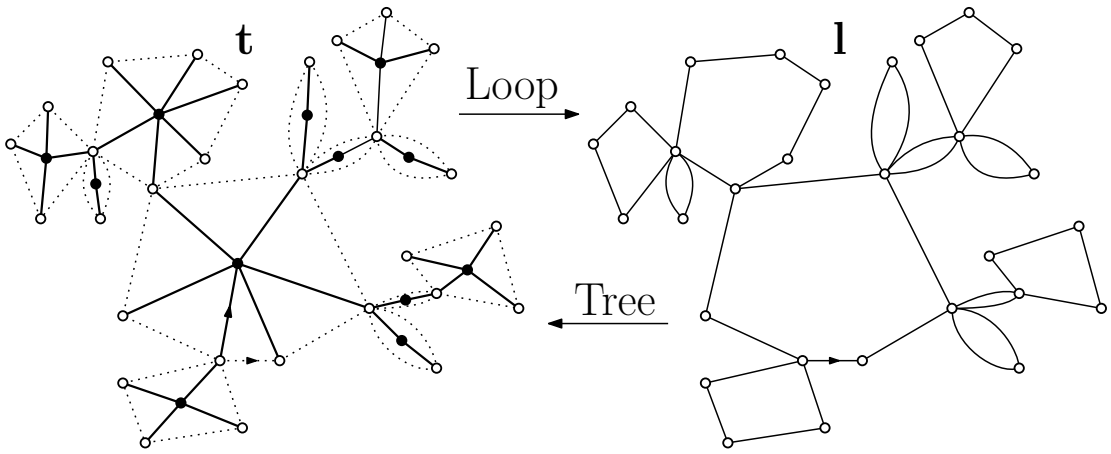

Figure 5.8: A looptree $\mathbf{l}$ and the associated tree of components $\mathbf{t}$.

This definition of looptree slightly differs from that of [CK14b, CK14a], that we now recall. Given a plane tree $\mathbf{t} \in \mathcal{T}_f$, the looptree $\mathbf{Loop}(\mathbf{t})$ (or $\mathbf{Loop}'(\mathbf{t})$ in [CK14b]) is build from $\mathbf{t}$ as follows. For every $u, v \in \mathbf{t}$, there is an edge between u and v iff one of the following conditions is fulfilled: u and v are consecutive siblings in $\mathbf{t}$, or v is either the first or the last child of u in $\mathbf{t}$. We will also need $\overline{\mathbf{Loop}}(\mathbf{t})$, which is obtained from $\mathbf{Loop}(\mathbf{t})$ by contracting the edges linking a vertex of $\mathbf{t}$ and its last child

in $\mathbf{t}$. These objects are rooted at the oriented edge between the origin of $\mathbf{t}$ and its last child in $\mathbf{t}$ (resp. penultimate for $\overline{\mathbf{Loop}}$). See Figure 5.9 for an example. We use the bold print **Loop** to distinguish this construction from Loop. Note that $\mathbf{Loop}(\mathbf{t})$ is a looptree and can be obtained as the image of a plane tree by Loop, but the converse does not hold: **Loop** does not allow several loops to be glued at the same vertex.

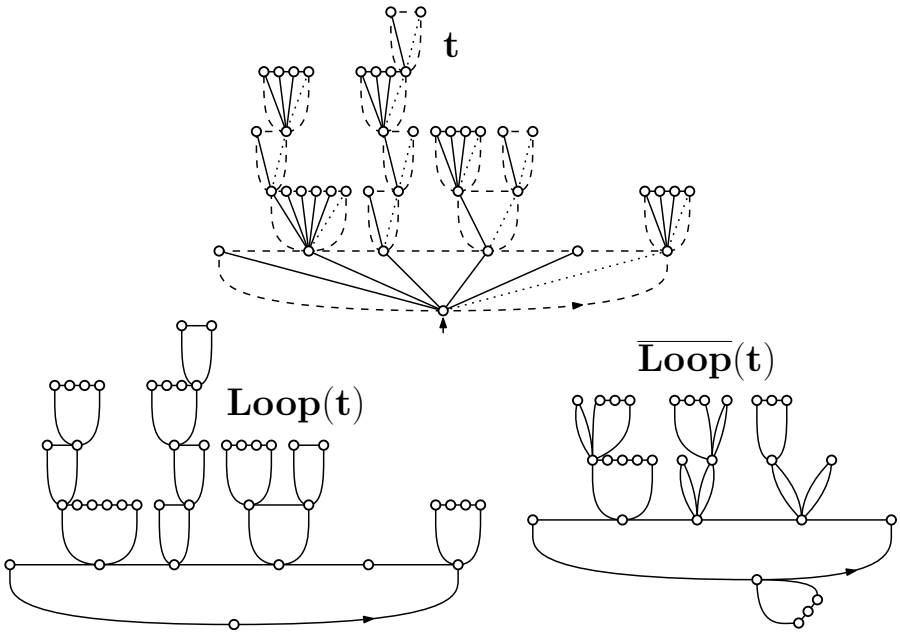

Figure 5.9: A tree $\mathbf{t}$ and the looptrees $\mathbf{Loop}(\mathbf{t})$ and $\overline{\mathbf{Loop}}(\mathbf{t})$.

The scooped-out map. The *scooped-out* map of a planar map $\mathbf{m}$ was defined in [CK14a] as the looptree $\mathrm{Scoop}(\mathbf{m})$ obtained from the boundary $\partial\mathbf{m}$ by duplicating the edges whose both sides belong to the root face. We call tree of components of $\mathbf{m}$ the tree of components of $\mathrm{Scoop}(\mathbf{m})$, denoted by $\mathbf{Tree}(\mathbf{m}) := \mathrm{Tree}(\mathrm{Scoop}(\mathbf{m}))$.

Any planar map $\mathbf{m}$ is recovered from $\mathrm{Scoop}(\mathbf{m})$ by gluing into the internal faces of $\mathrm{Scoop}(\mathbf{m})$ the proper maps with a simple boundary, which are the irreducible components of $\mathbf{m}$ (using Remark 5.3.2). Otherwise said, to every black vertex u of $\mathbf{t} := \mathbf{Tree}(\mathbf{m})$ corresponds a cycle of $\mathrm{Scoop}(\mathbf{m})$, and thus a planar map with a simple boundary of perimeter $\deg(u)$. This construction provides a bijection

$$\Phi_{\mathrm{TC}} : \mathbf{m} \mapsto (\mathbf{Tree}(\mathbf{m}), (\widehat{\mathbf{m}}_u : u \in \mathbf{Tree}(\mathbf{m})_\bullet))$$

that associates to a bipartite map $\mathbf{m} \in \mathcal{B}_f$ the plane tree $\mathbf{t} = \mathbf{Tree}(\mathbf{m})$, whose vertices at odd height have even degree, and a collection $(\widehat{\mathbf{m}}_u : u \in \mathbf{t}_\bullet)$ of bipartite maps with a simple boundary of respective perimeter $\deg(u)$. See Figure 5.10 for an example. The following relations between the perimeter of a map and the size of its tree of components will be useful:

$$|\mathbf{t}| = \#\partial\mathbf{m} + 1 \quad \text{and} \quad \sum_{u \in \mathbf{t}_\bullet} \deg(u) = \#\partial\mathbf{m} \quad (\mathbf{t} = \mathbf{Tree}(\mathbf{m})). \tag{5.31}$$

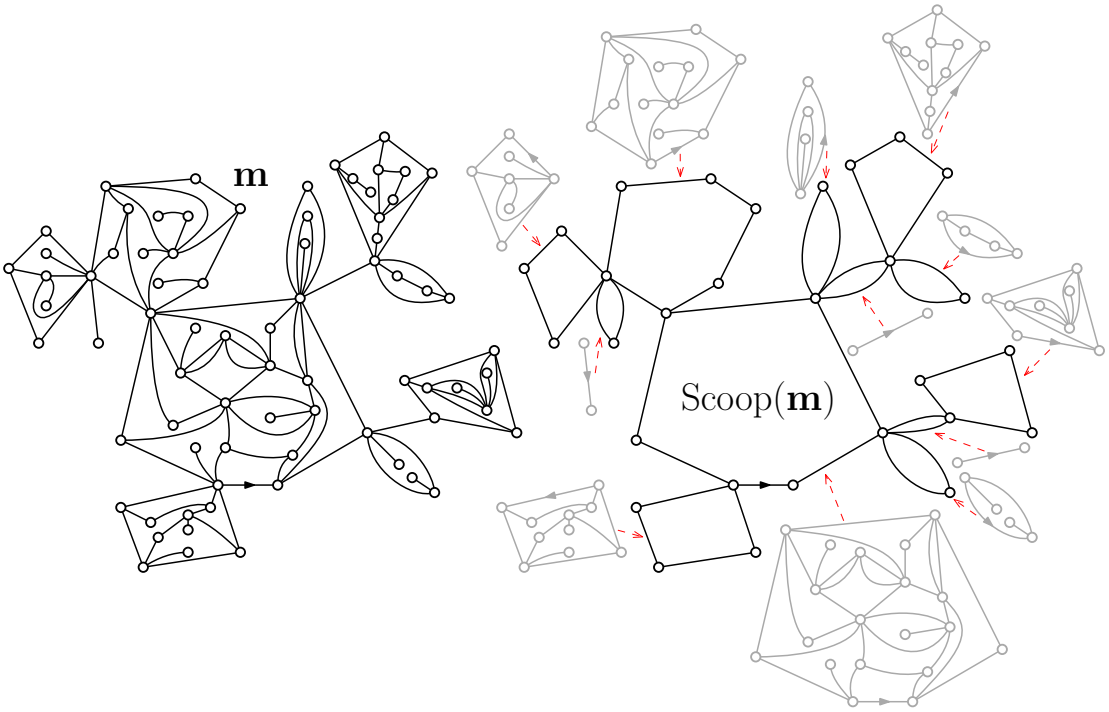

Figure 5.10: A planar map $\mathbf{m}$ and the associated scooped-out map $\mathrm{Scoop}(\mathbf{m})$.

5.3.3 Distribution of the tree of components

The purpose of this section is to provide the distribution of the tree of components of a bipartite map under the probability measure $\mathbb{P}_{\mathsf{q},r_\mathsf{q}}$ defined by

$$\mathbb{P}_{\mathsf{q},r_\mathsf{q}}(\mathbf{m}) := \frac{r_\mathsf{q}^{\#\partial\mathbf{m}/2} w_\mathsf{q}^*(\mathbf{m})}{F(r_\mathsf{q})}, \quad \mathbf{m} \in \mathcal{B}_f. \tag{5.32}$$

It is related to $\mathbb{P}_\mathsf{q}^{(k)}$ by conditioning with respect to the perimeter of the map: for every $k \geq 0$,

$$\mathbb{P}_{\mathsf{q},r_\mathsf{q}}\left(\mathbf{m} \mid \mathcal{B}_f^{(k)}\right) = \mathbb{P}_\mathsf{q}^{(k)}(\mathbf{m}), \quad \mathbf{m} \in \mathcal{B}_f. \tag{5.33}$$

The main result of this section generalizes Proposition 4.6.1 that deals with quadrangulations.

Proposition 5.3.3. *Let* q *be a weight sequence of type* $a \in [3/2, 5/2]$. *Under* $\mathbb{P}_{\mathsf{q},r_\mathsf{q}}$, $\mathbf{Tree}(M)$ *is a two-type Galton-Watson tree with offspring distribution* $(\nu_\circ, \nu_\bullet)$ *defined by*

$$\nu_\circ(k) = \frac{1}{F(r_\mathsf{q})}\left(1 - \frac{1}{F(r_\mathsf{q})}\right)^k \text{ and } \nu_\bullet(2k+1) = \frac{1}{F(r_\mathsf{q}) - 1}\left(r_\mathsf{q} F^2(r_\mathsf{q})\right)^{k+1} \widehat{F}_{k+1},\ k \in \mathbb{Z}_+.$$

(With $\nu_\bullet(k) = 0$ *for* k *even.) Moreover, conditionally on* $\mathbf{Tree}(M)$, *the bipartite maps with a simple boundary* $(\widehat{M}_u : u \in \mathbf{Tree}(M)_\bullet)$ *associated to* M *by* Φ_{TC} *are independent Boltzmann bipartite maps with a simple boundary, having respective distribution* $\widehat{\mathbb{P}}_\mathsf{q}^{(\deg(u)/2)}$.

Remark 5.3.4. The probability measure $\nu_\bullet$ is supported by odd integers, so the internal faces of $\mathrm{Scoop}(M)$ have even degree. This is consistent with the fact that $\mathbb{P}_{\mathsf{q},r_\mathsf{q}}$

is supported by bipartite maps. Note that M may have edges whose both sides are incident to the external face: this corresponds to a vertex of degree 2 of $\mathbf{Tree}(M)$ associated to the bipartite map with a simple boundary made of a single oriented edge.

Proof. Let us check that $\nu_\circ$ and $\nu_\bullet$ are probability measures. This is clear for $\nu_\circ$ which is a geometric distribution. For $\nu_\bullet$, we get recalling that $1 < F(r_\mathsf{q}) = \widehat{F}(r_\mathsf{q} F^2(r_\mathsf{q}))$

$$\sum_{k\in\mathbb{Z}_+} \nu_\bullet(k) = \frac{1}{F(r_\mathsf{q})-1}\left(\widehat{F}(r_\mathsf{q}F^2(r_\mathsf{q}))-1\right) = 1.$$

Let $\mathbf{m}\in\mathcal{B}_f$, and recall that Φ_{TC} associates to $\mathbf{m}$ its tree of components $\mathbf{t}=\mathbf{Tree}(\mathbf{m})$ and a collection $(\widehat{\mathbf{m}}_u : u\in\mathbf{t}_\bullet)$ of bipartite maps with a simple boundary and perimeter $\deg(u)$. Moreover, vertices of $\mathbf{t}_\bullet$ have even degree. Using (5.32) and (5.31), we have

$$\mathbb{P}_{\mathsf{q},r_\mathsf{q}}(\mathbf{m}) = \frac{r_\mathsf{q}^{\#\partial\mathbf{m}/2} w_\mathsf{q}^*(\mathbf{m})}{F(r_\mathsf{q})} = \frac{1}{F(r_\mathsf{q})}\prod_{u\in\mathbf{t}_\bullet} r_\mathsf{q}^{\deg(u)/2} w_\mathsf{q}^*(\widehat{\mathbf{m}}_u).$$

Then, for every $c>0$

$$1 = \prod_{u\in\mathbf{t}_\circ} c^{k_u}\left(\frac{1}{c}\right)^{|\mathbf{t}_\bullet|} \quad\text{and}\quad \frac{1}{c} = \prod_{u\in\mathbf{t}_\bullet} c^{k_u}\left(\frac{1}{c}\right)^{|\mathbf{t}_\circ|}.$$

Applying the first identity with $c = 1-1/F(r_\mathsf{q})$ and the second one with $c=F(r_\mathsf{q})$ yields

$$\begin{aligned}\mathbb{P}_{\mathsf{q},r_\mathsf{q}}(\mathbf{m}) &= \prod_{u\in\mathbf{t}_\circ}\frac{1}{F(r_\mathsf{q})}\left(1-\frac{1}{F(r_\mathsf{q})}\right)^{k_u}\prod_{u\in\mathbf{t}_\bullet}\frac{1}{F(r_\mathsf{q})-1}\left(r_\mathsf{q}F^2(r_\mathsf{q})\right)^{(k_u+1)/2} w_\mathsf{q}^*(\widehat{\mathbf{m}}_u)\\ &= \prod_{u\in\mathbf{t}_\circ}\nu_\circ(k_u)\prod_{u\in\mathbf{t}_\bullet}\nu_\bullet(k_u) w_\mathsf{q}^*(\widehat{\mathbf{m}}_u)\frac{1}{\widehat{F}_{(k_u+1)/2}}.\end{aligned}$$

By convention, we agree that both sides equal zero if there exists $u\in\mathbf{t}_\bullet$ such that $\widehat{F}_{(k_u+1)/2}=0$. Finally,

$$\begin{aligned}\mathbb{P}_{\mathsf{q},r_\mathsf{q}}\left(\mathbf{Tree}(M)=\mathbf{t}, \widehat{M}_u=\widehat{\mathbf{m}}_u : u\in\mathbf{t}_\bullet\right) &= \mathbb{P}_{\mathsf{q},r_\mathsf{q}}(M=\mathbf{m})\\ &= \mathsf{GW}_{\nu_\circ,\nu_\bullet}(\mathbf{t})\prod_{u\in\mathbf{t}_\bullet}\widehat{\mathbb{P}}_\mathsf{q}^{(\deg(u)/2)}(\widehat{\mathbf{m}}_u),\end{aligned}$$

which is the expected result. □

By Proposition 5.3.1, we obtain the following.

Corollary 5.3.5. *Let q be a weight sequence of type $a\in[3/2,5/2]$. Under $\mathbb{P}_{\mathsf{q},r_\mathsf{q}}$, the random tree $\Phi_{\mathrm{JS}}(\mathbf{Tree}(M))$ is a Galton-Watson tree with offspring distribution ν defined by*

$$\nu(2k) = \frac{1}{F(r_\mathsf{q})}\left(r_\mathsf{q}F^2(r_\mathsf{q})\right)^k\widehat{F}_k, \quad k\in\mathbb{Z}_+ \quad \textit{(and } \nu(k)=0 \textit{ for } k \textit{ odd)}.$$

As a consequence, the generating function of ν reads

$$G_\nu(s) = \frac{1}{F(r_\mathsf{q})} \sum_{k=0}^{\infty} s^{2k} \left(r_\mathsf{q} F^2(r_\mathsf{q})\right)^k \widehat{F}_k = \frac{1}{F(r_\mathsf{q})} \widehat{F}\left(r_\mathsf{q} F^2(r_\mathsf{q}) s^2\right), \quad s \in [0,1]. \tag{5.34}$$

From Lemma 5.2.10, we easily deduce the following formula for the mean of ν

$$m_\nu = G'_\nu(1) = \frac{1}{F(r_\mathsf{q})} 2 r_\mathsf{q} F^2(r_\mathsf{q}) \widehat{F}'\left(r_\mathsf{q} F^2(r_\mathsf{q})\right) = \frac{1}{1 + \frac{F(r_\mathsf{q})}{2 r_\mathsf{q} F'(r_\mathsf{q})}}. \tag{5.35}$$

Similarly, the generating function of $\nu_\bullet$ satisfies $G_{\nu_\bullet}(0) = 0$ and

$$G_{\nu_\bullet}(s) = \frac{1}{F(r_\mathsf{q}) - 1} \cdot \frac{1}{s} \left(\widehat{F}\left(r_\mathsf{q} F^2(r_\mathsf{q}) s^2\right) - 1\right), \quad s \in (0,1]. \tag{5.36}$$

We also have $m_{\nu_\circ} = F(r_\mathsf{q}) - 1$, so that by Proposition 5.3.1 and (5.35),

$$m_{\nu_\bullet} = \frac{m_\nu}{1 - \frac{1}{F(r_\mathsf{q})}} - 1 = \frac{1}{1 + \frac{F(r_\mathsf{q})}{2 r_\mathsf{q} F'(r_\mathsf{q})}} \cdot \frac{F(r_\mathsf{q})}{F(r_\mathsf{q}) - 1} - 1. \tag{5.37}$$

The next result is a consequence of (5.18).

Lemma 5.3.6. *The offspring distribution ν as well as the pair of offspring distributions $(\nu_\circ, \nu_\bullet)$ are critical if $a \in [3/2, 2]$ and subcritical if $a \in (2, 5/2]$.*

We now describe the tail of the measures ν and $\nu_\bullet$. The following is obtained by Proposition 5.2.8, (5.34) and (5.36). For $a = 3/2$, as $t \to 0^+$

$$L_\nu(t) = 1 - t + \left(1 + 4\widehat{c}_{3/2}\right) t^2 + o(t^2), \tag{5.38}$$

$$L_{\nu_\bullet}(t) = 1 - \left(\frac{1}{F(r_\mathsf{q}) - 1}\right) t + \left(\frac{1}{2} + 4\widehat{c}_{3/2} \frac{F(r_\mathsf{q})}{F(r_\mathsf{q}) - 1}\right) t^2 + o(t^2). \tag{5.39}$$

For $a \in (3/2, 2)$, as $t \to 0^+$

$$L_\nu(t) = 1 - t + 2^{\frac{1}{a-1}} t^{\frac{1}{a-1}} \widehat{\ell}(1/t) + o\left(t^{\frac{1}{a-1}} \widehat{\ell}(1/t)\right), \tag{5.40}$$

$$L_{\nu_\bullet}(t) = 1 - \left(\frac{1}{F(r_\mathsf{q}) - 1}\right) t + \frac{F(r_\mathsf{q})}{F(r_\mathsf{q}) - 1} 2^{\frac{1}{a-1}} t^{\frac{1}{a-1}} \widehat{\ell}(1/t) + o\left(t^{\frac{1}{a-1}} \widehat{\ell}(1/t)\right). \tag{5.41}$$

Finally, for $a \in (2, 5/2]$, as $t \to 0^+$,

$$L_\nu(t) = 1 - \widehat{c}_a t + 2^{a-1} t^{a-1} \widehat{\ell}(1/t) + o\left(t^{a-1} \widehat{\ell}(1/t)\right), \tag{5.42}$$

$$L_{\nu_\bullet}(t) = 1 - \left(1 - \widehat{c}_a \frac{F(r_\mathsf{q})}{F(r_\mathsf{q}) - 1}\right) t + \frac{F(r_\mathsf{q})}{F(r_\mathsf{q}) - 1} 2^{a-1} t^{a-1} \widehat{\ell}(1/t) + o\left(t^{a-1} \widehat{\ell}(1/t)\right). \tag{5.43}$$

The function $\widehat{\ell}(x) = \widehat{\ell}_1((1 - \exp(-2/x))^{-1})$ is slowly varying by [BGT89, Proposition 1.5.7]. Note that we recover formulas (5.35) and (5.37) from the definitions of $\widehat{c}_a$ (5.27) and C_q (5.23).

For $a = 3/2$, (5.38) and (5.27) entail that ν and $\nu_\bullet$ have finite variance equal to

$$\sigma_\nu^2 = \left(\frac{2P(r_{\mathsf{q}})}{\kappa'_{3/2}}\right)^2 = \left(\frac{F(r_{\mathsf{q}})}{Z_{\mathsf{q}}(1-m_\mu)}\right)^2 \quad \text{and} \quad \sigma_{\nu_\bullet}^2 = \frac{F(r_{\mathsf{q}})}{F(r_{\mathsf{q}})-1}\left(\left(\frac{F(r_{\mathsf{q}})}{Z_{\mathsf{q}}(1-m_\mu)}\right)^2 - 1\right). \tag{5.44}$$

If we assume additionally that $\widehat{r_{\mathsf{q}}} > r_{\mathsf{q}}F^2(r_{\mathsf{q}})$, there exists $s > 1$ such that $G_\nu(s) < \infty$ and $G_{\nu_\bullet}(s) < \infty$, so that ν and $\nu_\bullet$ have small exponential moments.

For $a \in (3/2, 2)$, Karamata's Tauberian theorem [BGT89, Theorem 8.1.6], (5.40) and (5.41) give

$$\nu([k,\infty)) \underset{k\to\infty}{\sim} \frac{2^{\frac{1}{a-1}}}{\left|\Gamma\left(\frac{a-2}{a-1}\right)\right|} \cdot \frac{\widehat{\ell}(k)}{k^{\frac{1}{a-1}}} \quad \text{and} \quad \nu_\bullet([k,\infty)) \underset{k\to\infty}{\sim} \frac{F(r_{\mathsf{q}})}{F(r_{\mathsf{q}})-1} \cdot \frac{2^{\frac{1}{a-1}}}{\left|\Gamma\left(\frac{a-2}{a-1}\right)\right|} \cdot \frac{\widehat{\ell}(k)}{k^{\frac{1}{a-1}}}. \tag{5.45}$$

Finally, when $a \in (2, 5/2]$, the same version of Karamata's Tauberian theorem gives

$$\nu([k,\infty)) \underset{k\to\infty}{\sim} \frac{2^{a-1}}{|\Gamma(2-a)|} \cdot \frac{\widehat{\ell}(k)}{k^{a-1}} \quad \text{and} \quad \nu_\bullet([k,\infty)) \underset{k\to\infty}{\sim} \frac{F(r_{\mathsf{q}})}{F(r_{\mathsf{q}})-1} \cdot \frac{2^{a-1}}{|\Gamma(2-a)|} \cdot \frac{\widehat{\ell}(k)}{k^{a-1}}. \tag{5.46}$$

Proposition 5.3.7. *For $a = 3/2$, ν and $\nu_\bullet$ have finite variance (and small exponential moments iff $\widehat{r_{\mathsf{q}}} > r_{\mathsf{q}}F^2(r_{\mathsf{q}})$). For $a \in (3/2, 2)$, ν and $\nu_\bullet$ are in the domain of attraction of a stable distribution with parameter $1/(a-1) \in (1,2)$ and for $a \in (2, 5/2]$, ν and $\nu_\bullet$ are in the domain of attraction of a stable distribution with parameter $a - 1 \in (1, 3/2]$.*

Remark 5.3.8. Again, the value $a = 2$ has to be excluded, even when an analogue of Proposition 5.2.6 holds. In this case, the expansion of the Laplace transform of ν is expected to have a singularity of integer order, for which Karamata's Tauberian theorem [BGT89, Theorem 8.1.6] provides a weaker result. This issue can be circumvented by using De Haan theory [BGT89, Chapter 3], as we will see in Section 5.7 (under additional assumptions on the weight sequence).

The results of Proposition 5.3.3 and Corollary 5.3.5 transfer to $\mathbb{P}_{\mathsf{q}}^{(k)}$. For every $n \geq 1$, we denote by $\mathsf{GW}_\rho^{(n)}$ (resp. $\mathsf{GW}_{\rho_\circ,\rho_\bullet}^{(n)}$) the law of a Galton-Watson tree with offspring distribution ρ (resp. $(\rho_\circ, \rho_\bullet)$) conditioned to have n vertices, provided this makes sense.

Corollary 5.3.9. *Let q be a weight sequence of type $a \in [3/2, 5/2]$. For every $k \geq 0$, under $\mathbb{P}_{\mathsf{q}}^{(k)}$, $\mathbf{Tree}(M)$ has distribution $\mathsf{GW}_{\nu_\circ,\nu_\bullet}^{(2k+1)}$, and $\Phi_{\mathsf{JS}}(\mathbf{Tree}(M))$ has distribution $\mathsf{GW}_\nu^{(2k+1)}$. Moreover, conditionally on $\mathbf{Tree}(M)$, the maps $(\widehat{M}_u : u \in \mathbf{Tree}(M)_\bullet)$ associated to M by Φ_{TC} are independent with respective distribution $\widehat{\mathbb{P}}_{\mathsf{q}}^{(\deg(u)/2)}$.*

Proof. Recall from (5.31) that for every $\mathbf{m} \in \mathcal{B}_f$, the size of $\mathbf{t} = \Phi_{\mathsf{JS}}(\mathbf{Tree}(\mathbf{m}))$ (or equivalently of $\mathbf{Tree}(\mathbf{m})$) equals $\#\partial\mathbf{m} + 1$. Then, by Proposition 5.3.3, for every $k \geq 1$,

$$\mathsf{GW}_\rho(\{|\mathbf{t}| = 2k+1\}) = \mathsf{GW}_{\rho_\circ,\rho_\bullet}(\{|\mathbf{t}| = 2k+1\}) = \mathbb{P}_{\mathsf{q},r_{\mathsf{q}}}\left(\mathcal{B}_f^{(k)}\right) = \frac{r_{\mathsf{q}}^k F_k}{F(r_{\mathsf{q}})},$$

which is positive by the results of Section 5.2.2. We conclude by applying Proposition 5.3.3. □

5.4 Scaling limits of the boundary of Boltzmann maps

This section deals with the scaling limits of the boundary of Boltzmann bipartite maps, in the Gromov-Hausdorff sense.

5.4.1 Continuum random trees and looptrees

The Gromov-Hausdorff topology. The Gromov-Hausdorff distance between two compact metric spaces (E_1, d_1) and (E_2, d_2) is defined by

$$d_{\mathrm{GH}}(E_1, E_2) := \inf\{d_{\mathrm{H}}(\varphi_1(E_1), \varphi_2(E_2))\},$$

where the infimum is taken over all choices of metric space (E, d) and all the isometric embeddings $\varphi_1 : E_1 \to E$ and $\varphi_2 : E_2 \to E$ of E_1 and E_2 into E, and d_{H} stands for the Hausdorff distance between compact sets in E. The set of compact metric spaces seen up to isometry equipped with d_{GH} is a Polish space.

A *correspondence* between (E_1, d_1) and (E_2, d_2) is a subset $\mathcal{R}$ of $E_1 \times E_2$ such that for every $x_1 \in E_1$, there exists $x_2 \in E_2$ such that $(x_1, x_2) \in \mathcal{R}$ and for every $x_2 \in E_2$, there exists $x_1 \in E_1$ such that $(x_1, x_2) \in \mathcal{R}$. The *distortion* of $\mathcal{R}$ with respect to d_1 and d_2 is defined by

$$\mathrm{dis}(\mathcal{R}) := \sup\{|d_1(x_1, y_1) - d_2(x_2, y_2)| : (x_1, x_2), (y_1, y_2) \in \mathcal{R}\}.$$

Then, the Gromov-Hausdorff distance between (E_1, d_1) and (E_2, d_2) also equals

$$d_{\mathrm{GH}}(E_1, E_2) = \frac{1}{2} \inf_{\mathcal{R} \subset E_1 \times E_2} \mathrm{dis}(\mathcal{R}),$$

where the infimum is over all correspondences. We refer to [BBI01] for further details on this topology.

Continuum random trees and looptrees. Let us describe the limiting objects that will appear in the remaining of this section. First, recall the coding of a real tree by its contour function (see [DLG05, LG05]). Given a nonnegative continuous function g on $[0, 1]$ with $g(0) = g(1) = 0$ (which is usually called a *normalized excursion*), let

$$d_g(s, t) := g(s) + g(t) - 2 \inf_{s \wedge t \le r \le s \vee t} g(r), \quad s, t \in [0, 1].$$

We introduce the equivalence relation $s \sim t$ iff $d_g(s, t) = 0$. The real tree coded by g is the quotient space $\mathscr{T}_g := [0, 1]/\sim$, equipped with the distance d_g. By [DLG05, Lemma 2.3] or [LG05, Lemma 2.4] we have

$$d_{\mathrm{GH}}\left(\mathscr{T}_{g_1}, \mathscr{T}_{g_2}\right) \le 2\|g_1 - g_2\|, \tag{5.47}$$

where $\|\cdot\|$ stands for the uniform norm and g_1, g_2 are arbitrary normalized excursions.

A plane tree $\mathbf{t} \in \mathcal{T}_f$ can be coded by its *contour function* $C = C(\mathbf{t})$, defined for $k \in \{0, \dots, 2(|\mathbf{t}| - 1)\}$ by $C_k = |u_k|$, where $(u_0, \dots, u_{2(|\mathbf{t}|-1)})$ is the sequence of vertices of $\mathbf{t}$ in contour order. We usually extend C on $\mathbb{R}_+$ by linear interpolation

(and the value zero beyond $2(|\mathbf{t}|-1)$). The real tree coded by $(C_{2(|\mathbf{t}|-1)s} : 0 \le s \le 1)$ is a continuous version of $\mathbf{t}$ (with edges of unit length). We will also deal with the *height function* $H = H(\mathbf{t})$ of a plane tree, defined for $k \in \{0, \dots, |\mathbf{t}|-1\}$ by $C_k = |\tilde{u}_k|$, where $(\tilde{u}_0, \dots, \tilde{u}_{|\mathbf{t}|-1})$ is the sequence of vertices of $\mathbf{t}$ in lexicographical order. Finally, the *Lukasiewicz path* $W = W(\mathbf{t})$ of the plane tree $\mathbf{t}$ is defined by $W_0 = 0$ and $W_{k+1} = W_k - 1 + k_{\tilde{u}_k}$, for $k \in \{0, \dots, |\mathbf{t}|-1\}$. The height function and the Lukasiewicz path are extended on $\mathbb{R}_+$ in the same way as the contour function.

The Brownian Continuum Random Tree (CRT) has been introduced by Aldous in [Ald91, Ald93]. It is the random compact real tree $\mathscr{T}_{\mathbb{e}}$ coded by the normalized brownian excursion $(\mathbb{e}_t : 0 \le t \le 1)$ (see [LG05] for details). The CRT is also the universal scaling limit of critical Galton-Watson trees with finite variance conditioned to survive. When the finite variance assumption is released but the offspring distribution is in the domain of attraction of a stable law with parameter $\beta \in (1,2)$, the scaling limit is the β-stable continuum random tree [Duq03]. The β-stable trees $(\mathscr{T}_\beta : \beta \in (1,2))$ were introduced by Duquesne & Le Gall [DLG02, DLG05]. They are real trees coded by the normalized excursion of the *continuous height processes* of [DLG02], that we denote by $(H^\beta_t : 0 \le t \le 1)$ (see [Duq03, Section 3.2] or [DLG05, Section 3] for details).

In [CK14b], Curien & Kortchemski introduced the random β-stable looptrees $(\mathscr{L}_\beta : \beta \in (1,2))$. These can intuitively be seen as dual to the stable trees, and appear as the scaling limit of discrete looptrees (see [CK14b, Theorem 4.1]). The β-stable trees and looptrees can be defined from the normalized excursion of a standard spectrally positive β-stable process, that we will denote by $(X^\beta_t : 0 \le t \le 1)$ (see [CK14b, Section 2.1], [LGM11a, Section 4.3] and [Ber98, Chapter VIII]).

5.4.2 Scaling limits for trees

We first deal with scaling limits for the tree of components under Φ_{JS}. For every metric space (E,d) and every $\lambda > 0$, $\lambda \cdot E$ stands for the metric space $(E, \lambda d)$.

Proposition 5.4.1. *Let* q *be a weight sequence of type* $a \in [3/2, 2)$. *For every* $k \ge 0$, *let* M_k *be a random planar map with distribution* $\mathbb{P}^{(k)}_{\mathsf{q}}$ *and set* $T_k := \Phi_{\mathrm{JS}}(\mathbf{Tree}(M_k))$. *Then, the following convergences hold in distribution for the Gromov-Hausdorff topology: For* $a = 3/2$,

$$\frac{\sigma_\nu}{2\sqrt{2k}} \cdot T_k \xrightarrow[k\to\infty]{(d)} \mathscr{T}_{\mathbb{e}},$$

while for $a \in (3/2, 2)$, *there exists a slowly varying function* $\ell_1^{\#}$ *such that*

$$\frac{2\ell_1^{\#}(k)}{(2k)^{2-a}} \cdot T_k \xrightarrow[k\to\infty]{(d)} \mathscr{T}_{\frac{1}{a-1}}.$$

Proof. Let $(X_i : i \ge 1)$ be a collection of i.i.d. random variables with law ν, and set $S_n = X_1 + \ldots + X_n$, for every $n \ge 1$. For $a = 3/2$, the central limit theorem yields

$$\frac{S_n - n}{\sigma_\nu \sqrt{n}} \xrightarrow[n\to\infty]{(d)} \mathcal{N}(0,1). \tag{5.48}$$

Using the De Bruijn conjugate of slowly varying functions [BGT89, Theorem 1.5.13], we find that for every $\gamma \in (1,2)$, there exists a slowly varying function $\ell_1^{\#}$ such that

$$\left(\ell_1^{\#}(x)\right)^{-\gamma} \widehat{\ell}\left(x^{1/\gamma}\ell_1^{\#}(x)\right) \underset{x\to\infty}{\longrightarrow} 1. \tag{5.49}$$

We let $\ell_1^{\#}$ be such a function with $\gamma := 1/(a-1)$, for every $a \in (3/2, 2)$. Then, by [Fel71, Theorem XVII.5.3] (see also [BGT89, Chapter 8] or [Jan11, Theorem 5.4]) we get for $a \in (3/2, 2)$

$$\frac{S_n - n}{2\ell_1^{\#}(n)n^{a-1}} \underset{n\to\infty}{\overset{(d)}{\longrightarrow}} \mathcal{S}^+_{\frac{1}{a-1}}, \tag{5.50}$$

where $\mathcal{S}^+_\gamma$ stands for the standard positive stable distribution with parameter γ, characterized by $E(\exp(-t\mathcal{S}^+_\gamma)) = \exp(t^\gamma)$, for $t \geq 0$.

We now apply the convergence results of [Ald93, Duq03]. By Corollary 5.3.9, T_k is a Galton-Watson tree with offspring distribution ν conditioned to have $2k+1$ vertices. The probability measure ν is periodic, which is excluded in [Ald93, Duq03]. However, as mentioned in [Kor13], the results still hold by considering subsequences as we will do. When $a = 3/2$, by [Ald93, Theorem 23],

$$\left(\frac{\sigma_\nu}{2\sqrt{2k+1}} C_{(4k)t}(T_k) : 0 \leq t \leq 1\right) \underset{k\to\infty}{\overset{(d)}{\longrightarrow}} (\mathbb{e}_t : 0 \leq t \leq 1), \tag{5.51}$$

in distribution for the topology of uniform convergence. For $a \in (3/2, 2)$, by [Duq03, Proposition 4.3] and the proof of [Duq03, Theorem 3.1], we have

$$\left(\left(2\ell_1^{\#}(2k+1)(2k+1)^{a-1}\right)^{-1} W_{(2k+1)t}(T_k) : 0 \leq t \leq 1\right) \underset{k\to\infty}{\overset{(d)}{\longrightarrow}} \left(X_t^{1/(a-1)} : 0 \leq t \leq 1\right), \tag{5.52}$$

in distribution for Skorokhod's topology. Moreover, by [Duq03, Theorem 3.1],

$$\left(2\ell_1^{\#}(2k+1)(2k+1)^{a-2} C_{(4k)t}(T_k) : 0 \leq t \leq 1\right) \underset{k\to\infty}{\overset{(d)}{\longrightarrow}} \left(H_t^{1/(a-1)} : 0 \leq t \leq 1\right), \tag{5.53}$$

in distribution for the topology of uniform convergence. The expected result follows from (5.53) and (5.47). □

Remark 5.4.2. For $a \in (2, 5/2]$, the situation is very different, because the offspring distribution ν is heavy-tailed and subcritical. This results in the so-called *condensation* phenomenon, first observed by Jonsson & Stefánsson in [JS10], and studied in greater detail in [Jan12, Kor15]. We will discuss this at the end of this section.

Remark 5.4.3. The scaling limit of the tree of components itself can be studied using [Ber16, Theorem 3]. However, the conditioning has to relate to the number of vertices at even (or odd) height in the tree, which amounts to conditioning the boundary of the map to have k vertices, instead of $2k$ edges. Precisely, for every $k \geq 1$, let M'_k be a planar map with distribution $\mathbb{P}_{\mathsf{q},r_\mathsf{q}}$ conditioned to have k vertices on its boundary. Then, under the proper rescaling, **Tree**(M'_k) converges in distribution for the Gromov-Hausdorff topology towards $\mathscr{T}_\mathbb{e}$ (if $a = 3/2$) or $\mathscr{T}_{\frac{1}{a-1}}$ (if $a \in (3/2, 2)$).

5.4.3 Scaling limits of the boundary of Boltzmann maps

This section deals with the scaling limits of the boundary of Boltzmann planar maps. We start with a preliminary result directly adapted from [CK14a], and illustrated in Figure 5.11.

Lemma 5.4.4. [CK14a, Lemma 4.3] *On the set $\mathcal{T}_f$ of finite plane trees, we have $\Phi_{\mathrm{JS}}^{-1} = \mathrm{Tree} \circ \overline{\mathbf{Loop}}$. In particular, for every $\mathbf{m} \in \mathcal{B}_f$, the planar maps $\mathrm{Scoop}(\mathbf{m})$ and $\overline{\mathbf{Loop}}(\Phi_{\mathrm{JS}}(\mathbf{Tree}(\mathbf{m})))$ are equal.*

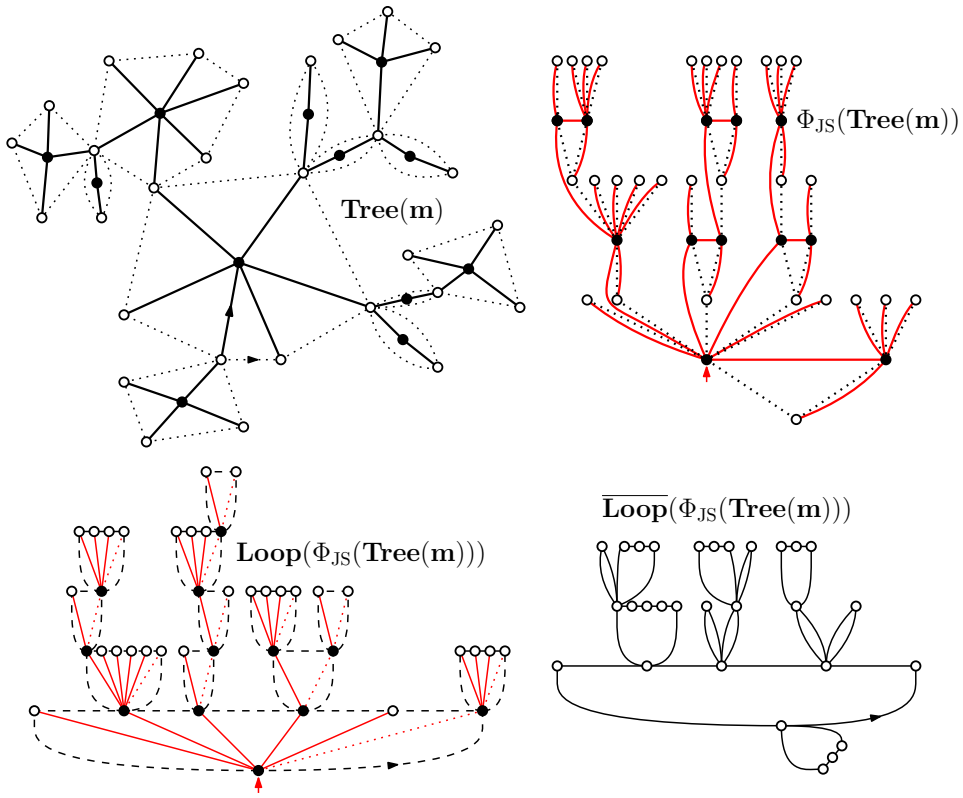

Figure 5.11: The tree of components of a bipartite map $\mathbf{m}$, its image $\Phi_{\mathrm{JS}}(\mathbf{Tree}(\mathbf{m}))$ under the Janson–Stefánsson bijection, and the associated looptrees $\mathbf{Loop}(\Phi_{\mathrm{JS}}(\mathbf{Tree}(\mathbf{m})))$ and $\overline{\mathbf{Loop}}(\Phi_{\mathrm{JS}}(\mathbf{Tree}(\mathbf{m})))$.

Scaling limits for the boundary: the dense regime. We first focus on the dense phase $a \in (3/2, 2)$ and prove Theorem 5.1.1. Our proof is based on scaling limits results of [CK14b] concerning looptrees, and parallels the proof of [CK14a, Theorem 1.2].

Proof of Theorem 5.1.1. For every $k \geq 0$, let M_k be a random planar map with distribution $\mathbb{P}_{\mathsf{q}}^{(k)}$ and set $T_k := \Phi_{\mathrm{JS}}(\mathbf{Tree}(M_k))$. First of all, by definition of $\overline{\mathbf{Loop}}$, we have

$$d_{\mathrm{GH}}\left(\mathbf{Loop}(T_k), \overline{\mathbf{Loop}}(T_k)\right) \leq 2\|H(T_k)\|_\infty. \tag{5.54}$$

Indeed, the longest path of vertices of T_k identified in $\overline{\mathbf{Loop}}(T_k)$ has length at most $\|H(T_k)\|_\infty$, which is the overall height of T_k. By Proposition 5.4.1 and (5.53), we also

get that

$$\frac{\|H(T_k)\|_\infty}{k^{a-1}} \underset{k\to\infty}{\longrightarrow} 0 \quad \text{in probability.} \tag{5.55}$$

Together with (5.52), this ensures that the invariance principle of [CK14b, Theorem 4.1] applies, which proves that

$$\frac{2^{2-a}}{\ell_1^{\#}(k)k^{a-1}} \cdot \mathbf{Loop}(T_k) \overset{(d)}{\underset{k\to\infty}{\longrightarrow}} \mathscr{L}_{\frac{1}{a-1}},$$

in the Gromov-Hausdorff sense. Applying (5.54), (5.55) and Lemma 5.4.4, we deduce that

$$\frac{2^{2-a}}{\ell_1^{\#}(k)k^{a-1}} \cdot \mathrm{Scoop}(M_k) \overset{(d)}{\underset{k\to\infty}{\longrightarrow}} \mathscr{L}_{\frac{1}{a-1}},$$

in the Gromov-Hausdorff sense. This concludes the proof since for any planar map $\mathbf{m}$, $\partial\mathbf{m}$ and $\mathrm{Scoop}(\mathbf{m})$ define the same metric space. □

Scaling limits for the boundary: the subcritical regime. We now consider the subcritical case. However, we need a more restrictive assumptions on the partition function $\widehat{F}_k$.

Proposition 5.4.5. *Let* q *be a subcritical weight sequence (of type* $a = 3/2$*), and assume that* $\widehat{r}_\mathsf{q} > r_\mathsf{q}F^2(r_\mathsf{q})$*. For every* $k \geq 0$*, let* M_k *be a random planar map with distribution* $\mathbb{P}_\mathsf{q}^{(k)}$*. Then, we have in distribution for the Gromov-Hausdorff topology*

$$\frac{K_\mathsf{q}}{\sqrt{2k}} \cdot \partial M_k \overset{(d)}{\underset{k\to\infty}{\longrightarrow}} \mathscr{T}_{\mathbb{e}}, \quad \textit{where} \quad K_\mathsf{q} = \frac{2F(r_\mathsf{q})Z_\mathsf{q}(1-m_\mu)}{Z_\mathsf{q}^2(1-m_\mu)^2 + F(r_\mathsf{q})^2}.$$

Proof. For every $k \geq 0$, let M_k be a planar map with distribution $\mathbb{P}_\mathsf{q}^{(k)}$ and set $T_k := \Phi_{\mathrm{JS}}(\mathbf{Tree}(M_k))$. By Corollary 5.3.9, T_k is a Galton-Watson tree with offspring distribution ν conditioned to have $2k+1$ vertices. Moreover, by Lemma 5.3.6 and Proposition 5.3.7, ν is critical with small exponential moments, and by (5.44) its variance reads

$$\sigma_\nu^2 = \left(\frac{F(r_\mathsf{q})}{Z_\mathsf{q}(1-m_\mu)}\right)^2.$$

Then, we can apply [CHK15, Theorem 14] which yields that

$$\frac{1}{\sqrt{2k}} \cdot \overline{\mathbf{Loop}}(T_k) \overset{(d)}{\underset{k\to\infty}{\longrightarrow}} \frac{\sigma_\nu^2+1}{2\sigma_\nu} \cdot \mathscr{T}_{\mathbb{e}},$$

in the Gromov-Hausdorff sense. We conclude the proof by Lemma 5.4.4 and the fact that for any planar map $\mathbf{m}$, $\partial\mathbf{m}$ and $\mathrm{Scoop}(\mathbf{m})$ define the same metric space. □

Remark 5.4.6. As we mentioned in Remark 5.2.9, it is not clear whether or not the assumption $\widehat{r}_\mathsf{q} > r_\mathsf{q}F^2(r_\mathsf{q})$ holds for any subcritical sequence q. However, we believe that [CHK15, Theorem 14] holds without the finite exponential moments assumption, and hope to investigate this in a future work. This would prove that Proposition 5.4.5 holds in full generality.

Still, by Remark 5.2.9 once again, the assumption $\widehat{r_{\mathsf{q}}} > r_{\mathsf{q}}F^2(r_{\mathsf{q}})$ is satisfied for subcritical Boltzmann quadrangulations. Furthermore, we believe that in this case, an adaptation of [Bet15, Theorem 5] shows that

$$\frac{1}{\sqrt{2k}} \cdot M_k \xrightarrow[k\to\infty]{(d)} \mathscr{T}_{\mathbb{e}},$$

in the Gromov-Hausdorff sense. As a consequence, the constant $1/K_{\mathsf{q}}$ can be interpreted as the asymptotic average diameter of a simple component in M_k.

Scaling limits for the boundary: the generic and dilute regimes. We finally deal with the generic and dilute regimes. We prove a partial result whose proof needs extra assumptions on the partition function $\widehat{F}_k$.

Proposition 5.4.7. *Let* q *be a weight sequence of type* $a = (2, 5/2]$*, and assume that there exists a slowly varying function* ℓ_d *such that*

$$\widehat{F}_k \underset{k\to\infty}{\sim} \frac{\ell_d(k)}{k^a} \widehat{r_{\mathsf{q}}}^{-k}. \tag{5.56}$$

For every $k \geq 0$*, let* M_k *be a random planar map with distribution* $\mathbb{P}_{\mathsf{q}}^{(k)}$*, and denote by* $\mathbb{S}_1$ *the unit circle. Then, we have in distribution for the Gromov-Hausdorff topology*

$$\frac{K_{\mathsf{q}}}{2k} \cdot \partial M_k \xrightarrow[k\to\infty]{(d)} \mathbb{S}_1, \quad \textit{where} \quad K_{\mathsf{q}} = 2\pi \left(1 + \frac{2r_{\mathsf{q}}F'(r_{\mathsf{q}})}{F(r_{\mathsf{q}})}\right).$$

Proof. The proof follows that of [CK14a, Theorem 1.2]. For every $k \geq 0$, let M_k be a map with distribution $\mathbb{P}_{\mathsf{q}}^{(k)}$ and set $T_k := \Phi_{\mathrm{JS}}(\mathbf{Tree}(M_k))$. By Corollary 5.3.9, T_k is a Galton-Watson tree with offspring distribution ν conditioned to have $2k+1$ vertices, and by Lemma 5.3.6, assumption (5.56) and Corollary 5.3.5, ν is subcritical and satisfies

$$\nu(2k) \underset{k\to\infty}{\sim} \frac{\ell_d(k)}{F(r_{\mathsf{q}})k^a}.$$

Under these hypotheses, [JS10, Theorem 5.5] (slightly adapted to our periodic setting $\nu(2\mathbb{Z}) = 1$ by considering a subsequence) ensures that there is an asymptotically unique vertex $u_k^* \in T_k$ with maximal degree, such that

$$\frac{\deg(u_k^*)}{2k} \xrightarrow[k\to\infty]{} 1 - m_\nu \quad \text{in probability.}$$

Moreover, by [Kor15, Corollary 2], if $\{T_j^* : 1 \leq j \leq \deg(u_k^*)\}$ are the connected components of $T_k \backslash \{u_k^*\}$ we have

$$\frac{1}{k} \sup_{1\leq j\leq \deg(u_k^*)} |T_j^*| \xrightarrow[k\to\infty]{} 0 \quad \text{in probability.}$$

Since $\nu_\circ$ is geometric, u_k^* is a black vertex of $\mathbf{Tree}(M_k)$ with probability tending to one as $k \to \infty$. Then, by properties of the Janson–Stefánsson bijection, $\mathrm{Scoop}(M_k)$ has a unique loop of perimeter $(1 - m_\nu)2k + o(k)$, and the largest connected component of $\mathrm{Scoop}(M_k)$ deprived of this loop has size $o(k)$. We conclude the proof using the formula (5.35) for m_ν. □

Remark 5.4.8. As we mentioned in Remark 5.2.9, we do not have an equivalent of the partition function $\widehat{F}_k$ itself, which is needed to apply the results of [JS10, Kor15]. However, we believe that Proposition 5.4.7 holds independently of assumption (5.56) and also hope to investigate this in a future work. By Remark 5.2.9, the assumption (5.56) is satisfied for critical Boltzmann quadrangulations (for which q is generic critical ($a = 5/2$)). In this case, [BM15, Theorem 8] also proves that

$$\sqrt{\frac{3}{2k}} \cdot M_k \xrightarrow[k\to\infty]{(d)} \mathsf{FBD}_1,$$

in the Gromov-Hausdorff sense. The random compact metric space FBD_1 is the Free Brownian Disk with perimeter 1, and is proved in [BM15] to have the topology of the unit disk (which is consistent with Proposition 5.4.7).

5.5 Local limits of the boundary of Boltzmann maps

In this section, we are interested in local limits of Boltzmann planar maps and their boundary.

5.5.1 Local limits of Galton-Watson trees

The local topology. The *local topology* on the set $\mathcal{B}_f$ is induced by the local distance

$$d_{\mathrm{loc}}(\mathbf{m}, \mathbf{m}') := \left(1 + \sup\left\{R \geq 0 : \mathbf{B}_R(\mathbf{m}) = \mathbf{B}_R(\mathbf{m}')\right\}\right)^{-1}, \quad \mathbf{m}, \mathbf{m}' \in \mathcal{B}_f. \tag{5.57}$$

Here, $\mathbf{B}_R(\mathbf{m})$ is the ball of radius R in $\mathbf{m}$ for the graph distance, centered at the origin vertex. More precisely, $\mathbf{B}_0(\mathbf{m})$ is the origin of $\mathbf{m}$, and for every $R \in \mathbb{N}$, $\mathbf{B}_R(\mathbf{m})$ contains all the vertices of $\mathbf{m}$ at distance less than R from the origin, and all the edges whose endpoints are in this set.

Equipped with d_{loc}, $\mathcal{B}_f$ is a metric space whose completion is denoted by $\mathcal{B}$. The elements of $\mathcal{B}_\infty := \mathcal{B}\backslash\mathcal{B}_f$ are called infinite bipartite planar maps and are represented by a consistent sequence of balls of radius R, for $R \geq 0$. However, an infinite (bipartite) planar map with one end (as a graph) can be seen as the equivalence class (up to orientation preserving homeomorphisms) of proper embeddings of an infinite graph in the plane $\mathbb{R}^2$ such that every compact intersects finitely many edges (see [Cur16a, Proposition 2]). In what follows, we restrict our attention to infinite planar maps that are one-ended or have a canonical embedding in the plane, so that we may always view elements of $\mathcal{B}_\infty$ as such equivalence classes. Then, the boundary $\partial\mathbf{m}$ of an infinite planar map $\mathbf{m} \in \mathcal{B}_\infty$ is the embedding of edges and vertices of its root face. When the boundary is infinite, it is called simple if isomorphic to $\mathbb{Z}$.

The set $\mathcal{T}_{\mathrm{loc}}$ of locally finite trees is the completion of $\mathcal{T}_f$ for d_{loc}. It is also obtained by extending the definition of a finite plane tree to possibly infinite trees, but whose vertices all have finite degree (i.e., $k_u(\mathbf{t}) < \infty$ for every $u \in \mathbf{t}$).

In order to take account of convergence towards plane trees with vertices of infinite degree, a weaker form of local convergence has been introduced in [JS10] (see

also [Jan12, Section 6] for a detailed presentation). The idea is to replace the ball $\mathbf{B}_R(\mathbf{t})$ in (5.57) by the sub-tree $\mathbf{B}_R^{\leftarrow}(\mathbf{t})$, called the *left ball* of radius R of $\mathbf{t}$. Formally, the root vertex belongs to $\mathbf{B}_R^{\leftarrow}(\mathbf{t})$, and a vertex $u = \widehat{u}k \in \mathbf{t}$ belongs to $\mathbf{B}_R^{\leftarrow}(\mathbf{t})$ iff $\widehat{u} \in \mathbf{t}$, $k \leq R$ and $|u| \leq R$.

For our purposes, a slightly stronger form of convergence is needed. We introduce a notation. For every $\mathbf{t} \in \mathcal{T}_f$ and every $u \in \mathbf{t}$, we denote by $(-u1, -u2, \ldots, -uk_u) = (uk_u, u(k_u - 1), \ldots, u1)$ the children of u in counterclockwise order. For every $\mathbf{t} \in \mathcal{T}_f$ and every $R \geq 0$, the *left-right ball* of radius R in $\mathbf{t}$ is the sub-tree $\mathbf{B}_R^{\leftrightarrow}(\mathbf{t})$ defined as follows. First, $\emptyset \in \mathbf{B}_R^{\leftrightarrow}(\mathbf{t})$. Then, a vertex $u \in \mathbf{t}$ belongs to $\mathbf{B}_R^{\leftrightarrow}(\mathbf{t})$ iff $\widehat{u} \in \mathbf{B}_R^{\leftrightarrow}(\mathbf{t})$, $|u| \leq 2R$ and $u \in \{\widehat{u}1, \ldots, \widehat{u}R\} \cup \{-\widehat{u}1, \ldots, -\widehat{u}R\}$ (i.e., u is among the R first or last children of its parent).

We call *local-$*$ topology* the topology on $\mathcal{T}_f$ induced by the distance

$$d^*_{\mathrm{loc}}(\mathbf{t}, \mathbf{t}') := \left(1 + \sup\left\{R \geq 0 : \mathbf{B}_R^{\leftrightarrow}(\mathbf{t}) = \mathbf{B}_R^{\leftrightarrow}(\mathbf{t}')\right\}\right)^{-1}, \quad \mathbf{t}, \mathbf{t}' \in \mathcal{T}_f.$$

The set $\mathcal{T}$ of general plane trees is the completion of $\mathcal{T}_f$ for d^*_{loc}. An element of $\mathcal{T}$ can also be seen as a tree embedded in the plane. In restriction to $\mathcal{T}_{\mathrm{loc}}$, the local and local-$*$ topologies coincide.

Local limits of conditioned Galton-Watson trees. We next recall results concerning local limits of Galton-Watson trees conditioned to survive.

The critical case. The critical setting was first investigated by Kesten in [Kes86b] (see also [LP16]) for monotype trees and extended by Stephenson in [Ste16, Theorem 3.1] to multi-type trees. Let $(\rho_\circ, \rho_\bullet)$ be a critical pair of offspring distributions, and recall that for every probability measure ρ on $\mathbb{Z}_+$ with mean $m_\rho \in (0, \infty)$, the size-biased distribution $\bar{\rho}$ is defined by

$$\bar{\rho}(k) := \frac{k\rho(k)}{m_\rho}, \quad k \in \mathbb{Z}_+.$$

The infinite random tree $\mathbf{T}_\infty^{\circ,\bullet} = \mathbf{T}_\infty^{\circ,\bullet}(\rho_\circ, \rho_\bullet)$ is defined as follows in [Ste16]. It has a.s. a unique infinite spine, i.e., a distinguished sequence of vertices $(u_0 = \emptyset, u_1, \ldots)$ such that $\widehat{u}_k = u_{k-1}$ for every $k \geq 1$. White (resp. black) vertices of the spine have offspring distribution $\bar{\rho}_\circ$ (resp. $\bar{\rho}_\bullet$), and a unique child in the spine chosen uniformly at random among their offspring. Outside of the spine, white (resp. black) vertices have offspring distribution $\rho_\circ$ (resp. $\rho_\bullet$), and all the number of offspring are independent. The tree $\mathbf{T}_\infty^{\circ,\bullet}$ is illustrated in Figure 5.12, and its distribution is denoted by $\mathsf{GW}^{(\infty)}_{\rho_\circ,\rho_\bullet}$.

Proposition 5.5.1. [Ste16, Theorem 3.1] *Let $(\rho_\circ, \rho_\bullet)$ be a critical pair of offspring distributions. For every $k \geq 1$, assume that $\mathsf{GW}_{\rho_\circ,\rho_\bullet}(\{|\mathbf{t}| = k\}) > 0$ and let $T_k^{\circ,\bullet}$ be a tree with distribution $\mathsf{GW}^{(k)}_{\rho_\circ,\rho_\bullet}$. Then, we have in distribution for the local topology*

$$T_k^{\circ,\bullet} \xrightarrow[k\to\infty]{(d)} \mathbf{T}_\infty^{\circ,\bullet}(\rho_\circ, \rho_\bullet).$$

The condition $\mathsf{GW}_{\rho_\circ,\rho_\bullet}(\{|\mathbf{t}| = k\}) > 0$ for every $k \geq 1$ can be relaxed, provided we consider subsequences along which it is satisfied. A similar result holds for critical

monotype Galton-Watson trees conditioned to survive. Then, the limiting tree is called *Kesten's tree*.

The subcritical case. We first deal with subcritical monotype trees, first considered in [JS10], and studied in full generality in [Jan12, Theorem 7.1]. Let ρ be a subcritical offspring distribution (such that $\rho(0) \in (0,1)$). The infinite random tree $\mathbf{T}_\infty = \mathbf{T}_\infty(\rho)$ is defined as follows in [JS10, Jan12]. It has a.s. a unique finite spine of random size L, such that

$$P(L = k) = (1 - m_\rho)m_\rho^{k-1}, \quad k \in \mathbb{N}.$$

The last vertex of the spine has infinite degree. The $L-1$ first vertices of the spine have offspring distribution $\bar{\rho}$, and a unique child in the spine chosen uniformly among the offspring. Outside of the spine, vertices have offspring distribution ρ, and all the number of offsprings are independent. This defines a random element of $\mathcal{T}$.

Proposition 5.5.2. [Jan12, Theorem 7.1] *Let ρ be a subcritical offspring distribution with no exponential moment (and $\rho(0) \in (0,1)$). For every $k \geq 1$, assume that $\mathsf{GW}_\rho(\{|\mathbf{t}| = k\}) > 0$ and let T_k be a tree with distribution $\mathsf{GW}_\rho^{(k)}$. Then, in distribution for the local-$*$ topology,*

$$T_k \xrightarrow[k\to\infty]{(d)} \mathbf{T}_\infty(\rho).$$

Proof. The proof follows from [Jan12, Theorem 7.1]. However, the notion of convergence in this result is equivalent to the convergence of left-balls of any radii (see [Jan12, Lemma 6.3]), which is weaker than our statement. Then, observe that for every $\mathbf{t} \in \mathcal{T}_f$, $k \geq 0$ and $R \geq 0$ we have

$$\mathsf{GW}_\rho^{(k)}\left(\mathbf{B}_R^{\leftrightarrow}(T) = \mathbf{t}\right) = \mathsf{GW}_\rho^{(k)}\left(\mathbf{B}_{2R}^{\leftarrow}(T) = \mathbf{t}\right).$$

Indeed, $\mathsf{GW}_\rho^{(k)}$ is invariant under the operation consisting in exchanging the descendants of $(u(R+1), \dots u(2R))$ and $(-u1, \dots -uR)$ for every $u \in T$ such that $k_u(T) > 2R$ (which exchanges $\mathbf{B}_R^{\leftrightarrow}(T)$ and $\mathbf{B}_{2R}^{\leftarrow}(T)$). This concludes the argument. □

We extend Proposition 5.5.2 to a two-type Galton-Watson tree. Let $(\rho_\circ, \rho_\bullet)$ be a subcritical pair of offspring distributions. We define a two-type version $\mathbf{T}_\infty^{\circ,\bullet} = \mathbf{T}_\infty^{\circ,\bullet}(\rho_\circ, \rho_\bullet)$ of $\mathbf{T}_\infty$ as follows. It has a.s. a unique spine, with random number of vertices $2L'$ satisfying

$$P(L' = k) = (1 - m_{\rho_\circ} m_{\rho_\bullet})(m_{\rho_\circ} m_{\rho_\bullet})^{k-1}, \quad k \in \mathbb{N}.$$

The topmost (black) vertex of the spine has infinite degree. The $2L'-1$ first vertices of the spine have offspring distribution $\bar{\rho}_\circ$ (if white) and $\bar{\rho}_\bullet$ (if black), with a unique child in the spine chosen uniformly among the offspring. Outside of the spine, white (resp. black) vertices have offspring distribution $\rho_\circ$ (resp. $\rho_\bullet$), and all the number of offsprings are independent. We keep the notation $\mathsf{GW}_{\rho_\circ,\rho_\bullet}^{(\infty)}$ for the distribution of $\mathbf{T}_\infty^{\circ,\bullet}$. See Figure 5.12 for an illustration.

Proposition 5.5.3. *Let $(\rho_\circ, \rho_\bullet)$ be a subcritical pair of offspring distributions, such that $\rho_\circ$ has geometric distribution with parameter $1-p \in (0,1)$: $\rho_\circ(k) = (1-p)p^k$ for*

every $k \geq 0$, and such that $\rho_\bullet$ has no exponential moment. For every $k \geq 1$, assume that $\mathsf{GW}_{\rho_\circ,\rho_\bullet}(\{|\mathbf{t}| = k\}) > 0$ and let $T_k^{\circ,\bullet}$ be a tree with distribution $\mathsf{GW}^{(k)}_{\rho_\circ,\rho_\bullet}$. Then, in distribution for the local-$*$ topology,

$$T_k^{\circ,\bullet} \xrightarrow[k\to\infty]{(d)} \mathbf{T}_\infty^{\circ,\bullet}(\rho_\circ, \rho_\bullet).$$

The condition $\mathsf{GW}_{\rho_\circ,\rho_\bullet}(\{|\mathbf{t}| = k\}) > 0$ for every $k \geq 1$ can be relaxed by considering subsequences. For every $\mathbf{t} \in \mathcal{T}_f$ and every $u \in \mathbf{t}$, we denote by $[\emptyset, u]$ (resp. $[\emptyset, u)$) the ancestral line of u in $\mathbf{t}$, u included (resp. excluded).

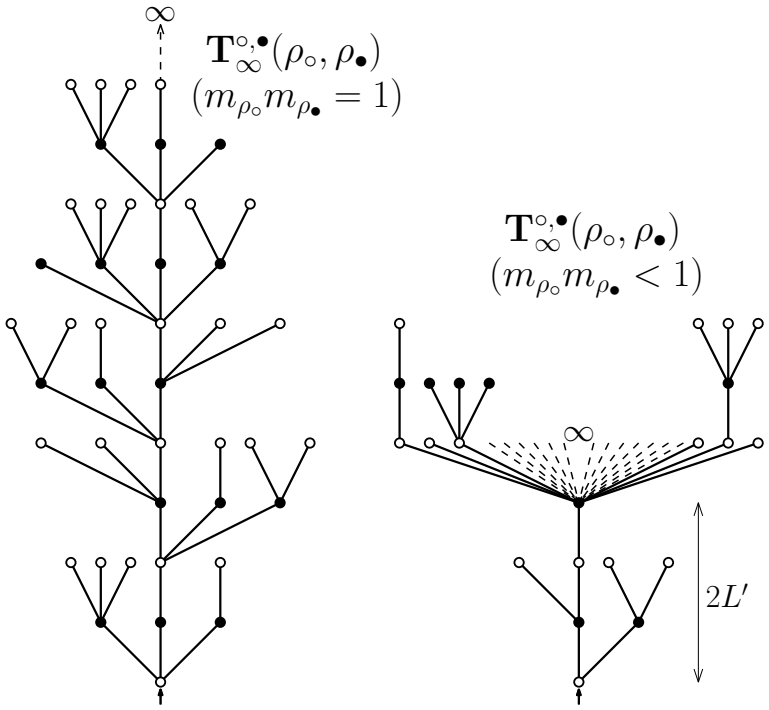

Figure 5.12: The local limits of two-type Galton-Watson trees conditioned to survive.

Proof. For every $k \geq 1$, let $T_k := \Phi_{\mathrm{JS}}(T_k^{\circ,\bullet})$. By Proposition 5.3.1, T_k has distribution $\mathsf{GW}_\rho^{(k)}$, where ρ satisfies

$$\rho(0) = 1 - p \quad \text{and} \quad \rho(k) = p \cdot \rho_\bullet(k-1), \quad k \in \mathbb{N}.$$

In particular, ρ satisfies the hypothesis of Proposition 5.5.2. For every $N \geq 1$, let $u_N = u_N(T_k)$ be the first vertex of $\mathbf{B}_N^{\leftrightarrow}(T_k)$ in contour order having $2N$ offspring (or the root vertex if such a vertex does not exist). For every $R \geq 0$, we also let $T_k\langle u_N, R\rangle$ be the collection of subtrees of T_k containing all the children of u_N different from $\{\pm u_N 1, \dots \pm u_N R\}$, as well as their descendants. Finally, set $T_k[N, R] := \mathbf{B}_N^{\leftrightarrow}(T_k) \backslash T_k\langle u_N, R\rangle$, and extend these definitions to $\mathbf{T}_\infty = \mathbf{T}_\infty(\rho)$. We denote by u_∞ the a.s. unique vertex with infinite degree of $\mathbf{T}_\infty$, and let $\mathbf{T}_\infty[R]$ be the subtree of $\mathbf{T}_\infty$ in which children of u_∞ different from $\{u_\infty 1, \dots u_\infty R\}$ and their descendants are discarded. This definition immediately extends to $\mathbf{T}_\infty^{\circ,\bullet}$.

Fix $R \geq 0$. By Proposition 5.5.2 and the definition of $\mathbf{T}_\infty$, we have in the local sense

$$T_k[N, R+1] \xrightarrow[k\to\infty]{(d)} \mathbf{T}_\infty[N, R+1], \quad \text{and} \quad \mathbf{T}_\infty[N, R+1] \xrightarrow[N\to\infty]{(d)} \mathbf{T}_\infty[2(R+1)]. \tag{5.58}$$

In particular, the event (measurable with respect to $\mathbf{B}_N^{\leftrightarrow}(T_k)$)

$$\mathcal{E}(R, N, k) := \left\{ \sup_{u \in T_k[N, R+1]} (|u| \vee k_u) < N \right\}$$

has probability tending to one when k and then N go to infinity. On the event $\mathcal{E}(R, N, k)$, one has $T_k \backslash T_k[N, R+1] \subseteq T_k\langle u_N, R+1\rangle$, which in turn enforces

$$\mathbf{B}_R^{\leftrightarrow}(T_k^{\circ,\bullet}) = \mathbf{B}_R^{\leftrightarrow}(\Phi_{\mathrm{JS}}^{-1}(T_k)) \subseteq \Phi_{\mathrm{JS}}^{-1}(T_k[N, R+1]). \tag{5.59}$$

Indeed, under this assumption, the images of vertices of $T_k \backslash T_k[N, R+1]$ in $\Phi_{\mathrm{JS}}^{-1}(T_k)$ are descendants of the children of $u'_N := \Phi_{\mathrm{JS}}^{-1}(u_N)$ that are not in $\{\pm u'_N 1, \dots \pm u'_N R\}$. (See Section 5.3.1 for details on the inverse Janson–Stefánsson bijection, and Figure 5.13 for an illustration.)

Let $d \geq 0$, and keep the notation u_∞ for the pointed vertex with d children in $\mathbf{T}_\infty[d]$ and $\mathbf{T}_\infty^{\circ,\bullet}[d]$. We denote by $\mathsf{GW}_\rho^{[d]}$ the distribution of $(\mathbf{T}_\infty[d], u_\infty)$, and by $\mathsf{GW}_{\rho_\circ,\rho_\bullet}^{[d]}$ the distribution of $(\mathbf{T}_\infty^{\circ,\bullet}[d], u_\infty)$. Then, the image of $\mathsf{GW}_{\rho_\circ,\rho_\bullet}^{[d]}$ under Φ_{JS} reads

$$\Phi_{\mathrm{JS}}\left(\mathsf{GW}_{\rho_\circ,\rho_\bullet}^{[d]}\right) = \mathsf{GW}_\rho^{[d+1]}. \tag{5.60}$$

We temporarily admit (5.60) and conclude the proof. Let A be a Borel set for the local-$*$ topology. We have by (5.59) that for every $k \geq 1$ and $N \geq 1$

$$\left|P\left(\mathbf{B}_R^{\leftrightarrow}\left(T_k^{\circ,\bullet}\right) \in A\right) - P\left(\mathbf{B}_R^{\leftrightarrow}\left(\Phi_{\mathrm{JS}}^{-1}(T_k[N, R+1])\right) \in A\right)\right| \leq 2P(\mathcal{E}(R, N, k)^c).$$

Next, for every $N \geq 1$, (5.58) entails

$$\left|P\left(\mathbf{B}_R^{\leftrightarrow}\left(\Phi_{\mathrm{JS}}^{-1}(T_k[N, R+1])\right) \in A\right) - P\left(\mathbf{B}_R^{\leftrightarrow}\left(\Phi_{\mathrm{JS}}^{-1}(\mathbf{T}_\infty[N, R+1])\right) \in A\right)\right| \underset{k\to\infty}{\longrightarrow} 0.$$

Then, by (5.58) again and the fact that $\mathbf{T}_\infty[2(R+1)]$ is a.s. finite,

$$\left|P\left(\mathbf{B}_R^{\leftrightarrow}\left(\Phi_{\mathrm{JS}}^{-1}(\mathbf{T}_\infty[N, R+1])\right) \in A\right) - P\left(\mathbf{B}_R^{\leftrightarrow}\left(\Phi_{\mathrm{JS}}^{-1}(\mathbf{T}_\infty[2(R+1)])\right) \in A\right)\right| \underset{N\to\infty}{\longrightarrow} 0.$$

Finally, for every $R \geq 0$, $\mathbf{B}_R^{\leftrightarrow}\left(\mathbf{T}_\infty^{\circ,\bullet}\right) = \mathbf{B}_R^{\leftrightarrow}\left(\mathbf{T}_\infty^{\circ,\bullet}[2R+1]\right)$ so that by (5.60),

$$\begin{aligned} P\left(\mathbf{B}_R^{\leftrightarrow}\left(\Phi_{\mathrm{JS}}^{-1}(\mathbf{T}_\infty[2(R+1)])\right) \in A\right) &= P\left(\mathbf{B}_R^{\leftrightarrow}\left(\mathbf{T}_\infty^{\circ,\bullet}[2R+1]\right) \in A\right) \\ &= P\left(\mathbf{B}_R^{\leftrightarrow}\left(\mathbf{T}_\infty^{\circ,\bullet}\right) \in A\right). \end{aligned}$$

As a conclusion, by letting k and then N go to infinity, we have

$$\lim_{k\to\infty} \left|P\left(\mathbf{B}_R^{\leftrightarrow}\left(T_k^{\circ,\bullet}\right) \in A\right) - P\left(\mathbf{B}_R^{\leftrightarrow}\left(\mathbf{T}_\infty^{\circ,\bullet}\right) \in A\right)\right| = 0,$$

which ends the proof.

Let us now prove assertion (5.60). Let $(\mathbf{t}, u^*)$ be a pointed plane tree such that $k_{u^*}(\mathbf{t}) = d+1$. By definition, $(\mathbf{t}', v^*) := \Phi_{\mathrm{JS}}^{-1}(\mathbf{t}, u^*)$ is a pointed plane tree satisfying $k_{v^*}(\mathbf{t}') = d$, and $v^* \in \mathbf{t}'_\bullet$. Then, we have by definition of $\rho_\circ$ and the identity $\sum_{u\in\mathbf{t}'_\circ} k_u(\mathbf{t}') = |\mathbf{t}'_\bullet|$,

$$\begin{aligned}
\mathsf{GW}^{[d]}_{\rho_\circ,\rho_\bullet}\left(\Phi_{\mathrm{JS}}^{-1}((\mathbf{t},u^*))\right) &= \mathsf{GW}^{[d]}_{\rho_\circ,\rho_\bullet}\left((\mathbf{t}',v^*)\right)\\
&= \frac{1-m_{\rho_\circ}m_{\rho_\bullet}}{m_{\rho_\circ}} \prod_{u\in\mathbf{t}'_\circ}(1-p)p^{k_u(\mathbf{t}')} \prod_{\substack{u\in\mathbf{t}'_\bullet\\ u\neq v^*}} \rho_\bullet(k_u(\mathbf{t}'))\\
&= \frac{p(1-m_{\rho_\circ}m_{\rho_\bullet})}{m_{\rho_\circ}} \prod_{u\in\mathbf{t}'_\circ}(1-p) \prod_{\substack{u\in\mathbf{t}'_\bullet\\ u\neq v^*}} p\cdot\rho_\bullet(k_u(\mathbf{t}')).
\end{aligned}$$

Vertices of $\mathbf{t}'_\circ$ are mapped to leaves of $\mathbf{t}$ by Φ_{JS}, while vertices of $\mathbf{t}'_\bullet$ with k children are mapped to vertices of $\mathbf{t}$ with $k+1$ children. By the formula $m_\rho - p = (1-p)m_{\rho_\circ}m_{\rho_\bullet}$, we get

$$\begin{aligned}
\mathsf{GW}^{[d]}_{\rho_\circ,\rho_\bullet}\left(\Phi_{\mathrm{JS}}^{-1}((\mathbf{t},u^*))\right) &= (1-m_\rho) \prod_{\substack{u\in\mathbf{t}\\ k_u(\mathbf{t})=0}}(1-p) \prod_{\substack{u\in\mathbf{t}\setminus\{u^*\}\\ k_u(\mathbf{t})>0}} p\cdot\rho_\bullet(k_u(\mathbf{t})-1)\\
&= (1-m_\rho)\prod_{u\in\mathbf{t}\setminus\{u^*\}}\rho(k_u(\mathbf{t})),
\end{aligned}$$

which is $\mathsf{GW}^{[d+1]}_\rho((\mathbf{t},u^*))$, as expected. □

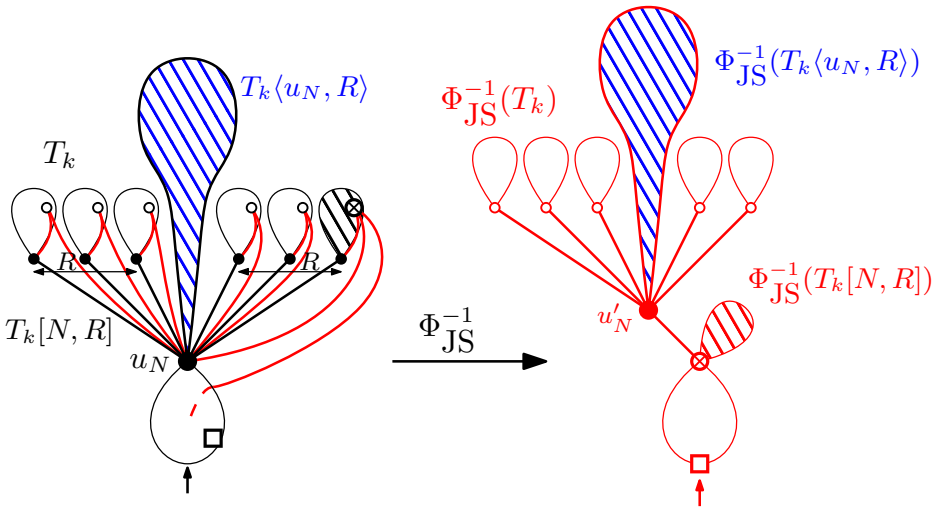

Figure 5.13: The image of T_k by Φ_{JS}^{-1}, on the event $\mathcal{E}(R,N,k)$. The boxed vertex is the last leaf of T_k in contour order, while the crossed vertex is the last leaf among the descendants of u_N.

We conclude with a property of $\mathbf{T}_\infty^{\circ,\bullet}$ under the assumptions of Proposition 5.5.3. Let u_∞ be the a.s. unique vertex with infinite degree of $\mathbf{T}_\infty^{\circ,\bullet}$, and $\widehat{u}_\infty$ its parent. There exists $j \in \{1,\dots,k_{\widehat{u}_\infty}\}$ such that $u_\infty = \widehat{u}_\infty j$. We define the vertex $u_\infty^{\leftarrow}$ as $\widehat{u}_\infty(j-1)$ if $j>1$, and $\widehat{u}_\infty$ itself if $j=1$. The vertex u_∞ and its incident edges disconnect $\mathbf{T}_\infty^{\circ,\bullet}$ in infinitely many connected components that we denote by $(\mathbf{T}_i : i\in\mathbb{Z})$. For

every $i \neq 0$, $\mathbf{T}_i$ is the connected component containing $u_\infty i$, rooted at the oriented edge going from $u_\infty i$ to its first child in $\mathbf{T}_\infty^{\circ,\bullet}$. Finally, $\mathbf{T}_0$ is the connected component containing the root vertex of $\mathbf{T}_\infty^{\circ,\bullet}$, and has the same root edge as $\mathbf{T}_\infty^{\circ,\bullet}$. Note that $u_\infty^{\leftarrow}$ is a vertex of $\mathbf{T}_0$.

Lemma 5.5.4. *The plane trees $(\mathbf{T}_i : i \in \mathbb{Z})$ are independent. For every $i \neq 0$, $\mathbf{T}_i$ has distribution $\mathsf{GW}_{\rho_\circ,\rho_\bullet}$, while $\mathbf{T}_0$ has the size-biased distribution $\overline{\mathsf{GW}_{\rho_\circ,\rho_\bullet}}$ defined by*

$$\overline{\mathsf{GW}_{\rho_\circ,\rho_\bullet}}(\mathbf{t}) = \frac{|\mathbf{t}|\mathsf{GW}_{\rho_\circ,\rho_\bullet}(\mathbf{t})}{\mathsf{GW}_{\rho_\circ,\rho_\bullet}(|T|)}, \quad \mathbf{t} \in \mathcal{T}_f.$$

Moreover, conditionally on $\mathbf{T}_0$, $u_\infty^{\leftarrow}$ has uniform distribution on $\mathbf{T}_0$.

Proof. We focus on $\mathbf{T}_0$. Let $(\mathbf{t}, u^*)$ be a pointed plane tree, and let u° be either the parent of u^* in $\mathbf{t}$ if $u^* \in \mathbf{t}_\bullet$, or u^* itself otherwise. Then, $(\mathbf{T}_0, u_\infty^{\leftarrow}) = (\mathbf{t}, u^*)$ enforces $\widehat{u}_\infty = u^\circ$. Since $k_{\widehat{u}_\infty}(\mathbf{T}_0) = k_{\widehat{u}_\infty}(\mathbf{T}_\infty^{\circ,\bullet}) - 1$ a.s. and by definition of $\rho_\circ$, we obtain

$$\begin{aligned}
&P\left((\mathbf{T}_0, u_\infty^{\leftarrow})\right) = (\mathbf{t}, u^*)) \\
&= \prod_{\substack{u \in \mathbf{t}_\circ \\ u \in [\emptyset, u^\circ)}} \frac{\bar\rho_\circ(k_u(\mathbf{t}))}{k_u(\mathbf{t})} \prod_{\substack{u \in \mathbf{t}_\bullet \\ u \in [\emptyset, u^\circ)}} \frac{\bar\rho_\bullet(k_u(\mathbf{t}))}{k_u(\mathbf{t})} \prod_{\substack{u \in \mathbf{t}_\circ \\ u \notin [\emptyset, u^\circ]}} \rho_\circ(k_u(\mathbf{t})) \prod_{\substack{u \in \mathbf{t}_\bullet \\ u \notin [\emptyset, u^\circ]}} \rho_\bullet(k_u(\mathbf{t})) \\
&\qquad \times \bar\rho_\circ(k_{u^\circ}(\mathbf{t}) + 1) \frac{1}{k_{u^\circ}(\mathbf{t}) + 1} (1 - m_{\rho_\circ} m_{\rho_\bullet})(m_{\rho_\circ} m_{\rho_\bullet})^{\frac{|u^\circ|}{2}} \\
&= \frac{p(1 - m_{\rho_\circ} m_{\rho_\bullet})}{m_{\rho_\circ}} \prod_{u \in \mathbf{t}_\circ} \rho_\circ(k_u(\mathbf{t})) \prod_{u \in \mathbf{t}_\bullet} \rho_\bullet(k_u(\mathbf{t})) = (1 - m_\rho)\mathsf{GW}_{\rho_\circ,\rho_\bullet}(\mathbf{t}).
\end{aligned}$$

Proposition 5.3.1 gives $\mathsf{GW}_{\rho_\circ,\rho_\bullet}(|T|) = \mathsf{GW}_\rho(|T|) = (1 - m_\rho)^{-1}$. This concludes the proof. □

5.5.2 Random infinite looptrees.

We now define infinite maps out of the infinite random trees $\mathbf{T}_\infty^{\circ,\bullet} = \mathbf{T}_\infty^{\circ,\bullet}(\rho_\circ, \rho_\bullet)$.

The critical case. When $(\rho_\circ, \rho_\bullet)$ is critical, $\mathbf{T}_\infty^{\circ,\bullet}$ is a.s. locally finite. We extend the mapping Loop to any locally finite plane tree $\mathbf{t} \in \mathcal{T}_{\text{loc}}$ by defining $\text{Loop}(\mathbf{t})$ as the consistent sequence of maps $(\text{Loop}(\mathbf{B}_{2R}(\mathbf{t})) : R \geq 0)$. This mapping is continuous on $\mathcal{T}_{\text{loc}}$ for the local topology. When $\mathbf{t}$ is infinite and one-ended (i.e., with a unique infinite spine), $\text{Loop}(\mathbf{t})$ is an infinite looptree, that is, an infinite edge-outerplanar map whose root face is the unique infinite face (and thus one-ended). Then, the random infinite looptree $\mathbf{L}_\infty = \mathbf{L}_\infty(\rho_\circ, \rho_\bullet)$ is defined by

$$\mathbf{L}_\infty := \text{Loop}(\mathbf{T}_\infty^{\circ,\bullet}).$$

See Figure 5.14 for an illustration.

The subcritical case. When $(\rho_\circ, \rho_\bullet)$ is subcritical, $\rho_\circ$ geometric and $\rho_\bullet$ has no exponential moment, $\mathbf{T}_\infty^{\circ,\bullet}$ has a.s. a unique vertex u_∞ with infinite degree. Since u_∞ has odd height, the sequence $(\mathbf{B}_r(\text{Loop}(\mathbf{B}_R^{\leftrightarrow}(\mathbf{T}_\infty^{\circ,\bullet}))) : R \geq 0)$ is eventually stationary, for every $r \geq 0$. Consequently, we define $\mathbf{L}_\infty = \mathbf{L}_\infty(\rho_\circ, \rho_\bullet)$ as the local limit

$$\mathbf{L}_\infty := \lim_{R \to \infty} \text{Loop}(\mathbf{B}_R^{\leftrightarrow}(\mathbf{T}_\infty^{\circ,\bullet})). \tag{5.61}$$

Although $\mathbf{L}_\infty$ is not a looptree in the aforementioned sense, we keep the notation $\mathbf{L}_\infty = \mathrm{Loop}(\mathbf{T}_\infty^{\circ,\bullet})$. By Lemma 5.5.4, $\mathbf{L}_\infty$ can be obtained as follows. We associate to $u_\infty^{\leftarrow}$ the oriented edge $e_\infty^{\leftarrow}$ of $\mathbf{T}_0$ that links either $\widehat{u}_\infty$ to $u_\infty^{\leftarrow}$ if $u_\infty^{\leftarrow}$ has odd height, or $\widehat{u}_\infty$ to its parent otherwise. For every $i \in \mathbb{Z}$, we define the looptree $\mathbf{L}_i := \mathrm{Loop}(\mathbf{T}_i)$ (with root edge e_i). Following the rooting convention of Section 5.3.2, to $e_\infty^{\leftarrow}$ is associated an oriented edge $e_0^{\leftarrow}$ of $\mathbf{L}_0$. We now consider the graph of $\mathbb{Z}$ embedded in the plane. For every $i \neq 0$, we embed $\mathbf{L}_i$ in the lower half-plane such that the vertex i of $\mathbb{Z}$ matches the origin vertex of $\mathbf{L}_i$, and the edges $(i-1, i)$ and e_i are consecutive in counterclockwise order around i. We apply the same construction to $\mathbf{L}_0$, but use $e_0^{\leftarrow}$ instead of e_0. We finally pick e_0 as the root edge. We get a proper embedding of the infinite planar map $\mathbf{L}_\infty = \mathrm{Loop}(\mathbf{T}_\infty^{\circ,\bullet})$ in the plane. See Figure 5.14 for an illustration.

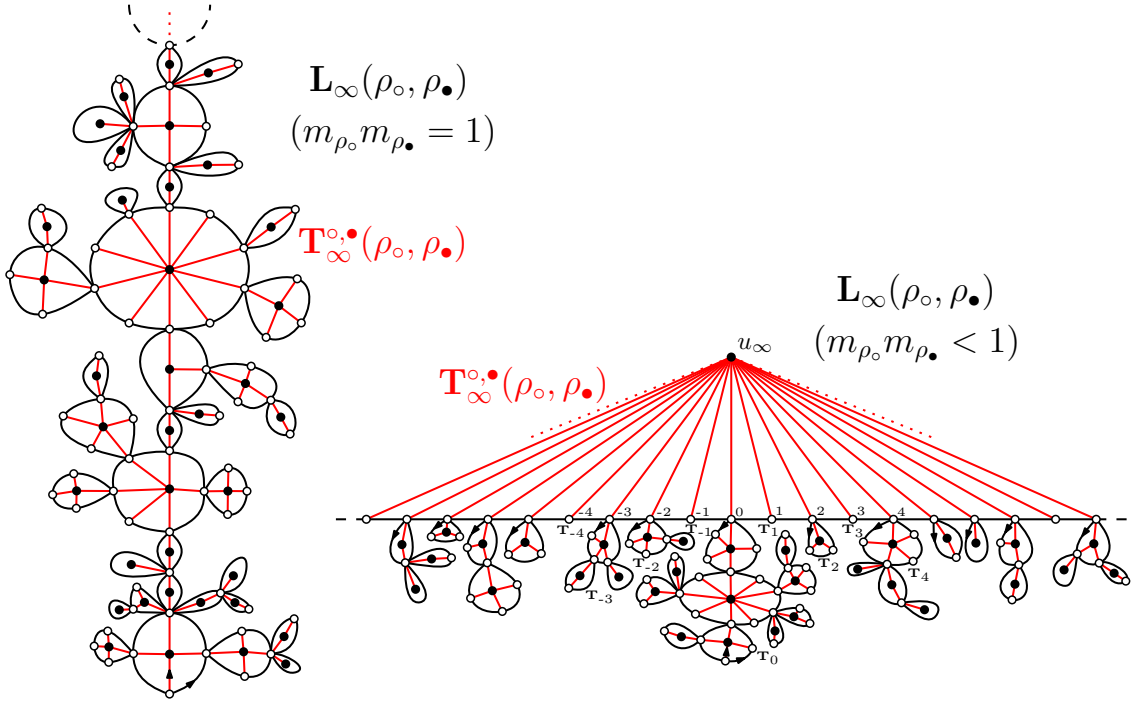

Figure 5.14: The infinite planar map $\mathbf{L}_\infty$ and the associated tree $\mathbf{T}_\infty^{\circ,\bullet}$.

Using the continuity of the mapping Loop and Proposition 5.5.1 in the critical case, and (5.61) and Proposition 5.5.2 in the subcritical case we get the following result.

Lemma 5.5.5. *Let $(\rho_\circ, \rho_\bullet)$ be a (sub)critical pair of offspring distributions such that $\rho_\circ$ has a geometric distribution and $\rho_\bullet$ has no exponential moment. Assume that for every $k \geq 1$, $\mathsf{GW}_{\rho_\circ,\rho_\bullet}(\{|\mathbf{t}| = k\}) > 0$ and let $T_k^{\circ,\bullet}$ be a tree with distribution $\mathsf{GW}_{\rho_\circ,\rho_\bullet}^{(k)}$. Then, in distribution for the local topology*

$$L_k := \mathrm{Loop}(T_k^{\circ,\bullet}) \xrightarrow[k\to\infty]{(d)} \mathbf{L}_\infty(\rho_\circ, \rho_\bullet).$$

The internal faces of $\mathbf{L}_\infty = \mathrm{Loop}(\mathbf{T}_\infty^{\circ,\bullet})$ are all finite in the critical case, while there is a unique infinite internal face in the subcritical case. In both regimes, the internal faces of $\mathbf{L}_\infty$ are in bijection with black vertices of $\mathbf{T}_\infty^{\circ,\bullet}$, so that the degree of the face and the degree of the vertex match.

5.5.3 Local limits of Boltzmann planar maps with a boundary

The local limits of Boltzmann bipartite maps with a boundary have been studied in [Cur16a].

Proposition 5.5.6. [Cur16a, Theorem 7] *Let* q *be an admissible weight sequence. Then, we have the weak convergence for the local topology*

$$\mathbb{P}_{\mathsf{q}}^{(k)} \underset{k\to\infty}{\Longrightarrow} \mathbb{P}_{\mathsf{q}}^{(\infty)}.$$

The probability measure $\mathbb{P}_{\mathsf{q}}^{(\infty)}$ *is supported on one-ended infinite bipartite planar maps with an infinite boundary (in particular, the root face is the unique infinite face).*

We let $\mathbf{M}_\infty = \mathbf{M}_\infty(\mathsf{q})$ be a planar map with distribution $\mathbb{P}_{\mathsf{q}}^{(\infty)}$, called the Infinite Boltzmann Half-Planar Map with weight sequence q (q-IBHPM in short). In the quadrangular case, $\mathbf{M}_\infty$ is a Uniform Infinite Half-Planar Quadrangulation with skewness UIHPQ$_p$ considered in Chapter 4 (which includes the standard UIHPQ with a general boundary of [CM15]).

Note that the definition of the scooped-out map, as well as that of the irreducible components, readily extend to any infinite bipartite map $\mathbf{m} \in \mathcal{B}_\infty$ (and $\mathrm{Scoop}(\mathbf{m})$ has a canonical embedding in the plane). As in the finite case, $\mathbf{m} \in \mathcal{B}_\infty$ is recovered from $\mathrm{Scoop}(\mathbf{m})$ by gluing its irreducible components into the internal faces of the latter. We are now interested in the continuity of Scoop with respect to the local topology.

Lemma 5.5.7. *Let* $(\mathbf{m}_k : k \in \mathbb{N})$ *be a sequence of finite bipartite maps, and* $\mathbf{m}_\infty \in \mathcal{B}_\infty$ *a one-ended infinite bipartite map such that in the local sense*

$$\mathbf{m}_k \underset{k\to\infty}{\longrightarrow} \mathbf{m}_\infty.$$

Then, in the local sense,

$$\mathrm{Scoop}(\mathbf{m}_k) \underset{k\to\infty}{\longrightarrow} \mathrm{Scoop}(\mathbf{m}_\infty).$$

Proof. First, if $(\#\partial\mathbf{m}_k : k \geq 1)$ is bounded, there exists $R \geq 0$ such that for every $k \geq 1$, $\partial\mathbf{m}_k \subseteq \mathbf{B}_R(\mathbf{m}_k)$ and the result follows. Thus, we can assume that $\#\partial\mathbf{m}_k \to \infty$ as $k \to \infty$.

For every $k \in \mathbb{N} \cup \{\infty\}$, we let $p(k) := \#\partial\mathbf{m}_k/2$ be the half-perimeter of $\mathbf{m}_k$ and denote by $(v_k(0), v_k(1), \ldots, v_k(p(k)))$ the sequence of vertices associated with the corners of the root face of $\mathbf{m}_k$, starting at the origin, in right contour order. We use the notation $(v_k(0), v_k(-1), \ldots, v_k(-p(k)))$ for the left contour order, so that $v_k(p(k)) = v_k(-p(k))$.

Let $r \geq 0$. We now prove that there exists $R \geq 0$ and $K \geq 1$ such that for every $k \geq K$,

$$\mathrm{V}(\mathbf{B}_r(\mathbf{m}_k)) \cap \{v_k(l) : |l| > R\} = \emptyset. \tag{5.62}$$

We proceed by contradiction. Because of the local convergence assumption, the sequence $(\#\mathrm{V}(\mathbf{B}_r(\mathbf{m}_k)) : k \geq 0)$ is bounded. Moreover, for every $v \in \mathrm{V}(\mathbf{B}_r(\mathbf{m}_k))$ we have

$$\#\{-p(k) \leq l \leq p(k) : v_k(l) = v\} \leq \deg_{\mathbf{m}_k}(v) \leq \sup_{u\in\mathrm{V}(B_r(\mathbf{m}_k))} \deg_{\mathbf{m}_k}(u),$$

which is also bounded. Therefore, there exists $M \geq 0$ such that for every $k \geq 0$,

$$\#\{-p(k) \leq l \leq p(k) : v_k(l) \in \mathrm{V}(\mathbf{B}_r(\mathbf{m}_k))\} \leq M.$$

Let $N \geq 0$. By assumption, there exists infinitely many k such that $p(k) > 2M(N+2)$ and

$$\mathrm{V}(\mathbf{B}_r(\mathbf{m}_k)) \cap \{v_{\mathbf{m}_k}(l) : |l| > M(N+2)\} \neq \emptyset.$$

As a consequence, in the cycle $(-p(k), \dots, p(k))$, there exists two distinct sequences of consecutive indices $(i, \dots, i+x)$ and $(j, \dots, j+y)$ such that $x, y \geq N+2$ and

$$\mathrm{V}(\mathbf{B}_r(\mathbf{m}_k)) \cap \{v_k(l) : i \leq l \leq i+x\} = \{v_k(i), v_k(i+x)\},$$

and similarly for $(j, \dots, j+y)$. In particular, the sets of vertices $E_1 := \{v_k(i+1), \dots, v_k(i+x-1)\}$ and $E_2 := \{v_k(j+1), \dots, v_k(j+y-1)\}$ are disjoint. Indeed, a vertex $v \in E_1 \cap E_2$ would disconnect $\mathrm{Scoop}(\mathbf{m}_k)$ in two submaps each containing a vertex at distance less than r from the origin, which is in contradiction with $v \notin \mathbf{B}_r(\mathbf{m}_k)$. Now, for every $-p(k) \leq i < p(k)$, $(v_k(i), v_k(i+1))$ is an edge of $\mathrm{Scoop}(\mathbf{m}_k)$. Therefore, the sets of edges $\{((v_k(l), v_k(l+1)) : i < l \leq i+N+1\}$ and $\{((v_k(l), v_k(l+1)) : j < l \leq j+N+1\}$ are disjoint sets of N half-edges contained in $\mathbf{B}_{r+N}(\mathbf{m}_k) \backslash \mathbf{B}_r(\mathbf{m}_k)$. This holds for infinitely many $k \geq 1$, thus for $\mathbf{m}_\infty$ by local convergence. Since $\mathbf{m}_\infty$ has one end and N is arbitrary, this is a contradiction.

Let us choose R and K such that assertion (5.62) holds for every $k \geq K$. By local convergence, (5.62) holds for $\mathbf{m}_\infty$ as well. For every $k \geq K$, let $\langle v_k(-R), \dots, v_k(R)\rangle$ be the sub-map induced by the R first half-edges of $\mathrm{Scoop}(\mathbf{m}_k)$ in left and right contour order. Let H be the measurable function such that $\langle v_k(-R), \dots, v_k(R)\rangle = H(\mathbf{m}_k) = H(\mathbf{B}_R(\mathbf{m}_k))$. By (5.62) and local convergence, we have for every $k \geq K$

$$\mathbf{B}_r(\mathrm{Scoop}(\mathbf{m}_k)) = \mathbf{B}_r(H(\mathbf{B}_R(\mathbf{m}_k)) \underset{k\to\infty}{\longrightarrow} \mathbf{B}_r(H(\mathbf{B}_R(\mathbf{m}_\infty)) = \mathbf{B}_r(\mathrm{Scoop}(\mathbf{m}_\infty)),$$

which concludes the proof. □

When an infinite bipartite map $\mathbf{m} \in \mathcal{B}_\infty$ has a unique infinite irreducible component, it is called the *core* of $\mathbf{m}$ and denoted by $\mathrm{Core}(\mathbf{m})$. Then, $\mathbf{m}$ is recovered from $\mathrm{Core}(\mathbf{m})$ by gluing finite bipartite maps (with a general boundary) on the vertices of the boundary of $\mathrm{Core}(\mathbf{m})$. Note that the boundary of $\mathrm{Core}(\mathbf{m})$ may be finite or infinite. We are now ready to prove Theorem 5.1.2.

Proof of Theorem 5.1.2. For every $k \geq 1$, let M_k be a planar map with distribution $\mathbb{P}_{\mathsf{q}}^{(k)}$. By Corollary 5.3.9, $T_k^{\circ,\bullet} := \mathbf{Tree}(M_k)$ is a two-type Galton-Watson tree with offspring distribution $(\nu_\circ, \nu_\bullet)$ conditioned to have $2k+1$ vertices. By Proposition 5.5.6 and Lemma 5.5.7, we have

$$\mathrm{Scoop}(M_k) \underset{k\to\infty}{\overset{(d)}{\longrightarrow}} \mathrm{Scoop}(\mathbf{M}_\infty).$$

On the other hand, by Lemma 5.5.5,

$$\mathrm{Scoop}(M_k) = \mathrm{Loop}(T_k^{\circ,\bullet}) \underset{k\to\infty}{\overset{(d)}{\longrightarrow}} \mathbf{L}_\infty(\nu_\circ, \nu_\bullet),$$

in distribution for the local topology. Lemma 5.3.6 and Proposition 5.3.7 conclude the first part of the proof. For $a \in [3/2, 2]$, Scoop$(\mathbf{M}_\infty)$ has only finite internal faces, which are the boundaries of the irreducible components of $\mathbf{M}_\infty$. Since Scoop$(\mathbf{M}_\infty)$ and $\mathbf{M}_\infty$ are one-ended, these irreducible components are necessarily finite. For $a \in (2, 5/2]$, Scoop$(\mathbf{M}_\infty)$ has a unique infinite internal face, which is the boundary of an infinite irreducible component. Since $\mathbf{M}_\infty$ is one-ended, the other irreducible components are finite, and $\mathbf{M}_\infty$ has a well-defined core. Moreover, the infinite map Core$(\mathbf{M}_\infty)$ is one-ended with an infinite simple boundary, and thus homeomorphic to the half-plane. □

Local limits: the subcritical and dense regimes. When q is of type $a \in [3/2, 2]$, $\mathbf{M}_\infty(\mathsf{q})$ can be entirely described by the looptree $\mathbf{L}_\infty(\nu_\circ, \nu_\bullet)$ and a collection of independent Boltzmann maps. This generalizes Theorem 4.2.10 which deals with subcritical quadrangulations.

Let us introduce some notation. Following Remark 5.3.2, we define a fill-in mapping that associates to a one-ended locally finite tree $\mathbf{t} \in \mathcal{T}_{\text{loc}}$ and a collection $(\widehat{\mathbf{m}}_u : u \in \mathbf{t}_\bullet)$ of finite bipartite maps with a simple boundary of respective perimeter $\deg(u)$ the infinite bipartite map

$$\Phi_{\text{TC}}^{-1}\left(\mathbf{t}, (\widehat{\mathbf{m}}_u : u \in \mathbf{t}_\bullet)\right),$$

obtained from $\mathbf{l} := \text{Loop}(\mathbf{t})$ by gluing the map $\widehat{\mathbf{m}}_u$ in the face of $\mathbf{l}$ associated to u, for every $u \in \mathbf{t}_\bullet$. We keep the notation Φ_{TC}^{-1} by consistency, although we consider infinite trees. This mapping is continuous with respect to the natural topology.

Proposition 5.5.8. *Let q be a weight sequence of type $a \in [3/2, 2]$, and let $\mathbf{T}_\infty^{\circ,\bullet} = \mathbf{T}_\infty^{\circ,\bullet}(\nu_\circ, \nu_\bullet)$. Conditionally on $\mathbf{T}_\infty^{\circ,\bullet}$, let $(\widehat{M}_u : u \in (\mathbf{T}_\infty^{\circ,\bullet})_\bullet)$ be a collection of independent bipartite maps with a simple boundary and distribution $\widehat{\mathbb{P}}_{\mathsf{q}}^{(\deg(u)/2)}$. Then, the infinite bipartite map*

$$M_\infty = \Phi_{\text{TC}}^{-1}\left(\mathbf{T}_\infty^{\circ,\bullet}, \left(\widehat{M}_u : u \in (\mathbf{T}_\infty^{\circ,\bullet})_\bullet\right)\right)$$

has distribution $\mathbb{P}_{\mathsf{q}}^{(\infty)}$, the law of the q-IBHPM.

Proof. The proof closely follows that of Theorem 4.2.10. For every $\mathbf{t} \in \mathcal{T}_{\text{loc}}$ and every $R \geq 1$, let $\text{Cut}_R(\mathbf{t})$ be the subtree of $\mathbf{t}$ made of vertices $u \in \mathbf{t}$ such that $|u| \leq 2R$. Consistently, if $\mathbf{m} = \Phi_{\text{TC}}^{-1}(\mathbf{t}, (\widehat{\mathbf{m}}_u : u \in \mathbf{t}_\bullet))$, $\text{Cut}_R(\mathbf{m})$ is the bipartite map $\Phi_{\text{TC}}^{-1}(\text{Cut}_R(\mathbf{t}), (\widehat{\mathbf{m}}_u : u \in \text{Cut}_R(\mathbf{t})_\bullet))$.

Let $R \geq 1$ and for every $k \geq 0$, let M_k be a bipartite map with distribution $\mathbb{P}_{\mathsf{q}}^{(k)}$. Let $\mathbf{m} \in \mathcal{B}_f$ and $(\mathbf{t}, (\widehat{\mathbf{m}}_u : u \in \mathbf{t}_\bullet)) = \Phi_{\text{TC}}(\mathbf{m})$. By Proposition 5.3.3 and 5.5.1, we have

$$\begin{aligned}
\mathbb{P}_{\mathsf{q}}^{(k)}(\text{Cut}_R(M) = \mathbf{m}) &= \text{GW}_{\nu_\circ,\nu_\bullet}^{(2k+1)}(\text{Cut}_R(T) = \mathbf{t}) \prod_{u \in \mathbf{t}_\bullet} \widehat{\mathbb{P}}_{\mathsf{q}}^{(\deg(u)/2)}(\widehat{\mathbf{m}}_u) \\
&\underset{k\to\infty}{\longrightarrow} \text{GW}_{\nu_\circ,\nu_\bullet}^{(\infty)}(\text{Cut}_R(T) = \mathbf{t}) \prod_{u \in \mathbf{t}_\bullet} \widehat{\mathbb{P}}_{\mathsf{q}}^{(\deg(u)/2)}(\widehat{\mathbf{m}}_u) \\
&= P(\text{Cut}_R(M_\infty) = \mathbf{m}).
\end{aligned}$$

This concludes the proof since $\mathbf{B}_R(\mathbf{m}) = \mathbf{B}_R(\text{Cut}_R(\mathbf{m}))$ if $\mathbf{m} = \Phi_{\text{TC}}^{-1}(\mathbf{t}, (\widehat{\mathbf{m}}_u : u \in \mathbf{t}_\bullet))$ with $\mathbf{t} \in \mathcal{T}_{\text{loc}}$. □

Remark 5.5.9. The tree-like structure of $\mathbf{M}_\infty$ when $a \in [3/2, 2]$ makes statistical mechanics models on it easier to study. In particular, the simple random walk on $\mathbf{M}_\infty$ is a.s. recurrent (see Corollary 4.2.13 for a proof) and the critical thresholds for Bernoulli site, bond and face percolation on $\mathbf{M}_\infty$ equal one a.s..

Local limits: the dilute and generic regimes. When q is of type $a \in (2, 5/2]$, $\mathbf{M}_\infty = \mathbf{M}_\infty(\mathsf{q})$ cannot be fully described using finite bipartite maps. By the construction of Section 5.5.2, Scoop$(\mathbf{M}_\infty)$ is obtained from the infinite simple boundary of Core$(\mathbf{M}_\infty)$ by attaching to its vertices independent looptrees $(\mathbf{L}_i : i \in \mathbb{Z})$ whose trees of components have distribution $\mathrm{GW}_{\nu_\circ,\nu_\bullet}$, except for that looptree containing the root edge of $\mathbf{M}_\infty$, whose tree of components has distribution $\overline{\mathrm{GW}_{\nu_\circ,\nu_\bullet}}$. We believe that the finite irreducible components of $\mathbf{M}_\infty$ are independent Boltzmann bipartite maps with a simple boundary (conditionally on $\partial\mathbf{M}_\infty$). Moreover, given Propositions 5.3.3 and 5.5.3, we conjecture that there exists a distribution $\widehat{\mathbb{P}}_{\mathsf{q}}^{(\infty)}$ supported on one-ended infinite bipartite planar maps with an infinite simple boundary such that $\widehat{\mathbb{P}}_{\mathsf{q}}^{(k)} \Rightarrow \widehat{\mathbb{P}}_{\mathsf{q}}^{(\infty)}$ as $k \to \infty$, and that Core$(\mathbf{M}_\infty)$ has distribution $\widehat{\mathbb{P}}_{\mathsf{q}}^{(\infty)}$. This would provide a complete description of the q-IBHPM, and has been achieved in the special case of the UIHPQ in [CM15, Proposition 6]. However, our techniques are not sufficient to prove these assertions.

5.6 Application to the rigid $O(n)$ loop model on quadrangulations

We now give applications to the rigid $O(n)$ loop model on quadrangulations, building on [BBG12c].

The rigid $O(n)$ loop model on quadrangulations. We now describe the setup of [BBG12c] (see also [CCM17]). A *quadrangulation with a boundary* is a planar map with a boundary whose internal faces all have degree 4. Given a quadrangulation with a boundary $\mathbf{q}$, a *loop configuration* on $\mathbf{q}$ is a collection $\boldsymbol{\ell} = (\ell_k : k \in \mathbb{N})$ of disjoint closed simple paths in the dual of $\mathbf{q}$ that do not visit the root face f_*. The loop configuration is known as *rigid* if moreover every loop crosses a quadrangle through opposite sides. See Figure 5.4 for an illustration. The pair $(\mathbf{q}, \boldsymbol{\ell})$ is then called a (rigid) *loop-decorated quadrangulation with a boundary*. The set of all such pairs $(\mathbf{q}, \boldsymbol{\ell})$ is denoted by $\mathcal{O}$ (resp. $\mathcal{O}_k$ if additionally $\mathbf{q}$ has perimeter $2k$). The set $\mathcal{O}_1$ is in bijection with loop-decorated quadrangulations of the sphere. For every $(\mathbf{q}, \boldsymbol{\ell}) \in \mathcal{O}$, we denote by $\#\boldsymbol{\ell}$ the number of loops in $\boldsymbol{\ell}$, by $|\boldsymbol{\ell}|$ the total length (i.e., the total number of edges) of the loops of $\boldsymbol{\ell}$, and by $|\ell|$ the number of edges, or perimeter, of a loop $\ell \in \boldsymbol{\ell}$.

For every $n \in (0, 2)$ and every $g, h \geq 0$, we define the measure $W_{(n;g,h)}$ on $\mathcal{O}$ by

$$W_{(n;g,h)}((\mathbf{q}, \boldsymbol{\ell})) := g^{\#\mathrm{F}(\mathbf{q})-|\boldsymbol{\ell}|} h^{|\boldsymbol{\ell}|} n^{\#\boldsymbol{\ell}}, \quad (\mathbf{q}, \boldsymbol{\ell}) \in \mathcal{O}. \tag{5.63}$$

In other words, we put a weight g per empty quadrangle of $\mathbf{q}$, a weight h per quadrangle crossed by a loop, and a weight n per loop. We also define the partition

function

$$F_k^\circ := \sum_{(\mathbf{q},\boldsymbol{\ell})\in\mathcal{O}_k} W_{(n;g,h)}((\mathbf{q},\boldsymbol{\ell})), \quad k \in \mathbb{Z}_+. \tag{5.64}$$

When this partition function is finite (which does not depend on k), we say that $(n;g,h)$ is admissible and define the $O(n)$ probability measure on $\mathcal{O}_k$ with parameters $(n;g,h)$ by

$$\mathbf{P}^{(k)}_{(n;g,h)}((\mathbf{q},\boldsymbol{\ell})) := \frac{W_{(n;g,h)}((\mathbf{q},\boldsymbol{\ell}))}{F_k^\circ}, \quad (\mathbf{q},\boldsymbol{\ell}) \in \mathcal{O}_k, \quad k \in \mathbb{Z}_+. \tag{5.65}$$

$\mathbf{P}_{(n;g,h)} := \mathbf{P}^{(1)}_{(n;g,h)}$ is the $O(n)$ distribution on loop-decorated quadrangulations of the sphere.

The gasket decomposition. The work [BBG12c] is based on the *gasket decomposition* of loop-decorated quadrangulations with a boundary, that we now recall (see also [CCM17]). First, for every $(\mathbf{q},\boldsymbol{\ell}) \in \mathcal{O}$ and every $\ell \in \boldsymbol{\ell}$, the interior and exterior of ℓ are well-defined thanks to the root edge of $\mathbf{q}$. Then, the *inner* (resp. *outer*) contour of ℓ is formed by the edges of $\mathbf{q}$ that are incident to faces of $\mathbf{q}$ crossed by ℓ, and that belong to the interior (resp. exterior) of ℓ.

The gasket decomposition of $(\mathbf{q},\boldsymbol{\ell}) \in \mathcal{O}_k$ consists in discarding the outer-most loops $(\ell_i : i \in \mathcal{I})$ of $\boldsymbol{\ell}$ (i.e., that are not contained in the interior of another loop) as well as the edges crossed by these loops. This disconnects $(\mathbf{q},\boldsymbol{\ell})$ in $\#\mathcal{I}+1$ connected components, as shown in Figure 5.15. The gasket is the connected component $\mathrm{Gasket}(\mathbf{q},\boldsymbol{\ell})$ containing the root edge of $\mathbf{q}$. It is the element of $\mathcal{B}_f^{(k)}$ formed by the edges of $\mathbf{q}$ that are exterior to all loops. The faces of $\mathrm{Gasket}(\mathbf{q},\boldsymbol{\ell})$ are either quadrangles of $\mathbf{q}$, or *holes* corresponding to the loops $(\ell_i : i \in \mathcal{I})$ (with degree $|\ell_i|$). The other connected components are the interiors of the outer-most loops, which are loop-decorated quadrangulations $((\mathbf{q}_i,\boldsymbol{\ell}_i) : i \in \mathcal{I})$ with perimeter $|\ell_i|$. By convention, the root edge of $\mathbf{q}_i$ lies on the leftmost shortest path from the root edge of $\mathbf{q}$ to $\mathbf{q}_i$ (with the convention that ℓ_i lies on its right).

Given $\mathbf{m} \in \mathcal{B}_f^{(k)}$ and $(\mathbf{q},\boldsymbol{\ell}) \in \mathcal{O}_k$ such that $\mathrm{Gasket}(\mathbf{q},\boldsymbol{\ell}) = \mathbf{m}$, $(\mathbf{q},\boldsymbol{\ell})$ is recovered by gluing into each face of $\mathrm{Gasket}(\mathbf{q},\boldsymbol{\ell})$ of degree $2p$ the proper elements of $\mathcal{O}_p$, with in-between a *ring* or *necklace* of $2p$ quadrangles crossed by a loop. When $p=2$, we can also glue an empty quadrangle. The following result is proved in [BBG12c], see in particular [BBG12c, Equation 2.3].

Proposition 5.6.1. [BBG12c] *Let $(n;g,h)$ be admissible, $k \geq 0$ and (Q,L) a loop-decorated quadrangulation with distribution $\mathbf{P}^{(k)}_{(n;g,h)}$. Denote by $(l_i : i \in \mathcal{I})$ the outer-most loops of (Q,L), and by $((Q_i,L_i) : i \in \mathcal{I})$ the associated loop-decorated quadrangulations. Then, $\mathrm{Gasket}(Q,L)$ has distribution $\mathbb{P}^{(k)}_{\mathsf{q}}$, where the weight sequence $\mathsf{q} = \mathsf{q}(n;g,h) = (q_k : k \in \mathbb{N})$ satisfies*

$$q_k = g\delta_2(k) + nh^{2k}F_k^\circ(n;g,h). \tag{5.66}$$

Moreover, conditionally on $(|l_i| : i \in \mathcal{I})$, $((Q_i,L_i) : i \in \mathcal{I})$ are independent loop-decorated quadrangulations with distribution $\mathbf{P}^{(|l_i|)}_{(n;g,h)}$.

Remark 5.6.2. We are interested in limits of large loops in the rigid $O(n)$ model on quadrangulations. Due to the rigidity constraint on loops, we can substitute loops (that are paths in the dual map) for their inner contours (in the primal map). Proposition 5.6.1 ensures that for every $k \geq 0$, in the rigid $O(n)$ loop model on $\mathcal{O}_k$, every loop of perimeter $2p$ is distributed as the boundary of a Boltzmann bipartite map with law $\mathbb{P}_{\mathsf{q}}^{(p)}$ for a suitable value of q. Therefore, the study of large loops reduces to the study of the boundary of a large Boltzmann bipartite map. For instance, consider the rigid $O(n)$ loop model on $\mathcal{O}_1$ with parameters $(n; g, h)$, and pick a loop using a deterministic criterion (e.g. the loop that is the closest to the root edge). Now, condition this loop to have perimeter $2p$ (which is an event of positive probability). Then, its inner contour is the boundary of a map with law $\mathbb{P}_{\mathsf{q}}^{(p)}$, for q satisfying (5.66).

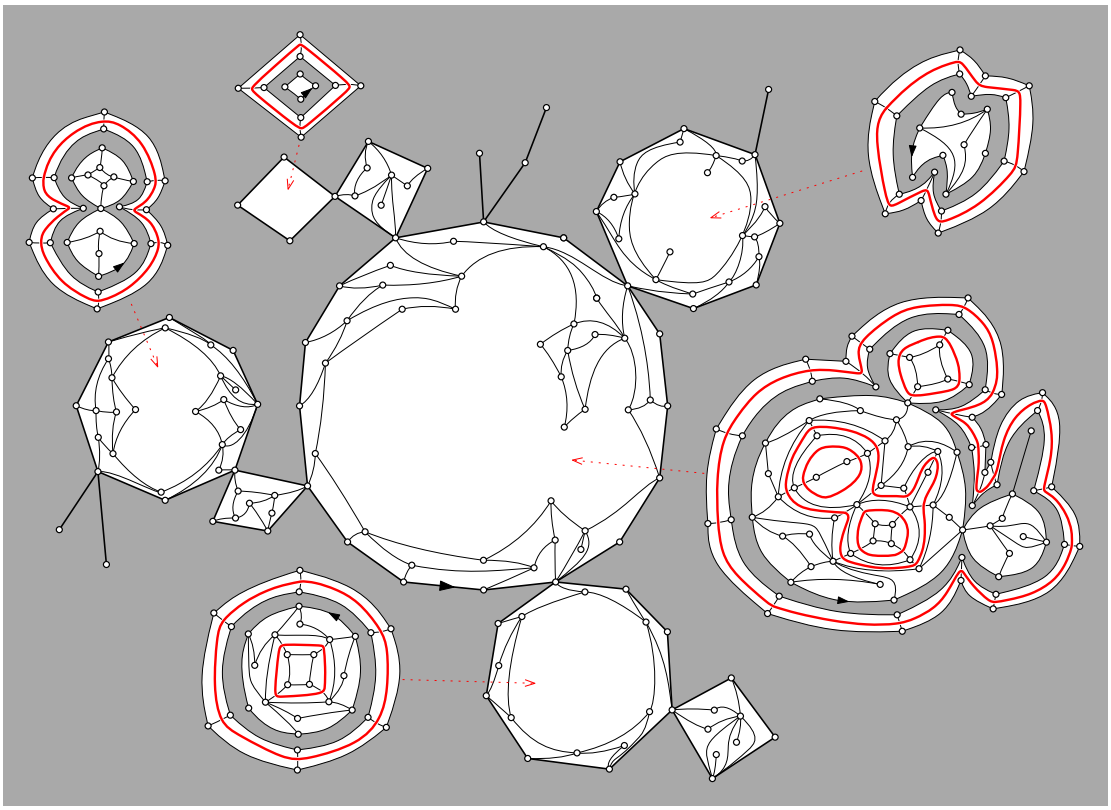

Figure 5.15: The gasket decomposition of the loop-decorated quadrangulation $(\mathbf{q}, \boldsymbol{\ell})$ of Figure 5.4. Note that holes may be non-simple faces of Gasket$(\mathbf{q}, \boldsymbol{\ell})$.

The phase diagram. In [BBG12c], the parameters of the $O(n)$ model have been classified according to the distribution of the gasket. A triplet $(n; g, h)$ is called *subcritical*, *generic critical* or *non-generic critical with parameter* α if the weight sequence q associated to $(n; g, h)$ by (5.66) is subcritical, generic critical or non-generic critical with parameter α. This results in the exact phase diagram of Figure 5.5 (see also [BBG12c, Figure 12]). As mentioned in [CCM17], the work [BBG12c] must be completed by [Bud17, Appendix] to get this diagram. Let $n \in (0, 2)$, and set

$$b := \frac{1}{\pi} \arccos\left(\frac{n}{2}\right).$$

Then, we have a critical line $h = h_c(n; g)$ that separates the region where the model is subcritical ($a = 3/2$) and the pairs (g, h) such that $(n; g, h)$ is non-admissible. The critical line has two parts. First, an arc of parabola that links $(g = 0, h = 2b^2/(2-n))$ to the special point $(g^*, h^*) = (g^*(n), h^*(n))$, with explicit equation [BBG12c, Equation (6.18)]. Then, a second part that links (g^*, h^*) to $(g = 1/12, h = 0)$ (corresponding to pure quadrangulations) with a more intricate parametrization [BBG12c, Equation (6.14)]. The regime changes along the critical line: for $g < g^*$, the parameters are non-generic critical with parameter $a = 2 - b \in (3/2, 2)$, which corresponds to the dense phase, while for $g > g^*$, the parameters are generic critical ($a = 5/2$). Finally the special point (g^*, h^*) is non-generic critical with parameter $a = 2 + b \in (2, 5/2)$, which corresponds to the dilute phase.

The situation is simpler in the non-generic critical cases. In [BBG12c] (as in [LGM11a, BC16]), the definition of a non-generic critical weight sequence q is less general than our, and implies that there exists a constant χ_{q} such that

$$F_k \underset{k\to\infty}{\sim} \chi_{\mathsf{q}} \frac{(4Z_{\mathsf{q}})^k}{k^a},$$

see [BBG12c, Equation (3.15)], [BC16, Equation (6)] or [Cur16a, Equation (5.8)]. In particular, the slowly varying function ℓ defined in Definition 5.2.4 is equivalent to a constant. Using this in the computations of Sections 5.2.2, 5.2.3 and 5.4, we finally obtain that the slowly varying function Λ of Theorem 5.1.2 can be replaced by a constant $C = C(\mathsf{q}) = C(n, g, h)$. Then, Theorems 5.1.3 and 5.1.4 follow from Proposition 5.6.1 and the phase diagram, by applying Theorems 5.1.1 and 5.1.2. By Remark 5.6.2, these results extend to any loop conditioned to be large in the rigid $O(n)$ loop model on quadrangulations (possibly with a boundary).

5.7 The non-generic critical case with parameter $3/2$

We have seen in Remarks 5.2.7 and 5.3.8 that the critical parameter $\alpha = 3/2$ ($a = 2$) plays a special role. In particular, Karamata's Tauberian theorem does not yield an equivalent for the tail of the probability measure ν. We now provide such an estimate by calling on De Haan theory [BGT89, Chapter 3] and using a special weight sequence introduced in [ABM16].

The special weight sequence. We recall the definition of the special weight sequence of [ABM16]. Here, we draw on [BC16, Section 5] and define the weight sequence $\mathsf{q}^* = (q^*_k : k \in \mathbb{N})$ by

$$q^*_k := \frac{1}{4} 6^{1-k} \frac{\Gamma(k - 3/2)}{\Gamma(k + 5/2)} \mathbf{1}_{k\geq 2} \quad k \in \mathbb{N}.$$

Then, q^* is admissible, critical, and of type $a = 2$. There exists a continuous family of such sequences covering all the values of $a \in (3/2, 5/2]$ (the case $a = 5/2$ corresponding to critical quadrangulations). This weight sequence is convenient because we

obtain an explicit formula for the partition function F_k by combining [BC16, Lemma 14] and [BC16, Equation (7)]:

$$F_k = \frac{3}{4}\frac{6^k}{(k+3/2)(k+1/2)}, \quad k \in \mathbb{Z}_+.$$

Consequently, $r_{\mathsf{q}} = 1/6$ and we have the explicit formula

$$F(x) = \frac{1}{4x} - \frac{3}{4(6x)^{3/2}}(1-6x)\log\left(\frac{1+\sqrt{6x}}{1-\sqrt{6x}}\right), \tag{5.67}$$

from which we deduce the asymptotic expansions as $x \to r_{\mathsf{q}}^-$

$$F(x) = \frac{3}{2} + \frac{3}{4}\left(1-\frac{x}{r_{\mathsf{q}}}\right)\log\left(1-\frac{x}{r_{\mathsf{q}}}\right) + \frac{3}{2}(1-\log(2))\left(1-\frac{x}{r_{\mathsf{q}}}\right)(1+o(1)), \tag{5.68}$$

$$F'(x) = -\frac{9}{2}(3-2\log(2)) - \frac{9}{2}\log\left(1-\frac{x}{r_{\mathsf{q}}}\right) + o(1). \tag{5.69}$$

The generating function of bipartite maps with a simple boundary. We now focus on estimates for the generating function $\widehat{F}$. Unlike the previous cases, an asymptotic expansion of $\widehat{F}$ itself is not sufficient; we rather need an expansion of its derivative. As in Section 5.2.3, the function $P(x) = xF^2(x)$ is continuous increasing from $[0, r_{\mathsf{q}}]$ onto $[0, P(r_{\mathsf{q}})]$ with inverse denoted by P^{-1}, and $P(r_{\mathsf{q}}) = 3/8$. Moreover, we have as $x \to r_{\mathsf{q}}^-$

$$P(x) = P(r_{\mathsf{q}}) + P(r_{\mathsf{q}})\left(1-\frac{x}{r_{\mathsf{q}}}\right)\log\left(1-\frac{x}{r_{\mathsf{q}}}\right) + P(r_{\mathsf{q}})(2\log(2)-1)\left(1-\frac{x}{r_{\mathsf{q}}}\right)(1+o(1)). \tag{5.70}$$

In what follows, we put $c^* = 2\log(2) - 1$. We define the function

$$R(x) := \frac{1}{P(r_{\mathsf{q}})}\left(P(r_{\mathsf{q}}) - P(r_{\mathsf{q}}(1-x))\right), \quad x \in [0,1],$$

which is continuous increasing onto $[0,1]$, with inverse R^{-1} defined by

$$R^{-1}(y) = 1 - \frac{1}{r_{\mathsf{q}}}P^{-1}\left(P(r_{\mathsf{q}})(1-y)\right), \quad y \in [0,1]. \tag{5.71}$$

The asymptotic expansion of R reads

$$R(x) = -x\log(x) - c^*x + o(x) \quad \text{as } x \to 1^-. \tag{5.72}$$

We now need the Lambert W function, defined as the (multivalued) inverse function of $x \mapsto xe^x$. Here, we use the lower branch W_{-1}, continuous decreasing from $[-e^{-1}, 0)$ onto $(-\infty, -1]$, which satisfies the identities

$$W_{-1}(-x) = \log\left(\frac{-x}{W_{-1}(-x)}\right) \quad \text{and} \quad W_{-1}(x\log(x))\log(x), \quad x \in (0, e^{-1}]. \tag{5.73}$$

We also have the asymptotic expansion

$$W_{-1}(-x) = \log(x) - \log(-\log(x)) + o(1) \quad \text{as } x \to 0^+. \tag{5.74}$$

The Lambert W function has a principal branch W_0, but the lower branch is more suitable to our needs. We introduce the function

$$Q(x) := R\left(\frac{-x}{W_{-1}(-x)}\right), \quad x \in (0, e^{-1}],$$

which is continuous increasing from $(0, e^{-1}]$ onto $(0, R(e^{-1})]$. By (5.73), its inverse function Q^{-1} satisfies

$$Q^{-1}(y) = -R^{-1}(y)\log\left(R^{-1}(y)\right) \quad \text{and} \quad R^{-1}(y) = \frac{-Q^{-1}(y)}{W_{-1}(-Q^{-1}(y))}, \quad y \in (0, R(e^{-1})]. \tag{5.75}$$

Using (5.72), (5.73) and (5.74) we get

$$Q(x) = x - c^*\frac{x}{\log(x)} + o\left(\frac{x}{\log(x)}\right) \quad \text{as } x \to 0^+. \tag{5.76}$$

Then, $Q'(0^+) = 1$, $(Q^{-1})'(0^+) = 1$ and $Q^{-1}(y) \sim y$ as $y \to 0^+$. Back to (5.76), we have

$$Q^{-1}(y) = y - c^*\frac{y}{\log(y)} + o\left(\frac{y}{\log(y)}\right) \quad \text{as } y \to 0^+. \tag{5.77}$$

Together with (5.75) and (5.74), this yields

$$R^{-1}(y) = -\frac{y}{\log(y)} - \frac{y\log(-\log(y))}{\log^2(y)} - c^*\frac{y}{\log^2(y)} + o\left(\frac{y}{\log^2(y)}\right) \quad \text{as } y \to 0^+. \tag{5.78}$$

Finally, by (5.71) we obtain

$$\begin{aligned} P^{-1}(y) = {} & \\ & r_{\mathsf{q}} + r_{\mathsf{q}}\left(1 - \frac{y}{P(r_{\mathsf{q}})}\right)\frac{1}{\log\left(1 - \frac{y}{P(r_{\mathsf{q}})}\right)} + r_{\mathsf{q}}\left(1 - \frac{y}{P(r_{\mathsf{q}})}\right)\frac{\log\left(-\log\left(1 - \frac{y}{P(r_{\mathsf{q}})}\right)\right)}{\log^2\left(1 - \frac{y}{P(r_{\mathsf{q}})}\right)} \\ & + r_{\mathsf{q}}c^*\left(1 - \frac{y}{P(r_{\mathsf{q}})}\right)\frac{1}{\log^2\left(1 - \frac{y}{P(r_{\mathsf{q}})}\right)}(1 + o(1)) \quad \text{as } y \to P(r_{\mathsf{q}})^-. \end{aligned} \tag{5.79}$$

This proves that $\widehat{r}_{\mathsf{q}} = P(r_{\mathsf{q}})$ by Lemma 5.2.10. The next step is to derive the asymptotic expansion of $\widehat{F}'$. By differentiating both sides in the equation of Lemma 5.2.10 we find

$$\widehat{F}'(y) = \frac{1}{y}\left(\frac{1}{P^{-1}(y)F'(P^{-1}(y))} + \frac{2}{F(P^{-1}(y))}\right)^{-1}, \quad y \in (0, P(r_{\mathsf{q}})). \tag{5.80}$$

Using (5.68), (5.69) and (5.79) we obtain the wanted expansion: as $y \to P(r_{\mathsf{q}})^-$,

$$\widehat{F}'(y) = 2 + \frac{2}{\log\left(1 - \frac{y}{P(r_{\mathsf{q}})}\right)} + \frac{2\log\left(-\log\left(1 - \frac{y}{P(r_{\mathsf{q}})}\right)\right)}{\log^2\left(1 - \frac{y}{P(r_{\mathsf{q}})}\right)} - \frac{2(3 - 2\log(2))}{\log^2\left(1 - \frac{y}{P(r_{\mathsf{q}})}\right)}(1 + o(1)). \tag{5.81}$$

The tree of components. We are now interested in properties of the tail of the probability measures ν and $\nu_\bullet$ of Section 5.3.3. To do so, we need estimates on the derivative of the Laplace transform L_ν. Recalling the form of the generating function of ν from (5.34), we get

$$L'_\nu(t) = -\frac{2P(r_{\mathsf{q}})}{F(r_{\mathsf{q}})} e^{-2t} \widehat{F}' \left(P(r_{\mathsf{q}})e^{-2t}\right), \quad t > 0. \tag{5.82}$$

By (5.81), we obtain

$$-L'_\nu(t) = 1 + \frac{1}{\log(2t)} + \frac{\log\left(-\log\left(2t\right)\right)}{\log^2\left(2t\right)} - \frac{3 - 2\log(2)}{\log^2\left(2t\right)} + o\left(\frac{1}{\log^2\left(t\right)}\right), \quad \text{as } t \to 0^+. \tag{5.83}$$

Since ν is critical, the Laplace transform $L_{\bar\nu}$ of the size-biased measure $\bar\nu$ is $-L'_\nu$. As a consequence,

$$\frac{L_{\bar\nu}\left(\frac{1}{\lambda x}\right) - L_{\bar\nu}\left(\frac{1}{x}\right)}{\log^2(x)} \underset{x\to\infty}{\longrightarrow} \log(\lambda), \quad \forall\, \lambda > 0. \tag{5.84}$$

Let us introduce a notation for the tail of the probability measure $\bar\nu$, say

$$T(x) := \sum_{k\geq x} k\nu(k), \quad x \in \mathbb{R}.$$

By De Haan's Tauberian theorem [BGT89, Theorem 3.9.1], (5.84) is equivalent to

$$\frac{T(\lambda x) - T(x)}{\log^2(x)} \underset{x\to\infty}{\longrightarrow} \log(\lambda), \quad \forall\, \lambda > 0. \tag{5.85}$$

The function T is said to be in the class $\Pi_{\log^2}$ with index 1. By an integration by parts (see also the last line in the proof of [BGT89, Theorem 8.1.6]), we have for every $x > 0$

$$x\nu((x,\infty)) = T(x) - x\int_x^\infty \frac{T(t)}{t^2}\mathrm{d}t. \tag{5.86}$$

Finally, by De Haan's Theorem [BGT89, Theorem 3.7.3], (5.85) and (5.86) we obtain the following.

Proposition 5.7.1. *Let q^* be the special weight sequence of type $a = 2$. Then, we have*

$$\nu([k,\infty)) \underset{k\to\infty}{\sim} \frac{1}{k\log^2(k)} \quad \text{and} \quad \nu_\bullet([k,\infty)) \underset{k\to\infty}{\sim} \frac{3}{k\log^2(k)}.$$

In particular, ν and $\nu_\bullet$ are in the domain of attraction of a Cauchy distribution (stable with parameter $a - 1 = 1$).

Remark 5.7.2. We have seen in Theorem 5.1.2 that when $a = 2$, the local limits of the boundary of Boltzmann bipartite maps behave as in the dense phase. However, Proposition 5.7.1 suggests that $\nu_\bullet$ has a very heavy tail, meaning that the local limit of the boundary has very large loops. We believe that the scaling limits of the boundary behave as in the dilute phase when $a = 2$, meaning that we expect the limit to be a circle, but the normalizing sequence to be negligible compared to the perimeter $2k$ of the map (typically of order $k/\log(k)$).

Acknowledgements. Many thanks to Grégory Miermont for enlightening discussions and his careful reading of this work. I would also like to thank warmly Erich Baur, Jérémie Bouttier, Timothy Budd, Nicolas Curien and Igor Kortchemski for very useful discussions and comments.

III

Percolation sur de grandes cartes à bord aléatoires

6

Universal aspects of percolation on random half-planar maps

We study a large class of Bernoulli percolation models on random lattices of the half-plane, obtained as local limits of uniform planar triangulations or quadrangulations. We first compute the exact value of the site percolation threshold in the quadrangular case using the so-called peeling techniques. Then, we generalize a result of Angel about the scaling limit of crossing probabilities, that are a natural analogue to Cardy's formula in (non-random) plane lattices. Our main result is that those probabilities are universal, in the sense that they do not depend on the percolation model neither on the degree of the faces of the map.

This Chapter is adapted from the work [3] (Electronic Journal of Probability, Vol. 20, 2015). It contains the proof of Theorems 12 and 13.

Contents

6.1 Introduction

In this work, we consider several aspects of Bernoulli percolation models (site, bond and face percolation) on Uniform Infinite Half-Planar Maps, more precisely on the Uniform Infinite Planar Triangulation and Quadrangulation of the half-plane (UIHPT and UIHPQ in short), which are defined as the so-called *local limit* of random planar maps. Those maps, or rather their infinite equivalents (UIPT and UIPQ), were first introduced by Angel & Schramm ([AS03]) in the case of triangulations and by Krikun ([Kri05]) in the case of quadrangulations (see also [CD06], [Mé10] and [CMM13] for an alternative approach). Angel later defined in [Ang04] the half-plane models, which have nicer properties. The Bernoulli percolation models on these maps are defined as follows: conditionally on the map, every site (respectively edge, face) is open with probability p and closed otherwise, independently of every other sites (respectively edges, faces). All the details concerning the map and percolation models are postponed to Section 6.2. More specifically, we will focus on the site percolation threshold for quadrangulations and the scaling limits of crossing probabilities.

In Section 6.3, we compute the site percolation threshold on the UIHPQ, denoted by $p_{c,\text{site}}^{\square}$. This problem was left open in [AC15], where percolation thresholds are given for any percolation and map model (site, bond and face percolation on the UIHPT and UIHPQ), except for the site percolation on the UIHPQ (see also [Ang03] and [MN14], where percolation thresholds are studied in the full-plane models). Roughly speaking, it is made harder by the fact that standard exploration processes of the map do not provide relevant information concerning percolation, as we will discuss later. This value is also useful in order to study the problem of the last section in the special case of site percolation on the UIHPQ. Namely, we will prove the following.

Theorem 6.1.1. *For Bernoulli site percolation on the* UIHPQ*, we have*

$$p_{c,site}^{\square} = \frac{5}{9}.$$

Moreover, there is no percolation at the critical point almost surely.

Due to the fact that Uniform Infinite Half-Planar Maps have a boundary, it is natural to consider boundary conditions. Here, the result holds for a free boundary condition. We believe that the percolation threshold is independent of these boundary conditions but did not investigate this further. We will discuss this again in Section 6.3.

The last section focuses on percolation models on Uniform Infinite Half-Planar Maps at their critical point, more precisely on crossing events. We work conditionally on the boundary condition of Figure 6.1 (in the case of bond percolation), where black edges are open, a, b are fixed and positive and λ is a positive scaling parameter.

Starting from now, we use the notation of [AC15] and let $*$ denote either of the symbols $\triangle$ or $\square$, where $\triangle$ stands for triangulations and $\square$ for quadrangulations.

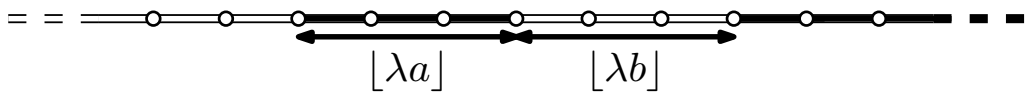

Figure 6.1: The boundary condition for the crossing probabilities problem.

The so-called *crossing event* we are interested in is the event that the two black segments are part of the same percolation cluster. We denote by $\mathsf{C}^*(\lambda a, \lambda b)$ this event and study the *scaling limit* of its probability when λ goes to infinity. The first result was proved by Angel in the case of site percolation on triangulations.

Theorem. ([Ang04, Theorem 3.3]) *Let $a, b \geq 0$. For site percolation at the critical point on the* UIHPT*,*

$$\lim_{\lambda \to +\infty} \mathbf{P}\left(\mathsf{C}^{\triangle}_{site}(\lambda a, \lambda b)\right) = \frac{1}{\pi} \arccos\left(\frac{b-a}{a+b}\right).$$

Our motivation is that this problem is a natural analogue to the famous *Cardy's formula* in regular lattices, which has been proved by Smirnov in the case of the triangular lattice (see [Smi01]). We are interested in the *universal* aspect of this scaling limit, in the sense that it is preserved for site, bond and face percolation on the UIHPT and the UIHPQ. Our main result is the following.

Theorem 6.1.2. *Let $a, b \geq 0$. We have for critical site, bond and face percolation models on the* UIHPT *and the* UIHPQ*,*

$$\lim_{\lambda \to +\infty} \mathbf{P}\left(\mathsf{C}^*(\lambda a, \lambda b)\right) = \frac{1}{\pi} \arccos\left(\frac{b-a}{a+b}\right).$$

In other words, asymptotic crossing probabilities are equal for site, bond and face percolation on the UIHPT *and the* UIHPQ *at their critical percolation threshold.*

The question of the universality of Cardy's formula for periodic plane graphs is an important open problem in probability theory, known as *Cardy's universality conjecture*. Here, the randomness of the planar maps we consider makes the percolation models easier to study.

Remark 6.1.3. We believe that for both the computation of the site percolation threshold and the asymptotics of crossing probabilities, our methods apply in more general settings as long as the *spatial Markov property* of Section 6.2.2 holds. This includes the generalized half-planar maps of [AR15], see also [Ray14] (in the "tree-like" phase of these maps, the critical point is 1 while in the "hyperbolic" phase, although the crossing probability vanishes at criticality, its rate of convergence could be investigated), and also covers the models defined in [BS14] and [Ste16], which have recently been proved to satisfy a version of the spatial Markov property in [Bud15]. In particular, we are able to compute the site percolation threshold in the UIHPT, which is already provided in [AC15]. The difference is that our method is less sensitive to boundary conditions, and also furnishes a universal formula for the site

percolation thresholds, in the spirit of [AC15]. We will discuss this in greater detail in Section 6.3.

Moreover, as we were finishing writing this paper, we became aware of the very recent preprint [BS15] by Björnberg and Stefánsson, that also deals with site percolation on the UIHPQ. This paper provides upper and lower bounds for the percolation threshold $p_{c,\text{site}}^{\square}$, but not the exact value $5/9$. Our study of the universality of crossing probabilities is also totally independent of [BS15].

6.2 Random planar maps and percolation models

We first recall the construction of the random planar maps we will focus on in the next part, and some important properties of these maps.

6.2.1 Definitions and distributions on planar maps

Let us first consider finite planar maps, i.e., proper embeddings of finite connected graphs in the sphere $\mathbb{S}^2$ (more precisely their equivalence class up to orientation-preserving homeomorphisms of the sphere). The faces of a planar map are the connected components of the complement of the embedding, and the degree of a face is the number of oriented edges this face is incident to (with the convention that the face incident to an oriented edge is the face on its left). Every planar map we consider is *rooted*: there is a distinguished oriented edge called the *root* of the map, and the tail vertex of this edge is the *origin* of the map.

We focus more precisely on p-*angulations* (the case $p = 3$ corresponds to *triangulations* and $p = 4$ to *quadrangulations*), i.e., finite planar maps whose faces all have the same degree p, and *generalized* p-angulations, i.e., planar maps whose faces all have degree p except possibly for a finite number of distinguished faces which can have arbitrary degrees. These faces are called *external faces* of the p-angulation (by contrast with *internal faces*), and are constrained to have a simple boundary (meaning that their embeddings are cycles without self-intersections). In this setting, an inner vertex of the map is a vertex that do not belong to an external face. Finally, triangulations are supposed to be 2-connected (or type 2), that is to say, multiple edges are allowed but loops are not.

Let $\mathcal{M}_f$ be the set of planar maps. We endow this set with the *local* topology, induced by the distance d_{loc} defined for every $\mathbf{m}, \mathbf{m}' \in \mathcal{M}_f$ by

$$d_{\text{loc}}(\mathbf{m}, \mathbf{m}') := (1 + \sup\{R \geq 0 : \mathbf{B}_R(\mathbf{m}) = \mathbf{B}_R(\mathbf{m}')\})^{-1},$$

where $\mathbf{B}_R(\mathbf{m})$ is the planar map given by the ball of radius R around the origin for the usual graph distance in the following sense: $\mathbf{B}_0$ contains only the origin of the map, and $\mathbf{B}_R$ is made of all the vertices at graph distance less than R from the origin, with all the edges linking them.

With this distance, $(\mathcal{M}_f, d_{\text{loc}})$ is a metric space, and we denote by $\mathcal{M}$ the completed space of $(\mathcal{M}_f, d_{\text{loc}})$. The elements of $\mathcal{M}_\infty := \mathcal{M} \backslash \mathcal{M}_f$ are called infinite planar maps, and are represented by a consistent sequence of balls of radius R for $R \geq 0$.

However, infinite planar maps that have one end (as a graph) are also the proper embedding of an infinite graph in the plane $\mathbb{R}^2$ such that every compact of $\mathbb{R}^2$ intersects finitely many edges, seen up to orientation-preserving homeomorphisms (see [CMM13, Appendix] and [Cur16a, Proposition 2] for greater details). In the next part, the infinite maps we consider all are one-ended.

Recall that $*$ stands for either of the symbols $\triangle$ or $\square$, where $\triangle$-angulations stands for type 2 triangulations and $\square$-angulations for quadrangulations. The first result of convergence in law of random maps for the local topology ([AS03, Theorem 1.8] for triangulations, [Kri05, Theorem 1] for quadrangulations) states as follows. For $n \geq 1$, let $\mathbb{P}_n^*$ be the uniform measure on the set of $*$-angulations with n vertices $(\triangle)$, respectively n faces $(\square)$. We have

$$\mathbb{P}_n^* \underset{n\to+\infty}{\Longrightarrow} \mathbb{P}_\infty^*,$$

in the sense of weak convergence, for the local topology. The probability measure $\mathbb{P}_\infty^*$ is supported on infinite $*$-angulations of the plane, and called the law of the Uniform Infinite Planar $*$-angulation (UIPT and UIPQ respectively in short). Note that there is an alternative construction in the quadrangular case, for which we refer to [CD06], [Mé10] and [CMM13].

In the next part, we will focus on a slightly different model introduced by Angel in [Ang04], that has an infinite boundary and nicer properties.

For $m \geq 2$, a generalized $*$-angulation with a unique external face of degree m is called $*$-angulation of the m-gon. Then, the edges of the external face are interpreted as the *boundary* of the map. For $n \geq 0$ and $m \geq 2$, we denote by $\widehat{\mathcal{M}}_{n,m}^*$ the set of $*$-angulations of the m-gon with n inner vertices *rooted on the boundary* (such that the external face lies on the right of the root), and $\varphi_{n,m}^*$ its cardinality. The set $\widehat{\mathcal{M}}_{0,2}$ contains the map with a single oriented edge. Note that $\varphi_{n,m}^{\square} = 0$ for m odd, so that we implicitly restrict ourselves to the cases where m is even for quadrangulations. The quantity $\varphi_{n,m}^*$ being positive and finite for $n \geq 0$ and $m \geq 2$ (see [Tut68] for exact enumerative formulas), we can define the uniform probability measure on $\widehat{\mathcal{M}}_{n,m}^*$, denoted by $\widehat{\mathbb{P}}_{n,m}^*$. Asymptotics for the numbers $(\varphi_{n,m}^*)_{n\geq 0, m\geq 2}$ are known and universal in the sense that

$$\varphi_{n,m}^* \underset{n\to+\infty}{\sim} C_*(m)\rho_*^n n^{-5/2} \quad \text{and} \quad C_*(m) \underset{m\to+\infty}{\sim} K_* \alpha_*^m \sqrt{m},$$

where $\rho_\triangle = 27/2$, $\alpha_\triangle = 9$, $\rho_\square = 12$, $\alpha_\square = \sqrt{54}$ and $K_* > 0$ (see for instance the work of Gao, or more precisely [Kri07] for 2-connected triangulations, and [BG09] for quadrangulations).

We now recall the construction of the uniform infinite half-planar maps. The Uniform Infinite Planar $*$-angulation of the Half-Plane, or UIHP-$*$, is a probability measure supported on infinite half-planar $*$-angulations defined by the following limits.

Theorem. ([AS03, Theorem 5.1] and [Ang04, Theorem 2.1]) *For every $m \geq 2$, we have*

$$\widehat{\mathbb{P}}_{n,m}^* \underset{n\to+\infty}{\Longrightarrow} \widehat{\mathbb{P}}_{\infty,m}^*,$$

in the sense of weak convergence, for the local topology. The probability measure $\widehat{\mathbb{P}}^*_{\infty,m}$ *is supported on infinite* $*$*-angulations of the* m*-gon and called the law of the* UIPT *and* UIPQ *of the* m*-gon, respectively. Moreover, we have*

$$\widehat{\mathbb{P}}^*_{\infty,m} \underset{m\to+\infty}{\Longrightarrow} \widehat{\mathbb{P}}^*_{\infty,\infty},$$

in the sense of weak convergence, for the local topology. The probability measure $\widehat{\mathbb{P}}^*_{\infty,\infty}$ *is called the law of the Uniform Infinite Half-Planar* $*$*-angulation (half-plane* UIPT *and* UIPQ*, or also* UIHPT *and* UIHPQ *respectively in short).*

This result is stated in [Ang04] for triangulations but easily extends to the quadrangular case, for which an alternative construction is provided in Section 6.1 of [CM15]. See also [AR15] for a characterization of these distributions.

We now give important properties of the previous measure, which justifies in particular the naming "half-plane". The proof of such a result is based upon the inductive construction of the measure $\widehat{\mathbb{P}}^*_{\infty,\infty}$ by a *peeling process*, as described in [Ang04]. This is also illustrated in Figure 6.2.

Proposition. *The probability measure* $\widehat{\mathbb{P}}^*_{\infty,\infty}$ *is supported on infinite* $*$*-angulations of the half-plane with an infinite simple boundary (and rooted on the boundary).*

Namely, these maps can be defined as the proper embedding of an infinite, locally finite connected graph in the upper half-plane $\mathbb{H}$ *such that all the faces are finite and have degree 3* $(* = \triangle)$*, respectively degree 4* $(* = \square)$*. (In the case of triangulations, there are also no self-loops.) In particular, the restriction of this embedding to the real line* $\mathbb{R}$ *is isomorphic to the graph of* $\mathbb{Z}$ *and the triangles (respectively quadrangles) exhaust the whole half-plane.*

Finally, the probability measure $\widehat{\mathbb{P}}^*_{\infty,\infty}$ *enjoys a re-rooting invariance property, in the sense that it is preserved under the natural shift operation for the root edge along the boundary.*

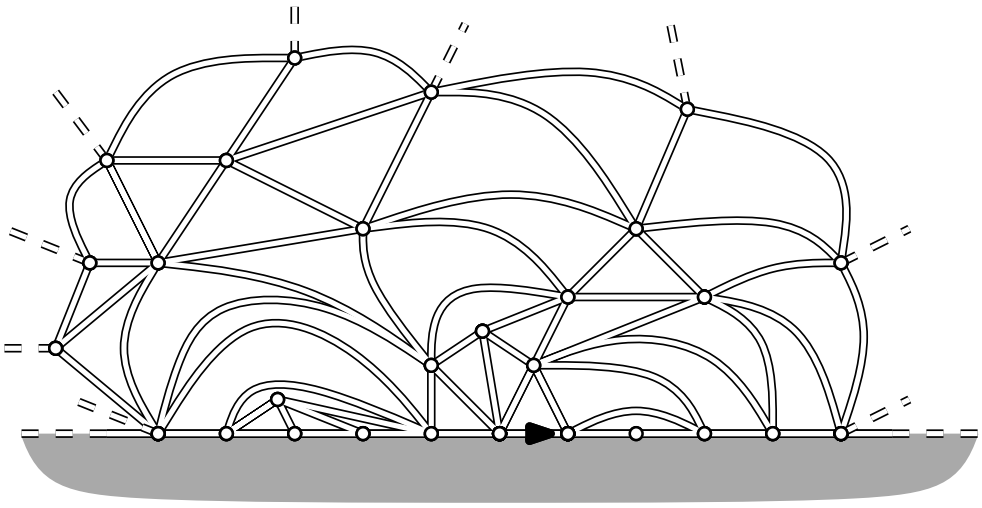

Figure 6.2: An embedding of the UIHPT in the upper half-plane.

In order to detail the outstanding properties of the measure $\widehat{\mathbb{P}}^*_{\infty,\infty}$, we have to define another measure on finite planar maps, which gives an equal weight to maps with a fixed number of faces or, equivalently, of inner vertices. This measure is called the *Boltzmann measure* (or *free measure* in [Ang03]). Let $m \geq 2$ and set

$$W^*_m := \sum_{n\geq 0} \varphi^*_{n,m} \rho_*^{-n}, \tag{6.1}$$

which is exactly the generating function of $*$-angulations of the m-gon at the radius of convergence. Now, let us interpret the quantities $(W^*_m : m \geq 2)$ as partition functions of a probability measure. This yields to the $*$-Boltzmann distribution of the m-gon, denoted by $\mathbb{W}^*_m$, which is the probability measure on finite $*$-angulations of the m-gon defined for every $\mathbf{m} \in \widehat{\mathcal{M}}^*_{n,m}$ and every $n \geq 0$ by

$$\mathbb{W}^*_m(\mathbf{m}) := \frac{\rho_*^{-n}}{W^*_m}. \tag{6.2}$$

A random variable with law $\mathbb{W}^*_m$ is called a Boltzmann $*$-angulation of the m-gon. Moreover, the asymptotic behaviour of $(W^*_m)_{m\geq 2}$ is also known and given by

$$W^*_m \underset{m\to+\infty}{\sim} \iota_* m^{-5/2} \alpha_*^m, \tag{6.3}$$

for some constant $\iota_* > 0$ and α_* as above.

The Boltzmann measures are particularly important because these objects satisfy a branching property, that we will identify on our uniform infinite $*$-angulations of the half-plane as the *spatial* (or *domain*) *Markov property*. The reason why we will get this property on our infinite map is that the UIHP-$*$ can also be obtained as the limit of Boltzmann measures of the m-gon when m becomes large.

Theorem. ([Ang04, Theorem 2.1]) *We have* $\mathbb{W}^*_m \underset{m\to+\infty}{\Longrightarrow} \widehat{\mathbb{P}}^*_{\infty,\infty}$ *in the sense of weak convergence, for the local topology.*

6.2.2 Spatial Markov property and configurations

We now describe the so-called *peeling* argument (introduced by Angel), whose principle is to suppose the whole map unknown and to reveal it face by face.

Let us consider a random map M which has the law of the UIHP-$*$, and a face A of M which is incident to the root. Then, we *reveal* or *peel* the face A, in the sense that we suppose the whole map unknown and work conditionally on the configuration of this face. We now consider the map $M\backslash$A, which is the map M deprived of the edges of A that belong to the boundary (in that sense, we also say that we *peel* the root edge). By convention, the connected components of this map are the submaps obtained by cutting at a single vertex of A that belongs to the boundary.

We can now state a remarkable property of the UIHPT and the UIHPQ that will be very useful for our purpose, and which is illustrated in Figure 6.3. This should be interpreted as a branching property of the measure $\widehat{\mathbb{P}}^*_{\infty,\infty}$.

Theorem. (Spatial Markov property, [Ang04, Theorem 2.2]) *Let M be a random variable with law $\widehat{\mathbb{P}}^*_{\infty,\infty}$, and* A *the face incident to the root edge of M.*

Then, $M\backslash$A has a unique infinite connected component, say M', and at most one ($* = \triangle$) or two ($* = \square$) finite connected components, say $\tilde{M}_1$ and $\tilde{M}_2$. Moreover, M' has the law $\widehat{\mathbb{P}}^*_{\infty,\infty}$ of the UIHP-$*$*, and $\tilde{M}_1$ and $\tilde{M}_2$ are Boltzmann $*$-angulations of a m-gon (for the appropriate value of $m \geq 2$ which is given by the configuration of the face* A*).*

Finally, all those $*$-angulations are independent, in particular M' is independent of $M\backslash M'$. This property still holds replacing the root edge by another oriented edge on the boundary, chosen independently of M.

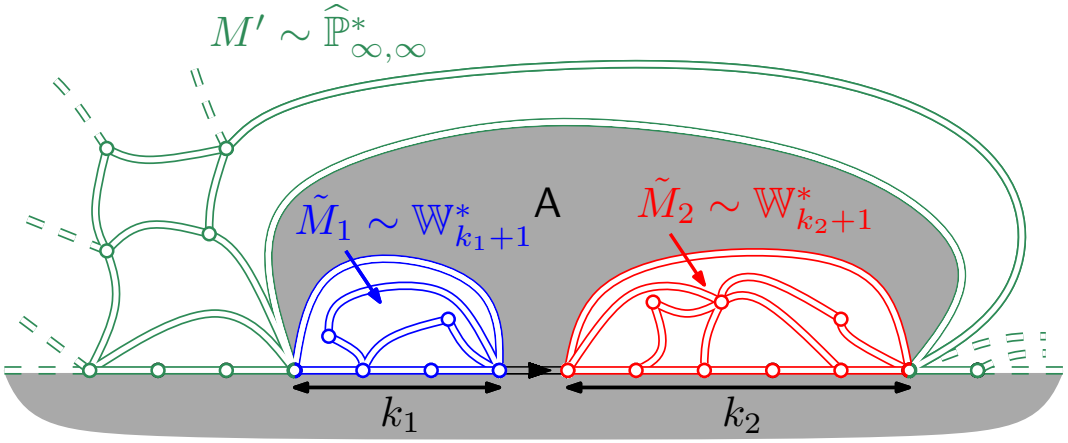

Figure 6.3: The spatial Markov property.

The peeling argument can now be extended to a *peeling* or *exploration* process, by revealing a new face in the unique infinite connected component of the map deprived of the last discovered face. The spatial Markov property ensures that the configurations for this face have the same probability at each step, and the re-rooting invariance of the UIHP-$*$ allows a complete freedom on the choice of the next edge to peel (as long as it does not depend on the unrevealed part of the map). This is the key idea in order to study percolation on the maps we consider, and has been used extensively in [Ang04] and [AC15].

We now describe all the possible configurations for the face A incident to the root in the UIHP-$*$, and the corresponding probabilities. Let us introduce some notations. On the one hand, some edges may lie on the boundary of the infinite connected component of $M\backslash$A. These edges are called *exposed* edges, and the (random) number of exposed edges is denoted by $\mathcal{E}^*$. On the other hand, some edges of the boundary may be enclosed in a finite connected component of the map $M\backslash$A. We call them *swallowed* edges, and the number of swallowed edges is denoted by $\mathcal{R}^*$. We will sometimes use the notation $\mathcal{R}^*_l$ (respectively $\mathcal{R}^*_r$) for the number of swallowed edges on the left (respectively right) of the root edge. (Note that the definitions of these random variables are robust with respect to the map model, but we may sometimes add the symbol $*$ to avoid confusion when the law of the map is not explicitly men-

tioned.) Finally, in the infinite maps we consider, an inner vertex is a vertex that do not belong to the boundary. The results are the followings.

Proposition 6.2.1. (Triangulations case, [AC15]) *There exists two configurations for the triangle incident to the root in the* UIHPT *(see Figure 6.4).*

1. *The third vertex of the face is an inner vertex* $(\mathcal{E}^{\triangle} = 2, \mathcal{R}^{\triangle} = 0)$. *This event has probability* $q^{\triangle}_{-1} = 2/3$.

2. *The third vertex of the face is on the boundary of the map,* $k \geq 1$ *edges on the left (respectively right) of the root* $(\mathcal{E}^{\triangle} = 1, \mathcal{R}^{\triangle} = k)$. *This event has probability* $q^{\triangle}_{k} = W^{\triangle}_{k+1} 9^{-k}$.

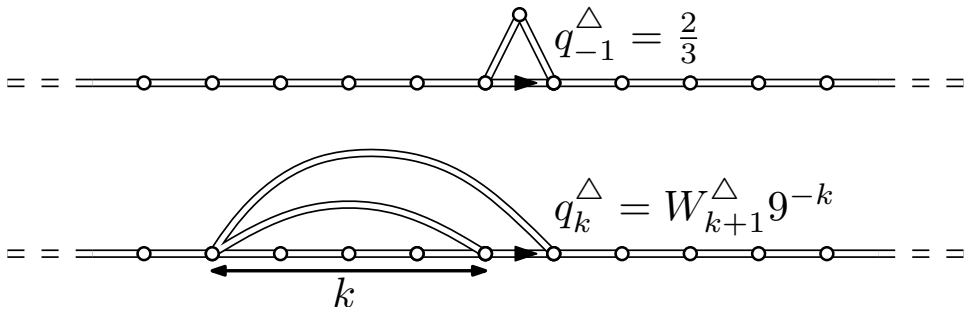

Figure 6.4: The configurations of the triangle incident to the root (up to symmetries).

Proposition 6.2.2. (Quadrangulations case, [AC15]) *There exists three configurations for the quadrangle* A *incident to the root in a map* M *which has the law of the* UIHPQ *(see Figure 6.5).*

1. *The face has two inner vertices* $(\mathcal{E}^{\square} = 3, \mathcal{R}^{\square} = 0)$. *This event has probability* $q^{\square}_{-1} = 3/8$

2. *The face has three vertices on the boundary of the map, the third one being* $k \geq 0$ *edges on the left (respectively right) of the root. This event has probability* $q^{\square}_{k}$, *given by the following subcases:*

   - *If* k *is odd, the fourth vertex belongs to the infinite connected component of* $M \backslash \mathsf{A}$ $(\mathcal{E}^{\square} = 2, \mathcal{R}^{\square} = k)$. *Then*

$$q^{\square}_{k} = \frac{W^{\square}_{k+1} \alpha_{\square}^{1-k}}{\rho_{\square}}.$$

   - *If* k *is even, the fourth vertex belongs to the finite connected component of* $M \backslash \mathsf{A}$ $(\mathcal{E}^{\square} = 1, \mathcal{R}^{\square} = k)$. *Then*

$$q^{\square}_{k} = \frac{W^{\square}_{k+2} \alpha_{\square}^{-k}}{\rho_{\square}}.$$

3. *The face has all of its four vertices on the boundary of the map, and the quadrangle defines two segments along the boundary of length k_1 and k_2 - both odd ($\mathcal{E}^{\square} = 1, \mathcal{R}^{\square} = k_1 + k_2$). This event has probability $q^{\square}_{k_1,k_2} = W^{\square}_{k_1+1} W^{\square}_{k_2+1} \alpha_{\square}^{-k_1-k_2}$.*

   (This configuration should be splitted in two subcases, depending on whether or not the vertices of the face are all on the same side of the root edge - up to symmetries).

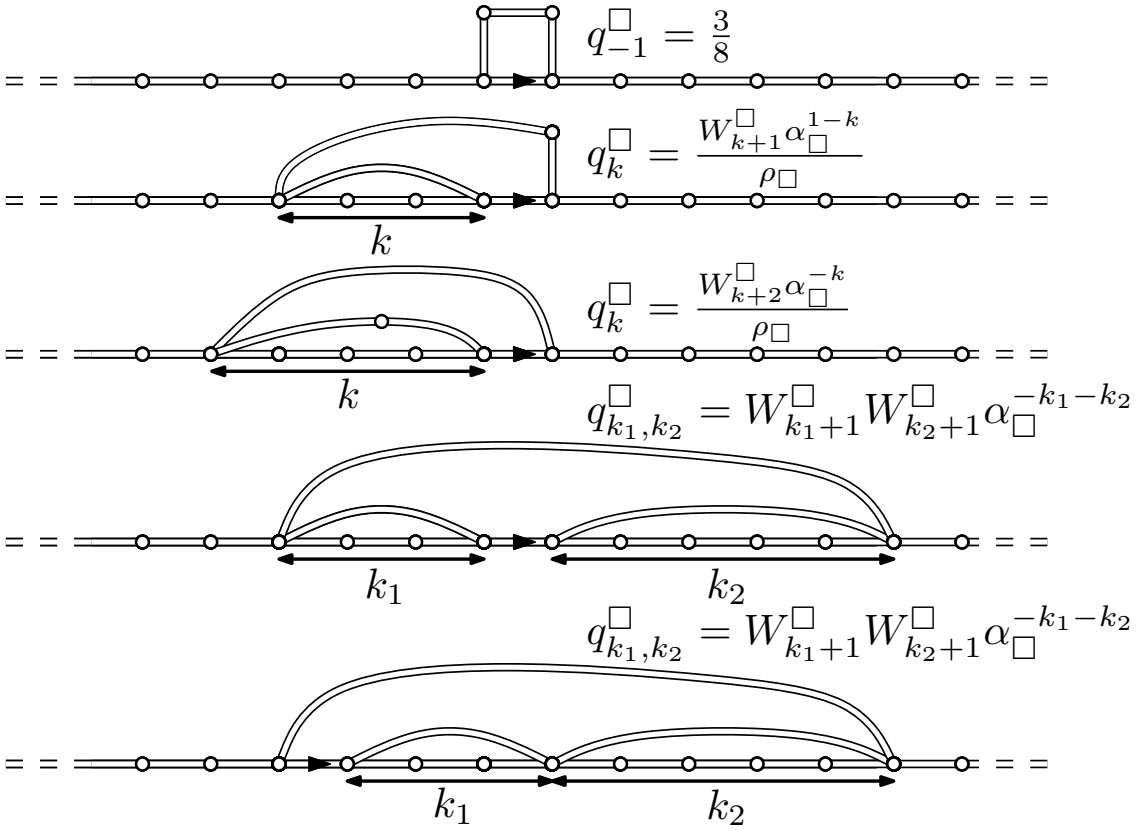

Figure 6.5: The configurations of the quadrangle incident to the root (up to symmetries).

We finally give the expectations of $\mathcal{E}^*$ and $\mathcal{R}^*$, obtained by direct computation using exact formulas for the partition function (6.1), see [AC15, Section 2.2].

Proposition 6.2.3. ([AC15, Proposition 3]) *We have*

- $\mathbf{E}(\mathcal{E}^{\triangle}) = 5/3$ *and* $\mathbf{E}(\mathcal{R}^{\triangle}) = 2/3$.
- $\mathbf{E}(\mathcal{E}^{\square}) = 2$ *and* $\mathbf{E}(\mathcal{R}^{\square}) = 1$.

Moreover, the distribution of $\mathcal{E}^{\square}$ can be explicitly computed.

$$\mathcal{E}^{\square} = \begin{cases} 3 & \text{with probability } 3/8 \\ 2 & \text{with probability } 1/4 \\ 1 & \text{with probability } 3/8 \end{cases}.$$

Remark 6.2.4. The configurations being completely symmetric, we have $\mathcal{R}_l^* \overset{(d)}{=} \mathcal{R}_r^*$, so that $\mathbf{E}(\mathcal{R}_l^*) = \mathbf{E}(\mathcal{R}_r^*) = \mathbf{E}(\mathcal{R}^*)/2$.

6.2.3 Percolation models

We now specify the percolation models we focus on. Recall that we are interested in Bernoulli percolation on the random maps we previously introduced, i.e., every site (respectively edge, face) is open (we will say coloured black, or refer to the value 1 in the following) with probability p and closed (coloured white, or taking value 0) otherwise, independently of every other sites (respectively edges, faces). Note that this colouring convention is the same as in [Ang03], but opposed to that of [AC15]. The convention for face percolation is that two faces are adjacent if they share an edge.

Here is a more precise definition of the probability measure $\mathbf{P}_p$ induced by our model. Recall that $\mathcal{M}$ is the set of (possibly infinite) planar maps, and for a given map $\mathbf{m} \in \mathcal{M}$, define the following measure on the set $\{0,1\}^{e(\mathbf{m})}$ of colourings of this map (where $e(\mathbf{m})$ is the set of the "elements" (vertices, edges or faces) of $\mathbf{m}$):

$$\mathcal{P}_p^{e(\mathbf{m})} := (p\delta_1 + (1-p)\delta_0)^{\otimes e(\mathbf{m})}.$$

We then define $\mathbf{P}_p$ as the measure on the set $\left\{(\mathbf{m}, c) : \mathbf{m} \in \mathcal{M}, c \in \{0,1\}^{e(\mathbf{m})}\right\}$ of coloured maps:

$$\mathbf{P}_p(\mathrm{d}\mathbf{m}\mathrm{d}c) := \widehat{\mathbb{P}}^*_{\infty,\infty}(\mathrm{d}\mathbf{m})\mathcal{P}_p^{e(\mathbf{m})}(\mathrm{d}c).$$

In other words, $\mathbf{P}_p$ is the measure on coloured planar maps such that the map has the law of the UIHP-$*$ and conditionally on this map, the colouring is a Bernoulli percolation with parameter p. We slightly abuse notation here, since we denote by $\mathbf{P}_p$ the probability measure induced by every map and percolation model considered in this paper, but there is little risk of confusion - if there is, we assign the notation $*$ to the random variables we consider. In what follows, we will often work conditionally on the colouring of the boundary of the map, which we call the boundary condition.

We finally define the percolation threshold (or critical point) in this model. Denote by $\mathcal{C}$ the open percolation cluster of the origin of the map we consider (respectively the root edge for face percolation) and recall that the percolation event is the event that $\mathcal{C}$ is infinite. The percolation probability is defined for $p \in [0,1]$ by

$$\Theta^*(p) := \mathbf{P}_p(|\mathcal{C}| = +\infty).$$

A standard coupling argument proves that the function Θ^* is non-decreasing, so that there exists a critical point p_c^*, called the percolation threshold, such that

$$\begin{cases} \Theta^*(p) = 0 & \text{if} \quad p < p_c^* \\ \Theta^*(p) > 0 & \text{if} \quad p > p_c^* \end{cases}.$$

Thus, the percolation threshold p_c^* can also be defined by the identity $p_c^* := \inf\{p \in [0,1] : \Theta^*(p) > 0\} = \sup\{p \in [0,1] : \Theta^*(p) = 0\}$. Note that both Θ^* and p_c^* depend on the law of the infinite planar map and on the percolation model we consider.

In our setting, we can use the peeling argument to derive a zero-one law under $\mathbf{P}_p$ for every $p \in [0,1]$, in the sense that every event invariant to finite changes in the coloured map has probability 0 or 1 under $\mathbf{P}_p$. The idea is to assign i.i.d. random variables to each step of peeling and to apply Kolmogorov's zero-one law (see [Ang03, Theorem 7.2] for a proof in the full-plane case). A fortiori, we have that the probability of such an event is 0 or 1 under $\mathcal{P}_p^{e(\mathbf{m})}$ for $\widehat{\mathbb{P}}^*_{\infty,\infty}(\mathrm{d}\mathbf{m})$-almost every map. Following usual arguments of percolation theory (see [Gri99, Theorem 1.11]), this yields that the event that there exists an infinite open cluster has probability 0 or 1 under $\mathbf{P}_p$ and then if we introduce the function defined for $p \in [0,1]$ by

$$\Psi^*(p) := \mathbf{P}_p\left(\exists\, x \in e'(\mathbf{m}) : |\mathcal{C}(x)| = +\infty\right),$$

where $\mathcal{C}(x)$ is the open percolation cluster of the site (respectively edge for face percolation) x of the map, we get that

$$\begin{cases} \Psi^*(p) = 0 & \text{if} \quad \Theta^*(p) = 0 \\ \Psi^*(p) = 1 & \text{if} \quad \Theta^*(p) > 0 \end{cases}.$$

Of course, we also get this result under $\mathcal{P}_p^{e(\mathbf{m})}$ for $\widehat{\mathbb{P}}^*_{\infty,\infty}(\mathrm{d}\mathbf{m})$-almost every map.

The map on which we study percolation being itself random, one should take care of the distinction between *annealed* and *quenched* statements concerning percolation. The above percolation threshold p_c^* is annealed, or averaged on all maps, since it is also the infimum of values of p such that a positive measure of maps under $\widehat{\mathbb{P}}^*_{\infty,\infty}$ satisfy that the percolation event has positive probability under $\mathcal{P}_p^{e(\mathbf{m})}$. We should then denote this threshold by $p_c^{(*,\mathrm{A})}$.

The quenched percolation threshold $p_c^{(*,\mathrm{Q})}$ is defined as the infimum of values of p such that for $\widehat{\mathbb{P}}^*_{\infty,\infty}(\mathrm{d}\mathbf{m})$-*almost every map*, the percolation event has positive probability under $\mathcal{P}_p^{e(\mathbf{m})}$. In other words, if we introduce the function defined for every $p \in [0,1]$ by

$$\tilde{\Theta}^*(p) := \widehat{\mathbb{P}}^*_{\infty,\infty}\left(\left\{\mathbf{m} \in \mathcal{M} : \mathcal{P}_p^{e(\mathbf{m})}\left(|\mathcal{C}| = +\infty\right) > 0\right\}\right),$$

then the critical thresholds $p_c^{(*,\mathrm{A})}$ and $p_c^{(*,\mathrm{Q})}$ are defined by

$$\begin{cases} \tilde{\Theta}^*(p) = 0 & \text{if} \quad p < p_c^{(*,\mathrm{A})} \\ \tilde{\Theta}^*(p) = 1 & \text{if} \quad p > p_c^{(*,\mathrm{Q})} \\ \tilde{\Theta}^*(p) \in (0,1) & \text{otherwise} \end{cases}.$$

These can be proved to exist by using again the coupling argument. Now, if $p > p_c^{(*,\mathrm{A})}$, we have from the above observation that

$$\Psi^*(p) = \int_{\mathcal{M}} \mathcal{P}_p^{e(\mathbf{m})}\left(\exists\, x \in e(\mathbf{m}) : |\mathcal{C}(x)| = +\infty\right) \widehat{\mathbb{P}}^*_{\infty,\infty}(\mathrm{d}\mathbf{m}) = 1,$$

which in turn yields that $\mathcal{P}_p^{e(\mathbf{m})}\left(\exists\, x \in e(\mathbf{m}) : |\mathcal{C}(x)| = +\infty\right) = 1$. Thus, we get that $\mathcal{P}_p^{e(\mathbf{m})}\left(|\mathcal{C}| = +\infty\right) > 0$ for $\widehat{\mathbb{P}}^*_{\infty,\infty}(\mathrm{d}\mathbf{m})$-almost every map. This proves that $\tilde{\Theta}^*(p) = 1$, and the identity

$$p_c^{(*,\mathrm{A})} = p_c^{(*,\mathrm{Q})}.$$

In the next part, we will thus use the notation p_c^* and give only annealed statements concerning percolation thresholds. Note that in particular, the absence of percolation at criticality of Theorem 6.1.1 implies that for $\widehat{\mathbb{P}}^*_{\infty,\infty}(\mathrm{d}\mathbf{m})$-almost every map, there is no percolation at the critical point under $\mathcal{P}_p^{e(\mathbf{m})}$.

6.2.4 Lévy $3/2$-stable process

Let us define the (spectrally negative) $3/2$-stable process and give some important properties that will be used later. All the results can be found in [Ber98].

Definition 6.2.5. The Lévy spectrally negative $3/2$-stable process is the Lévy process $(\mathcal{S}_t)_{t\geq 0}$ whose Laplace transform is given by $E(e^{\lambda \mathcal{S}_t}) = e^{t\lambda^{3/2}}$, for every $\lambda \geq 0$. Its Lévy measure is supported on $\mathbb{R}_-$ and given by

$$\Pi(dx) = \frac{3}{4\sqrt{\pi}}|x|^{-5/2}dx\mathbf{1}_{\{x<0\}}.$$

In particular, this process has no positive jumps. Finally, the Lévy spectrally negative $3/2$-stable process has a scaling property with parameter $3/2$, i.e for every $\lambda > 0$ the processes $(\mathcal{S}_t)_{t\geq 0}$ and $(\lambda^{-3/2}\mathcal{S}_{\lambda t})_{t\geq 0}$ have the same law.

Note that this process is also called Airy-stable process (ASP in short). We will need the so-called *positivity parameter* of the process $\mathcal{S}$, defined by

$$\rho := P(\mathcal{S}_1 \geq 0)$$

Applying results of [Ber98] in our setting, we get the following.

Lemma 6.2.6. ([Ber98, Chapter 8]) *The positivity parameter of the Lévy $3/2$-stable process is given by $\rho = 2/3$.*

This process will be very useful for our purpose because it is the scaling limit of a large class of random walks whose steps are in the domain of attraction of a stable distribution with parameter $3/2$.

Proposition 6.2.7. ([AC15, Section 4], [BGT89, Chapter 8], [Ber06]) *Let X being a **centered** real-valued random variable such that $P(X > t) = o(t^{-3/2})$ and $P(X < -t) = ct^{-3/2} + o(t^{-3/2})$, for a positive constant c. Then, if S is a random walk with steps distributed as X, i.e., $S_0 = 0$ and for every $n \geq 1$, $S_n = \sum_{i=1}^n X_i$ where the random variables $(X_i)_{i\geq 1}$ are independent and have the same law as X, we have*

$$\left(\frac{S_{\lfloor \lambda t \rfloor}}{\lambda^{2/3}}\right)_{t\geq 0} \xrightarrow[\lambda\to+\infty]{(d)} \kappa(\mathcal{S}_t)_{t\geq 0},$$

in the sense of convergence in law for Skorokhod's topology, where κ is an explicit constant (proportional to c).

We end this section with an important property of the $3/2$-stable process, which concerns the distribution of the so-called *overshoot* at the first entrance in $\mathbb{R}_-$. It is a consequence of the fact that the so-called *ladder height process* of $-(\mathcal{S}_t)_{t\geq 0}$ is a stable subordinator with index $1/2$ (see [Ber98] for details). We use the notation P_a for the law of the process started at a.

Proposition 6.2.8. ([Ang04, Section 3.3], [Ber98, Chapter 3], [DK06, Example 7]) *Let $\tau := \inf\{t \geq 0 : \mathcal{S}_t \leq 0\}$ denote the first entrance time of the $3/2$-stable process $\mathcal{S}$ in $\mathbb{R}_-$. Then, the distribution of the overshoot $|\mathcal{S}_\tau|$ of $\mathcal{S}$ at the first entrance in $\mathbb{R}_-$ is given for every $a, b > 0$ by*

$$P_a(|\mathcal{S}_\tau| > b) = \frac{1}{\pi} \arccos\left(\frac{b-a}{a+b}\right).$$

Moreover, the joint distribution of the undershoot and the overshoot $(\mathcal{S}_{\tau-}, |\mathcal{S}_\tau|)$ of $\mathcal{S}$ at the first entrance in $\mathbb{R}_-$ is absolutely continuous with respect to the Lebesgue measure on $(\mathbb{R}_+)^2$.

6.3 Site percolation threshold on the UIHPQ

Throughout this section, we consider Bernoulli site percolation on a random map which has the law of the UIHPQ, and focus on the computation of the site percolation threshold, denoted by $p_{c,\text{site}}^{\square}$.

First of all, let us state roughly why is computing the site percolation threshold different on triangulations and quadrangulations. The main idea of the proof in the triangular case in [Ang04] is to follow the percolation interface between the open origin and the closed neighbours on its right, say, using an exploration process. When dealing with quadrangulations, with positive probability the revealed quadrangle has the configuration of Figure 6.6. From there, one should try to follow the interface drawn on the figure, but the circled black vertex should not be ignored, because it is also possibly part of the open percolation cluster of the origin. Roughly speaking, keeping track of those revealed open vertices on the boundary makes the size of the revealed part of the cluster hard to study through the exploration.

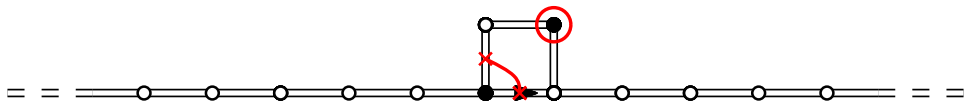

Figure 6.6: Exploration process in the UIHPQ.

Our aim is now to prove Theorem 6.1.1. In this statement, there is no condition on the initial colouring of the boundary, which is completely *free* (a free vertex is by definition open with probability p, closed otherwise, independently of all other vertices in the map). In order to simplify the proof, but also for the purpose of Section 6.4, we first work conditionally on the "Free-Black-White" boundary condition presented in Figure 6.7.

Figure 6.7: The boundary condition for the site percolation threshold problem.

The key here is to keep as much randomness as we can on the colour of the vertices and still to use an appropriate peeling process, following the ideas of [AC15].

Since we work on the UIHPQ and in order to make the notation less cluttered, we omit the symbol $\square$ in what follows.

6.3.1 Peeling process

We want to reveal the map face by face in a proper way, which will define our peeling or exploration process. The strategy here is to reveal one by one the colour of the free vertices of the boundary, and to "discard" or "peel" the white vertices that are discovered in a sense we now make precise. To do so, we need an alternative peeling process, that we call "vertex-peeling process". This process is well-defined independently of the boundary condition, as long as we have a marked vertex on the boundary.

ALGORITHM 6.3.1. (Vertex-peeling process) Consider a half-plane map which has the law of the UIHPQ and a marked vertex on the boundary.

Reveal the face incident to the edge of the boundary that is incident to the marked vertex on the left, and denote by R_r the number of swallowed edges on the right of this edge (without revealing the colour of the vertices that are discovered).

- If $\mathsf{R}_r > 0$, the algorithm ends.
- If $\mathsf{R}_r = 0$, repeat the algorithm on the unique infinite connected component of the map deprived of the revealed face.

Let us now give the main properties of this algorithm, which is illustrated in Figure 6.8 for the boundary condition that we will focus on in the next part (the arrow is pointed at the marked vertex).

Proposition 6.3.2. *The vertex-peeling process is well-defined, in the sense that the marked vertex is on the boundary as long as the algorithm does not end, which occurs in finite time almost surely. Moreover, when the algorithm ends:*

- *The number of swallowed edges on the right of the marked vertex in the initial map has the law $\mathbf{P}_p(\mathcal{R}_r \in \cdot \mid \mathcal{R}_r > 0)$ of the random variable $\mathcal{R}_r$ conditioned to be positive.*
- *The unique infinite connected component of the map deprived of the revealed faces has the law of the* UIHPQ *and the marked vertex does not belong to this map. In that sense, this vertex has been peeled by the process.*

Proof. The conservation of the marked vertex, say v, on the boundary is a consequence of the fact that $\mathsf{R}_r = 0$ at each step as long as the process is not over. Moreover, the spatial Markov property implies that the sequence of swallowed edges to the right of v is an i.i.d. sequence of random variables which have the same law as $\mathcal{R}_r$. The algorithm ends when the first positive variable in that sequence is reached (which happens in finite time almost surely), whose law is thus $\mathbf{P}_p(\mathcal{R}_r \in \cdot \mid \mathcal{R}_r > 0)$. It also equals the number of swallowed edges to the right of v in the initial map by

construction. Finally, since $R_r > 0$ at the last step, the marked vertex v is not on the boundary of the unique infinite connected component we consider when the process ends. □

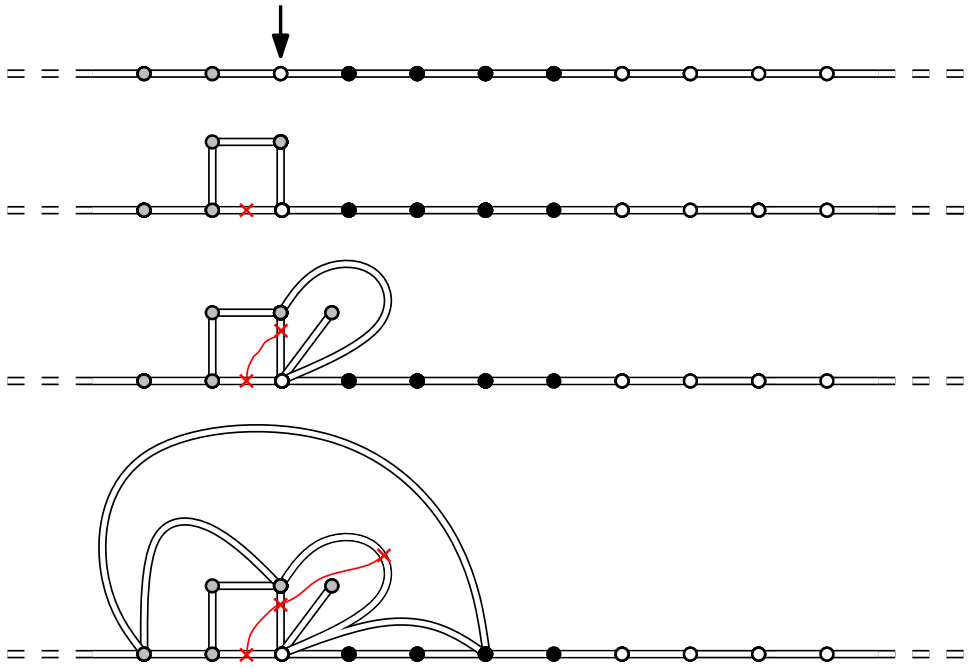

Figure 6.8: An example of execution of the vertex-peeling process.

We are now able to describe the complete peeling process we focus on. In what follows, a "Free-Black-White" boundary condition means in general that there are infinite free and white segments on the boundary (on the left and on the right respectively), and a finite black segment between them (Figure 6.7 is an example).

ALGORITHM 6.3.3. (Peeling process) Consider a half-plane map which has the law of the UIHPQ with a "Free-Black-White" boundary condition.

Reveal the colour of the rightmost free vertex on the boundary.

- If it is black, repeat the algorithm.
- If it is white, mark this vertex and execute the vertex-peeling process.

After each step, repeat the algorithm on the unique infinite connected component of the map deprived of the revealed faces. The algorithm ends when the initial open vertex of the boundary has been swallowed - i.e., does not belong to the map on which the algorithm should process.

Remark 6.3.4. In the previous algorithms, the map we consider at each step of the peeling process is implicitly rooted at the next edge we have to peel, which is determined by the colouring of the boundary.

As a consequence of the properties of the vertex-peeling process, we get that the whole peeling process is well-defined, in the sense that the pattern of the boundary (Free-Black-White) is preserved as long as the algorithm does not end. Moreover, at each step, the planar map we consider has the law of the UIHPQ and does not depend on the revealed part of the map: the transitions of the peeling process are independent and have the same law. In particular, if we denote by $\mathcal{H}_n$, c_n the number of swallowed edges at the right of the root edge and the colour of the revealed vertex at step n of the exploration respectively, then $(\mathcal{H}_n, c_n)_{n\geq 0}$ are i.i.d. random variables.

The quantity we are interested in is the **length of the finite black segment** on the boundary of the map at step n of the process, denoted by B_n. The process $(B_n)_{n\geq 0}$ is closely related to the percolation event by the following lemma.

Lemma 6.3.5. *Denote by $\mathcal{C}$ the open cluster of the origin (open) vertex in our map. Then,*

$$\left\{B_n \underset{n\to+\infty}{\longrightarrow} +\infty\right\} \subset \{|\mathcal{C}| = +\infty\} \quad \text{and} \quad \{\exists\, n \geq 0 : B_n = 0\} \subset \{|\mathcal{C}| < +\infty\}\,.$$

Proof. Let us start with the first point. It is easy to see that as long as the peeling algorithm is not over, any black vertex discovered on the boundary is connected by an explicit open path to the origin of the map, and thus belongs to $\mathcal{C}$. Then, if B_n goes to infinity (which implies that the algorithm do not end), we get that $\mathcal{C}$ is also infinite.

The second statement is less obvious. The point is to see that at any step of the process, the open percolation cluster $\mathcal{C}$ of the origin in the initial map is infinite if and only if the open percolation cluster $\mathcal{C}_n$ of the finite black segment *in the infinite connected component that we consider at step n of the process* is itself infinite. To see that, note that when a white vertex is discovered and peeled, the black vertices of the boundary that are swallowed are enclosed in a finite Boltzmann map and thus provide a finite number of vertices to the percolation cluster $\mathcal{C}$ (out of $\mathcal{C}_n$). To conclude, note that if $B_n = 0$ for a fixed $n \geq 0$, then at the last step the finite black segment is enclosed in a finite region of the map (see Figure 6.9) and thus $\mathcal{C}_n$ is also finite, which ends the proof. □

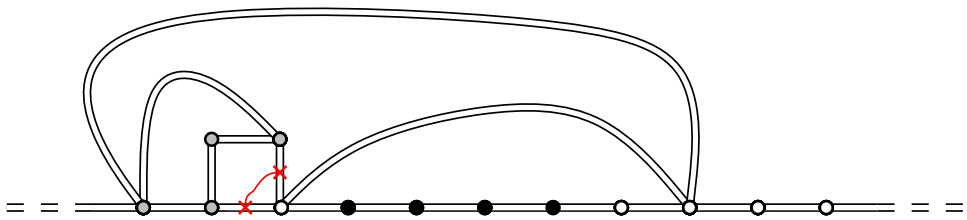

Figure 6.9: The situation when the algorithm ends.

It is now sufficient to determine the behaviour of the process $(B_n)_{n\geq 0}$, which is remarkably simple as a consequence of the very definition of the peeling process and Proposition 6.3.2.

Proposition 6.3.6. *The process $(B_n)_{n\geq 0}$ is a Markov chain with initial law δ_1, whose transitions are given for $n \geq 0$ by*

$$B_{n+1} = (B_n + 1 - \mathbf{1}_{c_n=0}\mathcal{H}_n)_+,$$

and which is absorbed at zero. Moreover, $(\mathcal{H}_n)_{n\geq 0}$ is a sequence of i.i.d. random variables and for every $n \geq 0$, conditionally on the event $\{c_n = 0\}$, $\mathcal{H}_n$ has the law of $\mathcal{R}_r$ conditioned to be positive.

In particular, the process $(B_n)_{n\geq 0}$ has the same law as a random walk started at 1 and killed at its first entrance in $\mathbb{Z}_-$, with steps distributed as the random variable $1 - \mathbf{1}_{c_0=0}\mathcal{H}_0$.

6.3.2 Computation of the percolation threshold

We now compute the percolation threshold for the "Free-Black-White" boundary condition of Figure 6.7.

Proposition 6.3.7. *For Bernoulli site percolation on the* UIHPQ *and conditionally on the "Free-Black-White" boundary condition with a single open vertex, we have*

$$p^{\square}_{c,site} = \frac{5}{9}.$$

Moreover, there is no percolation at the critical point almost surely: $\Theta^{\square}_{site}\left(p^{\square}_{c,site}\right) = 0$.

Proof. The quantity which rules the behaviour of $(B_n)_{n\geq 0}$ is the expectation of its steps, $\mathbf{E}_p(1-\mathbf{1}_{c_0=0}\mathcal{H}_0)$. It is obvious that $\mathbf{E}_p(c_0) = p$. Now the law of $\mathcal{H}_0$ conditionally on $\{c_0 = 0\}$ do not depend on p by construction and we have (see Proposition 6.2.3 and the following remark for details):

$$\mathbf{E}_p(\mathcal{H}_0 \mid c_0 = 0) = \mathbf{E}(\mathcal{R}_r|\mathcal{R}_r > 0) = \frac{\mathbf{E}(\mathcal{R}_r\mathbf{1}_{\{\mathcal{R}_r>0\}})}{\mathbf{P}(\mathcal{R}_r > 0)} = \frac{\mathbf{E}(\mathcal{R}_r)}{\mathbf{P}(\mathcal{R}_r > 0)} = \frac{9}{4}.$$

Thus,

$$\mathbf{E}_p(1 - \mathbf{1}_{c_0=0}\mathcal{H}_0) = 1 - (1-p)\mathbf{E}_p(\mathcal{H}_0 \mid c_0 = 0) = 1 - \frac{9}{4}(1-p).$$

We get that $\mathbf{E}_p(1 - \mathbf{1}_{c_0=0}\mathcal{H}_0) = 0$ if and only if $p = 5/9$. In the case where $p \neq 5/9$, standard arguments on the behaviour of simple random walks combined with Lemma 6.3.5 yield the first statement. Finally, when $p = 5/9$, the random walk with steps distributed as $1 - \mathbf{1}_{c_0=0}\mathcal{H}_0$ is null recurrent, so that almost surely, there exists $n \geq 0$ such that $B_n = 0$. This concludes the proof of the second assertion. □

Remark 6.3.8. A crucial quantity in the above computation of the percolation threshold is $\mathbf{P}(\mathcal{R}_r > 0)$. Let us describe in greater detail how to get the exact value for this probability. Recall that we work in the UIHPQ, and let $\mathcal{V}$ be the number of vertices of the face incident to the root that lie on the boundary. In particular, we have $\mathcal{V} \in \{2, 3, 4\}$. We also let $\mathcal{V}_l$ and $\mathcal{V}_r$ be the number of such vertices (strictly) on the left and on the right of the root edge respectively. Combined with the quantities $\mathcal{E}$

and $\mathcal{R}$, this allows to distinguish all the possible configurations of the face. Using the fact that the sum of the quantities $(q_k^{\square})_{k\geq 0}$ is the same for even and odd values and Proposition 6.2.3, we get

$$\mathbf{P}(\mathcal{E}=2)=\mathbf{P}(\mathcal{E}=1,\mathcal{V}<4)=\frac{1}{4}.$$

Thus, $\mathbf{P}(\mathcal{E}=1,\mathcal{V}=4)=1/8$, and using the symmetries of the configurations, we obtain

$$\mathbf{P}(\mathcal{E}=1,\mathcal{V}_l=\mathcal{V}_r=1)=\mathbf{P}(\mathcal{E}=1,\mathcal{V}_r=2)=\frac{1}{24}\quad\text{and}\quad\mathbf{P}(\mathcal{E}=2,\mathcal{V}_r=1)=\frac{1}{8}.$$

In the case where $\mathcal{E}=1$ and $\mathcal{V}<4$, one should take care of the fact that the number of swallowed edges can be zero on both sides with positive probability. We get

$$\mathbf{P}(\mathcal{E}=1,\mathcal{V}<4,\mathcal{V}_r=1)=\frac{1}{8}-q_0^{\square}.$$

Now,

$$\mathbf{P}(\mathcal{R}_r>0)=\mathbf{P}(\mathcal{V}_r>0)=\frac{1}{4}+\frac{1}{12}-q_0^{\square}=\frac{2}{9},$$

where we use the exact formulas for $q_0^{\square}$ and for the partition function (6.1) given in Section 2.2 of [AC15], or in [BG09] (we find $W_2^{\square}=4/3$, and thus $q_0^{\square}=1/9$).

6.3.3 Universality of the percolation threshold

We now want to discuss the *universal* aspects of the above result. The first one is the universality of the percolation threshold with respect to the boundary condition. Namely, we now consider Bernoulli site percolation on the UIHPQ in the most natural setting which is the free boundary condition, and prove Theorem 6.1.1.

Proof of Theorem 6.1.1. First of all, we can work without loss of generality conditionally on the fact that the origin vertex of the map is open. We then use a peeling process which is heavily based on the previous one.

Namely, we execute Algorithm 6.3.3 with the convention that we reveal the colour of the rightmost free vertex on the left of the origin (on the boundary).

The algorithm is paused when the finite black segment on the boundary has been completely swallowed. When this happens, two situations may occur, depending on the colour of the rightmost vertex v_0 of the boundary that is part of the last revealed face. By properties of the vertex-peeling process, such a vertex exists and lies on the right of the root edge (see Figure 6.10).

1. If v_0 is white, then the open cluster of the origin is enclosed in a finite region of the map and the algorithm ends: the percolation event does not occur.

2. If v_0 is black, then the percolation event occurs if and only if the open cluster of v_0 in the unrevealed infinite connected component is itself infinite. Then, the algorithm goes on executing Algorithm 6.3.3 on this map, with v_0 as origin vertex.

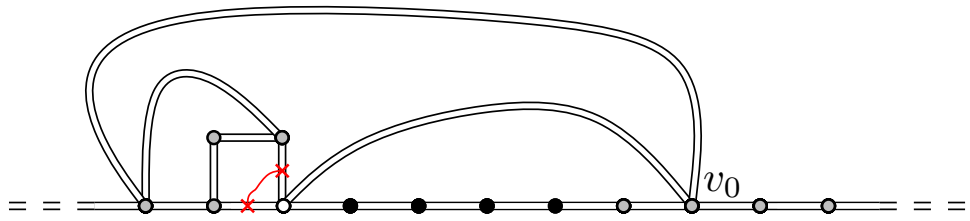

Figure 6.10: The situation when the finite black segment on the boundary is swallowed.

We let $(v_k)_{k\geq 0}$ be the sequence of vertices defined as v_0 at each time the algorithm is paused.

We are now able to conclude the proof. First, if $p > 5/9$, we know that $\Theta^{\square}_{\text{site}}(p) > 0$ using directly Proposition 6.3.7 and a standard monotone coupling argument. On the other hand, if $p \leq 5/9$, we know from Proposition 6.3.7 that the above algorithm is paused in finite time almost surely. By induction, we already stated that if there exists a vertex v_k which is white, the percolation event cannot occur. However, the colouring of the vertices $(v_k)_{k\geq 0}$ form an i.i.d. sequence with Bernoulli law of parameter $1-p > 0$, which yields that $\Theta^{\square}_{\text{site}}(p) = 0$ and the expected result. □

Let us finally detail the universality of our methods with respect to the law of the map. First, the previous arguments can be easily adapted to the case of the UIHPT. In particular, we have that for a free boundary condition

$$p^{\triangle}_{c,\text{site}} = \frac{1}{2},$$

and that there is no percolation at the critical point almost surely. This result has already been proved in [AC15] for a closed boundary condition (except the origin vertex). The interesting fact is that we can derive from our proof a universal formula for the site percolation thresholds, exactly as it was done in [AC15], Theorem 1, for bond and face percolation. Following this idea, we introduce the following notations:

$$\delta^* := \mathbf{E}(\mathcal{R}^*) = 2\mathbf{E}(\mathcal{R}^*_r) \qquad \text{and} \qquad \eta^* := \mathbf{P}(\mathcal{R}^*_r > 0),$$

where $*$ still denotes either of the symbols $\triangle$ or $\square$. From the results of Section 6.2 and the Remark following Proposition 6.3.7 we get that

$$\eta^{\triangle} = \frac{1}{6}, \quad \eta^{\square} = \frac{2}{9}, \quad \delta^{\triangle} = \frac{2}{3} \quad \text{and} \quad \delta^{\square} = 1.$$

Note that the computation of $\eta^{\triangle}$ is immediate from the symmetry of the configurations and the fact that there are no self-loops. The arguments of the proof of Theorem 6.1.1 yield the following result.

Theorem 6.3.9. *For site percolation on the* UIHPT *and the* UIHPQ*, we have that*

$$p^*_{c,site} = 1 - \frac{2\eta^*}{\delta^*}.$$

Of course, this formula is believed to hold in greater generality, for any infinite random half-planar map satisfying the spatial Markov property. Note that two parameters are needed to describe the site percolation threshold, while δ^* is sufficient for bond and face percolation as proved in [AC15].

6.4 Scaling limits of crossing probabilities in half-plane random maps

Throughout this section, we focus on the problem of scaling limits of crossing probabilities, and aim at generalizing the results of [Ang04]. Despite the fact that we also use a peeling process, the problem is much harder because the models we consider are less well-behaved than site percolation on the UIHPT.

More precisely, we consider site, bond and face percolation on the UIHPT and the UIHPQ, and work conditionally on the boundary condition represented on Figure 6.11 (for the bond percolation case). In other words, the boundary is "White-Black-White-Black", with two infinite segments and two finite ones, of lengths $\lfloor \lambda a \rfloor$ and $\lfloor \lambda b \rfloor$ respectively. The crossing event we focus on is the following: "there exists a black path linking the two black segments of the boundary", or equivalently "the two black segments are part of the same percolation cluster". We denote by $\mathsf{C}^*_{\text{bond}}(\lambda a, \lambda b)$ (respectively $\mathsf{C}^*_{\text{face}}(\lambda a, \lambda b)$ and $\mathsf{C}^*_{\text{site}}(\lambda a, \lambda b)$) this event where $*$ denote either of the symbols $\triangle$ or $\square$ (see Figure 6.11).

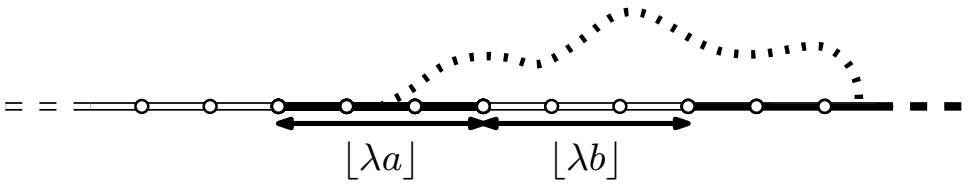

Figure 6.11: The boundary condition and the crossing event $\mathsf{C}^*(\lambda a, \lambda b)$.

Again, although the dependence on the map and percolation models are rather supported by the probability measure in this setting, we keep using the notation $*$ for the sake of simplicity. The quantity we are interested in is the scaling limit of the crossing probability $\mathbf{P}_p(\mathsf{C}^*(\lambda a, \lambda b))$,

$$\lim_{\lambda \to +\infty} \mathbf{P}_p\left(\mathsf{C}^*(\lambda a, \lambda b)\right),$$

which we expect to be universal following Cardy's universality conjecture if we consider the percolation models at their critical point, i.e., when p is exactly the percolation threshold. We recall those values that can be found in [AC15] and the previous section.

Theorem. ([AC15, Theorem 1], [Ang03], Theorem 6.1.1) *The percolation thresholds on the* UIHPT *are given by*

$$p^{\triangle}_{c,site} = \frac{1}{2}, \quad p^{\triangle}_{c,bond} = \frac{1}{4} \quad \textit{and} \quad p^{\triangle}_{c,face} = \frac{4}{5}.$$

The percolation thresholds on the UIHPQ *are given by*

$$p_{c,site}^{\square} = \frac{5}{9}, \quad p_{c,bond}^{\square} = \frac{1}{3} \quad \textit{and} \quad p_{c,face}^{\square} = \frac{3}{4}.$$

Starting from now, the probability p that an edge (respectively face, vertex) is open is always set at $p^*_{c,\text{bond}}$ (respectively $p^*_{c,\text{face}}$, $p^*_{c,\text{site}}$), in every model we consider. Most of the arguments being valid for both the UIHPT and the UIHPQ, we will treat those cases simultaneously and omit the notation $*$, underlying the differences where required. For technical reasons, we have to treat the cases of bond, face and site percolation separately, even though the proof always uses a similar general strategy. Our aim is now to prove Theorem 6.1.2.

6.4.1 Crossing probabilities for bond percolation

Peeling process and scaling limit. We start with the case of bond percolation. In order to compute the crossing probability we are interested in, we again use a peeling process that we now describe. The purpose of this process is to follow a closed path in the dual map, which is the map that has a vertex in each face of the initial (primal) map, and edges between neighboring faces (see [Gri99], Section 11.2 for details). The reason is that dual closed and primal open crossings between the segments of the boundary are almost surely complementary events.

The algorithm starts with revealing the face incident to the rightmost white edge of the infinite white segment (see Figure 6.12), without discovering the colour of its incident edges, which are thus free. (The rightmost white edge is then peeled in the sense that it is no longer in the infinite connected component of the map deprived of the revealed face.)

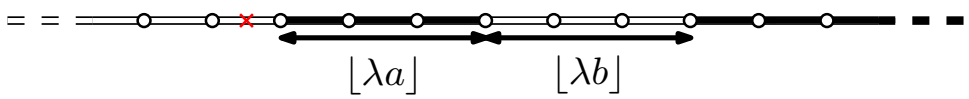

Figure 6.12: The initial boundary and the first edge to peel.

In general, the algorithm is well-defined as soon as the boundary has a "White-(Free)-Any" colouring, meaning that there is an infinite white segment and (possibly) a finite free segment on the left of the boundary, but no specific condition on the colouring of the right part. Although the right part will turn out to be coloured "Black-White-Black" in what follows, it will be helpful to have an algorithm which is defined independently of the colouring of the right part of the boundary.

ALGORITHM 6.4.1. Consider a half-plane map which has the law of the UIHP-$*$ with a "White-(Free)-Any" boundary condition.

- Reveal the colour of the rightmost free edge, if any:
  - If it is black, repeat the algorithm.

  - If it is white, reveal the face incident to this edge (without revealing the colour of the other edges of the face).

- If there is no free edge on the boundary of the map, as in the first step, reveal the face incident to the rightmost white edge of the infinite white segment (without revealing the colour of the other edges of the face).

After each step, repeat the algorithm on the UIHP-$*$ given by the unique infinite connected component of the current map, deprived of the revealed face.

We will call *revealed part* of the map all the vertices and edges that are not in this infinite connected component (even if all of them may not have been revealed, but rather swallowed in an independent finite connected component). The map we obtain is still implicitly rooted at the next edge we have to peel.

Let us now give some properties of Algorithm 6.4.1, which are essentially the same as that of Algorithm 6.3.3, apart from the fact that the algorithm never ends. We omit the proof of these properties, that are direct consequences of the spatial Markov property.

Proposition 6.4.2. *The peeling process is well-defined, in the sense that the pattern of the boundary (White-(Free)-Any) is preserved. Moreover, at each step, the planar map we consider has the law of the* UIHP-$*$ *and is independent of the revealed part of the map.*

Starting from now, we denote by $\mathcal{E}_n$, respectively $\mathcal{R}_n, c_n$, the number of exposed edges, respectively the number of swallowed edges and the color of the revealed edge at step n of the exploration, for every $n \geq 0$. By convention, we set $c_n = 0$ when there is no free edge on the boundary and $\mathcal{E}_n = \mathcal{R}_n = 0$ when no edge is peeled $(c_n = 1)$. Recall that $\mathcal{R}_{l,n}$ (respectively $\mathcal{R}_{r,n}$) denotes the number swallowed edges at the left (respectively right) of the root edge at step n of the exploration. The quantity we are interested in is the size of the finite black segment at step n. In order to study this quantity, we now introduce two random processes.

First, for every $n \geq 0$, we let F_n be the **length of the free segment** on the boundary at step n of the peeling process. Then, we have $F_0 = 0$ and for every $n \geq 0$,

$$F_{n+1} = \begin{cases} F_n - 1 & \text{if } \ c_n = 1 \\ \mathcal{E}_n + (F_n - \mathcal{R}_{l,n} - 1)_+ & \text{if } \ c_n = 0 \end{cases}. \tag{6.4}$$

The process $(F_n)_{n\geq 0}$ is a Markov chain with respect to the canonical filtration of the exploration process, and we have $c_n = 0$ when $F_n = 0$.

Remark 6.4.3. The Markov chain $(F_n)_{n\geq 0}$ takes value zero at step n only if we have $F_{n-1} = 1$ and $c_n = 1$. Moreover, if the whole free segment is swallowed by a jump of the peeling process at step n, then $F_n = \mathcal{E}_n$ (see Propositions 6.2.1 and 6.2.2).

Then, we let $B_0 = \lfloor \lambda a \rfloor$ and for every $n \geq 0$,

$$B_{n+1} = \begin{cases} B_n + 1 & \text{if } \ c_n = 1 \\ B_n - \mathcal{R}_{r,n} & \text{if } \ c_n = 0 \end{cases}. \tag{6.5}$$

Like $(F_n)_{n\geq 0}$, the process $(B_n)_{n\geq 0}$ is a Markov chain with respect to the canonical filtration of the exploration process. Moreover, if we denote by $T := \inf\{n \geq 0 : B_n \leq 0\}$ the first entrance time of $(B_n)_{n\geq 0}$ in $\mathbb{Z}_-$, then for every $n \in \{0, 1, \dots, T-1\}$, B_n is the **length of the finite black segment** at step n of the exploration process.

An important point is that for every $n < T$, the edges of the finite black segment are all part of the open cluster of the initial segment, while for $n \geq T$, the initial finite black segment has been swallowed by the peeling process. (However, the algorithm can continue because the infinite white and finite free segments are still well-defined.)

As we will see, and as was stressed in [Ang04], the so-called *overshoot* B_T of the process $(B_n)_{n\geq 0}$ at the first entrance in $\mathbb{Z}_-$ is the central quantity, which governs the behaviour of crossing events.

We now need to describe the law of the random variables involved in the previous definitions of the processes $(F_n)_{n\geq 0}$ and $(B_n)_{n\geq 0}$. This can be done using the very definition of the peeling algorithm and Section 6.2.2. Note that one has to be careful with the fact that $\mathcal{E}_n = \mathcal{R}_n = 0$ when $c_n = 1$. Thus, we let $(t_k)_{k\geq 1}$ be the sequence of consecutive stopping times such that $c_{t_k} = 0$ (i.e., the times at which a face is peeled), and $(s_k)_{k\geq 1}$ the sequence of consecutive stopping times such that $F_{s_k} > 0$ (i.e., the times at which there is an edge whose colour is revealed). In what follows, we let $(\mathcal{E}, \mathcal{R}_l, \mathcal{R}_r)$ be defined as in Section 6.2 (notation $*$ omitted). A simple application of the spatial Markov property yields the following result.

Lemma 6.4.4. *The random variables $(\mathcal{E}_{t_k}, \mathcal{R}_{l,t_k}, \mathcal{R}_{r,t_k})_{k\geq 1}$ are i.i.d. and have the same law as $(\mathcal{E}, \mathcal{R}_l, \mathcal{R}_r)$. Moreover, the random variables $(c_{s_k})_{k\geq 1}$ are i.i.d. and have the Bernoulli law of parameter $p^*_{c,bond}$.*

In the following, we denote by c a random variable which has the Bernoulli law of parameter $p^*_{c,\text{bond}}$, independent of $(\mathcal{E}, \mathcal{R}_l, \mathcal{R}_r)$. We are now able to describe the behaviour of the processes $(F_n)_{n\geq 0}$ and $(B_n)_{n\geq 0}$.

The process $(F_n)_{n\geq 0}$. The Markov chain $(F_n)_{n\geq 0}$ is not exactly a random walk, but has the same behaviour when it is far away from zero. More precisely, note that $F_1 > 0$ almost surely and let $\hat{\sigma} := \inf\{n \geq 1 : F_n - 1 - \mathbf{1}_{\{c_n=0\}}\mathcal{R}_{l,n} < 0\}$ be the first time at which the free segment is swallowed (possibly by a revealed face). Note that $F_{\hat{\sigma}}$ is not zero in general, but if $F_n = 0$ for $n \geq 1$, then $\hat{\sigma} \leq n$. By construction, as long as $n \leq \hat{\sigma}$, we have

$$F_n = F_1 + \sum_{k=1}^{n-1} \big(\mathbf{1}_{\{c_k=0\}}(\mathcal{E}_k - \mathcal{R}_{l,k}) - 1\big).$$

Thus, $(F_n - F_1)_{1\leq n\leq \hat{\sigma}}$ is a random walk killed at the random time $\hat{\sigma}$, whose steps are distributed as $\hat{X}$ defined by

$$\hat{X} := \mathbf{1}_{\{c=0\}}(\mathcal{E} - \mathcal{R}_l) - 1,$$

where we use the definition of $\hat{\sigma}$ and Lemma 6.4.4. Moreover, we obtain from Proposition 6.2.3 that

$$\mathbf{E}(\hat{X}) = -p^*_{c,\text{bond}} + (1-p^*_{c,\text{bond}})(\mathbf{E}(\mathcal{E}-\mathcal{R}_l)-1) = \begin{cases} \frac{1}{3} - \frac{4}{3}p^*_{c,\text{bond}} \ (* = \triangle) \\ \\ \frac{1}{2} - \frac{3}{2}p^*_{c,\text{bond}} \ (* = \square) \end{cases}.$$

Using the percolation thresholds given at the beginning of Section 6.4, we get that $\mathbf{E}(\hat{X}) = 0$. As a consequence, since $\hat{\sigma} < \sigma := \inf\{k \geq 1 : F_k = 0\}$, we get that $\hat{\sigma}$ is almost surely finite. It is finally easy to check that the random variable $\hat{X}$ satisfies the conditions of Proposition 6.2.7. In particular, if we denote by $(\hat{S}_n)_{n\geq 0}$ a random walk with steps distributed as $\hat{X}$ we get

$$\left(\frac{\hat{S}_{\lfloor \lambda t \rfloor}}{\lambda^{2/3}}\right)_{t\geq 0} \xrightarrow[\lambda\to+\infty]{(d)} \kappa(\mathcal{S}_t)_{t\geq 0}, \tag{6.6}$$

in the sense of convergence in law for Skorokhod's topology, where $\mathcal{S}$ is the Lévy $3/2$-stable process of Section 6.2.4, and $\kappa > 0$.

The process $(B_n)_{n\geq 0}$. Exactly as before, $(B_n)_{n\geq 0}$ is not a random walk, but behaves the same way when F_n is not equal to zero. Let us be more precise here. First, let $\sigma_0 = 0$, and inductively for every $k \geq 1$,

$$\sigma_k := \inf\{n \geq \sigma_{k-1} + 1 : F_n = 0\}. \tag{6.7}$$

From the above description of the process $(F_n)_{n\geq 0}$, we know that started from any initial size, the free segment is swallowed in time $\hat{\sigma}$, which is almost surely finite. When this happens, either a black edge has been revealed and $F_{\hat{\sigma}} = 0$, or a revealed face has swallowed the free segment. In this case, with probability bounded away from zero, $F_{\hat{\sigma}+1} = 0$. Applying the strong Markov property, we get that all the stopping times $(\sigma_k)_{k\geq 0}$ are almost surely finite.

Since $F_1 > 0$ by construction, as long as $1 \leq n \leq \sigma = \sigma_1$ we have

$$B_n = B_1 + \sum_{k=1}^{n-1} \left(\mathbf{1}_{\{c_k=1\}} - \mathbf{1}_{\{c_k=0\}}\mathcal{R}_{r,k}\right).$$

Thus, $(B_n - B_1)_{1\leq n\leq \sigma}$ is a random walk killed at the random time σ, whose steps are distributed as X defined by

$$X := \mathbf{1}_{\{c=1\}} - \mathbf{1}_{\{c=0\}}\mathcal{R}_r.$$

From the strong Markov property, we see that this also holds for the processes $(B_{\sigma_k+n} - B_{\sigma_k+1})_{1\leq n\leq \sigma_{k+1}-\sigma_k}$, noticing that $F_{\sigma_k+1} > 0$ for every $k \geq 0$ by definition. As a consequence of Proposition 6.2.3, we get that

$$\mathbf{E}(X) = p^*_{c,\text{bond}} - (1-p^*_{c,\text{bond}})\mathbf{E}(\mathcal{R}_r) = \begin{cases} \frac{4}{3}p^{\triangle}_{c,\text{bond}} - \frac{1}{3} \ (* = \triangle) \\ \\ \frac{3}{2}p^{\square}_{c,\text{bond}} - \frac{1}{2} \ (* = \square) \end{cases}.$$

Since we work at the critical point, $\mathbf{E}(X) = 0$ for both the UIHPT and the UIHPQ, and properties of the random variable X also yield that if $(S_n)_{n\geq 0}$ is a random walk with steps distributed as X,

$$\left(\frac{S_{\lfloor \lambda t \rfloor}}{\lambda^{2/3}}\right)_{t\geq 0} \xrightarrow[\lambda\to+\infty]{(d)} \kappa(\mathcal{S}_t)_{t\geq 0}, \tag{6.8}$$

in the sense of convergence in law for Skorokhod's topology, where $\mathcal{S}$ is the Lévy $3/2$-stable process of Section 6.2.4 and $\kappa > 0$.

We are now interested in the scaling limit of the process $(B_n)_{n\geq 0}$. We want to prove the following result:

Proposition 6.4.5. *We have, in the sense of convergence in law for Skorokhod's topology:*

$$\left(\frac{B_{\lfloor \lambda^{3/2} t \rfloor}}{\lambda}\right)_{t\geq 0} \xrightarrow[\lambda\to+\infty]{(d)} \kappa(\mathcal{S}_t)_{t\geq 0},$$

where $\mathcal{S}$ is the Lévy spectrally negative $3/2$-stable process started at a, and $\kappa > 0$.

The idea is to couple a random walk $(S_n)_{n\geq 0}$ with steps distributed as the random variable X and the process $(B_n)_{n\geq 0}$ in such a way that S_n and B_n are close. To do so, let us set $S_0 = B_0$, and introduce an independent sequence $(\beta_n)_{n\geq 0}$ of i.i.d. random variables with Bernoulli law of parameter $p^*_{c,\text{bond}}$. We then define $(S_n)_{n\geq 0}$ recursively as follows. For every $n \geq 0$:

$$S_{n+1} = S_n + \begin{cases} B_{n+1} - B_n = \mathbf{1}_{\{c_n=1\}} - \mathbf{1}_{\{c_n=0\}}\mathcal{R}_{r,n} & \text{if } F_n > 0 \\ \\ \beta_n + (1-\beta_n)(B_{n+1} - B_n) = \mathbf{1}_{\{\beta_n=1\}} - \mathbf{1}_{\{\beta_n=0\}}\mathcal{R}_{r,n} & \text{if } F_n = 0 \end{cases}.$$

Otherwise said, as long as $F_n > 0$, $(S_n)_{n\geq 0}$ performs the same steps as $(B_n)_{n\geq 0}$ and when $F_n = 0$, S_{n+1} takes value $S_n + 1$ if $\beta_n = 1$, and does the same transition as $(B_n)_{n\geq 0}$ otherwise. Using the previous discussion and the fact that $c_n = 0$ when $F_n = 0$, we get that $(S_n)_{n\geq 0}$ is a random walk started from B_0 with steps distributed as the random variable X, as wanted.

Let us also define the set $\Xi_n := \{0 \leq k < n : F_n = 0\}$ of zeros of $(F_n)_{n\geq 0}$ before time $n \geq 0$, and set $\xi_n := \#\Xi_n$ for every $n \geq 0$. The steps of $(S_n)_{n\geq 0}$ and $(B_n)_{n\geq 0}$ are the same except when $F_n = 0$, in which case, since $S_{n+1} - S_n$ for every $n \geq 0$, we have $S_{n+1} - S_n \leq 1 - (B_{n+1} - B_n)$. Hence, we get that almost surely for every $n \geq 0$,

$$S_n - R_n \leq B_n \leq S_n, \tag{6.9}$$

where for every $n \geq 0$,

$$R_n := \sum_{k\in\Xi_n} (1 - (B_{k+1} - B_k)).$$

Then, if $(r_n)_n$ is a sequence of i.i.d. random variables with the same law as $\mathcal{R}_r$, we have for every $n \geq 0$ that

$$R_n \overset{(d)}{=} \sum_{k=1}^{\xi_n} (1 + r_k).$$

In order to prove that $(B_n)_{n\geq 0}$ has the same scaling limit as $(S_n)_{n\geq 0}$, the idea is to establish that the process $(R_n)_{n\geq 0}$ is small compared to $(S_n)_{n\geq 0}$.

Recall from (6.7) the definition of the stopping times $(\sigma_k)_{k\geq 0}$. In other words, σ_k is the time of the k^{th} return of $(F_n)_{n\geq 0}$ to zero, and $\sigma_{k-1}+1$ is the first time after σ_{k-1} when $(F_n)_{n\geq 0}$ reaches $\mathbb{Z}_+$ (by construction). Notice that the total number of returns of the process to 0 before time n equals $\xi_n = \#\{k \geq 0 : \sigma_k < n\}$. The following lemma gives a bound on the asymptotic behaviour of this quantity.

Lemma 6.4.6. *For every $\alpha > 0$, we have the convergence in probability*

$$\frac{\xi_n}{n^{1/3+\alpha}} \xrightarrow[n\to+\infty]{\mathbf{P}} 0.$$

Proof. The strong Markov property applied to the stopping times $(\sigma_k)_{k\geq 0}$ yields that for every $k \geq 0$ and $n \geq 0$,

$$\mathbf{P}(\xi_n > k) \leq \prod_{j=1}^{k} \mathbf{P}(\sigma_j - \sigma_{j-1} \leq n). \tag{6.10}$$

Now, we may simplify the computation with the following remark: for every $k \geq 1$, $\sigma_k - \sigma_{k-1}$ stochastically dominates the time needed by the random walk $(\hat{S}_n)_{n\geq 0}$ started from 0 with steps distributed as $\hat{X}$ to reach $\mathbb{Z}_-\backslash\{0\}$. Indeed, due to the fact that $F_{\sigma_{k-1}+1} \geq 1$ almost surely we have (for instance by a coupling argument) that for every $k \geq 1$ and $n \geq 0$,

$$\mathbf{P}(\sigma_k - \sigma_{k-1} \leq n) \leq \mathbf{P}(\sigma' \leq n),$$

where σ' is defined exactly as $\sigma = \sigma_1$, but for the Markov chain $(F_n)_{n\geq 0}$ with initial distribution δ_1.

Then, observe that when started at length 1, the process $(F_n)_{n\geq 0}$ is bounded from below by a random walk with steps distributed as $\hat{X}$, also started at 1 and up to the first entrance of this random walk into $\mathbb{Z}_-$ (using again a coupling argument which consists in not taking the positive part in (6.4)). In other words, for every $k \geq 1$ and $n \geq 0$,

$$\mathbf{P}(\sigma_k - \sigma_{k-1} \leq n) \leq \mathbf{P}(\bar{\sigma} \leq n),$$

where $\bar{\sigma} := \inf\{n \geq 0 : \hat{S}_n + 1 \leq 0\}$. Thus, we get from (6.10) that $\mathbf{P}(\xi_n > k) \leq (\mathbf{P}(\bar{\sigma} \leq n))^k$, and now want to apply a result due to Rogozin that we recall for the sake of completeness.

Theorem. ([Don82, Theorem 0], [Rog71]) *Let $(X_k)_{k\geq 0}$ be a sequence of i.i.d. random variables, $S_0 := 0$ and for every $n \geq 1$, $S_n := \sum_{k=1}^{n} X_k$. Let $\sigma_+ := \inf\{n \geq 1 \mid S_n > 0\}$ be the first strict ascending ladder epoch of the random walk $(S_n)_{n\geq 0}$, and assume that*

$$\sum_{k=1}^{+\infty} k^{-1} P(S_k > 0) = \sum_{k=1}^{+\infty} k^{-1} P(S_k \leq 0) = +\infty. \tag{6.11}$$

Then, the following assertions are equivalent:

1. $n^{-1}\sum_{k=1}^{n} P(S_k > 0) \underset{n\to+\infty}{\longrightarrow} \gamma \in [0,1]$.
2. *There exists a slowly varying function* L_+ *such that* $P(\sigma_+ \geq n) \underset{n\to+\infty}{\sim} n^{-\gamma} L_+(n)$.

Let us check the assumptions of this result. Using the convergence (6.6), we get

$$\mathbf{P}(\hat{S}_n > 0) = \mathbf{P}\left(\frac{\hat{S}_n}{n^{2/3}} > 0\right) \underset{n\to+\infty}{\longrightarrow} P_0(\kappa \mathcal{S}_1 > 0) = \rho = \frac{2}{3},$$

where $\mathcal{S}$ is the spectrally negative $3/2$-stable process. It is thus clear that the identity (6.11) is satisfied by the process $(-\hat{S}_n)_{n\geq 0}$. Moreover, Césaro's Lemma ensures that

$$\frac{1}{n}\sum_{k=1}^{n} \mathbf{P}(-\hat{S}_k > 0) \underset{n\to+\infty}{\longrightarrow} \gamma = \frac{1}{3}.$$

Thus, the theorem applies and yields

$$\mathbf{P}(\bar{\sigma} \geq n) \underset{n\to+\infty}{\sim} n^{-1/3} L_+(n), \tag{6.12}$$

where L_+ is a slowly varying function at infinity. In particular, for every $\alpha > 0$ and $\varepsilon > 0$,

$$\mathbf{P}(\xi_n > n^{1/3+\alpha}\varepsilon) \leq (\mathbf{P}(\bar{\sigma} \leq n))^{n^{1/3+\alpha}\varepsilon} = (1 - \mathbf{P}(\bar{\sigma} > n))^{n^{1/3+\alpha}\varepsilon} \underset{n\to+\infty}{\longrightarrow} 0,$$

as wanted. □

Let us come back to the scaling limit of the process $(B_n)_{n\geq 0}$. We have for every $\alpha > 0$ and n large enough

$$\frac{R_n}{n^{1/3+\alpha}} \overset{(d)}{=} \frac{1}{n^{1/3+\alpha}} \sum_{k=1}^{\xi_n} (1 + r_k) = \frac{\xi_n}{n^{1/3+\alpha}} \frac{1}{\xi_n} \sum_{k=1}^{\xi_n} (1 + r_k). \tag{6.13}$$

We observed that all the $(\sigma_k)_{k\geq 0}$ are almost surely finite, and thus the quantity ξ_n goes to infinity almost surely with n. Using the previous lemma and the law of large numbers, we get that

$$\frac{R_n}{n^{2/3}} \underset{n\to+\infty}{\overset{\mathbf{P}}{\longrightarrow}} 0,$$

and then

$$\left(\frac{R_{\lfloor \lambda^{3/2} t \rfloor}}{\lambda}\right)_{t\geq 0} \underset{\lambda\to+\infty}{\overset{\mathbf{P}}{\longrightarrow}} 0$$

for the topology of uniform convergence on compact sets, and thus for Skorokhod's topology. Recalling the inequality (6.9) and the convergence (6.8), we immediately have

$$\left(\frac{B_{\lfloor \lambda t \rfloor}}{\lambda^{2/3}}\right)_{t\geq 0} \underset{\lambda\to+\infty}{\overset{(d)}{\longrightarrow}} \kappa(\mathcal{S}_t)_{t\geq 0},$$

and thus the proof of Proposition 6.4.5 with an obvious substitution, using that $\lambda^{-1} B_0 \underset{\lambda\to+\infty}{\longrightarrow} a$ to identify the starting point of the stable process.

Stopped peeling process. We now focus on the possible situations when the process $(B_n)_{n\geq 0}$ reaches $\mathbb{Z}_-$, which happens almost surely since $(B_n)_{n\geq 0}$ is bounded from above by the recurrent random walk $(S_n)_{n\geq 0}$ we previously introduced. Throughout this section, we denote by T the first time when $(B_n)_{n\geq 0}$ reaches nonpositive values:

$$T := \inf\{n \geq 0 : B_n \leq 0\}.$$

We now split our study into two cases, depending on the value $|B_T|$ of the so-called *overshoot* of the process $(B_n)_{n\geq 0}$ at its first entrance into $\mathbb{Z}_-$. We implicitly exclude the events $\{|B_T| = 0\}$ and $\{|B_T| = \lfloor \lambda b \rfloor\}$, whose probability will be proved to vanish when λ goes to infinity in Section 6.4.1.

Case 1: $|B_T| < \lfloor \lambda b \rfloor$. In this situation, only a fraction of the finite white segment on the boundary is swallowed, see Figure 6.13. Notice that the swallowed finite black segment has size B_{T-1}, since it is the black segment just before the last face is revealed, i.e., at time $T-1$. Unless explicitly mentioned, we now work conditionally on the event $\{|B_T| < \lfloor \lambda b \rfloor\}$.

In each case, the crossing event $\mathsf{C}^*(\lambda a, \lambda b)$ implies the existence of an open path linking the rightmost revealed vertex on the boundary, denoted by v^*, and the infinite black segment on the boundary (see the dashed path on Figure 6.13). Indeed, the exploration process has the property that the open connected component of the initial finite black segment is entirely swallowed by the last face that is revealed. (For the crossing event to occur, one also needs that some bottom edges of this face are open, see Figure 6.13, but an upper bound is enough for our purpose.)

The situation may again be simplified using the spatial Markov property, because this event has the same probability as the following: consider a map which has the law of the UIHP-$*$, and let C^1_λ be the event that there exists a path linking the origin of the map and the infinite black segment of the boundary, where the boundary of the map has the colouring of Figure 6.14 (the crossing event C^1_λ is again represented with a dashed path). Notice that the free segment on the boundary can have arbitrary but finite length (depending on the previous peeling steps) but this plays no role in our discussion.

Roughly speaking, the idea here is that when λ becomes large, so does the length $d^\lambda := \lfloor \lambda b \rfloor - |B_T|$ of the white segment that separates the origin from the black segment and the event C^1_λ becomes unlikely. To be precise, the following lemma holds.

Lemma 6.4.7. *Conditionally on $|B_T| < \lfloor \lambda b \rfloor$, we have*

$$\lfloor \lambda b \rfloor - |B_T| \xrightarrow[\lambda \to +\infty]{\mathbf{P}} +\infty.$$

Proof. Recall that $B_0 = \lfloor \lambda a \rfloor$ almost surely by definition, and let

$$\tilde{T} := \inf\left\{t \geq 0 : \lambda^{-1} B_{\lfloor \lambda^{3/2} t \rfloor} \leq 0\right\}. \tag{6.14}$$

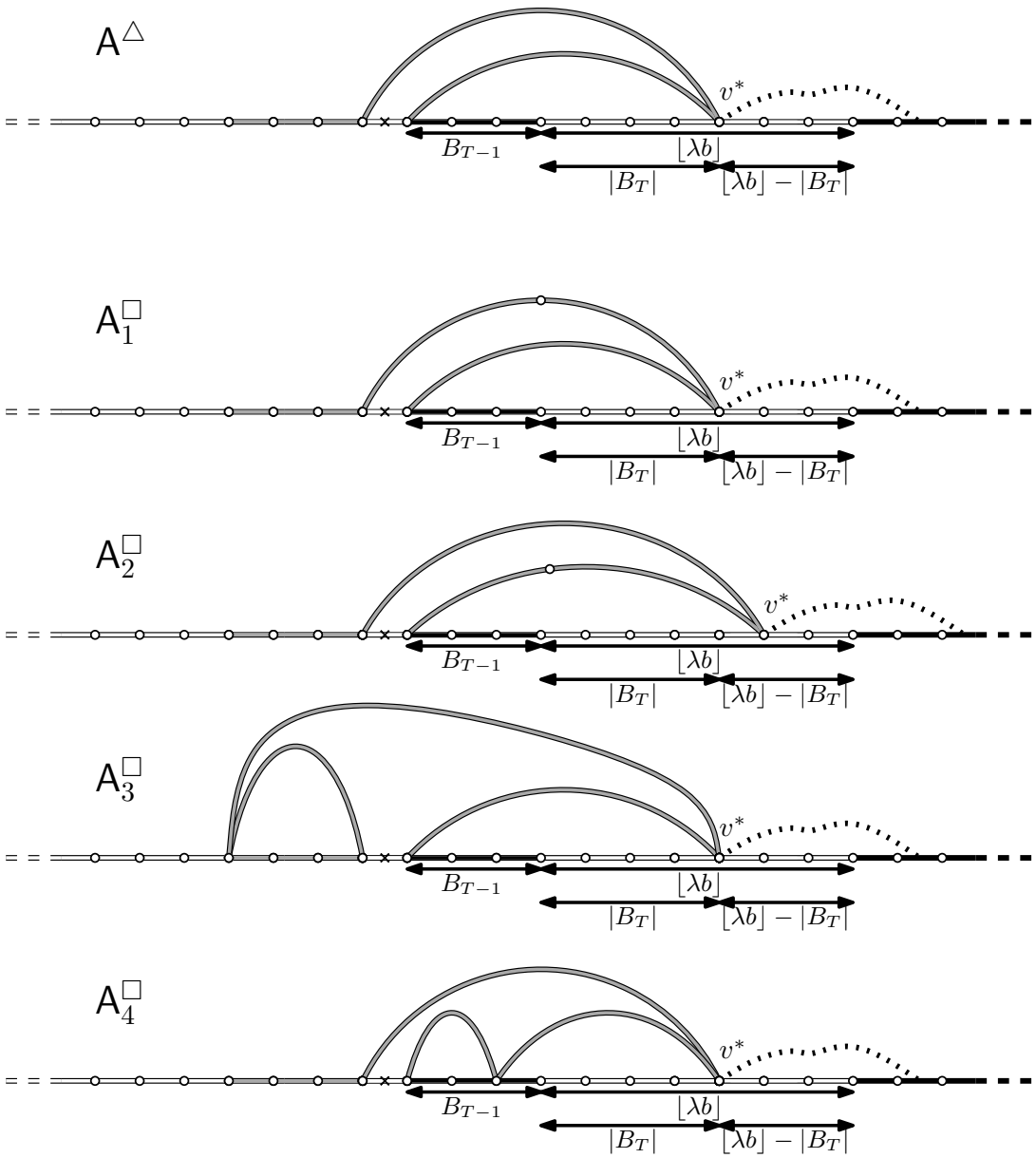

Figure 6.13: Configurations when $|B_T| < \lfloor \lambda b \rfloor$.

Then, we have $\lfloor \lambda^{3/2} \tilde{T} \rfloor = T$ and using Proposition 6.4.5, we get that conditionally given $|B_T| < \lfloor \lambda b \rfloor$,

$$\lambda^{-1} B_T \xrightarrow[\lambda \to +\infty]{(d)} \kappa \mathcal{S}_\tau \ \text{(given } \kappa |\mathcal{S}_\tau| < b) \,,$$

where $\tau := \inf\{t \geq 0 : \mathcal{S}_t \leq 0\}$ and $\mathcal{S}$ is the spectrally negative Lévy $3/2$-stable process started at a. As a consequence, we have that conditionally given $|B_T| < \lfloor \lambda b \rfloor$,

$$\lambda^{-1}(\lfloor \lambda b \rfloor - |B_T|) \xrightarrow[\lambda \to +\infty]{(d)} b - \kappa \mathcal{S}_\tau \ \text{(given } \kappa |\mathcal{S}_\tau| < b) \,,$$

Now, following Proposition 6.2.8, the distribution of the overshoot of the process $\mathcal{S}$ is absolutely continuous with respect to the Lebesgue measure on $\mathbb{R}_+$, which yields the expected result. □

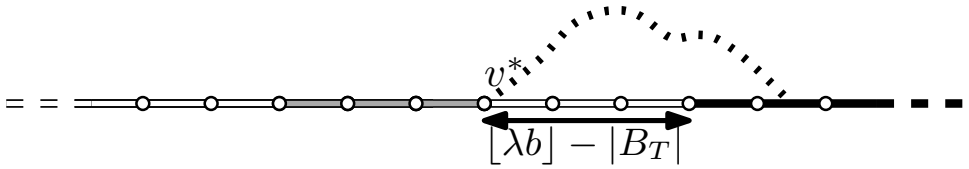

Figure 6.14: The crossing event C^1_λ.

Case 2: $|B_T| > \lfloor \lambda b \rfloor$. In this situation, the whole finite white segment of the boundary has been swallowed by the last revealed face, which divides the problem into different subcases shown in Figure 6.15. Unless explicitly mentioned, we now work conditionally on the event $\{|B_T| > \lfloor \lambda b \rfloor\}$.

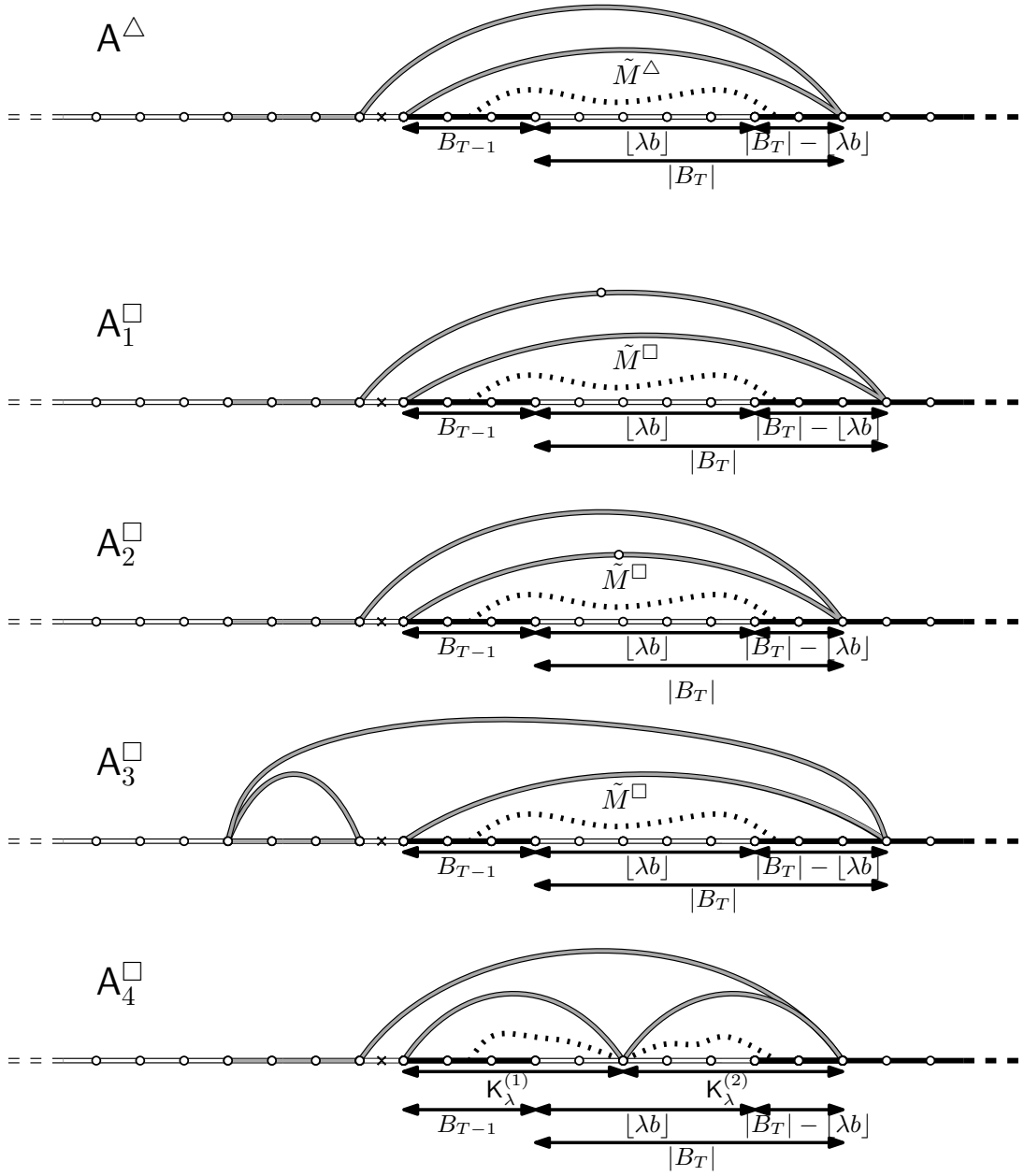

Figure 6.15: Configurations when $|B_T| > \lfloor \lambda b \rfloor$.

In the first four cases ($\mathsf{A}^{\triangle} - \mathsf{A}_3^{\square}$), either the crossing event is realized by bottom edges of the last revealed face (which occurs with probability less than one), or it depends on a crossing event between black segments of the boundary in a submap $\tilde{M}^*$, which is a Boltzmann $*$-angulation of the $(B_{T-1} + |B_T| + 1)$-gon (or $(B_{T-1} + |B_T| + 2)$-gon, depending on the configuration). Those events are represented by a dashed path on Figure 6.15. The reason for this is that the finite black segment on the boundary at the second to last step of the peeling process is in the same cluster as the initial one (those even share edges).

Roughly speaking, the idea here is that when λ becomes large, this Boltzmann $*$-angulation converges in law towards the UIHP-$*$ with infinite black segments on the boundary, so that the above crossing event occurs almost surely asymptotically. The fifth case $\mathsf{A}_4^{\square}$ is slightly different, because the crossing represented by the dashed path seems unlikely. In fact, this fifth case does not occur asymptotically in a sense we will make precise. We will need the following analogue of Lemma 6.4.7 concerning the size of the black segments that appear in the Boltzmann map.

Lemma 6.4.8. *Conditionally on $|B_T| > \lfloor \lambda b \rfloor$, we have*

$$|B_T| - \lfloor \lambda b \rfloor \xrightarrow[\lambda \to +\infty]{\mathbf{P}} +\infty \quad \textit{and} \quad B_{T-1} \xrightarrow[\lambda \to +\infty]{\mathbf{P}} +\infty,$$

and for every $\beta > 1$,

$$\lambda^{-\beta}(|B_T| - \lfloor \lambda b \rfloor) \xrightarrow[\lambda \to +\infty]{\mathbf{P}} 0 \quad \textit{and} \quad \lambda^{-\beta} B_{T-1} \xrightarrow[\lambda \to +\infty]{\mathbf{P}} 0.$$

Proof. The proof is analogous to that of Lemma 6.4.7. Again, recall that $B_0 = \lfloor \lambda a \rfloor$ almost surely by definition and that if $\tilde{T} := \inf\{t \geq 0 : \lambda^{-1} B_{\lfloor \lambda^{3/2} t \rfloor} \leq 0\}$, then $\lfloor \lambda^{3/2} \tilde{T} \rfloor = T$. Applying Proposition 6.4.5, we get that conditionally given $|B_T| > \lfloor \lambda b \rfloor$,

$$\lambda^{-1}(B_{T-1}, B_T) \xrightarrow[\lambda \to +\infty]{(d)} \kappa(\mathcal{S}_{\tau-}, \mathcal{S}_\tau) \ \text{(given } \kappa|\mathcal{S}_\tau| > b), \tag{6.15}$$

where $\tau := \inf\{t \geq 0 : \mathcal{S}_t \leq 0\}$ and $\mathcal{S}$ is the spectrally negative Lévy $3/2$-stable process started at a. Therefore, we have that conditionally given $|B_T| > \lfloor \lambda b \rfloor$,

$$\lambda^{-1}(B_{T-1}, |B_T| - \lfloor \lambda b \rfloor) \xrightarrow[\lambda \to +\infty]{(d)} (\kappa \mathcal{S}_{\tau-}, \kappa \mathcal{S}_\tau - b) \ \text{(given } \kappa|\mathcal{S}_\tau| > b),$$

We conclude the proof exactly as before, using the absolute continuity of the joint distribution of the undershoot and the overshoot of the process $\mathcal{S}$ with respect to the Lebesgue measure, given by Proposition 6.2.8. □

We now treat the fifth configuration, denoted by $\mathsf{A}_4^{\square}$ in Figure 6.15, which occurs only in the quadrangular case. Precisely, we work on the event (still denoted $\mathsf{A}_4^{\square}$) that the last revealed quadrangle has all of its four vertices lying on the boundary of the map, two of them being on the right of the root edge. On this event, we can introduce $\mathsf{K}_\lambda^{(1)}$ and $\mathsf{K}_\lambda^{(2)}$, which are the (random) lengths of the two finite segments determined on the right boundary by the last revealed quadrangle (see Figure 6.15 and a formal definition in (6.16)).

Lemma 6.4.9. *Conditionally on $|B_T| > \lfloor \lambda b \rfloor$ and on the event $\mathsf{A}_4^{\square}$, we have*

$$\lambda^{-1} \min\left(\mathsf{K}_\lambda^{(1)}, \mathsf{K}_\lambda^{(2)}\right) \xrightarrow[\lambda\to+\infty]{\mathbf{P}} 0.$$

As a consequence,

$$\max\left(B_{T-1} - \mathsf{K}_\lambda^{(1)}, |B_T| - \lfloor \lambda b \rfloor - \mathsf{K}_\lambda^{(2)}\right) \xrightarrow[\lambda\to+\infty]{\mathbf{P}} +\infty.$$

Proof. Let us introduce the sequence of random variables $(K_n^{(1)}, K_n^{(2)})_{n\geq 0}$, that describe the length of the two finite segments determined on the right boundary by the quadrangle revealed at step n of the exploration process. We adopt the convention that $K_n^{(1)} = K_n^{(2)} = 0$ if there are less than two segments determined on the right boundary. In particular, these random variables are i.i.d., and on the event $A_4^{\square}$, we have the identity

$$\left(\mathsf{K}_\lambda^{(1)}, \mathsf{K}_\lambda^{(2)}\right) := \left(K_{T-1}^{(1)}, K_{T-1}^{(2)}\right). \tag{6.16}$$

Now, for every $x > 0$,

$$\mathbf{P}\left(K_0^{(1)} \geq x, K_0^{(2)} \geq x\right) = \sum_{k_1,k_2\geq x} q^{\square}_{k_1,k_2},$$

and $q^{\square}_{k_1,k_2}$ is equivalent to $\iota_{\square} k_1^{-5/2} k_2^{-5/2}$ when k_1, k_2 go to infinity, using the estimation (6.3). Thus, if x is large enough, we have $q^{\square}_{k_1,k_2} \leq C k_1^{-5/2} k_2^{-5/2}$ for every $k_1, k_2 \geq x$, where C is a positive constant. This yields

$$\mathbf{P}\left(K_0^{(1)} \geq x, K_0^{(2)} \geq x\right) \leq C \sum_{k_1,k_2\geq x} k_1^{-5/2} k_2^{-5/2} \leq C' x^{-3}, \tag{6.17}$$

for another positive constant C', provided that x is large enough. Then, for every $\lambda > 0$, $\varepsilon > 0$ and $\delta > 0$ we have

$$\mathbf{P}\left(K_{T-1}^{(1)} \geq \lambda\varepsilon, K_{T-1}^{(2)} \geq \lambda\varepsilon\right) \leq \mathbf{P}\left(T > \lambda^{3/2+\delta}\right) + \mathbf{P}\left(\exists\, 0 \leq n < \lambda^{3/2+\delta} \mid K_n^{(1)} \geq \lambda\varepsilon, K_n^{(2)} \geq \lambda\varepsilon\right).$$

For the first term, using the random variable $\tilde{T} := \inf\{t \geq 0 : \lambda^{-1} B_{\lfloor \lambda^{3/2} t \rfloor} \leq 0\}$ introduced in (6.14), we have $\lfloor \lambda^{3/2} \tilde{T} \rfloor = T$ and from Proposition 6.4.5

$$\lambda^{-3/2} T \xrightarrow[\lambda\to+\infty]{(d)} \tau,$$

where $\tau := \inf\{t \geq 0 : \mathcal{S}_t \leq 0\}$ and $\mathcal{S}$ is the spectrally negative Lévy $3/2$-stable process. The random variable τ being almost surely finite by standard properties of this process, we obtain that

$$\mathbf{P}\left(T > \lambda^{3/2+\delta}\right) \xrightarrow[\lambda\to+\infty]{} 0.$$

The second term can be controlled straightforwardly from (6.17) using an union bound, giving

$$\mathbf{P}\left(\exists\, 0 \leq n < \lambda^{3/2+\delta} \mid K_n^{(1)} \geq \lambda\varepsilon, K_n^{(2)} \geq \lambda\varepsilon\right) \leq \lambda^{3/2+\delta} C' (\lambda\varepsilon)^{-3} \xrightarrow[\lambda\to+\infty]{} 0.$$

We can now conclude that

$$\lambda^{-1} \min\left(K^{(1)}_{T-1}, K^{(2)}_{T-1}\right) \xrightarrow[\lambda\to+\infty]{\mathbf{P}} 0, \tag{6.18}$$

convergence which still holds conditionally on $|B_T| > \lfloor \lambda b \rfloor$, observing that the probability of this event converges when λ goes to infinity by Proposition 6.2.8 and the convergence in law of Proposition 6.4.5 (see a precise statement in (6.23)).

On the other hand, using the convergence in law (6.15), conditionally given $|B_T| > \lfloor \lambda b \rfloor$ we get that

$$\begin{aligned}
&\lambda^{-1} \max\left(B_{T-1} - K^{(1)}_{T-1}, |B_T| - \lfloor \lambda b \rfloor - K^{(2)}_{T-1}\right) \\
&\geq \lambda^{-1} \min\left(B_{T-1}, |B_T| - \lfloor \lambda b \rfloor\right) - \lambda^{-1} \min\left(K^{(1)}_{T-1}, K^{(2)}_{T-1}\right) \\
&\xrightarrow[\lambda\to+\infty]{(d)} \min\left(\kappa \mathcal{S}_{\tau-}, \kappa \mathcal{S}_\tau - b\right) \ \text{(given } \kappa|\mathcal{S}_\tau| > b\text{)}
\end{aligned}$$

and thus by the very same argument as in Lemma 6.4.8, conditionally on $|B_T| > \lfloor \lambda b \rfloor$,

$$\max\left(B_{T-1} - K^{(1)}_{T-1}, |B_T| - \lfloor \lambda b \rfloor - K^{(2)}_{T-1}\right) \xrightarrow[\lambda\to+\infty]{\mathbf{P}} +\infty. \tag{6.19}$$

Applying the identity (6.16), the expected result follows from the convergences in probability (6.18) and (6.19), restricted on $\mathsf{A}^{\square}_4$. □

Intuitively, the consequence of this lemma is that only two situations may occur on the event $\mathsf{A}^{\square}_4$: either $B_{T-1} - \mathsf{K}^{(1)}_\lambda$ or $|B_T| - \lfloor \lambda b \rfloor - \mathsf{K}^{(2)}_\lambda$ is large, or more precisely, respectively $\mathsf{K}^{(1)}_\lambda$ or $\mathsf{K}^{(2)}_\lambda$ is small with respect to λ. This corresponds to the subcases $\mathsf{A}^{\square}_{4,1}$ and $\mathsf{A}^{\square}_{4,2}$ of Figure 6.16. Roughly speaking, this means that quadrangles "look like" triangles when λ is large.

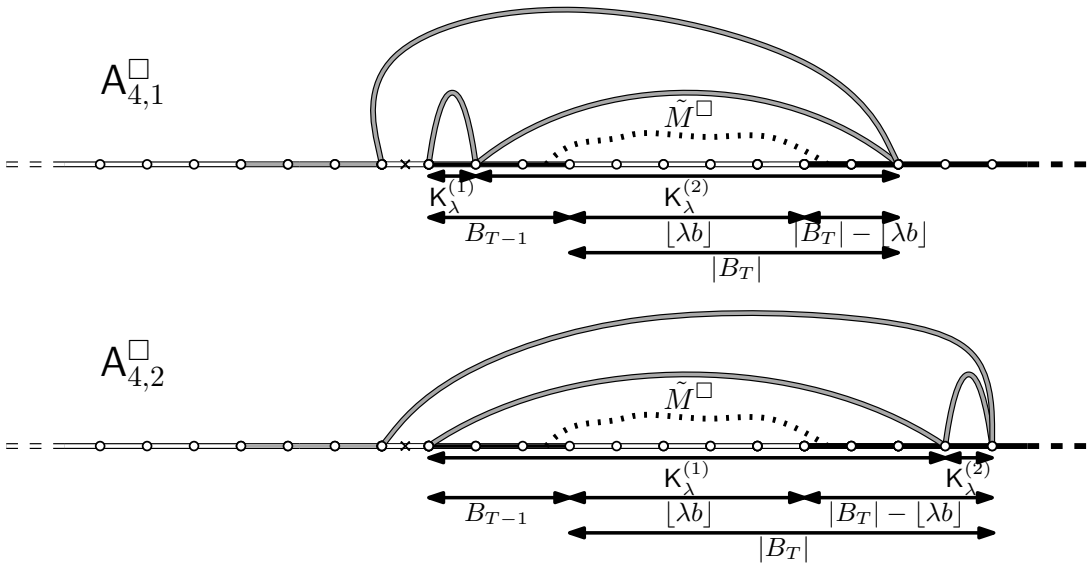

Figure 6.16: The likely subcases on the event $\mathsf{A}^{\square}_4$.

Let us be more precise here. The events $\mathsf{A}^{\square}_{4,1}$ and $\mathsf{A}^{\square}_{4,2}$ are defined as follows:

$$\mathsf{A}^{\square}_{4,1} := \mathsf{A}^{\square}_4 \cap \left\{\mathsf{K}^{(1)}_\lambda < B_{T-1}\right\} \quad \text{and} \quad \mathsf{A}^{\square}_{4,2} := \mathsf{A}^{\square}_4 \cap \left\{\mathsf{K}^{(2)}_\lambda < |B_T| - \lfloor \lambda b \rfloor\right\}.$$

Lemma 6.4.9 ensures that the probability of the event $\mathsf{A}_4^{\square} \cap \{\mathsf{K}_\lambda^{(1)} \geq B_{T-1}, \mathsf{K}_\lambda^{(2)} \geq |B_T| - \lfloor \lambda b \rfloor\}$ vanishes when λ becomes large, so that we can restrict our attention to the events $\mathsf{A}_{4,1}^{\square}$ and $\mathsf{A}_{4,2}^{\square}$ instead of $\mathsf{A}_4^{\square}$ in the next part, recalling that all the statements hold conditionally on the event $\{|B_T| > \lfloor \lambda b \rfloor\}$.

Looking at the dashed paths on Figure 6.16 and using the above discussion, one gets that in every likely case, the crossing event $\mathsf{C}^*(\lambda a, \lambda b)$ depends on the simple crossing event in the submap $\tilde{M}^*$, which is always a Boltzmann $*$-angulation of a proper polygon thanks to the spatial Markov property.

The key quantities are d_l^λ and d_r^λ, defined as the lengths of the two open segments on the boundary of that map (say with d_r^λ the segment that is closer from the last edge we peeled), whose boundary condition is thus that represented on Figure 6.17. In the first four configurations $(\mathsf{A}^{\triangle} - \mathsf{A}_3^{\square})$ described in Figure 6.15, we had $d_l^\lambda = B_{T-1}$ and $d_r^\lambda = |B_T| - \lfloor \lambda b \rfloor$. The situation is a bit more complicated in the cases of Figure 6.16, but with the convention that $\mathsf{K}_\lambda^{(1)} = \mathsf{K}_\lambda^{(2)} = +\infty$ out of the event $\mathsf{A}_4^{\square}$, we have the identities

$$d_l^\lambda = B_{T-1} \mathbf{1}_{\left\{\mathsf{K}_\lambda^{(1)} > B_{T-1} + \lfloor \lambda b \rfloor\right\}} + \left(B_{T-1} - \mathsf{K}_\lambda^{(1)}\right) \mathbf{1}_{\left\{\mathsf{K}_\lambda^{(1)} < B_{T-1}\right\}},$$

and

$$d_r^\lambda = (|B_T| - \lfloor \lambda b \rfloor) \mathbf{1}_{\left\{\mathsf{K}_\lambda^{(2)} > |B_T|\right\}} + \left(|B_T| - \lfloor \lambda b \rfloor - \mathsf{K}_\lambda^{(2)}\right) \mathbf{1}_{\left\{\mathsf{K}_\lambda^{(2)} < |B_T| - \lfloor \lambda b \rfloor\right\}}.$$

We now invoke Lemmas 6.4.8 and 6.4.9, together with the fact that $\mathsf{K}_\lambda^{(1)} + \mathsf{K}_\lambda^{(2)} = B_{T-1} + |B_T|$ on the event $\mathsf{A}_4^{\square}$, to get that (still conditionally on $|B_T| > \lfloor \lambda b \rfloor$),

$$d_l^\lambda \xrightarrow[\lambda \to +\infty]{\mathbf{P}} +\infty \quad \text{and} \quad d_r^\lambda \xrightarrow[\lambda \to +\infty]{\mathbf{P}} +\infty. \tag{6.20}$$

To sum up, we thus proved that conditionally on $|B_T| > \lfloor \lambda b \rfloor$, the crossing event $\mathsf{C}^*(\lambda a, \lambda b)$ occurs almost surely when there is an open path between the two black segments on the boundary of the map of Figure 6.17, which is a Boltzmann $*$-angulation. In what follows, we denote by C_λ^2 this event. Note that the length of the free segment on the boundary can either be 1 or 2 depending on the situation, and is thus uniformly bounded.

Asymptotic probabilities for submap crossings. Throughout this section, we discuss the asymptotic probabilities of the events C_λ^1 and C_λ^2 we previously introduced.

1. The event C_λ^1. Recall that the event C_λ^1 is the crossing event given by the existence of a path linking the origin of a UIHP-$*$ and the infinite open segment of the boundary, where the boundary of the map is coloured as in Figure 6.14 (the free segment has arbitrary but finite length). We denote by v^* the origin of the map, and recall that the length of the white segment located at the right of the origin satisfies from Lemma 6.4.7 (we implicitly still work conditionally on $|B_T| < \lfloor \lambda b \rfloor$)

$$d^\lambda := \lfloor \lambda b \rfloor - |B_T| \xrightarrow[\lambda \to +\infty]{\mathbf{P}} +\infty. \tag{6.21}$$

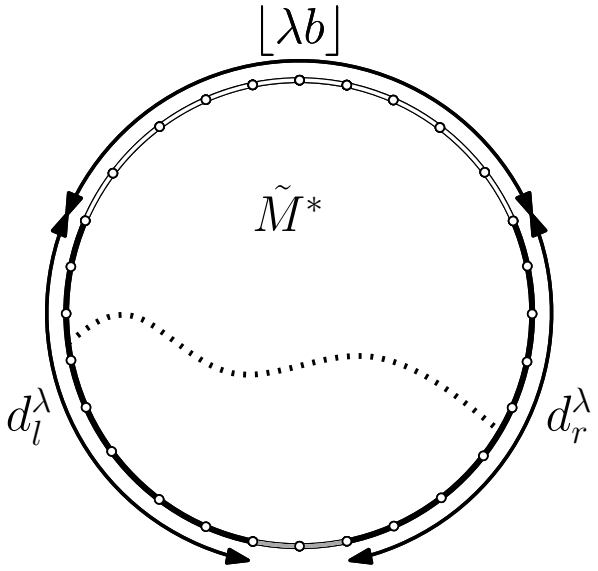

Figure 6.17: The crossing event C_λ^2.

For every $x \geq 0$, let $\partial_{x,\infty}^{(r)}$ be the set of vertices of the map that are located on the boundary, at least x vertices away on the right of v^*. We are now able to compute the asymptotic probability we are interested in.

Proposition 6.4.10. *Conditionally on $|B_T| < \lfloor \lambda b \rfloor$, we have*

$$\mathbf{P}\left(\mathsf{C}_\lambda^1\right) \underset{\lambda \to +\infty}{\longrightarrow} 0.$$

As a consequence, $\mathbf{P}(\mathsf{C}^*(\lambda a, \lambda b) \mid |B_T| < \lfloor \lambda b \rfloor) \underset{\lambda \to +\infty}{\longrightarrow} 0.$

Proof. We first introduce the sequence of events $(\mathrm{V}_x)_{x \geq 0}$, where for every $x \geq 0$, V_x is the event that an open path links the origin v^* of the map to the set of vertices $\partial_{x,\infty}^{(r)}$, without using edges of the right boundary. Then, we have that for every $\lambda > 0$,

$$\mathbf{P}\left(\mathsf{C}_\lambda^1\right) = \mathbf{P}\left(\mathrm{V}_{d^\lambda}\right).$$

(We implicitly used that from any open path realizing C_λ^1, we can extract one that does not use edges of the right boundary.) Now, $(\mathrm{V}_x)_{x \geq 0}$ is a decreasing sequence of events, so that for every $x \geq 0$ and $\lambda > 0$,

$$\mathbf{P}\left(\mathsf{C}_\lambda^1\right) \leq \mathbf{P}\left(\mathrm{V}_x\right) + \mathbf{P}\left(d^\lambda \leq x\right).$$

Moreover, the limiting event

$$\mathrm{V} := \bigcap_{x \geq 0} \mathrm{V}_x$$

is the event that infinitely many open paths from the origin intersect the right boundary (implicitly, at different vertices), again without using any edge of the right boundary. This event implies in particular that the cluster $\mathcal{C}$ of our map is still infinite if we set closed all the edges of the right boundary. Thus, the convergence (6.21) yields that

$$\limsup_{\lambda \to +\infty} \mathbf{P}\left(\mathsf{C}_\lambda^1\right) \leq \mathbf{P}\left(\mathrm{V}\right) \leq \Theta_{\text{bond}}^*\left(p_{c,\text{bond}}^*\right) = 0.$$

The fact that there is no percolation at the critical point almost surely is straightforward from [AC15], Theorem 7. This result holds for a "Free-White" boundary condition, and thus in our setting using the above remarks and a coupling argument. This ends the proof, using for the second statement the discussion of Section 6.4.1. □

2. The event C^2_λ. We now focus on the crossing event C^2_λ, which is defined by the existence of an open path linking the two open segments on the boundary of a Boltzmann $*$-angulation, whose boundary is represented in Figure 6.17. Recall that the law of this map is denoted by $\mathbb{W}^*_{v(\lambda)}$, where $v(\lambda)$ is the number of vertices on the boundary. The lengths of the open segments on the boundary are given by d^λ_l and d^λ_r. For the sake of clarity, we may now assume that the free segment on the boundary has unit length, this single edge being chosen as the root of the map and denoted w^* (the extension to the case with a free segment of length 2 - or simply bounded - is immediate). For every $x \geq 0$, we let $\partial^{(l)}_x$ and $\partial^{(r)}_x$ be the sets of x edges of the boundary of the map located immediately on the left and on the right of w^*. Finally, we set $d^\lambda := \min(d^\lambda_l, d^\lambda_r)$. Using the previous arguments, in particular (6.20) it is obvious that (again, we implicitly still work conditionally on $|B_T| > \lfloor \lambda b \rfloor$)

$$v(\lambda) \underset{\lambda\to+\infty}{\longrightarrow} +\infty \quad \text{and} \quad d^\lambda \underset{\lambda\to+\infty}{\overset{\mathbf{P}}{\longrightarrow}} +\infty. \tag{6.22}$$

In the next part, we will consider dual bond percolation on planar maps (i.e., bond percolation on the dual map), with the convention that the colour of a dual edge is the colour of the unique primal edge it crosses. We denote by $\Theta^*_{\text{bond}'}$ and $p^*_{c,\text{bond}'}$ the dual bond percolation probability and the dual bond percolation threshold on the UIHP-$*$. We can now prove that the event C^2_λ occurs asymptotically almost surely.

Proposition 6.4.11. *Conditionally on* $|B_T| > \lfloor \lambda b \rfloor$*, we have*

$$\mathbf{P}\left(\mathsf{C}^2_\lambda\right) \underset{\lambda\to+\infty}{\longrightarrow} 1.$$

As a consequence, $\mathbf{P}(\mathsf{C}^*(\lambda a, \lambda b) \mid |B_T| > \lfloor \lambda b \rfloor) \underset{\lambda\to+\infty}{\longrightarrow} 1.$

Proof. Let us first introduce the sequence of events $(\mathsf{V}_x)_{x\geq 0}$, where for every $x \geq 0$, V_x is the event that an open path links a vertex of $\partial^{(l)}_x$ to a vertex of $\partial^{(r)}_x$, without using edges of the boundary of the map (except possibly the root edge). Then, we have

$$\mathbf{P}\left(\mathsf{C}^2_\lambda\right) \geq \mathbf{P}\left(\mathsf{C}^2_\lambda, d^\lambda > x\right) \geq \mathbf{P}\left(\mathsf{V}_x, d^\lambda > x\right) \geq \mathbf{P}\left(\mathsf{V}_x\right) - \mathbf{P}\left(d^\lambda \leq x\right).$$

We emphasize that the quantity $\mathbf{P}\left(\mathsf{V}_x\right)$ still depends on λ through the law of the map we consider, whose boundary has size $v(\lambda)$. We now want to restrict the events $(\mathsf{V}_x)_{x\geq 0}$ to a finite subset of the map. To do so, we introduce for every $x \geq 0$ and $R \geq 0$ the event $\mathsf{V}_{x,R}$, which is defined exactly as V_x with the additional condition that the crossing event occurs in the ball of radius R of the map for the graph distance (and from the origin). We still have for every $x \geq 0$ and $R \geq 0$ that

$$\mathbf{P}\left(\mathsf{C}^2_\lambda\right) \geq \mathbf{P}\left(\mathsf{V}_{x,R}\right) - \mathbf{P}\left(d^\lambda \leq x\right).$$

Now, the event $\mathsf{V}_{x,R}$ is by construction measurable with respect to the ball of radius R of the map, so that the convergence in law $\mathbb{W}^*_{v(\lambda)} \underset{\lambda\to+\infty}{\Longrightarrow} \widehat{\mathbb{P}}^*_{\infty,\infty}$ for the local topology implies that for every fixed $x \geq 0$ and $R \geq 0$,

$$\mathbf{P}\left(\mathsf{V}_{x,R}\right) \underset{\lambda\to+\infty}{\longrightarrow} \widehat{\mathbb{P}}^*_{\infty,\infty}\left(\mathsf{V}_{x,R}\right).$$

Using also the convergence (6.22), we get

$$\liminf_{\lambda\to+\infty} \mathbf{P}\left(\mathsf{C}^2_\lambda\right) \geq \widehat{\mathbb{P}}^*_{\infty,\infty}\left(\mathsf{V}_{x,R}\right),$$

and from the increasing property of the sequence $(\mathsf{V}_{x,R})_{R\geq 0}$ for every fixed $x \geq 0$, by letting R go to infinity,

$$\liminf_{\lambda\to+\infty} \mathbf{P}\left(\mathsf{C}^2_\lambda\right) \geq \widehat{\mathbb{P}}^*_{\infty,\infty}\left(\mathsf{V}_{x}\right).$$

At this point, let us introduce the complementary ∂^∞_x of the sets of edges $\partial^{(l)}_x$ and $\partial^{(r)}_x$ on the boundary (i.e., the edges that are at least x edges away from the root on the boundary) and notice that almost surely, the complementary event $(\mathsf{V}_x)^c$ is exactly the existence of a dual closed crossing between the dual of the root edge and dual edges of the set ∂^∞_x that do not use dual edges of $\partial^{(l)}_x \cup \partial^{(r)}_x$, using standard properties of dual bond percolation on planar maps. Up to extraction, we can assume that such a path do not uses dual edges of the boundary at all (out of its endpoints).

Following the same idea as in Proposition 6.4.10, we introduce the decreasing sequence of events $(\mathsf{V}'_x)_{x\geq 0}$, where for every $x \geq 0$, V'_x is precisely the event that a closed dual path links the dual edge of the root to the set ∂^∞_x (without using other dual edges of the boundary than its endpoints). Thus, for every $x \geq 0$,

$$\limsup_{\lambda\to+\infty} \mathbf{P}\left(\left(\mathsf{C}^2_\lambda\right)^c\right) \leq \widehat{\mathbb{P}}^*_{\infty,\infty}\left(\mathsf{V}'_x\right).$$

Again, the limiting event

$$\mathsf{V}' := \bigcap_{x\geq 0} \mathsf{V}'_x$$

is the event that infinitely many dual paths from the dual of the root edge intersect the boundary (at different edges), without using dual edges of the boundary out of their endpoints. This event implies in particular that the dual closed percolation cluster $\mathcal{C}'$ is infinite, even if we do not allow dual paths to use boundary edges - or equivalently if we suppose that the boundary is totally open, except the root edge which is free. Thus,

$$\limsup_{\lambda\to+\infty} \mathbf{P}\left(\left(\mathsf{C}^2_\lambda\right)^c\right) \leq \widehat{\mathbb{P}}^*_{\infty,\infty}\left(\mathsf{V}'\right) \leq \Theta^*_{\text{bond}'}(1 - p^*_{c,\text{bond}}) = 0.$$

Indeed, the parameter for dual bond percolation equals $1 - p^*_{c,\text{bond}}$ because we work at criticality, and we can invoke the fact that $p^*_{c,\text{bond}'} = 1 - p^*_{c,\text{bond}}$ and that there is no percolation at the critical point (see [AC15, Section 3.4.1] for details). One should notice here that this result holds for a "Free-Black" boundary as proved in [AC15], but we easily conclude by the standard coupling argument and the above discussion. This ends the proof, using again for the second statement the discussion of Section 6.4.1. □

Proof of Theorem 6.1.2: bond percolation case. We now prove the main result of this section. Recall that $\mathsf{C}^*(\lambda a, \lambda b)$ denotes the crossing event between the two black segments on the boundary in a UIHP-$*$ with the boundary condition of Figure 6.11.

First, using again the stopping time $\tilde{T} := \inf\{t \geq 0 : \lambda^{-1} B_{\lfloor \lambda^{3/2} t \rfloor} \leq 0\}$, we get the convergence

$$\lambda^{-1} B_{\lfloor \lambda^{3/2} \tilde{T} \rfloor} \xrightarrow[\lambda \to +\infty]{(d)} \kappa \mathcal{S}_\tau,$$

where $\tau := \inf\{t \geq 0 : \mathcal{S}_t \leq 0\}$. Then, the distribution of the overshoot of the process $\mathcal{S}$ given in Proposition 6.2.8, which is absolutely continuous with respect to the Lebesgue measure, implies on the one hand that

$$\mathbf{P}(|B_T| > \lfloor \lambda b \rfloor) \underset{\lambda \to +\infty}{\longrightarrow} P_{\frac{a}{\kappa}}(\kappa |\mathcal{S}_\tau| > b) = \frac{1}{\pi} \arccos\left(\frac{b-a}{a+b}\right), \tag{6.23}$$

and on the other hand that the probability of the events $\{|B_T| = 0\}$ and $\{|B_T| = \lfloor \lambda b \rfloor\}$ vanish when λ becomes large. We can thus split up the problem conditionally on the value of $|B_T|$, namely the crossing probability $\mathbf{P}(\mathsf{C}^*(\lambda a, \lambda b))$ has the same limit when λ goes to infinity as the quantity

$$\mathbf{P}(\mathsf{C}^*(\lambda a, \lambda b) \mid |B_T| < \lfloor \lambda b \rfloor) \mathbf{P}(|B_T| < \lfloor \lambda b \rfloor) + \mathbf{P}(\mathsf{C}^*(\lambda a, \lambda b) \mid |B_T| > \lfloor \lambda b \rfloor) \mathbf{P}(|B_T| > \lfloor \lambda b \rfloor).$$

The results of Propositions 6.4.10 and 6.4.11 thus yield that

$$\lim_{\lambda \to +\infty} \mathbf{P}\left(\mathsf{C}^{\triangle}_{\text{bond}}(\lambda a, \lambda b)\right) = \lim_{\lambda \to +\infty} \mathbf{P}\left(\mathsf{C}^{\square}_{\text{bond}}(\lambda a, \lambda b)\right) = \frac{1}{\pi} \arccos\left(\frac{b-a}{a+b}\right),$$

which is exactly Theorem 6.1.2 in the bond percolation case on the UIHPT and the UIHPQ.

6.4.2 Crossing probabilities for face percolation

We now consider the crossing events for face percolation. We will see that although the peeling process is slightly different, the same method as for bond percolation applies in order to compute the scaling limits we are interested in. Recall that two faces are adjacent in this model if they share an edge. We still work conditionally on a "White-Black-White-Black" boundary condition. Here, this means that the crossing event $\mathsf{C}^*_{\text{face}}(\lambda a, \lambda b)$ has to occur between the two black segments of the boundary, such that one can imagine faces lying on the other side of the boundary as in Figure 6.18.

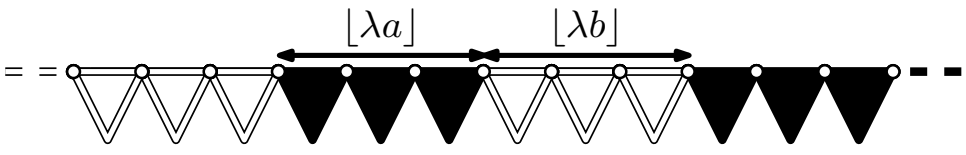

Figure 6.18: The boundary condition for the face percolation problem.

The arguments being very similar to the previous section, we do not give as many details, except for the remarkable differences.

Peeling process and scaling limit. The main argument is again to define the appropriate peeling process, which is here simpler because we do not have to deal with a free segment on the boundary. However, a subtlety arising in this context is that the right thing to do is to peel the leftmost black edge instead of the rightmost white. The reason is that this exploration follows the rightmost percolation interface between the open and closed clusters, which is the correct one as far as the crossing event is concerned.

ALGORITHM 6.4.12. Consider a half-plane map which has the law of the UIHP-$*$ with a "White-Black-White-Black" boundary condition (the outmost segments being infinite).

Reveal the face incident to the leftmost black edge of the boundary, including its colour.

After each step, repeat the algorithm on the UIHP-$*$ given by the unique infinite connected component of the current map, deprived of the revealed face. The exposed edges of the initial map form the boundary of the infinite connected component, whose colour is inherited from the adjacent revealed faces.

Note that this algorithm never ends because there is always a leftmost black edge on the boundary, although we are only interested in cases where the finite black segment has positive length.

The properties of this algorithm are the same as before, due to the spatial Markov property. In particular, the random variables $(\mathcal{E}_n, \mathcal{R}_{r,n}, c_n)_{n\geq 0}$, defined exactly as in Section 6.4.1, are i.i.d. and have the law of $\mathcal{E}, \mathcal{R}_r$ and c (which has the Bernoulli law of parameter $p^*_{c,\text{face}}$) respectively, where c_n denotes the colour of the face revealed at step n of the process and the other notations are the same as before. We again need the process $(B_n)_{n\geq 0}$, defined as follows.

We let $B_0 = \lfloor \lambda a \rfloor$ and for every $n \geq 0$:

$$B_{n+1} = B_n + \mathbf{1}_{\{c_n=1\}}\mathcal{E}_n - \mathcal{R}_{r,n} - 1. \tag{6.24}$$

The process $(B_n)_{n\geq 0}$ is a Markov chain with respect to the canonical filtration of the exploration process. Moreover, if we denote by $T := \inf\{n \geq 0 : B_n \leq 0\}$ the first entrance time of $(B_n)_{n\geq 0}$ in $\mathbb{Z}_-$, then for every $0 \leq n < T$, B_n is the **length of the finite black segment** at step n of the exploration process. As long as $n < T$, it still holds that all the (black) faces incident to this segment are part of the open cluster of the initial finite black segment, due to the fact that our algorithm follows the rightmost percolation interface, while for $n \geq T$, the initial finite black segment has been swallowed.

The process $(B_n)_{n\geq 0}$. The properties of the peeling process yields that $(B_n)_{n\geq 0}$ is a random walk with steps distributed as X defined by

$$X := \mathbf{1}_{c=1}\mathcal{E} - \mathcal{R}_r - 1.$$

In particular, using the same arguments as before, we get

$$\mathbf{E}(X) = p^*_{c,\text{face}}\mathbf{E}(\mathcal{E}) - \mathbf{E}(\mathcal{R}_r) - 1 = \begin{cases} \frac{5}{3}p^{\triangle}_{c,\text{face}} - \frac{4}{3} \ (* = \triangle) \\ \\ 2p^{\square}_{c,\text{face}} - \frac{3}{2} \ (* = \square) \end{cases}.$$

Thus, we have $\mathbf{E}(X) = 0$ in both the UIHPT and the UIHPQ, and this yields the convergence

$$\left(\frac{B_{\lfloor \lambda t \rfloor}}{\lambda^{2/3}}\right)_{t\geq 0} \xrightarrow[\lambda\to+\infty]{(d)} \kappa(\mathcal{S}_t)_{t\geq 0}$$

in the sense of Skorokhod, where $\mathcal{S}$ is the Lévy spectrally negative $3/2$-stable process started at a.

Stopped peeling process and asymptotics. Let us focus on the first time when $(B_n)_{n\geq 0}$ reaches $\mathbb{Z}_-$. Again, two cases are likely to happen:

Case 1: $|B_T| < \lfloor \lambda b \rfloor$. In this situation, a finite part of the white segment on the boundary is swallowed. If the last revealed face is white, the crossing event cannot occur, while if it is black, the crossing event implies the existence of an open path linking the rightmost edge of the finite black segment and the infinite black segment on the boundary. This event, still denoted by C^1_λ, is similar to that of the bond case. We again have that

$$\lfloor \lambda b \rfloor - |B_T| \xrightarrow[\lambda\to+\infty]{\mathbf{P}} +\infty,$$

so that the crossing event C^1_λ has probability bounded by the percolation probability in this model and we get

$$\lim_{\lambda\to+\infty} \mathbf{P}\left(\mathsf{C}^1_\lambda\right) \leq \Theta^*_{\text{face}}(p^*_{c,\text{face}}) = 0,$$

using [AC15, Theorem 6].

Case 2: $|B_T| > \lfloor \lambda b \rfloor$. In this situation, the whole white segment on the boundary is swallowed. We have

$$|B_T| - \lfloor \lambda b \rfloor \xrightarrow[\lambda\to+\infty]{\mathbf{P}} +\infty \quad \text{and} \quad B_{T-1} \xrightarrow[\lambda\to+\infty]{\mathbf{P}} +\infty,$$

as in the bond percolation case. Whether the last revealed face is open or closed, the crossing event is implied by a crossing event in a Boltzmann map, whose boundary has the colouring of Figure 6.17. We denote by C^2_λ this event, and we have that

$$d^\lambda_l \xrightarrow[\lambda\to+\infty]{\mathbf{P}} +\infty \quad \text{and} \quad d^\lambda_r \xrightarrow[\lambda\to+\infty]{\mathbf{P}} +\infty$$

in every likely case. Then, when λ goes to infinity, we have that $(\mathsf{C}^2_\lambda)^c$ implies the closed dual face percolation event - dual face percolation being face percolation where adjacent faces share a vertex, or equivalently site percolation on the dual map with the same adjacency rules. This is analogous to the star-lattice in the case of $\mathbb{Z}^d$, and we have that $1 - p^*_{c,\text{face}'} = p^*_{c,\text{face}}$, with no percolation at the critical point,

see [AC15, Section 3.4.2] (with a fully open boundary condition). As a consequence, we get:

$$\lim_{\lambda\to+\infty} \mathbf{P}\left(\left(\mathsf{C}^2_\lambda\right)^c\right) \leq \Theta^*_{\text{face}'}(1-p^*_{c,\text{face}}) = 0.$$

The statements we obtained up to this point yield, using the same arguments as in Section 6.4.1, that

$$\lim_{\lambda\to+\infty} \mathbf{P}\left(\mathsf{C}^{\triangle}_{\text{face}}(\lambda a,\lambda b)\right) = \lim_{\lambda\to+\infty} \mathbf{P}\left(\mathsf{C}^{\square}_{\text{face}}(\lambda a,\lambda b)\right) = \frac{1}{\pi}\arccos\left(\frac{b-a}{a+b}\right),$$

which is exactly Theorem 6.1.2 in the case of face percolation on the UIHPT and the UIHPQ.

6.4.3 Crossing probabilities for site percolation

The last case we study is site percolation on the UIHPQ. We work conditionally on the same "White-Black-White-Black" boundary condition, represented in Figure 6.19.

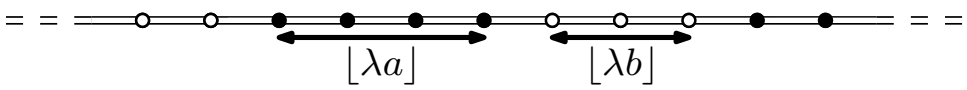

Figure 6.19: The boundary condition for the site percolation problem.

We are still interested in the scaling limit of the probability of the crossing event that the two black segments are part of the same percolation cluster, denoted by $\mathsf{C}^{\square}_{\text{site}}(\lambda a,\lambda b)$, at the critical point $p^{\square}_{c,\text{site}}$.

Peeling process and scaling limit. Here, the appropriate peeling process follows the same idea as in the bond percolation case, but we use the vertex-peeling process (Algorithm 6.3.1) introduced in Section 6.3 in order to peel vertices instead of edges. Recall that a "White-(Free)-Any" boundary condition means that we have an infinite white segment on the left, and then (possibly) a finite free segment, with no specific condition on the right part. Again, the right part will turn out to be coloured "Black-White-Black" due to the boundary condition we are interested in, but we define the algorithm in the general setting.

ALGORITHM 6.4.13. Consider a half-plane map which has the law of the UIHPQ with a "White-(Free)-Any" boundary condition.

- Reveal the colour of the rightmost free vertex, if any:
  - If it is black, repeat the algorithm.
  - If it is white, mark this vertex and execute the vertex-peeling process, without revealing the colour of the vertices.
- If there is no free vertex on the boundary of the map, as in the first step, mark the rightmost white vertex of the infinite white segment and execute the vertex-peeling process, without revealing the colour of the vertices.

After each step, repeat the algorithm on the unique infinite connected component of the current map, deprived of the revealed faces. The map we obtain is again implicitly rooted at the next edge we have to peel.

As usual, the algorithm is well-defined in the sense that the pattern of the boundary (White-(Free)-Any) is preserved.

Following the strategy of Section 6.4.1, we now define the two processes $(F_n)_{n\geq 0}$ and $(B_n)_{n\geq 0}$. Let us first recall some familiar notation. For every $n \geq 0$, we denote by c_n the color of the revealed vertex at step n of the exploration, with the convention that $c_n = 0$ when there is no free vertex on the boundary. When $c_n = 0$, the vertex-peeling process is executed and we let $\sigma_n + 1$ be the number of steps of this process (so that $\sigma_n \geq 0$). Then, for every $0 \leq i \leq \sigma_n$, we denote by $E_i^{(n)}$, respectively $R_i^{(l,n)}$, $R_i^{(r,n)}$ the number of exposed edges, respectively swallowed edges on the left and right of the root edge at step i of the vertex-peeling process (in particular, $R_i^{(r,n)} = 0$ for $i < \sigma_n$). All of those variables are set to zero when $c_n = 1$ by convention.

Thanks to the spatial Markov property and the definition of the vertex-peeling process, if we restrict ourselves to the consecutive stopping times when $c_n = 0$, the random variables $(\sigma_n)_{n\geq 0}$ are i.i.d., with geometric law of parameter $\mathbf{P}(\mathcal{R}_r = 0)$: they have the same law as σ, defined for every $k \geq 0$ by $\mathbf{P}(\sigma = k) = (\mathbf{P}(\mathcal{R}_r = 0))^k(1 - \mathbf{P}(\mathcal{R}_r = 0))$.

Conditionally on $(\sigma_n)_{n\geq 0}$, the variables $(E_i^{(n)})_{n\geq 0, 0\leq i\leq \sigma_n - 1}$ and $(R_i^{(l,n)})_{n\geq 0, 0\leq i\leq \sigma_n - 1}$ are i.i.d. and have the law of $\mathcal{E}$ and $\mathcal{R}_l$ conditionally on $\mathcal{R}_r = 0$ respectively, and moreover, $(E_{\sigma_n}^{(n)})_{n\geq 0}$, $(R_{\sigma_n}^{(l,n)})_{n\geq 0}$ and $(R_{\sigma_n}^{(r,n)})_{n\geq 0}$ are i.i.d. and have the law of $\mathcal{E}$,$\mathcal{R}_l$ and $\mathcal{R}_r$ conditionally on $\mathcal{R}_r > 0$ respectively. Finally, all those variables independent for different values of n.

In what follows, we let $(\tilde{E}_i)_{i\geq 0}$, $(\tilde{R}_{l,i})_{i\geq 0}$, $\bar{E}$, $\bar{R}_l$ and $\bar{R}_r$ be independent random variables having the law of $\mathcal{E}$, $\mathcal{R}_l$ and $\mathcal{R}_r$ conditionally on $\mathcal{R}_r = 0$ and $\mathcal{R}_r > 0$ respectively. We also define c that has the Bernoulli law of parameter $p_{c,\text{site}}^{\square}$. We can now define the processes $(F_n)_{n\geq 0}$ and $(B_n)_{n\geq 0}$.

First, for every $n \geq 0$, we let F_n be the **length of the free segment** on the boundary at step n of the peeling process.

In this setting, this quantity is harder to study because of the vertex-peeling process that we (possibly) execute. Let us provide an alternative description of the process $(F_n)_{n\geq 0}$. We first have $F_0 = 0$. Then, let $F_0^{(0)} = 0$ and for every $n \geq 0$, set inductively $F_0^{(n)} := (F_n - 1)_+$. We let for every $n \geq 0$ and $0 \leq i \leq \sigma_n$,

$$F_{i+1}^{(n)} := \begin{cases} F_i^{(n)} + E_i^{(n)} - R_i^{(l,n)} - 1 & \text{if} \quad F_i^{(n)} - R_i^{(l,n)} - 1 \geq 0 \\ E_i^{(n)} - 1 & \text{otherwise} \end{cases}.$$

On the event $\{c_n = 0\}$, this quantity describes the evolution of the length of the finite free segment during the execution of the vertex-peeling process. Then, we have for every $n \geq 0$,

$$F_{n+1} = \begin{cases} F_n - 1 & \text{if} \quad c_n = 1 \\ F_{\sigma_n+1}^{(n)} & \text{if} \quad c_n = 0 \end{cases}. \tag{6.25}$$

The process $(F_n)_{n\geq 0}$ is a Markov chain with respect to the canonical filtration of the exploration process, and $c_n = 0$ when $F_n = 0$.

Remark 6.4.14. Contrary to the bond percolation case, the process $(F_n)_{n\geq 0}$ can reach zero even when $c_n = 0$, and can also take value zero at consecutive times with positive probability.

Then, we also let $B_0 = \lfloor \lambda a \rfloor$ and for every $n \geq 0$:

$$B_{n+1} = \begin{cases} B_n + 1 & \text{if } \ c_n = 1 \\ B_n + 1 - R^{(r,n)}_{\sigma_n} & \text{if } \ c_n = 0 \end{cases}. \tag{6.26}$$

The process $(B_n)_{n\geq 0}$ is a Markov chain with respect to the canonical filtration of the exploration process. Moreover, if we denote by $T := \inf\{n \geq 0 : B_n \leq 0\}$ the first entrance time of $(B_n)_{n\geq 0}$ in $\mathbb{Z}_-$, then for every $0 \leq n < T$, B_n is the **length of the finite black segment** at step n of the exploration process. Again, while $n < T$, the vertices of this segment are part of the open cluster of the initial black segment, while this initial segment has been swallowed for $n \geq T$.

The process $(F_n)_{n\geq 0}$. Exactly as in Section 6.4.1, the process $(F_n)_{n\geq 0}$ is not a random walk, but has the same behaviour when it is far away from zero. More precisely, let us define $\hat{\sigma}_+ := \inf\{n \geq 0 : F_n > 0\}$ and $\hat{\sigma}_- := \inf\{n \geq \hat{\sigma}_+ : \exists\, 0 \leq i \leq \sigma_n : F^{(n)}_i - R^{(l,n)}_i - 1 < 0\}$, which is the first time after $\hat{\sigma}_+$ the finite free segment is swallowed (possibly during the vertex-peeling process). Note that $F_{\hat{\sigma}_-}$ is not zero in general, but if $F_n = 0$ for $n \geq \hat{\sigma}_+$, then $\hat{\sigma}_- \leq n$. By construction, as long as $\hat{\sigma}_+ \leq n < \hat{\sigma}_-$, we have

$$F_{n+1} = F_n - 1 + \mathbf{1}_{\{c_n=0\}} \left(\sum_{i=0}^{\sigma_n} \left(E^{(n)}_i - R^{(l,n)}_i - 1 \right) \right),$$

and $(F_{\hat{\sigma}_+ + n} - F_{\hat{\sigma}_+})_{0\leq n\leq \hat{\sigma}_- - \hat{\sigma}_+}$ is a killed random walk with steps distributed as the random variable $\hat{X}$ defined by

$$\hat{X} := \mathbf{1}_{\{c=0\}} \left(\sum_{i=0}^{\sigma-1} (\tilde{E}_i - \tilde{R}_{l,i} - 1) + \bar{E} - \bar{R}_l - 1 \right) - 1.$$

We get from the definitions that

$$\begin{aligned} \mathbf{E}(\hat{X}) &= (1 - p^{\square}_{c,\text{site}})[\mathbf{E}(\sigma)\mathbf{E}(\tilde{E}_0 - \tilde{R}_{l,0} - 1) + \mathbf{E}(\bar{E} - \bar{R}_l - 1)] - 1 \\ &= \frac{4}{9} \left(\frac{7}{2} \left[\mathbf{E}(\tilde{E}_0) - \mathbf{E}(\tilde{R}_{l,0}) - 1 \right] + 9 - \frac{7}{2}\mathbf{E}(\tilde{E}_0) - \frac{9}{4} + \frac{7}{2}\mathbf{E}(\tilde{R}_{l,0}) - 1 \right) - 1 = 0, \end{aligned}$$

using computations similar to that of Proposition 6.3.7 and the associated remark. This implies in particular that $\hat{\sigma}_-$ is almost surely finite (since it is bounded from above by the first return time of the process to zero). It is again easy to check that the random variable $\hat{X}$ satisfies the assumptions of Proposition 6.2.7, so that if we denote by $(\hat{S}_n)_{n\geq 0}$ a random walk with steps distributed as $\hat{X}$, we have

$$\left(\frac{\hat{S}_{\lfloor \lambda t \rfloor}}{\lambda^{2/3}} \right)_{t\geq 0} \xrightarrow[\lambda\to+\infty]{(d)} \kappa(\mathcal{S}_t)_{t\geq 0}, \tag{6.27}$$

in the sense of convergence in law for Skorokhod's topology, where $\mathcal{S}$ is the Lévy $3/2$-stable process.

The process $(B_n)_{n\geq 0}$. As before, $(B_n)_{n\geq 0}$ is not a random walk but behaves the same way when F_n is not equal to zero. More precisely, let $\sigma_0^{(0)} = 0$, $\sigma_0^{(1)} := \inf\{n \geq 0 : F_n > 0\}$ and recursively for every $k \geq 1$,

$$\sigma_k^{(0)} := \inf\{n \geq \sigma_{k-1}^{(1)} : F_n = 0\} \quad \text{and} \quad \sigma_k^{(1)} := \inf\{n \geq \sigma_k^{(0)} : F_n > 0\}.$$

From the fact that the vertex-peeling process exposes a positive number of vertices with positive probability, we know that $\sigma_0^{(1)}$ is almost surely finite. Moreover, using the above description of the process $(F_n)_{n\geq 0}$, it holds that started from any initial length, the free segment is swallowed in time $\hat{\sigma}_-$ which is also finite. This possibly happens during the vertex-peeling process, but in this case, with probability bounded away from zero, the vertex-peeling process ends at the next step with no exposed vertices and $F_{\hat{\sigma}_-} = 0$. From there, we get that $\sigma_1^{(0)}$, and thus all the stopping times $(\sigma_k^{(0)})_{k\geq 0}$ and $(\sigma_k^{(1)})_{k\geq 0}$ are almost surely finite.

Using the strong Markov property and the definition of $(B_n)_{n\geq 0}$, for every $k \geq 0$, the process $(B_{\sigma_k^{(1)}+n} - B_{\sigma_k^{(1)}})_{0\leq n\leq \sigma_{k+1}^{(0)}-\sigma_k^{(1)}}$ is a killed random walk with steps distributed as the random variable X defined by

$$X := \mathbf{1}_{\{c=1\}} - \mathbf{1}_{\{c=0\}}(\bar{R}_r - 1).$$

In particular, we have $\mathbf{E}(X) = p_{c,\text{site}}^{\square} - (1 - p_{c,\text{site}}^{\square})(\mathbf{E}(\mathcal{R}_r \mid \mathcal{R}_r > 0) - 1) = 0$ and properties of the random variable X yields that if $(S_n)_{n\geq 0}$ is a random walk with steps distributed as X, then

$$\left(\frac{S_{\lfloor \lambda t \rfloor}}{\lambda^{2/3}}\right)_{t\geq 0} \xrightarrow[\lambda\to+\infty]{(d)} \kappa(\mathcal{S}_t)_{t\geq 0} \tag{6.28}$$

in the sense of Skorokhod, where $\mathcal{S}$ is the Lévy $3/2$-stable process.

At this point, we are in the exact situation of Section 6.4.1, and the point is to get the following analogue of Proposition 6.4.5.

Proposition 6.4.15. *We have, in the sense of convergence in law for Skorokhod's topology*

$$\left(\frac{B_{\lfloor \lambda^{3/2} t \rfloor}}{\lambda}\right)_{t\geq 0} \xrightarrow[\lambda\to+\infty]{(d)} \kappa(\mathcal{S}_t)_{t\geq 0},$$

where $\mathcal{S}$ is the Lévy spectrally negative $3/2$-stable process started at a.

The proof of this result is analogous to that of Proposition 6.4.5, but some notable differences exist as we now explain. Let again $S_0 = B_0$ and introduce a sequence $(\beta_n)_{n\geq 0}$ of i.i.d. random variables with Bernoulli law of parameter $p_{c,\text{site}}^{\square}$. For every $n \geq 0$, we set

$$S_{n+1} = S_n + \begin{cases} B_{n+1} - B_n = \mathbf{1}_{\{c_n=1\}} - \mathbf{1}_{\{c_n=0\}}(R_{\sigma_n}^{(r,n)} - 1) & \text{if } F_n > 0 \\ \beta_n + (1-\beta_n)(B_{n+1} - B_n) = \mathbf{1}_{\{\beta_n=1\}} - \mathbf{1}_{\{\beta_n=0\}}(R_{\sigma_n}^{(r,n)} - 1) & \text{if } F_n = 0 \end{cases}$$

Let also for every $n \geq 0$, $\Xi_n := \{0 \leq k < n : F_n = 0\}$ and $\xi_n := \#\Xi_n$. Using arguments similar to that of Section 6.4.1, we see that $(S_n)_{n\geq 0}$ is a random walk started from B_0 with steps distributed as the random variable X we previously introduced, and that almost surely for every $n \geq 0$,

$$S_n - R_n \leq B_n \leq S_n,$$

where $R_n := \sum_{k\in\Xi_n} (1 - (B_{k+1} - B_k))$. The only thing that remains to check is that for every $\alpha > 0$,

$$\frac{\xi_n}{n^{1/3+\alpha}} \xrightarrow[n\to+\infty]{\mathbf{P}} 0. \tag{6.29}$$

We will then use the arguments of the proof of Proposition 6.4.5 to conclude that $(R_n)_{n\geq 0}$ is small with respect to $(S_n)_{n\geq 0}$ and does not affect the scaling limit of the process $(B_n)_{n\geq 0}$.

Here, the argument stands apart from the bond percolation case because the process $(F_n)_{n\geq 0}$ is slightly different from that of Section 6.4.1 in the sense that it can stay at value zero for consecutive steps with positive probability (see the previous remark). However, if we introduce for $n \geq 0$ the quantity $\chi_n := \#\{k \geq 0 : \sigma_k^{(0)} \leq n\}$, then the convergence (6.27) yield with the same proof as in Lemma 6.4.6 that

$$\frac{\chi_n}{n^{1/3+\alpha}} \xrightarrow[n\to+\infty]{\mathbf{P}} 0.$$

Indeed, for every $k \geq 0$, the random interval $\sigma_{k+1}^{(0)} - \sigma_k^{(1)}$ is still stochastically dominating the entrance time into $\mathbb{Z}_-$ of a random walk started at 1, with steps distributed as $\hat{X}$.

Moreover, thanks to the strong Markov property, the random variables $(\sigma_k^{(1)} - \sigma_k^{(0)})_{k\geq 0}$ are i.i.d. with geometric law of parameter $\theta \in (0, 1)$, where θ is the probability that the vertex-peeling process expose a positive number of vertices (for instance bounded from below by $\mathbf{P}(\mathcal{E} > 1 \mid \mathcal{R}_r > 0) > 0$). Then, for every $n \geq 0$, we have by construction

$$\xi_n \leq \sum_{k=0}^{\chi_n - 1} (\sigma_k^{(1)} - \sigma_k^{(0)}),$$

and we get the expected convergence (6.29) using the very same identity as in (6.13), combined with the law of large numbers. This concludes the proof of Proposition 6.4.15.

Stopped peeling process and asymptotics. Let us now focus on the situation when $(B_n)_{n\geq 0}$ reaches $\mathbb{Z}_-$. Two cases are likely to happen.

Case 1: $|B_T| < \lfloor \lambda b \rfloor$. In this situation, only a part of the white segment of size $\lfloor \lambda b \rfloor$ on the boundary of the initial map is swallowed by the peeling process, see Figure 6.20 for an illustration.

It is easy to see that for any possible configuration of the last revealed face, $|B_T| < \lfloor \lambda b \rfloor$ implies that the percolation cluster of the finite black segment is confined in a finite region of the space, disconnected from the infinite one. Thus, the crossing event does not occur: $\mathbf{P}(\mathsf{C}^{\square}(\lambda a, \lambda b) \mid |B_T| < \lfloor \lambda b \rfloor) = 0$.

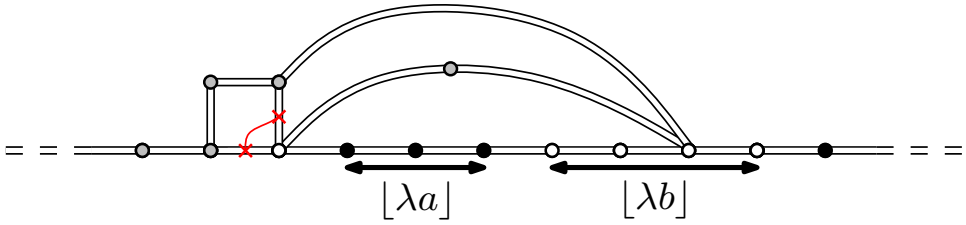

Figure 6.20: A possible configuration when $|B_T| < \lfloor \lambda b \rfloor$.

Case 2: $|B_T| > \lfloor \lambda b \rfloor$. In this situation, the whole white segment of size $\lfloor \lambda b \rfloor$ lying on the boundary of the initial map is swallowed by the peeling process, see Figure 6.21 for an illustration.

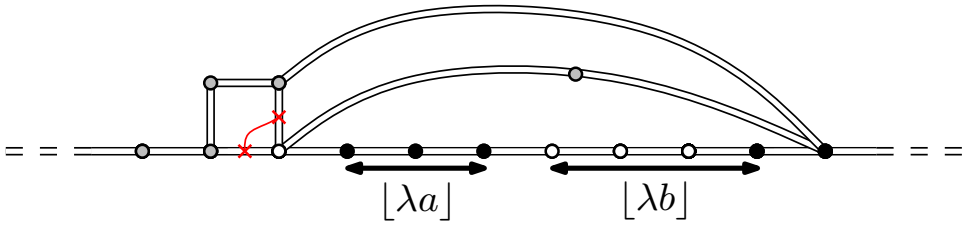

Figure 6.21: The situation when $|B_T| > \lfloor \lambda b \rfloor$.

First, we can treat the cases where four vertices of the last revealed face are lying on the boundary at the right of the origin vertex (the equivalent of the event $\mathsf{A}_4^{\square}$ of Section 6.4.1) exactly as before, and we get that the crossing event $\mathsf{C}^{\square}(\lambda a, \lambda b)$ is implied by the crossing event between the open segments on the boundary in a Boltzmann map with the boundary condition of Figure 6.22.

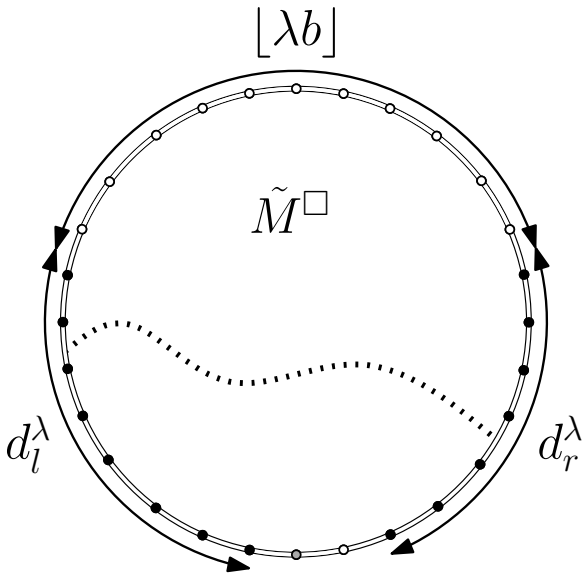

Figure 6.22: The event C_{λ}^{2}.

Again, the segment on the boundary may have size 1 or 2, but we suppose that it is made of a single white vertex which is the origin of the map v^* for the sake

of clarity (the extension being straightforward). We still denote by C^2_λ this crossing event. Recall that this map has law $\mathbb{W}^{\square}_{v(\lambda)}$, where $v(\lambda)$ is the number of vertices on its boundary.

For every $x \geq 0$, let $\partial_x^{(l)}$ and $\partial_x^{(r)}$ be the sets of x vertices of the boundary of the map located immediately on the left and on the right of v^*. Finally, we can prove the same way as for bond percolation that the lengths d_l^λ, d_r^λ of the finite black segments satisfy

$$d^\lambda := \min(d_l^\lambda, d_r^\lambda) \xrightarrow[\lambda\to+\infty]{\mathbf{P}} +\infty. \tag{6.30}$$

The main problem is now to prove that the event C^2_λ occurs almost surely asymptotically. The proof is here very different from the bond percolation case, because we have no information on the dual percolation model. (More precisely, the analogue of the dual graph for site percolation should be the so-called *matching graph*, which is in general non-planar.)

Proposition 6.4.16. *Conditionally on $|B_T| > \lfloor \lambda b \rfloor$, we have*

$$\mathbf{P}\left(\mathsf{C}^2_\lambda\right) \underset{\lambda\to+\infty}{\longrightarrow} 1.$$

As a consequence, $\mathbf{P}(\mathsf{C}^*(\lambda a, \lambda b) \mid |B_T| > \lfloor \lambda b \rfloor) \underset{\lambda\to+\infty}{\longrightarrow} 1.$

Proof. Recall the definition of the sequence of events $(\mathsf{V}_x)_{x\geq 0}$, where for every $x \geq 0$, V_x is the event that an open path links a vertex of $\partial_x^{(l)}$ to a vertex of $\partial_x^{(r)}$, without using vertices of the boundary of the map. Then, we have

$$\mathbf{P}\left(\mathsf{C}^2_\lambda\right) \geq \mathbf{P}\left(\mathsf{C}^2_\lambda, d^\lambda > x\right) \geq \mathbf{P}\left(\mathsf{V}_x, d^\lambda > x\right) \geq \mathbf{P}\left(\mathsf{V}_x\right) - \mathbf{P}\left(d^\lambda \leq x\right).$$

Again, the quantity $\mathbf{P}\left(\mathsf{V}_x\right)$ still depends on λ through the law of the map we consider, whose boundary has size $v(\lambda)$. We use the same restriction of the events $(\mathsf{V}_x)_{x\geq 0}$ to the ball of radius R of the map as in Proposition 6.4.11, and with the same arguments, including the convergence (6.30), we get

$$\liminf_{\lambda\to+\infty} \mathbf{P}\left(\mathsf{C}^2_\lambda\right) \geq \widehat{\mathbb{P}}^*_{\infty,\infty}\left(\mathsf{V}_x\right).$$

Since the sequence of events $(\mathsf{V}_x)_{x\geq 0}$ is increasing,

$$\liminf_{\lambda\to+\infty} \mathbf{P}\left(\mathsf{C}^2_\lambda\right) \geq \widehat{\mathbb{P}}^*_{\infty,\infty}\left(\mathsf{V}\right).$$

Here, the limiting event

$$\mathsf{V} := \bigcup_{x\geq 0} \mathsf{V}_x$$

is the event that there exists a crossing between the left and right boundaries in the UIHPQ with a closed origin vertex. With the current definitions, this crossing cannot use vertices of the boundary. However, if it was the case, we could extract from the crossing a subpath which do not intersect the boundary. In other words, we can focus on the crossing event between the two infinite black segments in a UIHPQ with a totally open boundary condition, excluding the origin which is closed.

It is easy to see, using the standard coupling argument, that the event V has probability bounded from below by the probability that there exists a crossing between the left and right boundaries in the UIHPQ with closed origin, an infinite free segment on the left and an infinite black segment on the right, as in Figure 6.23.

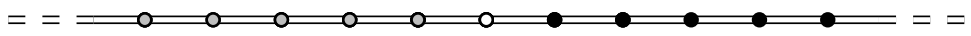

Figure 6.23: The colouring of the boundary for the coupling argument.

The idea is now to use the same peeling process as in Section 6.3, *with reversed colours*. It is defined as follows.

Reveal the colour of the rightmost free vertex on the boundary.

- If it is white, repeat the algorithm.
- If it is black, mark this vertex and execute the vertex-peeling process. Then, repeat the algorithm on the unique infinite connected component of the map deprived of the faces revealed by the vertex-peeling process.

The algorithm ends when the initial finite white segment (here a single vertex) has been swallowed.

We can check that the pattern of the boundary is preserved and that the steps of this process are i.i.d. exactly as before. For every $n \geq 0$, let W_n be the length of the finite white segment at step n of the exploration. Since $1 - p_{c,\text{site}}^{\square} < p_{c,\text{site}}^{\square}$, the percolation model is subcritical for closed vertices and we have that the stopping time $T' := \inf\{n \geq 0 : W_n = 0\}$ is almost surely finite, using the arguments of Section 6.3. Then, two cases may occur at time T':

- There is an explicit black crossing (which occurs with positive probability), see Figure 6.24.

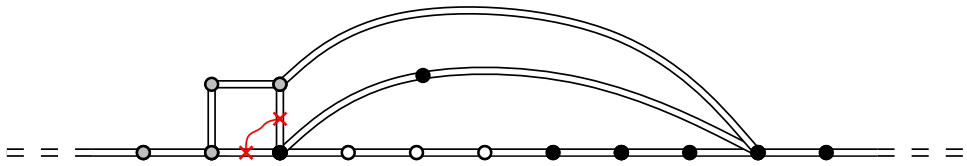

Figure 6.24: A black crossing occurs.

- There is no black crossing, see Figure 6.25.

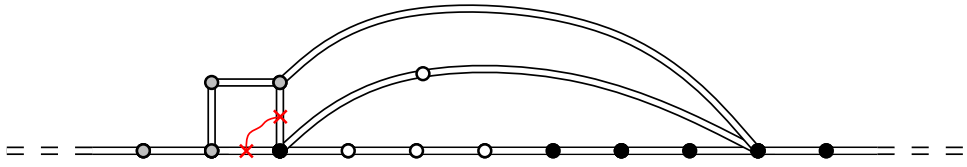

Figure 6.25: No black crossing occurs.

Let us focus on the case where there is no crossing. The total number F of (free) vertices discovered by the peeling process up to time T' is almost surely finite (because T' also is), so that the probability of the crossing event we are interested in is now bounded from below by the probability of the same event in a planar map which has the law of the UIHPQ and the boundary condition of Figure 6.26. Note that even though the F vertices discovered by the peeling process are free, it is helpful to suppose that they are closed vertices because they do not lie on the initial boundary of the map on which we want to exhibit a crossing event - in other words, the crossing now has to occur *across* this finite closed segment.

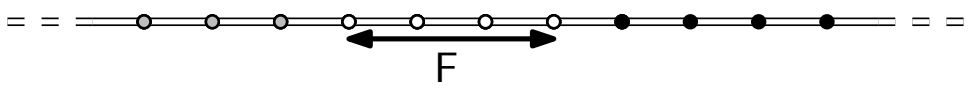

Figure 6.26: The situation when no black crossing occurred.

We now repeat the peeling process we previously introduced, with an initial white segment of size F. Since F is almost surely finite, this process ends in finite time almost surely. The point is now to observe that the probability that a black crossing occurs at time T' is bounded from below by $p_{c,\text{site}}^{\square}$, which is the probability that the free vertex between the two black vertices in the last revealed face (if any) is black. The successive executions of this process being independent, we end up with a black crossing in finite time almost surely, i.e., $\widehat{\mathbb{P}}^{*}_{\infty,\infty}(\mathsf{V}) = 1$, which ends the proof. □

Using the same arguments as in Section 6.4.1, the statements we obtained yield that

$$\mathbf{P}\left(\mathsf{C}_{\text{site}}^{\square}(\lambda a, \lambda b)\right) \underset{\lambda\to+\infty}{\longrightarrow} \frac{1}{\pi}\arccos\left(\frac{b-a}{a+b}\right),$$

which is exactly Theorem 6.1.2 in the case of site percolation on the UIHPQ, and thus ends the proof of the main result.

Acknowledgements. I deeply thank Grégory Miermont for his help, and a lot of very stimulating discussions and ideas. I am also very grateful to Nicolas Curien for his remarks that led to Theorem 6.3.9, and to the anonymous referee whose suggestions significantly improved this work.

7

The incipient infinite cluster of the uniform infinite half-planar triangulation

We introduce the Incipient Infinite Cluster (IIC) in the critical Bernoulli site percolation model on the Uniform Infinite Half-Planar Triangulation (UIHPT), which is the local limit of large random triangulations with a boundary. The IIC is defined from the UIHPT by conditioning the open percolation cluster of the origin to be infinite. We prove that the IIC can be obtained by adding within the UIHPT an infinite triangulation with a boundary whose distribution is explicit.

This Chapter is adapted from the work [4] (preprint). It contains the proof of Theorems 14 and 15.

Contents

7.1 Introduction

The purpose of this work is to describe the geometry of a large critical percolation cluster in the (type 2) Uniform Infinite Half-Planar Triangulation (UIHPT for short), which is the *local limit* of random triangulations with a boundary, upon letting first the volume and then the perimeter tend to infinity. Roughly speaking, rooted planar graphs, or maps, are close in the local sense if they have the same ball of a large radius around the root. The study of local limits of large planar maps goes back to Angel & Schramm, who introduced in [AS03] the Uniform Infinite Planar Triangulation (UIPT), while the half-plane model was defined later on by Angel in [Ang04]. Given a planar map, the Bernoulli site percolation model consists in declaring independently every site open with probability p and closed otherwise.

Local limits of large planar maps equipped with a percolation model have been studied extensively. Critical thresholds and critical exponents were provided for the UIPT [Ang03, GMSS17] and the UIHPT [Ang04, AC15] as well as for their quadrangular equivalents ([MN14, AC15], Chapter 6). The central idea of these papers is a Markovian exploration of the maps introduced by Angel and called the *peeling process*, which turns out to be much simpler in half-plane models. In this setting, the scaling limits of crossing probabilities ([Ang04], Chapter 6) can also be derived.

A natural goal in percolation theory is the description of the geometry of percolation clusters at criticality. In the UIPT, such a description has been achieved by Curien & Kortchemski in [CK14a]. They identified the *scaling limit* of the boundary of a critical percolation cluster conditioned to be large as a random *stable looptree* with parameter $3/2$, previously introduced in [CK14b]. Here, our aim is to understand not only the local limit of a percolation cluster conditioned to be large, but also the local limit of the whole UIHPT under this conditioning. This is inspired by the work of Kesten [Kes86a] in the two-dimensional square lattice.

Precisely, we consider a random map distributed as the UIHPT, equipped with a site percolation model with parameter $p \in [0,1]$, and denote the resulting probability measure by $\mathbf{P}_p$ (details are postponed to Section 7.2). Angel proved in [Ang04] that the critical threshold p_c equals $1/2$, and that there is no infinite connected component at the critical point almost surely. We also work conditionally on a "White-Black-White" boundary condition, meaning that all the vertices on the infinite simple boundary of the map are closed, except the origin which is open. We denote by $\mathcal{C}$ the open cluster of the origin, and by $|\mathcal{C}|$ its number of vertices or *volume*. The exploration of the percolation interface between the origin and its left neighbour on the boundary reveals an open path in the UIHPT. The maximal length of the *loop-erasure* of this path throughout the exploration is interpreted as the *height* $h(\mathcal{C})$ of the cluster $\mathcal{C}$. Theorem 7.2.5 states the existence of a probability measure $\mathbf{P}_{\text{IIC}}$ such that

$$\mathbf{P}_p(\cdot \mid |\mathcal{C}| = \infty) \underset{p \downarrow p_c}{\Longrightarrow} \mathbf{P}_{\text{IIC}} \quad \text{and} \quad \mathbf{P}_{p_c}(\cdot \mid h(\mathcal{C}) \geq n) \underset{n \to \infty}{\Longrightarrow} \mathbf{P}_{\text{IIC}}$$

in the sense of weak convergence, for the local topology. The probability measure $\mathbf{P}_{\text{IIC}}$ is called (the law of) the Incipient Infinite Cluster of the UIHPT (IIC for short)

and is supported on triangulations of the half-plane. As in [Kes86a], the limit is universal in the sense that it arises under at least two distinct and natural ways of conditioning $\mathcal{C}$ to be large.

The proof of Theorem 7.2.5 unveils a decomposition of the IIC into independent sub-maps with an explicit distribution. We first consider the percolation clusters of the origin and its neighbours on the boundary. By filling in their finite holes, we obtain the associated percolation *hulls*. The boundaries of the percolation hulls are random infinite *looptrees*, that is, a collection of cycles glued along a tree structure introduced in [CK14b]. The percolation hulls are rebuilt from their boundaries by filling in the cycles with independent *Boltzmann triangulations* with a simple boundary. Finally, the IIC is recovered by gluing the percolation hulls along *uniform infinite necklaces*, which are random triangulations of a semi-infinite strip first introduced in [BBG12c].

In Theorem 7.2.3, we decompose the UIHPT into two infinite sub-maps distributed as the closed percolation hulls of the IIC, and glued along a uniform necklace. The idea of such a decomposition goes back to [DMS14]. Together with Theorem 7.2.5, this describes how the geometry of the UIHPT is altered by the conditioning to have an infinite open percolation cluster. The IIC is obtained by cutting the UIHPT along the uniform necklace, and gluing inside, *ex-nihilo*, the infinite open percolation hull.

7.2 Definitions and results

Notation. In the following, we use the notation

$$\mathbb{N} := \{1, 2, \ldots\}, \quad \mathbb{Z}_+ := \mathbb{N} \cup \{0\}, \quad \mathbb{Z}_- := \{0, -1, \ldots\} \quad \text{and} \quad \mathbb{Z}^* := \mathbb{Z} \backslash \{0\}.$$

7.2.1 Random planar maps and percolation

Maps. A planar map is the proper embedding of a finite connected graph in the two-dimensional sphere, up to orientation-preserving homeomorphisms. For technical reasons, the planar maps we consider are always *rooted*, meaning that an oriented edge called the *root* is distinguished. The *origin* is the tail vertex of the root. The faces of a planar map are the connected components of the complement of the embedding of the edges. The degree of a face is the number of its incident oriented edges (with the convention that the face incident to an oriented edge lies on its left). The face incident to the right of the root edge is called the *root face*, and the other faces are called *internal*. The set of all planar maps is denoted by $\mathcal{M}_f$, and a generic element of $\mathcal{M}_f$ is usually denoted by $\mathbf{m}$.

In the next part, we will consider planar maps *with a boundary*. This means that the embedding of the edges and vertices of the root face is interpreted as the boundary $\partial\mathbf{m}$ of $\mathbf{m}$. When the edges of the root face form a cycle without self-intersection, the planar map is said to have a *simple boundary*. The degree of the root face is then the *perimeter* of the map. Any vertex that does not belong to the root face

is an *inner* vertex. The set of planar maps with a boundary of perimeter k is denoted by $\mathcal{M}_f^{(k)}$ (resp. $\widehat{\mathcal{M}}_f^{(k)}$ if additionally the boundary is simple).

In this paper, we deal with *triangulations*, which are planar maps whose faces all have degree three. We will also consider *triangulations with a boundary*, in which all the faces are triangles except possibly the root face. We make the technical assumption that triangulations are 2-connected (or type 2), meaning that multiple edges are allowed but self-loops are not.

Local topology. The *local topology* on $\mathcal{M}_f$ is induced by the distance d_{loc} defined by

$$d_{\mathrm{loc}}(\mathbf{m},\mathbf{m}') := (1+\sup\{R\geq 0 : \mathbf{B}_R(\mathbf{m})=\mathbf{B}_R(\mathbf{m}')\})^{-1}, \quad \mathbf{m},\mathbf{m}'\in\mathcal{M}_f.$$

Here, $\mathbf{B}_R(\mathbf{m})$ is the ball of radius R in $\mathbf{m}$ for the graph distance, centered at the origin vertex. Precisely, $\mathbf{B}_0(\mathbf{m})$ is the origin of the map, and for every $R>0$, $\mathbf{B}_R(\mathbf{m})$ contains vertices at graph distance less than R from the origin, and all the edges whose endpoints are in this set.

Equipped with the distance d_{loc}, $\mathcal{M}_f$ is a metric space whose completion is denoted by $\mathcal{M}$. The elements of $\mathcal{M}_\infty := \mathcal{M}\backslash\mathcal{M}_f$ are called infinite planar maps, and are represented by a coherent sequence of balls of radius R, for $R\geq 0$. Nevertheless, an infinite planar map with one end (as a graph) can always be seen as the equivalence class (up to orientation preserving homeomorphisms of the plane) of proper embeddings of an infinite graph in the plane $\mathbb{R}^2$ such that every compact of $\mathbb{R}^2$ intersects finitely many edges (see [Cur16a, Proposition 2]). In the next part, we restrict our attention to infinite planar maps that are one-ended (or have a canonical embedding in the plane), so that we may always view an element of $\mathcal{M}_\infty$ as such an equivalence class. Then, the boundary of an infinite planar map is the embedding of edges and vertices of its root face. When the root face is infinite, its vertices and edges on the left (resp. right) of the origin form the left (resp. right) boundary of the map, and the boundary is called simple if it is isomorphic to $\mathbb{Z}$. An infinite planar map whose faces are all triangles (except the root face) is called an infinite triangulation (with a boundary).

The uniform infinite half-planar triangulation. The study of the convergence of random planar triangulations in the local topology goes back to Angel and Schramm [AS03, Theorem 1.8], whose result states as follows. For $n\in\mathbb{N}$, let $\mathbb{P}_n^\triangle$ be the uniform measure on the set of rooted triangulations of the sphere with n vertices. Then, in the sense of weak convergence for the local topology,

$$\mathbb{P}_n^\triangle \underset{n\to\infty}{\Longrightarrow} \mathbb{P}_\infty^\triangle.$$

The probability measure $\mathbb{P}_\infty^\triangle$ is called (the law of) the Uniform Infinite Planar Triangulation (UIPT) and is supported on infinite triangulations of the plane (i.e., infinite one-ended triangulations). An analogous result has been proved in the quadrangular case by Krikun in [Kri05]. In this setting, there exists an alternative construction using bijective techniques for which we refer to [CD06, Mé10, CMM13].

Later on, Angel introduced in [Ang04] a model of infinite triangulation with an infinite boundary that has nicer properties. For $n\geq 0$ and $k\geq 2$, let $\widehat{\mathcal{M}}_{n,k}^\triangle$ be the

set of rooted triangulations of the k-gon (i.e., with a simple boundary of perimeter k) having n inner vertices. Let $\widehat{\mathbb{P}}^{\triangle}_{n,k}$ be the uniform probability measure on $\widehat{\mathcal{M}}^{\triangle}_{n,k}$. Then, first by [AS03, Theorem 5.1] and then by [Ang04, Theorem 2.1], in the sense of weak convergence for the local topology,

$$\widehat{\mathbb{P}}^{\triangle}_{n,k} \underset{n\to\infty}{\Longrightarrow} \widehat{\mathbb{P}}^{\triangle}_{\infty,k} \quad \text{and} \quad \widehat{\mathbb{P}}^{\triangle}_{\infty,k} \underset{k\to\infty}{\Longrightarrow} \widehat{\mathbb{P}}^{\triangle}_{\infty,\infty}.$$

The probability measure $\widehat{\mathbb{P}}_{\infty,k}$ is called (the law of) the UIPT of the k-gon, while $\widehat{\mathbb{P}}_{\infty,\infty}$ is (the law of) the Uniform Infinite Half-Planar Triangulation (UIHPT). The measure $\widehat{\mathbb{P}}_{\infty,\infty}$ is supported on infinite triangulations of the upper half-plane, that is, infinite one-ended triangulations with an infinite simple boundary (such a map can be properly embedded in the upper half-plane $\mathbb{H}$, dissecting the latter into a collection of finite simply connected regions). See Figure 7.1 for an illustration. It also enjoys a re-rooting invariance property, in the sense that it is preserved under the natural shift operation for the root edge along the boundary. This result extends to the quadrangular case, for which an alternative construction is also provided in [CM15, Section 6.1].

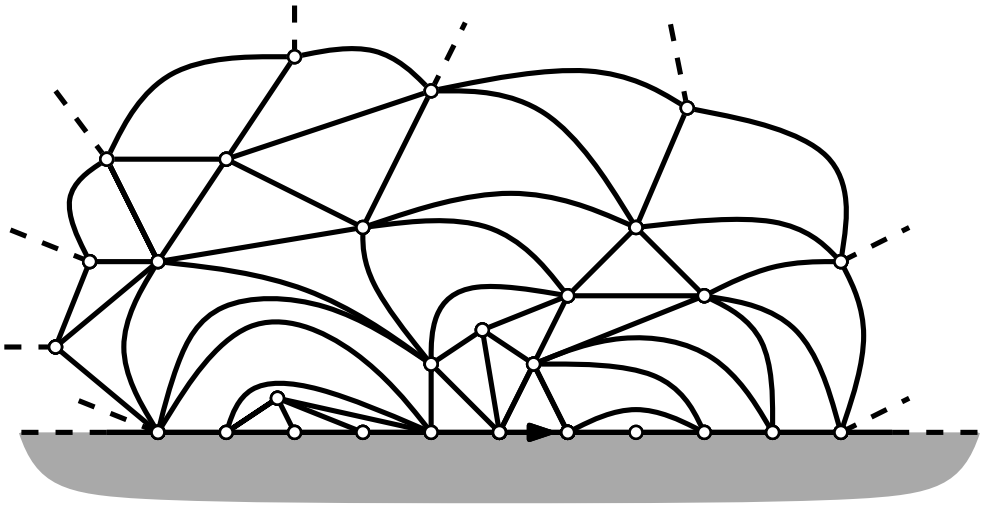

Figure 7.1: An embedding of the UIHPT in the upper half-plane.

The properties of the UIHPT are best understood using a probability measure supported on triangulations with fixed perimeter called the *Boltzmann measure* (or *free measure* in [Ang03]). Let $k \geq 2$ and introduce the *partition function*

$$W^{\triangle}_k := \sum_{n\in\mathbb{Z}_+} \#\widehat{\mathcal{M}}^{\triangle}_{n,k} \left(\frac{2}{27}\right)^n. \tag{7.1}$$

This is the generating function of triangulations with a simple boundary of perimeter k and (critical) weight $2/27$ per inner vertex. For further use, recall the asymptotics [AC15, Section 2.2]

$$W^{\triangle}_k \underset{k\to\infty}{\sim} \kappa k^{-5/2} 9^k, \quad (\kappa > 0). \tag{7.2}$$

The Boltzmann measure on the set of triangulations with a simple boundary of perimeter k is defined by

$$\mathbb{W}_k^{\triangle}(\mathbf{m}) := \frac{1}{W_k^{\triangle}} \left(\frac{2}{27}\right)^n, \quad \mathbf{m} \in \widehat{\mathcal{M}}_{n,k}^{\triangle}, \quad n \in \mathbb{Z}_+. \tag{7.3}$$

This object is of particular importance because it satisfies a branching property, that we will identify on the UIHPT as the *spatial* (or *domain*) *Markov property*. The tight relations between Boltzmann triangulations and the UIHPT are no coincidence, since the latter can be obtained as a limit of the first when the perimeter goes to infinity. Precisely, [Ang04, Theorem 2.1] states that

$$\mathbb{W}_k^{\triangle} \underset{k\to\infty}{\Longrightarrow} \widehat{\mathbb{P}}_{\infty,\infty}^{\triangle}$$

in the sense of weak convergence, for the local topology.

The spatial Markov property. In this paragraph, we detail the so-called *peeling* technique introduced by Angel. The general idea is to suppose the whole map unknown and to reveal its faces one after another. To do so, consider a map M distributed as the UIHPT and the face A of M incident to the root. To *reveal* or *peel* the face A means that we suppose the whole map unknown and work conditionally on the *configuration* of this face (see the definition below). We now consider the map $M\backslash$A, obtained by removing the root edge of M (in that sense, we also say that we peel the root edge). This map has at most one cut-vertex on the boundary, which defines sub-maps that we call the (connected) components of $M\backslash$A.

The spatial Markov property has been introduced in [Ang04, Theorem 2.2] and states as follows: $M\backslash$A has a unique infinite component M' with law $\widehat{\mathbb{P}}_{\infty,\infty}^{\triangle}$, and at most one finite component $\tilde{M}$ with law $\mathbb{W}_l^{\triangle}$ (and perimeter $l \geq 2$ given by the configuration of the face A). Moreover, $\tilde{M}$ is independent of M'. This is illustrated in Figure 7.2.

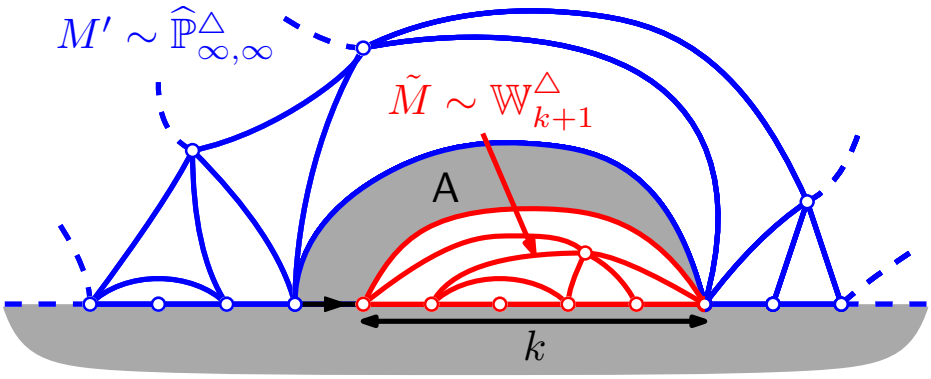

Figure 7.2: The spatial Markov property.

The peeling technique is extended to a *peeling process* by successively revealing a new face in the unique infinite component of the map deprived of the discovered face. The spatial Markov property ensures that the configuration of the revealed face

has the same distribution at each step, while the re-rooting invariance of the UIHPT allows a complete freedom on the choice of the next edge to peel on the boundary (as long as it does not depend on the unrevealed part of the map). This is the cornerstone to study percolation on uniform infinite half-planar maps, see [Ang04, AC15] and Chapter 6. Note that random half-planar triangulations satisfying the spatial Markov property and translation invariance have been classified in [AR15].

The peeling technique enlightens the crucial role played by the possible configurations for the face A incident to the root in the UIHPT and their probabilities. Let us introduce some notation. On the one hand, some edges of A, called *exposed*, belong to the boundary of the infinite component of $M\backslash$A. On the other hand, some edges of the boundary, called *swallowed*, may be enclosed in a finite component of $M\backslash$A. The number of exposed and swallowed edges are denoted by $\mathcal{E}$ and $\mathcal{R}$. We may use the notations $\mathcal{R}_l$ and $\mathcal{R}_r$ for the number of swallowed edges on the left and on the right of the root edge. The probabilities of the two possible configurations for the face incident to the root edge in the UIHPT are provided in [AC15, Section 2.3.1]:

1. The third vertex of A is an inner vertex $(\mathcal{E}=2,\mathcal{R}=0)$ with probability $q_{-1}=2/3$.

2. The third vertex of A is on the boundary of the map, $k\in\mathbb{N}$ edges on the left (or right) of the root $(\mathcal{E}=1,\mathcal{R}=k)$ with probability $q_k=W^{\triangle}_{k+1}9^{-k}$.

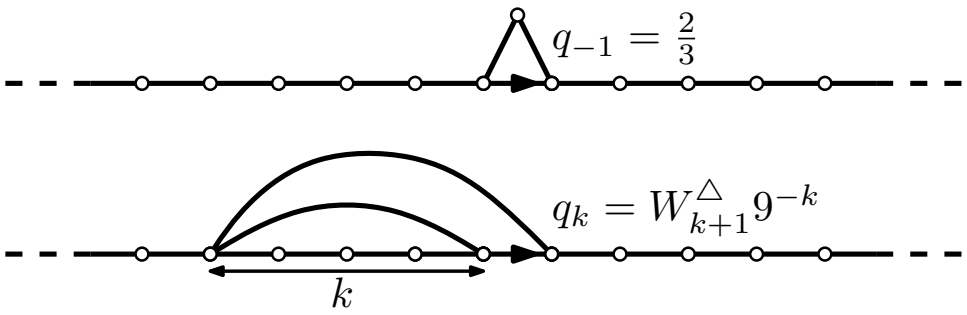

Figure 7.3: The configurations of the triangle incident to the root (up to symmetries).

Note that we have $\sum_{k\in\mathbb{N}}q_k=1/6$ and $\sum_{k\in\mathbb{N}}kq_k=1/3$. By convention, we set $q_0=0$.

Percolation. We now equip the UIHPT with a Bernoulli site percolation model, meaning that every site is open (coloured black, taking value 1) with probability p and closed (coloured white, taking value 0) otherwise, independently of every other site. This colouring convention is identical to that of [Ang03], but opposed to that of [AC15]. Let us define the probability measure $\mathbf{P}_p$ induced by this model. For a given map $\mathbf{m}\in\mathcal{M}$, we define a measure on the set of colourings of $\mathbf{m}$ by

$$\mathcal{P}_p^{V(\mathbf{m})}:=(p\delta_1+(1-p)\delta_0)^{\otimes V(\mathbf{m})},$$

where $V(\mathbf{m})$ is the set of vertices of $\mathbf{m}$. Then, $\mathbf{P}_p$ is the measure on the set of coloured (or percolated) maps $\{(\mathbf{m}, \mathrm{c}) : \mathbf{m} \in \mathcal{M}, \mathrm{c} \in \{0,1\}^{V(\mathbf{m})}\}$ defined by

$$\mathbf{P}_p(\mathrm{d}\mathbf{m}\mathrm{dc}) := \widehat{\mathbb{P}}^{\triangle}_{\infty,\infty}(\mathrm{d}\mathbf{m})\mathcal{P}_p^{V(\mathbf{m})}(\mathrm{dc}).$$

In other words, the map has the law of the UIHPT and conditionally on it, the colouring is a Bernoulli percolation with parameter p. We emphasize that this probability measure is annealed, so that conditioning on events depending only on the colouring may still affect the geometry of the underlying random lattice. We implicitly extend the definition of the local topology to coloured maps. In what follows, we will work conditionally on the colouring of the boundary of the map, which we call the *boundary condition*.

The open *percolation cluster* of a vertex v of the map is the set of open vertices connected to v by an open path, together with the edges connecting them (and similarly for closed clusters). If $\mathcal{C}$ is the open percolation cluster of the origin and $|\mathcal{C}|$ its number of vertices, the percolation probability is

$$\Theta(p) := \mathbf{P}_p(|\mathcal{C}| = \infty), \quad p \in [0,1].$$

A coupling argument shows that Θ is nondecreasing, so that there exists a critical point p_c, called the percolation threshold, such that $\Theta(p) > 0$ if $p > p_c$ and $\Theta(p) = 0$ if $p < p_c$. Under the natural boundary condition that all the vertices of the boundary are closed except the origin vertex which is open, Angel proved in [Ang04] (see also [AC15, Theorem 5]) that

$$p_c = \frac{1}{2}.$$

We will regularly work at criticality and use the notation $\mathbf{P}$ instead of $\mathbf{P}_{p_c}$. We slightly abuse notation here and use $\mathbf{P}$ for several boundary conditions. For every $k \geq 2$, we also denote by $\mathbf{W}_k^{\triangle}$ the measure induced by the Bernoulli site percolation model with parameter $1/2$ on a Boltzmann triangulation with distribution $\mathbb{W}_k^{\triangle}$ (and a boundary condition to be defined).

We end with some definition. Let $\mathcal{C}$ be a percolation cluster of a vertex v of the boundary in the UIHPT. The *hull* $\mathcal{H}$ of $\mathcal{C}$ is the coloured planar map obtained by filling in the finite holes of $\mathcal{C}$. In other words, $\mathcal{H}$ is the union of $\mathcal{C}$ and the finite connected components of its complement in the whole map, see Figure 7.4 for an example. This defines a (possibly infinite) planar map, which we root at the rightmost edge of $\mathcal{H}$ whose origin is v.

7.2.2 Random trees and looptrees

Plane trees. We use the formalism of [Nev86]. A finite plane tree $\mathfrak{t}$ as a finite subset of the set of finite sequences of positive integers

$$\mathcal{U} := \bigcup_{n=0}^{\infty} \mathbb{N}^n$$

satisfying the following properties.

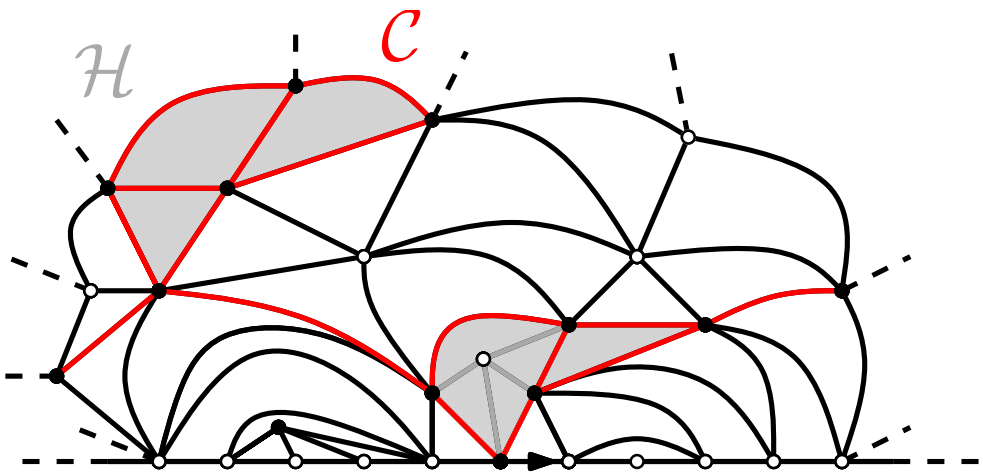

Figure 7.4: The percolation cluster of the origin and its hull.

First, the empty word $\emptyset$ is an element of $\mathbf{t}$ ($\emptyset$ is the root of $\mathbf{t}$). Next, for every $n \in \mathbb{N}$, if $v = (v_1, \dots, v_n) \in \mathbf{t}$, then $(v_1, \dots v_{n-1}) \in \mathbf{t}$ ($(v_1, \dots v_{n-1})$ is the parent of v in $\mathbf{t}$). Finally, for every $v = (v_1, \dots, v_n) \in \mathbf{t}$, there exists $k_v(\mathbf{t}) \in \mathbb{Z}_+$ such that $(v_1, \dots, v_n, j) \in \mathbf{t}$ iff $1 \leq j \leq k_v(\mathbf{t})$ ($k_v(\mathbf{t})$ is the number of children of v in $\mathbf{t}$).

For every $v = (v_1, \dots, v_n) \in \mathbf{t}$, $|v| = n$ is the height of v in $\mathbf{t}$. Vertices of $\mathbf{t}$ at even height are called white, and those at odd height are called black. We let $\mathbf{t}_\circ$ and $\mathbf{t}_\bullet$ denote the corresponding sets of vertices. The set of finite plane trees is denoted by $\mathcal{T}_f$.

We will also deal with the set $\mathcal{T}_{\text{loc}}$ of *locally finite* plane trees which is the completion of $\mathcal{T}_f$ with respect to the local topology. Equivalently, the set $\mathcal{T}_{\text{loc}}$ is obtained by extending the definition of $\mathcal{T}_f$ to infinite trees whose vertices have finite degree ($k_v(\mathbf{t}) < \infty$ for every $v \in \mathbf{t}$). A *spine* in a tree $\mathbf{t}$ is an infinite sequence $\{s_k : k \in \mathbb{Z}_+\}$ of vertices of $\mathbf{t}$ such that $s_0 = \emptyset$ and for every $k \in \mathbb{Z}_+$, s_k is the parent of s_{k+1}.

Looptrees. Looptrees have been introduced in [CK14b, CK14a] in order to study the boundary of percolation hulls in the UIPT. Here, we closely follow the presentation of [CK14a]. Let us start with a formal definition. A (finite) *looptree* is a finite planar map whose edges are incident to two distinct faces, one of them being the root face (such a map is also called *edge-outerplanar*). The set of finite looptrees is denoted by $\mathcal{L}_f$. Informally, a looptree is a collection of simple cycles glued along a tree structure. Consistently, there is a way to construct looptrees from trees and conversely, that we now describe.

To every plane tree $\mathbf{t} \in \mathcal{T}_f$ we associate a looptree $\mathbf{l} := \text{Loop}(\mathbf{t})$ as follows. Vertices of $\mathbf{l}$ are vertices of $\mathbf{t}_\circ$, and around each vertex $u \in \mathbf{t}_\bullet$, we connect the incident (white) vertices with edges in cyclic order. The looptree $\mathbf{l}$ is the planar map obtained by discarding the edges of $\mathbf{t}$ and its black vertices. The root edge of $\mathbf{l}$ connects the origin of $\mathbf{t}$ to the last child of its first offspring in $\mathbf{t}$. The inverse mapping associates to a looptree $\mathbf{l} \in \mathcal{L}_f$ the plane tree $\mathbf{t} := \text{Tree}(\mathbf{l})$ called the *tree of components* in [CK14a]. It is obtained by first adding an extra vertex into each inner face (or *loop*) of $\mathbf{l}$, and then connecting this vertex by an edge to all the vertices of the corresponding face (the

edges of $\mathbf{l}$ are discarded). The plane tree $\mathbf{t}$ is rooted at the oriented edge between the origin of $\mathbf{l}$ and the vertex lying inside the face on the left of the root edge. Our definition of looptree as well as the mappings Tree and Loop slightly differ from [CK14b, CK14a]. In particular, we allow several loops to be glued at the same vertex. See Figure 7.5 for an illustration.

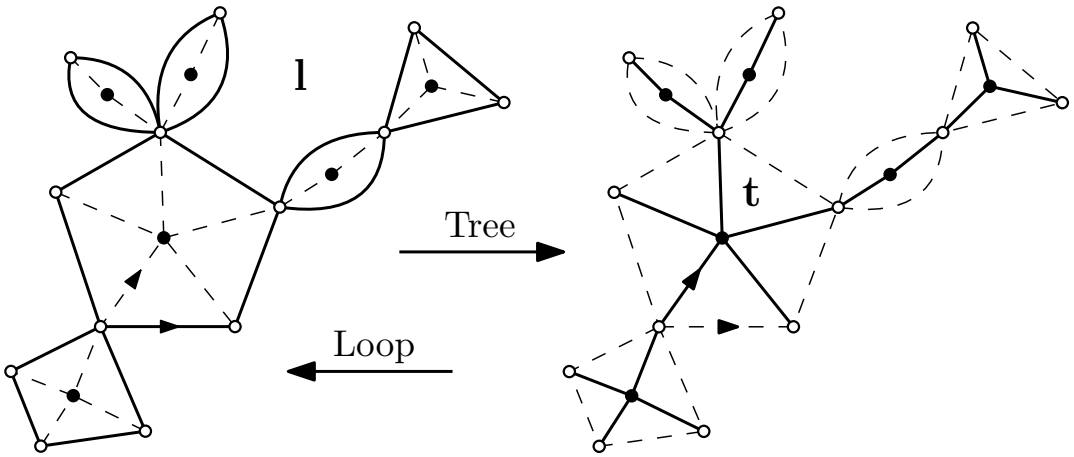

Figure 7.5: The mappings Tree and Loop.

We now extend our definition to infinite looptrees. Formally, an infinite looptree is an infinite edge-outerplanar map whose root face is the unique infinite face (it is thus one-ended). The set of finite and infinite looptrees is denoted by $\mathcal{L}$. The application Loop extends to any locally finite plane tree $\mathbf{t} \in \mathcal{T}_{\text{loc}}$ by using the consistent sequence of planar maps $\{\text{Loop}(\mathbf{B}_{2R}(\mathbf{t})) : R \in \mathbb{Z}_+\}$. When $\mathbf{t}$ is infinite and one-ended (i.e., with a unique spine), $\text{Loop}(\mathbf{t})$ is an infinite looptree. The inverse mapping Tree also extends to any infinite looptree $\mathbf{l} \in \mathcal{L}$ by using the consistent sequence of planar maps $\{\text{Tree}(\mathbf{B}'_R(\mathbf{l})) : R \in \mathbb{Z}_+\}$, where $\mathbf{B}'_R(\mathbf{l})$ is the finite looptree made of all the internal faces of $\mathbf{l}$ having a vertex at distance less than R from the origin. Note that the mappings Tree and Loop are both continuous with respect to the local topology.

Remark 7.2.1. Every internal face of a looptree $\mathbf{l}$ inherits a rooting from the branching structure. Namely, the root of a loop is the edge whose origin is the closest to the origin of $\mathbf{l}$, and such that the external face lies on its right. As a consequence, for every loop l of perimeter k in $\mathbf{l}$ and every map with a simple boundary of perimeter k, the gluing of $\mathbf{m}$ in the loop l is the operation which consists in identifying the boundary of $\mathbf{m}$ with the edges of l (with the convention that the root edges are identified).

Let us make use of these definitions to describe the branching structure of planar maps with a boundary. Let $\mathbf{m} \in \mathcal{M}$ be a map with a boundary. By splitting $\mathbf{m}$ at the cut-vertices (or pinch-points) of its boundary, we obtain a collection of connected components that are maps with a simple boundary, called the *irreducible components* of $\mathbf{m}$ in [BG09], see also [CM15, Section 2.2]. The irreducible components are rooted at the oriented edge whose origin is the closest to that of $\mathbf{m}$, and such that the root face of $\mathbf{m}$ lies on its right. We also define the so-called *scooped-out map*

$\mathrm{Scoop}(\mathbf{m})$, which is the (possibly infinite) planar map obtained from the boundary of $\mathbf{m}$ by duplicating the edges whose sides both belong to the root face.

Let us assume that the map $\mathbf{m} \in \mathcal{M}$ has no infinite irreducible component. Then, $\mathrm{Scoop}(\mathbf{m})$ is a looptree and we call *tree of components* of $\mathbf{m}$ the locally finite plane tree $\mathbf{Tree}(\mathbf{m}) := \mathrm{Tree}(\mathrm{Scoop}(\mathbf{m}))$ (see Figure 7.6 for an example). By construction, to every vertex v at odd height in $\mathbf{Tree}(\mathbf{m})$ with degree $k \geq 2$ corresponds an internal face of $\mathrm{Scoop}(\mathbf{m})$ with the same degree. Moreover, to this face is associated a map $\mathbf{m}_v \in \widehat{\mathcal{M}}_f^{(k)}$ with a simple boundary of perimeter k, which is the irreducible component of $\mathbf{m}$ delimited by the face. Thus, $\mathbf{m}$ is recovered from $\mathrm{Scoop}(\mathbf{m})$ by gluing the map $\mathbf{m}_v$ in the associated face of $\mathrm{Scoop}(\mathbf{m})$, as explained in Remark 7.2.1. This results in an application

$$\Phi_{\mathrm{TC}} : \mathbf{m} \mapsto (\mathbf{t} = \mathbf{Tree}(\mathbf{m}), \{\mathbf{m}_v : v \in \mathbf{t}_\bullet\})$$

that associates to the planar map with a boundary $\mathbf{m} \in \mathcal{M}$ its tree of components $\mathbf{t} = \mathbf{Tree}(\mathbf{m})$ together with a collection $\{\mathbf{m}_v : v \in \mathbf{t}_\bullet\}$ of maps with a simple boundary having respective perimeter $\deg(v)$ attached to vertices at odd height of $\mathbf{t}$ (which are the irreducible components of $\mathbf{m}$). Note that the inverse mapping Φ_{TC}^{-1} that consists in filling in the loops of $\mathrm{Loop}(\mathbf{t})$ with the collection $\{\mathbf{m}_v : v \in \mathbf{t}_\bullet\}$ is continuous with respect to the natural topology.

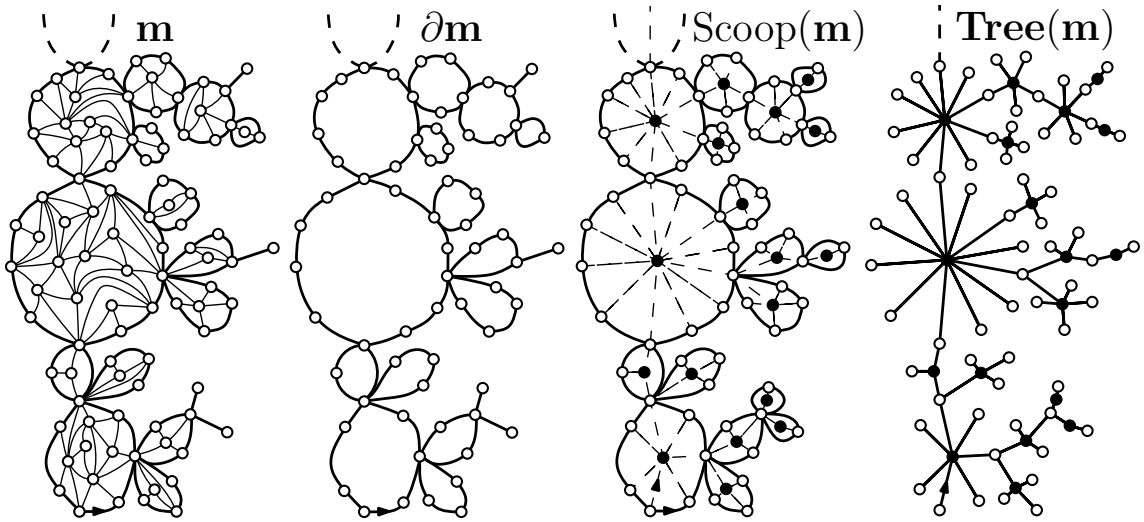

Figure 7.6: A triangulation with a boundary $\mathbf{m}$, its scooped-out map $\mathrm{Scoop}(\mathbf{m})$ and the associated tree of components $\mathbf{Tree}(\mathbf{m})$.

Remark 7.2.2. The tree of components $\mathbf{Tree}(\mathbf{m})$ is also obtained by adding a vertex into each internal face of $\mathrm{Scoop}(\mathbf{m})$, and connecting this vertex to all the vertices of the associated face (the edges of $\mathrm{Scoop}(\mathbf{m})$ are erased). Defined in this way, the mapping **Tree** extends to any planar map with a boundary $\mathbf{m} \in \mathcal{M}$. Moreover, $\mathbf{m} \in \mathcal{M}$ is still recovered from $\mathrm{Scoop}(\mathbf{m})$ by gluing its irreducible components into the internal faces of the latter, so that the mapping Φ_{TC} also extends to $\mathcal{M}$. Nonetheless, $\mathbf{Tree}(\mathbf{m})$ is not a locally finite plane tree in general, and has possibly a vertex of

infinite degree. In what follows, we only deal with maps $\mathbf{m} \in \mathcal{M}$ whose irreducible components are all finite.

Multi-type Galton-Watson trees. Let $\nu_\circ$ and $\nu_\bullet$ be probability measures on $\mathbb{Z}_+$. A random plane tree is an (alternated two-type) Galton-Watson tree with offspring distribution $(\nu_\circ, \nu_\bullet)$ if all the vertices at even (resp. odd) height have offspring distribution $\nu_\circ$ (resp. $\nu_\bullet$) all independently of each other. From now on, we assume that the pair $(\nu_\circ, \nu_\bullet)$ is critical (i.e. its mean vector $(m_{\nu_\circ}, m_{\nu_\bullet})$ satisfies $m_{\nu_\circ} m_{\nu_\bullet} = 1$). Then, the law $\mathsf{GW}_{\nu_\circ,\nu_\bullet}$ of such a tree is characterized by

$$\mathsf{GW}_{\nu_\circ,\nu_\bullet}(\mathbf{t}) = \prod_{v \in \mathbf{t}_\circ} \nu_\circ\left(k_v(\mathbf{t})\right) \prod_{v \in \mathbf{t}_\bullet} \nu_\bullet\left(k_v(\mathbf{t})\right), \quad \mathbf{t} \in \mathcal{T}_f.$$

The construction of *Kesten's tree* [Kes86b, LP16] has been generalized in [Ste16, Theorem 3.1] to multi-type Galton-Watson trees conditioned to survive as follows. Assume that the critical pair $(\nu_\circ, \nu_\bullet)$ satisfies $\mathsf{GW}_{\nu_\circ,\nu_\bullet}(\{|\mathbf{t}| = n\}) > 0$ for every $n \in \mathbb{Z}_+$. Let T_n be a plane tree with distribution $\mathsf{GW}_{\nu_\circ,\nu_\bullet}$ conditioned to have n vertices. Then, in the sense of weak convergence, for the local topology

$$T_n \xrightarrow[n\to\infty]{(d)} \mathbf{T}_\infty^{\circ,\bullet}.$$

The random infinite plane tree $\mathbf{T}_\infty^{\circ,\bullet} = \mathbf{T}_\infty^{\circ,\bullet}(\nu_\circ, \nu_\bullet)$ is a multi-type version of Kesten's tree, whose law is denoted by $\mathsf{GW}^{(\infty)}_{\nu_\circ,\nu_\bullet}$. Let us describe the alternative construction of $\mathbf{T}_\infty^{\circ,\bullet}$ as explained in [Ste16]. For every probability measure ν on $\mathbb{Z}_+$ with mean $m_\nu \in (0, \infty)$, the size-biased distribution $\bar{\nu}$ reads

$$\bar{\nu}(k) := \frac{k\nu(k)}{m_\nu}, \quad k \in \mathbb{Z}_+.$$

The tree $\mathbf{T}_\infty^{\circ,\bullet}$ has a.s. a unique spine, in which white vertices have offspring distribution $\bar{\nu}_\circ$ while black vertices have offspring distribution $\bar{\nu}_\bullet$. Each vertex of the spine has a unique child in the spine, chosen uniformly at random among the offspring. Out of the spine, white and black vertices have offspring distribution $\nu_\circ$ and $\nu_\bullet$ respectively, and the number of offspring are all independent. We will use two variants of $\mathbf{T}_\infty^{\circ,\bullet}$, which are obtained by discarding all the vertices and edges on the left (resp. right) of the spine, excluding the children of black vertices of the spine. Their distributions are denoted by $\mathsf{GW}^{(\infty,l)}_{\nu_\circ,\nu_\bullet}$ and $\mathsf{GW}^{(\infty,r)}_{\nu_\circ,\nu_\bullet}$ respectively.

For technical reasons related to forthcoming rooting conventions, all of these random infinite plane trees are implicitly re-rooted at the last outgoing edge of the root vertex (i.e., we shift the root by one edge on the left). The infinite looptree $\mathbf{L}_\infty(\nu_\circ, \nu_\bullet) := \mathrm{Loop}(\mathbf{T}_\infty^{\circ,\bullet})$ plays a special role in the following, and may be called *Kesten's looptree* with offspring distribution $(\nu_\circ, \nu_\bullet)$. It has a unique spine of finite loops (a chain of internal faces that all disconnect the root from infinity), associated to black vertices of the spine of $\mathbf{T}_\infty^{\circ,\bullet}$.

7.2.3 Statement of the results

Uniform infinite necklace. Necklaces are maps that were introduced in [BBG12c] for studying the $O(n)$ model on random maps, see also [CK14a]. Formally, an infinite necklace is a triangulation of the upper half-plane $\mathbb{H}$ with no inner vertex (and an infinite simple boundary).

Consider the graph of $\mathbb{Z}$ embedded in the plane, and rooted at the oriented edge $(0,1)$. Let $\{z_i : i \in \mathbb{N}\}$ be a sequence of independent random variables with Bernoulli distribution of parameter $1/2$, and define the simple random walk

$$S_k := \sum_{i=1}^{k} z_i, \quad k \in \mathbb{N}.$$

The uniform infinite necklace is the random rooted map obtained from $\mathbb{Z}$ by adding the set of edges $\{(-S_k, k+1-S_k) : k \in \mathbb{N}\}$ in a non-crossing manner. It is a.s. an infinite necklace in the aforementioned sense, and can also be interpreted as a gluing of triangles along their sides, with the tip oriented to the left or to the right equiprobably and independently. Its distribution is denoted by $\mathsf{UN}(\infty,\infty)$. See Figure 7.7 for an illustration.

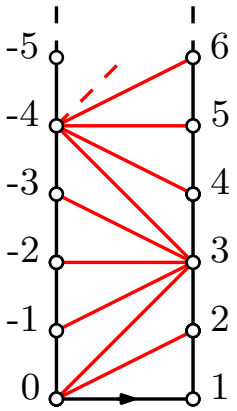

Figure 7.7: The uniform infinite necklace.

In the next part, we will perform gluing operations of planar maps with a boundary along infinite necklaces. Let $\mathbf{m}, \mathbf{m}' \in \mathcal{M}_\infty$ be maps with an infinite boundary. Let $\{e_i : i \in \mathbb{N}\}$ be the sequence of half-edges of the root face of $\mathbf{m}$ on the right of the origin vertex, listed in contour order. Similarly, the left boundary of $\mathbf{m}'$ defines the sequence of half-edges $\{e'_i : i \in \mathbb{N}\}$. Let $\mathbf{n}$ be an infinite necklace, with a boundary identified to $\mathbb{Z}$. The gluing $\Psi_{\mathbf{n}}(\mathbf{m}, \mathbf{m}')$ of $\mathbf{m}$ and $\mathbf{m}'$ along $\mathbf{n}$ is the infinite map defined as follows. For every $i \in \mathbb{N}$, we identify the half-edge $(i, i+1)$ of $\mathbf{n}$ with e'_i, and the half-edge $(-i, -i+1)$ of $\mathbf{n}$ with e_i. The root edge of $\Psi_{\mathbf{n}}(\mathbf{m}, \mathbf{m}')$ is the root edge of $\mathbf{n}$. An example is given in Figure 7.9.

Note that $\Psi_{\mathbf{n}}(\mathbf{m}, \mathbf{m}')$ is still a planar map with an infinite boundary. In particular, our construction extends to the gluing $\Psi_{(\mathbf{n},\mathbf{n}')}(\mathbf{m}, \mathbf{m}', \mathbf{m}'')$ of three maps with an infinite boundary $\mathbf{m}$, $\mathbf{m}'$ and $\mathbf{m}''$ along the pair of infinite necklaces $(\mathbf{n}, \mathbf{n}')$. To do so,

first define the map with an infinite boundary $\mathbf{m}^* := \Psi_{\mathbf{n}}(\mathbf{m}, \mathbf{m}')$, but keep the root edge of $\mathbf{m}'$ as the root edge of $\mathbf{m}^*$. Then, set $\Psi_{(\mathbf{n},\mathbf{n}')}(\mathbf{m}, \mathbf{m}', \mathbf{m}'') := \Psi_{\mathbf{n}'}(\mathbf{m}^*, \mathbf{m}'')$. See Figure 7.11 for an example. These gluing operations are continuous with respect to the local topology.

Decomposition of the UIHPT**.** We consider the UIHPT decorated with a critical percolation model, and work conditionally on the "Black-White" boundary condition of Figure 7.8. We let $\mathcal{H}_b$ and $\mathcal{H}_w$ be the hulls of the percolation clusters of the origin and the target of the root. We denote by $\mathbf{Tree}(\mathcal{H}_b)$ and $\mathbf{Tree}(\mathcal{H}_w)$ their respective tree of components, and by

$$\{M_v^b : v \in \mathbf{Tree}(\mathcal{H}_b)_\bullet\} \quad \text{and} \quad \{M_v^w : v \in \mathbf{Tree}(\mathcal{H}_w)_\bullet\}$$

their irreducible components (i.e. the second components of $\Phi_{\text{TC}}(\mathcal{H}_b)$ and $\Phi_{\text{TC}}(\mathcal{H}_w)$). The boundary conditions of the irreducible components are determined by the hull. We define the probability measures $\mu_\circ$ and $\mu_\bullet$ by

$$\mu_\circ(k) := \frac{2}{3}\left(\frac{1}{3}\right)^k \quad \text{and} \quad \mu_\bullet(k) := 6q_k, \quad k \in \mathbb{Z}_+. \tag{7.4}$$

By the properties established in Section 7.2.1, we get that the pair $(\mu_\circ, \mu_\bullet)$ is critical.

Figure 7.8: The "Black-White" boundary condition.

Theorem 7.2.3. *In the critical Bernoulli percolation model on the* UIHPT *with "Black-White" boundary condition:*

- *The trees of components* $\mathbf{Tree}(\mathcal{H}_b)$ *and* $\mathbf{Tree}(\mathcal{H}_w)$ *are independent with respective distribution* $\mathsf{GW}^{(\infty,l)}_{\mu_\circ,\mu_\bullet}$ *and* $\mathsf{GW}^{(\infty,r)}_{\mu_\circ,\mu_\bullet}$.
- *Conditionally on* $\mathbf{Tree}(\mathcal{H}_b)$ *and* $\mathbf{Tree}(\mathcal{H}_w)$*, the irreducible components* $\{M_v^b : v \in \mathbf{Tree}(\mathcal{H}_b)_\bullet\}$ *and* $\{M_v^w : v \in \mathbf{Tree}(\mathcal{H}_w)_\bullet\}$ *are independent critically percolated Boltzmann triangulations with respective distribution* $\mathbf{W}^{\triangle}_{\deg(v)}$.

Finally, the UIHPT *is recovered as the gluing* $\Psi_{\mathbf{N}}(\mathcal{H}_b, \mathcal{H}_w)$ *of* $\mathcal{H}_b$ *and* $\mathcal{H}_w$ *along a uniform infinite necklace* $\mathbf{N}$ *with distribution* $\mathsf{UN}(\infty,\infty)$ *independent of* $(\mathcal{H}_b, \mathcal{H}_w)$.

Remark 7.2.4. The result of Theorem 7.2.3 can be seen as a discrete counterpart to [DMS14, Theorem 1.16-1.17], as we will discuss in Section 7.6. It could also be stated without reference to percolation: By discarding the colouring of the vertices, we obtain a decomposition of the UIHPT into two independent looptrees filled in with Boltzmann triangulations and glued along a uniform necklace. An illustration is provided in Figure 7.9.

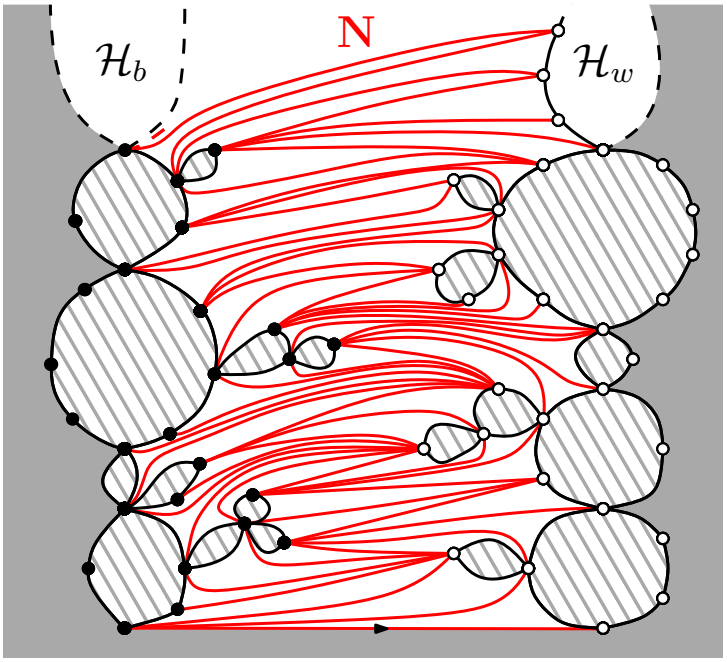

Figure 7.9: The decomposition of the UIHPT into its percolation hulls and the uniform infinite necklace. The hatched areas are filled-in with independent critically percolated Boltzmann triangulations of the given boundary length.

The incipient infinite cluster. We now consider the UIHPT decorated with a Bernoulli percolation model with parameter p conditionally on the "White-Black-White" boundary condition of Figure 7.10. In a map with such a boundary condition, we let $\mathcal{H}$, $\mathcal{H}_l$ and $\mathcal{H}_r$ be the hulls of the clusters of the origin and its left and right neighbours on the boundary. We let **Tree**$(\mathcal{H})$, **Tree**$(\mathcal{H}_l)$ and **Tree**$(\mathcal{H}_r)$ be their respective tree of components, and denote by

$$\{M_v : v \in \textbf{Tree}(\mathcal{H})_\bullet\}, \quad \{M_v^l : v \in \textbf{Tree}(\mathcal{H}_l)_\bullet\} \quad \text{and} \quad \{M_v^r : v \in \textbf{Tree}(\mathcal{H}_r)_\bullet\}$$

their irreducible components (i.e. the second components of $\Phi_{\text{TC}}(\mathcal{H})$, $\Phi_{\text{TC}}(\mathcal{H}_l)$ and $\Phi_{\text{TC}}(\mathcal{H}_r)$). Again, the boundary conditions of the components are forced by the hulls.

The *height* $h(\mathcal{C})$ of the open percolation cluster of the origin $\mathcal{C}$ will be defined in Section 7.5.1. It corresponds to the maximal length of the open segment revealed when exploring the percolation interface between the origin and its left neighbour on the boundary.

Figure 7.10: The "White-Black-White" boundary condition.

Theorem 7.2.5. *Let $\mathbf{P}_p$ be the law of the* UIHPT *equipped with a Bernoulli percolation model with parameter p and "White-Black-White" boundary condition. Then, there exists a probability measure $\mathbf{P}_{\text{IIC}}$ such that in the sense of weak convergence for the local topology,*

$$\mathbf{P}_p(\cdot \mid |\mathcal{C}| = \infty) \underset{p \downarrow p_c}{\Longrightarrow} \mathbf{P}_{\text{IIC}} \quad \textit{and} \quad \mathbf{P}_{p_c}(\cdot \mid h(\mathcal{C}) \geq n) \underset{n \to \infty}{\Longrightarrow} \mathbf{P}_{\text{IIC}}.$$

The probability measure $\mathbf{P}_{\mathsf{IIC}}$ *is called (the law of) the Incipient Infinite Cluster of the* UIHPT *or* IIC. *The* IIC *is a.s. a percolated triangulation of the half-plane with an infinite simple boundary and "White-Black-White" boundary condition. Moreover, in the* IIC*:*

- *The trees of components* $\mathbf{Tree}(\mathcal{H})$, $\mathbf{Tree}(\mathcal{H}_l)$ *and* $\mathbf{Tree}(\mathcal{H}_r)$ *are independent with respective distribution* $\mathsf{GW}^{(\infty)}_{\mu_\circ,\mu_\bullet}$, $\mathsf{GW}^{(\infty,l)}_{\mu_\circ,\mu_\bullet}$ *and* $\mathsf{GW}^{(\infty,r)}_{\mu_\circ,\mu_\bullet}$.
- *Conditionally on* $\mathbf{Tree}(\mathcal{H})$, $\mathbf{Tree}(\mathcal{H}_l)$ *and* $\mathbf{Tree}(\mathcal{H}_r)$, *the irreducible components* $\{M_v : v \in \mathbf{Tree}(\mathcal{H})_\bullet\}$, $\{M^l_v : v \in \mathbf{Tree}(\mathcal{H}_l)_\bullet\}$ *and* $\{M^r_v : v \in \mathbf{Tree}(\mathcal{H}_r)_\bullet\}$ *are independent critically percolated Boltzmann triangulations with respective distribution* $\mathbf{W}^{\triangle}_{\deg(v)}$.

Finally, the IIC *is recovered as the gluing* $\Psi_{(\mathbf{N}_l,\mathbf{N}_r)}(\mathcal{H}_l,\mathcal{H},\mathcal{H}_r)$ *of* $\mathcal{H}_l$, $\mathcal{H}$ *and* $\mathcal{H}_r$ *along an pair of independent uniform infinite necklaces* $(\mathbf{N}_l,\mathbf{N}_r)$ *with distribution* $\mathsf{UN}(\infty,\infty)$, *also independent of* $(\mathcal{H}_l,\mathcal{H},\mathcal{H}_r)$. *(The root edge of the* IIC *connects the origin of* $\mathcal{H}$ *to that of* $\mathcal{H}_r$*.)*

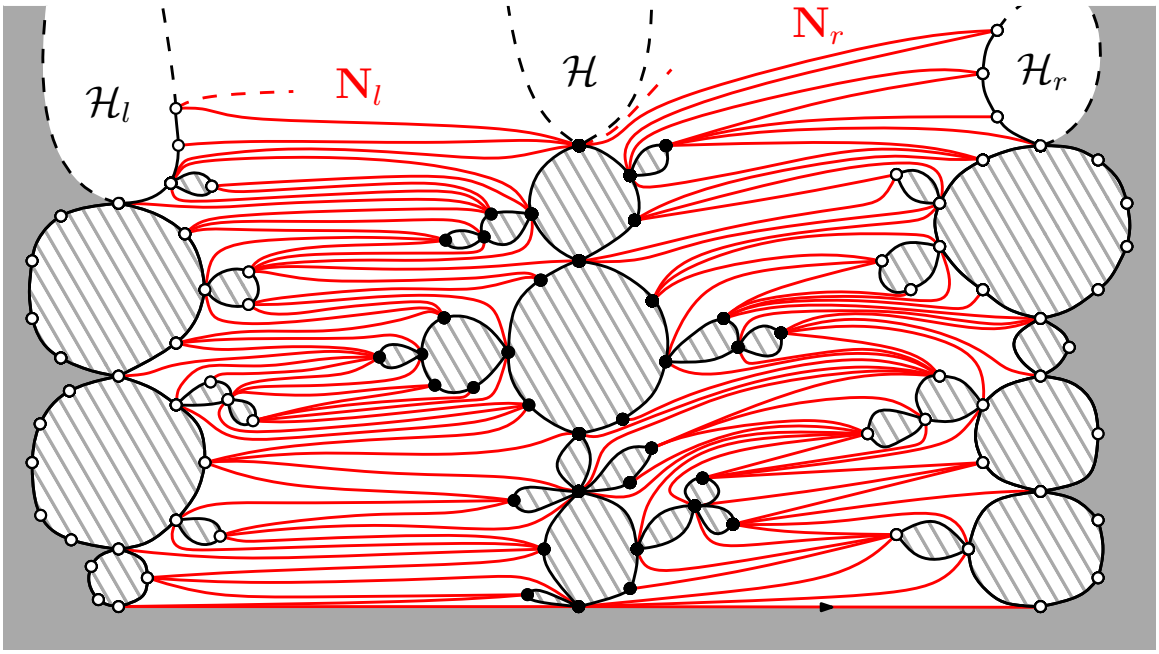

Figure 7.11: The decomposition of the IIC into its percolation hulls and the uniform necklaces. The hatched areas are filled-in with independent critically percolated Boltzmann triangulations of the given boundary length.

Remark 7.2.6. In the work of Kesten [Kes86a], the IIC is defined for bond percolation on $\mathbb{Z}^2$ by considering a supercritical open percolation cluster, and letting p decrease towards the critical point p_c. Equivalently, the IIC arises directly in the critical model when conditioning the open cluster of the origin to reach the boundary of $[-n,n]^2$, and letting n go to infinity. Theorem 7.2.5 is the analogous result for site percolation on the UIHPT; however, we use a slightly different conditioning in the critical setting, which is more adapted to the use of the peeling techniques.

Remark 7.2.7. Theorem 7.2.5 should be seen as a counterpart to Theorem 7.2.3. Indeed, the decomposition of the IIC shows that when conditioning the open cluster of the origin to be infinite, one adds ex-nihilo an infinite looptree in the UIHPT, as shown in Figure 7.11. This describes how the zero measure event we condition on twists the geometry of the initial random half-planar triangulation.

7.3 Coding of looptrees

7.3.1 The contour function

We first describe the encoding of looptrees via an analogue of the contour function for trees [Ald93, LG05]. This bears similarities with the coding of continuum random looptrees of [CK14a].

Finite looptrees. Let $n \in \mathbb{Z}_+$ and $C = \{C_k : 0 \leq k \leq n\}$ a discrete *excursion* with no positive jumps and no constant step, that is $C_0 = C_n = 0$, and for every $0 \leq k < n$, $C_k \in \mathbb{Z}_+$, $C_{k+1} - C_k \leq 1$ and $C_k \neq C_{k+1}$. The equivalence relation $\sim$ on $\{0, \dots, n\}$ is defined by

$$i \sim j \quad \text{iff} \quad C_i = C_j = \inf_{i \wedge j \leq k \leq i \vee j} C_k. \tag{7.5}$$

The quotient space $\{0, \dots, n\}/\sim$ inherits the graph structure of the chain $\{0, \dots, n\}$, and can be embedded in the plane as follows. Consider the graph of C (with linear interpolation), together with the set of edges E containing all the pairs $\{(i, C_i), (j, C_j)\}$ such that $i \sim j$. This defines a planar map $\mathbf{m}_C$, whose vertices are identified to $\{0, \dots, n\}$. The root edge of $\mathbf{m}_C$ connects the vertex n to $n-1$. The embedding of $\{0, \dots, n\}/\sim$ is obtained by contracting the edges of E as in Figure 7.12. We obtain a looptree denoted by $\mathbf{L}_C$. Let us describe the tree of components $\mathbf{T}_C := \mathrm{Tree}(\mathbf{L}_C)$. The black vertices of $\mathbf{T}_C$ are the internal faces of $\mathbf{m}_C$, and the white vertices of $\mathbf{T}_C$ are the equivalence classes of $\sim$. For every black vertex f, the white vertices incident to f are the classes that have a representative j incident to the face f in $\mathbf{m}_C$, with the natural cyclic order. The root edge of $\mathbf{T}_C$ connects the class of 0 to the the face on the left of the root of $\mathbf{m}_C$. See Figure 7.12 for an example. This construction extends to the case where $C_n > 0$, but the resulting map in not a looptree in general.

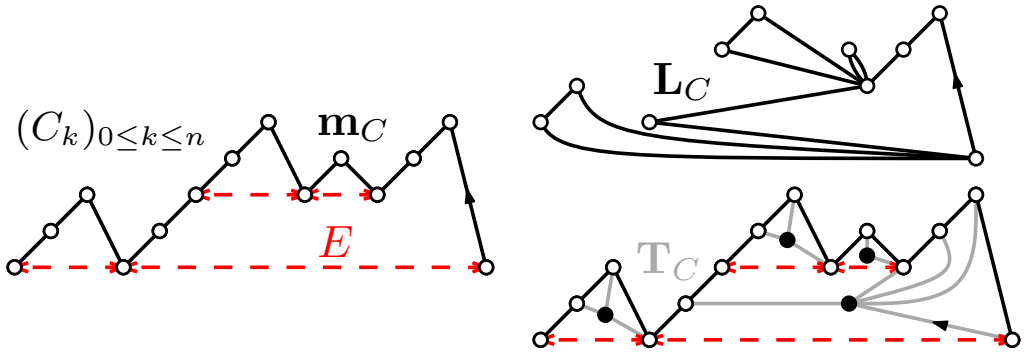

Figure 7.12: The construction of $\mathbf{L}_C$ and $\mathbf{T}_C$ from the excursion C.

Infinite looptrees. Let us extend the construction to infinite looptrees. Let $C : \mathbb{Z}_+ \to \mathbb{Z}$ be a function such that $C_0 = 0$, with no positive jump, no constant step and such that

$$\liminf_{k\to\infty} C_k = -\infty. \tag{7.6}$$

The function C is extended to $\mathbb{Z}$ by setting $C_k = k$ for $k \in \mathbb{Z}_-$. We define an equivalence relation $\sim$ on $\mathbb{Z}$ by applying (7.5) with the function C. The graph of $-C$ and the set of edges E containing all the pairs $\{(i, -C_i), (j, -C_j)\}$ such that $i \sim j$ define an infinite map $\mathbf{m}_C$, whose vertices are identified to $\mathbb{Z}$ (the root connects 0 to 1). By contracting the edges of E, we obtain the infinite looptree $\mathbf{L}_C$ (which is an embedding of $\mathbb{Z}/\sim$). The tree $\mathbf{T}_C := \mathrm{Tree}(\mathbf{L}_C)$ is defined as in the finite setting. By the assumption (7.6), internal faces of $\mathbf{m}_C$ (the black vertices) and equivalence classes of $\mathbb{Z}/\sim$ (the white vertices) are finite. Thus, $\mathbf{T}_C$ is locally finite. We let

$$\tau_0 = 0 \quad \text{and} \quad \tau_{k+1} := \inf\{i \geq \tau_k : C_i < C_{\tau_k}\}, \quad k \in \mathbb{Z}_+. \tag{7.7}$$

For every $k \in \mathbb{N}$, the white vertex of $\mathbf{T}_C$ associated to τ_k disconnects the root from infinity, as well as its (black) parent in $\mathbf{T}_C$. This exhibits the unique spine of $\mathbf{T}_C$ (and a spine of faces in $\mathbf{L}_C$). Since $C_k = k$ for negative k, there is no vertex on the left of the spine of $\mathbf{L}_C$.

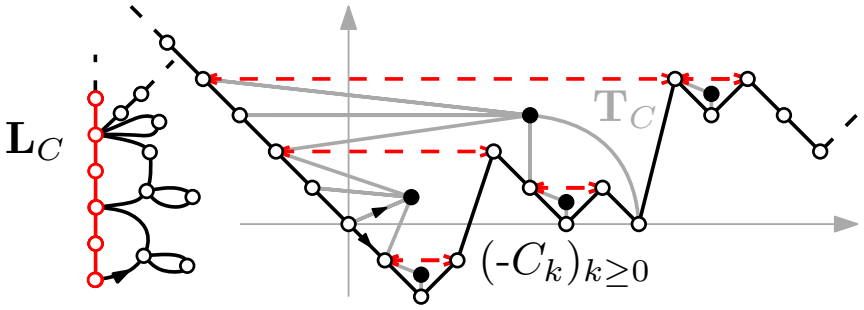

Figure 7.13: The construction of $\mathbf{L}_C$ and $\mathbf{T}_C$ from C.

We finally define a looptree out of a pair of functions $C, C' : \mathbb{Z}_+ \to \mathbb{Z}$, with $C_0 = C'_0 = 0$, no positive jumps, no constant steps and so that C satisfies (7.6) and C' is nonnegative. First define a looptree $\mathbf{L}_C$ as above, and let $\{e_i : i \in \mathbb{Z}_+\}$ be the half-edges of the left boundary of $\mathbf{L}_C$ in contour order. Then, we define an equivalence relation $\sim$ on $\mathbb{Z}_+$ by applying (7.5) with the function C'. Let $R_0 = -1$ and for every $k \in \mathbb{N}$, $R_k := \sup\{i \in \mathbb{Z}_+ : C'_i = k-1\}$. For every $k \in \mathbb{Z}_+$, the excursion $\{C'_{R_k+i+1} - k : 0 \leq i \leq R_{k+1} - R_k - 1\}$ of C' above its future infimum defines a looptree $\mathbf{L}_k$. We now consider the graph of $\mathbb{Z}_+$ embedded in the plane and for every $k \in \mathbb{Z}_+$, attach the looptree $\mathbf{L}_k$ on the left of the vertex $k \in \mathbb{Z}_+$ (so that the origin of $\mathbf{L}_k$ matches the vertex k and its root edge follows $(k, k+1)$ in counterclockwise order). We obtain a *forest* of looptrees $\mathbf{F}_{C'}$, isomorphic to $\mathbb{Z}_+/\sim$. The infinite looptree $\mathbf{L}_{C,C'}$ is obtained by gluing the left boundary of $\mathbf{L}_C$ to the right boundary of $\mathbf{F}_{C'}$ (i.e., by identifying the half-edge e_i with the half-edge $(i+1, i)$ of $\mathbb{N}$ for every $i \in \mathbb{N}$). The root edge of $\mathbf{L}_{C,C'}$ is the root edge of $\mathbf{L}_C$. The tree of components $\mathbf{T}_{C,C'} := \mathrm{Tree}(\mathbf{L}_{C,C'})$ has

a unique spine inherited from $\mathbf{T}_C$. We can also define a function $C^* : \mathbb{Z} \to \mathbb{Z}$ by

$$C^*_k = \begin{cases} -C_k & \text{if} \quad k \in \mathbb{Z}_+ \\ C'_{-k} & \text{if} \quad k \in \mathbb{Z}_- \end{cases} . \tag{7.8}$$

and an equivalence relation $\sim$ on $\mathbb{Z}$ by

$$i \sim j \quad \text{iff} \quad \begin{cases} i \vee j > 0 \quad \text{and} \quad \inf_{k \le i \wedge j} C^*_k \ge C^*_i = C^*_j \ge \sup_{(i\wedge j)\vee 0 \le k \le i \vee j} C^*_k \\ \quad \text{or} \\ i \vee j \le 0 \quad \text{and} \quad \inf_{i\wedge j \le k \le i\vee j} C^*_k \ge C^*_i = C^*_j \end{cases} \tag{7.9}$$

(with $\inf \emptyset = +\infty$ and $\sup \emptyset = -\infty$). Then, $\mathbf{L}_{C,C'}$ is isomorphic to $\mathbb{Z}/\sim$ (see Figure 7.14). In the next part, we let p_C and $p_{C,C'}$ denote the canonical projection on $\mathbf{L}_C$ and $\mathbf{L}_{C,C'}$.

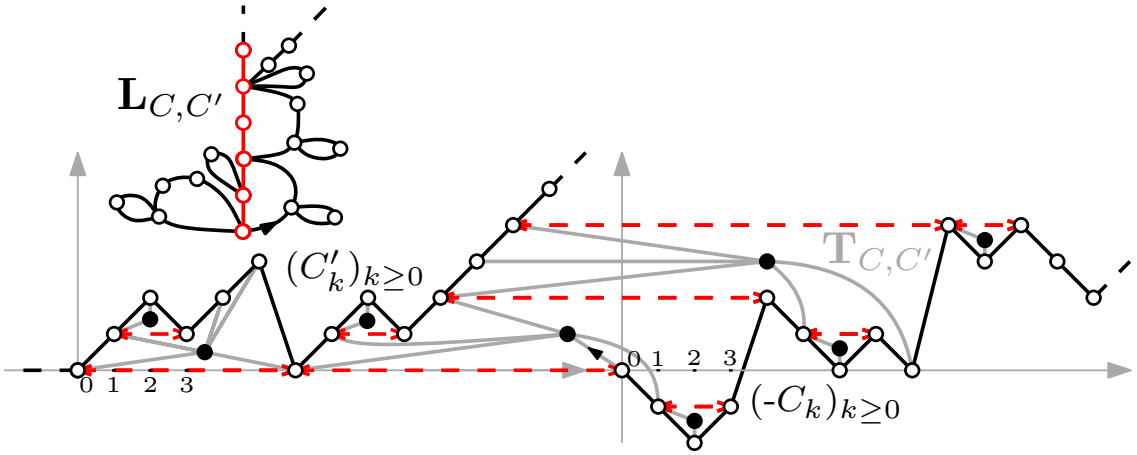

Figure 7.14: The construction of $\mathbf{L}_{C,C'}$ and $\mathbf{T}_{C,C'}$ from C and C'.

7.3.2 Random walks

We now gather results on random walks. For every probability measure ν on $\mathbb{Z}$ and every $x \in \mathbb{Z}$, let P^ν_x be the law of the simple random walk started at x with step distribution ν (we may omit the exponent ν). Let $Z = \{Z_k : k \in \mathbb{Z}_+\}$ be the canonical process and $T := \inf\{k \in \mathbb{Z}_+ : Z_k < 0\}$. We assume that ν is centered and $\nu((1, +\infty)) = 0$ (the random walk is called upwards-skip-free or with no positive jumps). For every $k \in \mathbb{Z}$, we let $\widehat{\nu}(k) = \nu(-k)$.

Overshoot. We start with a result on the *overshoot* at the first entrance in $(-\infty, 0)$.

Lemma 7.3.1. *We have*

$$P^\nu_0 (Z_{T-1} - Z_T = k) = \frac{k\nu(-k)}{\nu(1)}, \quad k \in \mathbb{Z}_+.$$

Conditionally on $Z_{T-1} - Z_T$, $-Z_T$ is uniform on $\{1, \dots, Z_{T-1} - Z_T\}$. Moreover, under P^ν_0 and conditionally on Z_{T-1}, the reversed process $\{\widehat{Z}_k : 0 \le k < T\} := \{Z_{T-1-k} : 0 \le k < T\}$ has the same law as $\{Z_k : 0 \le k < T\}$ under $P^{\widehat{\nu}}_{Z_{T-1}}$.

Proof. Let $n \in \mathbb{N}$ and $x_0, \dots, x_{n-1} \geq 0$. On the one hand

$$P_0^\nu(T = n, \widehat{Z}_0 = x_0, \dots, \widehat{Z}_{n-1} = x_{n-1}) = P_0^\nu\left(Z_0 = x_{n-1}, \dots, Z_{n-1} = x_0, Z_n < 0\right)$$
$$= \mathbf{1}_{\{x_{n-1}=0\}} \nu(x_{n-2} - x_{n-1}) \cdots \nu(x_0 - x_1)\nu((-\infty, -x_0))$$

and on the other hand since $\nu((1, +\infty)) = 0$,

$$P_{x_0}^{\widehat{\nu}}\left(T = n, Z_0 = x_0, \dots, Z_{n-1} = x_{n-1}\right)$$
$$= \mathbf{1}_{\{x_{n-1}=0\}} \nu(-(x_1 - x_0)) \cdots \nu(-(x_{n-1} - x_{n-2}))\nu(1).$$

Now, while computing the probability $P_0^\nu\left(Z_{T-1} = x_0\right)$ one gets

$$P_0^\nu\left(Z_{T-1} = x_0\right) = \nu((-\infty, -x_0)) \sum_{n \in \mathbb{N}} \sum_{x_1, \dots, x_{n-1} \geq 0} \mathbf{1}_{\{x_{n-1}=0\}} \nu(x_{n-2} - x_{n-1}) \cdots \nu(x_0 - x_1),$$

and still using $\nu((1, +\infty)) = 0$, we have

$$1 = P_{x_0}^{\widehat{\nu}}\left(Z_{T-1} = 0\right) = \nu(1) \sum_{n \in \mathbb{N}} \sum_{x_1, \dots, x_{n-1} \geq 0} \mathbf{1}_{\{x_{n-1}=0\}} \nu(x_{n-2} - x_{n-1}) \cdots \nu(x_0 - x_1).$$

The last assertion follows, as well as $P_0^\nu\left(Z_{T-1} = i\right) = \nu((-\infty, -i))/\nu(1)$ for every $i \in \mathbb{Z}_+$. By a direct computation, for every $i \in \mathbb{Z}_+$ and $j \in \mathbb{Z}_- \backslash \{0\}$,

$$P_0^\nu\left(Z_T = j \mid Z_{T-1} = i\right) = \frac{\nu(j - i)}{\nu((-\infty, -i))} \quad \text{and} \quad P_0^\nu\left(Z_{T-1} = i, Z_T = j\right) = \frac{\nu(j - i)}{\nu(1)}.$$

Then, for every $k \in \mathbb{Z}_+$ and $l \in \{1, \dots, k\}$,

$$P_0^\nu\left(Z_{T-1} - Z_T = k\right) = \frac{k\nu(-k)}{\nu(1)} \quad \text{and} \quad P_0^\nu\left(-Z_T = l \mid Z_{T-1} - Z_T = k\right) = \frac{1}{k},$$

which ends the proof. □

Remark 7.3.2. Since $\nu((1, +\infty)) = 0$, by putting $\widehat{Z}_T := \widehat{Z}_{T-1} - 1$ we have that under P_0^ν and conditionally on Z_{T-1}, $\{\widehat{Z}_k : 0 \leq k \leq T\}$ is distributed as $\{Z_k : 0 \leq k \leq T\}$ under $P_{Z_{T-1}}^{\widehat{\nu}}$.

Random walk conditioned to stay nonnegative. We now recall the construction of the so-called *random walk conditioned to stay nonnegative* of [BD94] (see also [Fel71, Spi01]). We let $T_n := \inf\{k \in \mathbb{N} : Z_k \geq n\}$ for every $n \in \mathbb{Z}_+$. Let $H := \{H_k : k \in \mathbb{Z}_+\}$ be the strict ascending ladder height process of $-Z$. Namely, let $L_0 = 0$ and

$$H_k = -Z_{L_k}, \quad L_{k+1} = \inf\{j > L_k : -Z_j > H_k\}, \quad k \in \mathbb{Z}_+.$$

Then, the *renewal function* associated with H is defined by

$$V(x) := \sum_{k=0}^{\infty} P_0(H_k \leq x) = E_0\left(\sum_{k=0}^{T_0-1} \mathbf{1}_{\{Z_k \geq -x\}}\right), \quad x \geq 0, \tag{7.10}$$

where the equality follows from the duality lemma. For every $x \geq 0$, we denote by $P_x^\uparrow$ the (Doob) h-transform of P_x by V. That is, for every $k \in \mathbb{Z}_+$ and every $F : \mathbb{Z}^{k+1} \to \mathbb{R}$,

$$E_x^\uparrow(F(Z_0, \dots, Z_k)) = \frac{1}{V(x)} E_x\left(V(Z_k)F(Z_0, \dots, Z_k)\mathbf{1}_{k<T}\right). \tag{7.11}$$

Theorem. [BD94, Theorem 1] *For every $x \geq 0$, in the sense of weak convergence of finite-dimensional distributions,*

$$P_x\left(\cdot \mid T_n < T\right) \underset{n\to+\infty}{\Longrightarrow} P_x^{\uparrow} \quad \text{and} \quad P_x\left(\cdot \mid T \geq n\right) \underset{n\to+\infty}{\Longrightarrow} P_x^{\uparrow}.$$

The probability measure $P_x^{\uparrow}$ is the law of the random walk conditioned to stay nonnegative.

We now recall Tanaka's pathwise construction. We let $T_+ := \inf\{k \in \mathbb{Z}_+ : Z_k > 0\}$.

Theorem. [Tan89, Theorem 1] *Let $\{w_k : k \in \mathbb{Z}_+\}$ be independent copies of the reversed excursion*

$$\left(0, Z_{T_+} - Z_{T_+-1}, \ldots, Z_{T_+} - Z_1, Z_{T_+}\right)$$

under P_0, with $w_k = (w_k(0), \ldots, w_k(s_k))$. Let for every $k \in \mathbb{Z}_+$

$$Y'_k := \sum_{j=0}^{i-1} w_j(s_j) + w_i\left(k - \sum_{j=0}^{i-1} w_j(s_j)\right) \quad \text{for} \quad \sum_{j=0}^{i-1} w_j(s_j) < k \leq \sum_{j=0}^{i} w_j(s_j),$$

and $Y_k := Y'_{k+1} - 1$. Then, the process $\{Y_k : k \in \mathbb{Z}_+\}$ has law $P_0^{\uparrow}$.

Remark 7.3.3. In [Tan89], $\{Y'_k : k \in \mathbb{Z}_+\}$ is the h-transform of P_0 by a suitable renewal function V'. This function differs from the function V of (7.10) and rather defines a random walk conditioned to stay positive. However, when the random walk is upwards-skip-free and we remove its first step (which gives $\{Y_k : k \in \mathbb{Z}_+\}$), the associated renewal function equals V up to a multiplicative constant. This ensures that $\{Y_k : k \in \mathbb{Z}_+\}$ has law $P_0^{\uparrow}$.

Let us rephrase this theorem. Let $R_0 = -1$ and $R_k := \sup\{i \in \mathbb{Z}_+ : Z_i \leq k-1\}$ for $k \in \mathbb{N}$.

Corollary 7.3.4. *Under $P_0^{\uparrow}$, the reversed excursions*

$$\left\{Z_i^{(k)},\ 0 \leq i < R_{k+1} - R_k\right\} := \left\{Z_{R_{k+1}-i} - k,\ 0 \leq i < R_{k+1} - R_k\right\}, \quad k \in \mathbb{Z}_+$$

are independent and distributed as $\{Z_k : 0 \leq k < T\}$ under $P_0^{\widehat{\nu}}$.

The law of the conditioned random walk stopped at a first hitting time is explicit.

Lemma 7.3.5. *Let $n \in \mathbb{Z}_+$. Under $P_0^{\uparrow}$, the process $\{Z_k : 0 \leq k \leq T_n\}$ has distribution $P_0\left(\cdot \mid T_n < T\right)$.*

Proof. Let $k \in \mathbb{Z}_+$ and $x_0, \ldots, x_k \geq 0$. By [BD94, Theorem 1],

$$P_0\left(T_n = k, Z_0 = x_0, \ldots, Z_k = x_k \mid T_m < T\right) \underset{m\to\infty}{\longrightarrow} P_0^{\uparrow}\left(T_n = k, Z_0 = x_0, \ldots, Z_k = x_k\right).$$

It is thus sufficient to prove that for m large enough,

$$P_0\left(T_n = k, Z_0 = x_0, \ldots, Z_k = x_k \mid T_m < T\right) = P_0\left(T_n = k, Z_0 = x_0, \ldots, Z_k = x_k \mid T_n < T\right).$$

We have $T_n < T_m$ whenever $m > n$, and $Z_{T_n} = n$ P_0-a.s.. The strong Markov property gives

$$P_0\left(T_n = k, Z_0 = x_0, \dots, T_m < T\right) = P_0\left(T_n = k, Z_0 = x_0, \dots, T_n < T\right) P_n\left(T_m < T\right).$$

We conclude the proof by using the identity $P_0\left(T_m < T\right) = P_0\left(T_n < T\right) P_n\left(T_m < T\right)$. □

We now deal with the conditioned random walk started at large values. For every $x \geq 0$, let ϕ_x be defined for every $y \in \mathbb{R}^{\mathbb{N}}$ by $\phi_x(y) = (y_i - x : i \in \mathbb{N})$. We use the notation $f_* P$ for the pushforward measure of P by the function f.

Lemma 7.3.6. *In the sense of weak convergence of finite-dimensional distributions,*

$$(\phi_x)_* P_x^{\uparrow} \underset{x\to\infty}{\Longrightarrow} P_0.$$

Proof. Let $k \in \mathbb{Z}_+$ and $x_0, \cdots, x_k \in \mathbb{Z}$. From (7.11), we have

$$(\phi_x)_* P_x^{\uparrow}(Z_0 = x_0, \dots, Z_k = x_k) = \frac{V(x + x_k)}{V(x)} P_x(k > T, Z_0 = x + x_0, \dots, Z_k = x + x_k).$$

Up to choosing x large enough, we can assume that $x_i + x \geq 0$ for $i \in \{0, \dots, k\}$ and get

$$(\phi_x)_* P_x^{\uparrow}(Z_0 = x_0, \dots, Z_k = x_k) = \frac{V(x + x_k)}{V(x)} P_0(Z_0 = x_0, \dots, Z_k = x_k).$$

We now assume that $x_k \in \mathbb{Z}_+$ (the case $x_k \in \mathbb{Z}_-$ can be treated similarly). We have

$$\frac{V(x + x_k)}{V(x)} = 1 + \frac{1}{V(x)} E_0\left(\sum_{k=0}^{T_0 - 1} \mathbf{1}_{\{-x - x_k \leq Z_k < -x\}}\right).$$

By monotone convergence, since $T_0 < \infty$ P_0-a.s.,

$$E_0\left(\sum_{k=0}^{T_0 - 1} \mathbf{1}_{\{-x - x_k \leq Z_k < -x\}}\right) \leq E_0\left(\sum_{k=0}^{T_0 - 1} \mathbf{1}_{\{Z_k < -x\}}\right) \underset{x\to\infty}{\longrightarrow} 0.$$

By (7.10) and monotone convergence once again, since $E_0(T_0) = \infty$, $V(x) \to \infty$ as $x \to \infty$, which concludes the proof. □

Random walk with positive drift. We consider random walks with positive drift conditioned to stay nonnegative. Let ν and $\{\nu_p : p \in \mathbb{Z}_+\}$ be upwards-skip-free probability measure, such that ν is centered, $m_{\nu_p} := E_0^{\nu_p}(Z_1) > 0$ and $\nu_p \Rightarrow \nu$ weakly as $p \to \infty$. The random walk conditioned to stay nonnegative is well-defined in the usual sense, since $P_0^{\nu_p}(T = \infty) > 0$ for $p \in \mathbb{Z}_+$. We denote its law by $P_x^{\nu_p \uparrow}$. It is also the h-transform of $P_x^{\nu_p}$ by the renewal function V_p associated to the strict ascending ladder height process of $-Z$, which satisfies

$$V_p(x) = \frac{P_x^{\nu_p}(T = \infty)}{P_0^{\nu_p}(T = \infty)}, \quad x \geq 0,\ p \in \mathbb{Z}_+.$$

We let $T_{-n} := \inf\{k \in \mathbb{N} : Z_k \leq -n\}$ for every $n \in \mathbb{N}$.

Lemma 7.3.7. *For $x \in \mathbb{Z}_+$, in the sense of weak convergence of finite-dimensional distributions,*

$$P_x^{\nu_p\uparrow} \underset{p\to+\infty}{\Longrightarrow} P_x^{\nu\uparrow}.$$

Proof. Let $x, k \in \mathbb{Z}_+$ and $x_0, \cdots, x_k \in \mathbb{Z}_+$. By (7.11),

$$P_x^{\nu_p\uparrow}(Z_0 = x_0, \ldots, Z_k = x_k) = \frac{V_p(x_k)}{V_p(x)} P_x^{\nu_p}(k > T, Z_0 = x_0, \ldots, Z_k = x_k). \tag{7.12}$$

Since $\nu_p \Rightarrow \nu$ weakly, we have

$$P_x^{\nu_p}(k > T, Z_0 = x_0, \ldots, Z_k = x_k) \underset{p\to\infty}{\longrightarrow} P_x^{\nu}(k > T, Z_0 = x_0, \ldots, Z_k = x_k).$$

By (7.10), for every $x, k \in \mathbb{Z}_+$,

$$\begin{aligned} V_p(x) &= E_0^{\nu_p}\left(\sum_{k=0}^{\infty} \mathbf{1}_{\{H_k \le x\}}\right) \\ &= E_0^{\nu_p}\left(\mathbf{1}_{\{T_{-x}\le K\}} \sum_{k=0}^{\infty} \mathbf{1}_{\{H_k\le x\}}\right) + E_0^{\nu_p}\left(\mathbf{1}_{\{T_{-x}> K\}} \sum_{k=0}^{\infty} \mathbf{1}_{\{H_k\le x\}}\right). \end{aligned}$$

The first variable being measurable with respect to the K first steps of Z, we get

$$E_0^{\nu_p}\left(\mathbf{1}_{\{T_{-x}\le K\}} \sum_{k=0}^{\infty} \mathbf{1}_{\{H_k\le x\}}\right) \underset{p\to\infty}{\longrightarrow} E_0^{\nu}\left(\mathbf{1}_{\{T_{-x}\le K\}} \sum_{k=0}^{\infty} \mathbf{1}_{\{H_k\le x\}}\right).$$

Since H is the *strict* ascending ladder height process of $-Z$ and Z takes only integer values,

$$E_0^{\nu_p}\left(\mathbf{1}_{\{T_{-x}> K\}} \sum_{k=0}^{\infty} \mathbf{1}_{\{H_k\le x\}}\right) \le (x+1) P_0^{\nu_p}\left(T_{-x} > K\right) \underset{p\to\infty}{\longrightarrow} (x+1) P_0^{\nu}\left(T_{-x} > K\right).$$

As a consequence, $\limsup_{p\to\infty} |V_p(x) - V(x)| \le 2(x+1)P_0^{\nu}(T_{-x} > K)$. Furthermore, T_{-x} is finite P_0^{ν}-a.s., so that $V_p(x) \to V(x)$ as $p \to \infty$ for every $x \ge 0$. Applying this to (7.12) together with (7.11) yields the expected result. □

7.3.3 Contour functions of random looptrees.

Let ν be a centered upwards-skip-free probability measure on $\mathbb{Z}$ such that $\nu(0) = 0$. We define the probability measures $\nu_\circ$ and $\nu_\bullet$ (with means $m_{\nu_\circ}$ and $m_{\nu_\bullet}$) by

$$\nu_\circ(k) := \nu(1)\,(1-\nu(1))^k \quad \text{and} \quad \nu_\bullet(k) := \frac{\nu(-k)}{1-\nu(1)}, \quad k \in \mathbb{Z}_+. \tag{7.13}$$

The fact that ν is centered entails $m_{\nu_\circ} m_{\nu_\bullet} = 1$, i.e. the pair $(\nu_\circ, \nu_\bullet)$ is critical.

Finite looptrees. We consider a random walk $\{\widehat{C}_k : k \in \mathbb{Z}_+\}$ with law $P_0^{\widehat{\nu}}$ (and $\widehat{\nu} := \nu(-\cdot)$). We let $T := \inf\{k \in \mathbb{Z}_+ : \widehat{C}_k < 0\}$, and $C = \{C_k : 0 \le k < T\} := \{\widehat{C}_{T-1-k} : 0 \le k < T\}$.

Lemma 7.3.8. *The tree of components* $\mathbf{T}_C = \mathrm{Tree}(\mathbf{L}_C)$ *of the looptree* $\mathbf{L}_C$ *has law* $\mathsf{GW}_{\nu_\circ,\nu_\bullet}$.

Proof. The excursion C satisfies a.s. the assumptions of Section 7.3.1 and defines a looptree $\mathbf{L}_C$. By construction, the number of offspring of the root vertex in $\mathbf{T}_C$ is the number of excursions of $\widehat{C}$ above zero before T: $k_\emptyset(\mathbf{T}_C) = \inf\{k \in \mathbb{Z}_+ : \widehat{C}_{\sigma_k+1} < 0\}$, where $\sigma_0 = 0$ and for every $k \in \mathbb{Z}_+$, $\sigma_{k+1} = \inf\{i > \sigma_k : \widehat{C}_i \leq 0\}$. By the strong Markov property, $k_\emptyset(\mathbf{T}_C)$ has geometric distribution with parameter $\widehat{\nu}(-1)$, which is exactly $\nu_\circ$. The descendants of the children of the root are coded by the excursions $\{\widehat{C}_{\sigma_{k+1}-i} : 0 \leq i \leq \sigma_{k+1} - \sigma_k\}$ for $0 \leq k < k_\emptyset(\mathbf{T}_C)$ and are i.i.d.. Thus, we focus on the child of the root v coded by the first of these excursions (i.e., the first child if $k_\emptyset(\mathbf{T}_C) = 1$, the second otherwise).

The number of offspring of v is $k_v(\mathbf{T}_C) = \widehat{C}_1$ (conditionally on $\{T > 1\}$, i.e., the root vertex has at least one child). Its law is $\widehat{\nu}$ conditioned to take positive values, which is $\nu_\bullet$. The descendants of the children of v are coded by the excursions $\{\widehat{C}_{\sigma'_{k+1}-i-1} : 0 \leq i < \sigma'_{k+1} - \sigma'_k\}$ for $0 \leq k < k_v(\mathbf{T}_C)$ (where $\sigma'_0 = 1$ and $\sigma'_{k+1} = \inf\{i \geq \sigma'_k : \widehat{C}_i < \widehat{C}_{\sigma'_k}\}$). These excursions are independent with the same law as $\{C_k : 0 \leq k < T\}$, which concludes the argument. □

Remark 7.3.9. We can extend Lemma 7.3.8 to $C = \{\widehat{C}_{T-1-k} : 0 \leq k < T\}$ where $\widehat{C}$ has distribution $P_x^{\widehat{\nu}}$ with $x > 0$ (using the construction of Section 7.3.1). By decomposing $\widehat{C}$ into its excursions above its infimum (as in (7.7)), we get a forest $\mathbf{F}_C$ of $x+1$ independent looptrees, whose trees of components have distribution $\mathsf{GW}_{\nu_\circ,\nu_\bullet}$ (see Figure 7.15 for an illustration).

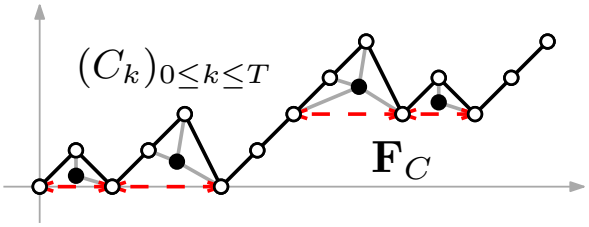

Figure 7.15: The construction of the forest $\mathbf{F}_C$ from the excursion C with $C_{T-1} = 4$.

Infinite looptrees. We first consider a random walk $C = \{C_k : k \in \mathbb{Z}_+\}$ with law P_0^ν.

Proposition 7.3.10. *The tree of components* $\mathbf{T}_C = \mathrm{Tree}(\mathbf{L}_C)$ *of the looptree* $\mathbf{L}_C$ *has law* $\mathsf{GW}^{(\infty,l)}_{\nu_\circ,\nu_\bullet}$.

Proof. The function C satisfies a.s. the assumptions of Section 7.3.1. We denote by $\{s_k : k \in \mathbb{Z}_+\}$ the a.s. unique spine of $\mathbf{T}_C$. For convenience, we shift the root by one edge on the right in $\mathbf{T}_C$ and $\mathsf{GW}^{(\infty,l)}_{\nu_\circ,\nu_\bullet}$ (so that the root edge belongs to the spine in both cases). Recall from (7.7) the definition of the excursions endpoints $\{\tau_k : k \in \mathbb{Z}_+\}$. The (white) vertices of the spine $\{s_{2k} : k \in \mathbb{Z}_+\}$ are also $\{p_C(\tau_k) : k \in \mathbb{Z}_+\}$. For every $k \in \mathbb{Z}_+$, let $\mathbf{T}_k$ be the sub-tree of $\mathbf{T}_C$ containing all the offspring of s_{2k} that are not offspring of s_{2k+2} (with the convention that s_{2k} and s_{2k+2} belong to $\mathbf{T}_k$). The tree $\mathbf{T}_k$

is coded by $\{C_{\tau_k+i} - C_{\tau_k} : 0 \le i \le \tau_{k+1} - \tau_k\}$, see Figure 7.16. By the strong Markov property, the trees $\{\mathbf{T}_k : k \in \mathbb{Z}_+\}$ are i.i.d. and it suffices to determine the law of $\mathbf{T}_0$.

The vertex s_1 is the unique black vertex of $\mathbf{T}_0$ that belongs to the spine of $\mathbf{T}_C$. Its number of offspring read $k_{s_1} = k_{s_1}(\mathbf{T}_C) = k_{s_1}(\mathbf{T}_0) = C_{\tau_1-1} - C_{\tau_1}$. Moreover, if $k_{s_1}^{(l)}$ (resp. $k_{s_1}^{(r)}$) is the number of offspring of s_1 on the left (resp. right) of the spine, we have $k_{s_1}^{(l)} = -C_{\tau_1} - 1$ and $k_{s_1}^{(r)} = C_{\tau_1-1}$. Thus, the position of the child $s_2 = p_C(\tau_1)$ of s_1 that belongs to the spine among its $C_{\tau_1-1} - C_{\tau_1}$ children is $-C_{\tau_1}$. By Lemma 7.3.1,

$$P(k_{s_1} = j) = \frac{j\nu(-j)}{\nu(1)} = \bar{\nu}_\bullet(j), \quad j \in \mathbb{N},$$

and conditionally on k_{s_1}, the rank of s_2 is uniform among $\{1, \dots, k_{s_1}\}$. We now work conditionally on $(C_{\tau_1} - 1, C_{\tau_1})$, and let $\{v_j : 0 \le j \le k_{s_1}\}$ be the neighbours of s_1 in counterclockwise order, v_0 being the root vertex of $\mathbf{T}_0$. Then, the descendants of $\{v_j : 0 \le j \le k_{s_1}^{(r)}\}$ are the trees of components of the finite forest coded by $\{C_i : 0 \le i < \tau_1\}$ (see Figure 7.16). By Lemma 7.3.1, conditionally on C_{τ_1-1}, the reversed excursion $\{C_{\tau_1-i-1} : 0 \le i < \tau_1\}$ has distribution $P^{\widehat{\nu}}_{C_{\tau_1-1}}$ and by Remark 7.3.9, the trees of components form a forest of $C_{\tau_1-1} + 1$ independent trees with distribution $\mathsf{GW}_{\nu_\circ,\nu_\bullet}$, that are grafted on the right of the vertices $\{v_j : 0 \le j \le k_{s_1}^{(r)}\}$. By construction, children of s_1 on the left of the spine have no offspring. It remains to identify the offspring distribution of the white vertex of the spine in $\mathbf{T}_0$, i.e. the root vertex. It has one (black) child s_1 on the spine, which is its leftmost offspring, and a tree with distribution $\mathsf{GW}_{\nu_\circ,\nu_\bullet}$ grafted on the right of it. As a consequence,

$$P(k_\emptyset(\mathbf{T}_C) = k) = \nu_\circ(k-1), \quad k \in \mathbb{N}.$$

By standard properties of the geometric distribution, this is the law of a uniform variable on $\{1, \dots, X\}$, with X of law $\bar{\nu}_\circ$. We get Kesten's multi-type tree with pruning on the left. □

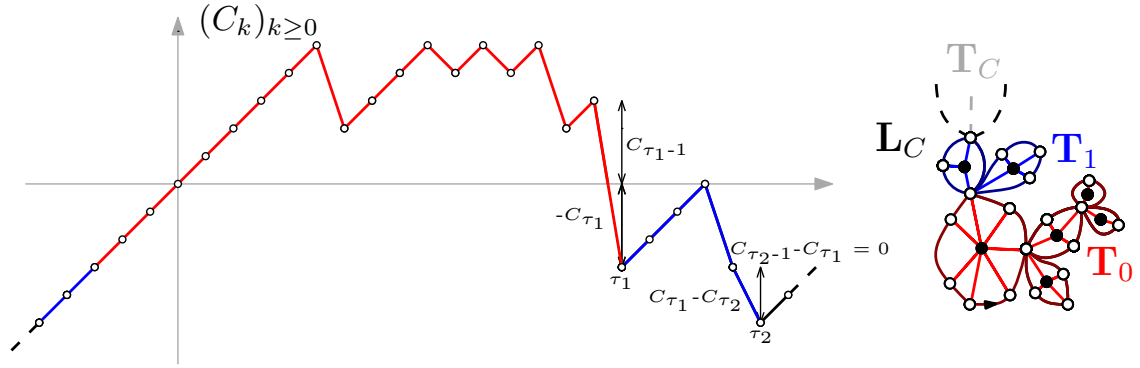

Figure 7.16: The decomposition of the tree $\mathbf{T}_C$.

Lastly, we consider a random walk $C = \{C_k : k \in \mathbb{Z}_+\}$ with law P_0^ν, together with an independent process $C' = \{C'_k : k \in \mathbb{Z}_+\}$ with law $P_0^{\nu\uparrow}$.

Proposition 7.3.11. *The tree of components* $\mathbf{T}_{C,C'} = \mathrm{Tree}(\mathbf{L}_{C,C'})$ *of* $\mathbf{L}_{C,C'}$ *has law* $\mathsf{GW}^{(\infty)}_{\nu_\circ,\nu_\bullet}$.

Proof. The processes C and C' satisfy a.s. the assumptions of Section 7.3.1. There, we defined $\mathbf{L}_{C,C'}$ as the gluing along their boundaries of $\mathbf{L}_C$ and the infinite forest $\mathbf{F}_{C'}$. By Proposition 7.3.10, $\mathbf{T}_C = \mathrm{Tree}(\mathbf{L}_C)$ has distribution $\mathrm{GW}^{(\infty,l)}_{\nu_\circ,\nu_\bullet}$. For convenience, we shift the root by one edge on the right in $\mathbf{T}_{C,C'}$, $\mathbf{T}_C$, $\mathrm{GW}^{(\infty)}_{\nu_\circ,\nu_\bullet}$ and $\mathrm{GW}^{(\infty,l)}_{\nu_\circ,\nu_\bullet}$ throughout the proof. Recall from Section 7.3.1 that the looptrees $\{\mathbf{L}_k : k \in \mathbb{Z}_+\}$ defining $\mathbf{F}_{C'}$ are coded by the excursions $\{C'_{R_k+i+1} - k : 0 \le i \le R_{k+1} - R_k - 1\}$. By Lemma 7.3.4, the time-reverse of these excursions are independent and distributed as $(Z_k)_{0\le k\le T-1}$ under $P_0^{\widehat{\nu}}$. By Lemma 7.3.8, $\mathbf{T}_k := \mathrm{Tree}(\mathbf{L}_k)$ has distribution $\mathrm{GW}_{\nu_\circ,\nu_\bullet}$. So vertices of $\mathbf{T}_{C,C'}$ have independent number of offspring, and offspring distribution $\nu_\circ$ and $\nu_\bullet$ out of the spine.

By Proposition 7.3.10, black vertices of the spine have offspring distribution $\bar{\nu}_\bullet$, and a unique child in the spine with uniform rank conditionally on the number of offspring. It remains to identify the offspring distribution of white vertices of the spine, and thus of the root vertex. By construction, we have $k_\emptyset(\mathbf{T}_{C,C'}) = k_\emptyset(\mathbf{T}_0) + k_\emptyset(\mathbf{T}_C)$, where the variables on the right hand side are independent with respective distribution $\nu_\circ(\cdot - 1)$ and $\nu_\circ$. Then,

$$P(k_\emptyset(\mathbf{T}_{C,C'}) = k) = \sum_{i=1}^{k} \nu_\circ(i-1)\nu_\circ(k-i) = \bar{\nu}_\circ(k), \quad k \in \mathbb{N}.$$

The child of the root that belongs to the spine of $\mathbf{T}_{C,C'}$ is the leftmost child of the root in $\mathbf{T}_C$. Its rank among the $k_\emptyset(\mathbf{T}_{C,C'})$ children of the root in $\mathbf{T}_{C,C'}$ is $k_\emptyset(\mathbf{T}_0) + 1$. Furthermore,

$$P(k_\emptyset(\mathbf{T}_0) + 1 = i \mid k_\emptyset(\mathbf{T}_{C,C'}) = k) = \nu_\circ(i-1)\nu_\circ(k-i)\frac{m_{\nu_\circ}}{k\nu_\circ(k)} = \frac{1}{k}, \quad k \in \mathbb{N},\ 1 \le i \le k,$$

so that this rank is uniform among the offspring. We obtain Kesten's multi-type tree. □

7.4 Decomposition of the UIHPT

In this section, we introduce a decomposition of the UIHPT along a percolation interface and prove Theorem 7.2.3. The idea of this decomposition first appears in [DMS14, Section 1.7.3], where it served as a discrete intuition for a continuous model (see Section 7.6 for details).

7.4.1 Exploration process

We consider a Bernoulli percolation model with parameter p on the UIHPT, conditionally on the "Black-White" boundary condition of Figure 7.8. The decomposition arises from the exploration of the percolation interface between the open and closed clusters of the boundary. Our approach is based on a peeling process introduced in [Ang04], notably to compute the critical threshold. Although we will only use this peeling process at criticality in the remainder of this section, we define it for any $p \in (0,1)$ in view of forthcoming applications.

ALGORITHM 7.4.1. ([Ang04]) Let $p \in (0,1)$, and consider a percolated UIHPT with distribution $\mathbf{P}_p$ and a "Black-White" boundary condition.

- Reveal the face incident to the edge of the boundary whose endpoints have different colour (the "Black-White" edge).
- Repeat the algorithm on the UIHPT given by the unique infinite connected component of the map deprived of the revealed face.

This peeling process is well-defined in the sense that the pattern of the boundary is preserved, and the spatial Markov property implies that its steps are i.i.d.. We now introduce a sequence of random variables describing the evolution of the peeling process. Let $\mathcal{E}_k$, $\mathcal{R}_{l,k}$, $\mathcal{R}_{r,k}$ and c_k be the number of exposed edges, swallowed edges on the left and right, and colour of the revealed vertex (if any, or a cemetery state otherwise) at step k of the peeling process.

Definition 7.4.2. For every $k \in \mathbb{N}$, let

$$Y_k = \left(Y_k^{(1)}, Y_k^{(2)}\right) := \left(\mathbf{1}_{\{c_k=1\}} - \mathcal{R}_{l,k}, \mathbf{1}_{\{c_k=0\}} - \mathcal{R}_{r,k}\right).$$

The exploration process $X = \{X_k = (X_k^{(1)}, X_k^{(2)}) : k \in \mathbb{Z}_+\}$ is defined by

$$X_0 = (0,0) \quad \text{and} \quad X_k := \sum_{i=1}^{k} Y_i, \quad k \in \mathbb{N}.$$

By the properties established in Section 7.2.1, the variables $\{Y_k : k \in \mathbb{N}\}$ are independent and distributed as $Y = \left(Y^{(1)}, Y^{(2)}\right)$ such that

$$Y = \begin{cases} (1,0) & \text{with probability} \quad 2p/3 \\ (0,1) & \text{with probability} \quad 2(1-p)/3 \\ (-k,0) & \text{with probability} \quad q_k \qquad (k \in \mathbb{N}) \\ (0,-k) & \text{with probability} \quad q_k \qquad (k \in \mathbb{N}) \end{cases}. \tag{7.14}$$

Let μ_p^0 be the law of $Y^{(1)}$, so that $Y^{(2)}$ has law μ_{1-p}^0. (This defines a probability measure since $\sum_{k\in\mathbb{N}} q_k = 1/6$.) Note that $Y^{(1)} = 0$ or $Y^{(2)} = 0$ but not both a.s., and $\mu_{1/2}^0$ is centered (since $\sum_{k\in\mathbb{N}} k q_k = 1/3$). We call the random walk X the *exploration process*, as it fully describes Algorithm 7.4.1. We now extract from X information on the percolation clusters. Let $\sigma_0^B = \sigma_0^W = 0$ and for every $k \in \mathbb{N}$,

$$\sigma_k^B := \inf\left\{i \geq \sigma_{k-1}^B : X_i^{(1)} \neq X_{\sigma_{k-1}^B}^{(1)}\right\} \quad \text{and} \quad \sigma_k^W := \inf\left\{i \geq \sigma_{k-1}^W : X_i^{(2)} \neq X_{\sigma_{k-1}^W}^{(2)}\right\}. \tag{7.15}$$

These stopping times are a.s. finite. We also let

$$z_k := \mathbf{1}_{\left\{Y_k^{(1)} \neq 0\right\}} = \mathbf{1}_{\left\{Y_k^{(2)} = 0\right\}}, \quad k \in \mathbb{N}, \tag{7.16}$$

In a word, $\{z_k : k \in \mathbb{N}\}$ is the sequence of colours of the third vertex of the faces revealed by the exploration. The processes $B = \{B_k : k \in \mathbb{Z}_+\}$ and $W = \{W_k : k \in \mathbb{Z}_+\}$ are defined by

$$B_k := X_{\sigma_k^B}^{(1)} \quad \text{and} \quad W_k := X_{\sigma_k^W}^{(2)}, \quad k \in \mathbb{Z}_+.$$

Lemma 7.4.3. *Let $p \in (0,1)$. Under $\mathbf{P}_p$, B and W are independent random walks started at 0 with step distribution*

$$\mu_p := \frac{\mu_p^0(\cdot \cap \mathbb{Z}^*)}{\mu_p^0(\mathbb{Z}^*)}.$$

Moreover, $\{z_k : k \in \mathbb{N}\}$ are independent with Bernoulli distribution of parameter $g(p) := 2p/3 + 1/6$, and independent of B and W.

Proof. As we noticed, for every $k \in \mathbb{Z}_+$, $Y_k^{(1)} = 0$ or $Y_k^{(2)} = 0$ a.s.. Thus, the sequences $\{\sigma_k^B : k \in \mathbb{N}\}$ and $\{\sigma_k^W : k \in \mathbb{N}\}$ induce a partition of $\mathbb{N}$. Moreover, we have

$$B_k = \sum_{i=0}^{k} Y^{(1)}_{\sigma_i^B} \quad \text{and} \quad W_k = \sum_{i=0}^{k} Y^{(2)}_{\sigma_i^W}, \quad k \in \mathbb{Z}_+.$$

The variables $\{Y_k : k \in \mathbb{N}\}$ being independent, B and W are independent. We also have

$$\sigma_k^B := \inf\left\{i \geq \sigma_{k-1}^B : Y_k^{(1)} \neq 0\right\} \quad \text{and} \quad \sigma_k^W := \inf\left\{i \geq \sigma_{k-1}^W : Y_k^{(2)} \neq 0\right\}, \quad k \in \mathbb{N}.$$

The strong Markov property applied at these times entails the first assertion. The distribution of the variables $\{z_k : k \in \mathbb{N}\}$ follows from the definition of the exploration process and the identity $\mu_p^0(0) = 2p/3 + 1/6$. Finally, for every $k \in \mathbb{N}$, σ_k^B (resp. σ_k^W) is independent of $Y_{\sigma_k^B}$ (resp. $Y_{\sigma_k^W}$) so that $\{z_k : k \in \mathbb{N}\}$ is independent of B and W. □

Note that for $p = p_c = 1/2$, $\mu := \mu_{p_c}$ is centered and $g(p_c) = 1/2$, while μ_p has positive mean if $p > p_c$. In the remainder of this section, we assume that $p = p_c$ and work under $\mathbf{P}$.

7.4.2 Percolation hulls and necklace

We now describe the percolation hulls $\mathcal{H}_b$ and $\mathcal{H}_w$ of the origin and the target of the root at criticality. Recall from (7.4) the definition of the probability measures $\mu_\circ$ and $\mu_\bullet$.

Proposition 7.4.4. *The trees of components* $\mathbf{Tree}(\mathcal{H}_b)$ *and* $\mathbf{Tree}(\mathcal{H}_w)$ *are independent with respective distribution* $\mathsf{GW}^{(\infty,l)}_{\mu_\circ,\mu_\bullet}$ *and* $\mathsf{GW}^{(\infty,r)}_{\mu_\circ,\mu_\bullet}$.

Moreover, conditionally on the trees $\mathbf{Tree}(\mathcal{H}_b)$ *and* $\mathbf{Tree}(\mathcal{H}_w)$*, the irreducible components $\{M_v^b : v \in \mathbf{Tree}(\mathcal{H}_b)_\bullet\}$ and $\{M_v^w : v \in \mathbf{Tree}(\mathcal{H}_w)_\bullet\}$ are independent critically percolated Boltzmann triangulations with a simple boundary and respective distribution* $\mathbf{W}^{\triangle}_{\deg(u)}$.

Remark 7.4.5. Galton-Watson trees conditioned to survive being a.s. locally finite and one-ended, $\mathrm{Scoop}(\mathcal{H}_b)$ and $\mathrm{Scoop}(\mathcal{H}_w)$ are infinite looptrees. In particular, $\mathcal{H}_b$ or $\mathcal{H}_w$ may have edges whose both sides are incident to their root face, corresponding to a loop of perimeter 2 in $\mathrm{Scoop}(\mathcal{H}_b)$ or $\mathrm{Scoop}(\mathcal{H}_w)$ that is filled in with the Boltzmann triangulation with a simple boundary consisting of a single edge.

Proof. We first deal with the open hull $\mathcal{H}_b$. The equivalence relation $\sim$ is defined by applying (7.5) with B. For every $k \in \mathbb{Z}_+$, let $\mathbf{L}_k$ be the quotient space of $(-\infty, k] \cap \mathbb{Z}$ by the restriction of $\sim$ to this set (with the embedding convention of Section 7.3.1). We also let $\mathbf{S}_k$ be the part of Scoop$(\mathcal{H}_b)$ discovered at step σ_k^B of the peeling process.

We now prove by induction that $\mathbf{S}_k$ is a map isomorphic to $\mathbf{L}_k$ for every $k \in \mathbb{Z}_+$. This is clear for $k = 0$, since the initial open cluster is isomorphic to $\mathbb{N}$. We assume that this holds for $k \in \mathbb{N}$, and denote by p_k the canonical projection on $\mathbf{L}_k$. The exploration steps between σ_k^B and σ_{k+1}^B reveal the face incident to $p_k(k)$ and the leftmost white vertex. They leave invariant the open cluster, so we restrict our attention to the step σ_{k+1}^B at which two cases are likely.

1. An inner open vertex is discovered ($Y^{(1)}_{\sigma^B_{k+1}} = 1$). Then, $\mathbf{S}_k$ is isomorphic to $\mathbf{L}_k$ plus an extra vertex in its external face connected only to $p_k(k)$. On the other hand, $B_{k+1} = B_k + 1$ so that $\mathbf{L}_{k+1}$ is isomorphic to $\mathbf{S}_k$.

2. The third vertex of the revealed triangle is on the (left) boundary and $l \in \mathbb{N}$ edges are swallowed ($Y^{(1)}_{\sigma^B_{k+1}} = -l$). Then, $\mathbf{S}_k$ is isomorphic to $\mathbf{L}_k$ plus an edge between $p_k(k)$ and l-th vertex after $p_k(k)$ in left contour order on the boundary of $\mathbf{L}_k$. Since $B_{k+1} = B_k - l$, $\mathbf{S}_k$ is isomorphic to $\mathbf{L}_{k+1}$.

In the second case, by the spatial Markov property, the loop of perimeter $l+1$ added to $\mathbf{L}_k$ is filled in with an independent percolated triangulation with a simple boundary having distribution $\mathbf{W}^{\triangle}_{l+1}$. This is the irreducible component $M_v^\bullet$ associated to this loop in Scoop$(\mathcal{H}_b)$. The peeling process follows the right boundary of $\mathcal{H}_b$. Since $\liminf_{k\to+\infty} B_k = -\infty$ a.s., the left and right boundaries of the hull intersect infinitely many times during the exploration. This ensures that the whole hull $\mathcal{H}_b$ is revealed by the peeling process (i.e. that $\mathbf{B}_R(\mathcal{H}_b)$ is eventually revealed for every $R \geq 0$). Moreover, the sequence $\{\mathbf{L}_k : k \in \mathbb{N}\}$ is a consistent exhaustion of the looptree $\mathbf{L}_B$. Thus, the scooped-out boundary Scoop$(\mathcal{H}_b)$ is isomorphic to $\mathbf{L}_B$. By Proposition 7.3.10, the tree of components $\mathbf{T}_B = \mathbf{Tree}(\mathcal{H}_b)$ has distribution $\mathsf{GW}^{(\infty,l)}_{\mu_\circ,\mu_\bullet}$.

The same argument shows that Scoop$(\mathcal{H}_w)$ is isomorphic to $\mathbf{L}_W$ (up to a reflection and a suitable rooting convention), and the independence of B and W concludes the proof. □

Remark 7.4.6. We proved in particular that $\mathcal{H}_b$ and $\mathcal{H}_w$ are one-ended triangulations with an infinite boundary. They have the same law up to a reflection, which is clear since $p_c = 1/2$. Note that $\mu_\bullet$ being supported on $\mathbb{N}$, there is no black leaf in the tree of components a.s. (this would correspond to a self-loop in the UIHPT, which is not allowed under our 2-connectedness assumption).

Let us explain how the hulls are connected in the UIHPT. We define a planar map with an infinite simple boundary $\mathbf{N}$ as follows. Let $\{c_i : i \in \mathbb{N}\}$ be the corners of the right boundary of $\mathcal{H}_b$ listed in contour order, and similarly for $\{c'_i : i \in \mathbb{N}\}$ with the left boundary of $\mathcal{H}_w$. Then, let $\mathbf{N}$ be the map with vertex set $\{c_i, c'_i : i \in \mathbb{N}\}$, such that two vertices are neighbours iff the associated corners are connected by an edge in the UIHPT. (Loosely speaking, we consider the sub-map of the UIHPT generated by

the right boundary of $\mathcal{H}_b$ and the left boundary of $\mathcal{H}_w$, but we split the pinch-points of these boundaries.)

Proposition 7.4.7. *The infinite planar map* $\mathbf{N}$ *has distribution* $\mathsf{UN}(\infty,\infty)$. *Otherwise said,* $\mathcal{H}_b$ *and* $\mathcal{H}_w$ *are glued along an independent uniform infinite necklace.*

Remark 7.4.8. Due to the "Black-White" boundary condition, Proposition 7.4.7 ensures that the infinite map generated by $\mathcal{H}_b$ and $\mathcal{H}_w$ in the UIHPT (i.e. the map revealed by the peeling process) is $\Psi_{\mathbf{N}}(\mathcal{H}_b,\mathcal{H}_w)$. Note that the edges of the uniform infinite necklace are exactly the edges that are peeled.

Proof. For every $k\in\mathbb{Z}_+$ such that $Y_k^{(1)}\neq 0$, the third vertex of the revealed face at step k of the peeling process is open, and defines the k-th corner of $\partial\mathcal{H}_b$ in right contour order. In such a situation, there is an edge between this corner and the last (closed) corner of $\partial\mathcal{H}_w$ that has been discovered. The converse occurs when $Y_k^{(2)}\neq 0$. By Lemma 7.4.3, the variables

$$z_k := \mathbf{1}_{\left\{Y_k^{(2)}=0\right\}} = \mathbf{1}_{\left\{Y_k^{(1)}\neq 0\right\}}, \quad k\in\mathbb{N},$$

are independent with Bernoulli distribution of parameter $1/2$, and independent of B and W. We obtain the uniform infinite necklace. □

7.4.3 Proof of the decomposition result

Proof of Theorem 7.2.3. The proof is based on Propositions 7.4.4 and 7.4.7. However, it remains to show that the percolation hulls $\mathcal{H}_b$ and $\mathcal{H}_w$, and the infinite necklace $\mathbf{N}$ cover the entire map, or in other words that the peeling process discovers the whole UIHPT.

For every $n\in\mathbb{N}$, let M_n be the map revealed at step n of the peeling process, and denote by M_∞ the underlying UIHPT (with origin vertex ρ). We denote by $\{\tau_k^\bullet : k\in\mathbb{Z}_+\}$ and $\{\tau_k^\circ : k\in\mathbb{Z}_+\}$ the endpoints of the excursions intervals of B and W above their infimums, defined as in (7.7), and set

$$\phi(n) := \sigma^B_{\tau_n^\bullet}\vee\sigma^W_{\tau_n^\circ}, \quad n\in\mathbb{N}.$$

We have $\phi(n)<\infty$ a.s. for every $n\in\mathbb{N}$. We consider the sequence of sub-maps of M_∞ given by $\{M_{\phi(n)} : n\in\mathbb{N}\}$. For every $n\in\mathbb{N}$, we let d_n stand for the graph distance on $M_{\phi(n)}$ and denote by $\partial M_{\phi(n)}$ the boundary of $M_{\phi(n)}$ as a sub-map of M_∞. More precisely,

$$\partial M_{\phi(n)} := \left\{v\in M_{\phi(n)} : \exists\, u\in M_\infty\backslash M_{\phi(n)} \text{ s.t. } u\sim v\right\}. \tag{7.17}$$

Let $\{v_k^\bullet : k\in\mathbb{Z}_+\}$ and $\{v_k^\circ : k\in\mathbb{Z}_+\}$ be the white vertices of the spine in $\mathbf{T}_B$ and $\mathbf{T}_W$, seen as vertices of $\mathbf{L}_B=\mathsf{Scoop}(\mathcal{H}_b)$ and $\mathbf{L}_W=\mathsf{Scoop}(\mathcal{H}_w)$ (and thus of $\mathcal{H}_b$ and $\mathcal{H}_w$). Namely,

$$v_k^\bullet := p_B\left(B_{\tau_k^\bullet}\right) \quad\text{and}\quad v_k^\circ := p_W\left(W_{\tau_k^\circ}\right), \quad k\in\mathbb{Z}_+.$$

Note that the vertices $v_0^\bullet,\dots,v_n^\bullet$ and $v_0^\circ,\dots,v_n^\circ$ can be identified in $M_{\phi(n)}$, since $\{\tau_k^\bullet : k\in\mathbb{Z}_+\}$ and $\{\tau_k^\circ : k\in\mathbb{Z}_+\}$ are stopping times in the filtration of the exploration process. Moreover, these vertices are cut-points: they disconnect the origin from infinity

in $\mathbf{L}_B$ (resp. $\mathbf{L}_W$). We now define an equivalence relation $\approx$ on the set $V(M_{\phi(n)})$ of vertices of $M_{\phi(n)}$ as follows:

For every $k \in \{0, \dots, n\}$ and every $v \in V(\mathcal{H}_b \cap M_{\phi(n)})$, $v \approx v_k^\bullet$ iff there exists a geodesic path from v to the origin of $\mathcal{H}_b$ that contains $v_k^\bullet$, but does not contain $v_{k+1}^\bullet$ if $k < n$.

We define symmetric identifications on $V(\mathcal{H}_w \cap M_{\phi(n)})$. Roughly speaking, for every $k \in \{0, \dots, n-1\}$, the vertices of $\mathcal{H}_b$ between $v_k^\bullet$ and $v_{k+1}^\bullet$ (excluded) are identified to $v_k^\bullet$, and all the vertices of $\mathcal{H}_b$ above $v_n^\bullet$ are identified to $v_n^\bullet$ (and similarly in $\mathcal{H}_w$). We denote the quotient map $M_{\phi(n)}/\approx$ by $M'_{\phi(n)}$ (the root edge of $M'_{\phi(n)}$ is the root edge of M_∞). The graph distance on $M'_{\phi(n)}$ is denoted by d'_n. The family $\{M'_{\phi(n)} : n \in \mathbb{N}\}$ is a consistent sequence of locally finite maps with origin $v_0^\bullet = \rho$. Moreover, for every $n \in \mathbb{N}$, the boundary of $M'_{\phi(n)}$ in $M'_{\phi(n+1)}$ is $\{v_n^\bullet, v_n^\circ\}$. Thus, the sequences $\{d'_n(\rho, v_n^\circ) : n \in \mathbb{N}\}$ and $\{d'_n(\rho, v_n^\bullet) : n \in \mathbb{N}\}$ are non-decreasing and diverge a.s.. By definition of $\approx$ and since we discover the finite regions swallowed by the peeling process, the representatives of $\partial M_{\phi(n)}$ in $M'_{\phi(n)}$ are $v_n^\bullet$ and v_n°. As a consequence,

$$d_n\left(\rho, \partial M_{\phi(n)}\right) \underset{n\to\infty}{\longrightarrow} \infty \quad \text{a.s..} \tag{7.18}$$

This implies that a.s. for every $R \in \mathbb{Z}_+$, the ball of radius R of the UIHPT $\mathbf{B}_R(M_\infty)$ is contained in $M_{\phi(n)}$ for n large enough, and concludes the argument. □

7.5 The incipient infinite cluster of the UIHPT

The goal of this section is to introduce the IIC probability measure, and prove the convergence and decomposition result of Theorem 7.2.5.

7.5.1 Exploration process

We consider a Bernoulli percolation model with parameter p on the UIHPT, conditionally on the "White-Black-White" boundary condition of Figure 7.10. From now on, we assume that $p \in [p_c, 1)$. As in Section 7.4 we use a peeling process of the UIHPT, which combines two versions of Algorithm 7.4.1.

ALGORITHM 7.5.1. Let $p \in [p_c, 1)$ and consider a percolated UIHPT with distribution $\mathbf{P}_p$ and "White-Black-White" boundary condition. Let $n, m \in \mathbb{N}$ such that $n \geq m$. The first part of the algorithm is called the *left peeling*.

1. **Left peeling.** While the finite open segment on the boundary has size less than $n+1$:
   - Reveal the face incident to the (leftmost) "White-Black" edge on the boundary. If there is no such edge, reveal the face incident to the leftmost exposed edge at the previous step.
   - Repeat the operation on the unique infinite connected component of the map deprived of the revealed face.

When the finite open segment on the boundary has size larger than $n+1$, we start a second part which we call the *right peeling*.

2. **Right peeling.** While the finite open segment on the boundary of the map has size greater than $n+1-m$:
   - Reveal the face incident to the (rightmost) "Black-White" edge on the boundary. If there is no such edge, reveal the face incident to the left-most exposed edge at the previous step.
   - Repeat the operation on the unique infinite connected component of the map deprived of the revealed face.

   The algorithm ends when the left and right peelings are completed.

Remark 7.5.2. By definition, the left and right peelings stop when the length of the open segment reaches a given value. However, it is convenient to define both peeling processes *continued forever*. We systematically consider such processes, and use the terminology *stopped peeling process* otherwise. Nevertheless, the right peeling is defined on the event that the left peeling ends, i.e. that the open segment on the boundary reaches size $n+1$.

Intuitively, the left and right peelings explore the percolation interface between the open cluster of the origin and the closed clusters of its left and right neighbours on the boundary. Note that the peeling processes are still defined when the open segment on the boundary is swallowed, although they do not follow any percolation interface in such a situation.

As for Algorithm 7.4.1, by the spatial Markov property, Algorithm 7.5.1 is well-defined and has i.i.d. steps. We use the notation of Section 7.4.1 for the number of exposed edges, swallowed edges on the left and right, and colour of the revealed vertex (if any) at step k of the left and right peeling processes. We use the exponents l and r to distinguish the quantities concerning the left and right peelings.

The peeling processes are fully described by the associated exploration processes $X^{(l)} = \{X_k^{(l)} = (X_k^{(l,1)}, X_k^{(l,2)}) : k \in \mathbb{Z}_+\}$ and $X^{(r)} = \{X_k^{(r)} = (X_k^{(r,1)}, X_k^{(r,2)}) : k \in \mathbb{Z}_+\}$, defined by

$$X_0^{(l)} = X_0^{(r)} = (0,0) \quad \text{and} \quad X_k^{(l)} := \sum_{i=1}^{k} Y_i^{(l)},\ X_k^{(r)} := \sum_{i=1}^{k} Y_i^{(r)}, \quad k \in \mathbb{N},$$

where for every $k \in \mathbb{N}$,

$$Y_k^{(l)} := \left(\mathbf{1}_{\left\{c_k^{(l)}=1\right\}} - \mathcal{R}_{l,k}^{(l)}, \mathbf{1}_{\left\{c_k^{(l)}=0\right\}} - \mathcal{R}_{r,k}^{(l)} \right)$$

and

$$Y_k^{(r)} := \left(\mathbf{1}_{\left\{c_k^{(r)}=1\right\}} - \mathcal{R}_{l,k}^{(r)}, \mathbf{1}_{\left\{c_k^{(r)}=0\right\}} - \mathcal{R}_{r,k}^{(r)} \right).$$

The exploration processes $X^{(l)}$ and $X^{(r)}$ have respective lifetimes

$$\sigma_n^{(l)} := \inf\left\{k \in \mathbb{Z}_+ : X_k^{(l,1)} \geq n\right\} \quad \text{and} \quad \sigma_m^{(r)} := \inf\left\{k \in \mathbb{Z}_+ : X_k^{(r,1)} \leq -m\right\}. \quad (7.19)$$

The right peeling process is defined on the event $\{\sigma_n^{(l)} < \infty\}$. However, the assumption $p \geq p_c$ guarantees that a.s. for every $n \in \mathbb{N}$, $\sigma_n^{(l)} < \infty$ and the left peeling ends. On the contrary, when $p > p_c$, with positive probability $\sigma_m^{(r)} = \infty$ and the right peeling does not end.

We now extract information on the percolation clusters, and introduce the processes $B^{(l)} = \{B_k^{(l)} : k \in \mathbb{Z}_+\}$, $W^{(l)} = \{W_k^{(l)} : k \in \mathbb{Z}_+\}$, $B^{(r)} = \{B_k^{(r)} : k \in \mathbb{Z}_+\}$ and $W^{(r)} = \{W_k^{(r)} : k \in \mathbb{Z}_+\}$ defined by

$$\left(B_k^{(l)}, W_k^{(l)}\right) := \left(X^{(l,1)}_{\sigma_k^{(B,l)}}, X^{(l,2)}_{\sigma_k^{(W,l)}}\right) \quad \text{and} \quad \left(B_k^{(r)}, W_k^{(r)}\right) := \left(X^{(r,1)}_{\sigma_k^{(B,r)}}, X^{(r,2)}_{\sigma_k^{(W,r)}}\right), \quad k \in \mathbb{Z}_+,$$

where we use the same definitions as in (7.15) for the stopping times. We define as in (7.16) the random variables $\{z_k^{(l)} : k \in \mathbb{N}\}$ and $\{z_k^{(r)} : k \in \mathbb{N}\}$. The exploration process $X^{(l)}$ is measurable with respect to $B^{(l)}$, $W^{(l)}$ and $z^{(l)}$ (and the same holds when replacing l by r). The lifetimes of the processes $B^{(l)}$ and $B^{(r)}$ are defined by

$$T_n^{(B,l)} := \inf\left\{k \in \mathbb{Z}_+ : B_k^{(l)} \geq n\right\} \quad \text{and} \quad T_m^{(B,r)} := \inf\left\{k \in \mathbb{Z}_+ : B_k^{(r)} \leq -m\right\}, \tag{7.20}$$

while the lifetimes of $W^{(l)}$ and $W^{(r)}$ read

$$T_n^{(W,l)} := \sigma_n^{(l)} - T_n^{(B,l)} \quad \text{and} \quad T_m^{(W,r)} := \sigma_m^{(r)} - T_m^{(B,r)}.$$

When $p > p_c$, $\sigma_m^{(r)} = \infty$ with positive probability, in which case $T_m^{(B,r)} = \infty$ (and by convention, $T_m^{(W,r)} = \infty$). Thus, $\{\sigma_m^{(r)} < \infty\}$ is measurable with respect to $T_m^{(B,r)}$ and $T_m^{(W,r)}$. For every $k \in \mathbb{N} \cup \{\infty\}$ and every $p \in (0,1)$, we denote by $\mathsf{NB}(k,p)$ the negative binomial distribution with parameters k and p (where $\mathsf{NB}(\infty, p)$ is a Dirac mass at infinity).

Lemma 7.5.3. *Let $p \in [p_c, 1)$ and $n, m \in \mathbb{N}$ such that $n \geq m$. The following hold under $\mathbf{P}_p$.*

- ***Left peeling.*** *$\{B_k^{(l)} : 0 \leq k \leq T_n^{(B,l)}\}$ is a random walk with step distribution μ_p, killed at the first entrance in $[n, +\infty)$. Conditionally on $T_n^{(B,l)}$, $T_n^{(W,l)}$ has distribution $\mathsf{NB}(T_n^{(B,l)}, g(p))$. Then, conditionally on $T_n^{(W,l)}$, $\{W_k^{(l)} : 0 \leq k \leq T_n^{(W,l)}\}$ is a random walk with step distribution μ_{1-p}, independent of $B^{(l)}$. Finally, conditionally on $T_n^{(B,l)}$ and $T_n^{(W,l)}$, $\{z_k^{(l)} : 1 \leq k \leq \sigma_n^{(l)} - 1\}$ is uniformly distributed among the set of binary sequences with $T_n^{(W,l)}$ zeros and $T_n^{(B,l)} - 1$ ones.*
- ***Right peeling.*** *The above results hold when replacing l by r, except that $\{B_k^{(r)} : 0 \leq k \leq T_m^{(B,r)}\}$ is killed at the first entrance in $(-\infty, -m]$. Moreover, $\sigma_m^{(r)}$ is possibly infinite: conditionally on $T_m^{(B,r)}$ and $T_m^{(W,r)}$, $\{z_k^{(r)} : 1 \leq k \leq \sigma_m^{(r)} - 1\}$ is uniformly distributed among the set of binary sequences with $T_m^{(W,r)}$ zeros and $T_m^{(B,r)} - 1$ ones on the event $\{\sigma_m^{(r)} < \infty\}$, and distributed as a sequence of i.i.d. variables with Bernoulli distribution of parameter $g(p)$ on the event $\{\sigma_m^{(r)} = \infty\}$.*

Lastly, $X^{(r)}$ is independent of $\{X_k^{(l)} : 0 \leq k \leq \sigma_n^{(l)}\}$. (However, it is not independent of the whole process $X^{(l)}$.)

Proof. By the spatial Markov property, $X^{(r)}$ is independent the map revealed by the left peeling process, i.e. of $\{X_k^{(l)} : 0 \leq k \leq \sigma_n^{(l)}\}$. Moreover, $X^{(l)}$ and $X^{(r)}$ are distributed as the process X of Definition 7.4.2. We restrict our attention to the left peeling. By Lemma 7.4.3, $B^{(l)}$ and $W^{(l)}$ are independent random walks with step distribution μ_p and μ_{1-p}, while $z^{(l)}$ is an independent sequence of i.i.d. variables with Bernoulli distribution of parameter $g(p)$. The first assertion follows from the definition of $T_n^{(B,l)}$. The random time $\sigma_n^{(l)}$ being measurable with respect to $X^{(l,1)}$, it is independent of $W^{(l)}$. Thus, conditionally on $T_n^{(B,l)}$ the lifetime of $W^{(l)}$ is exactly the number of failures before the $T_n^{(B,l)}$-th success in a sequence of independent Bernoulli trials with parameter $g(p)$. This is the second assertion. By definition, $Y^{(1,l)}_{\sigma_n^{(l)}} \neq 0$ so that $z^{(l)}_{\sigma_n^{(l)}} = 1$. Conditionally on $T_n^{(B,l)}$ and $T_n^{(W,l)}$, the binary sequence $\{z_k^{(l)} : 1 \leq k \leq \sigma_n^{(l)} - 1\}$ is uniform among all possibilities by definition of the negative binomial distribution. The properties of the right peeling follow from a slight adaptation of these arguments. □

We now describe the events we condition on to force an infinite critical open percolation cluster and define the IIC. As in [Kes86a], we use two distinct conditionings. Firstly, $B^{(l)}$ describes the length of the open segment on the boundary of the unexplored map (before the left peeling stops). This segment represents the revealed part of the left boundary of $\mathcal{C}$ (the open cluster of the origin). We define the height $h(\mathcal{C})$ of $\mathcal{C}$ by

$$h(\mathcal{C}) := \sup\left\{B_k^{(l)} : 0 \leq k \leq T\right\}, \quad \text{where} \quad T := \inf\left\{k \in \mathbb{Z}_+ : B_k^{(l)} < 0\right\}. \tag{7.21}$$

This is also the length of the loop-erasure of the open path revealed by the left peeling. Note that both the perimeter of the hull $\mathcal{H}$ of $\mathcal{C}$ and its size $|\mathcal{C}|$ are larger than $h(\mathcal{C})$. Consistently, we want to condition the height of the cluster to be larger than n. In terms of the exploration process, this exactly means that $B^{(l)}$ reaches $[n, +\infty)$ before $(-\infty, 0)$:

$$\{h(\mathcal{C}) \geq n\} = \left\{T_n^{(B,l)} < T\right\}.$$

We thus work under $\mathbf{P}(\cdot \mid h(\mathcal{C}) \geq n)$ and let n go to infinity. Secondly, we let $p > p_c = 1/2$ and condition $\mathcal{C}$ to be infinite (which is an event of positive probability under $\mathbf{P}_p$). In other words, we work under $\mathbf{P}_p(\cdot \mid |\mathcal{C}| = \infty)$ and let p decrease towards p_c.

We now describe the law of the exploration process under these conditional probability measures, starting with $\mathbf{P}(\cdot \mid h(\mathcal{C}) \geq n)$. In the next part, we voluntarily choose the same parameter n for the definition of the left peeling process and the conditioning $\{h(\mathcal{C}) \geq n\}$. This will make our argument simpler. The event $\{h(\mathcal{C}) \geq n\} = \{T_n^{(B,l)} < T\}$ is measurable with respect to $\{B_k^{(l)} : 0 \leq k \leq T_n^{(B,l)}\}$. By Lemma 7.5.3, it is then independent of the other variables involved in the stopped left peeling process.

Lemma 7.5.4. *Let $n, m \in \mathbb{N}$ such that $n \geq m$. Under $\mathbf{P}(\cdot \mid h(\mathcal{C}) \geq n)$, the statements of Lemma 7.5.3 (under $\mathbf{P}$) hold except that $\{B_k^{(l)} : 0 \leq k \leq T_n^{(B,l)}\}$ is a random walk conditioned to reach $[n, +\infty)$ before $(-\infty, 0)$ (and killed at that entrance time).*

We now describe the exploration process under $\mathbf{P}_p(\cdot \mid |\mathcal{C}| = \infty)$, for $p > p_c$.

Lemma 7.5.5. *Let $p > p_c$ and $n, m \in \mathbb{N}$ such that $n \geq m$. Under $\mathbf{P}_p(\cdot \mid |\mathcal{C}| = \infty)$, the statements of Lemma 7.5.3 (under $\mathbf{P}_p$) hold except that $\{B_k^{(l)} : 0 \leq k \leq T_n^{(B,l)}\}$ is a random walk conditioned to stay nonnegative killed at the first entrance in $[n, +\infty)$, and $\{B_k^{(r)} : 0 \leq k \leq T_m^{(B,r)}\}$ is a random walk conditioned to stay larger than $-n$ killed at the first entrance in $(-\infty, -m]$.*

Proof. We consider the left peeling first. From the proof of $p_c = 1/2$ in [Ang04], we get that

$$\{|\mathcal{C}| = \infty\} = \{T = \infty\} \quad \mathbf{P}_p\text{-a.s.}.$$

Indeed, with probability one, if T is finite the open segment on the boundary is swallowed by the exploration and $\mathcal{C}$ is confined in a finite region, while if T is infinite the exploration reveals infinitely many open vertices connected to the origin by an open path. In particular, the event $\{|\mathcal{C}| = \infty\}$ is measurable with respect to $B^{(l)}$, and thus independent of $W^{(l)}$ and $z^{(l)}$ by Lemma 7.4.3. The first assertion follows.

We now focus on the right peeling process and denote by M_∞ the underlying UIHPT. The event $\{T_n^{(B,l)} < \infty\} \cap \{T_n^{(B,l)} < T\}$ has probability one under $\mathbf{P}_p(\cdot \mid |\mathcal{C}| = \infty)$. Thus, the right exploration is performed in a half-planar triangulation M'_∞ with distribution $\mathbf{P}_p$ and a "White-Black-White" boundary condition (the open segment on the boundary has size $n+1$ and its rightmost vertex is the origin of M_∞). Since the stopped left peeling reveals a.s. finitely many vertices, the open cluster of the origin $\mathcal{C}$ in M_∞ is infinite iff the open cluster of the origin $\mathcal{C}'$ in M'_∞ is infinite. In other words, the right exploration is distributed as the exploration process of the UIHPT with the above boundary condition under $\mathbf{P}_p(\cdot \mid |\mathcal{C}| = \infty)$, and is independent of $\{X_k^{(l)} : 0 \leq k \leq \sigma_n^{(l)}\}$. By the same argument as above,

$$\{|\mathcal{C}| = \infty\} = \{T'_{-n} = \infty\} \quad \mathbf{P}_p\text{-a.s.}, \quad \text{where } T'_{-n} := \inf\left\{k \in \mathbb{Z}_+ : B_k^{(r)} < -n\right\}.$$

Again, $\{|\mathcal{C}| = \infty\}$ is measurable with respect to $B^{(r)}$, and thus independent of $W^{(r)}$ and $z^{(r)}$ by Lemma 7.4.3. This ends the proof. □

7.5.2 Distribution of the revealed map

We consider the peeling process of Algorithm 7.5.1 under the probability measures $\mathbf{P}(\cdot \mid h(\mathcal{C}) \geq n)$ and $\mathbf{P}_p(\cdot \mid |\mathcal{C}| = \infty)$. We let M_∞ be the underlying infinite triangulation of the half-plane.

We denote by $M_{n,m}$ the planar map that is revealed by the peeling process of Algorithm 7.5.1 with parameters $n, m \in \mathbb{N}$. Namely, the vertices and edges of $M_{n,m}$ are those discovered by the stopped peeling process (including the swallowed regions). However, by convention, we exclude the edges and vertices discovered at the last step of both the left and right (stopped) peeling processes. This will make our description simpler. The root edge of $M_{n,m}$ is the root edge of M_∞. By definition, $M_{n,m}$ is infinite on the event $\{\sigma_m^{(r)} = \infty\}$. The goal of this section is to provide a decomposition of the map $M_{n,m}$.

The percolation hulls. We now extend our definition of the percolation hulls to the possibly finite map $M_{n,m}$. The origin ρ of M_∞ and its left and right neighbours ρ_l and ρ_r on the boundary belong to $M_{n,m}$. The percolation hull $\mathcal{H}$ of ρ in $M_{n,m}$ is the cluster of ρ together with the connected components of its complement in $M_{n,m}$ that do not contain ρ_l or ρ_r. This extends to the hulls of ρ_l and ρ_r, for which we use the notation $\mathcal{H}_l$ and $\mathcal{H}_r$. We let

$$\underline{W}^{(l)} := \min_{0\le k\le T_n^{(W,l)}} W_k^{(l)} \quad \text{and} \quad \underline{W}^{(r)} := \min_{0\le k\le T_m^{(W,r)}} W_k^{(r)},$$

and define the finite sequences $w^{(l)}$ and $w^{(r)}$ by

$$w_k^{(l)} = \begin{cases} k & \text{if } -\underline{W}^{(l)} \le k < 0 \\ W_k^{(l)} & \text{if } 0 \le k \le T_n^{(W,l)} \end{cases} \quad \text{and} \quad w_k^{(r)} = \begin{cases} k & \text{if } -\underline{W}^{(r)} \le k < 0 \\ W_{-k}^{(r)} & \text{if } 0 \le k \le T_m^{(W,r)} \end{cases}. \tag{7.22}$$

We define equivalence relations on $\{-T_n^{(W,l)},\dots,-\underline{W}^{(l)}\}$ and $\{-T_m^{(W,r)},\dots,-\underline{W}^{(r)}\}$ by applying (7.5) with $w^{(l)}$ and $w^{(r)}$. By the construction of Section 7.3.1, this defines two planar maps which are not looptrees in general. Nonetheless, we denote them by $\mathbf{L}_{w^{(l)}}$ and $\mathbf{L}_{w^{(r)}}$ to keep the notation simple. We replace $\mathbf{L}_{w^{(l)}}$ by its image under a reflection. The left (resp. right) boundary of $\mathbf{L}_{w^{(l)}}$ is the projection of nonpositive (resp. nonnegative) integers of $\{-T_n^{(W,l)},\dots,-\underline{W}^{(l)}\}$ on $\mathbf{L}_{w^{(l)}}$. The same holds when replacing l by r, up to inverting left and right boundaries. We choose the root edges consistently. The sequence $w^{(l)}$ and $\mathbf{L}_{w^{(l)}}$ are a.s. finite, while $w^{(r)}$ and thus $\mathbf{L}_{w^{(r)}}$ are infinite on the event $\{\sigma_m^{(r)} = \infty\}$. We introduce the finite sequences $b^{(l)}$ and $b^{(r)}$ defined by

$$b_k^{(l)} = B_k^{(l)}, \quad 0 \le k < T_n^{(B,l)} \quad \text{and} \quad b_k^{(r)} = B_k^{(r)}, \quad 0 \le k < T_m^{(B,r)}. \tag{7.23}$$

We define an equivalence relation on $\{-T_n^{(B,l)}+1,\dots,T_m^{(B,r)}-1\}$ by applying (7.9), with $b^{(l)}$ (resp. $b^{(r)}$) playing the role of C' (resp. C). By the construction of Section 7.3.1, this defines a planar map that we denote by $\mathbf{L}_{b^{(l)},b^{(r)}}$, which is not a looptree either. (It is also obtained by defining $\mathbf{L}_{b^{(r)}}$ and the finite forest of looptrees $\mathbf{F}_{b^{(l)}}$ as above, and gluing them along their boundaries as in Section 7.3.1.) The left (resp. right) boundary of $\mathbf{L}_{b^{(l)},b^{(r)}}$ is the projection of nonpositive (resp. nonnegative) integers of $\{-T_n^{(B,l)}+1,\dots,T_m^{(B,r)}-1\}$ (and we choose the root edge consistently). Again, $\mathbf{L}_{b^{(l)},b^{(r)}}$ is infinite on the event $\{\sigma_m^{(r)} = \infty\}$.

Proposition 7.5.6. *Let $n, m \in \mathbb{N}$ such that $n \ge m$. Under $\mathbf{P}(\cdot \mid h(\mathcal{C}) \ge n)$ and $\mathbf{P}_p(\cdot \mid |\mathcal{C}| = \infty)$, in the map $M_{n,m}$, the percolation hulls $\mathcal{H}$, $\mathcal{H}_l$ and $\mathcal{H}_r$ are the independent random maps $\mathbf{L}_{b^{(l)},b^{(r)}}$, $\mathbf{L}_{w^{(l)}}$ and $\mathbf{L}_{w^{(r)}}$ in which each internal face of degree $l \ge 2$ is filled in with an independent triangulation with distribution $\mathbb{W}_l^\triangle$ equipped with a Bernoulli percolation model with parameter p_c (resp. p).*

Proof. The proof follows the same lines as Proposition 7.4.4, to which we refer for more details. We begin with the left peeling, which follows the percolation interface between $\mathcal{H}_l$ and $\mathcal{H}$. On the one hand, the right contour of $\mathcal{H}_l$ is encoded by $\{W_k^{(l)} : 0 \le k \le T_n^{(W,l)}\}$ and $-\underline{W}^{(l)}$ vertices are discovered on the left boundary of M_∞. We

obtain the map $\mathbf{L}_{w^{(l)}}$. On the other hand, the left contour of $\mathcal{H}$ is encoded by $b^{(l)}$, which defines the forest of finite looptrees $\mathbf{F}_{b^{(l)}}$ (by applying (7.5)). We now deal with the right peeling, that starts a.s. in a triangulation of the half-plane with an open segment of size $n+1$ on the boundary. This segment corresponds (up to the last vertex) to the right boundary of $\mathbf{F}_{b^{(l)}}$, i.e. to the set

$$\mathsf{V}_l := \left\{ 0 \le k < T_n^{(B,l)} : B_k^{(l)} = \inf_{k \le i < T_n^{(B,l)}} B_i^{(l)} \right\}. \tag{7.24}$$

The right peeling follows the percolation interface between $\mathcal{H}$ and $\mathcal{H}_r$. In particular, the right contour of $\mathcal{H}$ is encoded by $b^{(r)}$. By construction, vertices associated to the set

$$\mathsf{V}_r := \left\{ 0 \le k < T_m^{(B,r)} : B_k^{(r)} = \inf_{0 \le i \le k} B_i^{(r)} \right\} \tag{7.25}$$

are identified with the right boundary of $\mathbf{F}_{b^{(l)}}$. Precisely, every $k \in \mathsf{V}_r$ such that $B_k^{(r)} = -j$ is matched to the $(j+1)$-th element of V_l (note that $-\inf(b^{(r)}) \le m \le n$). We obtain the map $\mathbf{L}_{b^{(l)},b^{(r)}}$. Finally, $\{W_k^{(r)} : 0 \le k \le T_m^{(W,r)}\}$ encodes the left contour of $\mathcal{H}_r$ and $-\underline{W}^{(r)}$ vertices are discovered on the right boundary of M_∞, which gives the map $\mathbf{L}_{w^{(r)}}$.

The spatial Markov property shows that the finite faces of $\mathbf{L}_{b^{(l)},b^{(r)}}$, $\mathbf{L}_{w^{(l)}}$ and $\mathbf{L}_{w^{(r)}}$ are filled in with independent percolated Boltzmann triangulations with a simple boundary (the boundary conditions are fixed by the hulls and the percolation parameter by the underlying model). By definition of $M_{n,m}$, we then recover the whole percolation hulls $\mathcal{H}$, $\mathcal{H}_l$ and $\mathcal{H}_r$. □

We now focus on the connection between the percolation hulls in $M_{n,m}$. In order to make the next statement simpler, we generalize the definition of the uniform necklace.

Definition 7.5.7. Let $x, y \in \mathbb{N}$ and $\{z_i : 1 \le i \le x+y\}$ uniform among the set of binary sequence with x ones and y zeros. Define

$$S_k := \sum_{i=1}^{k} z_i, \quad 1 \le k \le x+y.$$

The uniform necklace of size (x,y) is obtained from the graph of $[-x, y+1] \cap \mathbb{Z}$ by adding the set of edges $\{(-S_k, k+1-S_k) : 1 \le k \le x+y\}$. Its distribution is denoted by $\mathsf{UN}(x,y)$.

By convention, for $x = y = \infty$, $\mathsf{UN}(\infty,\infty)$ is the uniform infinite necklace of Section 7.2.3.

We now use a construction similar to that preceding Proposition 7.4.7. Let $V_l := \{c_i : 1 \le i \le T_n^{(W,l)} + 1\}$ be the corners of the right boundary of $\mathcal{H}_l$ listed in contour order, and similarly for $V_r := \{c'_i : 1 \le i \le T_n^{(B,l)}\}$ with the left boundary of $\mathcal{H}$. Then, let N_l be the planar map with vertex set $V_l \cup V_r$, such that two vertices are neighbours iff the associated corners are connected by an edge in the UIHPT. The planar map N_r is defined symmetrically with the right boundary of $\mathcal{H}$ and the left boundary of $\mathcal{H}_r$.

Proposition 7.5.8. *Let $n, m \in \mathbb{N}$ such that $n \geq m$. Under $\mathbf{P}(\cdot \mid h(\mathcal{C}) \geq n)$ and $\mathbf{P}_p(\cdot \mid |\mathcal{C}| = \infty)$, conditionally on $T_n^{(B,l)}$, $T_m^{(B,r)}$, $T_n^{(W,l)}$ and $T_m^{(W,r)}$, the following holds: N_l and N_r are independent uniform necklaces with distribution $\mathsf{UN}(T_n^{(W,l)}, T_n^{(B,l)} - 1)$ and $\mathsf{UN}(T_m^{(B,r)} - 1, T_m^{(W,r)})$. Otherwise said, in the map $M_{n,m}$, $\mathcal{H}_l$, $\mathcal{H}$ and $\mathcal{H}_r$ are glued along a pair of independent uniform necklaces with respective size $(T_n^{(W,l)}, T_n^{(B,l)} - 1)$ and $(T_m^{(B,r)} - 1, T_m^{(W,r)})$.*

Proof. We follow the arguments of Proposition 7.4.7. For every $k \in \mathbb{Z}_+$ such that $Y_k^{(l,1)} \neq 0$, there is an edge between the revealed open corner of the left boundary of $\mathcal{H}$ and the last revealed closed corner of the right boundary of $\mathcal{H}_l$. The converse occurs when $Y_k^{(l,2)} \neq 0$. Then, N_l is the uniform necklace generated by $\{z_k^{(l)} : 1 \leq k < \sigma_n^{(l)}\}$. Similarly, N_r is the uniform necklace generated by $\{z_k^{(r)} : 1 \leq k < \sigma_m^{(r)}\}$. We conclude by Lemmas 7.5.4 and 7.5.5. □

Since $M_{n,m}$ is the map revealed by the peeling process, we obtain a decomposition of this map illustrated in Figure 7.17 (in the finite case). The map $M_{n,m}$ is measurable with respect to the processes $w^{(l)}$, $w^{(r)}$, $b^{(l)}$ and $b^{(r)}$, the variables $z^{(l)}$ and $z^{(r)}$ defining the uniform necklaces and the percolated Boltzmann triangulations with a simple boundary that fill in the internal faces.

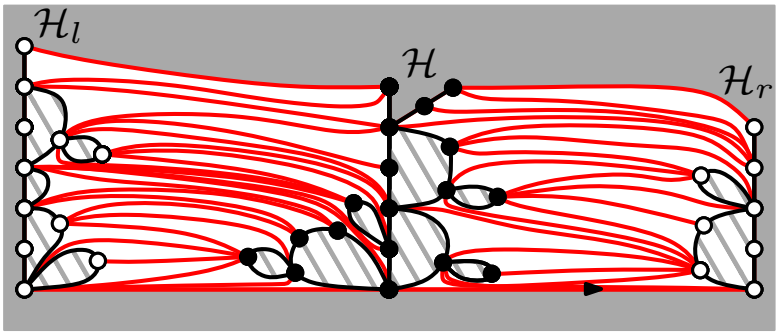

Figure 7.17: The decomposition of the map $M_{n,m}$ into percolation hulls and necklaces.

7.5.3 The IIC probability measure

In this section, we define a triangulation of the half-plane with distribution $\mathbf{P}_{\mathsf{IIC}}$. We use infinite looptrees, uniform necklaces and Boltzmann triangulations as building blocks.

Definition of the IIC. Let P be a probability measure and under P, let $A^{(l)} := \{A_k^{(l)} : k \in \mathbb{Z}_+\}$ be a random walk with law $P_0^{\mu\uparrow}$. Let also $A^{(r)} := \{A_k^{(r)} : k \in \mathbb{Z}_+\}$, $V^{(l)} := \{V_k^{(l)} : k \in \mathbb{Z}_+\}$ and $V^{(r)} := \{V_k^{(r)} : k \in \mathbb{Z}_+\}$ be random walks with law P_0^{μ}. Finally, let $y^{(l)} = \{y_k^{(l)} : k \in \mathbb{N}\}$ and $y^{(r)} = \{y_k^{(r)} : k \in \mathbb{N}\}$ be sequences of i.i.d. variables with Bernoulli distribution of parameter $1/2$. We assume that these processes are all independent under P.

Following Section 7.3.3, we define the looptrees $\mathbf{L}_{A^{(l)},A^{(r)}}$, $\mathbf{L}_{V^{(l)}}$ and $\mathbf{L}_{V^{(r)}}$. We replace $\mathbf{L}_{V^{(r)}}$ by its image under a reflection (with the root edge going from the vertex

0 to -1). By Propositions 7.3.10 and 7.3.11, the associated trees of components $\mathbf{T}_{A^{(l)},A^{(r)}}$, $\mathbf{T}_{V^{(l)}}$ and $\mathbf{T}_{V^{(r)}}$ have respective distribution $\mathsf{GW}^{\infty}_{\mu_\circ,\mu_\bullet}$, $\mathsf{GW}^{(\infty,l)}_{\mu_\circ,\mu_\bullet}$ and $\mathsf{GW}^{(\infty,r)}_{\mu_\circ,\mu_\bullet}$. We agree that the vertices of $\mathbf{L}_{A^{(l)},A^{(r)}}$ are open, while vertices of $\mathbf{L}_{V^{(l)}}$ and $\mathbf{L}_{V^{(r)}}$ are closed. For every vertex $v \in (\mathbf{T}_{A^{(l)},A^{(r)}})_\bullet$ (resp. $(\mathbf{T}_{V^{(l)}})_\bullet$, $(\mathbf{T}_{V^{(r)}})_\bullet$) we let M_v (resp. M_v^l, M_v^r) be a Boltzmann triangulation with distribution $\mathbf{W}^{\triangle}_{\deg(u)}$ (independent of all the other variables). Then, $\mathcal{H}$, $\mathcal{H}_l$ and $\mathcal{H}_r$ are defined by

$$\mathcal{H} := \Phi_{\mathsf{TC}}^{-1}\left(\mathbf{T}_{A^{(l)},A^{(r)}}, \left\{M_v : v \in \left(\mathbf{T}_{A^{(l)},A^{(r)}}\right)_\bullet\right\}\right), \ \mathcal{H}_l := \Phi_{\mathsf{TC}}^{-1}\left(\mathbf{T}_{V^{(l)}}, \left\{M_v^l : v \in (\mathbf{T}_{V^{(l)}})_\bullet\right\}\right)$$

and similarly for $\mathcal{H}_r$ replacing l by r. Finally, we let $\mathbf{N}_l$ and $\mathbf{N}_r$ be the uniform infinite necklaces with distribution $\mathsf{UN}(\infty,\infty)$ generated by $y^{(l)}$ and $y^{(r)}$. The infinite planar map M_∞ is defined by gluing $(\mathcal{H}_l, \mathcal{H}, \mathcal{H}_r)$ along $(\mathbf{N}_l, \mathbf{N}_r)$, i.e.

$$M_\infty := \Psi_{(\mathbf{N}_l,\mathbf{N}_r)}(\mathcal{H}_l, \mathcal{H}, \mathcal{H}_r).$$

In particular, the root edge of M_∞ connects the origin of $\mathbf{L}_{A^{(l)},A^{(r)}}$ to that of $\mathbf{L}_{V^{(r)}}$. The probability measure $\mathbf{P}_{\mathsf{IIC}}$ is the distribution of M_∞ under P.

The infinite planar map M_∞ is by construction one-ended, since infinite looptrees are one-ended themselves. It is also a (type 2) triangulation with an infinite simple boundary, and thus a triangulation of the upper half-plane. By definition, vertices of M_∞ are coloured and M_∞ has the "White-Black-White" boundary condition of Figure 7.10. Moreover, the planar maps $\mathcal{H}$, $\mathcal{H}_l$ and $\mathcal{H}_r$ are the percolation hulls of the origin vertex and its neighbours on the boundary in M_∞, which justifies the choice of notation.

Exploration of the IIC. For every $n, m \in \mathbb{N}$, we define a finite map $M_{n,m}$ under P, by replicating the construction of Section 7.5.2. Let

$$T_n^{(A,l)} := \inf\left\{k \in \mathbb{Z}_+ : A_k^{(l)} \geq n\right\} \quad \text{and} \quad T_m^{(A,r)} := \inf\left\{k \in \mathbb{Z}_+ : A_k^{(r)} \leq -m\right\}, \tag{7.26}$$

and conditionally on $T_n^{(A,l)}$ and $T_m^{(A,r)}$, let $T_n^{(V,l)}$ and $T_m^{(V,r)}$ be independent random variables with distribution $\mathsf{NB}(T_n^{(A,l)}, 1/2)$ and $\mathsf{NB}(T_m^{(A,r)}, 1/2)$. We let

$$\rho_n^{(l)} := T_n^{(A,l)} + T_n^{(V,l)} \quad \text{and} \quad \rho_m^{(r)} := T_m^{(A,r)} + T_m^{(V,r)}.$$

We define $v^{(l)}$ and $v^{(r)}$ as in (7.22) (replacing W by V), and $a^{(l)}$ and $a^{(r)}$ as in (7.23) (replacing B by A). Note that all the random times considered here are finite P-a.s.. Let us consider the finite planar maps $\mathbf{L}_{a^{(l)},a^{(r)}}$, $\mathbf{L}_{v^{(l)}}$ and $\mathbf{L}_{v^{(r)}}$, defined according to the construction of Section 7.5.2. As we will see in Proposition 7.5.9, these are possibly (though not always) sub-maps of the infinite looptrees $\mathbf{L}_{A^{(l)},A^{(r)}}$, $\mathbf{L}_{V^{(l)}}$ and $\mathbf{L}_{V^{(r)}}$. We now fill in each internal face of degree $l \geq 2$ of the finite maps with an independent percolated Boltzmann triangulation with distribution $\mathbf{W}_l^{\triangle}$. We agree that we use the same triangulations to fill in corresponding faces in the finite maps and their infinite counterparts when this is possible. Finally, we glue the right boundary of $\mathbf{L}_{v^{(l)}}$ and the left boundary of $\mathbf{L}_{a^{(l)},a^{(r)}}$ along the uniform necklace with size $(T_n^{(V,l)}, T_n^{(A,l)} - 1)$ generated by $\{y_k^{(l)} : 1 \leq k < \rho_n^{(l)}\}$. Similarly, we glue the left boundary of $\mathbf{L}_{v^{(r)}}$ and the right boundary of $\mathbf{L}_{a^{(l)},a^{(r)}}$ along the uniform necklace with size $(T_m^{(V,r)}, T_m^{(A,r)} - 1)$

generated by $\{y_k^{(r)} : 1 \le k < \rho_m^{(r)}\}$. These gluing operations are defined as in Section 7.2.3 provided minor adaptations to the finite setting. The resulting planar map is denoted by $M_{n,m}$.

Proposition 7.5.9. *A.s., for every $n \in \mathbb{N}$ and every $m \in \mathbb{N}$ such that $m \le \inf\{A_k^{(l)} : k \ge T_n^{(A,l)}\}$, $M_{n,m}$ is a sub-map of M_∞.*

Proof. Let $n, m \in \mathbb{N}$. We first consider the equivalence relation $\sim$ defined by applying (7.5) to $V^{(l)}$. The relation $i \sim j$ is determined by the values $\{V_k^{(l)} : i \wedge j \le k \le i \vee j\}$. Thus, the restriction of $\sim$ to $[-T_n^{(V,l)}, -\underline{V}^{(l)}] \cap \mathbb{Z}$ is isomorphic to $\mathbf{L}_{v^{(l)}}$, and $\mathbf{L}_{v^{(l)}}$ is a sub-map of $\mathbf{L}_{V^{(l)}}$. The same argument proves that $\mathbf{L}_{v^{(r)}}$ is a sub-map of $\mathbf{L}_{V^{(r)}}$, and that $\mathbf{F}_{a^{(l)}}$ (resp. $\mathbf{L}_{a^{(r)}}$) is a sub-map of the forest $\mathbf{F}_{A^{(l)}}$ (resp. the looptree $\mathbf{L}_{A^{(r)}}$). Moreover, the finite necklaces generated by $\{y_k^{(l)} : 1 \le k < \rho_n^{(l)}\}$ and $\{y_k^{(r)} : 1 \le k < \rho_m^{(r)}\}$ are sub-maps of the infinite uniform necklaces $\mathbf{N}_l$ and $\mathbf{N}_r$ generated by $y^{(l)}$ and $y^{(r)}$ in M_∞.

The only thing that remains to check is the gluing of $\mathbf{F}_{a^{(l)}}$ and $\mathbf{L}_{a^{(r)}}$ into $\mathbf{L}_{a^{(l)},a^{(r)}}$. Let $a := \{a_k : -T_n^{(A,l)} + 1 \le k \le T_m^{(A,r)} - 1\}$ and $A := \{A_k : k \in \mathbb{Z}\}$ be defined from $(a^{(l)}, a^{(r)})$ and $(A^{(l)}, A^{(r)})$ as in (7.8). We let $\sim_a$ and $\sim_A$ be the associated equivalence relations, defined from (7.9). When m is too large compared to n, $\sim_a$ is finer than the restriction of $\sim_A$ to $[-T_n^{(A,l)} + 1, T_m^{(A,r)} - 1] \cap \mathbb{Z}$ (see Figure 7.18 for an example). In other words, $\mathbf{L}_{a^{(l)},a^{(r)}}$ cannot be realized as a subset of $\mathbf{L}_{A^{(l)},A^{(r)}}$. By definition of $\sim_A$, such a situation occurs only if

$$-\inf_{0 \le k \le T_m^{(A,r)}-1} A_k^{(r)} > \inf_{k \ge T_n^{(A,l)}-1} A_k^{(l)}, \tag{7.27}$$

which is avoided for $m \le \inf\{A_k^{(l)} : k \ge T_n^{(A,l)}\}$. This concludes the proof. □

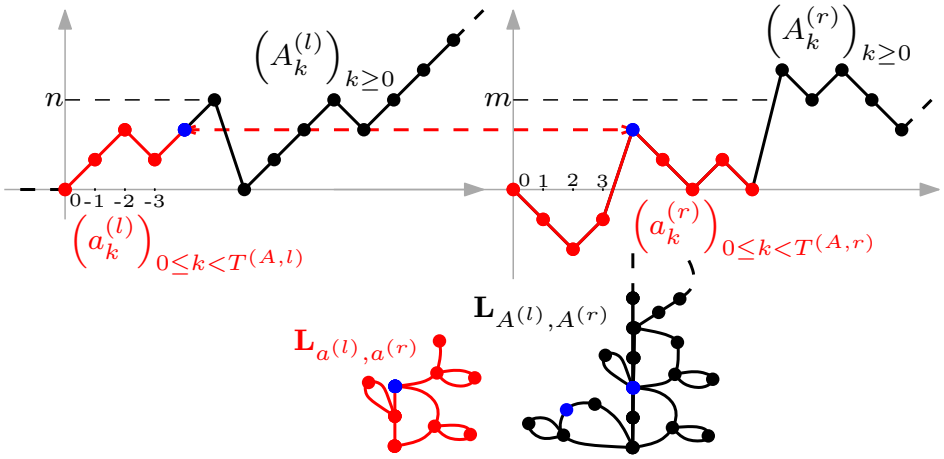

Figure 7.18: A configuration where $M_{n,m}$ cannot be realized as a subset of M_∞.

Convergence of the exploration processes. The goal of this paragraph is to prove that the distributions of the maps $M_{n,m}$ are close in total variation distance under $\mathbf{P}$, $\mathbf{P}(\cdot \mid h(\mathcal{C}) \ge n)$ and $\mathbf{P}_p(\cdot \mid |\mathcal{C}| = \infty)$ for a suitable choice of n, m, and p. In the next

part, $\mathcal{F}$ denotes the set of Borel functions from $\mathbb{Z}^{\mathbb{N}}$ to $[0,1]$. For every process Z and every stopping time T, $Z' := \{Z_k : 0 \leq k \leq T\}$ is interpreted as an element of $\mathbb{Z}^{\mathbb{N}}$ by putting $Z'_k = 0$ for $k > T$. We use the notation of Section 7.3.2 and start with two preliminary lemmas.

Lemma 7.5.10. *For every $n, m \in \mathbb{N}$ such that $n \geq m$,*

$$\limsup_{p \downarrow p_c} \sup_{F \in \mathcal{F}} \left| \mathbb{E}_p \left(F\left(B_k^{(l)} : 0 \leq k \leq T_n^{(B,l)}\right) \;\middle|\; |\mathcal{C}| = \infty \right) - E_0^{\mu\uparrow}\left(F\left(Z_k : 0 \leq k \leq T_n\right)\right) \right| = 0.$$

Proof. Let $\varepsilon > 0$, $n, m \in \mathbb{N}$ such that $n \geq m$ and $F \in \mathcal{F}$. By Lemma 7.5.5,

$$\mathbb{E}_p \left(F\left(B_k^{(l)} : 0 \leq k \leq T_n^{(B,l)}\right) \;\middle|\; |\mathcal{C}| = \infty \right) = E_0^{\mu_p\uparrow}\left(F\left(Z_k : 0 \leq k \leq T_n\right)\right).$$

Furthermore, by Lemma 7.3.7, for every $K \in \mathbb{N}$,

$$P_0^{\mu_p\uparrow}(T_n > K) \underset{p \downarrow p_c}{\longrightarrow} P_0^{\mu\uparrow}(T_n > K).$$

Since T_n is finite $P_0^{\mu\uparrow}$-a.s., up to choosing K large enough and then p close enough to p_c,

$$\max\left(P_0^{\mu_p\uparrow}(T_n > K), P_0^{\mu\uparrow}(T_n > K)\right) \leq \varepsilon.$$

Then,

$$\begin{aligned}
&\sup_{F \in \mathcal{F}} \left| \mathbb{E}_p \left(F\left(B_k^{(l)} : 0 \leq k \leq T_n^{(B,l)}\right) \;\middle|\; |\mathcal{C}| = \infty \right) - E_0^{\mu\uparrow}\left(F\left(Z_k : 0 \leq k \leq T_n\right)\right) \right| \\
&\qquad \leq 2\varepsilon + \sup_{F : \mathbb{Z}^{K+1} \to [0,1]} \left| E_0^{\mu_p\uparrow}\left(F\left(Z_0, \ldots, Z_K\right)\right) - E_0^{\mu\uparrow}\left(F\left(Z_0, \ldots, Z_K\right)\right) \right|
\end{aligned}$$

and by Lemma 7.3.7,

$$\sup_{F : \mathbb{Z}^{K+1} \to [0,1]} \left| E_0^{\mu_p\uparrow}\left(F\left(Z_0, \ldots, Z_K\right)\right) - E_0^{\mu\uparrow}\left(F\left(Z_0, \ldots, Z_K\right)\right) \right| \underset{p \downarrow p_c}{\longrightarrow} 0.$$

This concludes the proof since ε is arbitrary. □

Lemma 7.5.11. *For every $\varepsilon > 0$ and $m \in \mathbb{N}$, there exists $N \in \mathbb{N}$ such that for every $n \geq N$, the quantity*

$$\limsup_{p \downarrow p_c} \sup_{F \in \mathcal{F}} \left| \mathbb{E}_p \left(F\left(B_k^{(r)} : 0 \leq k \leq T_m^{(B,r)}\right) \;\middle|\; |\mathcal{C}| = \infty \right) - E_0^{\mu}\left(F\left(Z_k : 0 \leq k \leq T_{-m}\right)\right) \right|$$

is smaller than ε.

Proof. Let $\varepsilon > 0$, $m \in \mathbb{N}$, $n \in \mathbb{N}$ such that $n \geq m$ and $F \in \mathcal{F}$. By Lemma 7.5.5 and translation invariance,

$$\begin{aligned}
\mathbb{E}_p \left(F\left(B_k^{(r)} : 0 \leq k \leq T_m^{(B,r)}\right) \;\middle|\; |\mathcal{C}| = \infty \right) &= E_0^{\mu_p}\left(F\left(Z_k : 0 \leq k \leq T_{-m}\right) \mid T_{-n} = \infty\right) \\
&= E_n^{\mu_p}\left(F\left(Z_k - n : 0 \leq k \leq T_{n-m}\right) \mid T = \infty\right) \\
&= E_n^{\mu_p\uparrow}\left(F\left(Z_k - n : 0 \leq k \leq T_{n-m}\right)\right).
\end{aligned}$$

Furthermore, by Lemma 7.3.7 and then Lemma 7.3.6, for every $K \in \mathbb{N}$,

$$P_n^{\mu_p\uparrow}(T_{n-m} > K) \underset{p\downarrow p_c}{\longrightarrow} P_n^{\mu\uparrow}(T_{n-m} > K) \underset{n\to\infty}{\longrightarrow} P_0^{\mu}(T_{-m} > K).$$

Since T_{-m} is finite P_0^{μ}-a.s., up to choosing K large enough, then n large enough and finally p close enough to p_c,

$$\max\left(P_n^{\mu_p\uparrow}(T_{n-m} > K), P_0^{\mu}(T_{-m} > K)\right) \leq \varepsilon.$$

Then,

$$\begin{aligned}
&\sup_{F\in\mathcal{F}} \left| \mathbb{E}_p\left(F\left(B_k^{(r)} : 0 \leq k \leq T_m^{(B,r)}\right) \;\middle|\; |\mathcal{C}| = \infty\right) - E_0^{\mu}\left(F\left(Z_k : 0 \leq k \leq T_{-m}\right)\right)\right| \\
&\leq 2\varepsilon + \sup_{F:\mathbb{Z}^{K+1}\to[0,1]} \left| E_n^{\mu_p\uparrow}\left(F\left(Z_0 - n, \ldots, Z_K - n\right)\right) - E_0^{\mu}\left(F\left(Z_0, \ldots, Z_K\right)\right)\right| \\
&\leq 2\varepsilon + \sup_{F:\mathbb{Z}^{K+1}\to[0,1]} \left| E_n^{\mu_p\uparrow}\left(F\left(Z_0 - n, \ldots, Z_K - n\right)\right) - E_n^{\mu\uparrow}\left(F\left(Z_0 - n, \ldots, Z_K - n\right)\right)\right| \\
&\qquad + \sup_{F:\mathbb{Z}^{K+1}\to[0,1]} \left| E_n^{\mu\uparrow}\left(F\left(Z_0 - n, \ldots, Z_K - n\right)\right) - E_0^{\mu}\left(F\left(Z_0, \ldots, Z_K\right)\right)\right|
\end{aligned}$$

By Lemma 7.3.6, there exists $N \in \mathbb{N}$ such that for every $n \geq N$,

$$\sup_{F:\mathbb{Z}^{K+1}\to[0,1]} \left| E_n^{\mu\uparrow}\left(F\left(Z_0 - n, \ldots, Z_K - n\right)\right) - E_0^{\mu}\left(F\left(Z_0, \ldots, Z_K\right)\right)\right| \leq \varepsilon,$$

and by Lemma 7.3.7, for every $n \in \mathbb{N}$,

$$\sup_{F:\mathbb{Z}^{K+1}\to[0,1]} \left| E_n^{\mu_p\uparrow}\left(F\left(Z_0 - n, \ldots, Z_K - n\right)\right) - E_n^{\mu\uparrow}\left(F\left(Z_0 - n, \ldots, Z_K - n\right)\right)\right| \underset{p\downarrow p_c}{\longrightarrow} 0.$$

This concludes the proof. □

In what follows, $\mathcal{A}$ denotes the Borel σ-field of the local topology.

Proposition 7.5.12. *For every $\varepsilon > 0$ and $m \in \mathbb{N}$, there exists $N \in \mathbb{N}$ such that for every $n \geq N$,*

$$\limsup_{p\downarrow p_c} \sup_{A\in\mathcal{A}} |\mathbf{P}_p(M_{n,m} \in A \mid |\mathcal{C}| = \infty) - \mathsf{P}(M_{n,m} \in A)| \leq \varepsilon.$$

Moreover, for every $n, m \in \mathbb{N}$ such that $n \geq m$, the random planar map $M_{n,m}$ has the same law under $\mathbf{P}(\cdot \mid h(\mathcal{C}) \geq n)$ and P.

Proof. We start with the first assertion. Throughout this proof, we use $\mathbf{P}_p^{\infty} := \mathbf{P}_p(\cdot \mid |\mathcal{C}| = \infty)$ in order to shorten the notation. Let $\varepsilon > 0$ and $m \in \mathbb{N}$. By Lemma 7.5.11 and the definition of the IIC, there exists $N \in \mathbb{N}$ such that for every $n \geq N$,

$$\limsup_{p\downarrow p_c} \sup_{F\in\mathcal{F}} \left| \mathbb{E}_p^{\infty}\left(F\left(B_k^{(r)} : 0 \leq k \leq T_m^{(B,r)}\right)\right) - \mathsf{E}\left(F\left(A_k^{(r)} : 0 \leq k \leq T_m^{(A,r)}\right)\right)\right| \leq \varepsilon. \tag{7.28}$$

We now fix $n \geq N$, and by Lemma 7.5.10

$$\limsup_{p\downarrow p_c} \left| \mathbb{E}_p^{\infty}\left(F\left(B_k^{(l)} : 0 \leq k \leq T_n^{(B,l)}\right)\right) - \mathsf{E}\left(F\left(A_k^{(l)} : 0 \leq k \leq T_n^{(A,l)}\right)\right)\right| = 0. \tag{7.29}$$

Furthermore, by Lemma 7.5.5 and the definition of the IIC, for every $K \in \mathbb{N}$ and $F \in \mathcal{F}$,

$$\mathbb{E}_p^\infty \left(F\left(W_k^{(l)} : 0 \le k \le T_n^{(W,l)} \right) \,\middle|\, T_n^{(B,l)} = K \right) = \mathsf{E}\left(F\left(V_k^{(l)} : 0 \le k \le T_n^{(V,l)} \right) \,\middle|\, T_n^{(A,l)} = K \right). \quad (7.30)$$

For the same reason, for every $K, K' \in \mathbb{Z}_+$ and $F \in \mathcal{F}$,

$$\mathbb{E}_p^\infty \left(F\left(z_k^{(l)} : 0 \le k \le \sigma_n^{(l)} \right) \,\middle|\, \left(T_n^{(B,l)}, T_n^{(W,l)}\right) = (K, K') \right) = \mathsf{E}\left(F\left(y_k^{(l)} : 0 \le k \le \rho_n^{(l)} \right) \,\middle|\, \left(T_n^{(A,l)}, T_n^{(V,l)}\right) = (K, K') \right). \quad (7.31)$$

The assertions (7.30) and (7.31) hold when replacing l by r. Let $M'_{n,m}$ be the planar map obtained from the construction of $M_{n,m}$ in Sections 7.5.2 and 7.5.3 without filling the internal faces with Boltzmann triangulations with a simple boundary. Using (7.28), (7.29), (7.30) and (7.31), we get that

$$\limsup_{p \downarrow p_c} \sup_{A \in \mathcal{A}} \left| \mathbf{P}_p^\infty(M'_{n,m} \in A) - \mathsf{P}(M'_{n,m} \in A) \right| \le \varepsilon. \quad (7.32)$$

Since the colouring of the vertices in the Boltzmann triangulations filling in the faces of $M'_{n,m}$ is a Bernoulli percolation with parameter p (resp. p_c), for every finite map $\mathbf{m} \in \mathcal{M}_f$ we have

$$\limsup_{p \downarrow p_c} \sup_{A \in \mathcal{A}} \left| \mathbf{P}_p^\infty(M_{n,m} \in A \mid M'_{n,m} = \mathbf{m}) - \mathsf{P}(M_{n,m} \in A \mid M'_{n,m} = \mathbf{m}) \right| = 0.$$

Since $M'_{n,m}$ is P-a.s. finite, together with (7.32) this proves the first assertion.

For the second assertion, by Lemma 7.3.5, the above coding processes have the same law under $\mathbf{P}(\cdot \mid h(\mathcal{C}) \ge n)$ and P. The same arguments apply and conclude the proof. □

7.5.4 Proof of the IIC results

Proof of Theorem 7.2.5. Let $R \in \mathbb{Z}_+$ and $\varepsilon > 0$. We first prove that under P, $\mathbf{P}(\cdot \mid h(\mathcal{C}) \ge n)$ and $\mathbf{P}_p(\cdot \mid |\mathcal{C}| = \infty)$, $M_{n,m}$ contains $\mathbf{B}_R(M_\infty)$ with high probability for a good choice of the parameters, where M_∞ is the underlying infinite half-planar triangulation (with origin vertex ρ). This closely follows the proof of Theorem 7.2.3, to which we refer for more details.

We first restrict our attention to P, and define the random maps

$$M_N := M_{N,\xi_N}, \quad \xi_N := \inf\left\{ A_k^{(l)} : k \ge T_N^{(A,l)} \right\}, \quad N \in \mathbb{N}.$$

We denote by d_N the graph distance on M_N. By Proposition 7.5.9, M_N is P-a.s. a sub-map of M_∞ and we denote by ∂M_N its boundary as such (as in (7.17)). Recall that by Tanaka's theorem, we have $\xi_N \to \infty$ P-a.s. as $N \to \infty$. Let $\{\tau_k : k \in \mathbb{Z}_+\}$, $\{\tau_k^l : k \in \mathbb{Z}_+\}$ and $\{\tau_k^r : k \in \mathbb{Z}_+\}$ be the endpoints of the excursion intervals of $A^{(r)}$, $V^{(l)}$ and $V^{(r)}$ above their infimum processes, as in (7.7). They define cut-points that

disconnect the origin from infinity in $\mathbf{L}_{A^{(l)},A^{(r)}}$, $\mathbf{L}_{V^{(l)}}$ and $\mathbf{L}_{V^{(r)}}$ (and thus in $\mathcal{H}$, $\mathcal{H}_l$ and $\mathcal{H}_r$) respectively, by the identities

$$v_k := p_{A^{(r)}}\left(A^{(r)}_{\tau_k}\right),\ v^l_k := p_{V^{(l)}}\left(V^{(l)}_{\tau^l_k}\right) \text{ and } v^r_k := p_{V^{(r)}}\left(V^{(r)}_{\tau^r_k}\right), \quad k \in \mathbb{Z}_+.$$

The numbers of cut-points of $\mathcal{H}$ identified in M_N read

$$K(N) := \#\left\{k \in \mathbb{Z}_+ : \tau_k < T^{(A,r)}_{\xi_N}\right\},$$

and similarly for $\mathcal{H}_l$ and $\mathcal{H}_r$ with

$$K_l(N) := \#\left\{k \in \mathbb{Z}_+ : \tau^l_k < T^{(V,l)}_N\right\} \quad \text{and} \quad K_r(N) := \#\left\{k \in \mathbb{Z}_+ : \tau^r_k < T^{(V,r)}_{\xi_N}\right\}.$$

Since the processes $A^{(r)}$, $V^{(l)}$ and $V^{(r)}$ are centered random walks and $\xi_N \to \infty$ P-a.s., we get

$$K(N),\ K_l(N),\ K_r(N) \underset{N\to\infty}{\longrightarrow} \infty \quad \text{P-a.s..}$$

We define an equivalence relation $\approx$ as in Theorem 7.2.3, by identifying vertices between consecutive cut-points in $\mathcal{H}$, $\mathcal{H}_l$ and $\mathcal{H}_r$. We denote the quotient map $M_N/\approx$ by M'_N (the root edge of M'_N is the root edge of M_∞) and the graph distance on M'_N by d'_N. The family $\{M'_N : n \in \mathbb{N}\}$ is a consistent sequence of locally finite maps with origin $v_0 = \rho$. Moreover, for every $N \in \mathbb{N}$, the boundary of M'_N in M'_{N+1} is $\{v_{K(N)}, v^l_{K_l(N)}, v^r_{K_r(N)}\}$. Thus, the sequences

$$\left\{d'_N\left(\rho, v_{K(N)}\right) : N \in \mathbb{N}\right\},\ \left\{d'_N\left(\rho, v^l_{K_l(N)}\right) : N \in \mathbb{N}\right\} \text{ and } \left\{d'_N\left(\rho, v^r_{K_r(N)}\right) : N \in \mathbb{N}\right\}$$

are non-decreasing and diverge P-a.s.. By definition of $\approx$, since we discover the finite regions that are swallowed during the exploration, the representatives of ∂M_N in M'_N are $v_{K(N)}$, $v^l_{K_l(N)}$ and $v^r_{K_r(N)}$. As a consequence,

$$d_N\left(\rho, \partial M_N\right) \underset{N\to\infty}{\longrightarrow} \infty \quad \text{P-a.s..} \tag{7.33}$$

Let us choose $N \in \mathbb{N}$ such that $\mathsf{P}(d_N(\rho, \partial M_N) < R) \le \varepsilon$. By the proof of Proposition 7.5.9, we have that P-a.s., for every $n \ge N$ and $m \ge \xi_N$, M_N is a sub-map of $M_{n,m}$. Since ξ_N is P-a.s. finite, we can fix $m \in \mathbb{N}$ such that $\mathsf{P}(\xi_N > m) \le \varepsilon$, and thus for every $n \ge N$,

$$\mathsf{P}(M_N \subseteq M_{n,m}) \ge 1 - \varepsilon \tag{7.34}$$

Since $\xi_n \to \infty$ P-a.s., there exists $N_1 \ge N$ such that for every $n \ge N_1$, $\mathsf{P}(\xi_n < m) \le \varepsilon$. By Proposition 7.5.9, it follows that for every $n \ge N_1$,

$$\mathsf{P}(M_{n,m} \subseteq M_\infty) \ge 1 - \varepsilon. \tag{7.35}$$

By construction, when $M_N \subseteq M_{n,m} \subseteq M_\infty$, we have $d_N\left(\rho, \partial M_N\right) \le d\left(\rho, \partial M_{n,m}\right)$ (where d is the graph distance on $M_{n,m}$ and $\partial M_{n,m}$ its boundary in M_∞). Thus, for every $n \ge N_1$,

$$\mathsf{P}(M_{n,m} \subseteq M_\infty, d\left(\rho, \partial M_{n,m}\right) \ge R) \ge 1 - 3\varepsilon. \tag{7.36}$$

By Proposition 7.5.12, we find $N_2 \geq N_1$ such that for every $n \geq N_2$,

$$\limsup_{p \downarrow p_c} \sup_{A \in \mathcal{A}} |\mathbf{P}_p(M_{n,m} \in A \mid |\mathcal{C}| = \infty) - \mathsf{P}(M_{n,m} \in A)| \leq \varepsilon, \tag{7.37}$$

while $M_{n,m}$ has the same distribution under P and $\mathbf{P}(\cdot \mid h(\mathcal{C}) \geq n)$. Under $\mathbf{P}(\cdot \mid h(\mathcal{C}) \geq n)$ and $\mathbf{P}_p(\cdot \mid |\mathcal{C}| = \infty)$, $M_{n,m}$ is a.s. a sub-map of M_∞. By the construction of $M_{n,m}$, (7.36) and (7.37) we have for every $n \geq N_2$,

$$\limsup_{p \downarrow p_c} \mathbf{P}_p(d(\rho, \partial M_{n,m}) < R \mid |\mathcal{C}| = \infty) \leq 4\varepsilon, \quad \mathbf{P}(d(\rho, \partial M_{n,m}) < R \mid h(\mathcal{C}) \geq n) \leq 3\varepsilon. \tag{7.38}$$

Finally, on the event $\{M_{n,m} \subseteq M_\infty\}$, $d(\rho, \partial M_{n,m}) \geq R$ enforces that $\mathbf{B}_R(M_{n,m}) = \mathbf{B}_R(M_\infty)$, which concludes the first part of the proof.

Now, let $A \in \mathcal{A}$ be a Borel set for the local topology. By (7.38), for every $n \geq N_2$,

$$\begin{aligned}&\limsup_{p \downarrow p_c} |\mathbf{P}_p(\mathbf{B}_R(M_\infty) \in A \mid |\mathcal{C}| = \infty) - \mathbf{P}_p(\mathbf{B}_R(M_{n,m}) \in A \mid |\mathcal{C}| = \infty)| \\ &\leq 2 \limsup_{p \downarrow p_c} \mathbf{P}_p(d(\rho, \partial M_{n,m}) < R \mid |\mathcal{C}| = \infty) \leq 8\varepsilon.\end{aligned}$$

Then, by (7.37), for every $n \geq N_2$,

$$\limsup_{p \downarrow p_c} |\mathbf{P}_p(\mathbf{B}_R(M_{n,m}) \in A \mid |\mathcal{C}| = \infty) - \mathsf{P}(\mathbf{B}_R(M_{n,m}) \in A)| \leq \varepsilon.$$

Finally, by (7.36), for every $n \geq N_1$,

$$\begin{aligned}&|\mathsf{P}(\mathbf{B}_R(M_{n,m}) \in A) - \mathsf{P}(\mathbf{B}_R(M_\infty) \in A)| \\ &\qquad \leq 2\left(1 - \mathsf{P}(M_{n,m} \subseteq M_\infty, d(\rho, \partial M_{n,m}) \geq R)\right) \leq 6\varepsilon.\end{aligned}$$

This concludes the proof under $\mathbf{P}_p(\cdot \mid |\mathcal{C}| = \infty)$ since R and ε are arbitrary.

Under $\mathbf{P}(\cdot \mid h(\mathcal{C}) \geq n)$, the proof is simpler. By (7.38) once again, for every $n \geq N_2$,

$$\begin{aligned}&|\mathbf{P}(\mathbf{B}_R(M_\infty) \in A \mid h(\mathcal{C}) \geq n) - \mathbf{P}(\mathbf{B}_R(M_{n,m}) \in A \mid h(\mathcal{C}) \geq n)| \\ &\qquad \leq 2\mathbf{P}(d_{\mathrm{gr}}(\rho, \partial M_{n,m}) < R \mid h(\mathcal{C}) \geq n) \leq 6\varepsilon,\end{aligned}$$

and by Proposition 7.5.12,

$$\mathbf{P}(\mathbf{B}_R(M_{n,m}) \in A \mid h(\mathcal{C}) \geq n) = \mathsf{P}(\mathbf{B}_R(M_{n,m}) \in A).$$

This concludes the proof. □

Remark 7.5.13. In view of [BD94, Theorem 1], we believe that this proof can be adapted to show that in the sense of weak convergence, for the local topology

$$\mathbf{P}_{p_c}(\cdot \mid T \geq n) \underset{n \to \infty}{\Longrightarrow} \mathbf{P}_{\mathsf{IIC}}.$$

Otherwise said, the IIC arises as a local limit of a critically percolated UIHPT when conditioning the exploration process to survive a long time. It is also natural to conjecture that conditioning the open cluster of the origin to have large hull perimeter (as in [CK14a]) or to reach the boundary of a ball of large radius (as in [Kes86a]) yields the same local limit. However, our techniques do not seem to allow to tackle this problem.

7.6 Scaling limits and perspectives

In the recent work [BMR16] (see also [GM16]), Baur, Miermont and Ray introduced the scaling limit of the quadrangular analogous of the UIHPT, called the Uniform Infinite Half-Planar Quadrangulation (UIHPQ). Precisely, they consider a map $\mathbf{Q}_\infty^\infty$ having the law of the UIHPQ as a metric space equipped with its graph distance d_{gr}, and multiply the distances by a scaling factor λ that goes to zero, proving that [BMR16, Theorem 3.6]

$$(\mathbf{Q}_\infty^\infty, \lambda d_{\mathrm{gr}}) \xrightarrow[\lambda\to 0]{(d)} \mathsf{BHP},$$

in the local Gromov-Hausdorff sense (see [BBI01, Chapter 8] for more on this topology). The limiting object is called the *Brownian Half-Plane* and is a half-planar analog of the Brownian Plane of [CLG13]. Such a convergence is believed to hold also in the triangular case.

We now discuss the conjectural continuous counterpart of Theorem 7.2.3, and the connection with the BHP. On the one hand, the processes B and W introduced in Section 7.4.2 have a scaling limit. Namely, using the asymptotic (7.2) and standard results of convergence of random walks with steps in the domain of attraction of a stable law [BGT89, Chapter 8] one has

$$\left(\lambda^2 B_{\lfloor t/\lambda^3 \rfloor}\right)_{t\geq 0} \xrightarrow[\lambda\to 0]{(d)} (X_t)_{t\geq 0},$$

in distribution for Skorokhod's topology, where X is (up to a multiplicative constant) the spectrally negative $3/2$-stable process. This suggests that the looptrees $\mathbf{L}_B$ and $\mathbf{L}_W$ converge when distances are rescaled by the factor λ^2 towards a non-compact version of the random stable looptrees of [CK14b] (with parameter $3/2$), in the local Gromov-Hausdorff sense. This object is supposed to be coded by the process X extended to $\mathbb{R}$ by the relation $X_t = -t$ for every $t \leq 0$ and equivalence relation

$$s \sim t \quad \text{iff} \quad X_t = X_s = \inf_{s\wedge t \leq u \leq s\vee t} X_u. \tag{7.39}$$

On the other hand, one can associate to each negative jump of size ℓ of X (which codes a loop of the same length in the infinite stable looptree, see [CK14b]) a sequence of jumps of B (equivalently, of loops of $\mathbf{L}_B$) with sizes $\{\ell_\lambda : \lambda > 0\}$ satisfying

$$\lambda^2 \ell_\lambda \xrightarrow[\lambda\to 0]{} \ell.$$

With each negative jump of B is associated a Boltzmann triangulation M_λ with a simple boundary of size ℓ_λ and graph distance d_λ, that fills in the corresponding loop in the decomposition of the UIHPT. Inspired by [BM15, Theorem 8], we expect that there exists a constant $c > 0$ such that

$$\left(M_\lambda, (c\ell_\lambda)^{-1/2} d_\lambda\right) \xrightarrow[\lambda\to 0]{(d)} \mathsf{FBD}_1,$$

in the Gromov-Hausdorff sense, where FBD_1 is a compact metric space called the Free Brownian Disk with perimeter 1, originally introduced in [Bet15] (this result

has been proved for Boltzmann bipartite maps with a general boundary). By a scaling argument, we obtain

$$(M_\lambda, \lambda d_\lambda) \xrightarrow[\lambda \to 0]{(d)} \mathsf{FBD}_{c\ell},$$

where $\mathsf{FBD}_{c\ell}$ is the FBD with perimeter $c\ell$. From these observations, it is natural to conjecture that the looptrees $\mathbf{L}_B$ and $\mathbf{L}_W$ filled in with independent Boltzmann triangulations converge when rescaled by a factor that goes to zero, towards a collection of independent FBD with perimeters given by the jumps of a Lévy $3/2$-stable process, and glued together according to the looptree structure induced by this process. Based on Theorem 7.2.3, we believe that there is a way to glue two independent copies of the above looptrees of brownian disks along their boundaries so that the resulting object has the law of the BHP. Similarly, one may give a rigorous sense to the IIC embedded in the BHP, by passing to the scaling limit in Theorem 7.2.5. However, there are several possible metrics on the topological quotient, and it is not clear which metric should be chosen.

This question is connected to [DMS14, She10], where gluings of quantum surfaces are discussed. As we already mentioned, Theorem 7.2.3 can be seen as a discrete counterpart to [DMS14, Theorem 1.16-1.17]. Applying these results with the choice of parameter $\gamma = \sqrt{8/3}$, we obtain that the $\theta = \pi$ quantum wedge (which is believed to be a conformal version of the BHP) is obtain as the gluing of two independent forested wedges with parameter $\alpha = 3/2$ (an infinite counterpart to the $3/2$-stable looptree, where loops are filled in with disks equipped with a metric defined in terms of the Gaussian Free Field - a conformal version of the brownian disk). Moreover, the counterflow line that separates the forested wedges is a Schramm-Loewner Evolution with parameter 6, which is also the scaling limit of percolation interfaces in the triangular lattice [Sch00, Smi01]. In the recent work [GM17], Gwynne and Miller also proved the convergence of the percolation interface for face percolation on the UIHPQ towards Schramm-Loewner Evolution with parameter 6 on the BHP.

Acknowledgements. I would like to thank Gourab Ray for suggesting this question and interesting discussions, Grégory Miermont for insightful comments and many useful suggestions and Erich Baur for his helpful remarks. I am greatly indebted to Nicolas Curien for pointing out an inaccuracy on a preliminary version of this work.

Travaux présentés dans cette thèse

[1] Erich Baur, Grégory Miermont, and Loïc Richier. Geodesic rays in the uniform infinite half-planar quadrangulation return to the boundary. *ALEA : Latin American Journal of Probability and Mathematical Statistics*, XIII(2) :1123–1149, December 2016.

[2] Erich Baur and Loïc Richier. Uniform infinite half-planar quadrangulations with skewness. *arXiv :1612.08572 [math]*, December 2016.

[3] Loïc Richier. Universal aspects of critical percolation on random half-planar maps. *Electronic Journal of Probability*, 20(0), December 2015.

[4] Loïc Richier. The Incipient Infinite Cluster of the Uniform Infinite Half-Planar Triangulation. *arXiv :1704.01561 [math]*, April 2017.

[5] Loïc Richier. Limits of the boundary of random planar maps. *arXiv :1704.01950 [math]*, April 2017.

Bibliographie

[ABA13] Louigi Addario-Berry and Marie Albenque. The scaling limit of random simple triangulations and random simple quadrangulations. *arXiv :1306.5227 [math]*, June 2013.

[ABM16] Jan Ambjørn, Timothy Budd, and Yuri Makeenko. Generalized multicritical one-matrix models. *arXiv :1604.04522 [hep-th]*, April 2016.

[Abr16] Céline Abraham. Rescaled bipartite planar maps converge to the Brownian map. *Annales de l'Institut Henri Poincaré, Probabilités et Statistiques*, 52(2) :575–595, May 2016.

[AC15] Omer Angel and Nicolas Curien. Percolations on random maps I : Half-plane models. *Annales de l'Institut Henri Poincaré, Probabilités et Statistiques*, 51(2) :405–431, May 2015.

[AJD97] Jan Ambjørn, Þórður Jónsson, and Bergfinnur Durhuus. *Quantum Geometry : A Statistical Field Theory Approach*. Cambridge University Press, June 1997.

[AKM15] Omer Angel, Brett Kolesnik, and Grégory Miermont. Stability of geodesics in the Brownian map. *arXiv :1502.04576 [math]*, February 2015.

[Ald91] David Aldous. The Continuum Random Tree. I. *The Annals of Probability*, 19(1) :1–28, January 1991.

[Ald93] David Aldous. The Continuum Random Tree III. *The Annals of Probability*, 21(1) :248–289, January 1993.

[Ang03] Omer Angel. Growth and percolation on the uniform infinite planar triangulation. *Geometric & Functional Analysis GAFA*, 13(5) :935–974, October 2003.

[Ang04] Omer Angel. Scaling of Percolation on Infinite Planar Maps, I. *arXiv :math/0501006*, December 2004.

[AR15] Omer Angel and Gourab Ray. Classification of half-planar maps. *The Annals of Probability*, 43(3) :1315–1349, May 2015.

[AR16] Omer Angel and Gourab Ray. The half plane UIPT is recurrent. *arXiv :1601.00410 [math]*, January 2016.

[AS03] Omer Angel and Oded Schramm. Uniform Infinite Planar Triangulations. *Communications in Mathematical Physics*, 241(2-3) :191–213, October 2003.

[BBCK16] Jean Bertoin, Timothy Budd, Nicolas Curien, and Igor Kortchemski. Martingales in self-similar growth-fragmentations and their connections with random planar maps. *arXiv :1605.00581 [math-ph]*, May 2016.

[BBD16] Gaëtan Borot, Jérémie Bouttier, and Bertrand Duplantier. Nesting statistics in the O(n) loop model on random planar maps. *arXiv :1605.02239 [hep-th, physics :math-ph]*, May 2016.

[BBG12a] Gaëtan Borot, Jérémie Bouttier, and Emmanuel Guitter. Loop models on random maps via nested loops : case of domain symmetry breaking and application to the Potts model. *Journal of Physics A : Mathematical and Theoretical*, 45(49) :494017, December 2012.

[BBG12b] Gaëtan Borot, Jérémie Bouttier, and Emmanuel Guitter. More on the O(n) model on random maps via nested loops : loops with bending energy. *Journal of Physics A : Mathematical and Theoretical*, 45(27) :275206, July 2012.

[BBG12c] Gaëtan Borot, Jérémie Bouttier, and Emmanuel Guitter. A recursive approach to the O(n) model on random maps via nested loops. *Journal of Physics A : Mathematical and Theoretical*, 45(4) :045002, February 2012.

[BBI01] Dmitri Burago, Yuri Burago, and Sergei Ivanov. *A Course in Metric Geometry*. Graduate Studies in Mathematics. American Mathematical Society, 2001.

[BC16] Timothy Budd and Nicolas Curien. Geometry of infinite planar maps with high degrees. *arXiv :1602.01328 [math-ph]*, February 2016.

[BD94] Jean Bertoin and Ronald A. Doney. On Conditioning a Random Walk to Stay Nonnegative. *The Annals of Probability*, 22(4) :2152–2167, October 1994.

[BDFG04] Jérémie Bouttier, Philippe Di Francesco, and Emmanuel Guitter. Planar maps as labeled mobiles. *The Electronic Journal of Combinatorics*, 11(1) :R69, 27 p., 2004.

[BE11] Gaëtan Borot and Bertrand Eynard. Enumeration of maps with self avoiding loops and the O(n) model on random lattices of all topologies. *Journal of Statistical Mechanics : Theory and Experiment*, 2011(01) :P01010, January 2011.

[Ber98] Jean Bertoin. *Lévy Processes*. Cambridge University Press, October 1998.

[Ber06] Jean Bertoin. *Random Fragmentation and Coagulation Processes*. Cambridge University Press, August 2006.

[Ber16] Gabriel Berzunza. On scaling limits of multitype Galton-Watson trees with possibly infinite variance. *arXiv :1605.04810 [math]*, May 2016.

[Bet10] Jérémie Bettinelli. Scaling Limits for Random Quadrangulations of Positive Genus. *arXiv :1002.3682 [math]*, February 2010.

[Bet12] Jérémie Bettinelli. The topology of scaling limits of positive genus random quadrangulations. *The Annals of Probability*, 40(5) :1897–1944, September 2012.

[Bet15] Jérémie Bettinelli. Scaling limit of random planar quadrangulations with a boundary. *Annales de l'Institut Henri Poincaré, Probabilités et Statistiques*, 51(2) :432–477, May 2015.

[Bet16] Jérémie Bettinelli. Geodesics in Brownian surfaces (Brownian maps). *Annales de l'Institut Henri Poincaré, Probabilités et Statistiques*, 52(2) :612–646, May 2016.

[BG09] Jérémie Bouttier and Emmanuel Guitter. Distance statistics in quadrangulations with a boundary, or with a self-avoiding loop. *Journal of Physics A : Mathematical and Theoretical*, 42(46) :465208, November 2009.

[BG12] Jérémie Bouttier and Emmanuel Guitter. Planar maps and continued fractions. *Communications in Mathematical Physics*, 309(3) :623–662, February 2012.

[BGT89] Nicholas H. Bingham, Charles M. Goldie, and Jozef L. Teugels. *Regular Variation*. Cambridge University Press, July 1989.

[BH57] Simon R. Broadbent and John M. Hammersley. Percolation processes : I. Crystals and mazes. *Mathematical Proceedings of the Cambridge Philosophical Society*, 53(3) :629–641, July 1957.

[Bie45] Irénée-Jules Bienaymé. De la loi de multiplication et de la durée des familles. *Société Philomathique de Paris Extraits*, Série 5 :37–39, 1845.

[BIPZ78] Edouard Brézin, Claude Itzykson, Giorgio Parisi, and Jean-Bernard Zuber. Planar diagrams. *Communications in Mathematical Physics*, 59(1) :35–51, 1978.

[BJM14] Jérémie Bettinelli, Emmanuel Jacob, and Grégory Miermont. The scaling limit of uniform random plane maps, via the Ambjørn-Budd bijection. *Electronic Journal of Probability*, 19(0) :1–16, 2014.

[BLG13] Johel Beltran and Jean-François Le Gall. Quadrangulations with no pendant vertices. *Bernoulli*, 19(4) :1150–1175, 2013.

[BLR15] Nathanaël Berestycki, Benoît Laslier, and Gourab Ray. Critical exponents on Fortuin–Kasteleyn weighted planar maps. *arXiv :1502.00450 [math-ph]*, February 2015.

[BM15] Jérémie Bettinelli and Gregory Miermont. Compact Brownian surfaces I. Brownian disks. *arXiv :1507.08776 [math]*, July 2015.

[BMR16] Erich Baur, Grégory Miermont, and Gourab Ray. Classification of scaling limits of uniform quadrangulations with a boundary. *arXiv :1608.01129 [math]*, August 2016.

[BS01] Itai Benjamini and Oded Schramm. Recurrence of Distributional Limits of Finite Planar Graphs. *Electronic Journal of Probability*, 6(0), September 2001.

[BS14] Jakob E. Björnberg and Sigurdur Ö. Stefánsson. Recurrence of bipartite planar maps. *Electronic Journal of Probability*, 19(0), March 2014.

[BS15] Jakob E. Björnberg and Sigurdur Ö. Stefánsson. On Site Percolation in Random Quadrangulations of the Half-Plane. *Journal of Statistical Physics*, 160(2) :336–356, April 2015.

[Bud15] Timothy Budd. The peeling process of infinite Boltzmann planar maps. *arXiv :1506.01590 [gr-qc, physics :math-ph]*, June 2015.

[Bud16] Thomas Budzinski. The hyperbolic Brownian plane. *arXiv :1604.06622 [math]*, April 2016.

[Bud17] Timothy Budd, with an appendix jointly with L. Chen. The peeling process on random planar maps coupled to an O(n) loop model. *In preparation*, 2017.

[CC15] Alessandra Caraceni and Nicolas Curien. Geometry of the Uniform Infinite Half-Planar Quadrangulation. *arXiv :1508.00133 [math]*, August 2015.

[CCM17] Linxiao Chen, Nicolas Curien, and Pascal Maillard. The perimeter cascade in critical Boltzmann quadrangulations decorated by an O(n) loop model. *arXiv :1702.06916 [math-ph]*, February 2017.

[CD06] Philippe Chassaing and Bergfinnur Durhuus. Local limit of labeled trees and expected volume growth in a random quadrangulation. *The Annals of Probability*, 34(3) :879–917, May 2006.

[CD17] Guillaume Chapuy and Maciej Dołęga. A bijection for rooted maps on general surfaces. *Journal of Combinatorial Theory, Series A*, 145 :252–307, January 2017. arXiv : 1501.06942.

[Che15] Linxiao Chen. Basic properties of the infinite critical-FK random map. *arXiv :1502.01013 [math]*, February 2015.

[CHK15] Nicolas Curien, Bénédicte Haas, and Igor Kortchemski. The CRT is the scaling limit of random dissections. *Random Structures & Algorithms*, 47(2) :304–327, September 2015.

[CK14a] Nicolas Curien and Igor Kortchemski. Percolation on random triangulations and stable looptrees. *Probability Theory and Related Fields*, pages 1–35, December 2014.

[CK14b] Nicolas Curien and Igor Kortchemski. Random stable looptrees. *Electronic Journal of Probability*, 19(0), November 2014.

[CLG13] Nicolas Curien and Jean-François Le Gall. The Brownian Plane. *Journal of Theoretical Probability*, 27(4) :1249–1291, March 2013.

[CM15] Nicolas Curien and Grégory Miermont. Uniform infinite planar quadrangulations with a boundary. *Random Structures & Algorithms*, 47(1) :30–58, August 2015.

[CMM13] Nicolas Curien, Laurent Ménard, and Grégory Miermont. A view from infinity of the uniform infinite planar quadrangulation. *ALEA : Latin American Journal of Probability and Mathematical Statistics*, 10(1) :45–88, 2013.

[CMS07] Guillaume Chapuy, Michel Marcus, and Gilles Schaeffer. A bijection for rooted maps on orientable surfaces. *arXiv :0712.3649 [math]*, December 2007.

[CS04] Philippe Chassaing and Gilles Schaeffer. Random Planar Lattices and Integrated SuperBrownian Excursion. *Probability Theory and Related Fields*, 128(2) :161–212, 2004.

[Cur16a] Nicolas Curien. Peeling random planar maps, 2016. Cours Peccot, Collège de France.

[Cur16b] Nicolas Curien. Planar stochastic hyperbolic triangulations. *Probability Theory and Related Fields*, 165(3-4) :509–540, August 2016.

[CV81] Robert Cori and Bernard Vauquelin. Planar maps are well labeled trees. *Canadian Journal of Mathematics*, 33(5) :1023–1042, October 1981.

[DK88] Bertrand Duplantier and Ivan Kostov. Conformal Spectra of Polymers on a Random Surface. *Physical Review Letters*, 61(13) :1433–1437, September 1988.

[DK06] Ronald A. Doney and Andreas E. Kyprianou. Overshoots and undershoots of Lévy processes. *The Annals of Applied Probability*, 16(1) :91–106, February 2006.

[DLG02] Thomas Duquesne and Jean-François Le Gall. *Random trees, Lévy processes and spatial branching processes*. Société Mathématique de France, 2002.

[DLG05] Thomas Duquesne and Jean-François Le Gall. Probabilistic and fractal aspects of Lévy trees. *Probability Theory and Related Fields*, 131(4) :553–603, April 2005.

[DMS14] Bertrand Duplantier, Jason Miller, and Scott Sheffield. Liouville quantum gravity as a mating of trees. *arXiv :1409.7055 [math-ph]*, September 2014.

[Don82] Ronald A. Doney. On the exact asymptotic behaviour of the distribution of ladder epochs. *Stochastic Processes and their Applications*, 12(2) :203–214, March 1982.

[DS11] Bertrand Duplantier and Scott Sheffield. Liouville quantum gravity and KPZ. *Inventiones Mathematicae*, 185 :333–393, August 2011.

[Duq03] Thomas Duquesne. A limit theorem for the contour process of conditioned Galton–Watson trees. *The Annals of Probability*, 31(2) :996–1027, April 2003.

[EK95] Bertrand Eynard and Charlotte Kristjansen. Exact Solution of the O(n) Model on a Random Lattice. *Nuclear Physics B*, 455(3) :577–618, September 1995.

[EK96] Bertrand Eynard and Charlotte Kristjansen. More on the exact solution of the O(n) model on a random lattice and an investigation of the case $|n|>2$. *Nuclear Physics B*, 466(3) :463–487, May 1996.

[EZJ92] Bertrand Eynard and Jean Zinn-Justin. The O(n) model on a random surface : critical points and large order behaviour. *Nuclear Physics B*, 386(3) :558–591, November 1992.

[Fel68] William Feller. *An Introduction to Probability Theory and Its Applications, Vol. 1, 3rd Edition*. Wiley, New York, 3rd edition edition, 1968.

[Fel71] William Feller. *An Introduction to Probability Theory and Its Applications, Vol. 2*. Wiley, 2nd edition, 1971.

[FS09] Philippe Flajolet and Robert Sedgewick. *Analytic Combinatorics*. Cambridge University Press, January 2009.

[GGN12] Ori Gurel-Gurevich and Asaf Nachmias. Recurrence of planar graph limits. *arXiv :1206.0707 [math]*, June 2012.

[GM16] Ewain Gwynne and Jason Miller. Scaling limit of the uniform infinite half-plane quadrangulation in the Gromov-Hausdorff-Prokhorov-uniform topology. *arXiv :1608.00954 [math-ph]*, August 2016.

[GM17] Ewain Gwynne and Jason Miller. Convergence of percolation on uniform quadrangulations with boundary to SLE$_6$ on $\sqrt{8/3}$-Liouville quantum gravity. *arXiv :1701.05175 [math-ph]*, January 2017.

[GMS15] Ewain Gwynne, Cheng Mao, and Xin Sun. Scaling limits for the critical Fortuin-Kasteleyn model on a random planar map I : cone times. *arXiv :1502.00546 [math-ph]*, February 2015.

[GMSS17] Matthias Gorny, Édouard Maurel-Segala, and Arvind Singh. The geometry of a critical percolation cluster on the UIPT. *arXiv :1701.01667 [math]*, January 2017.

[Gri99] Geoffrey Grimmett. *Percolation*. Springer, Berlin ; New York, 2nd edition, June 1999.

[GS15a] Ewain Gwynne and Xin Sun. Scaling limits for the critical Fortuin-Kastelyn model on a random planar map II : local estimates and empty reduced word exponent. *arXiv :1505.03375 [math-ph]*, May 2015.

[GS15b] Ewain Gwynne and Xin Sun. Scaling limits for the critical Fortuin-Kastelyn model on a random planar map III : finite volume case. *arXiv :1510.06346 [math-ph]*, October 2015.

[GW75] Francis Galton and Henry W. Watson. On the Probability of the Extinction of Families. *The Journal of the Anthropological Institute of Great Britain and Ireland*, 4 :138–144, 1875.

[Jan11] Svante Janson. Stable distributions. *arXiv :1112.0220 [math]*, December 2011.

[Jan12] Svante Janson. Simply generated trees, conditioned Galton-Watson trees, random allocations and condensation. *Probability Surveys*, 9 :103–252, 2012.

[JS10] Thordur Jonsson and Sigurdur Ö. Stefánsson. Condensation in Nongeneric Trees. *Journal of Statistical Physics*, 142(2) :277–313, December 2010.

[JS15] Svante Janson and Sigurdur Orn Stefánsson. Scaling limits of random planar maps with a unique large face. *The Annals of Probability*, 43(3) :1045–1081, May 2015.

[Kes86a] Harry Kesten. The incipient infinite cluster in two-dimensional percolation. *Probability Theory and Related Fields*, 73(3) :369–394, September 1986.

[Kes86b] Harry Kesten. Subdiffusive behavior of random walk on a random cluster. *Annales de l'institut Henri Poincaré (B) Probabilités et Statistiques*, 22(4) :425–487, 1986.

[Kor13] Igor Kortchemski. A Simple Proof of Duquesne's Theorem on Contour Processes of Conditioned Galton–Watson Trees. *Séminaire de Probabilités XLV*, pages 537–558, 2013.

[Kor15] Igor Kortchemski. Limit theorems for conditioned non-generic Galton–Watson trees. *Annales de l'Institut Henri Poincaré, Probabilités et Statistiques*, 51(2) :489–511, May 2015.

[Kos89] Ivan K. Kostov. O(n) vector model on a planar random lattice : spectrum of anomalous dimensions. *Modern Physics Letters A*, 04(03) :217–226, February 1989.

[KPZ88] Vadim G. Knizhnik, Alexsandr M. Polyakov, and Alexander B. Zamolodchikov. Fractal structure of 2d-quantum gravity. *Modern Physics Letters A*, 03(08) :819–826, July 1988.

[Kri05] Maxim Krikun. Local structure of random quadrangulations. *arXiv :math/0512304*, December 2005.

[Kri07] Maxim Krikun. Explicit Enumeration of Triangulations with Multiple Boundaries. *The Electronic Journal of Combinatorics*, 14(1) :R61, August 2007.

[KS91] Ioannis Karatzas and Steven Shreve. *Brownian Motion and Stochastic Calculus*. Springer, New York, 2nd edition edition, August 1991.

[KS92] Ivan K. Kostov and Matthias Staudacher. Multicritical Phases of the O(n) Model on a Random Lattice. *Nuclear Physics B*, 384(3) :459–483, October 1992.

[LG99] Jean-François Le Gall. *Spatial Branching Processes, Random Snakes and Partial Differential Equations*. 1999.

[LG05] Jean-François Le Gall. Random trees and applications. *Probability Surveys*, 2 :245–311, 2005.

[LG07] Jean-François Le Gall. The topological structure of scaling limits of large planar maps. *Inventiones mathematicae*, 169(3) :621–670, September 2007.

[LG10] Jean-François Le Gall. Geodesics in large planar maps and in the Brownian map. *Acta Mathematica*, 205(2) :287–360, December 2010.

[LG13] Jean-François Le Gall. Uniqueness and universality of the Brownian map. *The Annals of Probability*, 41(4) :2880–2960, July 2013.

[LGLJ98] Jean-François Le Gall and Yves Le Jan. Branching processes in Lévy processes : the exploration process. *The Annals of Probability*, 26(1) :213–252, January 1998.

[LGM10] Jean-François Le Gall and Laurent Ménard. Scaling limits for the uniform infinite quadrangulation. *Illinois Journal of Mathematics*, 54(3) :1163–1203, 2010.

[LGM11a] Jean-François Le Gall and Grégory Miermont. Scaling limits of random planar maps with large faces. *The Annals of Probability*, 39(1) :1–69, January 2011.

[LGM11b] Jean-François Le Gall and Grégory Miermont. Scaling limits of random trees and planar maps. *arXiv :1101.4856 [math]*, January 2011.

[LGP08] Jean-François Le Gall and Frédéric Paulin. Scaling Limits of Bipartite Planar Maps are Homeomorphic to the 2-Sphere. *Geometric and Functional Analysis*, 18(3) :893–918, September 2008.

[LP16] Russell Lyons and Yuval Peres. *Probability on trees and networks*. Cambridge University Press, 2016.

[LZ04] Sergei K. Lando and Alexander K. Zvonkin. *Graphs on Surfaces and Their Applications*, volume 141 of *Encyclopaedia of Mathematical Sciences*. Springer, 2004.

[Mar16] Cyril Marzouk. Scaling limits of random bipartite planar maps with a prescribed degree sequence. *arXiv :1612.08618 [math]*, December 2016.

[Mie06] Grégory Miermont. An invariance principle for random planar maps. *DMTCS Proceedings*, 0(1), September 2006.

[Mie08] Grégory Miermont. On the sphericity of scaling limits of random planar quadrangulations. *Electronic Communications in Probability*, 13 :248–257, 2008.

[Mie09] Grégory Miermont. Tessellations of random maps of arbitrary genus. *Annales scientifiques de l'École Normale Supérieure*, 42(5) :725–781, 2009.

[Mie13] Grégory Miermont. The Brownian map is the scaling limit of uniform random plane quadrangulations. *Acta Mathematica*, 210(2) :319–401, June 2013.

[MM06] Jean-François Marckert and Abdelkader Mokkadem. Limit of normalized quadrangulations : The Brownian map. *The Annals of Probability*, 34(6) :2144–2202, November 2006.

[MM07] Jean-François Marckert and Grégory Miermont. Invariance principles for random bipartite planar maps. *The Annals of Probability*, 35(5) :1642–1705, September 2007.

[MN14] Laurent Ménard and Pierre Nolin. Percolation on uniform infinite planar maps. *Electronic Journal of Probability*, 19(0), September 2014.

[MS15] Jason Miller and Scott Sheffield. Liouville quantum gravity and the Brownian map I : The QLE(8/3,0) metric. *arXiv :1507.00719 [math-ph]*, July 2015.

[MS16a] Jason Miller and Scott Sheffield. Liouville quantum gravity and the Brownian map II : geodesics and continuity of the embedding. *arXiv :1605.03563 [math-ph]*, May 2016.

[MS16b] Jason Miller and Scott Sheffield. Liouville quantum gravity and the Brownian map III : the conformal structure is determined. *arXiv :1608.05391 [math-ph]*, August 2016.

[MT01] Bojan Mohar and Carsten Thomassen. *Graphs on Surfaces*. Johns Hopkins University Press, June 2001.

[MW08] Grégory Miermont and Mathilde Weill. Radius and profile of random planar maps with faces of arbitrary degrees. *Electronic Journal of Probability*, 13 :79–106, 2008.

[Mé10] Laurent Ménard. The two uniform infinite quadrangulations of the plane have the same law. *Annales de l'Institut Henri Poincaré, Probabilités et Statistiques*, 46(1) :190–208, February 2010.

[Nev86] Jacques Neveu. Arbres et processus de Galton-Watson. *Annales de l'institut Henri Poincaré (B) Probabilités et Statistiques*, 22(2) :199–207, 1986.

[Pit06] Jim Pitman. *Combinatorial Stochastic Processes*, volume 1875 of *Lecture Notes in Mathematics*. Springer, 2006.

[Pol81] Alexsandr M. Polyakov. Quantum geometry of bosonic strings. *Physics Letters B*, 103(3) :207–210, July 1981.

[Ray14] Gourab Ray. Geometry and percolation on half planar triangulations. *Electronic Journal of Probability*, 19(0) :1–28, May 2014.

[Rog71] Boris A. Rogozin. The Distribution of the First Ladder Moment and Height and Fluctuation of a Random Walk. *Theory of Probability & Its Applications*, 16(4) :575–595, January 1971.

[Sch98] Gilles Schaeffer. *Conjugaison d'arbres et cartes combinatoires aléatoires*. PhD thesis, Bordeaux 1, January 1998.

[Sch00] Oded Schramm. Scaling limits of loop-erased random walks and uniform spanning trees. *Israel Journal of Mathematics*, 118(1) :221–288, December 2000.

[Sch06] Oded Schramm. Conformally invariant scaling limits : an overview and a collection of problems. In *Proceedings of the International Congress of Mathematicians, Madrid, August 22–30, 2006*, volume 1, pages 513–543. European Mathematical Society, 2006.

[She10] Scott Sheffield. Conformal weldings of random surfaces : SLE and the quantum gravity zipper. *arXiv :1012.4797 [cond-mat, physics :math-ph]*, December 2010.

[She11] Scott Sheffield. Quantum gravity and inventory accumulation. *arXiv :1108.2241 [cond-mat, physics :hep-th, physics :math-ph]*, August 2011.

[Smi01] Stanislav Smirnov. Critical percolation in the plane : conformal invariance, Cardy's formula, scaling limits. *Comptes Rendus de l'Académie des Sciences - Series I - Mathematics*, 333(3) :239–244, August 2001.

[Spi01] Frank Spitzer. *Principles of Random Walk*. Springer, January 2001.

[Ste16] Robin Stephenson. Local convergence of large critical multi-type Galton-Watson trees and applications to random maps. *Journal of Theoretical Probability*, pages 1–47, 2016.

[Stu16] Benedikt Stufler. Limits of random tree-like discrete structures. *arXiv :1612.02580 [math]*, December 2016.

[Tan89] Hiroshi Tanaka. Time Reversal of Random Walks in One-Dimension. *Tokyo Journal of Mathematics*, 12(1) :159–174, June 1989.

[tH74] Gerardus 't Hooft. Planar Diagram Theory for Strong Interactions. *Nucl. Phys., B, v. B72, no. 3, pp. 461-473*, January 1974.

[Tut62a] William T. Tutte. A census of Hamiltonian polygons. *Canadian Journal of Mathematics*, 14(0) :402–417, January 1962.

[Tut62b] William T. Tutte. A census of planar triangulations. *Canadian Journal of Mathematics*, 14(0) :21–38, January 1962.

[Tut62c] William T. Tutte. A census of slicings. *Canadian Journal of Mathematics*, 14(0) :708–722, January 1962.

[Tut63] William T. Tutte. A census of planar maps. *Canadian Journal of Mathematics*, 15(0) :249–271, January 1963.

[Tut68] William T. Tutte. On the enumeration of planar maps. *Bulletin of the American Mathematical Society*, 74(1) :64–74, January 1968.

[Wat95] Yoshiyuki Watabiki. Construction of Non-critical String Field Theory by Transfer Matrix Formalism in Dynamical Triangulation. *Nuclear Physics B*, 441(1-2) :119–163, May 1995.

GÉOMÉTRIE ET PERCOLATION SUR DES CARTES À BORD ALÉATOIRES

Cette thèse porte sur des limites de grandes cartes à bord aléatoires.

Dans un premier temps, nous nous intéressons aux propriétés géométriques de telles cartes. Nous montrons d'abord des résultats concernant les limites d'échelle et les limites locales du bord de cartes de Boltzmann dont le périmètre tend vers l'infini, que nous appliquons à l'étude du modèle $O(n)$ rigide sur les quadrangulations. Ensuite, nous introduisons une famille de quadrangulations du demi-plan aléatoires avec un paramètre de torsion, dont on étudie les limites d'échelle et la structure de branchement. Enfin, nous établissons une propriété de confluence des géodésiques dans les cartes uniformes infinies du demi-plan, qui sont des limites locales de triangulations et quadrangulations à bord uniformes.

Dans un second temps, nous considérons des modèles de percolation de Bernoulli sur les cartes uniformes infinies du demi-plan. Nous calculons le seuil de percolation par site critique pour les quadrangulations, et établissons une propriété d'universalité de ces modèles de percolation au point critique à partir des probabilités de croisement. Pour finir, nous étudions la limite locale de grands amas de percolation critiques en construisant l'amas critique émergent, une triangulation uniforme infinie du demi-plan munie d'un amas de percolation critique infini.

Mots-clés. Cartes aléatoires, percolation, modèle $O(n)$, limites locales, limites d'échelle.

GEOMETRY AND PERCOLATION ON RANDOM MAPS WITH A BOUNDARY

This thesis deals with limits of large random planar maps with a boundary.

First, we are interested in geometric properties of such maps. We prove scaling and local limit results for the boundary of Boltzmann maps whose perimeter goes to infinity, which we apply to the study of the rigid $O(n)$ loop model on quadrangulations. Next, we introduce a family of random half-planar quadrangulations with a skewness parameter, and study their scaling limits and branching structure. Finally, we establish a confluence property of geodesics in uniform infinite half-planar maps, which are local limits of uniform triangulations and quadrangulations with a boundary.

Second, we consider Bernoulli percolation models on uniform infinite half-planar maps. We compute the critical site percolation threshold for quadrangulations, and prove a universality property of these percolation models at criticality involving crossing probabilities. To conclude, we study the local limit of large critical percolation clusters by defining the incipient infinite cluster, a uniform infinite half-planar triangulation equipped with an infinite critical percolation cluster.

Keywords. Random maps, percolation, $O(n)$ model, local limits, scaling limits.